P700US00

IN THE UNITED STATES PATENT AND TRADEMARK OFFICE

Application Number	:	10/482,914
Applicant	:	Nykjær et al
Filed	:	20 June 2005
Title	:	Modulation of Activity of Neurotrophins
Examiner:	:	MacFarlane, Stacey
Attorney Docket No.	:	NYKJAER1
Group Art Unit	:	1649
Confirmation Number	:	6823

Declaration of Prof. Dr. Thomas E. Willnow, Ph.D. under 37 CFR 1.132

I, Thomas E. Willnow, PhD, hereby declare and state that:

1. I am Professor of Molecular Cardiovascular Research and head of a research group at the Max-Delbrück-Center for Molecular Medicine in Berlin, focusing on functional characterization of endocytic receptors, cell surface proteins that transport metabolites, hormones or signaling molecules into cells. Further information can be retrieved from http://www.mdc-berlin.de/willnow/pages/research.htm. I have a dual appointment as full professor for Molecular Cardiovascular Research at the Charité, the Medical Faculty of the Universities of Berlin. In addition I serve as lecturer in Biochemistry at the Humbold-University in Berlin and hold the position as Scientific Director of ReceptIcon ApS of Aarhus, Denmark. I received a Diploma in Biology, University of Munich (1988) and Ph.D. in Biochemistry (with honors), University of Munich (1992).

My publications include:

a. Andersen, O.A., Reiche, R., Schmidt, V., Gotthardt, M., Spoelgen, R., Behlke, J., von Arnim, C.A. F., Breiderhoff, T., Jansen, P., Wu, X., Bales, K.R., Cappai, R., Masters, C.L., Gliemann, J., Mufson, E.J., Hyman, B.T., Paul, S.M., Nykjær, N. and T. E. Willnow. (2005) SorLA/LR11, a neuronal sorting receptor that regulates processing of the amyloid precursor protein. Proc. Natl. Acad. Sci. USA 102: 13461-13466

b. Hammes, A., Andreassen, T. K., Spoelgen, R., Raila, J., Huebner, N., Schulz, H., Metzger, J., Schweigert, F. J., Luppa, P. B., Nykjaerr, A. and T. E. Willnow. (2005) Impaired development of the reproductive organs in mice lacking megalin, an endocytic receptor for steroid hormones. Cell 122: 751-762

c. Spoelgen, R., Hammes, A., Anzenberger, U., Zechner, D., Jerchow, B., Andersen, O.M. and T.E. Willnow. (2005) LRP2/megalin is required for patterning of the ventral telencephalon. Development 132: 405-414

d. Nykjaer, A., Lee, R., Teng, T.T., Nielsen, M.S., Jansen, P., Madsen, P., Jacobsen, C., Kliemannel, M., Willnow, T.E., Hempstead, B. and C.M. Petersen. (2004) A novel neurotrophin receptor essential for proNGF induced neuronal cell death. Nature 427:843-848

e. Leheste, J., Melsen, F., Wellner, M., Jansen, P., Schlichting, U., Renner-Müller, I., Andreassen, T.T., Wolf, E., Bachmann, S., Nykjaer A. and T. E. Willnow. (2003). Hypocalcemia and osteopathy in mice with kidney-specific megalin gene defect. FASEB J. 17: 247-249

f. Nykjaer, A., Dragun, D., Walther, D., Vorum, H., Jacobsen, C.,Herz, J., Melsen, F., Christensen, E.I. and T.E. Willnow. (1999). An endocytic pathway essential for renal uptake and activation of the steroid 25-(OH) vitamin D3. Cell 96: 507-515

g. Willnow, T.E., Hilpert, J., Armstrong, S.A., Rohlmann, A., Hammer, R.E., Burns, D.K. and J. Herz. (1996). Defective forebrain development in mice lacking gp330/ megalin. Proc. Natl. Acad. Sci. USA 93: 8460-8464

h. Willnow, T.E., Rohlmann, A., Horton, J., Otani, H., Braun, J.R., Hammer, R.E. and J. Herz. (1996). RAP, a specialized chaperone, prevents ligand-induced ER-retention and degradation of LDL receptor-related receptors. EMBO J. 15: 2632-2639

i. Willnow, T.E., Armstrong, S.A., Hammer, R.E. and J. Herz. (1995). Functional expression of low density lipoprotein (LDL) receptor-related protein (LRP) is controlled by receptor-associated protein (RAP) in vivo. Proc. Natl. Acad. Sci. USA 92: 4537-4541

j. Willnow, T.E., Sheng, J., Ishibashi, S. and J. Herz. (1994). Inhibition of hepatic chylomicron remnant uptake by adenoviral gene transfer of a receptor antagonist. Science 264: 1472-1474

My CV is available online at: http://www.charite.de/for667/FOR%20667/CV%20Willnow.html

I am a consultant to the company NeuronIcon ApS of Aarhus, Denmark (the assignee of this application). I am an expert in functional characterization of Vps10p domain receptors, and highly knowledgeable in the field.

In my scientific work, I acquired extensive experience in the generation and application of antibodies for biomedical research. Successful applications include the use of antibodies to modulate (antagonize) target protein function in vitro (ligand binding), in cultured cells (ligand binding und uptake, signaling), as well as in vivo in laboratory animals (block of receptor activities in tissues).

2. I have reviewed the office action of 24 October 2007 and I understand that the Examiner has rejected claims 1-5, 7, 10-17, 33-37, 40-42 and 45 on the basis that the specification does not provide adequate direction to enable one of ordinary skill in the art to practice the invention set forth in the claims.

3. I make this declaration to rebut the Examiner's basis for the above declaration, with which I do not agree. First, I shall outline what skilled person would have known before the priority date of this application.

Neurotrophins are, as is indicated by the name itself, trophic factors, meaning that they ensure cell, specifically neuron or nerve cell, survival. Neurotrophins are essential for promoting survival, differentiation and myelination of neurons. Thus far, four mammalian neurotrophins have been identified: nerve growth factor (NGF), brain-derived neurotrophic factor (BDNF), neurotrophin 3 (NT3) and neurotrophin 4/5 (NT4/5).

Neurotrophins exert their positive effect on neurons by initiating intracellular signal transduction pathways that promote cell survival, synaptic plasticity and differentiation. These signal transduction pathways are activated by the binding of the neurotrophins to the receptor tyrosine kinases (Trk) -A, -B and -C with the p75 NT receptor ($p75^{NTR}$) functioning as a co-receptor to the Trk receptors. Neurotrophins, like other neurotrophic factors, are known to act through activation of two receptors, see the following scientific articles enclosed with this declaration: [1]Yano et al., [2]Airaksinen et al., [3]Dechant et al., [4]Chao et al. and [5]Bibel et al.

Neurotrophins are synthesized as pre-proneurotrophins and processed to proneurotrophins. These proneurotrophins, or neurotrophin precursors, carry an N-terminal domain, the pro-domain or propeptide, which is cleaved off proteolytically during processing of the proneurotrophin in the trans-Golgi network. Interestingly, not only the "mature" neurotrophins, but also the pro-neurotrophins are secreted from the cells.

This information was indeed known prior to the priority date of the present invention, as evidenced by the references disclosed on pages 1-4 of the present patent application as well as the text as such on those pages.

4. The Examiner, on page 8 of the office action, questions whether there is a nexus between modulation of the Vps10p-domain receptor family and neurotrophin or pro-neurotrophin activity.

The Vps10p-domain receptor family consists of the five members Sortilin, SorLA, SorCS1, SorCS2 and SorCS3, all comprising an N-terminally located Vps10p-domain, a single membrane spanning α-helix followed by an intracellularly located C-terminal domain.

As outlined in section 3 above, and demonstrated by [6]Yano et al., [7]Airaksinen et al., [8]Dechant et al., [9]Chao et al. and [10]Bibel et al, mature neurotrophins mediate cell survival through formation of a ternary complex with $p75^{NTR}$ and the receptors Trk A/B/C.

---

[1]Yano et al. (2000) Pharmaceutica Acta Helvetiae 74:253–260;
[2] Airaksinen and Saarma (2002) Nature Reviews - Neuroscience 3: 383-394
[3] Dechant et al. (2001) Cell Tissue Res 305:229–238;
[4] Chao (2003) Nature Reviews - Neuroscience 4: 299-309;
[5] Bibel et al (1999) EMBO J. 18(3): 616-622
[6]Yano et al. (2000) Pharmaceutica Acta Helvetiae 74:253–260;
[7] Airaksinen and Saarma (2002) Nature Reviews - Neuroscience 3: 383-394

The inventors of the discussed patent application have found that receptors in the Vps10p-domain family, are the main receptor for pro-neurotrophins, and thereby the inventors have confirmed that proneurotrophins, like neurotrophins, signal through two different receptors to exert their effect. This is demonstrated in the patent application figures 2-7. Of particular relevance is figure 3, where it is shown that proNGF binds with a higher affinity to Sortilin than to TrkA and p75.

Since it was already known in the art that pro-neurotrophins exert a pro-apoptotic effect, then knowing that receptors in the Vps10p-domain family are the main receptor for pro-neurotrophins inevitably leads to the conclusion that inhibition of binding of proNGF to receptors in the Vps10p-domain family leads to an inhibition of the pro-neurotrophic effect.

Therefore, from the finding presented in the present patent application it is clear to the person skilled in the art that inhibition of the binding of proneurotrophins to a Vps10p-domain receptor influences the balance between NGF and proNGF, since stimulation of the binding between proNGF and Sortilin leads to increased apoptotic effect of proNGF, whereas inhibition of the binding between proNGF and Sortilin leads to decreased apoptotic effects of proNGF. Thus, a stimulation of the activity of Sortilin will lead to an effect opposite the effect of NGF, i.e. increasing the pro-apoptotic effect of proNGF and therefore being neurodegenerative, whereas inhibition of the activity of Sortilin will lead to increasing effect of NGF, i.e. increase the beneficial effects of NGF in the treatment of neurodegenerative diseases.

The scientific importance of this finding is reflected by the fact that the article discussing the documentation of the present patent application was accepted and published by the highly reputed journal Nature in 2004, wherein a schematic presentation of the effect of NGF and proNGF, shown below, is found (Nykjær et al., 2004).

---

[8] Dechant et al. (2001) Cell Tissue Res 305:229–238;
[9] Chao (2003) Nature Reviews - Neuroscience 4: 299-309;
[10] Bibel et al (1999) EMBO J. 18(3): 616-622

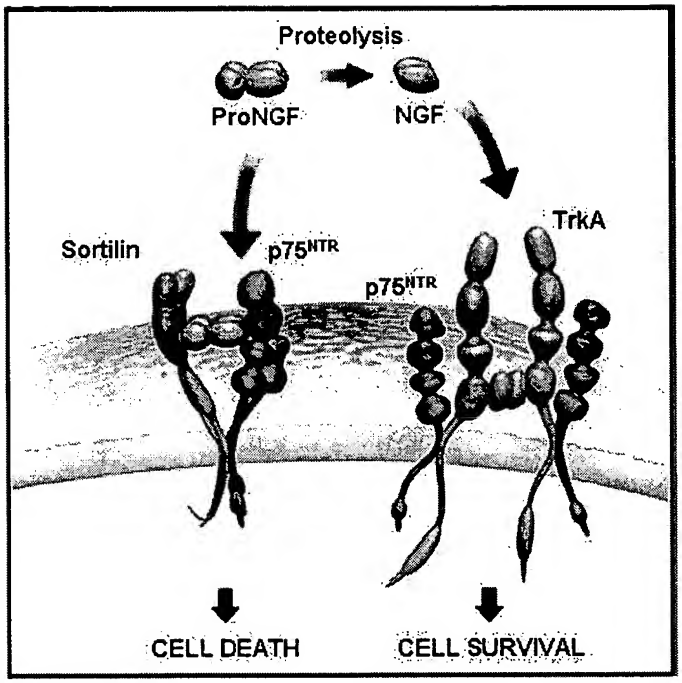

Nykjaer et al. (2004) Nature, Vol 427, p 843-848

The finding, that the Vps10p-domain receptors are the main receptors behind the death inducing capacity of the proneurotrophins, also explains how $p75^{NTR}$ can be involved in two pathways giving rise to complete opposite results: cell death and cell survival. $p75^{NTR}$ is a co-receptor that assists in the binding of selected ligands to either Trk receptors, thereby promoting cell proliferation, or Vps10p-domain family receptors and through these inducing cell death.

Accordingly, there is a clear nexus between modulation of the Vps10p-domain family and pro-neurotrophin activity.

5. On page 10 of the communication, Examiner states that "...at the time of filing, the state of the art with respect to function of these receptors was speculative at best...". As evidence thereof, Examiner cites the review paper by Mazella (2001) Cellular Signalling 13:1-6, wherein Examiner mentions that Mazella describes that Sortilin largely is located intracellularly. While it is correct that Sortilin performs an important role in intracellular sorting, especially in the late Golgi, Mazella et al on pages 3-4, section 5.1, clearly states that sortilin may act as endocytic or signalling receptor for ligands at the cell surface.

Furthermore, the enclosed paper by [11]Morinville et al., in the abstract, page 2153, lines 5-7 and 13-15, clearly states that approximately 8% of the receptor are at the cell surface at any given time. At the cell surface, Sortilin is described to acts as an endocytic receptor that binds neurotensin from the extracellular medium and mediates its endocytosis into the cells. In the same way, any other ligand such as the agent of the present invention would get access to sortilin.

In a further paper by [12]Nielsen et al., in the abstract, page 8832, lines 17-20 and 24-27, it is demonstrated that sortilin binds lipoprotein lipase (LpL). When expressed in CHO cells, the receptor Sortilin can mediate binding and endocytic uptake of the LpL. Thus, the receptor is accessible to extracellular molecules.

Taking the abovementioned papers individually or in combination, there is ample evidence in the literature that sortilin molecules shuttle between Golgi, cell surface and endosomes. Although at any given time, the pool of sortilin molecules at the cell surface may only be 10%, eventually all sortilin molecules recycle to the cell surface and will be targeted by the agents of the present invention.

Accordingly, on the contrary to what is stated by the examiner, the state of the art with respect to function of the receptors were far from speculative at the time of filing of the present application.

6. Examiner states that the instant specification does not provide any nexus between any disease/disorder and agents capable of (i) binding to a receptor of the Vps10p-domain receptor family and/or (ii) interfering with binding between a receptor of the Vps10p-domain receptor family and a neurotrophin and/or proneurotrophin and/or (iii) modulating the expression of a receptor of the Vps10p-domain receptor family.

The clinical implications of the neurotrophins are outlined on pages 2-3 of the specification, where it is disclosed that proNGF and its proteolytically processed and mature counterpart (NGF) product differentially activate pro- and anti-apoptotic cellular responses through preferential activation of $p75^{NTR}$ and Trk receptors, respectively - pro-NGF having enhanced affinity for $p75^{NTR}$ receptors and a reduced affinity for Trk receptors relative to the mature forms of NGF.

---

[11] Morinville et al. (2004) J. Biochem. and Cell Biol. 36: 2153-2168
[12] Nielsen et al. (1999) J. Biol. Chem 274(13): 8832-8836

It has been demonstrated by [13]Lee et al that pro-NGF induces $p75^{NTR}$-dependent apoptosis in cultured neurons with minimal activation of TrkA-mediated differentiation or survival. As demonstrated by e.g. [14]Mizuno et al and [15]Solary et al., the role of apoptosis in pathogenesis of disease and disorder such as AIDS, haematological diseases, neurogenerative disorders, ischaemic injury and reperfusion, and osteoporosis was indeed well known in the art well before the filing of the present application. Accordingly, the skilled person would have no problem in linking the clinical importance of modulation of apoptosis as demonstrated by embodiments of the present application, to the treatment of disease and disorder.

Additionally, neurotrophins are of clinical relevance as it is known that both upregulation of neurotrophins and increased $p75^{NTR}$ expression occur under pathological and inflammatory conditions, especially after nerve injury and damage to the vascular system. Indeed, [16]Soilu-Hanninen et al. have demonstrated that the pro-apoptotic functions of $p75^{NTR}$ are directly implicated in injury-induced apoptosis. [17]Beatty et al. demonstrated that proNGF induces p75 mediated death of oligodendrocytes following spinal cord injury.

In particular the article entitled "Regulation of Cell Survival by Secreted Proneurotrophins" by [6]Lee et al., cited at page 3, lines 12-13 of the present patent application, discusses neurotrophins and proneurotrophins and is one article amongst a variety of articles describing the general knowledge of neurotrophins and proneurotrophins before the priority date of the present invention.

It is clear from the article that neurotrophins are growth factors that promote neuronal survival and synaptic plasticity. As discussed herein above, there is ample evidence in the art that promotion of cell survival, i.e. inhibition of apoptosis would be beneficial in the treatment of disease and disorders related to excessive cell death including neurogenerative disorders such as Alzheimer's Disease and Parkinson's Disease or ischaemic injury and reperfusion e.g. during and subsequent to stroke. The Lee paper teaches that NGF exerts its beneficial effects on neurons by binding to TrkA, whereas proNGF does not bind to TrkA. On the other hand the article also shows that proNGF

[13] Lee et al. (2001) Science 294:1945-1948
[14] Mizuno et al. (1998) Internal Medicine 37(2):192-193
[15] Solary et al (1996) Eur Respir J.9:1293–1305
[16] Soilu-Hanninen , J. Neurosci. 19:4824-4838 (1999))
[17] Beattie et al (2002) Neuron 36: 375–386

binds with a greater affinity to $p75^{NTR}$ as compared with the binding affinity of NGF as such to $p75^{NTR}$. Thus, the article informs the skilled person that NGF is responsible for anti-apoptotic effects of the neurotrophins whereas proNGF is responsible for the pro-apoptotic effects of neurotrophins.

Furthermore, treatment of various diseases by administration of NGF was also known at the priority date of the present invention, for example neurodegenerative diseases, such as Parkinson's disease, Alzheimer's disease and amyotrophic lateral sclerosis.

The clinical importance of pro-neurotrophins, such as proNGF, is immediately clear from the Lee article cited above, in that promoting apoptosis of neurons lead to diseases associated with neuron degeneration or damage.

In an experiment, male rats were subjected to spinal cord injury as described by Harrington et al., Proc.Natl.Acad.Sci (2004), 101:6226-6230, in the absence (black column in figure below) or the presence of 1 ml/hrs of 100 mg/ml propeptide of proNGF (white column in the figure below). The receptor antagonist was applied by using osmotic minipumps for 7 days, after which the number of surviving motor neurons were scored. The propeptide of proNGF was fused to GST as described in Nykjaer et al, Nature (2004) 427:843-848.

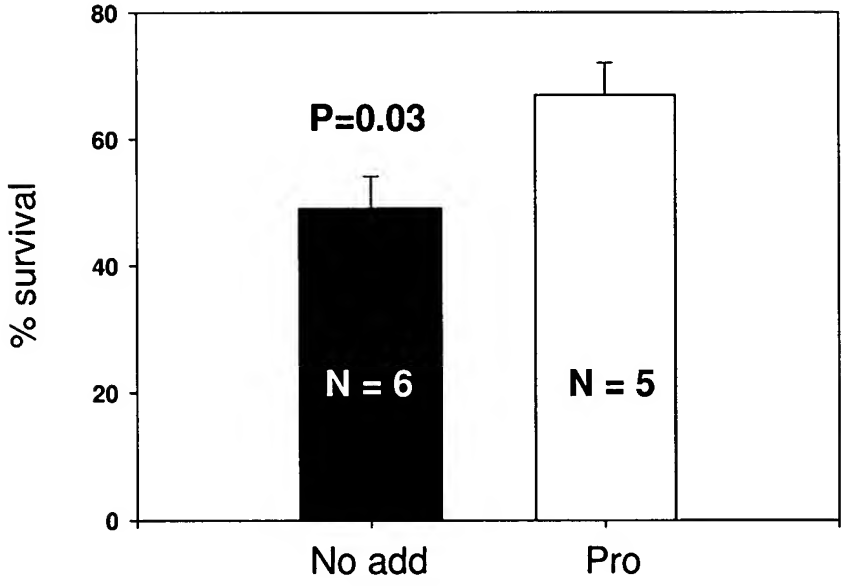

The results illustrated in the above figure demonstrate that whereas only 49% of the neurons

survive in the absence of a sortilin antagonist, 67% of the neurons stay alive in the presence of the proNGF propeptide which specifically inhibits binding of proneurotrophins to sortilin.

Accordingly, there is indeed a nexus between dysfunctions of the nervous system and inhibition of the pro-neurotrophin mediated pathway in accordance with the invention as claimed in the present application.

7. On page 9 (item 10) of the communication, Examiner states that it would require undue experimentation to discover how to practice the invention of the present patent application.

This is not correct for the following reasons. Testing compounds in an assay as described in the present patent application allows the skilled person to determine whether any compound fulfils the functional definition. Furthermore, an in vitro assay for evaluating ligand binding to Vps10p-domain receptors is outlined on page 40, line 26 to page 41, line 14. In this regard the skilled person may elect to use a commercial library comprising a large number of candidate (antibody) compounds for evaluation of binding to a receptor according to the in vitro screening method of the present invention. The inventors of this application have raised antibodies against several parts of the Vps10p-domain receptors. The present invention is directed to antibodies against the unifying feature of this receptor family – the Vps10p domain. The below sequence alignment of the Vps10p-domain demonstrate the conservation within this receptor family.

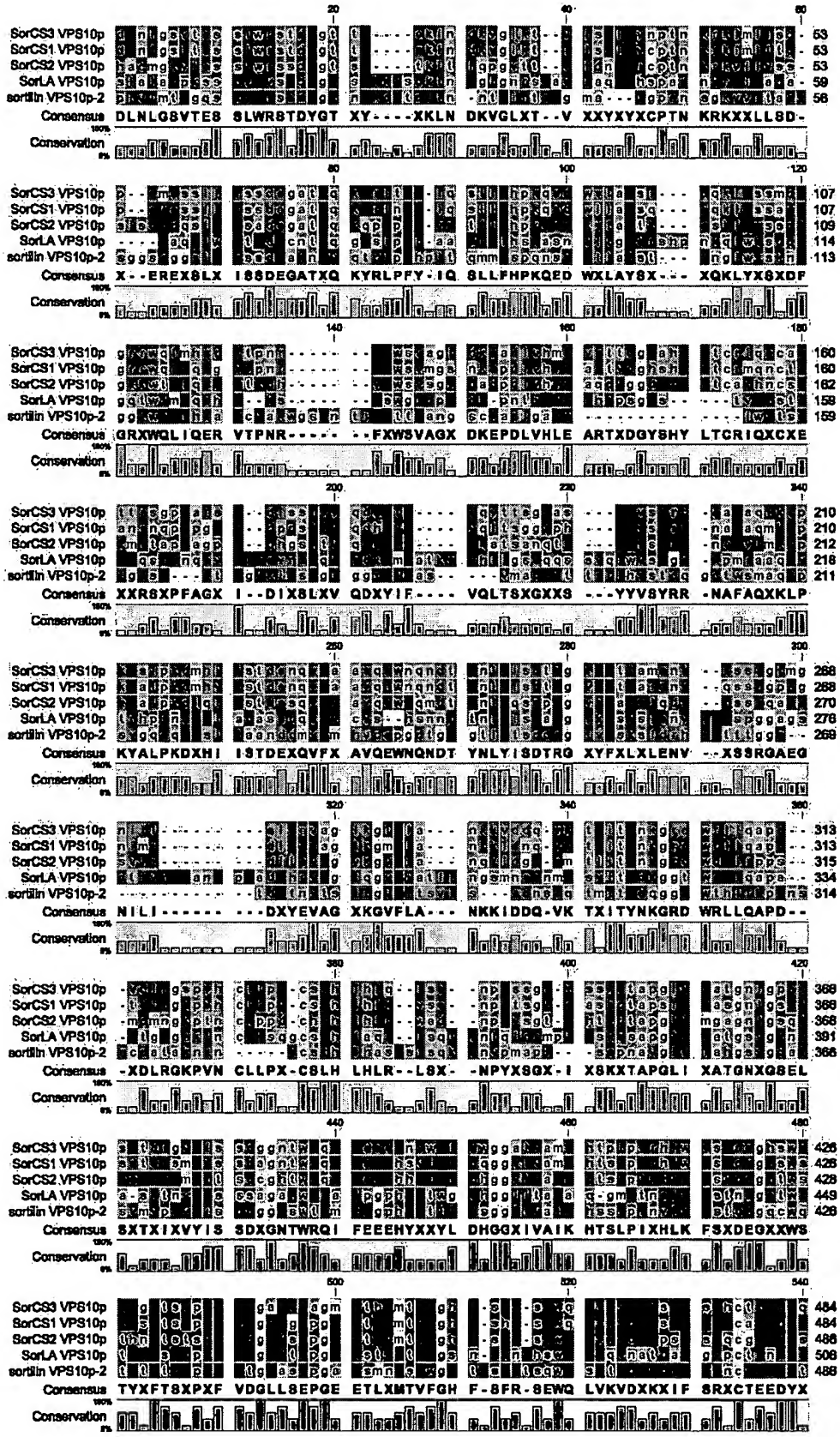
SorCS3 VPS10p
SorCS1 VPS10p
SorCS2 VPS10p
SorLA VPS10p
sortilin VPS10p-2
Consensus
Conservation

tors

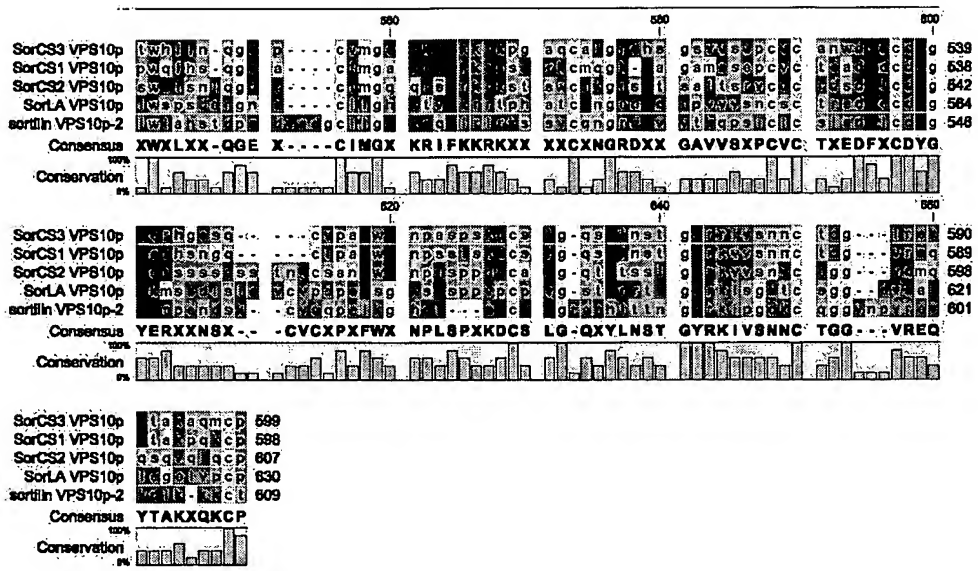

Generic use of an antibody to inhibit binding of a ligand

An antibody binds tightly to a particular target molecule, thereby either inactivating it directly or marking it for destruction. The antibody recognizes its target (antigen) with remarkable specificity and strength dictated by the sum of many chemical forces, including hydrogen bonds, hydrophobic and van der Waal's forces, as well as ionic interactions. In general, the more complex the target is chemically, the more immunogenic it will be. The antigenic determinant may encompass short linear amino acid stretches or a more complicated, three-dimensional protein module.

Conceptually, antibodies directed against a target receptor may inhibit ligand binding in two ways: competitive or allosteric. Competitive inhibition involves the direct binding of the antibody to or near the ligand binding site on the receptor, thereby displacing the ligand from its receptor or sterically inhibiting the approach of the ligand to the ligand binding site. Allosteric inhibition involves the binding of the antibody to a site on the receptor polypeptide that is distinct from the ligand binding epitope. However, binding to this site will induce a conformational change in the overall structure of the receptor that makes it more difficult or even impossible for the ligand to bind to its cognate recognition site.

Currently known antibodies against members of the Vps10p-domain receptor family

Receptor	Name	Antigen	Species	Western	IH/IC	Ref.
SorLA	SORLA goat	extracellular domain	goat	X	X	Schmidt et. al., J.Biol.Chem. 282:32956-67, 2007
	Hale SORLA	Cytoplasmic domain	rabbit	X		
	SORLA LA	Complement type repeat	rabbit	X		
	Sol SORLA	extracellular domain	rabbit	X	X	Andersen et al., PNAS 103:13461-6, 2005
	SORLA tail	Cytoplasmic domain	rabbit	X		
	SORLA VPS	VPS10p domain	rabbit	X		
	#606870	Peptide seq. in Vps10p-domain	rabbit	X		
	#642739	C-terminal	rabbit	X		
	#643739	Cytoplasmic tail	rabbit	X		
	20C11	Extracellular domain	mouse	X	X	
	AG4	Extracellular domain	mouse	X		
Sortilin	#5264	Extracellular domain	rabbit	X	X	Munck Petersen et al, EMBO J. 18 :595-604, 1999
	#5448	Cytoplasmic domain	rabbit	X	X	Jansen et al, Nature Neurosci. 10 :1449-1457, 2007
	#5287	Cytoplasmic domain	rabbit	X		
	CP 96 334 SR 96 204	propeptide	Rabbit	X		Munck Petersen et al, EMBO J. 18 :595-604, 1999
	#5438	Vps10p	rabbit	X		

	Sortilin goat /Laika	Extracellular domain	goat	X		
	F9	Extracellular domain	mouse	X	X	
	F11	Extracellular domain	mouse	X	X	
	AF2934	Extracellular domain	goat	X	X	R&D Systems, Jansen et al, Nature Neurosci. 10 :1449-1457, 2007
	AF3154	Extracellular domain	goat	X	X	R&D Systems; Jansen et al, Nature Neurosci. 10 :1449-1457, 2007
	anti-NTR3	Extracellular domain	mouse	X	X	BD Transduction Laboratories,
	ANT-009	Extracellular domain	mouse	X	X	Alomone Labs ; Nykjaer et al, Nature427 :843-848, 2004
SorCS1	AF3457	Extracellular domain	goat	X	X	BD Transduction Laboratories
	SorCS1 goat	Extracellular domain	goat	X		
	L-SorCS1	Extracellular domain	rabbit	X	X	Hermey et al, J.Biol.Chem. 279:50221-50229, 2003
	Leu-SorCS1	Leucine-rich domain	rabbit	X	X	Hermey et al, J.Biol.Chem. 279:50221-50229, 2003
	#5466	Extracellular domain	rabbit	X	X	
	1D	Extracellular domain	mouse	X		
	4H	Extracellular domain	mouse	X		
	6B	Extracellular domain	mouse	X		

	4A	Extracellular domain	mouse	X		
SorCS2	AF4237	Extracellular domain	sheep	X		BD Transduction Laboratories
	SorCS2 goat	Extracellular domain	goat	X	X	
	#5422	Extracellular domain	rabbit	X	X	Hermey et al, Biochem. J., 395:285-93, 2006
	#5431	28 C-terminal amino acids	rabbit	X	X	
	SorCS2-prp	propeptide	rabbit	X		Schousboe Sjoegaard, Dissertation, Aarhus University, 2005
	M1	Extracellular domain	mouse		X	Roland Holst, Master of Science Thesis, Aarhus University, 2006
	M3	Extracellular domain	mouse		X	Roland Holst, Master of Science Thesis, Aarhus University, 2006
	M4	Extracellular domain	mouse		X	Roland Holst, Master of Science Thesis, Aarhus University, 2006
	M7	Extracellular domain	mouse		X	Roland Holst, Master of Science Thesis, Aarhus University, 2006
	M9	Extracellular domain	mouse		X	Roland Holst, Master of

						Science Thesis, Aarhus University, 2006
	M10	Extracellular domain	mouse		X	Roland Holst, Master of Science Thesis, Aarhus University, 2006
	M13	Extracellular domain	mouse	X		Roland Holst, Master of Science Thesis, Aarhus University, 2006
	M15	Extracellular domain	mouse		X	Roland Holst, Master of Science Thesis, Aarhus University, 2006
	M18	Extracellular domain	mouse	X	X	Roland Holst, Master of Science Thesis, Aarhus University, 2006
	M19	Extracellular domain	mouse	X	X	Roland Holst, Master of Science Thesis, Aarhus University, 2006
	S21	Extracellular domain	mouse	X		Roland Holst, Master of Science Thesis, Aarhus University, 2006
	SorCS2-GST-73aa	Extracellular domain	rabbit	X		
	SorCS2-GST-100aa	Extracellular domain	rabbit	X		
	SorCS2-GST-172aa	Extracellular domain	rabbit	X		

SorCS3	SorCS3-N	extracellular domain	rabbit	X		
	SorCS3-C	15 C-terminal aa	rabbit	X		
	Sort3 N Term #5389	N-terminal domain	rabbit	X	X	Westergaard et al, FEBS Lett. 579:1172-6, 2005
	#5432	Extracellular domain	rabbit	X	X	
	MAB3067	Extracellular domain	mouse	X		BD Transduction Laboratories
	MAB30671	Extracellular domain	mouse	X		BD Transduction Laboratories
	AF3326	Extracellular domain	goat	X		BD Transduction Laboratories
	SorCS3 goat	Extracellular domain	goat	X		

Anti-SorLA (sol SorLA) immunhistochemistry of the neocortex from a wild-type mouse (left, +/+) and a sorLA knockout mouse (right, -/-). The inset depict a western blot of brain extracts of the respective genotypes.

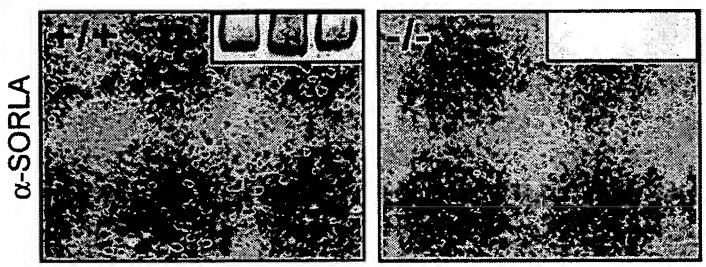

Anti-Sortilin (#5448) immunhistochemistry of the neocortex from a wild-type mouse (left, +/+) and a sortilin knockout mouse (right, -/-). Inset shows a western blot of superior cervical ganglia extracts using the same antibody.

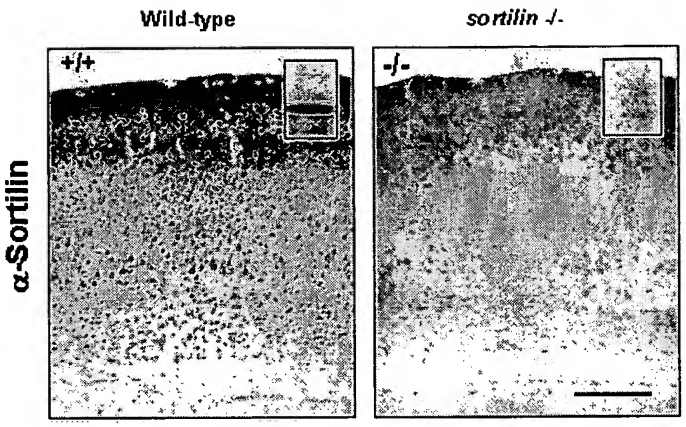

Procedures for making antibodies

Polyclonal and monoclonal antibodies directed against a specific antigen, or epitope of an antigen, can be produced according to standard procedures (see e.g. Antibodies – A laboratory Manual by Ed Harlow and David Lane, Cold Spring Harbor Laboratory 1998, ISBN 0-87969-314-2). The procedure for subsequent generation of humanized antibodies or fragments thereof has also been described (e.g. A. M. Scott et al, Cancer Research 60:3254-3261, 2000; A. Nissim and Y. Chernajovsky, Handb. Exp. Pharmacol. 181:3-18, 2008; A. Mountain and J. R. Adair, Biotechnol. Genet. Eng. Rev. 10:1-142, 1992).

General expectations of success in making antibodies

It is possible to generate antibodies against any peptide motif of choice using short synthetic oligopeptides that encompass the desired target epitope. Therefore, it is guaranteed that antibodies against ligand binding sites on receptors can be generated. Whether or not individual antibody species have the potential to inhibit ligand binding simply depends on the fact that the affinity of the immunoglobulin for the receptor exceeds that of the ligand. In the end, it is a matter of screening the inhibitory potential of a number of individual antibodies to find one with the desired properties.

Screening assays for inhibitory antibodies are common knowledge and typically involve a competitive enzyme linked immunosorbent assay (ELISA). In detail, the recombinant receptor or a fragment encompassing its ligand binding motif are immobilized in replicate wells of microtiter

plates. Subsequently, the wells are incubated with a solution containing the ligand. Binding of the ligand to the immobilized receptor is confirmed using an antibody that recognizes the ligand and that is coupled with a color dye reaction. Binding of the ligand to the receptor is tested in the presence of various antibodies to identify those immunoglobulin species that block ligand binding to the receptor and hence prevent color reaction in the respective microtiter plate well.

Successful clinical use of antibodies

A number of therapeutic antibodies are in clinical use. Examples include Genentech's Rituxan, an antibody directed against the CD20 receptor (used in rheumatoid arthritis), Johnson & Johnson's Remicade, an antibody directed against TNF alpha receptor (in Psoriasis), Roche's Avastin, an anti-VEGF antibody used for treatment of colorectal and lung cancer, as well as Herceptin, an antibody against the receptor HRE2 used in breast cancer therapy.

Assessing binding to a receptor is routine work for the person skilled in the biotechnical field. In this regard it has to be mentioned that pro-neurotrophins as well as the Vps10p-domain receptor family were known at the priority date of this invention and binding assays involving for example pro-neurotrophins has been mentioned in the prior art, for example in the article by Lee et al. mentioned above.

Furthermore, at page 41, line 31 to page 42, line 5 assays that can be used for measuring the binding of a pro-neurotrophin to a receptor of the Vps10p-domain receptor family are disclosed. In addition thereto, figure legends to Figures 2-6 describe how the binding to Sortilin is measured.

In summary, the present application discloses clear instructions of how to define the antibody agents, since the skilled person is able to apply an antibody to a binding assay specified in the patent description and test whether it inhibits binding of a neurotrophin to a Vps10p-domain receptor or not without employing any inventive skills.

Accordingly, a person skilled in the art is able to determine that the agents defined by the present invention may have an effect corresponding to the effect of a neurotrophin when used as a medicament, as stated at page 32, lines 29-30 of the patent description: "...to promote the survival or growth of neurons, or in whatever conditions are treatable with NGF, NT-3, BDNF, or NT-4/5",

due to the combined knowledge of the prior art and the finding presented in the present application that the Vps10p-domain receptor family is the main receptor for proneurotrophins.

8. On page 12 of the communication, Examiner cites a section of a paper by Pardridge as evidence of that administration of that large molecule drugs do not cross the blood brain barrier (BBB). While it is true that most large, water soluble molecules do not cross an undisrupted BBB, there are indeed examples of the opposite in the art such as paper by [18]Friden et al., entitled "Anti-transferrin receptor antibody and antibody-drug conjugates cross the blood-brain barrier".

Examiner furthermore fails to recognise that agents of the present invention are not administered to healthy individuals but to individuals in need of treatment of injury and/or dysfunction of the central and/or peripheral nervous system. It is well known in the art that during disease, the blood-brain barrier is leaky and thus allows passage of endogenous or exogenous molecules including anti-bodies.

One example of a disease state when sortilin antibodies would be applied to the CNS is in a state of acute distress such as stroke when the blood brain barrier is leaky. The following scientific journal articles describe breakdown of the BBB during disease states such as cerebral ischemia, stroke, multiple sclerosis, Alzheimer's disease and other indications treatable by agents of the present invention. The papers also describe states wherein the BBB is permeable and indicate the ability to deliver immunoglobulins to the brain in diseases addressed by the inventors of the present patent application.

[19]Rubin and Staddon on page 23 last three lines disclose that disruption of the BBB can be a relatively major part of the pathology following cerebral ischemia. On page 24, last line, the authors state that "...the hallmark of the BBB is its permeability, but we have already seen instances in which this feature is violated."

[18] Friden et al. , in PNAS (1991) 88(11): 4771–4775
[19] Rubin and Staddon (1999) Annu. Rev. Neurosci. 22:11–28

[20]Arshavsky on page 1697 in line 9-11 of the summary states that "Evidence emerging from recent literature indicates that AD may have an autoimmune nature associated with BBB impairments" which in other words mean that the BBB is permeable to immunoglobulins. Page 1698, left column, last paragraph states that "The growing bulk of evidence suggests that the development of AD might be related with impairments of the barrier function of the BBB..." and "It has been shown that among these effects the cardiovascular factors leading to AD is the interruption of the BBB."

On the same page, right column, last paragraph, last three lines, continuing on the next page 1699 it is stated that "The memory impairments in [..] mice developed around the age of 6-10 months, when the BBB was severely damaged but the plaques were not formed. All these results suggest that AD neuron pathology and memory deficit resulting from the mutation of the APP gene may be more closely related to a faulty BBB than to accumulation of Aβ in the brain."

On page 1699, left column it is further stated that "These findings, as well as results obtained on transgenic mice led some investigators to the suggestion that the primary cause for onset of AD (caused both cardiovascular disorders and genetic factors) is cerebral vascular pathology leading to the impairment of the barrier function of the BBB."

On page 1700 left column, second paragraph: " This concept is based on the results obtained in postmortem immunostaining studies of AD brains and "control" brains taken from individuals of a similar age. These studies have revealed significant penetration of blood proteins, including Igs, into the brain parenchyma of AD patients. [..] Strong immunostaining by the anti-immunoglobulin serum was observed in those cortical areas that contained numerous amyloid plaques, whereas only minor staining was observed in the areas where few plaques were found." Finally on page 1701, first and second line of the conclusion: "Recent findings strongly suggest that AD is an autoimmune disease resulting from a breakdown of the BBB...".

[21]De Boer and Gaillard in the abstract of their paper state that "Many (brain) diseases change the functionality and integrity of the BBB. Mostly this results in increased BBB permeability. [..] Many diseases with an inflammatory component like multiple sclerosis, meningitis, encephalitis, ischemic

[20] Arshavsky (2006) J Neural Transm 113: 1697–1707
[21] De Boer and Gaillard (2006) J Neural Transm 113: 455–462

stroke, head trauma, neurodegenerative diseases like Parkinson's and Alzheimer, AIDS-related dementia, change the functionality and/or integrity of the BBB and thus brain homeostasis."

The authors continue on page 457, right hand column, last paragraph by stating that "Increased BBB permeability for blood compounds has been observed under the influence of diseases, like multiple sclerosis [..], Alzheimer [..], AIDS-related dementia [..], encephalitis and meningitis [..], high blood pressure, seizures and by psychiatric disease.

In [22]Deli et al (2005), on page 83 under "Pathology" it is stated that the BBB permeability play a crucial role in brain edema formation and central nervous system injuries during human diseases, such as stroke, cerebral hypoxia-reoxygenation, head injuries, neurodegenerative diseases, and neurological infections including bacterial and viral meningitis, encephalitis, or HIV-1 infection. On page 84 it further stated that the mentioned models of BBB pathology may offer a suitable tool for testing efficacy and brain penetration of new drugs and it is also described that brain ischemia resulting e.g. from stroke, changes BBB permeability.

In [23]Ballabh et al (2004) on page 7, top of left column under "Opening of the BBB in pathophysiology" it is stated that during pathological conditions, the permeability of the BBB increases. On page 8, left column it is stated that hypoxia-ischemia sets in motion a series of events, which leads to disruption of TJ (tight junctions) and increases BBB permeability. On the very same page in the right column under "Break down of BBB in sepatic encephalopathy" it is declared that inflammation of the brain increases permeability of the BBB. On page 9, bottom left column it is disclosed that the BBB is leaky also in Alzheimer's disease, Parkinson's disease and in viral infection.

In [24]Neuwelt (2004) on page 136, right column it is disclosed that in multiple sclerosis, increased BBB permeability is an early event. On page 137, left column of the same paper it is disclosed that the BBB is disrupted as a consequence of stroke.

---

[22] Deli et al (2005) Cell and Mol Neurobiol 25(1): 59-127
[23] Ballabh et al (2004) Neurobiology of Disease 16:1-13
[24] Neuwelt (2004) Neurosurgury 54: 131-142

The papers by Rubin and Staddon, Arshavsky et al., De Boer and Gaillard, Deli, Ballabh et al. and Neuwelt, all disclose that the blood brain barrier is leaky during conditions such as e.g. stroke and ischemia, Alzheimer's disease and Parkinson's disease which are indications to be treated by administering agents of the present invention.

Thus, in conclusion there is overwhelming evidence in the art, both prior and subsequent to the priority date of the present patent application, of permeability of the blood-brain barrier, in particular during disease stages, including permeability to macromolecules such as immunoglobulins which are agents of the present invention.

I hereby declare that all statements made herein of my own knowledge are true and that all statements made on information and belief are believed to be true; and further that these statements and the like so made are punishable by fine or imprisonment, or both, under Section 1001 Title 18 of the United States Code, and that such willful false statements may jeopardize the validity of the application or any patent issuing thereon.

SIGNATURE:

Prof. Dr. Thomas E. Willnow, PhD

March 11, 2008
Date

ELSEVIER

Pharmaceutica Acta Helvetiae 74 (2000) 253–260

PHARMACEUTICA ACTA HELVETIAE

www.elsevier.com/locate/pharmactahelv

Neurotrophin receptor structure and interactions

Hiroko Yano, Moses V. Chao *

Molecular Neurobiology Program, Skirball Institute of Biomolecular Medicine Department of Cell Biology Department of Physiology and Neuroscience New York University School of Medicine 540 First Avenue New York, NY 10016, USA

Keywords: Neurotrophins; Brain derived neurotrophic factor (BDNF); p75 receptor; NGF; neurotrophin-3 (NT-3); neurotrophin-4/5 (NT-4)

1. Introduction

Neurotrophins represent a family of survival and differentiation factors that exert profound effects in the central and peripheral nervous systems (Levi-Montalcini, 1987; Barde, 1989; Thoenen, 1995). Nerve growth factor (NGF), brain derived neurotrophic factor (BDNF), neurotrophin-3 (NT-3), and neurotrophin-4/5 (NT-4) associate as non-covalent homodimers in a biologically active form. These target-derived trophic factors are active on distinct sets of embryonic neurons, whose dependence is restricted in duration during development (Davies, 1994). Neurotrophins have been proposed as therapeutic agents for the treatment of neurodegenerative disorders and nerve injury, either individually or in combination with other trophic factors, such as ciliary neurotrophic factor (CNTF), insulin-like growth factor and fibroblast growth factor (Lindsay et al., 1994; Nishi, 1994). Recent clinical efforts have met with disappointing results. Improvements in overcoming difficulties of delivery and pharmacokinetics in the central nervous system will provide more impetus for the application of neurotrophins for neurodegenerative diseases. An understanding of the mechanisms of neurotrophin action will provide insights into the use of this proteins therapeutically.

Responsiveness of neurons to neurotrophins is governed by the expression of two classes of cell surface receptors (Chao, 1992a). For NGF, they are $p75^{NTR}$ (p75) and the TrkA receptor tyrosine kinase. Three vertebrate *trk* receptor genes have been isolated, including numerous variants of *trk* structure (Barbacid, 1994). The related TrkB receptor tyrosine kinase binds both BDNF and NT-4, the most closely related neurotrophins from phylogenetic analysis, while TrkC receptor binds only NT-3. NT-3 can also bind to the TrkA receptor. The p75 receptor binds to all neurotrophins with similar affinities, but different kinetics (Rodriguez-Tebar et al., 1992). Hence, the neurotrophins can engage two separate receptors, which can act independently, or interact with each other.

The mechanism of action of neurotrophins has provided a challenging and formidable problem in signal transduction. In addition to promoting cell differentiation and survival, neurotrophins can induce cell death under certain conditions. Several mechanisms have been proposed to explain how NGF might act as a trophic factor and as a cell killer (Casaccia-Bonnefil et al., 1998). The survival and cell death properties of the receptors are dependent upon the relative ratio of receptors and the duration of the signalling events. Here we provide evidence that neurotrophin receptors exist as preformed multi-subunit complexes. Such complex formation by transmembrane receptors is likely to dictate biological responsiveness to neurotrophins.

2. Neurotrophin structure

Neurotrophins are produced as precursor proteins, which are cleaved at dibasic amino acids to form a mature form of 118–120 amino acids (Angeletti and Bradshaw, 1971; Leibrock et al., 1989; Maisonpierre et al., 1990). The X-ray crystal structure of NGF has been solved and provides a structural model for this family (McDonald et al., 1991). The conservation of structural features indicates that the neurotrophins will adopt similar conformations to that of NGF.

* Corresponding author. Tel.: +1-212-263-0761; fax: +1-212-263-0723; e-mail: chao-saturn.med.nyu.edu

PII: S0031-6865(99)00036-9

The dimeric NGF possesses a novel tertiary fold that results in a flat asymmetric molecule with dimensions of 60 Å by 25 Å by 30 Å (McDonald et al., 1991). Each NGF subunit is characterized by two pairs of anti-parallel β-strands that contribute to the molecule's flat, elongated shape. These β-strands are connected at one end of the neurotrophin by three short loops. These loops are known to be highly flexible and represent the regions in the neurotrophin structure where many amino acid differences exist between the neurotrophins.

The three disulfide bridges in each neurotrophin are clustered at the one end of molecule and provides rigidity to the structure. The arrangement of the disulfide linkages is unusual. The disulfide bridges and their connecting residues form a ring structure and a tightly packed cystine knot motif (McDonald and Hendrickson, 1993). This cystine knot allows the two pairs of β-strands from each neurotrophin to pack against each other, generating an extensive subunit interface. The interface has a largely hydrophobic character comprised primarily of aromatic residues, consistent with the tight association constant (10^{13} M) measured for NGF. The NGF tertiary fold and "cystine knot" motif have been identified in structures of transforming growth factor β (TGF-β), platelet-derived growth factor (PDGF) and more recently in human chorionic gonadotrophin (McDonald and Hendrickson, 1993). Members of this diverse structural superfamily of ligands typically form homo- or hetero-dimeric species.

The structural features of the neurotrophin family, in particular the dimer interface, are highly conserved, as evidenced in the ability of these members to form dimers in vitro (Arakawa et al., 1994; Jungbluth et al., 1994; Radziewjewski and Robinson, 1993). These heterodimeric proteins give functional activity in many cases, indicating there is overall compatibility of these structures.

3. Neurotrophin receptors

The neurotrophins are unusual among polypeptide growth factors in that two different transmembrane proteins serve as receptors for each neurotrophin. The structural features of Trk tyrosine kinases and the p75 neurotrophin receptor are displayed in Fig. 1. The Trk subfamily of receptor tyrosine kinases is distinguished by immunoglobulin-C2 domains and repeats rich in leucine and cysteine residues in the extracellular domain and a tyrosine kinase domain with a small interruption and a short cytoplasmic tail.

The p75 receptor contains four negatively charged cysteine-rich extracellular repeats, and a unique cytoplasmic domain which is highly conserved among species. There are no sequence similarities between the Trk and p75 receptors, in either ligand binding or cytoplasmic domains. The p75 receptor is the founding member of a superfamily of receptors, exemplified by tumor necrosis factor (TNF) and the Fas receptor (Smith et al., 1994). The TNF family of receptors is defined by canonical cysteine-rich domains in the extracellular region. Each cysteine-rich domain folds independently and is stabilized by extensive intrachain disulfide bonding. Other members include the lymphoid

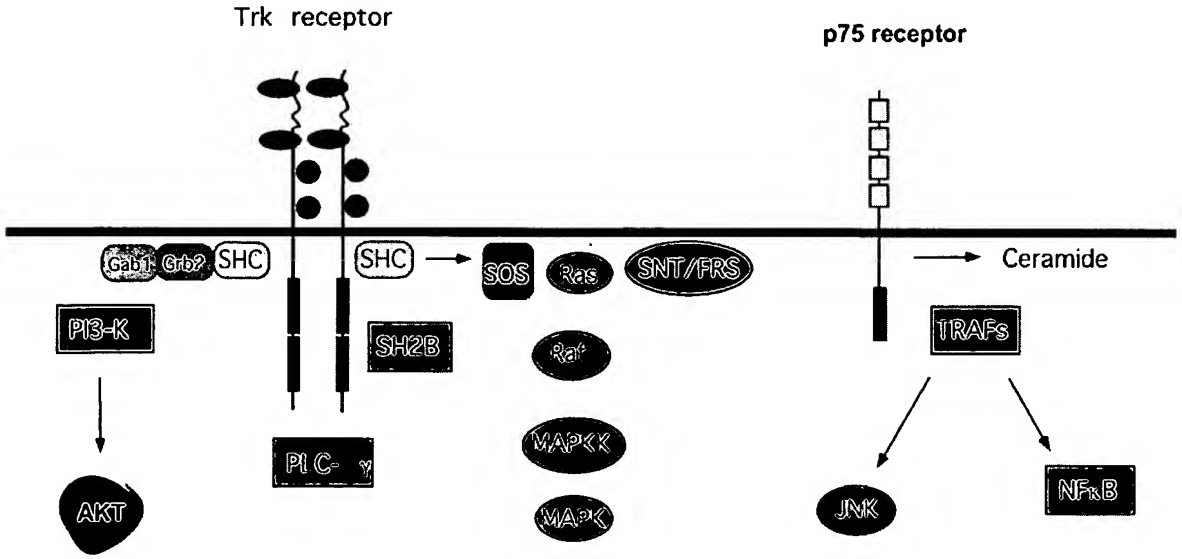

Fig. 1. Transmembrane receptors for NGF. Whereas the TrkA receptor is a member of tyrosine kinase family of receptor, the p75 neurotrophin receptor belongs to the TNF superfamily of receptors. A schematic representation of the TrkA and the p75 neurotrophin receptor is shown, together with their substrates and adaptor proteins Trk adaptor proteins include FRS II (Kouhara et al., 1997) and SH2B (Qian et al., 1998). Signal transduction by the neurotrophins involves recruitment of enzymatic activities, such as phosphatidylinositol 3′ kinase (PI3-K) and phospholipase C-γ for TrkA (Kaplan and Stephens, 1994) and TRAF6 for p75 (Khursigara et al., 1999).

cell-specific receptor CD30, CD40, CD27, and other diverse members, such as DR-3, DR-4, CAR-1 and GITR (Smith et al., 1994; Brojatsch et al., 1996; Chinnaiyan et al., 1996; Montgomery et al., 1996; Pan et al., 1997). All of these transmembrane proteins share in their extracellular domains a cysteine motif that spans 40 amino acids and is repeated two to six times.

Each class of receptors undergoes ligand-induced dimerization (Grob et al., 1985; Jing et al., 1992) that activates multiple signal transduction pathways. Neurotrophin binding to Trk family members produces biological responses through activation of the tyrosine kinase domain resulting in a rapid increase in the phosphorylation of selected effector enzymes, such as phospholipase C-γ and phosphatidylinositol 3′-kinase, PI3-K (Fig. 1). Increased *ras* activity, a common signal from all tyrosine kinase receptors, results from the stimulation of guanine nucleotide exchange factors coupled to SHC adaptor proteins which directly interact with Trk after ligand binding (Kaplan and Stephens, 1994). The p75 receptor signals via pathways involved with activation of sphingomyelinase activities (Dobrowsky et al., 1994), NFκB (Carter et al., 1996) and c-jun N-terminal Kinase, JNK (Casaccia-Bonnefil et al., 1996). More crucially, expression of p75 modulates Trk signalling activity at low concentration of neurotrophins (Barker and Shooter, 1994; Hantzopoulos et al., 1994; Verdi et al., 1994).

The substrates for neurotrophin Trk receptors-phospholipase C-γ, PI3-K SHC and Grb2 adaptor proteins-are utilized by many tyrosine kinase receptors. This raises the question of how these phosphorylation events lead to different biological outcomes (Chao, 1992b). There are several possibilities. First, the strength and duration of the receptor autophosphorylation events may determine downstream signalling outcomes. Second, differential signalling may be controlled by specific dephosphorylation events. Third, there may be unique second messengers or substrates which determine the specific nature of the response.

For neurotrophin factors, the timing of signalling has provided an important criteria for differential signalling. In PC12 cells, NGF induces a prolonged activation of Ras and MAP kinase activity, lasting for several hours, while EGF-mediated MAP kinase activation is transient in nature (Qui and Green, 1991, 1992). The duration signalling is one of the major differences that accounts for the differentiation program elicited by NGF vs. the action of other mitogenic growth factors, such as EGF. However, the magnitude of receptor signalling is not sufficient. Ligand-dependent autophosphorylation of the EGF receptor is higher than that of the TrkA NGF receptor in PC12 cells (Berg et al., 1992). Since EGF does not elicit neuronal differentiation as NGF, the level of receptor activation cannot solely account for the difference in trophic factor action.

Another mechanism is the recruitment of receptor substrates such as docking or adaptor proteins. FRS-2/SNT is an highly phosphorylated protein that contains an NH_2-terminal myristylation site, a phophotyrosine binding (PTB) domain and binding sites for SH2 and SH3 containing proteins (Kouhara et al., 1997). Other adaptor protein, SH2-B/rAPS, bind to Grb2 and promotes NGF-dependent activation of Ras and MAP kinases. These proteins interact with the catalytic domain of the TrkA receptor (Qian et al., 1998) and mediate signalling in a variety of neuronal populations. The large number of adaptor proteins that associate with Trk receptors suggest that there are multiple pathways for signal transduction.

4. Binding properties of Trk and p75 receptors

Two classes of NGF binding sites exist on the surface of responsive neurons (Sutter et al., 1979). These sites differ 100-fold in equilibrium binding constants, which can be further distinguished by the rates of ligand association and dissociation. The proteins responsible for the high affinity NGF binding site were a subject of considerable debate, since a small percentage of high affinity sites were detected for the TrkA receptor (Jing et al., 1992).

However, both p75 and TrkA receptors have been shown to contribute to the high affinity NGF binding site. Whereas p75 displays fast rates of association and dissociation with NGF, TrkA interacts with much slower on- and off-rates (Mahadeo et al., 1994). Due to its unusually slow on-rate, NGF binding to TrkA results in a relative low affinity K_d of 10^{-9}–10^{-10} M. A similar affinity has been determined for BDNF binding to TrkB receptors (Dechant et al., 1993). These affinities are lower than the high affinity binding site, $K_d = 10^{-11}$ M, measured in sensory neurons (Dechant et al., 1993; Sutter et al., 1979). When TrkA and p75 receptors are co-expressed, the on-rate is accelerated 25-fold, creating a new kinetic site whose features are consistent with the high affinity NGF binding site ($K_d = 10^{-11}$ M). This site requires an excess ratio of p75 to TrkA (Chao, 1994). Hence, one function of the p75 receptor is to increase the binding affinity of NGF for TrkA.

It is therefore not correct to refer to p75 and Trk receptors as low and high affinity receptors, since TrkA and TrkB displayed predominantly low affinity values (Hempstead et al., 1991; Dechant et al., 1993) and p75 receptors can exist in a high affinity state (Dechant and Barde, 1997). It is more correct to use the terms high and low affinity to refer to binding sites.

Other receptor systems exhibit similar behavior. At least two functional receptor subunits for IL-2, IL-6, and CNTF are required for high affinity ligand binding, with each subunit independently binding the ligand with a lower affinity. A difference of nearly a 100-fold in the equilibrium binding constants can be contributed by the existence

of a multisubunit receptor system (Nicola and Metcalf, 1992; Mahadeo et al., 1994).

After binding neurotrophins, the ligand-receptor complex is internalized and retrogradely transported in the axon to the cell body (Distefano et al., 1992). Both Trk and p75 receptors play a role in the retrograde transport of neurotrophins. For example, in the isthmo-optic nucleus, BDNF is taken up at the axon terminal and transported to the cell body by both p75 and TrkB receptors (von Bartheld et al., 1995).

Neurotrophin binding to Trk receptors requires the two extracellular immunoglobulin (Ig)-like domains, which may also be necessary for dimerization (Perez et al., 1995; Urfer et al., 1995). The identification of an immunoglobulin-like domain for neurotrophin binding is a recurrent theme for ligand-receptor signalling by receptor tyrosine kinase, such as FGF and c-kit receptors. Besides the IgC2-like domains, the region between the transmembrane and the Ig domain nearest to the membrane may be also critical to binding of neurotrophins (McDonald and Meakin, 1996). The localization of neurotrophin binding sites on their receptors will ultimately lead to the generation of small molecule agonists.

5. Interactions between Trk and p75 receptors

The ratio of p75 and Trk receptors dictates responsiveness to individual neurotrophins and their respective equilibrium binding properties (Benedetti et al., 1993; Wyatt and Davies, 1993; Verdi et al., 1994). The properties exhibited by neurotrophins for Trk tyrosine kinase receptors result in different consequences in the presence of p75, or other Trk isoforms.

Direct interactions between p75 and Trk receptors have been difficult to document biochemically. However, immunoprecipitation experiments carried out in crosslinked spinal cord and brain tissues with ^{125}I-NGF suggest that an association between the TrkA and p75 may take place (Huber and Chao, 1995). Photobleaching experiments following a fluorescently tagged p75 receptor have also revealed a potential physical interaction with TrkA receptors (Wolf et al., 1995).

Based upon these previous experiments, it is conceivable that the two receptors exist as part of a complex. The relative low abundance of the receptors found in most cells has made this difficult to assess. To test these possibility, TrkA and p75 receptor cDNAs have been transfected in human embryonic kidney 293T cells, subjected to immunoprecipitation with anti-Trk antibodies, followed by immunoblot analysis. After high level expression of the receptors in 293T cells, an association between the two receptors could be easily observed (Fig. 2). The results with p75 and TrkA receptors have also been detected using other cell expression systems and epitope-tagged versions of the receptors (Gargano et al., 1997; Bibel et al., 1999).

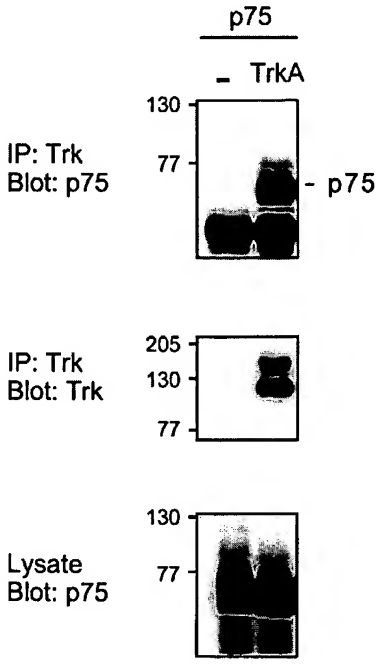

Fig. 2. TrkA associates with p75 receptor in 293T cells. 293T cells ($\sim 1 \times 10^6$) were co-transfected with $p75^{NTR}$ and either TrkA or empty vector. 36 h after transfection, the cells were harvested into TNE buffer [10 mM Tris (pH 8.0), 150 mM NaCl, 1 mM EDTA, and 1% NP40]. The lysates were immunoprecipitated with anti-pan Trk antibody (C14, Santa Cruz) which recognizes the C-terminus of Trk and subsequently subjected to Western blot analysis with an anti-$p75^{NTR}$ antiserum (9992), or anti-pan Trk antiserum. The amount of p75 protein for each transfection is assayed in the bottom panel. The protein visualized in both lanes of the top panel reflects reactivity of the heavy chain of IgG.

In addition to binding, signal transduction by TrkA can be influenced by p75 (Berg et al., 1991; Hantzopoulos et al., 1994; Verdi et al., 1994). Cell culture experiments indicate that p75 is capable of enhancing TrkA autophosphorylation (Barker and Shooter, 1994; Verdi et al., 1994). A potential function of the p75 receptor may be to increase the effective concentration of neurotrophin at the cell surface in order to enhance trkA binding. This is consistent with the limited amounts of neurotrophin available to competing neurons during development. Another model is that an altered conformation of Trk may be formed in the presence of p75 which facilitates ligand binding and subsequent signalling functions (Mahadeo et al., 1994).

An unexpected property that has emerged is that neurotrophins can, under certain circumstances, promote apoptotic cell death, in addition to a survival function (Casaccia-Bonnefil et al., 1996; Frade et al., 1996; Bamji et al., 1998). The similarity in the intracellular domains of the p75 with other family members, such as the Fas antigen and the p55 TNF receptor (Liepinsh et al., 1997), suggested that p75 might function as a cell death molecule. The Fas and TNF receptor share significant homology within their intracellular domains — an 80 amino acid region called the death domain which has been shown to be required for the apoptosis-promoting activities of Fas

and TNF receptors. The death domain is a novel protein–protein association motif found in several pro-apoptotic proteins (Feinstein et al., 1995).

The first report of a cell death activity for p75 was made in immortalized cerebellar neuronal cell lines (Rabizadeh et al., 1993). There are only a few examples in which neurotrophins have been directly shown to be responsible for apoptotic cell death. Many cell types express p75, but do not undergo apoptosis as a result of neurotrophin treatment. This suggests that cell context and history are important determinants and that p75 alone is not sufficient for this activity. The effect of p75 on cell death is highly dependent on the developmental stage of the cells and by their differentiative state in culture (Casaccia-Bonnefil et al., 1998).

Apoptosis mediated by p75 requires specific conditions, with regard to cell type, cell cycle stage, developmental stage, injury or stress. This could be due to time in culture, metabolic impairment, hypoxia, or other types of "stress" signals, such as nerve injury or trauma (Gu et al., 1999). Sensitive cells may be highly susceptible to injury and inflammation and may become more reactive to released growth factors and cytokines by upregulating receptor expression at the site of injury.

An important consequence is that Trk tyrosine kinase receptors can negate the signalling properties of p75, with respect to programmed cell death activities (Yoon et al., 1998). When both NGF receptors are co-expressed, as in the case of PC12 cells, TrkA exerts a suppressive effect upon p75, as assayed by ceramide production (Dobrowsky et al., 1995). Introduction of TrkA receptors into oligodendrocyte susceptible to cell death through p75 activation resulted in a reduction in JNK activation and NGF-induced apoptosis (Yoon et al., 1998). In the absence of TrkA expression, binding of NGF to p75 receptors can increase intracellular ceramide levels through increased sphingomyelin hydrolysis. Therefore, TrkA signalling can selectively down-regulate responses elicited from p75 activation. It should be emphasized that p75 co-expression is ordinarily associated with the ability to enhance NGF binding to TrkA (Hempstead et al., 1991; Barker and Shooter, 1994; Mahadeo et al., 1994).

To address the state of endogenous TrkA and p75 receptors in PC12 cells, co-immunoprecipitation experiments have been carried out in PC12 cells. A subline of PC12 (615) cells that expressed higher levels of TrkA receptors (Hempstead et al., 1992) was employed. The PC12 615 cell line was subjected to NGF treatment for 10

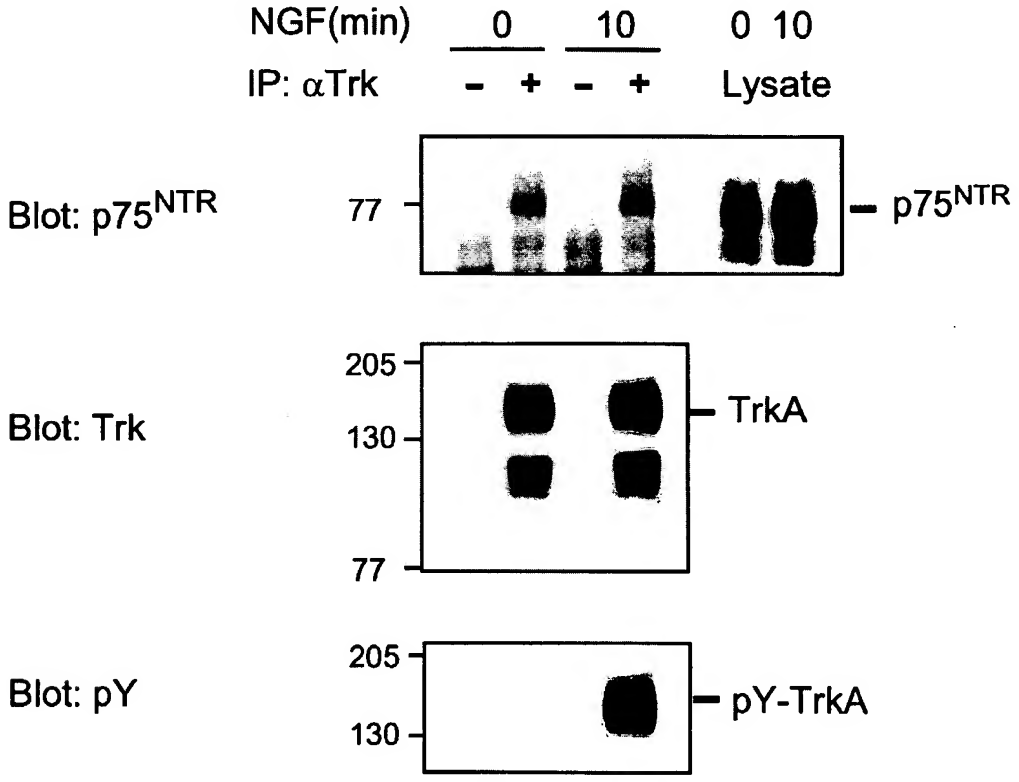

Fig. 3. Association of TrkA receptor with p75 in PC12 cells. TrkA-overexpressing PC12 (615) cells were treated with or without NGF (50 ng/ml, 10 min) and then harvested in TNE buffer. Cell lysates (18 mg of protein) were immunoprecipitated with either anti-pan Trk IgG or normal IgG as a negative control (as described - or - on top of the panel). The resulting immunocomplexes were analyzed by immunoblotting with anti-$p75^{NTR}$ antiserum (9992). The immunoprecipitation of TrkA was confirmed by immunoblotting of a portion of the immunocomplex with anti-pan Trk serum and reprobed with anti-phosphotyrosine antibody (pY99, Santa Cruz). The amount of p75 protein in each lysate was analyzed by western blot analysis on the two rightmost lanes of the top panel.

min and lysates were prepared. Interestingly, an association between the two receptors could be detected without NGF treatment. After addition of NGF, a similar interaction between the two receptors could be observed (Fig. 3). These results suggest a preformed complex of neurotrophin receptors exists at the cell membrane. A direct interaction between the two receptors has been difficult to observe. Recent studies indicate that both extracellular and intracellular domains of p75 and Trk receptors may be responsible for the co-immunoprecipitation results (Gargano et al., 1997; Bibel et al., 1999). These observations may be explained by additional cytoplasmic proteins that mediate the association of neurotrophin receptors.

There are several ways to account for an association between receptors. For the Trk receptors, SH2-containing proteins serve as adaptor molecules that link to enzymatic functions. For p75 receptors, signalling intermediates used by TNF and Fas receptors, such as FADD and TRADD proteins, downstream effectors, such as caspase-8 and the FLICE/MACH interacting enzyme (Cleveland and Ihle, 1995) may be functional. It remains to be seen whether p75 utilize these adaptor proteins, or other interacting proteins of different specificity.

A family of cytokine associated signaling intermediates, the TNF receptor-associated factors (TRAFs), have been described. Originally discovered as molecules associated with the p75 TNF receptor (Rothe et al., 1994), TRAF proteins represent a family of molecules that signal through activation of JNK and NFκB activities. Moreover, these proteins have been found to be associated with receptors required for different biological activities. These receptors include CD30, CD40, and lymphotoxin β (Gedrich et al., 1996; Nakano et al., 1996; Rothe et al., 1995) and the p55 TNF receptor (Hsu et al., 1996).

TRAF6 has been found to bind to p75 receptors and to modulate NFκB responses in Schwann cells (Khursigara et al., 1999). The TRAF6 protein contains several protein–protein binding motifs, such as a RING finger and TRAF domain, that may be instrumental in linking the p75 receptor to other cell surface proteins. Another protein that may be involved in linking Trk receptors with the p75 receptor is caveolin-1 (Bilderback et al., 1999). Caveolin-1 is localized to invaginations in the plasma membrane which are frequently sites where signaling molecules are found. A mutual interaction of caveolin-1 protein with an NGF/p75/TrkA complex may target neurotrophin responses locally in specialized membrane domains.

6. Summary

Although ligand-induced dimerization or oligomerization of receptors is a well established mechanism of growth factor signaling, increasing evidence indicates that biological responses are often mediated by receptor trans-signaling mechanisms involving two or more receptor systems. These include G protein-coupled receptors, cytokine, growth factor and trophic factor receptors. Greater flexibility is provided when different signaling pathways are merged through multiple receptor signaling systems.

Trophic factors exemplified by NGF and its family members, ciliary neurotrophic factor (CNTF) and glial derived neurotrophic factor (GDNF) all utilize increased tyrosine phosphorylation of cellular substrates to mediate neuronal cell survival. Actions of the NGF family of neurotrophins are not only dictated by *ras* activation through the Trk family of receptor tyrosine kinases, but also a survival pathway defined by phosphatidylinositol-3-kinase activity (Yao and Cooper, 1995), which gives rise to phosphoinositide intermediates that activate the serine/threonine kinase Akt/PKB (Dudek et al., 1997). Induction of the serine-threonine kinase activity is critical for cell survival, as well as cell proliferation. Hence, for many trophic factors, multiple proteins constitute a functional multisubunit receptor complex that activates *ras*-dependent and *ras*-independent intracellular signaling.

The NGF receptors provide an example of bidirectional crosstalk. In the presence of TrkA receptors, p75 can participate in the formation of high affinity binding sites and enhanced neurotrophin responsiveness leading to a survival or differentiation signal. In the absence of TrkA receptors, p75 can generate, in only specific cell populations, a death signal. These activities include the induction of NFκB (Carter et al., 1996); the hydrolysis of sphingomyelin to ceramide (Dobrowsky et al., 1995); and the pro-apoptotic functions attributed to p75.

Receptors are generally drawn and viewed as isolated integral membrane proteins which span the lipid bilayer, with signal transduction proceeding in a linear step-wise fashion. There are now numerous examples which indicate that each receptor acts not only in a linear, independent manner, but can also influence the activity of other cell surface receptors, either directly or through signaling intermediates. Which step and which intermediates are utilized for crosstalk between the receptors is a critical question. For neurotrophins, their primary function in sustaining the viability of neurons is counterbalanced by a receptor mechanism to eliminate cells by an apoptotic mechanism. It is conceivable that this bidirectional system may be utilized selectively during development and in neurodegenerative diseases.

Acknowledgements

This work was supported by grants from the NIH (MVC) and the American Heart Association (HY).

References

Angeletti, R.H., Bradshaw, R.A., 1971. The amino acid sequence of 2.5S mouse submaxillary gland nerve growth factor. Proc. Natl. Acad. Sci. 68, 2417–2420.

Arakawa, T., Haniu, M., Narhi, L.O., Miller, J.A., Talvenheimo, J., Philo,

J.S., Chute, H.T., Matheson, C., Carnahan, J., Louis, J.-C., Yan, Q., Welcher, A.A., Rosenfeld, R., 1994. Formation of heterodimers from three neurotrophins, nerve growth factor, neurotrophin-3 and brain-derived neurotrophic factor. J. Biol. Chem. 269, 27833–27839.

Bamji, S., Majdan, M., Pozniak, C.D., Belliveau, D.J., Aloyz R, J.K., Causing, C.G., Miller, F.D., 1998. The p75 neurotrophin receptor mediates neuronal apoptosis and is essential for naturally occurring sympathetic neuron death. J. Cell Biol. 140, 911–923.

Barbacid, M., 1994. The trk family of neurotrophin receptors. J. Neurobiol. 25, 1386–1403.

Barde, Y.A., 1989. Trophic factors and neuronal survival. Neuron 2, 1525–1534.

Barker, P.A., Shooter, E.M., 1994. Disruption of NGF binding to the low-affinity neurotrophin receptor p75 reduces NGF binding to trkA on PC12 cells. Neuron 13, 203–215.

Benedetti, M., Levi, A., Chao, M.V., 1993. Differential expression of nerve growth factor receptors leads to altered binding affinity and neurotrophin responsiveness. Proc. Natl. Acad. Sci. U.S.A. 90, 7859–7863.

Berg, M.M., Sternberg, D.W., Hempstead, B.L., Chao, M.V., 1991. The low affinity nerve growth factor (NGF) receptor mediates NGF-induced tyrosine phosphorylation. Proc. Natl. Acad. Sci. U.S.A. 88, 857–866.

Berg, M.M., Sternberg, D., Parada, L.F., Chao, M.V., 1992. K-252a inhibits NGF-induced trk proto-oncogene tyrosine phosphorylation and kinase activity. J. Biol. Chem. 267, 13–16.

Bibel, M., Hoppe, E., Barde, Y.-A., 1999. Biochemical and functional interactions between the neurotrophin receptors trk and $p75^{NTR}$. The EMBO J. 18, 616–622.

Bilderback, T.R., Gazula, V.-R., Lisanti, M.P., Dobrowsky, R.T., 1999. Caveolin interacts with TrkA and $p75^{NTR}$ and regulates neurotrophin signaling pathways. J. Biol. Chem. 274, 257–263.

Brojatsch, J., Naughton, J., Rolls, M.M., Zingler, K., Young, J.A.T., 1996. CAR1, a TNFR-related protein is a cellular receptor for cytopathic avian leukosis-sarcoma viruses and mediates apoptosis. Cell 87, 845–855.

Carter, B.D., Kaltschmidt, C., Kaltschmidt, B., Offenhauser, N., Bohm-Matthaei, R., Baeuerle, P.A., Barde, Y.-A., 1996. Selective activation of NK-κB by nerve growth factor through the neurotrophin receptor p75. Science 272, 542–545.

Casaccia-Bonnefil, P., Carter, B.D., Dobrowsky, R.T., Chao, M.V., 1996. Death of oligodendrocytes mediated by the interaction of nerve growth factor with its receptor p75. Nature 383, 716–719.

Casaccia-Bonnefil, P., Kong, H., Chao, M.V., 1998. Neurotrophins: the biological paradox of survival factors eliciting apoptosis. Cell Death and Differentiation 5, 357–364.

Chao, M.V., 1992a. Neurotrophin receptors: a window into neuronal differentiation. Neuron 9, 583–593.

Chao, M.V., 1992b. Growth factor signaling: where is the specificity? Cell 68, 995–997.

Chao, M.V., 1994. The p75 neurotrophin receptor. J. Neurobiol. 25, 1373–1385.

Chinnaiyan, A.M., O'Rourke, K., Yu, G.-L., Lyons, R.H., Garg, M., Duan, D.R., Xing, L., Gentz, R., Ni, J., Dixit, V.M., 1996. Signal transduction by DR3, a death domain-containing receptor related to TNFR-1 and CD95. Science 274, 990–992.

Cleveland, J.L., Ihle, J.N., 1995. Contenders in FasL/TNF death signaling. Cell 81, 479–482.

Davies, A.M., 1994. Neurotrophic factors — switching neurotrophin dependence. Curr. Biol. 4, 273–276.

Dechant, G., Barde, Y.-A., 1997. The neurotrophin receptor p75 binds neurotrophin-3 on sympathetic neurons with high affinity and specificity. J. Neurosci. 17, 5281–5287.

Dechant, G., Biffo, S., Okazawa, H., Kolbeck, R., Pottgiesser, J., Barde, Y.-A., 1993. Expression and binding characteristics of the BDNF receptor chick trkB. Development 119, 545–558.

Distefano, P.S., Friedman, B., Radziejewski, C., Alexander, C., Boland, P., Schick, C.M., Lindsay, R.M., Wiegand, S.J., 1992. The neurotrophins BDNF, NT-3 and NGF display distinct patterns of retrograde axonal-transport in peripheral and central neurons. Neuron 8, 983–993.

Dobrowsky, R.T., Werner, M.H., Castellino, A.M., Chao, M.V., Hannun, Y.A., 1994. Activation of the sphingomyelin cycle through the low-affinity neurotrophin receptor. Science 265, 1596–1599.

Dobrowsky, R.T., Jenkins, G.M., Hannun, Y.A., 1995. Neurotrophins induce sphingomyelin hydrolysis. J. Biol. Chem. 270, 22135–22142.

Dudek, H., Datta, S.R., Franke, T.F., Birnbaum, M.J., Yao, R., Cooper, G.M., Segal, R.A., Kaplan, D.R., Greenberg, M.E., 1997. Regulation of neuronal survival by the serine-threonine protein kinase Akt. Science 275, 661–665.

Feinstein, E., Kimchi, A., Wallach, D., Boldin, M., Varfolomeev, E., 1995. The death domain: a module shared by proteins with diverse cellular functions. TIBS 20, 342–344.

Frade, J.M., Rodriguez-Tebar, A., Barde, Y.-A., 1996. Induction of cell death by endogenous nerve growth factor through its p75 receptor. Nature 383, 166–168.

Gargano, N., Levi, A., Alema, S., 1997. Modulation of nerve growth factor internalization by direct interaction between p75 and TrkA receptors. J. Neurosci. Res. 50, 1–12.

Gedrich, R.W., Gilfillan, M.C., Duckett, C.S., Van Dongen, J.L., Thompson, C.B., 1996. CD30 contains two binding sites with different specificities for members of the tumor necrosis factor receptor-associated factor family of signal transducing proteins. J. Biol. Chem. 271, 12852–12858.

Grob, P.M., Ross, A.H., Koprowski, H., Bothwell, M., 1985. Characterization of the human melanoma nerve growth factor receptor. J. Biol. Chem. 260, 8044–8049.

Gu, C., Casaccia-Bonnefil, P., Srinivasan, A., Chao, M.V., 1999. Oligodendrocyte apoptosis mediated by caspase activation. J. Neurosci. 19, 3043–3049.

Hantzopoulos, P.A., Suri, C., Glass, D.J., Goldfarb, M.P., Yancopoulos, G.D., 1994. The low affinity NGF receptor, p75, can collaborate with each of the Trks to potentiate functional responses to the neurotrophins. Neuron 13, 187–207.

Hempstead, B.L., Martin-Zanca, D., Kaplan, D.R., Parada, L.F., Chao, M.V., 1991. High-affinity NGF binding requires co-expression of the trk proto-oncogene and the low-affinity NGF receptor. Nature 350, 678–683.

Hempstead, B.L., Rabin, S.J., Kaplan, L., Reid, S., Parada, L.F., Kaplan, D.R., 1992. Overexpression of the trk tyrosine kinase rapidly accelerates nerve growth factor-induced differentiation. Neurons 9, 883–896.

Hsu, H., Shu, H.-B., Pan, M.-P., Goeddel, D.V., 1996. TRADD-TRAF2 and TRADD-FADD interactions define two distinct TNF receptor-1 signal transduction pathways. Cell 84, 299–308.

Huber, L.J., Chao, M.V., 1995. A potential interaction of p75 and trkA NGF receptors revealed by affinity crosslinking and immunoprecipitation. J. Neurosci. Res. 40, 557–563.

Jing, S.Q., Tapley, P., Barbacid, M., 1992. Nerve growth-factor mediates signal transduction through trk homodimer receptors. Neuron 9, 1067–1079.

Jungbluth, S., Bailey, K., Barde, Y.A., 1994. Purification and characterization of a brain-derived neurotrophic factor neurotrophin-3 (bdnf/nt-3) heterodimer. Eur. J. Biochem. 221, 677–685.

Kaplan, D.R., Stephens, R.M., 1994. Neurotrophin signal transduction by the trk receptor. J. Neurobiol. 25, 1404–1417.

Khursigara, G., Orlinick, J.R., Chao, M.V., 1999. Association of TRAF6 with the p75 neurotrophin receptor. J. Biol. Chem. 274, 2597–2600.

Kouhara, H., Hadari, Y.R., Spivak-Kroizman, T., Schilling, J., Bar-Sagi, D., Lax, I., Schlessinger, J., 1997. A lipid-anchored Grb2-binding protein that links FGF-receptor activation to the Ras/MAPK signaling pathway. Cell 89, 693–702.

Leibrock, J., Lottspeich, F.H., Holn, A., Hofer, M., Hengerer, B., Masiakowski, P., Thoenen, H., Barde, Y.A., 1989. Molecular cloning and expression of brain-derived neurotrophic factor. Nature 341, 149–152.

Levi-Montalcini, R., 1987. The nerve growth factor: thirty-five years later. Science 237, 1154–1164.

Liepinsh, E., Ilag, L.L., Otting, G., Ibanez, C.F., 1997. NMR structure of the death domain of the p75 neurotrophin receptor. EMBO J. 16, 4999–5005.

Lindsay, R.M., Wiegand, S.J., Altar, C.A., Distefano, P.S., 1994. Neurotrophic factors — from molecule to man. Trends Neurosci. 17, 182–190.

Mahadeo, D., Kaplan, L., Chao, M.V., Hempstead, B.L., 1994. High affinity nerve growth factor binding displays a faster rate of association than p140(trk) binding-implications for multisubunit polypeptide receptors. J. Biol. Chem. 269, 6884–6891.

Maisonpierre, P.C., Belluscio, L., Squinto, S., Ip, N.Y., Furth, M.E., Lindsay, R.M., Yancopoulos, G.D., 1990. Neurotrophin-3: a neurotrophic factor related to NGF and BDNF. Science 247, 1446–1451.

McDonald, N.Q., Hendrickson, W.A., 1993. A new structural superfamily of growth factors defined by a cystine knot motif. Cell 73, 421–424.

McDonald, J.I., Meakin, S.O., 1996. Deletions in the extracellular domain of rat trkA lead to an altered differentiative phenotype in neurotrophin responsive cells. Mol. Cell. Neurosci. 7, 371–390.

McDonald, N.Q., Lapatto, R., Murray-Rust, J., Gunning, J., Wlodawer, A., Blundell, T.L., 1991. A new protein fold revealed by a 2.3 A resolution crystal structure of nerve growth factor. Nature 354, 411–414.

Montgomery, R.I., Warner, M.S., Lum, B.J., Spear, P.G., 1996. Herpes simplex virus-1 entry into cells mediated by a novel member of the TNF/NGF receptor family. Cell 87, 427–436.

Nakano, H., Oshima, H., Chung, W., Williams-Abbott, L., Ware, C.F., Yagita, H., Okumura, K., 1996. TRAF5, an activator of NF-κB and putative signal transducer for the lymphotoxin-β receptor. J. Biol. Chem. 271, 14661–14664.

Nicola, N.A., Metcalf, D., 1992. Subunit promiscuity among hemopoietic growth factor receptors. Cell 67, 1–4.

Nishi, R., 1994. Neurotrophic factors: two are better than one. Science 265, 1052–1053.

Pan, G., O'Rourke, K., Chinnaiyan, A.M., Gentz, R., Ebner, R., Ni, J., Dixit, V.M., 1997. The receptor for the cytotoxic ligand TRAIL. Science 276, 111–113.

Perez, P., Coll, P.M., Hempstead, B.L., Martin-Zanca, D., Chao, M.V., 1995. NGF binding to the trk tyrosine kinase receptor requires the extracellular immunoglobulin-like domains. Mol. Cell. Neurosci. 6, 97–105.

Qian, X., Riccio, A., Zhang, Y., Ginty, D.D., 1998. Identification and characterization of novel substrates of Trk receptors in developing neurons. Neuron 21, 1017–1029.

Qui, M.-S., Green, S.H., 1991. NGF and EGF rapidly activate p21ras in PC12 cells by distinct, convergent pathways involving tyrosine phosphorylation. Neuron 7, 937–946.

Qui, M.-S., Green, S.H., 1992. PC12 cell neuronal differentiation is associated with prolonged p21ras activity and consequent prolonged ERK activity. Neuron 9, 705–717.

Rabizadeh, S., Oh, J., Zhong, L.T., Yang, J., Bitler, C.M., Butcher, L.L., Bredesen, D.E., 1993. Induction of apoptosis by the low-affinity NGF receptor. Science 261, 345–348.

Radziewjewski, C., Robinson, R.C., 1993. Heterodimers of the neurotrophic factors-formation, isolation and differential stability. Biochemistry 32, 13350–13356.

Rodriguez-Tebar, A., Dechant, G., Gotz, R., Barde, Y.A., 1992. Binding of neurotrophin-3 to its neuronal receptors and interactions with nerve growth-factor and brain-derived neurotrophic factor. EMJO J. 11, 917–922.

Rothe, M., Wong, S.C., Henzel, W.J., Goeddel, D.V., 1994. A novel family of putative signal transducers associated with the cytoplasmic domain of the 75 kDa tumor necrosis factor receptor. Cell 78, 681–692.

Rothe, M., Sarma, V., Dixit, V.M., Goeddel, D.V., 1995. TRAF2-mediated activation of NF-kB by TNF receptor 2 and CD40. Science 269, 1424–1427.

Smith, C.A., Farrah, T., Goodwin, R.G., 1994. The TNF receptor superfamily of cellular and viral proteins: activation, costimulation and death. Cell 76, 959–962.

Sutter, A., Riopelle, R.J., Harris-Warrick, R.M., Shooter, E.M., 1979. NGF receptors. Characterization of two distinct classes of binding sites on thick embryo sensory ganglia cells. J. Biol. Chem. 254, 5972–5982.

Thoenen, H., 1995. Neurotrophins and neuronal plasticity. Science 270, 593–598.

Urfer, R., Tsoulfas, P., O'Connell, L., Shelton, D.L., Parada, L.F., Presta, L.G., 1995. An immunoglobulin-like domain determines the specificity of neurotrophin receptors. EMBO J. 14, 2795–2805.

Verdi, J.M., Birren, S.J., Ibanez, C.F., Persson, H., Kaplan, D.R., Benedetti, M., Chao, M.V., Anderson, D.J., 1994. p75(LNGFR) regulates trk signal transduction and NGF-induced neuronal differentiation in MAH cells. Neuron 12, 733–745.

von Bartheld, C.S., Williams, R., Lefcort, F., Clary, D.O., Reichardt, L.F., Bothwell, M., 1995. Retrograde transport of neurotrophins from the eye to the brain in chick embryos: roles of the $p75^{NTR}$ and trkB receptors. J. Neurosci. 16, 2995–3008.

Wolf, D.E., McKinnon, C.A., Daou, M.-C., Stephens, R.M., Kaplan, D.R., Ross, A.H., 1995. Interaction with trkA immobilizes gp75 in the high affinity nerve growth factor receptor complex. J. Biol. Chem. 270, 2133–2138.

Wyatt, S., Davies, A.M., 1993. Regulation of expression of mRNAs encoding the nerve growth factor receptors p75 and trkA mRNA in developing sensory neurons. Development 119, 635–647.

Yao, R., Cooper, G.M., 1995. Requirement for phosphatidylinositol-3 kinase in the prevention of apoptosis by nerve growth factor. Science 267, 2003–2006.

Yoon, S.O., Casaccia-Bonnefil, P., Carter, B., Chao, M.V., 1998. Competitive signaling between TrkA and p75 nerve growth factor receptors determines cell survival. J. Neurosci. 18, 3273–3281.

THE GDNF FAMILY: SIGNALLING, BIOLOGICAL FUNCTIONS AND THERAPEUTIC VALUE

Matti S Airaksinen and Mart Saarma

Members of the nerve growth factor (NGF) and glial cell line-derived neurotrophic factor (GDNF) families — comprising neurotrophins and GDNF-family ligands (GFLs), respectively — are crucial for the development and maintenance of distinct sets of central and peripheral neurons. Knockout studies in the mouse have revealed that members of these two families might collaborate or act sequentially in a given neuron. Although neurotrophins and GFLs activate common intracellular signalling pathways through their receptor tyrosine kinases, several clear differences exist between these families of trophic factors.

CYSTINE KNOT
A structural motif that consists of six cysteine residues that are linked together by three disulphide bonds. It is involved in protein stabilization and dimer formation.

HEPARAN SULPHATE
A glycosaminoglycan that consists of repeated units of hexuronic acid and glucosamine residues. It usually attaches to proteins through a xylose residue to form proteoglycans.

Programme of Molecular Neurobiology, Institute of Biotechnology, P.O. Box 56, Viikki Biocenter, FIN-00014, University of Helsinki, Finland.
e-mails: Matti.Airaksinen@helsinki.fi; Saarma@biocenter.helsinki.fi
DOI: 10.1038/nrn812

Glial cell line-derived neurotrophic factor (GDNF) was originally purified from a rat glioma cell-line supernatant as a trophic factor for embryonic midbrain dopamine neurons, and was later found to have pronounced effects on other neuronal subpopulations. Because GDNF protects dopamine neurons in animal models of Parkinson's disease, and rescues motor neurons *in vivo*, hopes have been raised that GDNF could be used as a therapeutic agent to treat several neurodegenerative diseases. In addition, GDNF has important roles outside the nervous system. It acts as a morphogen in kidney development and regulates the differentiation of spermatogonia. In this review, we focus on recent insights into GDNF-family ligand (GFL) receptor mechanisms, communication pathways and their functional implications in the nervous system.

GDNF family: distant relatives of the TGF-β kin

GFLs are synthesized, secreted and activated by a variety of tissues, and can bind to receptors on specific target cells, influencing their development or supporting their survival and differentiated phenotype in adult animals[1]. GDNF and neurturin (NRTN) were first purified biochemically by virtue of their biological activity. Thereafter, artemin (ARTN) and persephin (PSPN) were isolated by a database search and homology cloning[2]. GFLs belong to the transforming growth factor-β (TGF-β) superfamily, containing seven cysteine residues with the same relative spacing as other members of this family. Despite low amino-acid sequence homology, GDNF and other structurally characterized members of the TGF-β superfamily have similar conformations[3]. They all belong to the CYSTINE KNOT protein family, and they function as homodimers.

Typically for secreted proteins, GFLs are produced in the form of a precursor, preproGFL. The signal sequence is cleaved on secretion, and activation of the proGFL probably occurs by proteolytic cleavage. GFLs seem to bind HEPARAN SULPHATE side chains of extracellular-matrix proteoglycans, which might restrict their diffusion and raise their local concentration[4]. Although the sites of GFL synthesis have been studied extensively[5], our knowledge of the gene regulation and mechanisms of secretion of GFLs, and of the activation of GFL precursors, is very limited. The specific proteases that cleave and activate GFL precursors have not been identified. Interestingly, recent evidence indicates that secreted proneurotrophins are biologically active[6]. Secreted proforms of nerve growth factor (NGF) and brain-derived neurotrophic factor (BDNF) are cleaved extracellularly by the serine protease plasmin and selective matrix metalloproteinases. ProNGF binds with high affinity to $p75^{NTR}$, a receptor that induces apoptosis in cultured neurons, with minimal activation of the

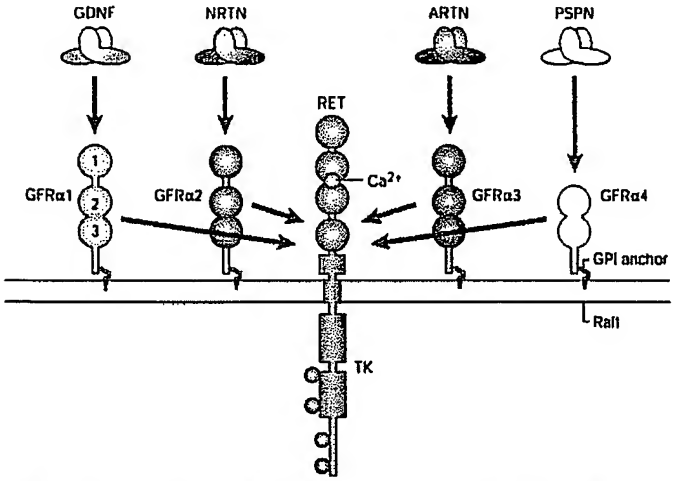

Figure 1 | GDNF-family ligands and receptor interactions. Homodimeric glial cell line-derived neurotrophic factor (GDNF)-family ligands (GFLs) activate RET tyrosine kinase (TK) by first binding their cognate GDNF-family receptor-α (GFRα) receptors. Arrows indicate the preferred ligand–receptor interactions that are known to occur physiologically *in vivo*. GFRα proteins are attached to the plasma membrane by a glycosyl phosphatidylinositol (GPI) anchor and are predicted to have three globular cysteine-rich domains (1,2,3) (except for GFRα4, which has only two), joined together by less conserved adaptor sequences[1]. GFLs bind mainly to the second domain of GFRα receptors, which is also crucial for RET binding[85]. Although the extracellular domain of RET interacts with all four GFL–GFRα complexes[88], the regions of RET that are involved in these interactions have not been delineated. Binding of Ca^{2+} ions to one of the four extracellular cadherin-like domains of RET is required for its activation by GFLs[87]. Four tyrosine residues in the RET intracellular part (Tyr905, Tyr1015, Tyr1062 and Tyr1096; red balls) serve as docking sites for different adaptors. One of them (Tyr1096) is in the carboxy-terminal end of the long isoform of RET (long). Membrane rafts are shown in yellow. ARTN, artemin; NRTN, neurturin; PSPN, persephin.

differentiation/survival pathway that is mediated by the tyrosine kinase A receptor (TrkA). It is now of interest to determine whether the biological actions of GFLs are also regulated by proteolytic cleavage, and whether pro-forms of GFLs have functions that are distinct from those of the mature ligands.

GDNF-family signalling

GFLs bind specific GFRα co-receptors and activate RET. All GFLs signal through the RET RECEPTOR TYROSINE KINASE, which was first discovered as a proto-oncogene (reviewed in REF. 7). It is activated only if the GFL is first bound to a novel class of proteins, known as GDNF-family receptor-α (GFRα) receptors, which are linked to the plasma membrane by a GLYCOSYL PHOSPHATIDYLINOSITOL (GPI) anchor. Four different GFRα receptors have been characterized (GFRα1–4), which determine the ligand specificity of the GFRα–RET complex. GDNF binds to GFRα1, then forms a complex with RET. NRTN binds to GFRα2, ARTN to GFRα3, and PSPN activates RET by binding to GFRα4 (FIG. 1). NRTN and ARTN might crosstalk weakly with GFRα1, and GDNF with GFRα2 and GFRα3. However, in mammals at least, PSPN can bind only to GFRα4 (REFS 1,2,7,8). GFRα receptors are usually bound to the plasma membrane, but cleavage by an unknown phospholipase or protease can produce soluble forms of these co-receptors[9]. Alternative splicing can also produce soluble forms, at least of GFRα4 (REF. 8). Analysis of The Genome Database, the near-complete public human genome databank, indicates that further functional GFL members are unlikely to exist (M.S.A., unpublished observations).

RET is a single-pass transmembrane protein that contains four cadherin-like repeats in the extracellular domain and a typical intracellular tyrosine kinase domain (FIG. 1). GFL–GFRα binding to the extracellular domain of RET leads to activation of the intracellular tyrosine kinase domain. According to the original model, a GDNF dimer first binds to either monomeric or dimeric GFRα1, and the GDNF–GFRα1 complex then interacts with two RET molecules, thereby inducing their homodimerization and tyrosine autophosphorylation[1]. However, the fact that GDNF mutants that are deficient in GFRα1 binding are able to activate RET indicates that at least some RET molecules are weakly associated with GFRα1 before GDNF binding[10] (FIG. 2a). The stoichiometry as well as the kinetics of ligand–receptor complex formation are not well understood. It is assumed that the other GFL members interact with their cognate co-receptor and activate RET in a similar manner to GDNF.

Division of labour within and outside lipid rafts. There is increasing evidence that the lipid microenvironment on the cell surface is crucial for signal transduction. Lipid rafts consist of dynamic assemblies of cholesterol and sphingolipids on the outer leaflet of the plasma membrane[11]. The inner leaflet is probably rich in phospholipids, with saturated fatty acids and cholesterol, but it is unclear how the inner and outer leaflets of the plasma membrane are coupled, although transmembrane proteins are probably essential. Importantly, proteins have been identified that are included in or excluded from the rafts. Lipid rafts, which contain interacting proteins, can change their size and composition in response to various stimuli. Several protein groups have high affinity for rafts, including GPI-anchored proteins, doubly acylated proteins such as cytoplasmic Src-family kinases (SFKs), cholesterol-linked and palmitylated proteins, as well as some transmembrane proteins.

The GPI anchor in GFRα receptors localizes them to the lipid rafts of the plasma membrane[12] (FIG. 2a). GDNF binding to lipid-anchored GFRα1 recruits RET to the lipid rafts and triggers its association with Src, which is required for effective downstream signalling[13]. Signal transduction depends on the colocalization of RET and GFRα1 in the lipid rafts, as cholesterol depletion significantly decreases signalling efficacy.

Stimulation of RET *in cis* or *in trans* by GDNF in a complex with GPI-anchored or soluble GFRα1, respectively, triggers different signalling pathways inside and outside the rafts (FIG. 2), although both types of stimulation activate (different) RET tyrosine phosphorylation sites with indistinguishable kinetics[14]. The activated RET protein interacts with the lipid-anchored adaptor protein FRS2 (fibroblast growth factor receptor substrate 2) only inside the rafts, and with soluble Shc (Src-homologous and collagen-like protein) mainly outside the rafts[9].

RECEPTOR TYROSINE KINASE
Any of a family of transmembrane receptors, the intracellular domains of which catalyse the phosphorylation, by ATP, of specific tyrosine residues on their target proteins.

GLYCOSYL PHOSPHATIDYLINOSITOL
A post-translational modification, the function of which is to attach proteins to the exoplasmic leaflet of membranes, possibly to specific domains therein. The anchor is made of one molecule of phosphatidylinositol to which a carbohydrate chain is linked through the C-6 hydroxyl of the inositol, and is attached to the protein through an ethanolamine phosphate moiety.

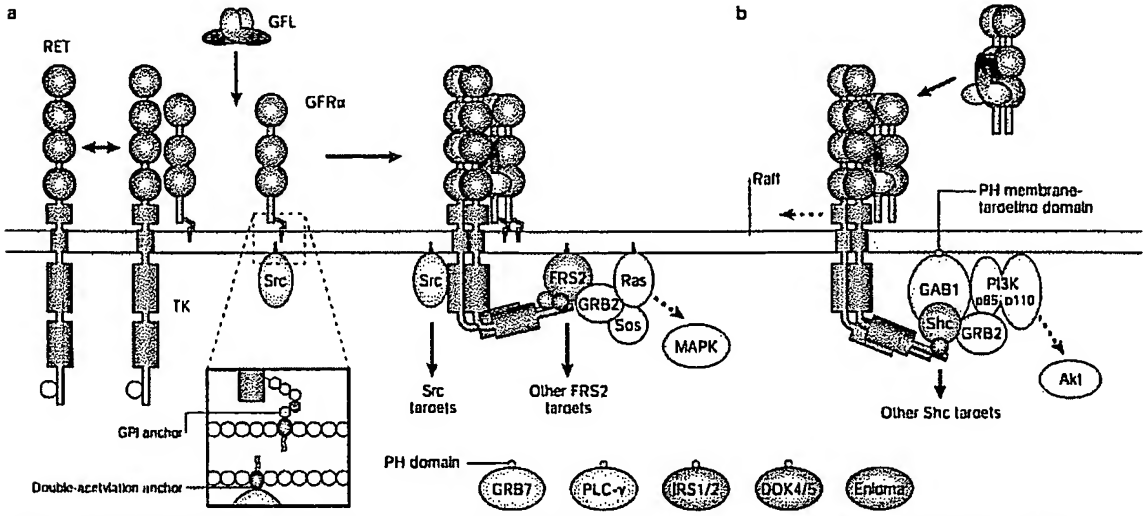

Figure 2 | Distinct GDNF-family ligand signalling inside and outside rafts. The model highlights the different intracellular RET-binding proteins (blue) and activated downstream signalling pathways (grey) when RET tyrosine kinase (TK) is stimulated a | in rafts (yellow) by glial cell line-derived neurotrophic factor (GDNF)-family ligand (GFL) in a complex with glycosyl phosphatidylinositol (GPI)-anchored GDNF-family receptor-α (GFRα) *in cis*, or b | outside rafts by a soluble GFL–GFRα complex *in trans*[9]. In the absence of ligand, most GPI-anchored GFRα molecules are in rafts, some weakly bound to RET, and most RET is outside the rafts. GFL might induce GFRα dimerization. The enhanced affinity of the GFL–GFRα complex to RET drags RET to the rafts and promotes its dimerization[13]. The phosphorylated tyrosine residue (Tyr1062) in RET that is used for docking is shown in red. RET stimulation *in trans* by GFL bound to soluble GFRα outside the rafts initially activates signalling pathways that are mediated by soluble adaptors such as Shc (Src-homologous and collagen-like protein). The soluble GFL–GFRα complex recruits RET to lipid rafts and triggers raft-specific signalling (broken arrow). Although both FRS2 (fibroblast growth factor receptor substrate 2) and Shc adaptors can bind to the same phosphotyrosine (Tyr1062), RET stimulation by GPI-anchored GFRα in rafts promotes the binding of lipid-anchored adaptors such as FRS2 and the activation of Src (green). Three other adaptor proteins — DOK4/5 (downstream of tyrosine kinase 4/5), IRS1/2 (insulin receptor substrate 1/2) and enigma — bind to the same Tyr1062 site. Binding of enigma to RET is independent of phosphorylation. The mechanism of Src activation (green) by RET is unclear. GAB1, GRB2-associated binding protein 1; GRB, growth factor receptor-bound protein; MAPK, mitogen-activated protein kinase; PH, plextrin homology; PI3K, phosphatidylinositol 3-kinase; PLC, phospholipase C.

So, the lipid rafts seem to compartmentalize signalling molecules on both sides of the plasma membrane, which allows them to interact with each other and prevents interactions with proteins that are excluded from the rafts.

Surprisingly, soluble GFRα1, which binds GDNF and activates RET *in trans* initially outside lipid rafts, can also recruit RET to the rafts with delayed kinetics[9]. RET stimulation, also *in trans* leads to sustained downstream signalling, both in and outside rafts, that potentiates neuronal survival and differentiation responses to the ligand[9,14,15]. Although RET tyrosine kinase activity is required, the mechanisms that bring the complex of GDNF, soluble GFRα1 and RET to rafts, and prolong signalling, are unclear.

GDNF-family receptors: multiple signalling pathways

Germ-line mutations in the *RET* proto-oncogene are responsible for two unrelated neural crest disorders in humans. Activating mutations in the *RET* gene cause several types of cancer, whereas inactivating mutations lead to Hirschsprung's disease (aganglionic megacolon). RET-related inherited diseases have recently been reviewed (see REFS 7,16). Although significant progress has been made in characterizing the biological consequences of *RET* mutations and changes in RET downstream signalling in pathological conditions, several challenges still remain. For example, it is not clear why different point mutations in the gene associate with particular types of cancer, what the pathogenetic role of GFRα receptors and GFLs is, and how these proteins contribute to disease phenotypes. As *RET* was first found as an oncogene, there are ample experimental data on RET activation and signalling pathways in disease, whereas information about the GFL-activated RET-signalling pathways is still limited.

Once phosphorylated, the tyrosine residues in the intracellular domain of activated RET serve as high-affinity binding sites for various intracellular signalling proteins in the target cells, as in the case of other receptor tyrosine kinases[17]. Intriguingly, Tyr1062 in the carboxy-terminal cytoplasmic tail of RET is the binding site of at least five different docking proteins — Shc, FRS2, DOK4/5 (downstream of tyrosine kinase 4/5), IRS1/2 (insulin receptor substrate 1/2) and enigma. Neurotrophins activate, through their Trk receptors, the phosphatidylinositol 3-kinase (PI3-kinase) and mitogen-activated protein kinase (MAPK) pathways, which both contribute to neuronal survival[18]. Furthermore, the activation of MAPK is crucial for neuritogenesis. Recent evidence indicates that PI3-kinase and phospholipase Cγ (PLC-γ) activation by neurotrophins are involved in the enhancement of neurotransmission[19].

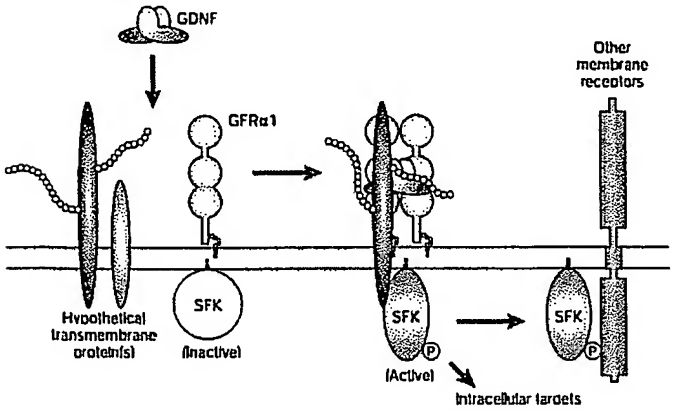

Figure 3 | Model of RET-independent GDNF–GFRα1 signalling. Glial cell line-derived neurotrophic factor (GDNF) induces phosphorylation (P) of Src-family kinase (SFK) that is anchored to rafts, by binding to GDNF-family receptor-α1 (GFRα1) and to an unknown transmembrane glycoprotein. SFK can then activate intracellular substrates and other plasma-membrane receptors.

These same routes are activated by GFLs, which signal through RET (reviewed in REF. 7). However, there are some differences in the signalling of neurotrophins and GFLs, such as the involvement of lipid rafts and IAPs (inhibitor of apoptosis proteins), as discussed later.

As different GFLs signal through the same RET receptor, it is of interest to know whether these factors trigger qualitatively or quantitatively different signalling pathways. In cultured sympathetic neurons, GDNF, NRTN and ARTN, by their cognate co-receptors, induce a coordinated phosphorylation of the same four key RET tyrosines (Tyr905, Tyr1015, Tyr1062 and Tyr1096) with similar kinetics[14], and are suggested to stimulate a similar profile of downstream signalling pathways. So, RET seems unable to trigger specific signalling by three different GFL–GFRα complexes. However, not all tyrosines in the RET cytoplasmic domain have been studied. Moreover, as the same phosphotyrosine (Tyr1062) can bind different adaptors, they could be selectively recruited by different GFL–GFRα complexes and produce distinct biological outcomes.

RET stimulation *in trans* is consistent with the finding that GFRα receptors are often expressed in tissues without RET. What might their role be *in vivo*? Soluble GFRα1 receptors are produced by cultured enteric neurons[15] and Schwann cells[9]. Soluble or extracellular-matrix-bound GFRα receptors might potentiate and alter the biological activities of GFLs by stimulating RET *in trans*. Neurons might require different RET-signalling mechanisms during different phases of their development, such as a relatively mobile GFL–GFRα gradient during precursor migration compared with a fixed local source during terminal axon growth and branching. Consistent with this, in neurons that express GFRα1 and RET, GDNF *cis/trans* signalling by immobilized GFRα1 elicits marked, localized expansions of axons and growth cones compared with signalling by soluble or GPI-anchored GFRα1 alone[9]. Soluble GFRα receptors, if released together with the ligand, seem to increase the ligand specificity in RET signalling[15], which, combined with restricted ligand expression, might explain why GFLs do not seem to crosstalk *in vivo* under physiological conditions. The mechanisms that regulate GFRα shedding and GFL–GFRα–RET internalization remain open to question.

RET exists as two main isoforms that differ in their carboxyl terminus. The docking adaptor GRB2 (growth factor receptor-bound protein 2) can also bind to Tyr1096, which is specific to the long isoform of RET (FIG. 1). Surprisingly, mice that lack the long RET isoform seem to be normal, whereas mice that lack the short isoform have kidney abnormalities and enteric aganglionosis, which are almost as severe as in *Ret*-null mice[20]. So, most RET signalling during embryonic development can be attributed to the short isoform. NGF can activate only the long isoform of RET in adult sympathetic neurons[21], which indicates a long-form-specific intracellular binding protein and a sympathetic neuron phenotype in mice that are deficient in the long form of RET.

Interestingly, an alternative, ligand-independent RET-signalling pathway has been suggested. In the absence of ligand, RET triggers cell death when overexpressed in some cell lines, and this pro-apoptotic activity is blocked by GDNF[22]. A pro-apoptotic fragment that is cleaved by caspases from the cytoplasmic domain of RET is sufficient to trigger apoptosis. This provocative result awaits verification by other studies.

Crosstalk with other growth factors and receptors. Unlike other members of the TGF-β superfamily, GFLs do not signal through receptor serine–threonine kinases. However, in a sympathoadrenal lesion paradigm, endogenous TGF-β is required as a cofactor for exogenous GDNF to be neuroprotective[1]. TGF-β and GDNF could cooperate during several crucial steps of signal transduction, including GFRα1 receptor membrane localization[23]. Although the significance of TGF-β in physiological GFL signalling is unknown, this synergy might have clinical relevance.

There is also cooperation between GDNF- and neurotrophin-family signalling. For example, in sensory neurons of the PETROSAL GANGLION, GDNF and BDNF act as target-derived trophic factors and are required simultaneously for survival[24], although the mechanism of this collaboration is not clear. Recent data from the Milbrandt and Johnson laboratory reveal a new communication pathway between RET and NGF signalling by the TrkA receptor[21]. During postnatal development, sympathetic neurons lose their dependence on NGF for survival, but continue to require NGF for soma growth and process maintenance, as well as for the development of a mature neurotransmitter phenotype. These authors show that RET phosphorylation increases with postnatal age in sympathetic neurons *in vitro* and *in vivo*. This RET phosphorylation is independent of both GFLs and GFRα co-receptors, but requires TrkA that is activated by NGF. So, NGF promotes phosphorylation of the heterologous receptor tyrosine kinase RET, resulting

PETROSAL GANGLION
A structure that contains the cell bodies of the sensory neurons of the glossopharyngeal nerve, which innervate the tongue, pharynx, middle ear and carotid body.

LAMELLIPODIA
Sheet-like extensions at the edge of cells that contain a crosslinked F-actin meshwork.

C-FOS
An immediate early gene that is rapidly turned on when many types of neuron increase their activity. It can therefore be used to identify responsive neurons

in enhanced growth, metabolism and gene expression. However, the functional relevance of this crosstalk *in vivo* and more detailed molecular mechanisms of the intracellular pathway between TrkA and RET, remain to be elucidated.

Cyclic AMP is an important regulator of neuronal survival, regeneration and growth cone remodelling that are mediated by neurotrophic factors[25]. The increase in the intracellular cAMP level activates protein kinase A (PKA), which influences a variety of biochemical events in neurons. Recent data from the Takahashi laboratory[26] show that Ser696 on RET is phosphorylated after the elevation of cAMP levels, apparently by PKA, and is required for GDNF-induced Rac activity and LAMELLIPODIA formation. This implies a new mechanism, in which receptor tyrosine kinase modulates actin dynamics by its cAMP-dependent serine phosphorylation. It indicates a crosstalk between RET and other receptors, such as G-protein-coupled receptors, which are known to activate PKA in neurons during migration, differentiation, target innervation and activity-dependent synaptic plasticity.

New GDNF receptors Recently, GDNF was shown to activate intracellular signalling pathways independently of RET, through GFRα1. In RET-deficient cell lines and primary neurons, GDNF triggers SFK activation and subsequent phosphorylation of MAPK, PLC-γ, cAMP response element-binding protein (CREB), as well as the induction of c-*fos*[22,27]. By contrast, it has been claimed that NRTN–GFRα2 cannot signal in the absence of RET[28]. The mechanism of RET-independent signal transduction is unclear, because GPI-anchored GFRα1 should not be able to interact directly with SFKs and other intracellular signalling effectors. So, non-RET signalling predicts the existence of a new transmembrane receptor or linker protein for GDNF–GFRα1 (FIG. 3). As there is no direct evidence for GDNF signalling in mice that lack RET, the physiological relevance of RET-independent signalling *in vivo* remains to be shown. Also, the new receptors might act postnatally or under pathological conditions; for example, in lesions or cancer.

Gene ablations show what GFLs really do
Mice that lack RET, GDNF or GFRα1 die soon after birth, whereas mice lacking other GFLs or co-receptors are viable and fertile. TABLE 1 provides a summary of the neuronal phenotypes of the different GFLs and their receptor-knockout mice. The very similar phenotypes of ligand and co-receptor knockouts indicate a specific pairing of each GFL and corresponding GFRα *in vivo*. Virtually all cells and tissues that are affected in GFL- or GFRα-knockout mice also express RET, indicating that this is the main signalling receptor of GFLs *in vivo*.

Table 1 | Phenotypes of mice that lack GDNF-family ligands or their receptors

Gene knockout	*Ret*	*Gdnf* or *Gfra1*	*Nrtn* or *Gfra2*	*Artn* or *Gfra3*	*Gfra4*
Gross phenotype	Lethal at birth[32]	Lethal at birth[1]	Pseudoptosis, fertile. *Gfra2*$^{-/-}$ mice grow poorly after weaning[1]	Ptosis, viable, fertile[29]	Viable, fertile[31]
Viscerosensory	Breathing defect	PG: 40% loss of neurons[24]; breathing defect	ND	ND	ND
Somatosensory	DRG: NS[32]	TG: loss of myelinated endings in whisker follicle DRG: neuron number NS[50], reduced soma size[49]	DRG: neuron number NS, reduced soma size, loss of heat sensitivity in a subpopulation[51]	DRG: NS[29]	ND
Sympathetic	SCG: migration and initial axon growth defect; subtle deficits in other ganglia[34]	SCG neurons: NS or subtle loss[1]	SCG neurons: NS[1]	SCG: migration and initial axon growth defect[29] or reduced proliferation[15], most neurons die by P60	ND
Parasympathetic	No SPG or OG; reduced number and soma size in SMG and other ganglia[38]	No SPG or OG; reduced number and soma size in SMG and other ganglia[38,40]	SPG neurons; number NS, but lack innervation; reduced number, soma size and innervation in other ganglia[38,40]	SMG neurons: NS[29]	ND
Enteric	No neurons in bowel below stomach[32]	No neurons in bowel below stomach[2]	Moderate loss of fibres in small intestine, reduced motility[1]	NS[29]	ND
Motor	Loss in various nuclei (see text)	Moderate loss in various nuclei[50,53]	No gross defects[53]	ND	ND
Brain	SN: NS[32]	SN: NS[1]; impaired learning in adult *Gdnf*$^{+/-}$ mice[52]	Subtle deficit in hippocampal synaptic transmission[71]	No gross defects[29]	No gross defects[31]
Other tissues	No kidneys[32], moderate C-cell loss[30]	No kidneys[2], testis degeneration in adult *Gdnf*$^{+/-}$ mice[59]	ND	ND	ND

Numbers in superscript refer to corresponding references in the bibliography. If not stated, the phenotype refers to the newborn in *Ret*, *Gdnf* and *Gfra1* knockouts, and to the adult in others. C cell, thyroid calcitonin-producing cell; DRG, dorsal root ganglion; GDNF, glial cell line-derived neurotrophic factor; ND, not determined; NS, not significantly different from wild type; OG, otic ganglion; P60, postnatal day 60; PG, petrosal ganglion; SCG, superior cervical ganglion; SMG, submandibular ganglion; SPG, sphenopalatine ganglion; SN, substantia nigra; TG, trigeminal ganglion.

Mice that lack GDNF, GFRα1 or RET share a phenotype of kidney agenesis, and an absence of many parasympathetic and enteric neurons (see REF. 1 for original references). Likewise, mice that lack NRTN or GFRα2 have similar deficits in enteric and parasympathetic innervation. However, *Gfra2*$^{-/-}$ mice show growth retardation after weaning, whereas *Nrtn*$^{-/-}$ mice grow normally. The growth retardation of *Gfra2*$^{-/-}$ mice is probably due to multiple innervation deficits along the alimentary tract, including the pancreas (M.S.A., unpublished observations). The discrepancy in growth between NRTN- and GFRα2-deficient mice might reflect differences in genetic background or feeding conditions (although GDNF crosstalk through GFRα2 cannot yet be excluded). Although mice that lack GFRα2 or GFRα3 seem to share a phenotype of droopy eyelids (ptosis), the underlying causes are completely different. *Gfra2*$^{-/-}$ mice lack parasympathetic innervation in the lacrimal gland, whereas *Gfra3*$^{-/-}$ mice lack sympathetic innervation to the lid elevator muscle[29]. PSPN supports embryonic rat[2], but not mouse, midbrain dopamine and spinal motor neurons *in vitro* (M.S.A. *et al.*, unpublished observations). This species difference seems to be due to a lack of messenger RNA that encodes the functional GFRα4 receptor in the mouse nervous system[30]. Accordingly, lack of GFRα4 signalling does not lead to any obvious defects in the mouse brain[31].

Each GFL seems to regulate the mRNA expression of its cognate co-receptor, as *Gfra1*, but not *Gfra2* or *Ret*, expression is reduced in the peripheral ganglia in *Gdnf*$^{-/-}$ mice, whereas the opposite is seen in *Nrtn*$^{-/-}$ mice[1]. Interestingly, this regulation might be independent of RET signalling, because GFRα expression in RET-deficient mice is unaltered[32]. This kind of feedback regulation would match changes in trophic factor production in target cells with changes in the neurotrophic responsiveness of neurons. It is not known whether this regulation of GFRα gene expression by GFLs is direct, or whether it is mediated by neuronal activity.

Neuronal-subtype-specific functions of GFLs

Sympathetic neurons. Analysis of GFRα3- and RET-deficient mice has revealed a crucial role for ARTN signalling by GFRα3–RET in the migration of superior cervical ganglion (SCG) sympathetic precursors[29]. ARTN is first produced locally in the vicinity of sympathetic ganglia, and later by large blood vessels — intermediate targets along which the developing sympathetic axons grow to their final destination. Sympathetic neurons in late embryos become independent of ARTN by down-regulating *Gfra3* expression, and become dependent on target-derived NGF. SCG neurons in *Gfra3*$^{-/-}$ mice die, apparently because the sympathetic axons fail to reach their proper targets (and consequently lack adequate trophic support). In addition, subtle migration and innervation defects in other ganglia along the sympathetic chain have been reported in mouse embryos that lack ARTN, GFRα3 (REF. 33) or RET[34]. However, it is not known whether these defects have any functional consequences in adult ARTN- or GFRα3-deficient mice. Taken together, the results indicate that sympathetic neuron development requires chemoattractant ARTN signalling through GFRα3–RET for migration and initial axon outgrowth (FIG. 4).

Several questions remain. There is some debate about the extent to which GFRα3–RET signalling is required for sympathetic precursor proliferation and survival before NGF dependence[35]. The role of GFRα3 in adult sympathetic neurons is contradictory — although *Gfra3* is not expressed by postnatal day 60 (P60) SCG neurons *in vivo*[29], ARTN can still support a subpopulation of these neurons *in vitro*[35]. However, the culture of freshly isolated neurons might represent an injury situation in which *Gfra3* expression is upregulated. Also, the role of GDNF in sympathetic development is still unclear: no loss of SCG neurons by birth in *Gfra1*$^{-/-}$, but a 30% loss in *Gdnf*$^{-/-}$ mice has been reported (see REF. 1 for original references). As discussed earlier, NGF signalling by TrkA promotes phosphorylation of the long RET isoform in mature sympathetic neurons[21]. However, the role of GFRα receptors that seem to be co-expressed with RET in sympathetic neurons, at least during the first postnatal week[29], is unclear.

In addition, it is not known whether RET is expressed by a specific subpopulation of sympathetic neurons postnatally. One possibility is that it is involved in the cholinergic differentiation of a subpopulation of sympathetic neurons, which seems to require neurotrophin 3 (NT-3)[36]. Interestingly, in cultured neonatal SCG neurons, NT-3 has a synergistic survival action with GDNF, and retinoic acid induces GDNF and NT-3 responsiveness and cholinergic differentiation[37].

Parasympathetic neurons. Postganglionic parasympathetic neurons are located in small ganglia close to or within the target tissue. In the cranial region, these include the ciliary, sphenopalatine, submandibular and otic ganglia. The otic and sphenopalatine ganglia are absent in newborn RET-, GFRα1- or GDNF-deficient mice, indicating that GDNF signalling by the GFRα1–RET receptor complex is essential for the development of these parasympathetic neurons during embryogenesis[38,39]. The ganglia are already missing at embryonic day 12, and their neuronal precursors show defects in migration and proliferation (but not increased apoptosis)[38]. Parasympathetic precursors express *Gfra1* and *Ret*, and GDNF is found within or around them during migration. So, GDNF signalling by GFRα1–RET is required for migration and proliferation of parasympathetic neuronal precursors during early embryonic development (FIG. 4).

Gfra1 mRNA expression in parasympathetic neurons is downregulated before birth, but the neurons continue to express *Ret* and *Gfra2* postnatally, while *Nrtn* is upregulated in the target tissues[38,39]. NRTN- or GFRα2-deficient mice have variable deficits in parasympathetic target innervation in all regions examined. As a striking example, the parasympathetic innervation of the lacrimal (Hadrenian) gland that arises from the sphenopalatine ganglion is virtually absent. However, the neuronal cell bodies in the ganglion are not reduced in number, but are slightly smaller. Interestingly,

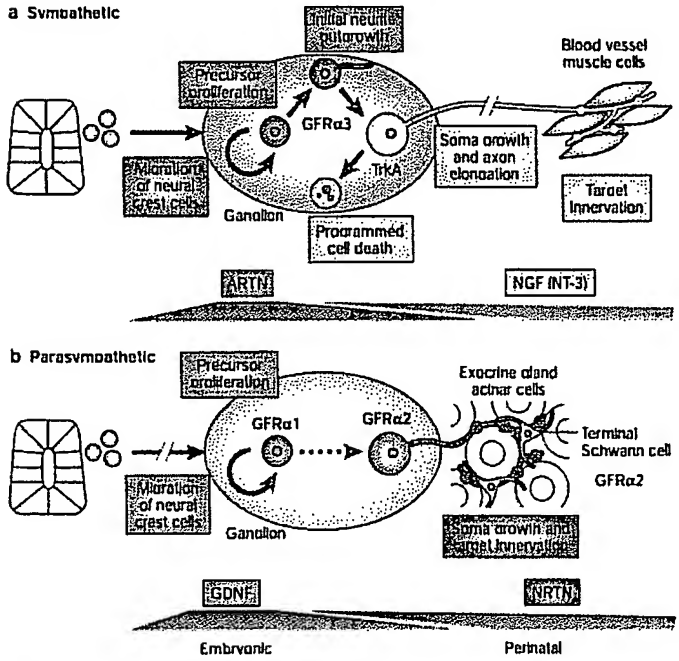

Figure 4 | Differences in trophic factor dependence between sympathetic and parasympathetic neurons. Shown is a schematic comparison of a | the sympathetic superior cervical (SCG) and b | the parasympathetic sphenopalatine ganglion (SPG) during development. In early embryos, neuronal precursors in the SCG require artemin (ARTN) for migration, proliferation and subsequent initial neurite outgrowth. SPG precursors require glial cell line-derived neurotrophic factor (GDNF), primarily for migration and proliferation. In late embryos and perinatally, sympathetic neurons require neurotrophins — nerve growth factor (NGF) and neurotrophin 3 (NT-3) — for survival, whereas parasympathetic neurons undergo a switch to require neurturin (NRTN) for target innervation and maintenance. In contrast to SCG sympathetic neurons, SPG parasympathetic neurons do not die in the absence of target-derived NRTN support. Note that non-myelinating glial support cells, which surround the neuron cell bodies and fibres, are thought to arise from the same autonomic neuronal precursors. In parasympathetic target tissue at least, the terminal Schwann cells express GDNF-family receptor-α2 (GFRα2) but not GFRα1. TrkA, tyrosine kinase A receptor.

Schwann cells in parasympathetic target tissues, which in wild-type mice express *Gfra2* (and not *Gfra1*) and are in close contact with parasympathetic fibres, are not affected (M.S.A., unpublished observations). So, the main role of NRTN in this ganglion, and presumably in other parasympathetic ganglia, is to support target innervation (including local axon guidance, branching and terminal formation) and to maintain neuronal size (trophic status).

Earlier studies in frog cardiac ganglia indicated that parasympathetic neurons within or close to the target tissue might not undergo programmed cell death, as they match the growing target size with increased proliferation[40]. By contrast, for chick ciliary ganglion neurons, limited amounts of target-derived NRTN seem to act as a classical survival factor[41]. Further studies of naturally occurring cell death in mammalian parasympathetic ganglia are needed. Nevertheless, the apparent lack of cell death in some parasympathetic neurons in the absence of target NRTN support is intriguing, and indicates differences in trophic signalling pathways that are activated by neurotrophins and GFLs. These surviving but atrophic neurons are reminiscent of neonatal Bax-deficient or mature sympathetic neurons, which atrophy and retract their neurites in the absence of NGF, but do not die.

In summary, GDNF and NRTN have distinct and sequential roles in developing parasympathetic neurons (FIG. 4). This shift from GDNF to NRTN signalling is also found in the enteric nervous system, indicating that common developmental mechanisms exist between the parasympathetic and enteric nervous systems.

Enteric neurons. Enteric neurons and glial cells that are derived from the vagal and sacral neural crest are missing below the stomach in mice that lack GDNF, GFRα1 or RET (reviewed in REF. 16). Mutations that affect the RET or ENDOTHELIN signalling pathways, as well as the transcription factors SOX10 or SIP1 (Smad-interacting protein 1), cause Hirschsprung's disease in humans [16]. *Gdnf*-heterozygous mutant mice have a variable enteric phenotype that might more closely resemble the human syndrome[42]. GDNF, expressed in gut mesenchymal cells, promotes the migration, proliferation, survival and differentiation of multipotent enteric precursor cells that express GFRα1 and RET[42]. As with other autonomic precursors, it is unclear whether all these effects of GDNF are direct, and what their relative contributions might be *in vivo*. Soluble GFRα1 is apparently produced by gut non-neuronal cells and promotes the effect of GDNF on precursor proliferation[43]. As expression of soluble GFRα1 ceases in late embryos, the GDNF response changes from mitogenic to trophic. Endothelin 3 (Edn3) signalling seems to modulate GDNF action by inhibiting the premature neuronal differentiation of migrating precursors[43]. The possibility of crosstalk between RET and endothelin receptor B (Ednrb) signalling has been suggested[44].

Mice that lack NRTN or GFRα2 show little if any loss of enteric neurons. However, these mice show a moderate but significant loss of the cholinergic, substance-P-containing fine myenteric nerve plexus in the small intestine, especially in the duodenum[3]. During late embryonic and early postnatal development, NRTN is expressed predominantly in the circular muscle layer, whereas the postnatal enteric neurons express GFRα2 and RET. Interestingly, although the density of the myenteric plexus in the GFRα2-deficient mouse colon is affected only slightly, the release of substance P *in vitro* from the NRTN-deficient mouse colon is reduced markedly. This implies that besides supporting enteric innervation, NRTN–GFRα2 signalling could regulate neurotransmitter release. Although GDNF, NRTN and their receptor components are also expressed in the adult gut[3], their role in the adult enteric nervous system and in functional disorders such as irritable bowel syndrome is unknown.

Somatic sensory neurons. *In vitro*, GFLs can support subpopulations of primary sensory neurons that serve different modalities, but, in most cases, their physiological role *in vivo* is poorly understood. Before birth, many

ENDOTHELIN
A molecule with potent vasoconstrictor activity. It is expressed by vascular cells, as well as in brain, kidney and lung.

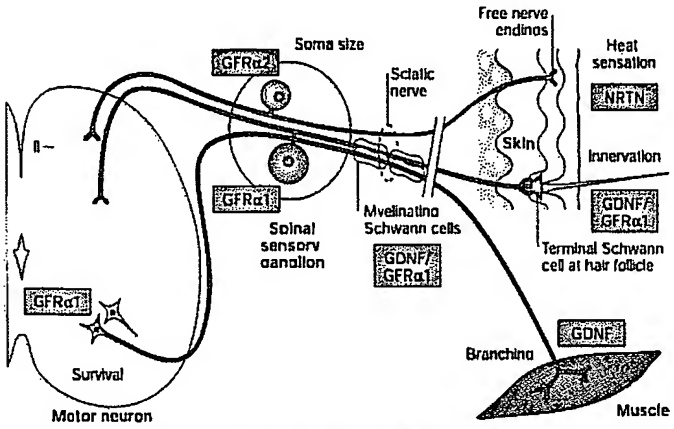

Figure 5 | *In vivo* functions of GDNF-family ligands in somatic sensory and motor neurons. The summary diagram shows a subpopulation of spinal primary sensory and motor neurons that are affected in knockout (or transgenic) mice at some developmental stage. A subpopulation of motor neurons requires glial cell line-derived neurotrophic factor (GDNF) for survival during embryonic development and possibly for terminal innervation during postnatal development. Terminal innervation of some myelinated mechanoceptors in the whisker follicle requires GDNF postnatally. The innervation deficit in the hair follicle is extrapolated from whisker-pad data[47]. Neurturin (NRTN) regulates heat sensitivity in a subpopulation of unmyelinated nociceptors. For details, see the main text. GFRα, GDNF-family receptor-α.

primary sensory neurons in the petrosal ganglion require target-derived GDNF (and BDNF) for survival[24]. These visceral chemoafferent sensory neurons innervate the CAROTID BODY and participate in breathing control. Accordingly, GDNF- and RET-deficient mice have disturbances in respiration, and point mutations in these genes are found in congenital central hypoventilation syndrome[15].

Most primary sensory neurons in the spinal and trigeminal ganglia require NGF for survival during embryonic development. Soon after birth, half of these neurons downregulate TrkA and start to express RET and cell-surface glycoproteins that bind the plant lectin IB4 (REF. 45). These small, unmyelinated neurons mediate pain and temperature sensation predominantly from the skin, and they terminate in the inner part of lamina II of the spinal cord (FIG. 5). During development, *Gfra1*, *Gfra2* and *Gfra3* mRNAs are expressed in peripheral nerves[5] (presumably in Schwann cells), and are co-expressed with *Ret* in partially overlapping subpopulations of sensory neurons[48], whereas sensory target areas, such as the epidermis and whisker follicles, express *Gdnf* and *Nrtn*[5,47]. GDNF is not detectable in adult skin[5], but it is present in Schwann cells and in the superficial layers of the spinal cord[48]. *Artn* mRNA is found in developing peripheral nerve roots, but its levels in adult nerves are low. *Gfra1* and *Ret* are also expressed in a subpopulation of large, myelinated mechanosensory neurons.

Consistent with the finding that the GDNF-dependence of somatosensory neurons *in vitro* starts after birth[49], the number of sensory neurons is not affected in the spinal and trigeminal ganglia of newborn *Gdnf*$^{-/-}$ (REF. 50) or *Gfra1*$^{-/-}$ (REF. 1) mice. Postnatally, GDNF signalling might be required for survival, target innervation and/or other functions in GFRα1/RET-expressing subpopulations of sensory neurons. *Gdnf*$^{+/-}$ mice show a postnatal loss of myelinated mechanoceptors (lanceolate and reticular endings), implying that GDNF supports cutaneous sensory innervation[47]. Intriguingly, terminal Schwann cells in the whisker follicles, but not in the adjacent myelinated nerve endings, show detectable GFRα1 immunoreactivity, indicating that GFRα1 in Schwann cells might be released locally or act *in trans*. By contrast, newborn *Gdnf*$^{+/-}$ or adult *Gdnf*$^{+/-}$ mice show no deficits in unmyelinated innervation in the whisker follicle. Why the large myelinated but not the small unmyelinated GFRα1/RET-expressing sensory neurons seem to require GDNF for innervation is unknown.

It seems that none of the small, unmyelinated RET/GFRα-expressing neurons requires GFLs for survival during normal development *in vivo*, because mice that lack GFRα2 (REF. 51) or GFRα3 (REF. 20) have normal numbers of spinal and trigeminal sensory neurons. The reason why the survival of these neurons in culture is supported by GFLs[49] could be related to axotomy-induced changes *in vitro*.

The functional identity and physiological role of NRTN-responsive somatosensory neurons has been studied using acute spinal sensory neuron cultures and SKIN-NERVE PREPARATIONS from adult GFRα2-deficient mice[51]. The results show that GFRα2 signalling regulates noxious heat transduction of an IB4-binding subpopulation of sensory neurons. Although NRTN promotes neurite outgrowth from GFRα2-expressing neurons in sensory ganglion explants before birth[1], the number of unmyelinated sensory axons in the cutaneous nerve is not reduced in adult GFRα2-deficient mice. However, it is not known whether the nerve terminals (free nerve endings) in the skin are affected. So, the development or maintenance of a functional heat-transduction apparatus in a subpopulation of nociceptors seems to require NRTN. Sensory function and target innervation in ARTN- or GFRα3-deficient mice have not been studied so far. Taken together, the results indicate that GFLs have roles that are probably not related to survival in several subpopulations of primary sensory neurons, but their specific *in vivo* roles are still poorly understood.

Motor neurons. Trophic factors that are produced by muscle and glial cells act synergistically to support motor neuron survival[52]. During development, GDNF is produced primarily by Schwann cells. There is a substantial loss of spinal and cranial motor neurons (20–40% depending on the region), and a corresponding increase in dying cells, in GDNF- and GFRα1-deficient mouse embryos compared with wild-type controls[53]. Accordingly, preliminary studies of *Ret*-knockout mice indicate significant losses in all motor neuron populations examined (R. Oppenheim, personal communication). Conversely, motor neuron survival is promoted by the muscle-specific overexpression of *Gdnf* or by GDNF treatment *in utero*, indicating that GDNF is indeed a physiological survival factor for a subpopulation of motor neurons[50]. Although exogenous NRTN supports motor neuron survival, this is largely mediated by

CAROTID BODY
A chemoreceptor organ that is located above the bifurcation of the common carotid artery. It monitors changes in blood O_2 and CO_2 content, and pH, thus helping to control respiratory activity.

SKIN-NERVE PREPARATION
An *in vitro* preparation that is used to study the functional properties of sensory neurons that innervate the skin. Single sensory afferents are isolated by recording from axons in microdissected filaments of a cutaneous nerve, and are classified on the basis of their conduction velocity, mechanical threshold and adaptation properties.

GFRα1, at least in culture. Accordingly, no clear loss of motor neurons is found in mice that lack GFRα2 (REF. 53).

Continued subcutaneous injections of GDNF (but not NRTN) during postnatal life[54], or transgenic overexpression of GDNF in skeletal muscle (starting after the period of programmed cell death)[55], produce hyperinnervation of neuromuscular junctions (with abnormal motor endplates), which is maintained in adults. GDNF seems to induce this extra innervation by promoting terminal branching that counteracts the ongoing multiple-synapse elimination, resulting in continuous synaptic remodelling at the neuromuscular junction (an equilibrium of axon extension and retraction). These results indicate that the main role of GDNF in postnatal motor neurons is to promote terminal axon branching and synapse formation[54] (FIG. 5).

Dopamine neurons. GDNF and NRTN are potent survival factors for midbrain dopamine neurons. However, only GDNF can promote axon growth and hypertrophy of these neurons[56]. Both factors seem to signal through the GFRα1–RET receptor complex, which is present on developing and mature dopamine neurons. However, analysis of knockout mice has shown that GFRα1–RET signalling is not essential for the embryonic development of dopamine neurons *in vivo*[1]. But GDNF could still be required for postnatal development, maintenance and/or plasticity of dopamine neurons, and for their striatal target innervation. This is indirectly supported by the observation that GDNF is expressed prominently in the striatum during the first few postnatal weeks, when dopamine neuron target innervation is taking place. Also, in contrast to neurons from wild-type mice, transplanted embryonic midbrain dopamine neurons from GDNF-deficient mice fail to survive and to innervate adult 1-methyl-4-phenyl-1,2,3,6-tetrahydropyridine (MPTP)-denervated striatal tissue[57]. Moreover, antisense inhibition of GDNF expression reduces dopamine axon sprouting on striatal injury[58]. Results from conditional-knockout mice that do not die after birth will be needed to determine whether endogenous GDNF signalling is required for postnatal survival or target innervation of dopamine neurons.

Clinical potential and pitfalls

Since their discovery, GFLs have received attention as potential therapeutic agents for the treatment of certain neurological diseases. Below, we discuss some recent findings that illustrate their clinical potential. Side effects, including weight loss and certain tumours[59], that might arise after systemic administration could be avoided by local delivery.

Motor neuron disease. Sciatic nerve axotomy increases the expression of GDNF in the denervated muscle, of GDNF and GFRα1 in the Schwann cells, and of RET and GFRα1 in the injured motor neurons. Axotomy also stimulates the release of soluble GFRα1 from Schwann cells[8]. Exogenously administered GDNF can support long-term motor neuron survival and axon regeneration after peripheral nerve injury in newborn or adult animals[60]. Whether GDNF, together with soluble or matrix-bound GFRα1, could further facilitate motor neuron regeneration would merit further study.

Recently, two related IAPs, NAIP (neuronal-apoptosis-inhibitory protein) and XIAP (X-linked inhibitor of apoptosis), were shown to be essential for the GDNF-mediated rescue of axotomized motor neurons[61]. The expression of these IAPs in motor neurons is upregulated by exogenous GDNF, but not by BDNF. Importantly, downregulation of IAP expression abolished the survival-promoting effect of GDNF, but not that of BDNF, indicating that intracellular survival mechanisms that are activated by GFLs and neurotrophins are different. It is not known whether IAPs have a role in the physiological cell death of GDNF-dependent motor neurons, or whether they control anti-apoptotic effects in other GFL-dependent neuronal populations.

Sensory regeneration and neuropathic pain. Peripheral nerve injury often leads to chronic neuropathic pain. The persistent nature of this symptom indicates abnormal plasticity changes in sensory pathways. Neurotrophins seem to be involved, as blocking antibodies can prevent hyperalgesia in models of neuropathic pain[62]. Recently, McMahon's group has shown that exogenous GDNF can prevent several abnormal axotomy-induced changes in sensory neurons, including A-fibre sprouting into lamina II. In response to peripheral nerve injury, RET-expressing sensory neurons also sprout around other sensory neurons, possibly as a response to local GFL production[63]. Importantly, INTRATHECAL GDNF produces potent analgesic effects in neuropathic models of pain, in part by reversing injury-induced changes in Na^+ channel subunit expression[64]. In contrast to NGF, intrathecal GDNF does not seem to affect pain sensation in normal animals[64].

Damaged sensory axons can normally regenerate in the peripheral nerve over long distances, but are unable to enter their central target area — the spinal cord. Surprisingly, chronic intrathecal treatment with NGF or GDNF can overcome this: after dorsal root injury, these factors cause sensory axons to regenerate back into the spinal cord and form functional connections with their normal target cells, thereby rescuing sensory function[65]. This study has clinical relevance for other sensory disorders, including diabetic neuropathy, in which the GDNF-responsive sensory axons are particularly vulnerable[66].

As different subpopulations of sensory neurons express receptors for GFLs and neurotrophins, the combination of growth factors from the two families would be expected to be beneficial for sensory regeneration. The combination of different GFLs, possibly with soluble GFRα receptors, might promote functional regeneration and prevent abnormal changes even better than GDNF can alone. However, this might also lead to complex interactions. For example, GFRα3, which is upregulated in most nociceptors after axotomy[16] and, in contrast to GFRα1 and GFRα2, is expressed little outside sensory neurons in adults, would seem an attractive drug target for pain-related studies. However, GFRα3 signalling might inhibit GFRα1 and GFRα2 signalling.

INTRATHECAL
Administered into the outer sheath of the spinal cord.

Box 1 | GDNF-family ligands and synaptic function

Apart from their roles in early neurogenesis, neurite outgrowth and target innervation, it seems that glial cell line-derived neurotrophic factor (GDNF)-family ligands (GFLs), in a manner similar to the neurotrophins (reviewed in REF. 25), are involved in activity-dependent synaptic plasticity. GDNF, neurturin (NRTN) and RET are expressed in many cortical areas, albeit at low levels, and their GDNF-family receptor-α (GFRα) receptors are abundant in the adult brain. Although messenger RNA expression of GDNF and NRTN in the brain is upregulated after seizure activity (see REF. 1 for original references), it is unclear whether GFL synthesis is regulated directly by neuronal activity. In addition, we do not know whether the secretion and uptake of GFLs is activity dependent, similar to that of neurotrophins. Depolarization that is induced by high concentrations of extracellular K^+ upregulates GFRα1 and downregulates GFRα2 expression in embryonic chick peripheral cranial sensory neurons *in vitro*[1]. This implies that neuronal activity evokes reciprocal changes in GFRα expression. Reciprocal changes in GFRα1 and GFRα2 are also seen in some brain regions after insults such as stroke and epilepsy[1]. Moreover, after peripheral nerve lesions, GFRα1 (and GFRα3) expression in primary sensory neurons is increased, whereas that of GFRα2 is reduced[16]. The mechanisms and significance of this reciprocal regulation remain unclear. Interestingly, intrathecal GDNF reverses the changes in GFRα1 expression, but also in GFRα2 expression, indicating that GFLs can also regulate co-receptor expression in the adult nervous system *in vivo*. Impairment in water-maze learning performance in *Gdnf*-heterozygous mutant mice[52], and in basal excitatory transmission at entorhinal afferent synapses to dentate granule cells in GFRα2-deficient mice[71], indicates that endogenous GFLs are involved in cognitive abilities and synaptic transmission.

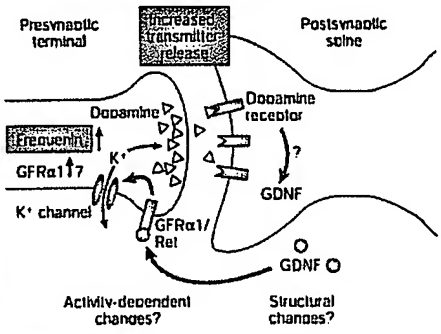

The figure shows a hypothetical model of a dopaminergic synapse in the striatum. GDNF might be produced by target neurons, and also by dopamine neurons that express GFRα1 and RET. GDNF and soluble GFRα1 might also be released from surrounding cells. GDNF has been shown to increase transmitter release from the axonal varicosities of midbrain dopamine neurons and from the neonatal mouse neuromuscular junction. Recently, Lu and co-workers[33] showed that GDNF potentiates Ca^{2+} channels and neurotransmitter release by the upregulation of frequenin, a Ca^{2+}-binding protein. Furthermore, GDNF acutely modulates A-type K^+ channels in, and therefore the excitability of, cultured midbrain dopamine neurons[34]. So, GDNF might acutely potentiate dopamine release (triangles) by modulating K^+ channels, and also modulate transmitter release by upregulating the Ca^{2+}-binding protein frequenin. GDNF could also promote structural changes, such as axon branching and synapse formation. In contrast to that of brain-derived neurotrophic factor (BDNF), GDNF signalling does not have very rapid (millisecond) effects on synaptic transmission. It is not clear whether GFLs other than GDNF can affect neuronal transmission by regulating transmitter release.

GDNF cannot prevent apoptotic cell death, but prevents excitotoxic (necrotic) neuronal death by reducing NMDA (N-methyl-D-aspartate)-receptor-mediated Ca^{2+} influx through an ERK (extracellular-signal-regulated kinase)-dependent pathway[70]. So, to be beneficial, GDNF would probably have to be administered in the early phase of stroke. Further work will be necessary to clarify the mechanisms of action of GDNF *in vivo*. Small-molecule compounds that act downstream of GDNF, such as NMDA receptor antagonists, could represent more practical therapeutic agents for ischaemia.

Epilepsy. After different types of seizure, GDNF, NRTN and their co-receptors are differentially regulated in neurons, and RET is upregulated also in seemingly non-neuronal cells in the hippocampus and other limbic structures[1]. Epileptogenesis, as assessed in the hippocampal KINDLING model, is markedly suppressed in GFRα2-deficient mice[71]. Although investigations in this area are still in their infancy, the results indicate that GFRα2 signalling contributes to the development and persistence of kindling epilepsy, and that GDNF and NRTN might modulate seizure susceptibility.

Parkinson's disease. Current therapy for Parkinson's disease is symptomatic — it does not slow down or reverse the underlying degeneration of midbrain dopamine neurons. In various animal models of Parkinson's disease, GDNF can prevent the neurotoxin-induced death of dopamine neurons and can promote functional recovery (reviewed in REF. 72). However, GDNF that was delivered into the lateral ventricles of a patient with Parkinson's disease was inefficient and caused severe side effects, including weight loss[73]. Recent improvements in GDNF delivery in animal models of Parkinson's disease include heparin co-administration, which increases GFL spread[4], novel viral vectors[74] and engrafted GDNF-producing neuronal stem cells[75], which maintain high levels of GDNF production. The site of GDNF administration is clearly important, because chronic delivery of GDNF into the striatum does not cause weight loss, can preserve dopamine terminals and promotes functional striatal dopamine innervation[76]. Combined with safety measures, including means to control gene expression, these new vehicles for GDNF delivery look promising for Parkinson's disease therapy[77]. However, it is unclear how well the neurodegenerative mechanisms in the models that have been used so far represent the natural disease process in the parkinsonian brain, stressing the need for new genetic models.

Addiction. The abuse of psychostimulant drugs induces behavioural sensitization, a form of dopamine-mediated neuronal plasticity[78]. Chronic administration of psychostimulants, such as cocaine or morphine, induces long-lasting neuronal changes in the ventral tegmental area (VTA), the origin of mesolimbic and mesocortical dopamine neurons. Learning, memory and drug addiction share certain intracellular signalling cascades, including dependence on the activation of the transcription factor CREB. So, neurotrophic factors that regulate as shown in postnatal sensory neurons *in vitro*[9]. Clearly, further studies — for example, using GFRα-knockout mice — are merited.

Ischaemia. In experimental models of focal ischaemia, exogenous GDNF administered before[67] or just after[68] anoxia can reduce ischaemic brain injury. The adult brain can respond to GDNF, as RET and GFRα1 show widespread upregulation in neurons, and in cells that seem to be non-neuronal, in the forebrain after ischaemia[69]. Interestingly, in cultures of cortical neurons,

KINDLING
An experimental model of epilepsy in which an increased susceptibility to seizures arises after daily focal stimulation of specific brain areas (for example, the amygdala) — stimulation that does not reach the threshold to elicit a seizure by itself.

dopamine neuronal plasticity might also regulate drug addiction. Recent data from the Nestler laboratory showed that infusion of GDNF into the VTA blocks certain biochemical adaptations to chronic cocaine and morphine, as well as the rewarding effects of cocaine[79]. *Gdnf*-heterozygous mice that were given morphine for several days showed enhanced locomotor sensitization after drug withdrawal compared with wild-type controls. Interestingly, chronic cocaine or morphine administration decreased RET phosphorylation levels, indicating that these drugs decrease signalling by endogenous GDNF pathways in the VTA. The intracellular signalling mechanisms through which GDNF inhibits drug addiction are not known. Finally, it would be of interest to test the effects on drug addiction of compounds that either inhibit or specifically activate RET signalling.

Conclusions and future directions

The picture of GFL signalling is still unclear, with many gaps in our understanding and some pieces of data that do not seem to fit with the rest. From the work discussed above, it might seem that GFLs are involved in almost every aspect of a neuron's life, from cell proliferation and migration to transmitter release and neuronal excitability (FIGS 4 and 5; BOX 1). This raises important questions about primary versus secondary roles of GFLs, and about the specificity of GFL signalling. Why should parasympathetic neurons need to switch their dependency from GDNF to NRTN if these factors can elicit the same biological responses by activating similar signalling pathways through RET? The evolution of this synergistic transcriptional switch indicates that different GFLs have unique skills. For example, GFLs might differ in their range of action (as determined by their affinity for the extracellular matrix), or in their ability to activate RET *in trans* or to signal independently of RET.

Another issue is how the same GFL induces different biological responses at different developmental stages or in different cell types. Presumably, mechanisms that influence GFL responses, including soluble GFRα receptors[15], intracellular signalling molecules, and synergistic factors and their receptors, show age- and cell-specific expression. Expression of *Ret* in autonomic neurons is regulated by a complex action of transcription factors, including Phox2b[80], Pax3 and Sox10 (REF 81), but we still know relatively little about the regulation, synthesis, secretion and extracellular-matrix association of the GFLs and GFRα receptors. Studies on the evolution and cell-biological aspects of GFLs and their receptors are also in an embryonic phase.

New tools, such as modern imaging approaches and knock-in mouse models, should help us to understand the *in vivo* functions of various RET- signalling components during development. Tissue-specific and inducible knockouts, as well as function-blocking antibodies, will allow us to explore the functions of RET signalling in the adult rodent nervous system. New technology, such as DNA arrays, will enable us to determine which genes regulate or are regulated by GFLs. Structural information about the GFL receptors and their complexes with GFLs will be needed if we are to understand the molecular details of ligand–receptor interactions, and is a prerequisite for rational drug design.

1. Airaksinen, M. S., Titievsky, A. & Saarma, M. GDNF family neurotrophic factor signaling: four masters, one servant? *Mol. Cell. Neurosci.* 13, 313–325 (1999).
2. Baloh, R. H., Enomoto, H., Johnson, E. M. Jr. & Milbrandt, J. The GDNF family ligands and receptors — implications for neural development. *Curr. Opin. Neurobiol.* 10, 103–110 (2000).
3. Ibáñez, C. F. Emerging themes in structural biology of neurotrophic factors. *Trends Neurosci.* 21, 438–444 (1998).
4. Hamilton, J. F. *et al.* Hexamin confusion during convection-enhanced delivery (CED) increases the distribution of the glial-derived neurotrophic factor (GDNF) ligand family in rat striatum and enhances the pharmacological activity of neurturin. *Exp. Neurol.* 168, 155–161 (2001).
5. Golden, J. P., DeMaro, J. A., Osborne, P. A., Milbrandt, J. & Johnson, E. M. Jr. Expression of neurturin, GDNF, and GDNF family-receptor mRNA in the developing and mature mouse. *Exp. Neurol.* 158, 504–528 (1999).
6. Lee, R., Kermani, P., Teng, K. K. & Hempstead, B. L. Regulation of cell survival by secreted proneurotrophins. *Science* 294, 1945–1948 (2001).
7. Takahashi, M. The GDNF/RET signaling pathway and human diseases. *Cytokine Growth Factor Rev.* 12, 361–373 (2001).
8. Lindahl, M. *et al.* Human glial cell line-derived neurotrophic factor receptor α4 is the receptor for persephin and is predominantly expressed in normal and malignant thyroid medullary cells. *J. Biol. Chem.* 276, 9344–9351 (2001).
9. Paratcha, G. *et al.* Released GFRα1 potentiates downstream signaling, neuronal survival, and differentiation via a novel mechanism of recruitment of c-Ret to lipid rafts. *Neuron* 29, 171–184 (2001).
   Together with reference 15, this paper shows that released GFRα1–GDNF potentiates RET signalling. Moreover, it shows that RET stimulation by immobilized GFRα1–GDNF enhances axonal growth cone formation, and that soluble GFRα1 can recruit RET to lipid rafts by a novel mechanism that requires the RET tyrosine kinase.
10. Ekerfalt, S., Fainzilber, M., Murray-Rust, J. & Ibáñez, C. F. Distinct structural elements in GDNF mediate binding to GFRα1 and activation of the GFRα1–c-Ret receptor complex. *EMBO J.* 18, 5901–5910 (1999).
11. Simons, K. & Toomre, D. Lipid rafts and signal transduction. *Nature Rev. Mol. Cell Biol.* 1, 31–39 (2000).
12. Poteryaev, D. *et al.* GDNF triggers a novel Ret-independent Src kinase family-coupled signaling via a GPI-linked GDNF receptor α1. *FEBS Lett.* 463, 63–66 (1999).
    Together with reference 27, this paper provides the first demonstration that GDNF signals in a RET-independent manner through GFRα1 in lipid rafts.
13. Tansey, M. G., Baloh, R. H., Milbrandt, J. & Johnson, E. M. Jr. GFRα-mediated localization of RET to lipid rafts is required for effective downstream signaling, differentiation, and neuronal survival. *Neuron* 25, 611–623 (2000).
    The first demonstration that the recruitment of RET to lipid rafts by GFL binding to GFRα is required for effective signalling.
14. Coulpier, M., Anders, J. & Ibáñez, C. F. Coordinated activation of autophosphorylation sites in the RET receptor tyrosine kinase: importance of tyrosine 1062 for GDNF mediated neuronal differentiation and survival. *J. Biol. Chem.* 277, 1991–1999 (2002).
15. Worley, D. S. *et al.* Developmental regulation of GDNF response and receptor expression in the enteric nervous system. *Development* 127, 4383–4393 (2000).
    The first demonstration of endogenous soluble GFRα1, which is released by cultured gut cells in a developmentally regulated manner.
16. Manie, S., Santoro, M., Fusco, A. & Billaud, M. The RET receptor: function in development and dysfunction in congenital malformation. *Trends Genet.* 17, 580–589 (2001).
17. Schlessinger, J. Cell signaling by receptor tyrosine kinases. *Cell* 103, 211–225 (2000).
18. Kaplan, D. R. & Miller, F. D. Neurotrophin signal transduction in the nervous system. *Curr. Opin. Neurobiol.* 10, 381–391 (2000).
19. Yano, F. *et al.* PI-3 kinase and IP3 are both necessary and sufficient to mediate NT3-induced synaptic potentiation. *Nature Neurosci.* 4, 19–28 (2001).
20. de Graaff, E. *et al.* Differential activities of the RET tyrosine kinase receptor isoforms during mammalian embryogenesis. *Genes Dev.* 15, 2433–2444 (2001).
    Using a knock-in approach, this study shows that the short RET isoform mediates most of the biological activities of RET *in vivo*.
21. Tsui-Pierchala, B. A., Milbrandt, J. & Johnson, E. M. NGF utilizes c-Ret via a novel GFL-independent, inter-RTK signaling mechanism to maintain the trophic status of mature sympathetic neurons. *Neuron* 33, 261–273 (2002).
    Identifies a new pathway for RET activation by NGF through TrkA.
22. Bordeaux, M. C. *et al.* The RET proto-oncogene induces apoptosis: a novel mechanism for Hirschsprung disease. *EMBO J.* 19, 4056–4063 (2000).
23. Peterziel, H., Unsicker, K. & Krieglstein, K. Molecular mechanisms underlying the cooperative effect of glial cell line-derived neurotrophic factor and transforming growth factor-β on neurons. *Soc. Neurosci. Abstr.* 27, 364.35 (2001).
24. Erickson, J. T., Brosenitsch, T. A. & Katz, D. M. Brain-derived neurotrophic factor and glial cell line-derived neurotrophic factor are required simultaneously for survival of dopaminergic primary sensory neurons *in vivo*. *J. Neurosci.* 21, 581–589 (2001).
25. Poo, M. M. Neurotrophins as synaptic modulators. *Nature Rev. Neurosci.* 2, 24–32 (2001).
26. Fukuda, T., Kiuchi, K. & Takahashi, M. Novel mechanism of regulation of Rac activity and lamellipodia formation by RET tyrosine kinase. *J. Biol. Chem.* 8 March 2002 (10.1074/jbc.M200643200).

27 Trupp, M., Scott, R., W Ilemore, S. R. & Ibanez, C. F Ret-dependent and -independent mechanisms of glial cell line-derived neurotrophic factor signaling in neuronal cells. *J Biol Chem.* 274, 20885–20894 (1999).

28 Pezeshki, G., Franke, B. & Enaele, J. Evidence for a ligand-specific signaling through GFRα-1, but not GFRα-2, in the absence of Ret. *J. Neurosci. Res.* 66, 390–395 (2001)

29. Nishino, J. *et al.* GFRα3, a component of the artemin receptor, is required for migration and survival of the superior cervical ganglion. *Neuron* 23, 725–736 (1999)
The first demonstration that ARTN–GFRα3 signalling controls the migration of sympathetic precursors *in vivo*.

30 Lindahl, M., Timmusk, T., Rossi, J., Saarma, M. & Airaksinen, M. S. Expression and alternative splicing of mouse *Gfra4* suggest roles in endocrine cell development. *Mol. Cell. Neurosci.* 15, 522–533 (2000)

31 Hiltunen, P. *et al.* Initial characterization of GDNF-family receptor GFRα4-deficient mice. *Soc. Neurosci. Abstr.* 27, 364.31 (2001).

32. Taraviras, S. *et al.* Signalling by the RET receptor tyrosine kinase and its role in the development of the mammalian enteric nervous system. *Development* 126, 2785–2797 (1999).

33 Homma, Y. *et al.* Artemin is required for the sympathetic nervous system development. *Soc. Neurosci. Abstr.* 27, 798.4 (2001).

34 Enomoto, H. *et al.* RET signaling is essential for migration, axonal growth and axon guidance of developing sympathetic neurons. *Development* 128, 3963–3974 (2001).

35. Andres, R. *et al.* Multiple effects of artemin on sympathetic neurone generation, survival and growth. *Development* 128, 3685–3695 (2001)

36. Brodski, C., Schmuch, H. & Dechant, G. Neurotrophin-3 promotes the cholinergic differentiation of sympathetic neurons. *Proc. Natl Acad. Sci. USA* 97, 9683–9688 (2000).

37. Thang, S. H., Kobayashi, M. & Matsuoka, I. Regulation of glial cell line-derived neurotrophic factor responsiveness in developing rat sympathetic neurons by retinoic acid and bone morphogenetic protein-2. *J. Neurosci.* 20, 2917–2925 (2000)

38. Enomoto, H., Heuckeroth, R. O., Golden, J. P., Johnson, E. M. & Milbrandt, J. Development of cranial parasympathetic ganglia requires sequential actions of GDNF and neurturin. *Development* 127, 4877–4889 (2000).
Together with reference 39, this paper indicates an early role for GDNF in parasympathetic precursor development.

39 Rossi, J., Tomac, A., Saarma, M. & Airaksinen, M. S. Distinct roles for GFRα1 and GFRα2 signaling in different cranial parasympathetic ganglia *in vivo*. *Eur. J. Neurosci.* 12, 3944–3952 (2000)

40. Heathcote, R. D. & Saraeni, P. B. Growth and morphogenesis of an autonomic ganglion. II. Establishment of neuron position. *J. Neurosci.* 7, 2502–2509 (1987)

41. Hashino, E. *et al.* GDNF and neurturin are target-derived factors essential for cranial parasympathetic neuron development. *Development* 128, 3773–3782 (2001)

42. Shen, L. *et al.* Gdnf haploinsufficiency causes Hirschsprung-like intestinal obstruction and early-onset lethality in mice. *Am. J. Hum. Genet.* 70, 435–447 (2002)

43 Gershon, M. D. Lessons from genetically engineered animal models. II. Disorders of enteric neuronal development: insights from transgenic mice. *Am. J. Physiol.* 277, G262–G267 (1999).

44 Auricchio, A. *et al.* Double heterozygosity for a RET substitution interfering with splicing and an *EDNRB* missense mutation in Hirschsprung disease. *Am. J. Hum. Genet.* 64, 1216–1221 (1999).

45 Snider, W. D. & McMahon, S. B. Tackling pain at the source: new ideas about nociceptors. *Neuron* 20, 629–632 (1998)

46 Bennett, D. L. *et al.* The glial cell line-derived neurotrophic factor family receptor components are differentially regulated within sensory neurons after nerve injury. *J. Neurosci.* 20, 427–437 (2000)

47 Fundin, B. T., Mikaels, A., Westphal, H. & Emfors, P. A rapid and dynamic regulation of GDNF-family ligands and receptors correlate with the developmental dependency of cutaneous sensory innervation. *Development* 126, 2597–2610 (1999)

48 Jongen, J. L., Dahm, F., Vechi, C. J. & Holstege, J. C. Depletion of GDNF from primary afferents in adult rat dorsal horn following peripheral axotomy. *Neuroreport* 10, 867–871 (1999).

49 Baudet, C. *et al.* Positive and negative interactions of GDNF, NTN and ART in developing sensory neuron subpopulations, and their collaboration with neurotrophins. *Development* 127, 4335–4344 (2000).

50 Oppenheim, R. W. *et al.* Glial cell line-derived neurotrophic factor and developing mammalian motoneurons: regulation of programmed cell death among motoneuron subtypes. *J. Neurosci.* 20, 5001–5011 (2000)

51. Stucky, C. L., Rossi, J., Airaksinen, M. S. & Lewin, G. R. The heat sensitivity of isolectin-B4 positive nociceptors is selectively lost in mice lacking the neurturin receptor GFRα2. *Soc. Neurosci. Abstr.* 94, 8 (1999)

52. Arce, V. *et al.* Synergistic effects of Schwann- and muscle-derived factors on motoneuron survival involve GDNF and cardiotrophin-1 (CT-1). *J. Neurosci.* 18, 1440–1448 (1998)

53 Garces, A. *et al.* GFRα1 is required for development of distinct subpopulations of motoneuron. *J. Neurosci.* 20, 4992–5000 (2000).

54. Keller-Peck, C. R. *et al.* Glial cell line-derived neurotrophic factor administration in postnatal life results in motor unit enlargement and continuous synaptic remodeling at the neuromuscular junction. *J. Neurosci.* 21, 6136–6146 (2001)

55 Zwick, M., Tena, L., Mu, X., Springer, J. E. & Davis, B. M. Overexpression of GDNF induces and maintains hyperinnervation of muscle fibers and multiple end-plate formation. *Exp. Neurol.* 171, 342–350 (2001).

56 Akerud, P., Alberch, J., Eketjall, S., Wagner, J. & Arenas, E. Differential effects of glial cell line-derived neurotrophic factor and neurturin on developing and adult substantia nigra dopaminergic neurons. *J. Neurochem.* 73, 70–78 (1999)

57 Granholm, A. C. *et al.* Glial cell line-derived neurotrophic factor is essential for postnatal survival of midbrain dopamine neurons. *J. Neurosci.* 20, 3182–3190 (2000).

58 Batchelor, P. E., Liberatore, G. T., Porritt, M. J., Donnan, G. A. & Howells, D. W. Inhibition of brain-derived neurotrophic factor and glial cell line-derived neurotrophic factor expression reduces dopaminergic sprouting in the injured striatum. *Eur. J. Neurosci.* 12, 3462–3468 (2000).

59 Mena, X. *et al.* Regulation of cell fate decision of undifferentiated spermatogonia by GDNF. *Science* 287, 1489–1493 (2000).
The first demonstration that GDNF regulates spermatogonia differentiation *in vivo*.

60 Hollinger, A. F., Azzouz, M., Deglon, N., Aebischer, P. & Zurn, A. D. Complete and long-term rescue of lesioned adult motoneurons by lentiviral-mediated expression of glial cell line-derived neurotrophic factor in the facial nucleus. *J. Neurosci.* 20, 5587–5593 (2000).

61 Perrelet, D. *et al.* IAPs are essential for GDNF-mediated neuroprotective effects in injured motor neurons *in vivo*. *Nature Cell Biol.* 4, 175–179 (2002).
The first demonstration of a difference in trophic signalling between GFLs and neurotrophins.

62. Zhou, X. F., Deng, Y. S., Xian, C. J. & Zhong, J. H. Neurotrophins from dorsal root ganglia induce allodynia after spinal nerve injury in rats. *Eur. J. Neurosci.* 12, 100–105 (2000).

63. Li, L. & Zhou, X. F. Pericellular Griffonia simplicifolia I isolectin B4-binding nerve structures in the dorsal root ganglia following peripheral nerve injury in rats. *J. Comp. Neurol.* 439, 259–274 (2001).

64 Boucher, T. J. *et al.* Potent analgesic effects of GDNF in neuropathic pain states. *Science* 290, 124–127 (2000)
Shows that GDNF supresses neuropathic pain, possibly by preventing the upregulation of Na^+ channel subunits.

65 Ramer, M. S., Priestley, J. V. & McMahon, S. B. Functional regeneration of sensory axons into the adult spinal cord. *Nature* 403, 312–316 (2000).
The first demonstration that axons can regenerate through the dorsal root entry zone into the spinal cord and form functional synapses if provided with the right growth factors.

66 Akkina, S. K., Patterson, C. L. & Wright, D. E. GDNF rescues nonpeptidergic unmyelinated primary afferents in streptozotocin-treated diabetic mice. *Exp. Neurol.* 167, 173–182 (2001).

67. Wang, Y., Lin, S. Z., Chiou, A. L., Williams, L. R. & Hofer, B. J. Glial cell line-derived neurotrophic factor protects against ischemia-induced injury in the cerebral cortex. *J. Neurosci.* 17, 4341–4348 (1997)

68 Kitagawa, H. *et al.* Reduction of ischemic brain injury by topical application of glial cell line-derived neurotrophic factor after permanent middle cerebral artery occlusion in rats. *Stroke* 29, 1417–1422 (1998).

69 Arvidsson, A., Kokaia, Z., Airaksinen, M. S., Saarma, M. & Lindvall, O. Stroke induces widespread changes of gene expression for glial cell line-derived neurotrophic factor family receptors in the adult rat brain. *Neuroscience* 106, 27–41 (2001).

70. Nicole, O. *et al.* Neuroprotection mediated by glial cell line-derived neurotrophic factor: involvement of a reduction of NMDA-induced calcium influx by the mitogen-activated protein kinase pathway. *J. Neurosci.* 21, 3024–3033 (2001)

71. Nanobashvili, A. *et al.* Development and persistence of limb/leg coleosy are impaired in mice lacking glial cell line-derived neurotrophic factor family receptor α2. *Proc. Natl Acad. Sci. USA* 97, 12312–12317 (2000).

72. Grondin, R. & Gash, D. M. Glial cell line-derived neurotrophic factor (GDNF) — a drug candidate for the treatment of Parkinson's disease. *J. Neurol.* 245, 35–42 (1998)

73. Kordower, J. H. *et al.* Clinicopathological findings following intraventricular glial-derived neurotrophic factor treatment in a patient with Parkinson's disease. *Ann. Neurol.* 46, 419–424 (1999).

74. Kordower, J. H. *et al.* Neurodegeneration prevented by lentiviral vector delivery of GDNF in primate models of Parkinson's disease. *Science* 290, 767–773 (2000)

75. Åkerud, P., Canals, J. M., Snyder, E. Y. & Arenas, E. Neuroprotection through delivery of glial cell line-derived neurotrophic factor by neural stem cells in a mouse model of Parkinson's disease. *J. Neurosci.* 21, 8108–8118 (2001).

76. Björklund, A. *et al.* Towards a neuroprotective gene therapy for Parkinson's disease: use of adenovirus, AAV and lentivirus vectors for gene transfer of GDNF to the nigrostriatal system in the rat Parkinson model. *Brain Res.* 886, 82–98 (2000).

77. Zurn, A. D., Widmer, H. R. & Aebischer, P. Sustained delivery of GDNF: towards a treatment for Parkinson's disease. *Brain Res. Brain Res. Rev.* 36, 222–229 (2001)

78. Nestler, E. J. Molecular basis of long-term plasticity underlying addiction. *Nature Rev. Neurosci.* 2, 119–128 (2001).

79 Messer, C. J. *et al.* Role for GDNF in biochemical and behavioral adaptations to drugs of abuse. *Neuron* 26, 247–257 (2000)
Indicates a role for endogenous GDNF in dopamine plasticity *in vivo* after cocaine or morphine exposure.

80 Pativn, A., Morin, X., Cremer, H., Gondo, C. & Brunet, J. F. The homeobox gene *Phox2b* is essential for the development of autonomic neural crest derivatives. *Nature* 399, 366–370 (1999).

81. Lang, D. *et al.* Pax3 is required for enteric ganglia formation and functions with Sox10 to modulate expression of c-ret. *J. Clin. Invest.* 106, 963–971 (2000).

82. Gerlai, R. *et al.* Impaired water maze learning performance without altered dopaminergic function in mice heterozygous for the GDNF mutation. *Eur. J. Neurosci.* 14, 1153–1163 (2001).

83 Wang, C. Y. *et al.* Ca^{2+} binding protein frequenin mediates GDNF-induced potentiation of Ca^{2+} channels and transmitter release. *Neuron* 32, 99–112 (2001).

84 Yang, F. *et al.* GDNF acutely modulates excitability and A-type K^+ channels in midbrain dopaminergic neurons. *Nature Neurosci.* 4, 1071–1078 (2001).

85. Scott, R. P. & Ibáñez, C. F. Determinants of ligand binding specificity in the glial cell line-derived neurotrophic factor family receptor αs. *J. Biol. Chem.* 276, 1450–1458 (2001).

86. Baloh, R. H., Tansey, M. G., Johnson, E. M. J. & Milbrandt, J. Functional mapping of receptor specificity domains of glial cell line-derived neurotrophic factor (GDNF) family ligands and production of GFRα1 RET-specific agonists. *J. Biol. Chem.* 275, 3412–3420 (2000)

87 Anders, J., Kjar, S. & Ibáñez, C. F. Molecular modeling of the extracellular domain of the RET receptor tyrosine kinase reveals multiple cadherin-like domains and a calcium-binding site. *J. Biol. Chem.* 276, 35808–35817 (2001)

Acknowledgements

We thank U. Arumae, M. Pavelev, J. Rossi and P. Runeberg-Roos for critical reading of the manuscript. Our work is supported by the Academy of Finland, TEKES, Biocentrum Helsinki and the Sigrid Juselius Foundation. Owing to space limitations, we have cited original references only from the last four years; we apologize for the omission of earlier papers.

Online links

DATABASES

The following terms in this article are linked online to:
LocusLink: http://www.ncbi.nlm.nih.gov/LocusLink/
ARTN | BDNF | CREB | DOK4/5 | Edn3 | Ednrb | enteric | frequenin | FRS2 | GDNF | GFRα | GRB2 | IRS1/2 | NAIP | NGF | NRTN | NT-3 | P75^{NTR} | Pax3 | Phox2b | PSPN | Rac | RET | Shc | SIP1 | SOX10 | Src | TGF-β1 | TrkA | XIAP
OMIM: http://www.ncbi.nlm.nih.gov/Omim/
congenital central hypoventilation syndrome | Hirschsprung's disease | Parkinson's disease

FURTHER INFORMATION

Encyclopedia of Life Sciences: http://www.els.net/
motor neuron diseases | Parkinson disease | trophic support
The Genome Database: http://gdbwww.gdb.org/gdb/
Access to this interactive links box is free online.

Cell Tissue Res (2001) 305:229–238
DOI 10.1007/s004410100378

REVIEW

Georg Dechant

Molecular interactions between neurotrophin receptors

Received: 2 January 2001 / Accepted: 12 February 2001 / Published online: 24 April 2001

Abstract Neurotrophins signal via a dual-receptor system comprising receptor tyrosine kinases, the Trks, and a tumor necrosis factor (TNF) receptor like molecule, p75. Interest in these receptors was spurred on by the finding that they are employed by their neurotrophin ligands to activate opposing cellular mechanisms. Signalling via Trk receptors promotes the survival of embryonic neurons, whereas activation of p75 can trigger apoptosis. However, this antagonistic view is an oversimplification. It is more accurate to refer to this system as a signalling network in which ligands, receptors and their intracellular target proteins are linked by balanced biochemical interactions. This article reviews recent advances in our understanding of these molecular mechanisms which critically determine many cell-type-specific responses to neurotrophins. Emphasis is given to the formation of receptor complexes, the generation of receptor diversity by alternative splicing and the influence exerted by the local membrane environment on neurotrophin signalling.

Keywords Trk · Receptor tyrosine kinase · Neurotrophins · p75 · Ceramide · Alternative splicing · Internalization · Retrograde transport

Introduction

Neurotrophins are vertebrate-specific growth factors which predominantly act on nerve cells. During development, they regulate neuronal survival and differentiation and control the chemotropic orientation of neurites in vivo (Tucker et al. 2001). In the mature nervous system, their role in activity-dependent neuronal plasticity defines them as prime candidates for regulators of higher systemic brain functions (Thoenen 1995; McAllister et al. 1999). The neurotrophins, their biological effects and also the intracellular signalling pathways of their receptors have been the subject of a number of recent reviews (Friedman and Greene 1999; Bibel and Barde 2000; Dobrowsky and Carter 2000b; Chao 2000; Kaplan and Miller 2000). In the following, I will focus on key mechanisms for determining the cellular responses to neurotrophins: the molecular interactions between ligands and receptors occurring at the plasma membrane of responsive cells.

G. Dechant (✉)
Department of Neurobiochemistry,
Max Planck Institute of Neurobiology,
Am Klopferspitz 18a, 82152 Martinsried, Germany
e-mail: dechant@neuro.mpg.de
Tel.: +49-89-85783623, Fax: +49-89-85783749

The neurotrophins and their receptors

At the cellular level, responses to neurotrophins are highly diverse, cell-type specific and not uncommonly seem paradoxical: neurotrophins can cause cells to proliferate or withdraw from the cell cycle, to grow or to shrink and they can protect cells from apoptosis or kill them. However, from a genetic point of view, the receptor/ligand system used to generate these diverse phenomena is simple. In higher vertebrates, it derives from only four genes encoding growth factor ligands (NGF, BDNF, NT3 and NT4/5), and another set of four genes encoding their receptors: the three *trk* receptor tyrosine kinase genes (*trkA, trkB* and *trkC*) and the single gene encoding the neurotrophin receptor $p75^{NTR}$, a member of the TNF receptor family (Fig. 1). The Trk receptors mediate the classical antiapoptic effects of the neurotrophins (but see Kim et al. 1999), whereas p75 can trigger apoptosis (for a review, see Dechant and Barde 1997).

The receptor-ligand relationships between the neurotrophins and their receptors were mostly elucidated with cell lines overexpressing the receptors in recombinant form. In such cell-line paradigms, p75 binds all neurotrophins with similar binding properties, while the Trk receptors are more selective in their ligand interactions, but to varying degrees. While TrkC binds only one neurotrophin (NT3), TrkA binds two (NGF, NT3) and TrkB three (BDNF, NT4/5, NT3).

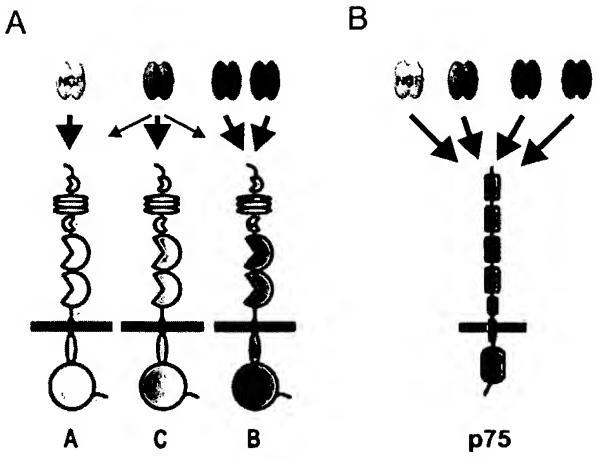

Fig. 1A, B Neurotrophins bind to two types of transmembrane receptors. **A** The Trk family of receptor tyrosine kinases (TrkA, B, C) is characterized by a specific combination of structural motives: In their extracellular domains three tandem repeat leucine-rich motives are flanked by two cysteine clusters. The main contacts between the Trk receptors and their ligands occur within two Ig-like C2 type domains. The protein sequences of the intracellular, enzymatically active, tyrosine kinase domains are highly conserved in the three receptors. **B** The second type of neurotrophin receptor is p75. This molecule, previously known under the name of NGF receptor or low-affinity neurotrophin receptor, interacts with all four neurotrophins. Its protein structure defines it as a member of the TNF-R/fas family of receptors. Binding of its neurotrophin ligands occurs mainly within the four cysteine-rich domains in its extracellular part. The intracellular domain remotely resembles the death domains found in several members of the TNF-R/fas family

For the Trk receptors, the physiological relevance of these biochemical interactions was unequivocally confirmed by the congruous phenotypes of mice with targeted mutations in genes encoding Trk receptors and their ligands, especially in the peripheral sensory nervous system. However, the analysis of these animals also left open a number of important questions. The brains of developing Trk knockout mice turned out to be surprisingly unaffected, despite a widespread expression of Trk receptors in the developing CNS. Even in PNS neurons, Trk receptor expression is not synonymous with neurotrophin responsiveness. Ectopic expression of TrkA in primary neurons failed to render these cells NGF responsive at a developmental stage in which they critically depend on trophic support (Allsopp et al. 1993). The observed cellular responses of many Trk-expressing cells are not uniform. Depending on the cell type, ligand specificity, binding affinities, dose response curves as well as duration and magnitude of Trk receptor activation can vary substantially. This fine-tuning in the biochemistry of the receptors is potentially highly significant for the physiology of the neurotrophins. Many cells have the intrinsic capacity to amplify differences in the magnitude and duration of tyrosine receptor kinase activation and to translate them into very different cellular responses (Bonni and Greenberg 1997).

The problem is even more pronounced in the case of p75, the second type of neurotrophin receptor. The p75 protein is expressed in a variety of tissues and the gene is highly regulated both during development and in adult neuronal lesion paradigms. While p75 was previously considered a simple accessory protein for the Trk receptors, it has now come to light that it is an actively signalling receptor, although lacking intrinsic enzymatic activity (reviewed in Dechant and Barde 1997). Yet, many cells expressing p75 at substantial levels show no obvious functional response upon stimulation with neurotrophin ligands. Moreover, many tissues in which p75 is expressed in a highly dynamic pattern during embryonic development appear perfectly intact in mice lacking full-length p75 (Lee et al. 1992). Furthermore, while p75 binds all neurotrophins with similar affinity in overexpression paradigms, its signalling can be highly ligand specific (Carter et al. 1996b). This is likely to reflect, at least in part, cell-type-specific differences in the biochemistry of p75 as opposed to differences in the expression of components of its signalling cascades. Many of the recently identified protein interactors of p75 appear to be widely, if not ubiquitously, expressed (for a review, see Bibel and Barde 2000). Hence, the expression pattern of these intracellular interactors can be used to predict responses to neurotrophins even less than that of p75 itself.

Hence, it seems that the reaction of cells to stimulation with a neurotrophin is strongly influenced by cell-type-specific interactions already occurring at the plasma membrane. For a comprehensive understanding of the biological effects of the neurotrophins, it is therefore crucial to investigate the molecular interactions of their receptors in specific cellular environments.

Receptor-receptor complexes

Biochemical experiments indicate that neurotrophin receptors form three different types of complexes: homodimers of Trk receptors, homomeric p75 receptors and a mixed complex of unknown stoichiometry containing both Trk and p75 (Fig. 2). In the frequently observed case of cells coexpressing Trk and p75 receptors, these complexes should coexist and may be linked through biochemical equilibria. Functionally, their signalling can be independent, synergistic or antagonistic. The response of a cell to neurotrophins may hence be determined by the quantitative and qualitative composition of its receptor complement in combination with biochemical equilibria between pools of active and inactive receptors.

Trk receptor dimerization

The signalling of Trk receptors is triggered by the formation of homodimeric complexes. Biochemical evidence was provided for functional dimeric TrkA receptors in the absence of p75 (Jing et al. 1992). In cell lines overexpressing Trk receptors but not p75, distinct binding sites are detected for the preferred ligands which differ

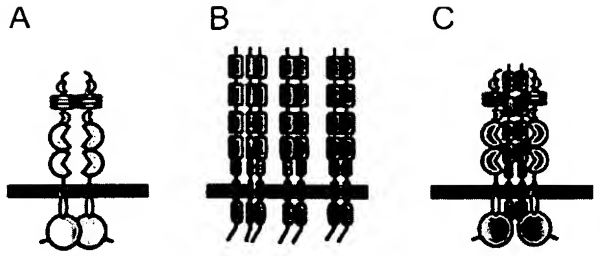

Fig. 2A–C Neurotrophin receptor complexes. The neurotrophin receptors form complexes within the plasma membrane. Biochemical evidence has been provided for homodimeric Trk receptors **(A)**, for complexes between p75 monomers **(B)**, and for mixed complexes containing both Trk and p75 receptors **(C)**. Formation of these complexes often correlates with higher ligand affinity and specificity

about 100-fold in their ligand affinities (Klein et al. 1991; Sqinto et al. 1991; Dechant et al. 1993; Lamballe et al. 1991). Although the affinities of monomeric and dimeric Trks have yet to be determined in direct binding experiments, it is likely that the high-affinity binding sites reflect dimeric receptors, whereas the low-affinity sites are monomeric. Cell-type-specific shifts in the monomer-dimer equilibrium of Trk receptors provide one reasonable explanation for the observed variability in the activation kinetics of Trk receptors by neurotrophins (Knüsel et al. 1994). While this equilibrium may be predominantly a function of Trk expression levels (Hempstead et al. 1992), work with other receptor tyrosine kinases suggests that it is also influenced by different cellular mechanisms, such as the activity of tyrosine phosphatases (reviewed in Weiss et al. 1997). Recently, crystal structures of the ligand interaction domains of all three trks have been solved (Ultsch et al. 1999). Although the stoichiometry between ligands and Trk receptors in the naturally occurring complexes is unknown, it is interesting to note that the structure of the NGF complex with the soluble second IgG domain of TrkA displays twofold symmetry with two identical TrkA interaction domains in the NGF dimer (Wiesmann et al. 1999). Thus, a single NGF dimer should be sufficient to stabilize one TrkA dimer.

p75 receptor complexes

The stoichiometry of actively signalling p75 complexes is elusive. The closest structural and functional p75 homologues, the receptors of the TNF-R/fas family, signal as trimers. By analogy, the formation of higher-order complexes or aggregates of p75 may be required for its signalling (but see Wang et al. 2000). This is also indicated by the finding that monomeric and dimeric p75 receptors interact with different intracellular proteins (Ye et al. 1999). Biophysical measurements revealed that p75 can form clusters (Venkatakrishnan et al. 1991). Biochemically, at least homodimeric complexes of p75 can be identified (Grob et al. 1985; Meakin and Shooter 1991; Carter et al. 1996a). The equilibrium between monomeric and dimeric p75 receptors appears to be shifted by serine-threonine phosphorylation of the receptor (Grob et al. 1985). The binding curve of neurotrophins to p75 on PCNA cells, a cell line which lacks Trk receptors, displays a ligand-specific allosteric behaviour indicative of equilibria between complexes of unknown stoichiometry (Dechant and Barde 1997). p75 sites of low and high affinity can be detected on primary neurons and cell lines in the absence of the corresponding Trk receptor (Dechant et al. 1997; Ross et al. 1998). At least for NT3, the high-affinity state of p75 receptors on neurons is linked to a higher ligand specificity (Dechant et al. 1997).

Mixed p75-Trk receptor complexes

The finding that p75 physically interacts with all three Trks receptors adds an interesting twist to the physiology of neurotrophin receptors (Huber and Chao 1995; Gargano et al. 1997; Ross et al. 1998; Bibel et al. 1998). For receptor tyrosine kinases, it is not unusual that they interact with accessory receptor proteins in order to achieve a higher binding affinity and ligand specificity, a prominent example being the ret tyrosine kinase and its alpha coreceptors. However, amongst the numerous TNFR/fas receptor family members, p75 is exceptional to date in its association with a receptor tyrosine kinase. The formation of mixed complexes may, at least in part, explain the well-documented reciprocal modulatory effect of Trk and p75 coexpression on ligand interactions and signalling functions (reviewed in Bothwell 1995; Majdan and Miller 1999). However, at present the physiological significance of the direct binding of Trk and p75 receptors remains to be firmly established. One important open question is whether heteromeric neurotrophin receptors exist on neurons. Furthermore, it will be crucial to answer the question of whether heteromeric p75/Trk complexes possess signalling capacities which are principally different from those of the homomeric Trk or p75 receptors. In vitro, the effects of coexpression with p75 on Trk receptor function are remarkably complex. For example, coexpression with p75 sensitizes TrkA for NGF and desensitizes it for NT3 (Benedetti et al. 1993; Verdi et al. 1994). Interestingly, the effect of p75 on TrkB appears to be variable and dependent on the cellular system (Bibel et al. 1998; Vesa et al. 2000). The autophosphorylation of TrkC in response to NT3 was reported to be not changed by coexpression with p75 (Vesa et al. 2000). These results clearly indicate that p75 interacts differently with the three types of Trk receptors and that results obtained with one type of Trk receptor should not be extrapolated to the others.

Trk and p75 receptors are coexpressed in embryonic primary sensory and sympathetic neurons, and mixed Trk/p75 complexes are the most likely explanation for the so-called high-affinity binding sites observed on these cells (reviewed in Dechant et al. 1994). These

cells are the classical targets for the anti-apoptotic function of the neurotrophins in the developing PNS and represent the most thoroughly investigated paradigm of neurotrophin receptors on primary neurons. For these cells, a correlation could be established between the presence of high-affinity binding sites and neurotrophin responsiveness. Binding data of neurotrophins to primary CNS neurons are sparse, but it is interesting to note that high-affinity binding sites for BDNF and NT3 could not be detected on cerebellar granular neurons expressing high levels of TrkB and TrkC but small amounts of p75 (Lindholm et al. 1993). Neuronal high-affinity receptors might be an adaptive and transient specialization of embryonic long projection neurons at a stage when they are in competition with their neighbours for trophic support. In mature and central neurons, neurotrophins regulate events occurring on a much faster time scale (Kafitz et al. 1999), and binding sites with lower affinity but faster kinetics might then be of advantage.

Interactions between neurotrophin receptor complexes

The different receptor types, sending distinct and sometimes opposing biological signals, make the neurotrophin signalling machinery a challenging model case to study. A likely scenario is that multiple components in this network are connected by biochemical equilibria, e.g. between pools of monomeric and multimeric receptors and between unoccupied and liganded receptors.

For the Trk receptors, ligand-dependent dimerization is the dominant, but not necessarily exclusive, means of activation since autoactivation in the absence of ligand is observed with cell lines. Much less evident is the role of ligand interactions for the activation of p75. Stimulation of cell death through p75 receptors has been reported in vitro both in the absence and presence of ligand, whereas ligand-induced cell death prevails in vivo (for a discussion, see Dechant and Barde 1997; Bibel and Barde 2000). Since p75 interacts physically with all three Trk receptors, it is conceivable that TrkA, TrkB and TrkC receptor complexes cross-talk to each other through p75, providing a physical link between them. An additional level of complexity is added by the ligand promiscuity of both p75 and Trk receptors. What, for example, is the impact of the presence or absence of p75 on the interaction of TrkA and TrkB with their non-preferred ligand NT3? While, at first glance, this might seem an academic question, it appears to be of physiological significance in vivo (see below). In cell culture models, the interplay between p75 and Trk receptors is different depending on which ligand is bound to p75. Saturation of p75 with BDNF reduces TrkA signalling on PC12 cells and kills sympathetic neurons (MacPhee and Barker 1997; Bamji et al. 1998), whereas p75/NGF interactions augment TrkA signalling and neuronal survival (Davies et al. 1993; Verdi et al. 1994; Barker and Shooter 1994). However, it must be clearly stated that interactions between p75 and Trk are not restricted to physical association of the proteins. Cross-talk of their downstream signalling mechanisms is now amply documented. Of particular relevance are antagonistic interactions between p75 and Trk signalling cascades for the regulation of apoptosis (reviewed in Majdan and Miller 1999).

For a genetic analysis of the cross-talk occurring between neurotrophin receptors, the mice lacking the full-length form of p75 proved to be extremely useful (Lee et al. 1992). In these mice, cell numbers are increased in neuronal structures both during development and in lesion paradigms by interference with two different p75-dependent mechanisms. Consistent with the role of p75 as a death receptor, cells survive in the p75 mutant mice which are actively killed by p75 in wild-type mice (Frade and Barde 1999). Along the same line, a recent report provides genetic evidence for the activation of caspase-3 through p75 in trigeminal neurons (Agerman et al. 2000). However, an increase in the number of neurons in mice lacking full-length p75 can also result from a completely different mechanism. Consistent with in vitro and in vivo results which have demonstrated that p75 impairs NT3 signalling through TrkA, the functional interactions of NT3 with TrkA are facilitated in the absence of full-length p75. This allows NT3 to substitute more efficiently for a missing NGF allele in p75 mutant mice compared with wild-type animals (Brennan et al. 1999).

Alternative splicing of neurotrophin receptors

All four neurotrophin receptor genes are expressed in multiple naturally occurring protein isoforms which are generated by alternative splicing of their primary gene transcripts (Fig. 3a).

Extracellular Trk receptor isoforms

Splicing of a small exon occurs in the extracellular domain of TrkA (Barker et al. 1993; Clary and Reichardt 1994) and TrkB (Strohmaier et al. 1996; Garner et al. 1996). Both the TrkA and the TrkB isoforms have altered ligand interactions compared with the full-length receptors. The TrkB splice variant binds BDNF with similar affinity to that of its wild-type counterpart, but has reduced affinities for NT4/5 and NT3. It is present in chick and man (Hackett et al. 1998), but could not be detected in rodents so far. In the chick, the two TrkB isoforms are differentially expressed in neuronal subpopulations (Boeshore et al. 1999). The corresponding TrkA variants differ in their interaction with the non-preferred ligand NT3 (Clary and Reichardt 1994). This effect is observed in PC12 cells but not in fibroblasts, and the difference may lie in the presence or absence of p75. The sterical mechanism for the changes in ligand affinity and

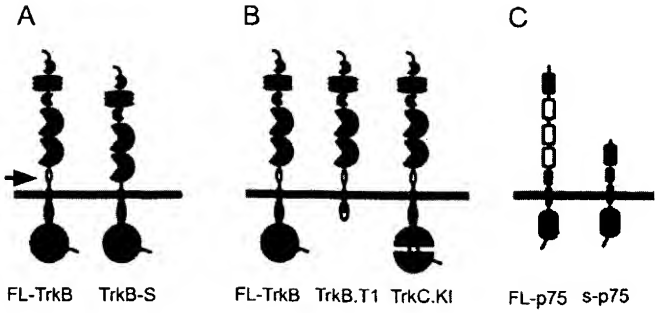

Fig. 3A–C Alternative splicing of Trk and p75 receptors. **A** Alternative splicing has been described for all Trk receptors. TrkA and TrkB transcripts are alternatively spliced at a small exon in their extracellular domain. The corresponding protein isoforms depicted here, full-length TrkB (*FL-TrkB*) and short TrkB (*TrkB-S*), differ in the absence or presence of a short peptide stretch (*arrow*) and in their interactions with non-preferred ligands. **B** Alternative splicing of exons coding for intracellular protein domains occurs at TrkB and TrkC transcripts. TrkB.T1 is an example of a protein isoform with a truncated tyrosine kinase domain. Such isoforms have been described for both TrkB and TrkC. In addition, TrkC isoforms exist such as TrKC.KI, which have peptide insertions in their tyrosine kinase domain. **C** Recently we have detected a protein isoform of p75 (s-p75) which lacks cysteine-rich domains 2, 3 and 4 due to alternative splicing of exon III of the full-length receptor (FL-p75)

specificity in these TrkA and TrkB variants remains to be established. The spliced exons encode short peptide stretches downstream of the second IgG domain, which forms the main binding pocket in all Trk receptors. Biochemical data suggest that this region of the wild-type TrkB receptor is functional in ligand binding (Haniu et al. 1997). Other TrkB variants with deletions in the leucine-rich domains completely lack ligand binding and signalling capacities (Ninkina et al. 1997).

Intracellular Trk receptor isoforms

Receptor isoforms have been described for TrkB and TrkC receptors with truncations or insertions in the tyrosine kinase domains (Klein et al. 1990; Lamballe et al. 1993) (Fig. 3b). Some of the corresponding transcripts are regulated in a very dynamic pattern and independently of the regular tyrosine kinase isoforms. TrkC receptors, which contain peptide insertions in the tyrosine kinase domain, are phosphorylated in response to their ligands, but are restricted in their signalling potential (see, for example, Garner and Large 1994). The truncated TrkB isoforms can act as dominant negative inhibitors of the TrkB tyrosine kinase if both isoforms are expressed in *cis* on the same cell (Ninkina et al. 1996; Eide et al. 1996). The same isoforms can also function as scavenger receptors in *trans*: they sequester BDNF and remove it from the extracellular space via internalization (Biffo et al. 1995; Alderson et al. 2000). Consequently, activation of the full-length TrkB tyrosine kinase is restricted both temporally and spatially. The interplay between the full-length and truncated variants of TrkB can be very intricate. The two forms regulate the dendritic growth of cortical neurons differentially. Expression of full-length TrkB in slice cultures favours growth of proximal dendrites, whereas the truncated variant promotes elongation of distal neurites (Yacoubian and Lo 2000). Recent studies strongly indicate that truncated Trk receptor isoforms have intrinsic signalling capacity. Expression of the truncated TrkB.T1 receptor triggers BDNF-mediated signalling in the absence of the full-length form, as detected by the acidification of medium (Baxter et al. 1997). Moreover, overexpression of the same variant leads to detectable morphological changes in a cell line (Haapasalo et al. 1999). A truncated form of TrkC promotes neuronal differentiation of neural crest cells, but only in the presence of p75 (Hapner et al. 1998).

Alternative splicing of the p75 gene

We have recently found that the p75 gene is also expressed in two isoforms (Dechant and Barde 1997). Alternative splicing of exon III occurs in human, mouse, rat and chick. The alternative transcript contains an open reading frame, which is translated into a novel, naturally occurring isoform of p75, which we have dubbed short-p75 (s-p75) (Fig. 3c). The spliced exon III encodes the cysteine-rich domains 2, 3 and 4 of the full-length protein, which are essential for the binding of neurotrophins. Consequently, s-p75 does not bind any of the neurotrophins with detectable affinity. The physiological role of s-p75 remains to be defined. Since the full-length receptor and s-p75 share an identical intracellular domain, it seems likely that s-p75 binds at least some of the intracellular interactors of full-length p75. s-p75 retains the capacity of FL-p75 to interact with Trk receptors (M. Bibel, unpublished observation). Therefore, s-p75 may act as a naturally occurring modulator of FL-p75, with which it is coexpressed in many tissues (our unpublished results). As mentioned above, the relationship between ligand binding and activation of signalling is not unambiguously defined for full-length p75. A ligand-independent activity of s-p75 is therefore also conceivable. The s-p75 transcript and protein are expressed from the available mutated p75 allele, in which the alternatively spliced exon III has been targeted (Lee et al. 1992). We are currently investigating a novel complete p75 knockout with a targeted exon IV (von Schack, Casademunt and Dechant, unpublished results).

Interactions of neurotrophin receptors with their local environment

The signalling of neurotrophin receptors is modified by dynamic cellular processes such as changes in the lipid environment, internalization into intracellular compartments, degradation and retrograde transport (Fig. 4).

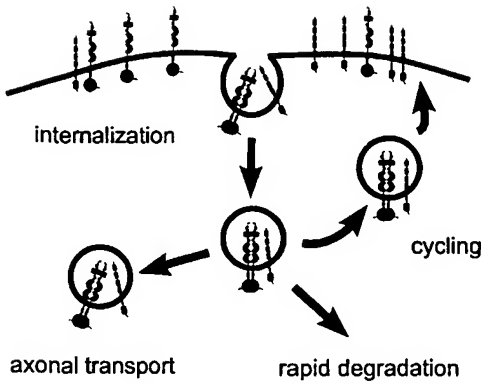

Fig. 4 Neurotrophin receptor internalization. Neurotrophins and their receptor are taken up via clathrin-dependent mechanisms into small vesicles of poorly defined origin, which are sometimes referred to as early endosomes. Endocytosed Trk receptors can be actively signalling inside the cell. Vesicular receptors have different fates. They can be recycled to the surface or undergo rapid degradation, most likely in proteasomes. Alternatively, they can be transferred via retrograde transport to the cell soma. Retrogradely transported neurotrophin signals are required for embryonic neuronal survival. Receptors and ligands are finally degraded in a lysosomal compartment in the cell soma of neurons

Trk receptor subcellular distribution

Neurotrophins predominantly act on nerve cells with their highly specialized and polarized shape. Hence the subcellular distribution of their receptors in synapses, dendrites and axons is potentially functionally relevant. However, evidence for highly localized expression was so far obtained only for TrkB in postsynaptic structures on muscle fibres (Gonzalez et al. 1999). In the hippocampus, TrkB is present in preparations of postsynaptic densities (Wu et al. 1994), but in overexpression experiments it appears to be only weakly enriched in this structure (Kryl et al. 1999). Overexpressed TrkC and TrkB are uniformly distributed in hippocampal neurons and cortical slice cultures (Kryl et al. 1999) and p75 is also not differentially sorted in hippocampal neurons (Jareb and Banker 1998). Interestingly, in overexpressing fibroblasts TrkB is colocalized with cadherin in sites of cell-cell contacts (Zhou et al. 1997).

Caveolae and caveolae-related domains

Dimerization and signalling of neurotrophin receptors are influenced by the lipid composition in the local membrane environment. Caveolae and caveolae-related domains (CRD) may represent hot spots of p75-Trk interactions (reviewed in Dobrowsky 2000a). p75 as well as Trk receptors and many of their downstream signalling targets have been detected in CRDs of fibroblasts, PC12 cells and neurons (Bilderback et al. 1997; Wu et al. 1997; Huang et al. 1999). Of particular interest in this context is ceramide, the product of sphingomyelin hydrolysis which is specifically produced in caveolae. Ceramide is involved in cellular responses to stress and participates in p55 TNF-receptor and fas signalling. p75 stimulates ceramide production in caveolae or CRD (Dobrowsky et al. 1994; Bilderback et al. 1997), while TrkA receptor signalling abolishes p75-dependent ceramide production (Dobrowsky et al. 1995). Caveolin-1 or caveolin-like proteins provide a potential link between these observations. Caveolin-1 binds directly to both p75 and TrkA, but with different domains (Bilderback et al. 1997, 1999). Overexpression of caveolin-1 in PC12 cells decreases TrkA signalling and neuritic growth in response to NGF and inhibits TrkA phosphorylation in vitro, whereas p75-mediated sphingomyelin hydrolysis is stimulated (Bilderback et al. 1999). Level and duration of TrkA phosphorylation in PC12 cells are influenced by ceramide in a biphasic manner. Signalling of NGF through TrkA is initially reduced in the presence of ceramide, whereas at later time points it is stimulated. The short-term inhibitory effect of ceramide appears to result from the activation of a serine threonine kinase that modifies TrkA (MacPhee and Barker 1997). In contrast, long-term ceramide treatment promotes the formation of TrkA homodimers and their autoactivation, even in the absence of NGF (MacPhee and Barker 1999).

Neurotrophin receptor internalization

Internalization of neurotrophin receptors into an intracellular compartment of small vesicles occurs via clathrin-dependent mechanisms (Grimes et al. 1997). TrkA strongly and rapidly stimulates its own internalization and the formation of clathrin-coated pits in PC12 cells (Beattie et al. 2000).

The vesicular organelles, into which the receptors are internalized, are not fully defined at present, but they may be of critical importance for neurotrophin signalling, especially in neurons. From this compartment the receptors can take different routes leading to reappearance on the surface, degradation or retrograde transport (Fig. 4).

The responsiveness of cells to neurotrophins is determined by the ligand-accessible receptors on their surface. These receptors can be either newly synthesized or recycled from an intracellular pool of receptors in submembranous vesicles (Eveleth and Bradshaw 1988).

The recruitment of stored intracellular receptor is regulated by membrane depolarization in CNS neurons (Meyer-Franke et al. 1998) and the cell cycle in PC12 cells (Urdiales et al. 1998). Whether a Trk receptor is localized on the surface or in vesicles determines not only its accessibility for ligand but also for intracellular proteins. Internalized and surface receptors are exposed to microenvironments which differ in their composition of lipids and signalling proteins. This provides an explanation for the finding that TrkA, depending on its rate of internalization, preferentially generates survival-promoting or neuritogenic signals (Zhang et al. 2000; Watson et al. 1999). Work performed with an NGF antibody complex, which interacts with TrkA but not p75, suggests a role of p75 in Trk receptor internalization (Saragovi et

al. 1998). The NGF complex is taken up more efficiently and faster compared to NGF alone (Saragovi et al. 1998). This is accompanied by reduced MAPK activation and neuronal differentiation. Hence, complexation with p75 might modulate TrkA internalization and thereby change its signalling spectrum (Gargano et al. 1997).

Some neurons rapidly desensitize for BDNF through a loss of surface-exposed TrkB (Carter et al. 1995). Interestingly, desensitization was not observed for NGF in this study. Activated and internalized TrkB, but not TrkA, receptors undergo rapid degradation in cerebellar granular neurons, which can be blocked by proteasome inhibitors. In domain-swapping experiments, the difference between the two receptors was mapped to the iuxtamembrane domain, since this region of the TrkB receptor conferred NGF-dependent downregulation to TrkA expressed in a neuronal cell line (Sommerfeld et al. 2000). The cellular mechanisms by which TrkB is targeted for degradation remain to be elucidated.

Retrograde transport

Another highly specialized neuronal mechanism which influences both temporal and spatial activity of neurotrophin signalling is retrograde transport. This mechanism separates local neurotrophin effects, for example, on the neuronal cytoskeleton, from effects on neuronal survival and gene expression. Hence it is especially important for neurons projecting over long distances (recently reviewed by Reynolds et al. 2000). All neurotrophins are retrogradely transported by receptor-dependent mechanisms. The composition of the retrogradely transported complexes appears to be different in a cell-type and neurotrophin-dependent manner. Evidence has been provided that both p75 and the Trk receptors can mediate retrograde transport alone and in combination (Curtis et al. 1995, 1998). Retrogradely transported complexes can be actively signalling and can contain phosphorylated Trk receptors together with neurotrophins (Ehlers et al. 1995; Riccio et al. 1997; Grimes et al. 1997; Bhattacharyya et al. 1997). The biochemical and signalling properties of the complexes, their sorting mechanisms, the precise origin of the retrogradely transported vesicle and the mechanisms by which they are linked to the retrograde transport machinery have been the subject of recent investigations (Johanson et al. 1995; Senger and Campenot 1997; Tsui-Pierchala and Ginty 1999). These processes, which occur in neurons at a considerable distance from the cell body, are rate-limiting determinants of the retrograde delivery of neurotrophic signals to the cell body and hence are crucial for life and death decisions of nerve cells (Ure and Campenot 1997).

Summary

The biochemical interactions of neurotrophins with their receptors are complex. This complexity is generated with only four receptor genes by binding of ligands to multiple receptors, the formation of complexes between receptor proteins, alternative splicing and interactions between receptor and their local membrane environment. These mechanisms determine ligand affinity, ligand specificity and subsequently intracellular signalling. The molecular and biochemical properties of the neurotrophin receptors on responsive cells are subject to precise developmental and cell-type specific regulation. These receptor modifications endow embryonic and adult neurons with the capacity to determine intrinsically when, how fast and at what concentration they respond to neurotrophins. Hence, cellular responses to neurotrophins, which can be as different as death or survival, are not exclusively generated by differences in the expression pattern of the receptors or their downstream signalling proteins. It appears that they are also profoundly influenced by rather subtle shifts in highly balanced biochemical equilibria. In the future, novel tools, which selectively interfere with the functions of the two types of neurotrophin receptors, will help further to dissect this intricate network of protein interactions. Promising results have been obtained not only with antibodies (Weskamp and Reichardt 1991; LeSauteur et al. 1996), but also with small molecular weight compounds (Jaen et al. 1995; Niederhauser et al. 2000) and peptides (Longo et al. 1997; Beglova et al. 2000).

Acknowledgements I thank H. Thoenen for critical reading of the manuscript and M. Ashdown for linguistic revision.

References

Agerman K, Baudet C, Fundin B, Willson C, Ernfors P (2000) Attenuation of a caspase-3 dependent cell death in NT4- and p75-deficient embryonic sensory neurons. Mol Cell Neurosci 16:258–268

Alderson RF, Curtis R, Alterman AL, Lindsay RM, Distefano PS (2000) Truncated TrkB mediates the endocytosis and release of BDNF and neurotrophin-4/5 by rat astrocytes and Schwann cells in vitro. Brain Res 871:210–222

Allsopp TE, Robinson M, Wyatt S, Davies AM (1993) Ectopic *trkA* expression mediates a NGF survival response in NGF-independent sensory neurons but not in parasympathetic neurons. J Cell Biol 123:1555–1566

Bamji SX, Majdan M, Pozniak CD, Belliveau DJ, Aloyz R, Kohn J, Causing CG, Miller FD (1998) The p75 neurotrophin receptor mediates neuronal apoptosis and is essential for naturally occurring sympathetic neuron death. J Cell Biol 140:911–923

Barker PA, Shooter EM (1994) Disruption of NGF binding to the low affinity neurotrophin receptor $p75^{LNTR}$ reduces NGF binding to TrkA on PC12 cells. Neuron 13:203–215

Barker PA, Lomen-Hoerth C, Gensch EM, Meakin SO, Glass DJ, Shooter EM (1993) Tissue-specific alternative splicing generates two isoforms of the *trkA* receptor. J Biol Chem 268: 15150–15157

Baxter GT, Radeke MJ, Kuo RC, Makrides V, Hinkle B, Hoang R, Medina-Selby-A, Coit D, Valenzuela P, Feinstein SC (1997) Signal transduction mediated by the truncated trkB receptor isoform trkB.T1 and trkB.T2. J Neurosci 17:2683–2690

Beattie EC, Howe CL, Wilde A, Brodsky FM, Mobley WC (2000) NGF signals through TrkA to increase clathrin at the plasma membrane and enhance clathrin-mediated membrane trafficking. J Neurosci 20:7325–7333

Beglova N, Maliartchouk S, Ekiel I, Zaccaro MC, Saragovi HU, Gehring K (2000) Design and solution structure of functional peptide mimetics of nerve growth factor. J Med Chem 43: 3530–3540

Benedetti M, Levi A, Chao MV (1993) Differential expression of nerve growth factor receptors leads to altered binding affinity and neurotrophin responsiveness. Proc Natl Acad Sci USA 90:7859–7863

Bhattacharyya A, Watson FL, Bradlee TA, Pomeroy SL, Stiles CD, Segal RA (1997) Trk receptors function as rapid retrograde signal carriers in the adult nervous system. J Neurosci 17:7007–7016

Bibel M, Barde Y-A (2000) Neurotrophins: key regulators of cell fate and cell shape in the vertebrate nervous system. Gen Dev 14:2919–2937

Bibel M, Hoppe E, Barde YA (1998) Biochemical and functional interactions between the neurotrophin receptors *trk* and p75^{NTR}. EMBO J 18:616–622

Biffo S, Offenhäuser N, Carter BD, Barde Y-A (1995) Selective binding and internalisation by truncated receptors restrict the availability of BDNF during development. Development 121:2461–2470

Bilderback TR, Grigsby RJ, Dobrowsky RT (1997) Association of p75^{NTR} with caveolin and localization of neurotrophin-induced sphingomyelin hydrolysis to caveolae. J Biol Chem 272: 10922–10927

Bilderback TR, Gazula VR, Lisanti MP, Dobrowsky RT (1999) Caveolin interacts with Trk A and p75(NTR) and regulates neurotrophin signaling pathways. J Biol Chem 274:257–263

Boeshore KL, Luckey CN, Zigmond RE, Large TH (1999) TrkB isoforms with distinct neurotrophin specificities are expressed in predominantly nonoverlapping populations of avian dorsal root ganglion neurons. J Neurosci 19:4739–4747

Bonni A, Greenberg ME (1997) Neurotrophin regulation of gene expression. Can J Neurol Sci 24:272–283

Bothwell M (1995) Functional interactions of neurotrophins and neurotrophin receptors. Annu Rev Neurosci 18:223–253

Brennan C, Rivas-Plata K, Landis SC (1999) The p75 neurotrophin receptor influences NT-3 responsiveness of sympathetic neurons in vivo. Nat Neurosci 2:699–705

Carter BD, Zirrgiebel U, Barde Y-A (1995) Differential regulation of p21^{ras} activation in neurons by nerve growth factor and brain-derived neurotrophic factor. J Biol Chem 270:21751–21757

Carter BD, Dechant G, Frade JM, Kaltschmidt C, Barde Y-A (1996a) Neurotrophins and their p75 receptor. Cold Spring Harb Symp Quant Biol 61:407–415

Carter BD, Kaltschmidt C, Kaltschmidt B, Offenhäuser N, Böhm-Matthaei R, Baeuerle PA, Barde YA (1996b) Selective activation of NF-kappaB by nerve growth factor through the neurotrophin receptor p75. Science 272:542–545

Chao MV (2000) Trophic factors: an evolutionary cul-de-sac or door into higher neuronal function? J Neurosci Res 59:353–355

Clary DO, Reichardt LF (1994) An alternatively spliced form of the nerve growth factor receptor TrkA confers an enhanced response to neurotrophin 3. Proc Natl Acad Sci USA 91:11133–11137

Curtis R, Adryan KM, Stark JL, Park JS, Compton DL, Weskamp G, Huber LJ, Chao MV, Jaenisch R, Lee KF (1995) Differential role of the low affinity neurotrophin receptor (p75) in retrograde axonal transport of the neurotrophins. Neuron 14: 1201–1211

Curtis R, Tonra JR, Stark JL, Adryan KM, Park JS, Cliffer KD, Lindsay RM, Distefano PS (1998) Neuronal injury increases retrograde axonal transport of the neurotrophins to spinal sensory neurons and motor neurons via multiple receptor mechanisms. Mol Cell Neurosci 12:105–118

Davies AM, Lee K-F, Jaenisch R (1993) p75-deficient trigeminal sensory neurons have an altered response to NGF but not to other neurotrophins. Neuron 11:565–574

Dechant G, Barde Y-A (1997) Signalling through the neurotrophin receptor p75^{NTR}. Curr Opin Neurobiol 7:413–418

Dechant G, Biffo S, Okazawa H, Kolbeck R, Pottgiesser J, Barde Y-A (1993) Expression and binding characteristics of the BDNF receptor chick trkB. Development 119:545–558

Dechant G, Rodríguez-Tébar A, Barde Y-A (1994) Neurotrophin receptors. Prog Neurobiol 42:347–352

Dechant G, Tsoulfas P, Parada LF, Barde Y-A (1997) The neurotrophin receptor p75 binds neurotrophin-3 on sympathetic neurons with high affinity and specificity. J Neurosci 17:5281–5287

Dobrowsky RT (2000a) Sphingolipid signalling domains floating on rafts or buried in caves? Cell Signal 12:81–90

Dobrowsky RT, Carter BD (2000b) p75 neurotrophin receptor signaling: mechanisms for neurotrophic modulation of cell stress? J Neurosci Res 61:237–243

Dobrowsky RT, Werner MH, Castellino AM, Chao MV, Hannun YA (1994) Activation of the sphingomyelin cycle through the low-affinity neurotrophin receptor. Science 265:1596–1599

Dobrowsky RT, Jenkins GM, Hannun YA (1995) Neurotrophins induce sphingomyelin hydrolysis – modulation by co-expression of p75^{NTR} with Trk receptors. J Biol Chem 270:22135–22142

Ehlers MD, Kaplan DR, Price DL, Koliatsos VE (1995) NGF-stimulated retrograde transport of trkA in the mammalian nervous system. J Cell Biol 130:145–156

Eide FF, Vining ER, Eide BL, Zang KL, Wang XY, Reichardt LF (1996) Naturally occurring truncated trkB receptors have dominant inhibitory effects on brain-derived neurotrophic factor signaling. J Neurosci 16:3123–3129

Eveleth DD, Bradshaw RA (1988) Internalization and cycling of nerve growth factor in PC12 cells: interconversion of type II (fast) and type I (slow) nerve growth factor receptors. Neuron 1:929–936

Frade JM, Barde YA (1999) Genetic evidence for cell death mediated by nerve growth factor and the neurotrophin receptor p75 in the developing mouse retina and spinal cord. Development 126:683–690

Friedman WJ, Greene LA (1999) Neurotrophin signaling via Trks and p75. Exp Cell Res 253:131–142

Gargano N, Levi A, Alema S (1997) Modulation of nerve growth factor internalization by direct interaction between p75 and TrkA receptors. J Neurosci Res 50:1–12

Garner AS, Large TH (1994) Isoforms of the avian TrkC receptor: a novel kinase insertion dissociates transformation and process outgrowth from survival. Neuron 13:457–472

Garner AS, Menegay HJ, Boeshore KL, Xie XY, Voci JM, Johnson JE, Large TH (1996) Expression of TrkB receptor isoforms in the developing avian visual system. J Neurosci 16: 1740–1752

Gonzalez M, Ruggiero FP, Chang Q, Shi YJ, Rich MM, Kraner S, Balice-Gordon RJ (1999) Disruption of TrkB-mediated signaling induces disassembly of postsynaptic receptor clusters at neuromuscular junctions. Neuron 24:567–583

Grimes ML, Beattie E, Mobley WC (1997) A signaling organelle containing the nerve growth factor-activated receptor tyrosine kinase, TrkA. Proc Natl Acad Sci USA 94:9909–9914

Grob PM, Ross AH, Koprowski H, Bothwell M (1985) Characterization of the human melanoma nerve growth factor receptor. J Biol Chem 260:8044–8049

Haapasalo A, Saarelainen T, Moshnyakov M, Arumäe U, Kiema T-R, Saarma M, Wong G, Castren E (1999) Expression of the naturally occurring truncated trkB neurotrophin receptor induces outgrowth of filopodia. Oncogene 18:1296

Hackett SF, Friedman Z, Freund J, Schoenfeld C, Curtis R, DiStefano PS, Campochiaro PA (1998) A splice variant of trkB and brain-derived neurotrophic factor are co-expressed in retinal pigmented epithelial cells and promote differentiated characteristics. Brain Res 789:201–212

Haniu M, Montestruque S, Bures EJ, Talvenheimo J, Toso R, Lewis-Sandy S, Welcher AA, Rohde MF (1997) Interactions between brain-derived neurotrophic factor and the TRKB receptor. J Biol Chem 272:25296–25303

Hapner SJ, Boeshore KL, Large TH, Lefcort F (1998) Neural differentiation promoted by truncated trkC receptors in collaboration with p75^{NTR}. Dev Biol 201:90–100

Hempstead BL, Rabin SJ, Kaplan L, Reid S, Parada LF, Kaplan DR (1992) Overexpression of the trk tyrosine kinase rapidly accelerates nerve growth factor-induced differentiation. Neuron 9:883–896

Huang C, Zhou J, Feng AK, Lynch CC, Klumperman J, DeArmond SJ, Mobley WC (1999) Nerve growth factor signaling in caveolae-like domains at the plasma membrane. J Biol Chem 274:36707–36714

Huber LJ, Chao MV (1995) A potential interaction of p75 and *trkA* NGF receptors revealed by affinity crosslinking and immunoprecipitation. J Neurosci Res 40:557–563

Jaen JC, Laborde E, Bucsh RA, Caprathe BW, Sorenson RJ, Fergus J, Spiegel K, Marks J, Dickerson MR, Davis RE (1995) Kynurenic acid derivatives inhibit the binding of nerve growth factor (NGF) to the low-affinity p75 NGF receptor. J Med Chem 38:4439–4445

Jareb M, Banker G (1998) The polarized sorting of membrane proteins expressed in cultured hippocampal neurons using viral vectors. Neuron 20:855–867

Jing S, Tapley P, Barbacid M (1992) Nerve growth factor mediates signal transduction through trk homodimer receptors. Neuron 9:1067–1079

Johanson S, Crouch M, Hendry I (1995) Retrograde transport of signal transduction proteins in rat sciatic nerve. Brain Res 690:55–63

Kafitz KW, Rose CR, Thoenen H, Konnerth A (1999) Neurotrophin-evoked rapid excitation through TrkB receptors. Nature 401:918–921

Kaplan DR, Miller FD (2000) Neurotrophin signal transduction in the nervous system. Curr Opin Neurobiol 10:381–391

Kim JY, Sutton ME, Lu DJ, Cho TA, Goumnerova LC, Goritchenko L, Kaufman JR, Lam KK, Billet AL, Tarbell NJ, Wu J, Allen JC, Stiles CD, Segal RA, Pomeroy SL (1999) Activation of neurotrophin-3 receptor TrkC induces apoptosis in medulloblastomas. Cancer Res 59:711–719

Klein R, Conway D, Parada LF, Barbacid M (1990) The trkB tyrosine protein kinase gene codes for a second neurogenic receptor that lacks the catalytic kinase domain. Cell 61:647–656

Klein R, Jing S, Nanduri V, O'Rourke E, Barbacid M (1991) The *trk* proto-oncogene encodes a receptor for nerve growth factor. Cell 65:189–197

Knüsel B, Rabin SJ, Hefti F, Kaplan DR (1994) Regulated neurotrophin receptor responsiveness during neuronal migration and early differentiation. J Neurosci 14:1542–1554

Kryl D, Yacoubian T, Haapasalo A, Castren E, Lo D, Barker PA (1999) Subcellular localization of full-length and truncated Trk receptor isoforms in polarized neurons and epithelial cells. J Neurosci 19:5823–5833

Lamballe F, Klein R, Barbacid M (1991) *trk*C, a new member of the *trk* family of tyrosine protein kinases, is a receptor for neurotrophin-3. Cell 66:967–979

Lamballe F, Tapley P, Barbacid M (1993) *trk*C encodes multiple neurotrophin-3 receptors with distinct biological properties and substrate specificities. EMBO J 12:3083–3094

Lee K-F, Li E, Huber LJ, Landis SC, Sharpe AH, Chao MV, Jaenisch R (1992) Targeted mutation of the gene encoding the low affinity NGF receptor p75 leads to deficits in the peripheral sensory nervous system. Cell 69:737–749

LeSauteur L, Maliartchouk S, Le Jeune H, Quirion R, Saragovi HU (1996) Potent human p140-TrkA agonists derived from an anti-receptor monoclonal antibody. J Neurosci 16:1308–1316

Lindholm D, Dechant G, Heisenberg C-P, Thoenen H (1993) Brain-derived neurotrophic factor is a survival factor for cultured rat cerebellar granule neurons and protects them against glutamate-induced neurotoxicity. Eur J Neurosci 5:1455–1464

Longo FM, Manthorpe M, Xie YM, Varon S (1997) Synthetic NGF peptide derivatives prevent neuronal death via a p75 receptor-dependent mechanism. J Neurosci Res 48:1–17

MacPhee IJ, Barker PA (1997) Brain-derived neurotrophic factor binding to the p75 neurotrophin receptor reduces TrkA signaling while increasing serine phosphorylation in the TrkA intracellular domain. J Biol Chem 272:23547–23551

MacPhee I, Barker PA (1999) Extended ceramide exposure activates the trkA receptor by increasing receptor homodimer formation. J Neurochem 72:1423–1430

Majdan M, Miller FD (1999) Neuronal life and death decisions: functional antagonism between the Trk and p75 neurotrophin receptors. Int J Dev Neurosci 17:153–161

McAllister AK, Katz LC, Lo DC (1999) Neurotrophins and synaptic plasticity. Ann Rev Neurosci 22:295–318

Meakin SO, Shooter EM (1991) Molecular investigations on the high-affinity nerve growth factor receptor. Neuron 6:153–163

Meyer-Franke A, Wilkinson GA, Kruttgen A, Hu M, Munro E, Hanson MG Jr, Reichardt LF, Barres BA (1998) Depolarization and cAMP elevation rapidly recruit TrkB to the plasma membrane of CNS neurons. Neuron 21:681–693

Niederhauser O, Mangold M, Schubenel R, Kusznir EA, Schmidt D, Hertel C (2000) NGF ligand alters NGF signaling via $p75^{NTR}$ and TrkA. J Neurosci Res 61:263–272

Ninkina N, Adu J, Fischer A, Pinon LGP, Buchman VL, Davies AM (1996) Expression and function of TrkB variants in developing sensory neurons. EMBO J 15:6385–6393

Ninkina N, Grashchuck M, Buchman VL, Davies AM (1997) TrkB variants with deletions in the leucine-rich motifs of the extracellular domain. J Biol Chem 272:13019–13025

Reynolds AJ, Bartlett SE, Hendry IA (2000) Molecular mechanisms regulating the retrograde axonal transport of neurotrophins. Brain Res Brain Res Rev 33:169–178

Riccio A, Pierchala BA, Ciarallo CL, Ginty DD (1997) An NGF-TrkA-mediated retrograde signal to transcription factor CREB in sympathetic neurons. Science 277:1097–1100

Ross GM, Shamovsky IL, Lawrance G, Solc M, Dostaler SM, Weaver DF, Riopelle RJ (1998) Reciprocal modulation of TrkA and $p75^{NTR}$ affinity states is mediated by direct receptor interactions. Eur J Neurosci 10:890–898

Saragovi HU, Zheng W, Maliartchouk S, DiGugliemo GM, Mawal YR, Kamen A, Woo SB, Cuello AC, Debeir T, Neet KE (1998) A TrkA-selective, fast internalizing nerve growth factor-antibody complex induces trophic but not neuritogenic signals. J Biol Chem 273:34933–34940

Senger DL, Campenot RB (1997) Rapid retrograde tyrosine phosphorylation of trkA and other proteins in rat sympathetic neurons in compartmented cultures. J Cell Biol 138:411–421

Sommerfeld MT, Schweigreiter R, Barde YA, Hoppe E (2000) Down-regulation of the neurotrophin receptor TrkB following ligand binding. Evidence for an involvement of the proteasome and differential regulation of TrkA and TrkB. J Biol Chem 275:8982–8990

Sqinto SP, Stitt TN, Aldrich TH, Davis S, Bianco SM, Radziejewski C, Glass DJ, Masiakowski P, Furth ME, Valenzuela DM, Distefano PS, Yancopoulos GD (1991) trkB encodes a functional receptor for brain-derived neurotrophic factor and neurotrophin-3 but not NGF. Cell 65:1–20

Strohmaier C, Carter BD, Urfer R, Barde YA, Dechant G (1996) A splice variant of the neurotrophin receptor trkB with increased specificity for brain-derived neurotrophic factor. EMBO J 15: 3332–3337

Thoenen H (1995) Neurotrophins and neuronal plasticity. Science 270:593–598

Tsui-Pierchala BA, Ginty DD (1999) Characterization of an NGF-P-TrkA retrograde-signaling complex and age-dependent regulation of TrkA phosphorylation in sympathetic neurons. J Neurosci 19:8207–8218

Tucker KL, Meyer M, Barde Y-A (2001) Neurotrophins are required for nerve growth during development. Nat Neurosci 4:29–37

Ultsch MH, Wiesmann C, Simmons LC, Henrich J, Yang M, Reilly D, Bass SH, De Vos AM (1999) Crystal structures of the neurotrophin-binding domain of TrkA, TrkB and TrkC. J Mol Biol 290:149–159

Urdiales JL, Becker E, Andrieu M, Thomas A, Jullien J, van Grunsven LA, Menut S, Evan GI, Martin-Zanca D, Rudkin BB (1998) Cell cycle phase-specific surface expression of nerve growth factor receptors TrkA and $p75^{NTR}$. J Neurosci 18:6767–6775

Ure DR, Campenot RB (1997) Retrograde transport and steady-state distribution of ^{125}I-nerve growth factor in rat sympathetic neurons in compartmented cultures. J Neurosci 17:1282–1290

Venkatakrishnan G, McKinnon C, Pilapil CG, Wolf DE, Ross AH (1991) Nerve growth factor receptors are preaggregated and immobile on responsive cells. Biochemistry 30:2748–2753

Verdi JM, Birren SJ, Ibáñez CF, Persson H, Kaplan DR, Benedetti M, Chao MV, Anderson DJ (1994) p75^{LNGFR} regulates Trk signal transduction and NGF-induced neuronal differentiation in MAH cells. Neuron 12:733–745

Vesa J, Krüttgen A, Shooter EM (2000) p75 reduces TrkB tyrosine autophosphorylation in response to brain-derived neurotrophic factor and neurotrophin 4/5. J Biol Chem 275:24414–24420

Wang JJL, Rabizadeh S, Tasinato A, Sperandio S, Ye X, Green M, Assa-Munt N, Spencer D, Bredesen DE (2000) Dimerization-dependent block of the proapoptotic effect of p75^{NTR}. J Neurosci Res 60:587–593

Watson FL, Porcionatto MA, Bhattacharyya A, Stiles CD, Segal RA (1999) TrkA glycosylation regulates receptor localization and activity. J Neurobiol 39:323–336

Weiss FU, Daub H, Ullrich A (1997) Novel mechanisms of RTK signal generation. Curr Opin Genet Dev 7:80–86

Weskamp G, Reichardt LF (1991) Evidence that biological activity of NGF is mediated through a novel subclass of high affinity receptors. Neuron 6:649–663

Wiesmann C, Ultsch MH, Bass SH, De Vos AM (1999) Crystal structure of nerve growth factor in complex with the ligand-binding domain of the TrkA receptor. Nature 401:184–188

Wu C, Butz S, Ying Y, Anderson RGW (1997) Tyrosine kinase receptors concentrated in caveolae-like domains from neuronal plasma membrane. J Biol Chem 272:3554–3559

Wu K, Xu JL, Suen PC, Levine E, Huang XY, Mount HT, Lin SY, Black IB (1994) Functional trkB neurotrophin receptors are intrinsic components of the adult brain postsynaptic density. Brain Res Mol Brain Res 43:286–290

Yacoubian T, Lo DC (2000) Truncated and-full-length TrkB receptors regulate distinct modes of dendritic growth. Nat Neurosci 3:342–349

Ye X, Mehlen P, Rabizadeh S, VanArsdale T, Zhang HY, Shin H, Wang JJL, Leo E, Zapata J, Hauser CA, Reed JC, Bredesen DE (1999) TRAF family proteins interact with the common neurotrophin receptor and modulate apoptosis induction. J Biol Chem 274:30202–30208

Zhang YZ, Moheban DB, Conway BR, Bhattacharyya A, Segal RA (2000) Cell surface Trk receptors mediate NGF-induced survival while internalized receptors regulate NGF-induced differentiation. J Neurosci 20:5671–5678

Zhou H, Welcher AA, Shooter EM (1997) BDNF/NT4–5 receptor TrkB and cadherin participate in cell-cell adhesion. J Neurosci Res 49:281–291

NEUROTROPHINS AND THEIR RECEPTORS: A CONVERGENCE POINT FOR MANY SIGNALLING PATHWAYS

Moses V. Chao

The neurotrophins are a family of proteins that are essential for the development of the vertebrate nervous system. Each neurotrophin can signal through two different types of cell surface receptor — the Trk receptor tyrosine kinases and the p75 neurotrophin receptor. Given the wide range of activities that are now associated with neurotrophins, it is probable that additional regulatory events and signalling systems are involved. Here, I review recent findings that neurotrophins, in addition to promoting survival and differentiation, exert various effects through surprising interactions with other receptors and ion channels.

LONG-TERM POTENTIATION (LTP). An enduring increase in the amplitude of excitatory postsynaptic potentials as a result of high-frequency (tetanic) stimulation of afferent pathways. It is measured both as the amplitude of excitatory postsynaptic potentials and as the magnitude of the postsynaptic-cell population spike. LTP is most often studied in the hippocampus and is often considered to be the cellular basis of learning and memory in vertebrates

Skirball Institute of Biomolecular Medicine, New York University School of Medicine, New York, New York 10016, USA.
e-mail: chao@saturn.med.nyu.edu
doi:10.1038/nrn1078

The era of growth factor research began fifty years ago with the discovery of nerve growth factor (NGF). Since then, the momentum to study the NGF — or neurotrophin — family has never abated because of their continuous capacity to provide new insights into neural function: the influence of neurotrophins spans from developmental neurobiology to neurodegenerative and psychiatric disorders. In addition to their classic effects on neuronal cell survival, neurotrophins can also regulate axonal and dendritic growth and guidance, synaptic structure and connections, neurotransmitter release, LONG-TERM POTENTIATION (LTP) and synaptic plasticity[1,2].

The surprising discovery that neurotrophins and their receptors do not exist in *Drosophila melanogaster* or *Caenorhabditis elegans* reinforced the idea that these proteins are not absolutely necessary for the development of neuronal circuits *per se*, but are involved in 'higher-order' activities. For example, neurotrophins and their receptors influence many aspects of neuronal activity that result in the generation of new synaptic connections, which can be long lasting[3]. Alterations in neurotrophin levels have profound effects on a wide variety of phenomena, including myelination, regeneration, pain, aggression, depression and substance abuse.

The actions of neurotrophins depend on two different transmembrane-receptor signalling systems[4] — the Trk receptor tyrosine kinases and the p75 neurotrophin receptor[5,6]. Despite considerable progress in understanding the roles of these receptors, additional mechanisms are needed to explain the many cellular and synaptic interactions that occur between neurons. An emerging view is that neurotrophin receptors act as sensors for various extracellular and intracellular inputs, and several new mechanisms have recently been put forward. Here, I will consider several ways in which Trk and p75 receptors might account for the unique effects of neurotrophins on behaviour and higher-order activities.

The levels of neurotrophins are important

It is well established that the overall levels of neurotrophins determine the balance between cell survival and APOPTOSIS during development. Neural activity has profound effects on the levels of neurotrophins. Indeed, the idea that neurotrophins are crucial for synaptic plasticity came from observations that they are synthesized and released in an activity-dependent manner[7–9]. NGF and brain-derived neurotrophic factor (BDNF) messenger RNAs (mRNAs) are highly regulated by electrical stimulation and epileptic activity[10], and BDNF in particular is rapidly released by neuronal activity during periods of activity-dependent synaptic remodelling[11–14].

Studies of mice that express reduced levels of neurotrophins have shown surprising effects on adult brain function and behaviour. Mice that completely

Box 1 | Haploinsufficiency of neurotrophins

***NGF*$^{+/-}$ mice**
- Decreased cholinergic innervation of the hippocampus[15]
- Deficiency in memory acquisition and retention[15]
- Loss of neurons of the peripheral nervous system[121]

***BDNF*$^{+/-}$ mice**
- Hyperphagia, obesity[16–18]
- Impairment of long-term potentiation[19,20,122]
- Elevated striatal dopamine levels[123]
- Loss of mechanosensitivity[124]
- Loss of neurons of the peripheral nervous system[125,126]

***NT3*$^{+/-}$ mice**
- Deficient amygdala KINDLING activity[127]
- Cardiovascular defects[128]
- Reduced mechanoreceptors[129]
- Loss of neurons of the peripheral nervous system[130]

lack neurotrophins die during the first few weeks following birth. Heterozygous mice in which neurotrophin levels are reduced by half are viable but, strikingly, they show other unanticipated deficits (BOX 1). For example, lowering the level of NGF leads to several deficits in memory acquisition and retention[15]. In the absence of normal levels of BDNF, mice show enhanced aggressiveness, hyperactivity and hyperphagia[16–18]. Intracerebroventricular infusion of BDNF or neurotrophin 4 (NT4) reverses the hyperphagic phenotype[17]. In *BDNF*$^{+/-}$ heterozygous mice, 5-HT (5-hydroxytryptamine, serotonin)-mediated neuronal function is abnormal in the forebrain, cortex, hippocampus and hypothalamus, and administration of the selective 5-HT-reuptake inhibitor fluoxetine reduces the aggressive behaviour, hyperphagia and hyperlocomotor activity[16]. A conditional deletion of BDNF in the brains of postnatal mice also leads to hyperphagia and hyperactivity, as well as to higher levels of anxiety as measured by a LIGHT/DARK EXPLORATION TEST[18]. Therefore, the feeding phenotype and the other behavioural abnormalities are mediated by the action of BDNF in the central nervous system (CNS), not in the periphery. Abnormal behaviours, indicative of impulse-control disorders, are also elicited by partial deletion of BDNF.

Lack of BDNF also causes deficits in memory tasks: for example, *BDNF*$^{+/-}$ mice show impairments in spatial memory. This is consistent with defects in LTP that are found in the hippocampus. Interestingly, *BDNF*$^{+/-}$ and *BDNF*$^{-/-}$ mice show the same deficits in LTP[19,20], indicating that not only the availability of BDNF, but also its levels, can profoundly alter plasticity.

Neurotrophins and their receptors

The neurotrophins are initially synthesized as precursors or pro-neurotrophins, which are cleaved to produce the mature proteins[22]. Pro-neurotrophins are cleaved intracellularly by FURIN or pro-convertases at a highly conserved dibasic amino-acid cleavage site to release carboxy-terminal mature proteins. The mature proteins, which are about 12 kDa in size, form stable, non-covalent dimers, and are normally expressed at very low levels during development. The amino-terminal half (or pro-domain) of the pro-neurotrophin is believed to be important for the proper folding and intracellular sorting of neurotrophins.

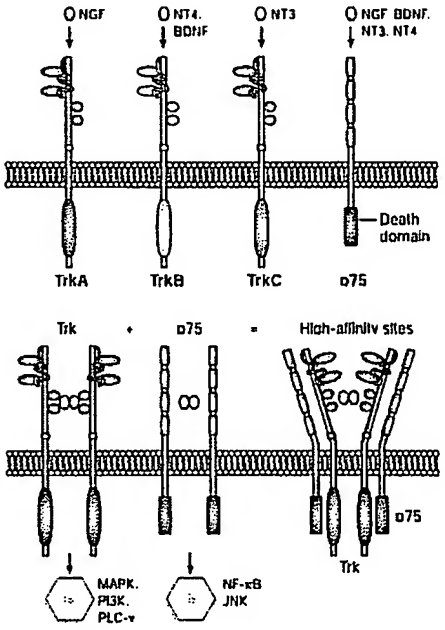

Figure 1 | Models of Trk and p75 receptor activation. Neurotrophin binding results in dimerization of each receptor. Neurotrophins bind selectively to specific Trk receptors, whereas all neurotrophins bind to p75. Trk receptors contain extracellular immunoglobulin G (IgG) domains for ligand binding and a catalytic tyrosine kinase sequence in the intracellular domain. Each receptor activates several signal transduction pathways[3,34,35]. The extracellular portion of p75 contains four cysteine-rich repeats, and the intracellular part contains a death domain. Neurotrophin binding to the p75 receptor mediates survival, cell migration and myelination[135] through several signalling pathways[36]. Interactions between Trk and p75 receptors can lead to changes in the binding affinity for neurotrophins[27]. BDNF, brain-derived neurotrophic factor; JNK, Jun N-terminal kinase; MAPK, mitogen-activated protein kinase; NGF, nerve growth factor; NT, neurotrophin; PI3K, phosphatidylinositol 3-kinase; PLC-γ, phospholipase Cγ.

Receptors encode specificity and responsiveness. Different neurotrophins show binding specificity for particular receptors — NGF binds preferentially to tyrosine receptor kinase A (TrkA); BDNF and NT4 to TrkB; and neurotrophin 3 (NT3) to TrkC (FIG. 1). These interactions have generally been considered to be of high affinity. However, in reality, the binding of NGF to TrkA, and of BDNF to TrkB is of low affinity[23–25], but it can be regulated by receptor dimerization, structural modifications

APOPTOSIS
The process of programmed cell death, characterized by distinctive morphological changes in the nucleus and cytoplasm, chromatin cleavage at regularly spaced sites, and the endonucleolytic cleavage of genomic DNA.

LIGHT/DARK EXPLORATION TEST
This test depends on the natural tendency of rodents to explore the environment in the absence of a threat and to retreat to an enclosed area when fearful. The animals are placed in an apparatus that has a dark and an illuminated compartment. Reduced exploration of the bright compartment and a reduced number of transitions between compartments are commonly interpreted as measures of anxiety.

FURIN
An endopeptidase with specificity for the consensus sequence Arg-X-Lys/Arg-Arg.

KINDLING
An experimental model of epilepsy in which an increased susceptibility to seizures arises after daily focal stimulation of specific brain areas (for example, the amygdala) — stimulation that does not reach the threshold to elicit a seizure by itself.

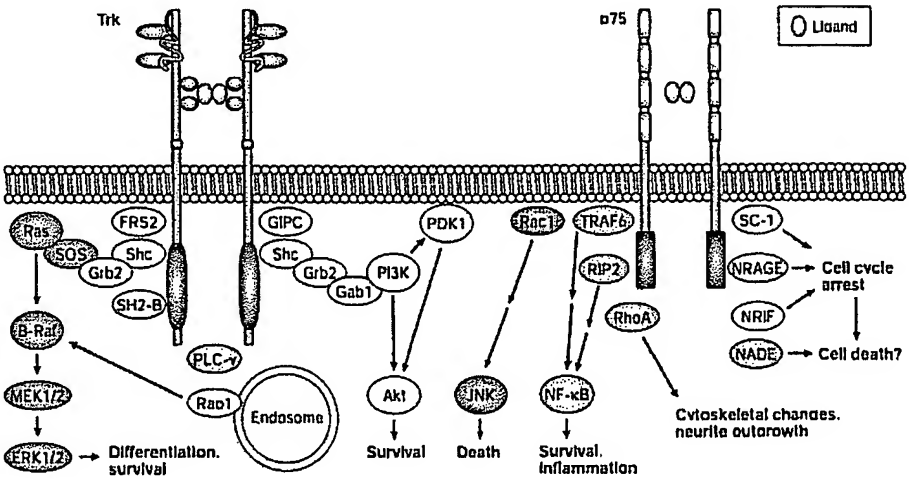

Figure 2 | Neurotrophin receptor signalling. Trk receptors mediate differentiation and survival signalling through extracellular signal-regulated kinase (ERK), phosphatidylinositol 3-kinase (PI3K) and phospholipase Cγ (PLC-γ) pathways[1,5]. Trk family members recruit and increase the phosphorylation of PLC-γ and Src homologous and collagen-like adaptor protein (Shc), which leads to activation of PI3K and ERK. Rap1 exerts its actions from an endosomal location[138]. The p75 receptor predominantly signals to activate NF-κB and Jun N-terminal kinase (JNK), and modulates RhoA activity. These responses are mediated through adaptor proteins that bind to the cytoplasmic domain of p75, including neurotrophin-receptor interacting factor (NRIF), neurotrophin-associated cell death executor (NADE), neurotrophin-receptor-interacting MAGE homologue (NRAGE), Schwann cell 1 (SC1) and receptor-interacting protein 2 (RIP2)[35,39], which can exert effects on apoptosis, survival, neurite elongation and growth arrest. Akt, protein kinase B; FRS2, fibroblast growth factor receptor substrate 2; Gab1, Grb2-associated binder-1; Grb2, growth factor receptor-bound protein 2; GIPC, GAIP interacting protein, C terminus; MEK, mitogen-activated protein kinase (MAPK)/ERK kinase; PDK1, phosphoinositide-dependent kinase 1; SH2B, Src homology 2-B; SOS, Son of Sevenless; TRAF6, tumour necrosis factor receptor-associated factor 6.

or association with the p75 receptor[26,27]. The p75 receptor can bind to each neurotrophin, and also acts as a co-receptor for Trk receptors (FIG. 1). Expression of p75 can increase the affinity of TrkA for NGF and can enhance its specificity for cognate neurotrophins[28–30]. As a result, increased ligand selectivity can be conferred on the Trk receptors by the p75 receptor.

The ability of Trk and p75 receptors to present different binding sites and affinities to particular neurotrophins determines both their responsiveness and specificity. The ratio of receptors is important in dictating the numbers of surviving cells, and interactions between p75 and Trk receptors provide greater discrimination between different neurotrophins. A similar mechanism is also observed in other ligand–receptor systems, such as the glial-derived neurotrophic factor (GDNF)–Ret receptor[31], in which preferential interactions between GDNF ligands and the Ret receptor are facilitated by expression of GDNF family receptor subunits (GFRα). Not surprisingly, Ret receptors use signalling pathways similar to those used by Trks.

The effects of neurotrophins on axon guidance can also be modulated by the intracellular location of the neurotrophin–receptor complex. During development, neurotrophins are produced and released from the target cells and become internalized into vesicles, which are then transported to the cell body. The biological effects of neurotrophins require that signals be conveyed over long distances, from the nerve terminal to the cell body[32]. Both Trk and p75 receptors undergo retrograde and anterograde transport. Several proteins are associated with the Trk and p75 receptors during transport, and signalling persists after internalization[33]. The proper distribution of these proteins in the growth cone could result from movement of the neurotrophin receptors.

These receptor functions do not necessarily provide an explanation for the numerous phenotypes that are shown by mice that are deficient in neurotrophins. In addition to forming complexes, Trk and p75 receptors show independent signalling properties[5,34–36], and downstream signal transduction pathways significantly contribute to individual physiological responses. Neurotrophins bind as dimers to p75- and Trk-family members. Trk receptor dimerization leads to *trans*-autophosphorylation and to the activation of intracellular signalling cascades. The Src homologous and collagen-like (Shc) adaptor protein links the activated Trk receptor to two separate intracellular signalling pathways (FIG. 2). Neuronal survival requires Shc binding to the Trk receptor, which results in increases in phosphatidylinositol 3-kinase (PI3K) and Akt (protein kinase B) activities (FIG. 2). Phosphorylation of Shc by Trk also leads to increases in the activity of Ras and the extracellular signal-regulated kinase (ERK). These events in turn influence transcriptional events, such as the induction of the cyclic AMP-response element binding (CREB) transcription factor. CREB has effects

Box 2 | Processing of the p75 receptor

The p75 receptor undergoes cleavage by metalloproteinases[131] — such as α-secretase — to produce an ectodomain piece and a fragment containing the transmembrane and cytoplasmic domains (see figure). Unexpectedly, this membrane-spanning region is further cleaved by a presenilin-dependent γ-secretase (REF. 132; T.-W. Kim, unpublished observations). The generation of proteins by regulated intramembrane proteolysis is a universal mechanism[133] that acts on several proteins, including the amyloid precursor protein, Notch and the ErbB4 receptor tyrosine kinase. Whether the proteolytic enzymes involved in these events are regulated is not known. However, the generation of a p75 intracellular domain implies that neurotrophins might use regulated intramembrane proteolysis to transmit an intracellular signal. Analogous to Notch, the p75 intracellular domain might function in the nucleus as a transcriptional modifier. The intracellular domain might be involved in activation or repression of neurotrophin-related genes. Several p75 adaptor proteins, such as neurotrophin-receptor interacting factor (NRIF), tumour necrosis factor receptor-associated factors (TRAFs), receptor-interacting protein 2 (RIP2) and Schwann cell 1 (SC1) (FIG. 2), are candidates for nuclear translocation.

As p75 is expressed after nerve damage, in inflammatory conditions such as multiple sclerosis and in neuronal populations that degenerate in Alzheimer's disease, it is tempting to speculate that the γ-secretase cleavage of p75 reflects an early event in the pathogenesis of neurodegenerative diseases that are characterized by a chronic inflammation reaction.

Together with the preponderance of proneurotrophins in Alzheimer's disease-affected tissues[134], proteolytic cleavage of neurotrophins and their receptors represent an intriguing regulatory mechanism for neuronal survival and regeneration during injury and ageing.

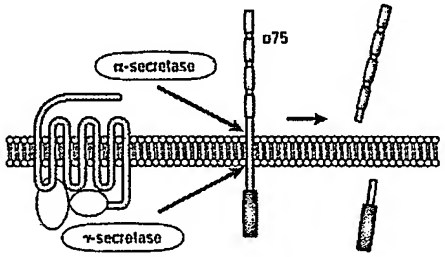

on the cell cycle, neurite outgrowth and synaptic plasticity[37]. The small G protein Rap1 accounts for the ability of neurotrophins to signal through ERK for sustained periods[38]. In addition, phospholipase Cγ (PLC-γ) binds to activated Trk receptors and initiates an intracellular signalling cascade, resulting in the release of inositol phosphates and activation of protein kinase C (PKC).

Through a different set of adaptor proteins (FIG. 2), p75 produces increases in Jun N-terminal kinase (JNK), NF-κB and ceramide[36]. One established function of p75 is to promote cell death[35]. This might provide a means for the refinement of correct target innervation during development and eliminate cells during periods of developmental cell death[39]. Apoptosis by p75 is also manifested after seizure or inflammation[40,41]. Injury to the spinal cord leads to oligodendrocyte death that is p75-dependent — a phenomenon that has also been observed in culture[42]. This apoptotic function is accompanied by an increase of Rac and JNK activities (FIG. 2), which are essential for NGF-dependent death[43]. Another function of p75 might be to mediate a non-apoptotic or survival response[44,45], similar to the behaviour of other tumour necrosis factor receptors.

Surprisingly, pro-neurotrophins are more selective ligands for the p75 receptor than mature forms[46], and are more effective at inducing p75-dependent apoptosis[47,48]. This indicates that the biological actions of neurotrophins can be regulated by proteolytic cleavage, with pro-forms preferentially activating p75 to mediate apoptosis and mature forms selectively activating Trk receptors to promote survival. Like the neurotrophins, the p75 receptor can also undergo cleavage (BOX 2).

Many of the components of the pathways that mediate neurotrophin signalling, such as ERK, Akt, PLC, PKC, Ras, JNK and NF-κB (FIG. 2), are not unique to neurotrophins. Each signalling component is used in many different contexts and by other growth factors and cytokines. This complicates the problem of ascribing specific mechanisms to a particular response[47]. Clearly, the effects of neurotrophins depend on various factors — their levels, their affinity of binding to transmembrane receptors, and the duration and intensity of downstream signalling cascades that are stimulated after receptor activation. From these considerations alone, it is still not evident how changes in behaviour and neuronal activity can be explained simply by a 50% reduction in levels of neurotrophins or their signalling components.

Neurotrophin-mediated plasticity

Many observations have indicated that neurotrophins influence both the frequency and amplitude of synaptic currents. Neurotrophins such as BDNF and NT3 produce rapid increases in synaptic strength in nerve-muscle synapses, as well as increases in excitatory post-synaptic currents in hippocampal neurons[48–50]. BDNF and NT3 also induce rapid and long-lasting enhancement of synaptic strength through LTP in hippocampal slices. These effects are not due to the nonspecific effects of using large amounts of proteins in electrophysiological recordings *in vitro*, as mice deficient in BDNF or NT4 show a notable impairment of LTP in hippocampal slices[19,51]. Similarly, the effects on LTP are not due to a developmental or structural alteration created by gene targeting, as normal LTP can be rescued by addition of exogenous BDNF[20,52].

Despite considerable evidence for the effects of neurotrophins on synaptic strength[53,54], there are few molecular and signalling mechanisms that could explain these effects. The use of protein kinase inhibitors has indicated that intracellular protein phosphorylation is important, as well as phosphatidylinositol lipids and inositol-1,4,5-triphosphate (Ins(1,4,5)P_3) receptors[55]. A CONDITIONAL MUTATION of the *TrkB* gene results in deficits in memory acquisition and consolidation in several hippocampus-dependent learning tasks[56]. These studies provide convincing evidence that signalling by TrkB receptors is directly responsible for promoting hippocampal LTP[57]. Mutagenesis of the Shc and PLC-γ binding sites in the *TrkB* gene shows that downstream activation of CREB and calcium/calmodulin-dependent kinase II is responsible for the ability of TrkB to modulate LTP. Although Trk receptors are implicated in many forms of neuronal plasticity, there are reports that p75 signalling might also exert some effects on behaviour. Analysis of mice deficient in the full-length p75 receptor

CONDITIONAL MUTATION
A mutation that can be selectively targeted to specific organs (or cell types within an organ) or induced at a specific developmental stage.

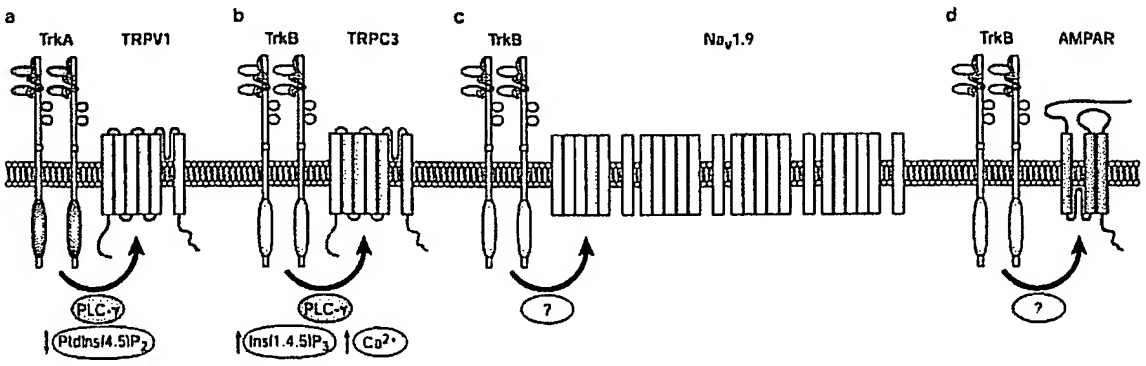

Figure 3 | Examples of ion channel interactions with Trk neurotrophin receptors. Several examples of interactions between Trk receptors and ion channels are known. a | TrkA with the transient receptor potential (TRP) channel TRPV1 (or VR1)[83]. b | TrkB with TRPC3 (REF. 65). c | TrkB with $Na_v1.9$ (REF. 77). d | α-Amino-3-hydroxy-5-methyl-4-isoxazole propionic acid receptor (AMPAR) activity can be modified by brain-derived neurotrophic factor (BDNF) binding and activation of TrkB receptors[77]. TrkA-mediated PLC-γ activation decreases levels of cellular PIP2, which leads to the opening of TRPV1 channels. In the case of TrkB and TRPC3, TrkB-mediated PLC-γ activity leads to the opening of TRPC3 through inositol-1,4,5-trisphosphate ($Ins(1,4,5)P_3$) generation and store-operated calcium release. These associations have been confirmed by co-immunoprecipitation experiments. $PtdIns(4,5)P_2$, phosphatidylinositol-4,5-bisphosphate

has revealed slight impairments in several learning tasks[58]. Another p75-mutant mouse that lacks both the full-length and the short isoform[59] shows a more severe phenotype and could provide additional insight into the role of p75 in higher-order functions.

However, full explanation of the ability of neurotrophins to regulate synaptic plasticity in the adult brain requires a better understanding of how neurotrophin-receptor signalling is linked to ion channel function. Recent analysis of the role of ephrins at synapses has shown that EphB2 receptors can regulate postsynaptic function through an interaction with NMDA (*N*-methyl-D-aspartate) receptors[60–63]. These studies highlight the possibility that other receptor tyrosine kinase systems might regulate ion channel function.

The study of transient receptor potential (TRP) ion channels has provided new insights into this question. The TRP superfamily includes more than twenty cation channels, some of which have been shown to be sensitive to cold and hot temperatures, and to pheromones[64]. TRPC3 is a non-voltage-gated, store-operated cation channel that is highly expressed in brain regions where TrkB receptors are found. Treatment of pontine neurons with BDNF resulted in a delayed inward current after 30 s (REF. 65). This response was specific to BDNF, as other ligands — such as fibroblast growth factor and insulin-like growth factor — did not elicit an increase in cation current. The BDNF-induced current depended on activation of TrkB and PLC (FIG. 3). The biological consequences of interactions between TrkB and TRPC3 have not been fully defined, but the increase in cation flux implies a unique neurotrophin-specific function. The abundant expression of TRPC3 during neonatal development indicates that it might have a role in neurotrophin-dependent plasticity.

Neurotrophins and pain

Another TRP family member that has intimate ties with the Trk receptor is the TRPV1 (VR1) channel or capsaicin receptor, a non-selective cation channel that is activated by heat, noxious vanilloid compounds such as capsaicin, and extracellular protons[66]. Previously, NGF was shown to potentiate the responses of nociceptive sensory neurons to capsaicin[67]. This indicated that crosstalk between capsaicin and NGF occurred within sensory neurons. The idea that TRPV1 channels are necessary for NGF-induced thermal hypersensitivity was also underscored by observations of mice lacking TRPV1. In contrast to NGF-injected normal mice, which showed a marked decrease in paw withdrawal latency in response to a thermal stimulus, injection of NGF into TRPV1-deficient mice did not produce any sensitization[68].

Strikingly, NGF produced an approximately 30-fold increase in proton-evoked currents in *Xenopus* oocytes that co-expressed TrkA and TRPV1. Diminution of phosphatidylinositol-4,5-bisphosphate levels through antibody sequestration or PLC-mediated hydrolysis mimicked the potentiating effects of NGF at the cellular level (FIG. 3). Moreover, recruitment of PLC-γ to TrkA was essential for NGF-mediated potentiation of channel activity (FIG 3). Co-immunoprecipitation studies indicated that TRPV1 associates with TrkA and PLC-γ to form a complex. As an interaction was also observed between TrkB and TRPC3 (REF. 65), it is likely that common sequences are required for these interactions.

Neurotrophins have been shown to produce acute pain as a side effect in clinical trials for neuropathy and neurodegeneration[69,70]. NGF is present at high levels after inflammation and promotes nociceptor sensitization. These responses might reflect the same process as potentiation of thermal sensitivity by TRPV1 or related heat-activated ion channels. In NGF-responsive

nociceptive sensory neurons. TrkA and TRPV1 are frequently co-expressed. In other neuronal populations, similar mechanisms might account for the pronounced pain that is observed when high levels of neurotrophins are administered in animal models or in human clinical trials.

Other ion channels

Increasing numbers of interactions between Trk receptors and ion channels are being discovered. Increased tyrosine phosphorylation of NMDA and voltage-gated potassium channels occurs as a result of treatment with BDNF[71,72]. In the hippocampus, Trk receptors are expressed both pre- and postsynaptically, and both pre- and postsynaptic mechanisms have been proposed to account for changes in synaptic activity[50,73–76]. Electrophysiological measurements show that BDNF can actually suppress $K_v1.3$ currents[72] and block postsynaptic α-amino-3-hydroxy-5-methyl-4-isoxazole propionic acid (AMPA) receptor-mediated currents[77]. The catalytic activity of TrkB receptors is required for the decrease in AMPA receptor activity, implying that there might be a close association between TrkB and AMPA receptors (FIG. 3). Alternatively, the exo- and endocytosis of AMPA receptors[78], which determine activity-dependent changes of synaptic efficacy, could be influenced by BDNF signalling.

One reason for suspecting a direct interaction between Trk receptors and ion channels comes from recent studies in which the sodium channel $Na_v1.9$ was activated by BDNF[79]. The effects of BDNF on hippocampal neurons of the CA1 region are remarkable for the rapidity of their response — an inward sodium current was detected within milliseconds of BDNF treatment. Curiously, the BDNF-mediated increase was blocked by K-252a, a Trk-specific inhibitor[80]. This requirement for receptor tyrosine kinase activity is difficult to reconcile with the time course of $Na_v1.9$ activation, as phosphorylation takes a considerably longer time than the patterns of activity that are stimulated by BDNF. For example, the earliest tyrosine phosphorylation events require nearly a minute of neurotrophin treatment[81]. Also, it takes up to a minute of exposure to NGF to elicit a change in sodium channel mRNA expression[82], a far longer time interval than is required for BDNF to activate the $Na_v1.9$ channel.

Although the exact mechanisms for receptor–ion channel interactions are unknown, the considerations outlined in the previous paragraph indicate that the TrkB BDNF receptor might exist in a complex with the $Na_v1.9$ channel (FIG. 3). Conformational changes in the receptor or the channel might account for the ability of sodium channels to be rapidly influenced by the binding of BDNF to TrkB. Previous studies have indicated that conformational changes in the TrkA receptor might account for changes in its NGF-binding properties[25]. In addition, TrkA receptor dimerization and activation might simply result from a point mutation in the extracellular domain of the receptor[83]. This raises the possibility that changes in Trk structure might be transmitted to neighbouring ion channels.

Transactivation through GPCRs

Although ligand-induced dimerization or oligomerization of receptors is a well-established mechanism for growth factor signalling, there is increasing evidence that biological responses can be mediated by two or more receptor systems. For some time, it has been appreciated that heterotrimeric G-protein-coupled receptors (GPCRs) produce similar responses (in terms of cell growth) to other growth factors that use receptor tyrosine kinases[84,85].

Activation of Trk neurotrophin receptors occurs after treatment with adenosine, a neuromodulator that acts through GPCRs. Trk receptor autophosphorylation is increased in hippocampal neurons and PC12 cells after treatment with adenosine. This transactivation requires adenosine A_{2A} receptors[86], and does not result from the production of neurotrophins. The increase in Trk activity was inhibited by protein kinase inhibitors, such as PP1 (4-amino-5-(4-methylphenyl)-7-(*t*-butyl)pyrazolo[3,4-*d*]-pyrimidine, which is specific for Src family members) or K-252a. The pituitary adenylate cyclase-activating polypeptide (PACAP), a neuropeptide, can also transactivate Trk receptors in a manner similar to transactivation by adenosine[87]. PACAP occurs in two forms, one of 38 and one of 27 amino acids, and is a member of the vasoactive intestinal peptide/secretin/glucagon family. The two PACAP peptides also interact with GPCRs.

The effects of adenosine and PACAP are specific, as other GPCR ligands do not participate in crosstalk with Trk receptors. Bradykinin, carbachol, ATP, apomorphine, quinpirole and angiotensin II do not cause TrkA activation[85], even though receptors for these ligands are expressed on the same cells as those for adenosine and PACAP. By contrast, many of these ligands can stimulate epidermal growth factor (EGF) receptors and other mitogenic growth factor receptors. Conversely, adenosine and its agonists do not activate EGF receptors.

These GPCR transactivation events are unique in other ways. Both adenosine and PACAP require a long period of time (more than 1–2 hours) to activate Trk tyrosine kinase activity. Both ligands produce an activation of PI3K and Akt, which results in enhanced cell survival after withdrawal of NGF. These results provide an explanation for the neuroprotective actions of adenosine and PACAP, and point to a therapeutic use for small-molecule GPCR agonists in neurodegenerative disorders. For example, activation of Trk receptors by PACAP was also observed in primary cultures of basal forebrain cholinergic neurons, and administration of PACAP effectively rescued these neurons after fimbria–fornix lesion *in vivo*[88]. These results are significant, because NGF-responsive cholinergic neurons in the basal forebrain degenerate in Alzheimer's disease[89].

What is the physiological relevance to neurotrophin action of transactivation by GPCR signalling? Transactivation might explain why neuronal survival in the CNS is not adversely affected by the lack of neurotrophins — GPCR ligands might compensate by providing a survival function through a neurotrophin-receptor signalling pathway. Also, other essential activities, such

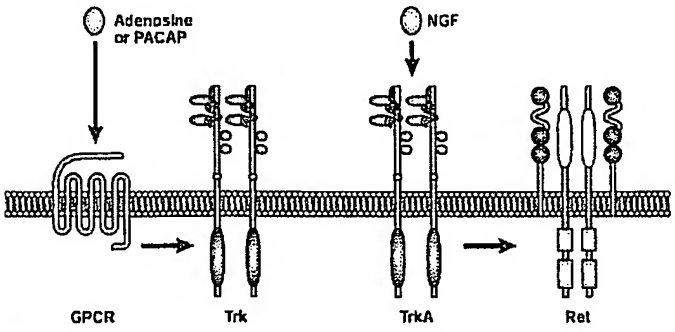

Figure 4 | Transactivation of receptor tyrosine kinases. Transactivation of Trk receptor by G-protein-coupled (GPC) ligands — such as adenosine and pituitary adenylate cyclase-activating polypeptide (PACAP) — results in neuroprotection[86,137]. In sympathetic neurons, binding of nerve growth factor (NGF) to TrkA results in the activation of Ret tyrosine kinase receptors[95]. GPCR, G-protein-coupled receptor.

as the regulation of ion channels, might be legitimate actions for transactivated receptor signalling. Indeed, dopamine–GPCR transactivation of platelet-derived growth factor receptors has an acute effect on NMDA ion channel activity in hippocampal neurons[90].

Importantly, mutations in components of the adenosine or PACAP signalling pathways give rise to behavioural problems in learning and memory[91,92] and heightened aggression[93], which are reminiscent of the effects of mutations in the BDNF and TrkB receptor genes[10,17,20,54,75]. These striking similarities imply that adenosine and PACAP signalling might work in parallel or converge with neurotrophin receptor action. These similarities also imply that Trk receptors act as convergence points for signals emanating from other receptor systems. In this manner, Trk receptors act to survey various inputs, in addition to those from neurotrophins.

Crosstalk between different transmembrane receptors might represent a more common signalling mechanism. Further to the influence that GPCRs exert upon Trk receptor activity, Trk receptors can activate other seemingly unrelated receptors. An unusual case is the Ret tyrosine kinase receptor (FIG. 4), which is a common signalling receptor for GDNF-related ligands that also include artemin, neurturin and persephin[94]. These ligands require specific GFRα subunits to confer ligand specificity. However, in postnatal sympathetic neurons, NGF produces an activation of Ret receptors over the course of 1–2 days, which does not require GDNF ligand binding[95]. Activation of Ret signalling provides additional survival advantages during postnatal periods when these sympathetic neurons become independent of NGF. Transactivation of Ret tyrosine kinases by binding of NGF to the TrkA receptor represents a new mechanism for transmitting survival signals within neurons.

Therefore, there are ways of activating Trk and Ret tyrosine kinase receptors other than direct ligand binding. Activation of the neurotrophin system through other receptor signalling systems is an alternative mechanism of communication in the nervous system, and examples of this crosstalk abound. For example, antidepressant agents that act through monoamine GPCRs can cause increased expression of both neurotrophins and neurotrophin receptors[96]. Notably, only the neurons that express the monoamine GPCRs have the capacity to enhance neurotrophin or Trk receptor levels. The results of studies with GPCR ligands raise the possibility of using small molecules to elicit neurotrophic effects in the treatment of neurodegenerative diseases[70]. This approach would allow selective targeting of neurons that express specific GPCRs and trophic factor receptors.

Regeneration

Proteins that modulate growth cone dynamics have an important role in axonal patterning during development, and in preventing regeneration of axons following injury. Considerable attention has been given to Nogo, myelin-associated glycoprotein (MAG) and semaphorin 3A — proteins that provide potent inhibitory signals for axonal growth. There is increasing evidence that places neurotrophin receptors in the realm of these inhibitory proteins.

Neurotrophins can modulate the response of growth cones to inhibitory axon-guidance molecules. For example, neurotrophins have been shown to affect the extent of the axonal response to MAG[97]. Moreover, semaphorin 3A induces the collapse of dorsal-root ganglion (DRG) and sympathetic growth cones[98], and neurotrophins can rapidly modulate the response of DRG growth cones to semaphorin 3A (REF. 99). The sensitivity of DRG growth cones to semaphorin 3A is influenced by BDNF and NGF in distinct ways — BDNF increases the sensitivity of DRG growth cones to semaphorin 3A, whereas NGF decreases it. These effects depend on Trk signalling, implying that TrkA and TrkB exert differential effects on semaphorin 3A signalling. Furthermore, the effects of NGF in opposing the inhibitory action of semaphorin 3A are highly dependent on ligand concentration and downstream signalling through the activities of protein kinase A and protein kinase G (REF 100). These observations indicate the operation of a mechanism in which the receptors for neurotrophins and semaphorins are functionally linked.

Like the Trk receptors, p75 interacts with some unlikely partners. Nogo-A is an important inhibitory protein that is expressed in oligodendrocytes. It binds to a glycosylphosphatidylinositol-linked receptor[101] that is recognized by a 66-amino-acid fragment of Nogo (Nogo-66). Unexpectedly, there are other ligands for this Nogo receptor, including oligodendrocyte myelin glycoprotein[102] and MAG[103,104]. The absence of a cytoplasmic domain in the structure of the Nogo receptor implies that other components are involved in signalling, and association of the Nogo receptor with the p75 receptor has proved to be a surprising and intriguing solution to this problem[105,106].

The identification of p75 as a co-receptor of the Nogo receptor was based on several key observations.

POLYMORPHISM
The simultaneous existence in the same population of two or more genotypes in frequencies that cannot be explained by recurrent mutations

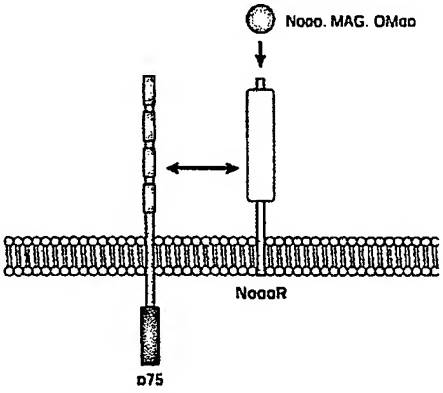

Figure 5 | Neurotrophins and p75 undergo site-specific cleavages. The Nogo and p75 receptors are found in a complex. Nogo[138], myelin-associated glycoprotein (MAG) and oligodendrocyte myelin glycoprotein (OMgp) are all ligands for the Nogo receptor (NogoR)[102,104]. Inhibition of neurite outgrowth by MAG is mediated by NogoR and the p75 receptor[105,106].

First, MAG serves as a ligand for the Nogo receptor. Second, the inhibitory effects of MAG were found to depend on the presence and action of the p75 receptor[107]. The Nogo receptor is closely associated with p75 through interactions between the extracellular domains of the two proteins (FIG. 5), and this association produces a repulsive effect on axonal growth. Together, these results indicate that myelin-dependent inhibition of axonal regeneration depends on the binding of MAG to a complex containing the Nogo and p75 receptors. Several different proteins bind to the cytoplasmic domain of p75 (FIG. 2); among them, RhoA is the most relevant to the inhibition of neurite outgrowth and growth cone collapse. Indeed, earlier work indicated that binding of p75 to RhoA influences axonal growth[108]. The inhibitory influence of MAG and Nogo might be explained by the recruitment of p75 into a complex that sends a repulsive signal in neurons. The participation of p75 in the prevention of regeneration following injury is plausible because the absence of p75 leads to sprouting and enhanced axonal growth and density[109].

Table 1 | Induction of p75 receptor expression after injury

Cell type	Injury
Motor neurons	Axotomy, regeneration[139–141]
Purkinje neurons	Traumatic injury[142]
Entorhinal neurons	Seizure[43]
Hippocampal neurons	Primary culture[143]
Striatal neurons	Ischaemia[144]
Cortical neurons	Zinc, ischaemia[145], Alzheimer's disease[146]
Schwann cells	Axotomy[147,148]
Oligodendrocytes	Spinal cord injury[42], multiple sclerosis lesions[40,149]

p75 expression is also induced in experimental allergic encephalomyelitis[150,151] and Alzheimer's disease[152].

The participation of p75 receptors in the axonal regeneration process provides further insight into the function of these receptors. There are many examples of elevated p75 expression in the adult brain and spinal cord after injury, inflammation and stress[6,110]. Interestingly, many cell types — including hippocampal and cortical neurons, oligodendrocytes and microglial cells — ordinarily show low levels of p75. However, after ischaemia, seizure, axotomy or other forms of stress, the expression of this receptor is considerably elevated in these types of cells (TABLE 1). Also, many cell types express p75 in culture, presumably owing to the change in environmental conditions. In fact, the magnitude of NF-κB signalling through p75 is highly dependent on whether cells have experienced stress, such as changes in serum, temperature or cell–cell contact[111].

Neurotrophins and disease

Few associations have been found between neurotrophin genes and neurological or psychiatric disorders, although a recent series of studies has linked a POLYMORPHISM in the pro-domain of BDNF with depression, bipolar disorders and schizophrenia. This polymorphism — which was identified from a single nucleotide polymorphism screen — is caused by a single amino-acid change, from valine (Val) to methionine (Met), at position 66 in the pro-domain of the BDNF protein[112–114]. In patients with bipolar disorder or depression, the *Val* allele seems to confer greater risk for the disease, whereas in patients with schizophrenia, the *Met* allele seems to be associated with impaired memory functions. The existence of mutations in BDNF — a highly conserved protein — implicates neurotrophins in the complex pathophysiology of psychiatric diseases[115], as well as neurodegenerative diseases such as Alzheimer's disease[116]. Cleavage of the p75 receptor has also been implicated in the pathogenesis of Alzheimer's disease (BOX 2).

An analysis of the Val→Met change in the pro-BDNF protein indicated that this alteration is responsible for abnormal sorting and secretion of BDNF[115]. The impact of this BDNF genotype was followed in human subjects who were examined for alterations in episodic memory. Individuals in which the pro-domain of BDNF has Met at position 66 performed relatively poorly in verbal episodic memory tests, and functional magnetic resonance imaging of hippocampal function showed an abnormal pattern of activation during cognitive tests. These effects of this polymorphism in BDNF indicate that neurotrophins can participate in hippocampal function and memory through a mechanism that relies on correct BDNF secretion. So, activity-dependent secretion of BDNF, and its subsequent effects on LTP and synaptic plasticity now have an important correlate in the human population.

An unexpected example of the involvement of neurotrophins in psychiatric disorders has come from the pathophysiology of depression, especially when depression is associated with stress. Several lines of evidence have implicated neurotrophins in depression. First, in animal models, restraint stress leads to decreased expression of BDNF in the hippocampus[117,118]. Second, the

LEARNED HELPLESSNESS
A commonly used model of depression in which animals are exposed to inescapable shock and subsequently tested for deficits in learning a shock-avoidance task. Learned helplessness is a rare example in which, rather than working from the psychiatric disorder to the model, the behavioural effect was originally discovered in experimental animals (dogs) and later invoked to explain depression.

administration of BDNF to the midbrain or hippocampus results in antidepressant effects in animal models of depression — forced swim and LEARNED HELPLESSNESS. This effect is comparable to chronic treatment with pharmacological antidepressants[118]. Third, BDNF has been shown to have trophic effects on 5-HT and noradrenergic neurons. Mutant mice with decreased levels of BDNF show a selective decrement in the function of 5-HT neurons and behavioural dysfunctions that are consistent with serotonergic abnormalities.

Many functions of the neurotrophic factors in the adult nervous system — other than their effects on neuronal survival — have now been elucidated. These functions include the maintenance of differentiated neuronal phenotypes, regulation of synaptic connections, activity-dependent synaptic plasticity, and neurotransmission. These additional functions show that neurotrophin receptors act as a point of convergence that might be involved in the integration of many environmental inputs. This can lead to alterations in neuronal circuitry and, ultimately, in behaviour. In particular, it has become clear that neurotrophins can produce long-term changes in the functionality of adult neurons through changes in transcription. As several psychotropic drugs affect neurotrophin signalling, this ability might help to explain the delay in therapeutic action of many psychiatric treatments.

Perspectives

To explain the complex behavioural effects that are related to the function of neurotrophins, an understanding of how local circuits and signal transduction pathways are integrated is required. Neurotrophins show both rapid and slow effects that are breathtaking in their scope and duration, but need to be further differentiated and defined. Cell-surface receptors are generally represented as isolated integral membrane proteins that span the lipid bilayer, with closely associated receptor components and with signal transduction proceeding in a linear stepwise fashion. This view of receptor function will undoubtedly be modified in the future. Neurotrophins provide an excellent example of how receptors can act not only in a linear manner, but can also influence the activity of other transmembrane molecules, either directly or through signalling intermediates. The description of these actions will require new methods of computational analysis, such as the effort to describe activity-dependent neurotrophic interactions by mathematical modelling[120].

Cell–cell communication represents the combined effects of many growth factors. Unlike studies that have been carried out *in vitro*, in which cell lines are treated with single factors, the growth and survival of cells *in vivo* are under the influence of the simultaneous actions of many polypeptide factors. Cooperativity between just two different transmembrane proteins implies that the possibilities for extracellular signalling are greatly expanded. In reality, the regulation of trophic activities is probably determined by the additive effects of many receptors and the duration of signalling events, as well as by protein cleavage events. The lack of a detectable effect on cell numbers in mice that are deficient in key growth factors also indicates that cell growth and survival are supported by multiple proteins. Interactions between neurotrophin receptors and ion channels and other cell-surface proteins provide a powerful mechanism for merging the actions of different ligand–receptor systems to achieve new cellular outcomes.

1. McAllister, A., Katz, L. & Lo, D. Neurotrophins and synaptic plasticity. *Annu. Rev. Neurosci.* **22**, 295–318 (1999)
2. Poo, M.-M. Neurotrophins as synaptic modulators. *Nature Rev. Neurosci.* **2**, 24–31 (2001)
3. Huang, E. & Reichardt, L. Neurotrophins: roles in neuronal development and function. *Annu. Rev. Neurosci.* **24**, 677–736 (2001)
4. Chao, M. V. & Hempstead, B. L. p75 and trk: a two-receptor system. *Trends Neurosci.* **19**, 321–326 (1995)
5. Kaplan, D. R. & Miller, F. D. Neurotrophin signal transduction in the nervous system. *Curr. Opin. Neurobiol.* **10**, 381–391 (2000)
6. Dechant, G. & Barde, Y.-A. The neurotrophin receptor p75NTR: novel functions and implications for diseases of the nervous system. *Nature Neurosci.* **5**, 1131–1136 (2002)
7. Gall, C. & Isackson, P. Limbic seizures increase neuronal production of messenger RNA for nerve growth factor. *Science* **234**, 758–761 (1986)
8. Blochl, A. & Thoenen, H. Characterization of nerve growth factor release from hippocampal neurons: evidence for a constitutive and an unconventional sodium-dependent regulated pathway. *Eur. J. Neurosci.* **7**, 1464–1472 (1995).
9. Wang, X. H. & Poo, M.-M. Potentiation of developing synapses by postsynaptic release of NT-4. *Neuron* **19**, 825–835 (1998)
10. Gall, C. Regulation of brain neurotrophin expression by physiological activity. *Trends Pharmacol. Sci.* **13**, 401–403 (1992).
11. Schoups, A., Elliott, R., Friedman, W. & Black, I. NGF and BDNF are differentially modulated by visual experience in the developing geniculocortical pathway. *Brain Res.* **86**, 326–334 (1995)
12. Lein, E., Hohn, A. & Shatz, C. Dynamic regulation of BDNF and NT-3 expression during visual system development. *J. Comp. Neurol.* **420**, 1–18 (2000)
13. Kohara, K., Kitamura, A., Morishima, M. & Tsumoto, T. Activity-dependent transfer of brain-derived neurotrophic factor to postsynaptic neurons. *Science* **291**, 2419–2423 (2001)
14. Balkowiec, A. & Katz, D. Cellular mechanisms regulating activity-dependent release of native brain-derived neurotrophic factor from hippocampal neurons. *J. Neurosci.* **22**, 10399–10407 (2002)
15. Chen, K. *et al.* Disruption of a single allele of the nerve growth factor gene results in atrophy of basal forebrain cholinergic neurons and memory deficits. *J. Neurosci.* **17**, 7288–7296 (1997).
16. Lyons, W. E. *et al.* Brain-derived neurotrophic factor-deficient mice develop aggressiveness and hyperphagia in conjunction with brain serotonergic abnormalities. *Proc. Natl Acad. Sci. USA* **96**, 15239–15244 (1999).
17. Kernie, S., Liebl, D. & Parada, L. BDNF regulates eating behavior and locomotor activity in mice. *EMBO J.* **19**, 1290–1300 (2000).
18. Rios, M. *et al.* Conditional deletion of brain-derived neurotrophic factor in the postnatal brain leads to obesity and hyperactivity. *Mol. Endocrinol.* **15**, 1748–1757 (2001)
Profound effects on feeding and aggressive behaviours have been observed in three different lines of mice with reduced levels of BDNF. These results indicate that a partial depletion of BDNF can have a key role in regulating behavioural responses, in this case, through serotonergic abnormalities.
19. Korte, M. *et al.* Hippocampal long-term potentiation is impaired in mice lacking brain-derived neurotrophic factor. *Proc. Natl Acad. Sci. USA* **92**, 8856–8860 (1995).
20. Patterson, S. *et al.* Recombinant BDNF rescues deficits in basal synaptic transmission and hippocampal LTP in BDNF knockout mice. *Neuron* **16**, 1137–1145 (1996)
21. Heymach, J. V. & Shooter, E. M. The biosynthesis of neurotrophin heterodimers by transfected mammalian cells. *J. Biol. Chem.* **270**, 12297–12304 (1995)
22. Mowla, S. J. *et al.* Biosynthesis and post-translational processing of the precursor to brain-derived neurotrophic factor. *J. Biol. Chem.* **276**, 12660–12666 (2001).
23. Dechant, G. *et al.* Expression and binding characteristics of the BDNF receptor chick trkB. *Development* **119**, 545–558 (1993)
24. Mahadeo, D., Kaplan, L., Chao, M. V. & Hempstead, B. L. High affinity nerve growth factor binding displays a faster rate of association than p140trk binding — implications for multisubunit polypeptide receptors. *J. Biol. Chem.* **269**, 6884–6891 (1994).
25. Schnopel, A., von Schack, D., Dechant, G. & Barde, Y.-A. Early expression of the nerve growth factor receptor chkA in chick sympathetic and sensory ganglia. *Mol. Cell. Neurosci.* **6**, 544–556 (1995)
26. Arevalo, J. *et al.* TrkA immunoglobulin-like ligand binding domains inhibit spontaneous activation of the receptor. *Mol. Cell Biol.* **20**, 5908–5916 (2000)
27. Esposito, D. *et al.* The cytoplasmic and transmembrane domains of the p75 and TrkA receptors regulate high affinity binding to nerve growth factor. *J. Biol. Chem.* **276**, 32687–32695 (2001)
28. Hempstead, B. L., Martin-Zanca, D., Kaplan, D. R., Parada, L. F. & Chao, M. V. High-affinity NGF binding requires co-expression of the trk proto-oncogene and the low-affinity NGF receptor. *Nature* **350**, 678–683 (1991)
29. Benedetti, M., Levi, A. & Chao, M. V. Differential expression of nerve growth factor receptors leads to altered binding affinity and neurotrophin responsiveness. *Proc. Natl Acad. Sci. USA* **90**, 7859–7863 (1993).
30. Bibel, M., Hoppe, E. & Barde, Y. Biochemical and functional interactions between the neurotrophin receptors trk and p75NTR. *EMBO J.* **18**, 616–622 (1999)

31 Baloh, R., Enomoto, H., Johnson, E. & Milbrandt, J. The GDNF family ligands and receptors — implications for neural development. *Curr. Opin. Neurobiol.* 10, 103–110 (2000)
32. Ginty, D. & Segal, R. Retrograde neurotrophin signaling: Trk-ing along the axon. *Curr. Opin. Neurobiol.* 12, 268–274 (2002).
33. Grimes, M., Beattie, E. & Mobley, W. A signaling organelle containing the nerve growth factor-activated receptor tyrosine kinase, TrkA. *Proc. Natl Acad. Sci. USA* 94, 9909–9914 (1997).
34. Patapoutian, A. & Reichardt, L. Trk receptors: mediators of neurotrophin action. *Curr. Opin. Neurobiol.* 11, 272–280 (2001).
35. Hempstead, B. The many faces of p75NTR. *Curr. Opin. Neurobiol.* 12, 260–267 (2002).
36. Roux, P. & Barker, P. Neurotrophin signaling through the p75 neurotrophin receptor. *Prog. Neurobiol.* 67, 203–233 (2002).
37. Lonze, B. & Ginty, D. Function and regulation of CREB family transcription factors in the nervous system. *Neuron* 35, 605–623 (2002).
38. York, R. *et al.* Rac1 mediates sustained MAP kinase activation induced by nerve growth factor. *Nature* 392, 622–626 (1998).
39. Maddan, M. & Miller, F. Neuronal life and death decisions: functional antagonism between the Trk and p75 neurotrophin receptors. *Int. J. Dev. Neurosci.* 17, 153–161 (1999).
40. Dowling, P. *et al.* Upregulated p75NTR neurotrophin receptor on glial cells in MS plaques. *Neurology* 53, 1676–1682 (1999).
41. Roux, P., Colicos, M., Barker, P. & Kennedy, T. p75 neurotrophin receptor expression is induced in apoptotic neurons after seizure. *J. Neurosci.* 19, 6887–6896 (1999).
42. Beattie, M. *et al.* ProNGF induces p75-mediated death of oligodendrocytes following spinal cord injury. *Neuron* 36, 375–386 (2002).
43. Harrington, A. W., Kim, J. Y. & Yoon, S. O. Activation of Rac GTPase by p75 is necessary for c-jun N-terminal kinase-mediated apoptosis. *J. Neurosci.* 22, 156–166 (2002).
44. Khursigara, G. *et al.* A pro-survival function for the p75 receptor death domain-mediated via the caspase recruitment domain receptor interacting protein 2. *J. Neurosci.* 21, 5854–5863 (2001).
45. DeFreitas, M., McQuillen, P. & Shatz, C. A novel p75NTR signaling pathway promotes survival, not death, of immunocytofilled neocortical subplate neurons. *J. Neurosci.* 21, 5121–5129 (2001).
46. Lee, R., Kermani, P., Teng, K. & Hempstead, B. Regulation of cell survival by secreted proneurotrophins. *Science* 294, 1945–1948 (2001).
The precursor forms of neurotrophins have been implicated in the folding and processing of the mature proteins. This paper indicates that the pro-sequence of NGF preferentially binds to the p75 receptor.
47. Chao, M. V. Growth factor signaling: where is the specificity? *Cell* 68, 995–997 (1992).
48. Lohof, A. M., Ip, N. & Poo, M.-M. Potentiation of developing neuromuscular synapses by the neurotrophins NT-3 and BDNF. *Nature* 363, 350–353 (1993).
49. Kang, H. & Schuman, E. M. Long-lasting neurotrophin-induced enhancement of synaptic transmission in the adult hippocampus. *Science* 267, 1658–1662 (1995).
50. Levine, E. S., Dreyfus, C. F., Black, I. B. & Plummer, M. R. Brain-derived neurotrophic factor rapidly enhances synaptic transmission in hippocampal neurons via postsynaptic tyrosine kinase receptors. *Proc. Natl Acad. Sci. USA* 92, 8074–8077 (1995).
51. Xie, C. *et al.* Deficient long-term memory and long-lasting long-term potentiation in mice with a targeted deletion of neurotrophin-4. *Proc. Natl Acad. Sci. USA* 97, 8116–8121 (2000).
52. Korte, M. *et al.* Virus-mediated gene transfer into hippocampal CA1 region restores long-term potentiation in brain-derived neurotrophic factor mutant mice. *Proc. Natl Acad. Sci. USA* 93, 12547–12552 (1996).
53. Schuman, E. Neurotrophin regulation of synaptic transmission. *Curr. Opin. Neurobiol.* 9, 105–109 (1999).
54. Schinder, A. & Poo, M.-M. The neurotrophin hypothesis for synaptic plasticity. *Trends Neurosci.* 23, 639–645 (2000).
55. Yano, F. *et al.* PI-3 kinase and IP3 are both necessary and sufficient to mediate NT3-induced synaptic potentiation. *Nature Neurosci.* 4, 19–28 (2001).
56. Minichiello, L. *et al.* Essential role for TrkB receptors in hippocampus-mediated learning. *Neuron* 24, 401–414 (1999).
57. Minichiello, L. *et al.* Mechanism of TrkB-mediated hippocampal long-term potentiation. *Neuron* 36, 121–137 (2002).
58. Peterson, D. A., Dickinson-Anson, H. A., Leppert, J. T., Lee, K.-F. & Gage, F. H. Central neuronal loss and behavioral impairment in mice lacking neurotrophin receptor p75. *J. Comp. Neurol.* 404, 1–20 (1999).
59. von Schack, D. *et al.* Complete ablation of the neurotrophin receptor p75NTR causes defects both in the nervous and the vascular system. *Nature Neurosci.* 4, 977–978 (2001).
60. Dalva, M. *et al.* EphB receptors interact with NMDA receptors and regulate excitatory synapse formation. *Cell* 103, 945–956 (2000).
61. Grunwald, I. *et al.* Kinase-independent requirement of EphB2 receptors in hippocampal synaptic plasticity. *Neuron* 32, 1027–1040 (2001).
62. Henderson, J. *et al.* The receptor tyrosine kinase EphB2 regulates NMDA-dependent synaptic function. *Neuron* 32, 1041–1056 (2001).
63. Takasu, M., Dalva, M., Zigmond, R. & Greenberg, M. Modulation of NMDA receptor-dependent calcium influx and gene expression through EphB receptors. *Science* 295, 491–495 (2002).
64. Montell, C., Birnbaumer, L. & Flockerzi, V. The TRP channels, a remarkably functional family. *Cell* 108, 595–598 (2002).
65. Li, H., Xu, X. & Montell, C. Activation of a TRPC3-dependent cation current through the neurotrophin BDNF. *Neuron* 24, 261–273 (1999).
BDNF binding to TrkB produced a rapid influx of cations through TRPC3 that was dependent on activation of phospholipase C. An interaction between TrkB receptors and TRPC3 ion channels was observed, indicating that ion channels might be closely associated with receptor tyrosine kinases.
66. Caterina, M. *et al.* The capsaicin receptor: a heat-activated ion channel in the pain pathway. *Nature* 389, 816–824 (1997).
67. Shu, X. & Mendell, L. Neurotrophins and hyperalgesia. *Proc. Natl Acad. Sci. USA* 96, 7693–7696 (1999).
68. Chuang, H.-h. *et al.* Bradykinin and nerve growth factor release the capsaicin receptor from PtdIns(4,5)P_2-mediated inhibition. *Nature* 411, 957–962 (2001).
This study shows that the capsaicin (TRPV1) receptor is activated through NGF binding to TrkA receptors. The interaction between a receptor tyrosine kinase and a pain-related channel provides a mechanism for the ability of sensory neurons to respond to NGF-mediated heat sensitivity and also points to a mechanism for the heightened hyperalgesia that is observed after administration of neurotrophins in clinical trials of neurodegenerative diseases.
69. Johansen, M. *et al.* Intracerebroventricular infusion of nerve growth factor in three patients with Alzheimer's disease. *Dement. Geriat. Cogn.* 9, 246–257 (1998).
70. Thoenen, H. & Sendtner, M. Neurotrophins: from enthusiastic expectations through sobering experiences to rational therapeutic approaches. *Nature Neurosci.* 5, S1046–S1050 (2002).
71. Lin, S. *et al.* BDNF acutely increases tyrosine phosphorylation of the NMDA receptor subunit 2B in cortical and hippocampal postsynaptic densities. *Brain Res. Mol. Brain Res.* 55, 20–27 (1998).
72. Tucker, K. & Fadool, D. Neurotrophin modulation of voltage-gated potassium channels in rat through TrkB receptors is time and sensory experience dependent. *J. Physiol. (Lond.)* 54, 413–429 (2002).
73. Figurov, A., Pozzo-Miller, L., Olafsson, I., Wang, B. & Lu, B. Regulation of synaptic responses to high-frequency stimulation and LTP by neurotrophins in the hippocampus. *Nature* 381, 706–709 (1996).
74. Gottschalk, W., Pozzo-Miller, L., Figurov, A. & Lu, B. Presynaptic modulation of synaptic transmission and plasticity by brain-derived neurotrophic factor in the developing hippocampus. *J. Neurosci.* 18, 6830–6839 (1998).
75. Xu, B. *et al.* The role of brain-derived neurotrophic factors in the mature hippocampus: modulation of long-term potentiation through a presynaptic mechanism involving TrkB. *J. Neurosci.* 20, 6888–6897 (2000).
76. Kovalchuk, Y., Hanse, E., Kafitz, K. & Konnerth, A. Postsynaptic induction of BDNF-mediated long-term potentiation. *Science* 295, 1729–1734 (2002).
77. Balkowiec, A., Kunze, D. & Katz, D. Brain-derived neurotrophic factor acutely inhibits AMPA-mediated currents in developing sensory relay neurons. *J. Neurosci.* 20, 1904–1911 (2000).
78. Carroll, R., Beattie, E., von Zastrow, M. & Malenka, R. Role of AMPA receptor endocytosis in synaptic plasticity. *Nature Rev. Neurosci.* 2, 315–324 (2001).
79. Blum, R., Kafitz, K. & Konnerth, A. Neurotrophin-evoked depolarization requires the sodium channel $Na_v1.9$. *Nature* 419, 687–693 (2002).
80. Kafitz, K., Rose, C., Thoenen, H. & Konnerth, A. Neurotrophin-evoked rapid excitation through TrkB receptors. *Nature* 401, 918–921 (1999).
A remarkably rapid response of a sodium channel by BDNF treatment is documented in references 79 and 80.
81. Choi, D.-Y., Toledo-Aral, J., Segal, R. & Halegoua, S. Sustained signaling by phospholipase C-γ mediates nerve growth factor-triggered gene expression. *Mol. Cell Biol.* 21, 2695–2705 (2001).
82. Toledo-Aral, J., Brehm, P., Halegoua, S. & Mandel, G. A single pulse of nerve growth factor triggers long-term neuronal excitability through sodium channel gene induction. *Neuron* 14, 607–611 (1995).
83. Arevalo, J. *et al.* A novel mutation within the extracellular domain of TrkA causes constitutive receptor activation. *Oncogene* 20, 1229–1234 (2001).
84. Daub, H., Weiss, F. U., Wallasch, C. & Ullrich, A. Role of transactivation of the EGF receptor in signalling by G-protein coupled receptors. *Nature* 379, 557–560 (1996).
85. Luttrell, L., Daaka, Y. & Lefkowitz, R. Regulation of tyrosine kinase cascades by G-protein-coupled receptors. *Curr. Opin. Cell Biol.* 11, 177–183 (1999).
86. Lee, F. & Chao, M. Activation of Trk neurotrophin receptors in the absence of neurotrophins. *Proc. Natl Acad. Sci. USA* 92, 3555–3560 (2001).
87. Lee, F. S., Rajagopal, R., Kim, A. H., Chang, P. & Chao, M. V. Activation of Trk neurotrophin receptor signaling by pituitary adenylate cyclase-activating polypeptides. *J. Biol. Chem.* 277, 9096–9102 (2002).
88 Takei, N. *et al.* Pituitary adenylate cyclase-activating polypeptide promotes the survival of basal forebrain cholinergic neurons *in vitro* and *in vivo*: comparison with effects of nerve growth factor. *Eur. J. Neurosci.* 12, 2273–2280 (2000).
89 Williams, L. R. *et al.* Continuous infusion of NGF prevents basal forebrain neuronal death after fimbria fornix transection. *Proc. Natl Acad. Sci. USA* 83, 9231–9235 (1986).
90 Kolecha, S. *et al.* A D2 class dopamine receptor transactivates a receptor tyrosine kinase to inhibit NMDA receptor transmission. *Neuron* 35, 1111–1122 (2002).
91. Otto, C. *et al.* Impairment of mossy fiber long-term potentiation and associative learning in pituitary adenylate cyclase activating polypeptide type I receptor-deficient mice. *J. Neurosci.* 21, 5520–5527 (2001).
92. Hashimoto, H., Shintani, N. & Baba, A. Higher brain functions of PACAP and a homologous *Drosophila* memory gene amnesiac: insights from knockouts and mutants. *Biochem. Biophys. Res. Commun.* 297, 427–432 (2002).
93. Ledent, C. *et al.* Aggressiveness, hyperalgesia and high blood pressure in mice lacking the adenosine A2a receptor. *Nature* 388, 674–678 (1997).
94 Airaksinen, M. & Saarma, M. The GDNF family: signalling, biological functions and therapeutic value. *Nature Rev. Neurosci.* 3, 383–394 (2002).
95. Tsui-Pierchala, B., Milbrandt, J. & Johnson, E. NGF utilizes c-Ret via a novel GFL-independent, inter-RTK signaling mechanism to maintain the trophic status of mature sympathetic neurons. *Neuron* 33, 261–273 (2002).
96 Duman, R., Heninger, G. & Nestler, E. A molecular and cellular theory of depression. *Arch. Gen. Psychiatry* 54, 597–606 (1997).
97 Cai, D., Shen, Y., DeBellard, M., Tang, S. & Filbin, M. Prior exposure to neurotrophins blocks inhibition of axonal regeneration by MAG and myelin via a cAMP-dependent mechanism. *Neuron* 22, 89–101 (1999).
98 Luo, Y., Raible, D. & Raper, J. Collapsin, a protein in brain that induces the collapse and paralysis of neuronal growth cones. *Cell* 75, 217–227 (1993).
99. Tuttle, R. & O'Leary, D. Neurotrophins rapidly modulate growth cone response in the axon guidance molecule, collapsin-1. *Mol. Cell. Neurosci.* 11, 1–8 (1998).
100 Dontchev, V. & Letourneau, P. Nerve growth factor and semaphorin 3A signaling pathways interact in regulating sensory neuronal growth cone motility. *J. Neurosci.* 22, 6659–6669 (2002).
101. Fournier, A., GrandPre, T. & Strittmatter, S. Identification of a receptor mediating Nogo-66 inhibition of axonal regeneration. *Nature* 409, 341–346 (2001).
102 Wang, K. *et al.* Oligodendrocyte-myelin glycoprotein is a Nogo receptor ligand that inhibits neurite outgrowth. *Nature* 417, 941–944 (2002).
103 Liu, B., Fournier, A., GrandPre, T. & Strittmatter, S. Myelin-associated glycoprotein as a functional ligand for the Nogo-66 receptor. *Nature* 297, 1190–1193 (2002).
104 Domeniconi, M. *et al.* Myelin-associated glycoprotein interacts with the Nogo-66 receptor to inhibit neurite outgrowth. *Neuron* 35, 283–290 (2002).
105. Wang, K., Kim, J., Sivasankaran, R., Segal, R. & He, Z. p75 interacts with the Nogo receptor as a co-receptor for Nogo, MAG and OMgp. *Nature* 420, 74–78 (2002).
106 Wong, S. *et al.* A $p75^{NTR}$ and Nogo receptor complex mediates repulsive signaling by myelin-associated glycoprotein. *Nature Neurosci.* 5, 1302–1308 (2002).
These papers merge neurotrophin receptor signalling to inhibition of regeneration in the CNS through the

actions of three unrelated proteins — Nogo, p75 and MAG.
107. Yamashita, T., Higuchi, H. & Tohyama, M. The p75 receptor transduces the signal from myelin-associated glycoprotein to Rho. *J. Cell Biol.* 157, 565–570 (2002)
An important link is made between the ability of MAG to block axonal growth and Rho activity through the p75 receptor. The results led to the experiments showing that the p75 and Nogo receptors act in a complex.
108. Yamashita, T., Tucker, K. & Barde, Y. Neurotrophin binding to the p75 receptor modulates Rho activity and axonal outgrowth. *Neuron* 24, 585–593 (1999).
109. Walsh, G., Krol, K., Crutcher, K. & Kawaja, M. Enhanced neurotrophin-induced axon growth in myelinated portions of the CNS in mice lacking the p75 neurotrophin receptor. *J. Neurosci.* 19, 4155–4168 (1999).
110. Dobrowsky, R. T. & Carter, B. D. p75 neurotrophin receptor signaling: mechanisms for neurotrophic modulation of cell stress? *J. Neurosci. Res.* 61, 237–243 (2000).
111. Cosgaya, J. & Shooter, E. Binding of nerve growth factor to its p75 receptor in stressed cells induces selective IκB-β degradation and NF-κB nuclear translocation. *J. Neurochem.* 79, 391–399 (2001).
112. Sklar, P. *et al.* Family-based association study of 76 candidate genes in bipolar disorder: BDNF is a potential risk locus. *Mol. Psychiatry* 7, 579–593 (2002).
113. Neves-Pereira, M. *et al.* The brain-derived neurotrophic factor gene confers susceptibility to bipolar disorder: evidence from a family-based association study. *Am. J. Hum. Genet.* 71, 651–655 (2002).
114. Sen, S. *et al.* A BDNF coding variant is associated with the NEO personality inventory domain neuroticism, a risk factor for depression. *Neuropsychopharmacology* 28, 397–401 (2003).
115. Egan, M. *et al.* The BDNF val66met polymorphism affects activity-dependent secretion of BDNF and human memory and hippocampal function. *Cell* 112, 257–269 (2003)
This study is the first to show that a human polymorphism in BDNF is associated with memory deficits. A single amino acid variation in the pro-domain of BDNF accounts for the ability of BDNF to undergo proper secretion.
116. Ventriglia, M. *et al.* Association between the BDNF 196 A/G polymorphism and sporadic Alzheimer's disease. *Mol. Psychiatry* 7, 136–137 (2002).
117. Smith, M., Makino, S., Kvetnansky, R. & Post, R. Stress alters the expression of brain-derived neurotrophic factor and neurotrophin-3 mRNAs in the hippocampus. *J. Neurosci.* 15, 1768–1777 (1995).
118. Uevama, T. *et al.* Immobilization stress reduced the expression of neurotrophins and their receptors in the rat brain. *Brain Res.* 28, 103–110 (1997).
119. Shirayama, Y., Chen, A., Nakagawa, S., Russell, D. & Duman, R. Brain-derived neurotrophic factor produces antidepressant effects in behavioral models of depression. *J. Neurosci.* 22, 3251–3261 (2002)
Administration of exogenous BDNF exerted profound positive effects in forced swim and learned helplessness assays, indicating that BDNF signalling might be related to depression.
120. Elliott, T. & Shadbolt, N. Competition for neurotrophic factors: mathematical analysis. *Neural Comput.* 10, 1939–1981 (1998).
121. Crowley, C. *et al.* Mice lacking nerve growth factor display perinatal loss of sensory and sympathetic neurons yet develop basal forebrain cholinergic neurons. *Cell* 76, 1001–1012 (1994).
122. Bartoletti, A. *et al.* Heterozygous knock-out mice for brain-derived neurotrophic factor show a pathway-specific impairment of long-term potentiation but normal critical period for monocular deprivation. *J. Neurosci.* 22, 10072–10077 (2002).
123. Dluzen, D. *et al.* Evaluation of nigrostriatal dopaminergic function in adult +/+ and +/– BDNF mutant mice. *Exp. Neurol.* 170, 121–128 (2001).
124. Carroll, P., Lewin, G., Koltzenburg, M., Toyka, K. & Thoenen, H. A role for BDNF in mechanosensation. *Nature Neurosci.* 1, 42–46 (1998).
125. Ernfors, P., Lee, K. F. & Jaenisch, R. Mice lacking brain-derived neurotrophic factor develop with sensory deficits. *Nature* 368, 147–150 (1994).
126. Bianchi, L. *et al.* Degeneration of vestibular neurons in late embryogenesis of both heterozygous and homozygous *BDNF* null mutant mice. *Development* 122, 1965–1973 (1996).
127. Elmer, E. *et al.* Suppressed kindling epileptogenesis and perturbed *BDNF* and *TrkB* gene regulation in *NT-3* mutant mice. *Exp. Neurol.* 145, 93–103 (1997).
128. Donovan, M., Hahn, R., Tessarollo, L. & Hempstead, B. Neurotrophin-3 is required for mammalian cardiac development: identification of an essential nonneuronal neurotrophin function. *Nature Neurosci.* 14, 210–213 (1996).
129. Airaksinen, M. *et al.* Specific subtypes of cutaneous mechanoreceptors require neurotrophin-3 following peripheral target innervation. *Neuron* 16, 287–295 (1996).
130. Ernfors, P., Lee, K.-F., Kucera, J. & Jaenisch, R. Lack of neurotrophin-3 leads to deficiencies in the peripheral nervous system and loss of limb proprioceptive afferents. *Cell* 77, 503–512 (1994).
131. DiStefano, P., Chelsea, D., Schick, C. & McKelvy, J. Involvement of a metalloprotease in low-affinity nerve growth factor receptor truncation: inhibition of truncation in vitro and in vivo. *J. Neurosci.* 13, 2405–2414 (1993).
132. Schecterson, L., Kanning, K., Hudson, M. & Bothwell, M. The neurotrophin receptor p75 is cleaved by regulated intramembranous proteolysis. *Soc. Neurosci. Abstr.* 27, 822.10 (2002)
Intramembranous cleavage of Notch, the amyloid precursor protein and ErbB4 receptors generates intracellular cytoplasmic fragments that produce marked changes in signalling and transcriptional activities. The cleavage of p75 by a γ-secretase reveals a new mechanism for transmitting neurotrophin signals from the cell surface to intracellular locations.
133. Brown, M., Yu, J., Rawson, R. & Goldstein, J. Regulated intramembrane proteolysis: a control mechanism conserved from bacteria to humans. *Cell* 100, 391–398 (2000).
134. Fahnestock, M., Michalski, B., Xu, B. & Coughlin, M. The precursor pro-nerve growth factor is the predominant form of nerve growth factor in brain and is increased in Alzheimer's disease. *Mol. Cell. Neurosci.* 18, 210–220 (2001).
135. Cosgaya, J. M., Chan, J. R. & Shooter, E. M. The neurotrophin receptor $p75^{NTR}$ as a positive modulator of myelination. *Science* 298, 1245–1248 (2002)
136. Wu, C., Lai, C. F. & Mobley, W. C. Nerve growth factor activates persistent Rap1 signaling in endosomes. *J. Neurosci.* 21, 5406–5416 (2001).
137. Lee, F., Rajagopal, R., Kim, A., Chang, P. & Chao, M. Activation of Trk neurotrophin receptor signaling by pituitary adenylate cyclase-activating polypeptides. *J. Biol. Chem.* 277, 9096–9102 (2002).
138. Chen, M. *et al.* Nogo-A is a myelin-associated neurite outgrowth inhibitor and an antigen for monoclonal antibody IN-1. *Nature* 403, 434–439 (2000).
139. Ernfors, P., Henschen, A., Olson, L. & Persson, H. Expression of nerve growth factor receptor mRNA is developmentally regulated and increased after axotomy in rat spinal cord motoneurons. *Neuron* 2, 1605–1613 (1989).
140. Kokaia, Z., Andsberg, G., Martinez-Serrano, A. & Lindvall, O. Focal cerebral ischemia in rats induces expression of p75 neurotrophin receptor in resistant striatal cholinergic neurons. *Neuroscience* 84, 1113–1125 (1998).
141. Hayes, R., Wiley, R. & Armstrong, D. Induction of nerve growth factor receptor (p75NGFr) mRNA within hypoglossal motoneurons following axonal injury. *Brain Res. Mol. Brain Res.* 15, 291–297 (1992).
142. Martinez-Murillo, R., Fernandez, A., Bentura, M. & Rodrigo, J. Subcellular localization of low-affinity nerve growth factor receptor-immunoreactive protein in adult rat Purkinje cells following traumatic injury. *Exp. Brain Res.* 119, 47–57 (1998).
143. Friedman, W. Neurotrophins induce death of hippocampal neurons via the p75 receptor. *J. Neurosci.* 20, 6340–6346 (2000).
144. Kokaia, Z., Andsberg, G., Martinez-Serrano, A. & Lindvall, O. Focal cerebral ischemia in rats induces expression of p75 neurotrophin receptor in resistant striatal cholinergic neurons. *Neuroscience* 84, 1113–1125 (1998).
145. Park, J., Lee, J., Sato, T. & Koh, J. Co-induction of p75NTR and p75NTR-associated death executor in neurons after zinc exposure in cortical culture or transient ischemia in the rat. *J. Neurosci.* 20, 9096–9103 (2000).
146. Mufson, E. & Kordower, J. Cortical neurons express nerve growth factor receptors in advanced age and Alzheimer's disease. *Proc. Natl Acad. Sci. USA* 89, 569–573 (1992).
147. Lemke, G. & Chao, M. V. Axons regulate Schwann cell expression of major myelin and NGF receptor genes. *Development* 102, 499–504 (1988).
148. Taniuchi, M., Clark, H., Schweitzer, J. & Johnson, E. Expression of nerve growth factor receptors by Schwann cells of axotomized peripheral nerves: ultrastructural location, suppression by axonal contact, and binding properties. *J. Neurosci.* 8, 664–681 (1988).
149. Chang, A., Nishiyama, A., Peterson, J., Prineas, J. & Trapp, B. NG2-positive oligodendrocyte progenitor cells in adult human brain and multiple sclerosis lesions. *J. Neurosci.* 20, 6404–6412 (2000).
150. Calza, L., Giardino, L., Pozza, M., Micera, A. & Aloe, L. Time-course changes of nerve growth factor, corticotropin-releasing hormone and nitric oxide synthase isoforms and their possible role in the development of inflammatory response in experimental allergic encephalomyelitis. *Proc. Natl Acad. Sci. USA* 94, 3368–3373 (1997).
151. Nataf, S. *et al.* Low affinity NGF receptor expression in the central nervous system during experimental allergic encephalomyelitis. *J. Neurosci. Res.* 52, 83–92 (1998).
152. Hu, X.-Y. *et al.* Increased $p75^{NTR}$ expression in hippocampal neurons containing hyperphosphorylated τ in Alzheimer patients. *Exp. Neurol.* 178, 104–111 (2002).

Acknowledgement
The assistance of Albert Kim is gratefully acknowledged.

Online links

DATABASES
The following terms in this article are linked online to:
Swiss-Prot: http://ca.expasy.org/sprot/
BDNF | CREB | GDNF | JNK1 | K_v1.3 | MAG | Na_v1.9 | NF-κB | NGF | Nogo | PACAP | Semaphorin 3A | Shc | TrkA | TrkB | TrkC | Tumour necrosis factor
OMIM: http://www.ncbi.nlm.nih.gov/Omim/
Alzheimer disease
Access to this interactive links box is free online.

The EMBO Journal Vol.18 No.3 pp.616–622, 1999

Biochemical and functional interactions between the neurotrophin receptors *trk* and p75^{NTR}

Miriam Bibel[1], Edmund Hoppe[2] and Yves-Alain Barde

Max-Planck Institute of Neurobiology, Department of Neurobiochemistry, 82152 Planegg-Martinsried, Germany

[2]Present address: Hoechst Marion Roussel, Fraunhoferstraße 22, 82152 Martinsried, Germany

[1]Corresponding author
e-mail: miriam@neuro.mpg.de

Neurotrophins bind to two structurally unrelated receptors, the *trk* tyrosine kinases and the neurotrophin receptor p75^{NTR}. Ligand activation of these two types of receptor can lead to opposite actions, in particular the prevention or activation of programmed cell death. Many cells co-express *trk* receptors and p75^{NTR}, and we found that p75^{NTR} was co-precipitated with *trk*A, *trk*B and *trk*C in cells transfected with both receptor types. Co-precipitation of p75^{NTR} was not observed with the epidermal growth factor receptor. Experiments with deletion constructs of *trk*B (the most abundant *trk* receptor in the brain) and p75^{NTR} revealed that both the extracellular and intracellular domains of *trk*B and p75^{NTR} contribute to the interaction. Blocking autophosphorylation of *trk*B substantially reduced the interactions between p75^{NTR} and *trk*B constructs containing the intracellular, but not the extracellular, domains. We also found that co-expression of p75^{NTR} with *trk*B resulted in a clear increase in the specificity of *trk*B activation by brain-derived neurotrophic factor, compared with neurotrophin-3 and neurotrophin-4/5. These results indicate a close proximity of the two neurotrophin receptors within cell membranes, and suggest that the signalling pathways they initiate may interact soon after their activation.

Keywords: BDNF/NT3/NT4/neurotrophins/receptors

Introduction

All known members of the nerve growth factor (NGF) family, designated the neurotrophins, bind to two different types of receptors, the *trk* tyrosine kinases and the neurotrophin receptor p75^{NTR} (Bothwell, 1991; Chao, 1992; Meakin and Shooter, 1992). In mammals, three different *trk* receptors have been identified and are activated by one or more of the four neurotrophins (for review see Barbacid, 1994). Binding of the neurotrophins to the *trk* receptors leads to receptor tyrosine phosphorylation, triggering the activation of pathways leading to the prevention of programmed cell death during development (Kaplan and Miller, 1997). Studies with antibodies and with mouse mutants have established that each neurotrophin and *trk* receptor is required during neural development, the elimination of any one of these components leading to specific deficits in the nervous system (Snider, 1994; Lewin and Barde, 1996).

All neurotrophins also bind to the neurotrophin receptor p75^{NTR}, a member of the tumour necrosis factor (TNF) receptor and FAS/Apo-1/CD95 family. Following the discovery of the *trk* receptors as mediators of the trophic effects of the neurotrophins, the role of p75^{NTR} was mostly discussed as that of an accessory receptor modulating the signalling of the *trk* receptors (Chao and Hempstead, 1995). Recently however, p75^{NTR} has also been shown to mediate cell death in a ligand-dependent fashion (Casaccia-Bonnefil *et al.*, 1996; Bamji *et al.*, 1998; Davey and Davies, 1998), a function similar to that demonstrated previously with the structural parents of p75^{NTR}, namely the TNF receptor 1 and CD95. Evidence for this new function of p75^{NTR} has also been obtained *in vivo* in the avian retina (Frade *et al.*, 1996; Frade and Barde, 1998), in mouse sympathetic ganglia (Bamji *et al.*, 1998) and in the developing spinal cord of mice carrying a mutation in the *nef* or the *p75* gene (Frade and Barde, 1999).

In view of these observations and the fact that many neuronal populations co-express *trk* receptors and p75^{NTR}, we tested to see whether an interaction between both receptor types could be demonstrated by immunoprecipitation in transfected cells. While this question has been addressed in previous studies, work has focused on p75^{NTR} and *trk*A using either cross-linking (Huber and Chao, 1995; Gargano *et al.*, 1997) or co-patching techniques (Ross *et al.*, 1996). As *trk*B can be activated by three different neurotrophins, namely brain-derived neurotrophic factor (BDNF), neurotrophin-4/5 (NT4/5) and neurotrophin-3 (NT3), we also investigated the extent to which co-expression of p75^{NTR} with *trk*B modulates the ligand specificity of this receptor.

Results

Co-immunoprecipitation of p75^{NTR} with trkA, trkB and trkC

Comparable conditions for immunoprecipitation of the rat receptors *trk*A, *trk*B and *trk*C were established by tagging the three receptors at their N-terminal ends using a nine amino acid hemagglutinin (HA) epitope. The ability of the tagged receptors to bind neurotrophins was determined in cross-linking experiments using radiolabelled neurotrophins and by ligand-induced receptor phosphorylation (data not shown). These three cDNAs were used to transfect A293 cells together with rat p75^{NTR} at a ratio of 1:1. Following cell lysis with 1.0% Triton X-100, the *trk* receptors were precipitated with anti-HA antibodies and the immunoprecipitates analysed by Western blotting with anti-p75 antibodies. These experiments revealed that

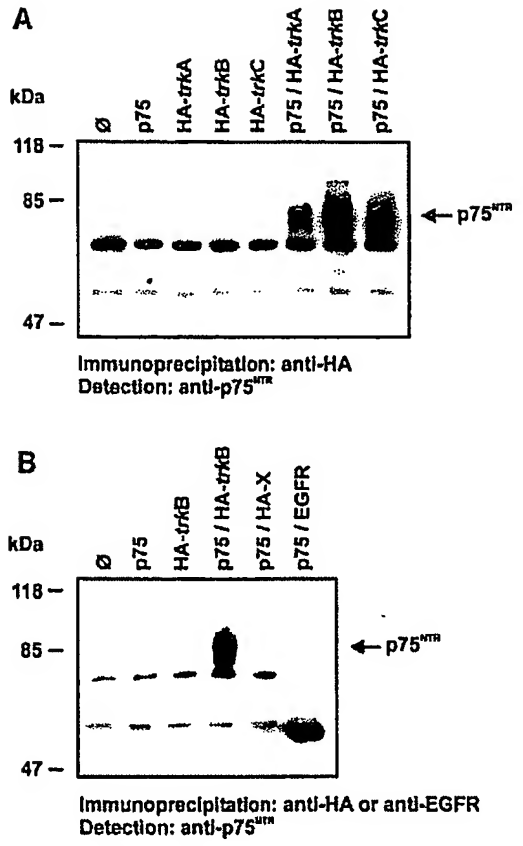

Fig. 1. Co-immunoprecipitation of p75^{NTR} with the *trk* receptors. (A) A293 cells were transiently transfected with the various constructs as indicated. Cells were lysed after 2 days and HA-tagged trk receptors were precipitated with an anti-HA mAb. Immunoprecipitates were run on a 7% acrylamide SDS gel followed by Western blotting. Detection was performed with a polyclonal anti-p75 antibody. (B) Co-immunoprecipitation was carried out as in (A) except that the EGF receptor (EGFR) was precipitated with a mAb to the EGF receptor. HA-X denotes a HA-tagged phosphodiesterase as a control. The signals observed in all lanes result from antibody cross-reactivities.

p75^{NTR} is co-immunoprecipitated with *trk*A, *trk*B and *trk*C (Figure 1A). Like rat p75^{NTR}, chick p75^{NTR} was also co-immunoprecipitated (data not shown).

When similar experiments were performed with the epidermal growth factor (EGF) receptor using a monoclonal antibody (mAb) to the EGF receptor, no co-immunoprecipitation of p75^{NTR} could be detected (Figure 1B).

To test whether expression of both receptors in the same cells is needed for the *trk*–p75^{NTR} interaction, the *trk* and p75^{NTR} constructs were expressed in separate sets of cells and the immunoprecipitation performed as above after mixing the cell extracts. No co-immunoprecipitation of p75^{NTR} could be detected under these conditions (data not shown).

Although all three *trk* receptors behaved similarly in their ability to associate and co-precipitate p75^{NTR}, subsequent investigations focused on *trk*B, as this is the most abundant of the *trk* receptors expressed in brain tissue. Also, previous studies have established that *trk*B can be activated in fibroblasts by three different neurotrophins (see below).

Mapping trkB and p75^{NTR} interacting domains

We were interested in delineating the receptor domains involved in the interaction and designed various deletion constructs of p75^{NTR} and *trk*B. The *trk*B receptor also exists as a splice-variant form lacking the tyrosine kinase domain, raising the question of whether the truncated form of this receptor would also interact with p75^{NTR}.

To facilitate comparisons between the constructs, the HA epitope was preserved in the *trk*B constructs, as was the p75^{NTR} detection epitope (Figure 2). Deletion mutants were constructed for each receptor lacking either most of the intracellular domain (ΔICD) or the extracellular domain (ΔECD). *trk*B ΔICD essentially corresponds to the naturally occurring *trk*B splice variant designated T1 and lacking the tyrosine kinase domain. p75^{NTR} ΔICD, as well as p75^{NTR} ΔECD, co-immunoprecipitated with full-length *trk*B (Figure 3A). Likewise, *trk*B ΔICD and *trk*B ΔECD co-immunoprecipitated with full-length p75^{NTR}. The weakest interaction was found between p75^{NTR} and *trk*B ΔECD (Figure 3B). Also, p75^{NTR} ΔECD and *trk*B ΔECD, as well as p75^{NTR} ΔICD and *trk*B ΔICD, co-immunoprecipitated, but no detectable interactions could be seen when p75^{NTR} ΔICD was expressed together with *trk*B ΔECD (Figure 3C). In sum, these mapping studies indicate that interaction between p75^{NTR} and *trk*B involves the extracellular, as well as intracellular, domains of both receptors. However, the transmembrane sequence (which is common to all the constructs tested) does not seem to be sufficient for a stable interaction under our experimental conditions.

The trkB–p75^{NTR} interaction is K-252a sensitive

The demonstration by immunoprecipitation of an interaction between *trk* receptors and p75^{NTR} necessitates receptor over-expression. This leads to phosphorylation of the *trk* receptors due to their propensity to dimerize in a ligand-independent fashion. As our results indicate that the intracellular domain of *trk*B interacts with p75^{NTR} (see above), the question arises as to whether the phosphorylation status of *trk*B influences the formation of the *trk*B–p75^{NTR} complex. This possibility was tested using the kinase inhibitor K-252a. A dose-dependent reduction of the *trk*B–p75^{NTR} interaction was observed, with a slight inhibition at 500 nM K-252a and a marked reduction at 1 μM K-252a (Figure 4). To test whether the effects of K-252a result from an action of the alkaloid on the intracellular domain of *trk*B, we used the *trk*B ΔECD construct with p75^{NTR}. The interaction between the two receptors was inhibited almost completely with 500 nM K-252a. In contrast, the interaction of *trk*B T1 with p75^{NTR} was not influenced by K-252a. Therefore these experiments indicate that the K252a-mediated inhibition of receptor interaction is due to its action on the intracellular domain of *trk*B, and that the phosphorylated form of *trk*B is predominantly involved in the interaction with p75^{NTR}.

p75^{NTR} influences the specificity of ligand-dependent phosphorylation of trkB

The close proximity of the two receptors may affect their ability to be activated by different ligands. As *trk*B can

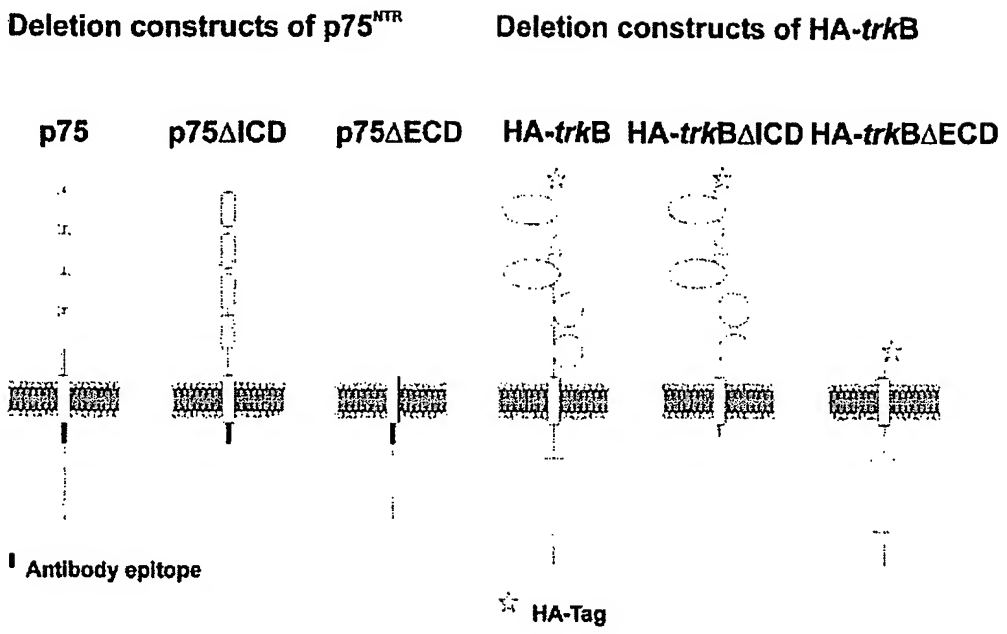

Fig. 2. Deletion constructs of p75^{NTR} and HA-*trk*B.

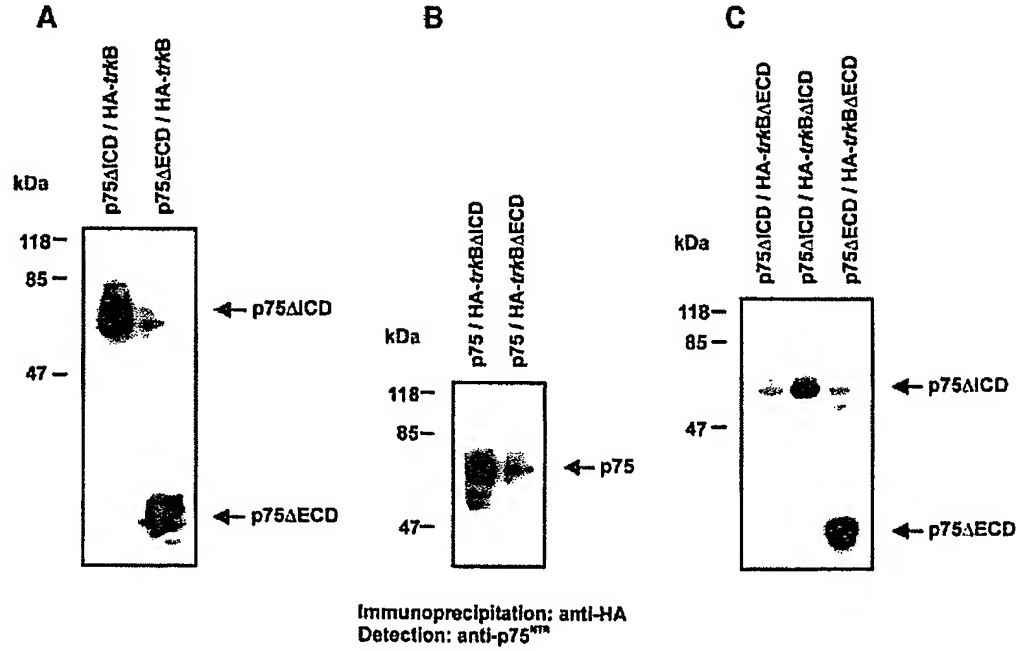

Fig. 3. Co-immunoprecipitation of the deletion constructs of p75^{NTR} and *trk*B. (A) Deletion constructs of p75^{NTR} co-immunoprecipitated with full-length HA-*trk*B. (B) Full-length p75^{NTR} co-immunoprecipitated with deletion constructs of HA-*trk*B. (C) Co-immunoprecipitation of deletion constructs of both receptors. The experiments were performed as described in Figure 1, except that 10% acrylamide SDS gels were used. Note that p75ΔICD and HA-*trk*BΔECD do not interact. The interaction of p75^{NTR} full-length with HA-*trk*BΔECD is significantly weaker.

be activated by BDNF, NT4/5 and NT3, we asked whether p75^{NTR} increases the ligand selectivity of *trk*B. Ligand-dependent *trk*B phosphorylation was investigated in A293 cells stably transfected with a *trk*B construct that can be readily activated by three different neurotrophins (*trk*B-L, Strohmaier *et al.*, 1996). These cells were transiently transfected with various p75^{NTR} constructs. Whereas the BDNF-induced phosphorylation of *trk*B remained unchanged with p75^{NTR} co-expression (Figure 5), that induced by NT4/5 and NT3 was clearly reduced. This increased selectivity was dose-dependent, being more prominent at lower neurotrophin concentrations and not readily apparent at 100 ng/ml neurotrophin (data not shown). p75^{NTR} ΔICD also mediated the increased ligand

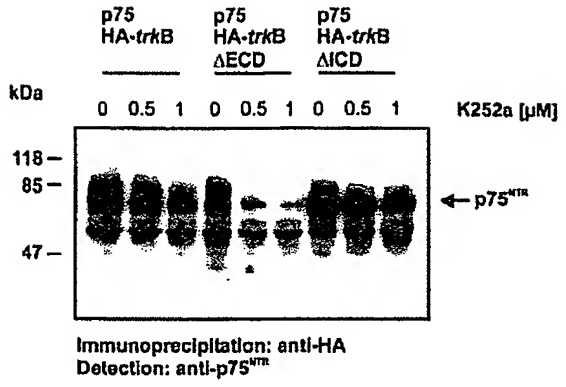

Fig. 4. Inhibition of the p75^{NTR}–HA-*trk*B interaction by K-252a. Transiently transfected A293 cells were treated with K-252a for 24 h before lysis. Co-immunoprecipitation was performed as in Figure 1.

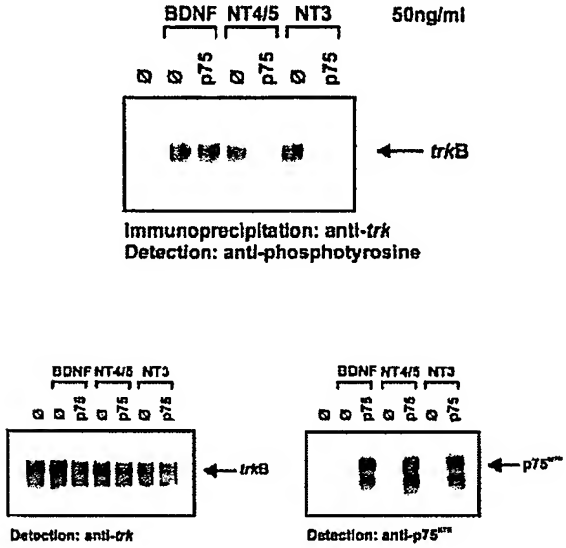

Fig. 5. Influence of p75^{NTR} on ligand-induced autophosphorylation of *trk*B. Following incubation in serum-free medium (see Materials and methods), cells stably transfected with *trk*B were incubated with neurotrophin (50 ng/ml) for 5 min at 37°C. Cell lysates were immunoprecipitated and analysed using a phosphotyrosine antibody. Following stripping, the blots were reprobed with a pantrk antibody to check for receptor expression levels. Cell lysates were also checked for p75^{NTR} expression levels.

specificity of *trk*B (data not shown). From these experiments we conclude that one of the consequences of the *trk*B–p75^{NTR} interaction is a marked increase in the selectivity of *trk*B for BDNF-mediated receptor phosphorylation, and that this effect is more likely to be accounted for by direct receptor interaction than by p75^{NTR}-mediated signalling.

Discussion

The possibility of *trk*–p75^{NTR} receptor association has been raised ever since two different receptors were shown to bind the neurotrophins. This question is all the more pressing since both receptors are now known to signal, and that this signalling may lead to results as different as cell death or cell survival. Our study provides evidence for a direct association between the *trk* receptors and p75^{NTR}, as demonstrated by co-immunoprecipitation. This association is relevant to the *trk* function in intact cells, as it leads to an increase in ligand specificity.

Previous biochemical studies on trk–p75^{NTR} interactions

The question of an association between the *trk* receptors and p75^{NTR} has already been addressed in previous studies with *trk*A. Chemical cross-linking was used, either with radiolabelled NGF (Huber and Chao, 1995), or by reversibly cross-linking receptors expressed in Sf9 insect cells (Gargano *et al.*, 1997). Also, co-patching studies with fluorescently labelled receptors (Wolf *et al.*, 1995; Ross *et al.*, 1996) suggested a co-localization of the receptors in cell membranes using Sf9 cells. Curiously, no such evidence could be obtained in similar experiments using *trk*B instead of *trk*A (Wolf *et al.*, 1995; Ross *et al.*, 1996). Functionally, co-operation between p75^{NTR} and all three *trk* receptors has been obtained in transfected cells by showing that co-expression increases responsiveness to low neurotrophin concentrations, but in these and other experiments the demonstration of co-immunoprecipitation of p75^{NTR} and *trk* failed (Hantzopoulos *et al.*, 1994). The explanation as to why we eventually succeeded in demonstrating a biochemical interaction between p75^{NTR} and all three *trk* receptors may lie in the tagging procedure. It is possible that antibodies used previously to test receptor association may have either interfered with the formation of a *trk*–p75^{NTR} receptor complex or did not recognise the receptor complex. In particular, we note that Gargano and colleagues documented the observation that, whereas antibodies to p75^{NTR} efficiently co-precipitated p75^{NTR} cross-linked to *trk*A, antibodies to *trk*A did not detectably co-precipitated p75^{NTR} (Gargano *et al.*, 1997). Also, it is conceivable that the A293 cells used in this study offer a favourable context to study the interactions between p75^{NTR} and *trk* receptors, for example by providing cytoplasmic proteins that stabilise the interaction. However, merely mixing detergent extracts of cells expressing only one receptor type does not lead to receptor association (see Results).

Functional evidence for a trk–p75^{NTR} association

Whereas there is no doubt that the *trk* receptors play a key role in mediating the trophic effects of neurotrophins, it is also clear that the expression of *trk* receptors does not account for all neurotrophin receptor properties on neurons. For example, NGF binds with high affinity to sensory neurons ($\sim 10^{-11}$ M; Sutter *et al.*, 1979), and most of the sites formed by *trk*A are of a low-affinity type (Mahadeo *et al.*, 1994). Similar observations were made with BDNF and *trk*B (compare for example Rodriguez-Tébar and Barde (1988) with Dechant *et al.* (1993)). In addition, co-expression of both p75^{NTR} and *trk*A in the same cells leads to the formation of high-affinity receptors (Hempstead *et al.*, 1991; Mahadeo *et al.*, 1994). That the formation of high-affinity binding sites is of functional significance is well established for NGF. For example, studies with PC12 cells indicate a reduced activation of *trk*A at low NGF concentrations when binding to p75^{NTR} is prevented (Barker and Shooter, 1994; see also Verdi *et al.*, 1994). Moreover, in mice carrying a deletion in

the NGF-binding domain of p75^{NTR}, substantial sensory deficits have been observed, and neurons isolated from such mice display a decreased sensitivity to low concentrations of NGF (Lee *et al.*, 1992, 1994; Davies *et al.*, 1993). In line with this, two recent studies have shown that a mutated form of NGF unable to bind to p75^{NTR}, but capable of activating *trk*A, is less active than wild-type NGF in supporting the survival of p75^{NTR}/trkA expressing neurons at low ligand concentrations (Horton *et al.*, 1997; Rydén *et al.*, 1997).

Of special relevance to the present study are previous indications that an additional function of the *trk*–p75^{NTR} association may be an increased ligand specificity. Thus, sympathetic neurons isolated from *p75$^{NTR-/-}$* animals are more responsive to NT3 than wild-type neurons (Lee *et al.*, 1994) and PC12 cells have an increased responsiveness to NT3 when p75^{NTR} levels are reduced (Benedetti *et al.*, 1993).

Finally, there is evidence for a modulation of p75^{NTR}-mediated sphingomyelin hydrolysis by *trk*A (Dobrowsky *et al.*, 1995).

Properties of the trk–p75^{NTR} association

Our experiments indicate that the interaction of p75^{NTR} with all three *trk* receptors is stable enough to resist detergent solubilization in a buffer containing 1% Triton X-100. It is thus unlikely that the association results from hydrophobic interactions within the membrane, and co-transfection with constructs only able to interact with their transmembrane domains are in line with this interpretation. In this context, it is interesting to note that a previous study using a reversible cross-linker of *trk*A and p75^{NTR} also concluded that transmembrane interaction is unlikely to participate significantly in receptor interactions (Gargano *et al.*, 1997). Our mapping experiments indicate that both the extracellular and intracellular domains of the receptors seem to be sufficient to drive a stable association of the two receptors. This result is in agreement with that of Gargano *et al.* (1997), who used deletion constructs of *trk*A and p75^{NTR}. However, the finding that the association with the intracellular domain of *trk*B is K252a-sensitive raises the possibility that in the absence of receptor phosphorylation, the interaction may be driven mainly by the extracellular domains of the receptor. The possibility therefore exists that the state of phosphorylation of the *trk* receptors modulates the strength of the interactions of the *trk* receptor with p75^{NTR}, and our findings suggest that phosphorylation of *trk* would reinforce the interaction with p75^{NTR}. Clearly not all tyrosine kinase receptors interact with p75^{NTR} as no co-immunoprecipitation could be demonstrated with the EGF receptor.

Beyond co-immunoprecipitation, the most direct indication for an interaction between *trk* receptors and p75^{NTR} is the increase in ligand specificity of *trk*B when p75^{NTR} is co-expressed with *trk*B. The details of the mechanisms by which p75^{NTR} increases ligand specificity are unclear. It is conceivable that the association of p75^{NTR} with the *trk* receptors changes their conformation leading to increased ligand-binding specificity. Such a mechanism could also be responsible for the enhanced binding of NGF to *trk*A in the presence of p75^{NTR} (Barker and Shooter, 1994; Verdi *et al.*, 1994). In theory, signalling through p75^{NTR} following ligand binding could also be a mechanism leading to increased ligand specificity. In particular, a recent report indicates that BDNF can activate p75^{NTR} to cause serine phosphorylation of *trk*A (MacPhee and Barker, 1997). But as our results with p75^{NTR} carrying a large deletion in the intracellular domain indicate, this construct is equally effective in increasing ligand specificity, compared with full-length p75^{NTR}, we consider this possibility unlikely. Previously we have reported that a chick *trk*B splice variant lacking exon 9 coding for 11 amino acids in the extracellular juxtamembrane domain of *trk*B also shows an increased selectivity for BDNF, compared with NT4/5 and NT3, even in the absence of expression of p75^{NTR} (Strohmaier *et al.*, 1996). A similar variant of *trk*B with increased selectivity for BDNF was also found in human retinal pigmented epithelium (Hackett *et al.*, 1998). Taken together, these results indicate that there are at least two different ways by which the selectivity of *trk*B for BDNF can be increased. This is particularly relevant in the context of numerous previous reports indicating that BDNF has trophic activities on a variety of neurons that differ from those of NT4/5, even though both ligands bind to *trk*B.

Conclusion

The results of this study point to a close association of *trk* and p75^{NTR} receptors in cellular membranes and that one outcome of receptor association is an increased ligand specificity. Close association of these two different receptor types suggests that their signalling pathways may interact with each other as soon as they are activated.

Materials and methods

Cell culture and reagents

A293 cells (Graham *et al.*, 1977) were cultured in Dulbecco's modified Eagle's medium (DMEM, Gibco-BRL) supplemented with 10% fetal calf serum (Boehringer Mannheim) at 37°C and 5% CO_2. The A293 cell line stably expressing chick *trk*B had been established previously and was used as described in Dechant *et al.* (1993). K-252a was from the Alexis Corporation.

Construction of p75^{NTR}- and trk-expression plasmids and deletion mutants

Rat p75^{NTR} full-length and the p75^{NTR} extracellular domain (ΔICD) were cloned in the mammalian expression vector pcDNA3 (Invitrogen). The intracellular domain of p75^{NTR} (ΔECD), rat *trk*B and the *trk*B constructs, as well as *trk*A and *trk*C, were cloned in the pRC/CMV AC7 vector, a derivative of the pRC/CMV vector (Invitrogen), which contains the BM40 signal peptide (Maver *et al.*, 1994). In all cases expression was driven from the CMV promoter.

Rat p75^{NTR} was isolated from the pGEM1 vector by cloning it with *Eco*RI and *Aval* in a pcDNA3 expression vector leaving the 5' and part of the 3' untranslated region (UTR) intact. Using rat p75^{NTR} subcloned in pcDNA3 as template, a one-step PCR strategy was performed to delete the 118 C-terminal amino acid residues (p75^{NTR}ΔICD). Primers were: 5'-CTGGAATTCCCGGGGATCCG; and the 3' antisense oligonucleotide with a translation stop codon inserted: 3'-GCCACGGGCCCT-CAGCCACTGTCGCTGTGCAGTT. The resulting cDNA for the construct was subcloned with *Eco*RI and *Aval* into the pcDNA3 vector and sequenced. The p75^{NTR}ΔECD construct was generated by performing PCR with the primers 5'-GCCCCGCTAGCTCGCGGCACCACCGAC-AACC and 3'-GATCAGTGCGGCCGCTCACACTGGGGATGTGGC-AG, which deletes the 245 N-terminal amino acid residues. The construct was subcloned with *Nhe*I and *Not*I into pRC/CMV AC7 and sequenced. Rat *trk*B with the fused HA tag was cloned in the pRC/CMV AC7 vector and used as a template to generate the construct *trk*BΔECD, in which the 398 N-terminal amino acid residues are deleted. The primers used were 5'-GCCCCGCTAGCTTATCCTTATGACGTGCCTGACT-ATGCCGGGGGACAAACCAATCGGGAGCATCTC and 3'-GATCA-

GTGCGGCCGCCTAGCCTAGGATGTCCAGGTA. *Nhe*I and *Not*I were used for subcloning into pRC/CMV AC7. The T1 isoform of *trk*B was cloned from a pCMV-5 *trk*B.T1 construct using *Hind*III and *Xba*I to fuse it to the HA-tagged N-terminus of *trk*B in the vector pB-KS followed by subcloning into pRC/CMV AC7 with *Nhe*I and *Not*I. Rat *trk*A and rat *trk*C were similarly cloned with the HA tag into the vector pRC/CMV AC7. The EGF receptor construct pRK5 was kindly provided by A.Ullrich.

Neurotrophins and antibodies

Recombinant BDNF, NT3 and NT4/5 produced in Chinese hamster ovary cells (CHO) were a gift from Genentech, Inc. In some experiments *Escherichia coli*-derived recombinant neurotrophins were also used (Regeneron Amgen Partners). The antibodies used included anti-human p75^{NTR} pAb (Promega) as well as a rabbit polyclonal antiserum #17 generated against a peptide corresponding to amino acids 248–274 of the cytoplasmic domain of chick p75^{NTR} (kindly provided by A.Rodriguéz-Tébar). Monoclonal anti-HA for immunoprecipitation was used from hybridoma supernatants (a kind gift from S.Werner). Western blotting was performed with anti-HA mouse mAb clone 12CA5 1 μg/μl (Boehringer Mannheim). A rabbit anti-*trk* antiserum (pantrk) recognising all *trk* proteins (raised against a peptide corresponding to the last 14 amino acids of the chick *trk*A sequence) had been established previously (Schröne *et al.*, 1995). Monoclonal anti-phosphotyrosine (clone 4G10) was purchased from Upstate Biotechnology. Anti-EGF receptor antibodies were #108 (Waterfield *et al.*, 1982) and RK2 (Kris *et al.*, 1985).

Transfection of cell lines

A293 cells were transfected by the calcium phosphate precipitation protocol using the method of Chen and Okayama (1987). Within one experiment, the amount of DNA was kept constant by supplementing samples with pcDNA3 vector DNA. For transient expression, cells were lysed 2 days after transfection. Transfection efficiency was analysed by parallel transfection with a pCMV-GFP vector (pEGFP-N1, Clontech).

Immunoprecipitation

Cells were washed with ice-cold phosphate-buffered saline (PBS) and lysed at 4°C in 1 ml lysis buffer (50 mM HEPES pH 7.5, 150 mM NaCl, 10% glycerol, 1% Triton X-100, 10 μg/ml Leupeptin and 1 mM PMSF) followed by centrifugation at 4°C with 10 000 *g* for 10 min. The supernatants were incubated with 200 μl anti-HA antibody for 2–5 h at 4°C followed by precipitation with protein A–Sepharose 6MB beads (Pharmacia Biotech) overnight at 4°C. The EGF receptor was precipitated with 2 μl antibody #108. After washing the beads three times with lysis buffer, containing 0.1% Triton X-100 instead of 1% and no Leupeptin and PMSF, the proteins were eluted by boiling in 30 μl Laemmli loading buffer for 5 min. Samples were subsequently processed by Western blotting.

Receptor phosphorylation studies

A293–*trk*B-L cells were grown in serum-free medium overnight, incubated in fresh serum-free medium for another 3–5 h and neurotrophins were added for 5 min at 37°C. Immunoprecipitation was performed as described above, except that the lysis buffer was supplemented with 5 mM orthovanadate and 3 mM EDTA. The beads were washed with a buffer containing 1 mM orthovandate. *trk*B was immunoprecipitated with 2 μl pantrk antiserum for 1–2 h at 4 C followed by the addition of protein A–Sepharose beads.

Western blotting

Proteins were separated on 7% or 10% polyacrylamide gels and subsequently transferred onto Immobilon (Millipore) membranes. Following incubation with 2% nonfat milk powder in Tris-buffered saline-Tween (TBST: 50 mM Tris pH 7.4, 150 mM NaCl, 0.1% Tween 20), the membranes were incubated overnight at 4°C with anti-human p75^{NTR} pAb (Promega), diluted at 1:2000 in blocking buffer or with the p75 antiserum #17, diluted at 1:500 in blocking buffer, followed by incubation for 1 h at room temperature with goat anti-rabbit IgG-POD (Pierce, 1:10 000 in TBST). The EGF receptor was similarly detected with the antibody RK2, diluted at 1:1000

After blocking with a gelatine solution (0.5% gelatine, 5 mM EDTA in TBST), phosphorylated *trk*B receptors were detected using the anti-phosphotyrosine antibody 4G10 overnight at room temperature, diluted at 1:400 in gelatine blocking buffer, followed by incubation for 1 h at room temperature with goat anti-mouse IgG-POD (Pierce, 1:10 000 in TBST). *trk* receptors were detected following overnight incubation at 4°C with the pantrk antibody, diluted at 1:1000 in TBST/2% milk or with the anti-HA antibody (Boehringer Mannheim), diluted at 1:1000 in TBST/2% milk.

The immune complexes were detected using the ECL detection system (Amersham) and exposure to autoradiographic film (Fuji).

Acknowledgements

We thank A.Ullrich for providing the EGF receptor construct and the anti-EGF receptor antibodies #108, and RK2 and G.Yancopoulos for the *trk*C cDNA. We are grateful to A.Rodriguez-Tébar for the anti-p75^{NTR} antiserum #17 and the pantrk antibody, and S.Werner for the anti-HA hybridoma supernatants.

References

Bamji,S.X., Maidan,M., Pozniak,C.D., Belliveau,D.J., Alovz,R., Kohn,J., Causing,C.G. and Miller,F.D. (1998) The p75 neurotrophin receptor mediates neuronal apoptosis and is essential for naturally occurring sympathetic neuron death. *J. Cell Biol.*, 140, 911–923.

Barbacid,M. (1994) The trk family of neurotrophin receptors. *J. Neurobiol.*, 25, 1386–1403.

Barker,P.A. and Shooter,E.M. (1994) Disruption of NGF binding to the low affinity neurotrophin receptor p75^{LNTR} reduces NGF binding to TrkA on PC12 cells. *Neuron*, 13, 203–215.

Benedetti,M., Levi,A. and Chao,M.V. (1993) Differential expression of nerve growth factor receptors leads to altered binding affinity and neurotrophin responsiveness. *Proc. Natl Acad. Sci. USA*, 90, 7859–7863.

Bothwell,M. (1991) Keeping track of neurotrophin receptors. *Cell*, 65, 915–918.

Casaccia-Bonnefil,P., Carter,B.D., Dobrowsky,R.T. and Chao,M.V. (1996) Death of oligodendrocytes mediated by the interaction of nerve growth factor with its receptor p75. *Nature*, 383, 716–719.

Chao,M.V. (1992) Neurotrophin receptors: a window into neuronal differentiation. *Neuron*, 9, 583–593.

Chao,M.V. and Hempstead,B.L. (1995) p75 and Trk: a two-receptor system. *Trends Neurosci.*, 18, 321–326.

Chen,C. and Okayama,H. (1987) High-efficiency transformation of mammalian cells by plasmid DNA. *Mol. Cell. Biol.*, 7, 2745–2752.

Davey,F. and Davies,A.M. (1998) TrkB signalling inhibits p75-mediated apoptosis induced by nerve growth factor in embryonic proprioceptive neurons. *Curr. Biol.*, 8, 915–918

Davies,A.M., Lee,K.-F. and Jaenisch,R. (1993) p75-deficient trigeminal sensory neurons have an altered response to NGF but not to other neurotrophins. *Neuron*, 11, 565–574.

Dechant,G., Biffo,S., Okazawa,H., Kolbeck,R., Pottgiesser,J. and Barde,Y.-A. (1993) Expression and binding characteristics of the BDNF receptor chick *trk*B. *Development*, 119, 545–558.

Dobrowsky,R.T., Jenkins,G.M. and Hannun,Y.A. (1995) Neurotrophins induce sphingomyelin hydrolysis. Modulation by co-expression of p75^{NTR} with Trk receptors. *J. Biol. Chem.*, 270, 22135–22142.

Frade,J.M. and Barde,Y.-A. (1998) Microglia-derived nerve growth factor causes cell death in the developing retina. *Neuron*, 20, 35–41.

Frade,J.M. and Barde,Y.-A. (1999) Genetic evidence for cell death mediated by nerve growth factor and the neurotrophin receptor p75 in the developing mouse retina and spinal cord. *Development*, in press.

Frade,J.M., Rodriguez-Tébar,A. and Barde,Y.-A. (1996) Induction of cell death by endogenous nerve growth factor through its p75 receptor. *Nature*, 383, 166–168.

Gargano,N., Levi,A. and Alema,S. (1997) Modulation of nerve growth factor internalization by direct interaction between p75 and TrkA receptors. *J. Neurosci. Res.*, 50, 1–12.

Graham,F.L., Smiley,J., Russell,W.C. and Nairn,R. (1977) Characteristics of a human cell line transformed by DNA from human adenovirus type 5. *J. Gen. Virol.*, 36, 59–72.

Hackett,S.F., Friedman,Z., Freund,J., Schoenfeld,C., Curtis,R., DiStefano,P.S. and Campochiaro,P.A. (1998) A splice variant of trkB and brain-derived neurotrophic factor are co-expressed in retinal pigmented epithelial cells and promote differentiated characteristics. *Brain Res.*, 789, 201–212.

Hantzopoulos,P.A., Suri,C., Glass,D.J., Goldfarb,M.P. and Yancopoulos,G.D. (1994) The low affinity NGF receptor, p75, can collaborate with each of the Trks to potentiate functional responses to the neurotrophins. *Neuron*, 13, 187–201

Hempstead,B.L., Martin-Zanca,D., Kaplan,D.R., Parada,L.F. and Chao,M.V. (1991) High-affinity NGF binding requires coexpression

of the *trk* proto-oncogene and the low-affinity NGF receptor. *Nature*, 350, 678–683.

Horton,A., Laramee,G., Wyatt,S., Shih,A., Winslow,J. and Davies,A.M. (1997) NGF binding to p75 enhances the sensitivity of sensory and sympathetic neurons to NGF at different stages of development. *Mol. Cell. Neurosci.*, 10, 162–172.

Huber,L.J. and Chao,M.V. (1995) A potential interaction of p75 and *trkA* NGF receptors revealed by affinity crosslinking and immunoprecipitation. *J. Neurosci. Res.*, 40, 557–563.

Kaplan,D.R. and Miller,F.D. (1997) Signal transduction by the neurotrophin receptors. *Curr. Opin. Cell Biol.*, 9, 213–221.

Kris,R.M., Lax,I., Gullick,W., Waterfield,M.D., Ullrich,A., Fridkin,M. and Schlessinger,J. (1985) Antibodies against a synthetic peptide as a probe for the kinase activity of the avian EGF receptor and v-erbB protein. *Cell*, 40, 619–625.

Lee,K.-F., Li,E., Huber,L.J., Landis,S.C., Sharpe,A.H., Chao,M.V. and Jaenisch,R. (1992) Targeted mutation of the p75 low affinity NGF receptor gene leads to deficits in the peripheral sensory nervous system. *Cell*, 69, 737–749.

Lee,K.-F., Davies,A.M. and Jaenisch,R. (1994) p75-deficient embryonic dorsal root sensory and neonatal sympathetic neurons display a decreased sensitivity to NGF. *Development*, 120, 1027–1033.

Lewin,G.R. and Barde,Y.-A. (1996) Physiology of the neurotrophins. *Annu. Rev. Neurosci.*, 19, 289–317.

MacPhee,I.J. and Barker,P.A. (1997) Brain-derived neurotrophic factor binding to the p75 neurotrophin receptor reduces TrkA signaling whereas increasing serine phosphorylation in the TrkA intracellular domain. *J. Biol. Chem.*, 272, 23547–23551.

Mahadeo,D., Kaplan,L., Chao,M.V. and Hempstead,B.L. (1994) High affinity nerve growth factor binding displays a faster rate of association than $p140^{trk}$ binding. Implications for multi-subunit polypeptide receptors. *J. Biol. Chem.*, 269, 6884–6891.

Maver,U., Pöschl,E., Nischt,R., Specks,U., Pan,T.-C., Chu,M.-L. and Timpl,R. (1994) Recombinant expression and properties of the Kunitz-type protease-inhibitor module from human type VI collagen α3 (VI) chain. *Eur. J. Biochem.*, 225, 573–580.

Meakin,S.O. and Shooter,E.M. (1992) The nerve growth factor family of receptors. *Trends Neurosci.*, 15, 323–331.

Rodriguez-Tébar,A. and Barde,Y.-A. (1988) Binding characteristics of brain-derived neurotrophic factor to its receptors on neurons from the chick embryo. *J. Neurosci.*, 8, 3337–3342.

Ross,A.H., Daou,M.C., McKinnon,C.A., Condon,P.J., Lachyankar,M.B., Stephens,R.M., Kaplan,D.R. and Wolf,D.E. (1996) The neurotrophin receptor, gp75, forms a complex with the receptor tyrosine kinase TrkA. *J. Cell Biol.*, 132, 945–953.

Rydén,M., Hempstead,B. and Ibáñez,C.F. (1997) Differential modulation of neuron survival during development by nerve growth factor binding to the p75 neurotrophin receptor. *J. Biol. Chem.*, 272, 16322–16328.

Schröpel,A., von Schack,D., Dechant,G. and Barde,Y.-A. (1995) Early expression of the nerve growth factor receptor ctrkA in chick sympathetic and sensory ganglia. *Mol. Cell. Neurosci.*, 6, 544–556.

Snider,W.D. (1994) Functions of the neurotrophins during nervous system development: What the knockouts are teaching us. *Cell*, 77, 627–638.

Strohmaier,C., Carter,B.D., Urfer,R., Barde,Y.-A. and Dechant,G. (1996) A splice variant of the neurotrophin receptor trkB with increased specificity for brain-derived neurotrophic factor. *EMBO J.*, 15, 3332–3337.

Sutter,A., Riopelle,R.J., Harris-Warrick,R.M. and Shooter,E.M. (1979) Nerve growth factor receptors. Characterization of two distinct classes of binding sites on chick embryo sensory ganglia cells. *J. Biol. Chem.*, 254, 5972–5982.

Verdi,J.M., Birren,S.J., Ibáñez,C.F., Persson,H., Kaplan,D.R., Benedetti,M., Chao,M.V. and Anderson,D.J. (1994) $p75^{LNGFR}$ regulates trk signal transduction and NGF-induced neuronal differentiation in MAH cells. *Neuron*, 12, 733–745.

Waterfield,M.D., Maves,E.L., Stroobant,P., Bennet,P.L., Young,S., Goodfellow,P.N., Banting,G.S. and Ozanne,B. (1982) A monoclonal antibody to the human epidermal growth factor receptor. *J. Cell. Biochem.*, 20, 149–161.

Wolf,D.E., McKinnon,C.A., Daou,M.-C., Stephens,R.M., Kaplan,D.R. and Ross,A.H. (1995) Interaction with TrkA immobilizes gp75 in the high affinity nerve growth factor receptor complex. *J. Biol. Chem.*, 270, 2133–2138.

Received October 12, 1998; revised December 3, 1998; accepted December 7, 1998

Available online at www.sciencedirect.com
SCIENCE DIRECT®
IJBCB
ELSEVIER
The International Journal of Biochemistry & Cell Biology 36 (2004) 2153–2168
www.elsevier.com/locate/biocel

Internalization and trafficking of neurotensin via NTS3 receptors in HT29 cells

Anne Morinville[a,b,1], Stéphane Martin[c,d,1], Mariette Lavallée[a], Jean-Pierre Vincent[c], Alain Beaudet[a], Jean Mazella[c,*]

[a] *Montreal Neurological Institute, McGill University, 3801 University Street, Montreal, Que., Canada H3A 2B4*
[b] *Department of Pharmacology and Therapeutics, McGill University, 3655 Promenade Sir William Osler, Montreal, Que., Canada H3G 1Y6*
[c] *Institut de Pharmacologie Moléculaire et Cellulaire, Unité Mixte de Recherche 6097 du Centre National de la Recherche Scientifique, 660 Route des Lucioles, 06560 Valbonne, France*
[d] *MRC Centre for Synaptic Plasticity, Department of Anatomy, School of Medical Sciences, Bristol University, Bristol BS8 1TD, UK*

Received 6 November 2003; received in revised form 17 March 2004; accepted 14 April 2004

Abstract

The neurotensin receptor-3, originally identified as sortilin, is unique among neuropeptide receptors in that it is a single trans-membrane domain, type I receptor. To gain insight into the functionality of neurotensin receptor-3, we examined the neurotensin-induced intracellular trafficking of this receptor in the human carcinoma cell line HT29, which expresses both neurotensin receptor-1 and -3 sub-types. At steady state, neurotensin receptor-3 was found by sub-cellular fractionation and electron microscopic techniques to be predominantly associated with intracellular elements. A small proportion (~10%) was associated with the plasma membrane, but a significant amount (~25%) was observed inside the nucleus. Following stimulation with neurotensin (NT), neurotensin/neurotensin receptor-3 complexes were internalized via the endosomal pathway. This internalization entailed no detectable loss of cell surface receptors, suggesting compensation through either recycling or intracellular receptor recruitment mechanisms. Internalized ligand and receptors were both sorted to the pericentriolar recycling endosome/Trans-Golgi Network (TGN), indicating that internalized neurotensin is sorted to this compartment via neurotensin receptor-3. Furthermore, within the Trans-Golgi Network, neurotensin was bound to a lower molecular form of the receptor than at the cell surface or in early endosomes, suggesting that signaling and transport functions of neurotensin receptor-3 may be mediated through different molecular forms of the protein. In conclusion, the present work suggests that the neurotensin receptor-3 exists in two distinct forms in HT29 cells: a high molecular weight, membrane-associated form responsible for neurotensin endocytosis from the cell surface and a lower molecular weight, intracellular form responsible for the sorting of internalized neurotensin to the Trans-Golgi Network.

Keywords: Neurotensin; Sortilin NTS3 receptor; Trafficking; Sub-cellular fractionation; Electron microscopy

1. Introduction

The tridecapeptide neurotensin (NT) is widely distributed in brain and periphery and is involved in a variety of neural, endocrine, cardiovascular, and diges-

* Corresponding author. Tel.: +33-4-93-95-77-61; fax: +33-4-93-95-77-08.
E-mail address: mazella@ipmc.cnrs.fr (J. Mazella).
[1] Contributed equally to this work.

1357-2725/$ – see front matter © 2004 Elsevier Ltd. All rights reserved.
doi:10.1016/j.biocel.2004.04.013

tive functions (for review, see Rostène & Alexander, 1997). Three different NT receptors, referred to as NTS1, NTS2, and NTS3 have so far been cloned (for reviews, see Mazella, 2001; Vincent, Mazella, & Kitabgi, 1999). Whereas, NTS1 and NTS2 are both seven trans-membrane domain receptors, NTS3 is a single trans-membrane domain type I receptor, which shows 100% homology with the sorting protein, sortilin (Mazella et al., 1998; Petersen et al., 1997). This receptor belongs to a new receptor family related to the yeast sorting receptor Vps10p and characterized by similar N-terminal luminal domains (Marcusson, Horazdovsky, Cereghino, Gharakhanian, & Emr, 1994). This receptor family includes, in addition to NTS3/sortilin, SorLA and SorCS-1, -2, and -3 (for review, see Hampe, Rezgaoui, Hermans-Borgmeyer, & Schaller, 2001). These receptors are produced as inactive precursors that are converted to mature forms upon cleavage by furin (Hampe et al., 2001; Petersen et al., 1999). Accordingly, NTS3 binds NT with considerably lower affinity when transfected in epithelial cell lines alone (K_d = 17 nM for hNTS3 and 45 nM for mNTS3) (Navarro et al., 2001) than together with furin (K_d = 0.3 nM for hNTS3) (Mazella et al., 1998). In addition to NT, NTS3/sortilin binds a variety of other ligands, including the receptor-associated protein (RAP) (Petersen et al., 1997; Tauris et al., 1998), lipoprotein lipase (LpL) (Nielsen, Jacobsen, Olivecrona, Gliemann, & Petersen, 1999), and the 44-amino-acid propeptide cleaved during maturation of the receptor precursor (Petersen et al., 1999).

In addition to its N-terminal and single trans-membrane domains, NTS3 comprises a short C-terminal cytoplasmic segment identical to the corresponding domain in the mannose 6-phosphate/insulin growth factor-II receptor (CI-M6PR) (Petersen et al., 1997). This C-terminal tail contains several sorting motifs, suggesting that NTS3/sortilin can engage in various types of trafficking, including endocytosis and transport between the Golgi and late endosomes (Nielsen et al., 2001). Indeed, a major pool of NTS3/sortilin was found to be associated with Golgi vesicles in adipocytes (Morris et al., 1998). Furthermore, only a small proportion of NTS3 appears to be present at the cell surface of either adipocytes or transfected cells under steady-state conditions (Morris et al., 1998; Navarro et al., 2001). However, in adipocytes, NTS3 is up-regulated at the plasma membrane upon stimulation with insulin, together with the glucose transporter GLUT4 (Lin, Pilch, & Kandror, 1997; Morris et al., 1998). Similarly, in neuronal cell cultures, NTS3 (identified at the time as a 100 kDa NT binding protein) was shown to be recruited at the cell membrane following stimulation with NT (Chabry, Gaudriault, Vincent, & Mazella, 1993).

The role of NTS3/sortilin in mediating central and/or peripheral effects of NT remains elusive. When transfected in epithelial cell lines, this receptor binds and efficiently internalizes NT (Navarro et al., 2001). Moreover, NT stimulates the growth of CHO cells stably transfected with NTS3, suggesting that the latter may behave as a signaling receptor regulating cell proliferation (Dal Farra et al., 2001). Accordingly, NTS3 was found to be expressed in a variety of human cancer cell lines derived from colon, pancreas and prostate (Dal Farra et al., 2001) upon which NT had been documented to exert a proliferative action (Iwase et al., 1996; Maoret et al., 1994; Seethalakshmi, Mitra, Dobner, Menon, & Carraway, 1997). However, the strongest evidence to date that NTS3 can behave as a true NT receptor lies with the recent demonstration that this protein may be involved in the NT-induced migration of human microglial cells, via stimulation of both MAP and Pi3-kinase-dependent pathways (Martin, Vincent, & Mazella, 2003).

Nonetheless, little is known regarding the effects of NT on endogenous NTS3 receptor trafficking. In particular, it remains to be determined whether endogenously expressed NTS3 receptors internalize NT and, if this is the case, to which intracellular compartments ligand and receptors are targeted. We recently demonstrated that NTS3 receptors are abundantly expressed in the human adenocarcinoma cell line HT29 (Martin, Navarro, Vincent, & Mazella, 2002), from which the human NTS1 receptor was originally cloned (Vita et al., 1993). Stimulation of HT29 cells with NT results in a robust down-regulation of cell surface NT binding sites and concomitant desensitization of the calcium mobilizing effects of NT (Turner, James-Kracke, & Camden, 1990). However, it is unclear whether this down regulation reflects a loss of NTS3 and/or NTS1 receptors from the cell surface and whether NT is internalized through NTS3 and/or NTS1 binding sites. The aim of the present study was therefore to address some of these issues by tracking

NTS3 and NT-labeled NTS3 receptors in HT29 cells by combined biochemical and immunocytochemical techniques.

2. Methods

2.1. Materials

Neurotensin (NT) was purchased from Bachem (Voisins-le-Bretonneux, France) and NT(2-13) was synthesized by Neosystem (Strasbourg, France). ^{125}I-Tyr$_3$-NT, α-azidobenzoyl-^{125}I-Tyr$_3$-NT(2-13), and *N*α-Bodipy-NT(2-13) were prepared and purified as described previously (Faure et al., 1995; Mazella, Kitabgi, & Vincent, 1985; Sadoul, Mazella, Amar, Kitabgi, & Vincent, 1984). Dulbecco's modified Eagle's medium (DMEM) was from Invitrogen, Inc. (Burlington, Ont., Canada) and fetal bovine serum (FBS) from BioWest (Nuaillé, France) or Invitrogen, Inc., Gentamycin, 1,10-phenanthroline, sucrose, EDTA, HEPES, bovine serum albumin (BSA), ovalbumin (OA), Mowiol, paraformaldehyde, mammalian protease inhibitor cocktail were from Sigma (Lyon, France). The antiserum against the luminal domain of NTS3/sortilin was a generous gift from Dr. C. M. Petersen (University of Aarhus, Aarhus, Denmark). The mouse monoclonal antibody directed against the Golgi cistern marker Giantin was kindly provided by Prof. H.-P. Hauri (Biocenter of the University of Basel, Department of Pharmacology, Basel, Switzerland). The mouse monoclonal anti-Lamp-1 antibody was kindly provided by Dr. Minoru Fukuda (The Burnham Institute, La Jolla, CA, USA). Mouse monoclonal anti-syntaxin-6 and anti-Na^+/K^+ ATPase α1 antibodies were purchased from Transduction Laboratories (Lexington, KY, USA) and Upstate Biotechnology (Lake Placid, NY, USA), respectively. Rabbit polyclonal anti-Rab5A and anti-HDAC-1 antibodies were purchased from Santa Cruz Biotechnology (Santa Cruz, CA, USA). Cy™ 5-conjugated donkey anti-mouse, Texas red- or FITC-conjugated donkey anti-rabbit antibodies were obtained from Jackson Immunoresearch Laboratories (supplied through BioCan Scientific, Mississauga, Ont., Canada). HRP-conjugated goat anti-rabbit and anti-mouse IgGs as well as goat anti-rabbit IgG-gold (AuroProbe One GAR) and IntenSE M Silver Enhancement Kit were from Amersham-Pharmacia Biotech, Inc. (Baie d'Urfé, Que., Canada). Human Alexa 568-Tranferrin was from Molecular Probes, Inc (Eugene, OR, USA).

2.2. Cell culture

HT29 cells, documented to express both NTS1 and NTS3 receptors (Martin et al., 2002) as well as furin (Khatib et al., 2001), were kindly supplied by Dr. P. Kitabgi (IPMC, CNRS, Valbonne, France). Cells were grown in 100 mm Petri dishes in DMEM supplemented with 10% FBS and 50 μg/mL gentamycin or 1% penicillin/streptomycin (Life Technologies, Inc.) at 37 °C under 5% CO_2.

2.3. Western blotting of cell homogenates

HT29 cells were rinsed with 0.1 M phosphate buffered saline (PBS), pH 7.4 and lysed in 10 mM Tris buffer containing 1 mM EDTA (TE) and protease inhibitors diluted 1/100. Samples were sonicated for 10 s prior to centrifugation at 13,000 × *g* for 30 min at 4 °C. The pellets were resuspended in TE buffer containing protease inhibitors. The protein content was determined using Bio-Rad protein assay dye reagent using the method of Bradford (Bradford, 1976) with OA as the protein standard. Proteins were denatured by boiling at 95 °C for 3 min using 2× Laemmli sample buffer. Samples (30–50 μg loaded per lane) were resolved by SDS–polyacrylamide gels using 8% gels followed by electroblotting onto nitrocellulose membranes. After blocking with 5% milk powder in PBS with 0.05% Tween-20 (PBS + T), the membranes were incubated for 1 h with the rabbit NTS3 antibody diluted 1:1000 in PBS + T with 5% milk powder at room temperature. Membranes were washed with PBS + T (3 × 5 min) prior to incubation with a goat anti-rabbit antibody conjugated to horseradish peroxidase for 45 min at room temperature. Membranes were subsequently washed with PBS + T (3 × 5 min) and PBS (5 min), incubated in the presence of Luminol® chemiluminescence reagents (Roche Diagnostics France S.A., Meylan, France) and exposed to film.

2.4. Sub-cellular fractionation

The protocol described by Clancy and Czech (1990) was employed to obtain the following fractions: plasma membrane (Mb); high density microsomes (HDM); low density microsomes (LDM); nucleus and mitochondria (N + M); and cytosol. Briefly, cells (from two 100 mm Petri dishes grown to 70–80% confluence for each condition) were collected in Solution A (250 mM sucrose, 20 mM HEPES, 1 mM EDTA and 1 mM PMSF at pH 7.4), homogenized with a Teflon pestle, and centrifuged at 16,000 × *g* for 20 min to yield Pellet 1 and Supernatant 1. Pellet 1 was resuspended in Solution B (20 mM HEPES and 1 mM EDTA at pH 7.4) using a Dounce homogenizer, deposited on a sucrose solution (1.12 M sucrose in Buffer B), and centrifuged at 100,000 × *g* for 60 min to yield Pellet 2 and Supernatant 2. Pellet 2 was re-suspended in Buffer B by sonication (5 s) and represents the N + M fraction. Supernatant 2 was collected at the interface between the sucrose solution and Buffer B and was resuspended in Buffer B and centrifuged at 30,000 × *g* for 30 min to yield Pellet 3; this pellet was resuspended in Buffer B and represents the Mb fraction. Meanwhile, Supernatant 1 was centrifuged at 30,000 × *g* for 30 min to produce Pellet 4 and Supernatant 3. Pellet 4 was resuspended in Buffer B and represents the HDM fraction. Supernatant 3 was centrifuged at 200,000 × *g* for 90 min to yield Pellet 5 and Supernatant 4. Pellet 5 was resuspended in Buffer B and represents the LDM fraction. Proteins were precipitated overnight at 4 °C from Supernatant 4 using 10% TCA to produce the cytosolic fraction.

2.5. Western blotting of sub-cellular fractions

Proteins from sub-cellular fractions were denatured by boiling at 95 °C for 3 min using 2× or 6× Laemmli sample buffer, resolved using 10% Tris–Glycine gels (Invitrogen, Burlington, Ont., Canada) and subsequently electroblotted onto nitrocellulose membranes. Membranes were blocked and incubated with primary antibody either overnight at 4 °C or for 2–4 h at room temperature. The bound antibody was visualised using an HRP-conjugated goat anti-rabbit or an HRP-conjugated goat anti-mouse followed by chemiluminescence reagents (Mandel Scientific, Guelph, Ont., Canada). Primary antibodies directed against NTS3, Na^+/K^+ ATPase α1, Rab5A, syntaxin-6, and HDAC-1 were employed. For quantification of NTS3 immunoreactivity, blots were digitized by scanning with an Agfa Duoscan T1200. Digital images were quantified using the ScionImage software program (Scion Corporation, Frederick, MD, USA). The integrated density (I.D.) for each band (arbitrary units) was divided by the amount (μg) of protein loaded on the gel for that respective sample (to yield I.D./μg). The I.D./μg for each sub-cellular fraction (Mb, HDM, LDM, N + M) was then multiplied by the total weight of that fraction (μg) and the resulting value was then divided by the sum of values from all fractions for each respective experiment ($n = 3$, expressed as a percentage). For assessing changes in NTS3 immunoreactivity within individual fractions over time, values from 3 to 4 independent experiments were pooled and expressed as a percentage of the I.D./μg of an internal standard (the steady-state HDM fraction of one experiment, which was loaded on all gels). Calculations and statistical analysis (Kruskal–Wallis test) was performed using Excel 97 (Microsoft Corp., San Francisco, CA, USA) and Prism 3.02 (Graph Pad Software Inc., San Diego, CA, USA). Images were processed using Adobe Photoshop 4.0.1 (Adobe Systems Inc., San Jose, CA, USA).

2.6. Binding and cross-linking of azido-^{125}I-NT

HT29 cells, grown in a 100 mm Petri dish to 70–80% confluence, were washed with Earle's buffer (25 mM HEPES, 140 mM NaCl, 5 mM KCl, 1.8 mM $CaCl_2$, 3.6 mM $MgCl_2$, 0.9 g/L glucose). Cells were subsequently incubated in the presence of 0.3 nM α-azidobenzoyl-^{125}I-Tyr_3-NT (6×10^6 cpm/Petri, two Petri for each condition) in an Earle's buffer containing 0.8 mM 1,10-phenanthroline for 5, 15 or 30 min at 37 °C. Cells were then washed at 4 °C with Earle's buffer and irradiated using an XL-1500 UV Crosslinker (Spectronics Corporation) to cross-link the radioligand to its receptors. Specificity of the binding was assessed by carrying the incubation in the presence of 1 μM unlabeled NT. Internalization specificity was assessed by pre-incubating the cells at 37 °C for 30 min with 0.45 M sucrose and subsequently incubating them at 37 °C with

azido-^{125}I-NT in the presence of 0.45 M sucrose for 30 min. For steady-state conditions, cells were washed with Earle's buffer on ice and extemporaneously irradiated (time: 0 min). Cells were then subjected to sub-cellular fractionation as described above.

The protein content of each fraction was determined using Bio-Rad protein assay dye reagent with ovalbumin as the protein standard. The samples were denatured by boiling at 95 °C for 3 min using 2× Laemmli sample buffer and were run on 8% SDS–PAGE gels. Proteins were electroblotted onto nitrocellulose membranes and these membranes were exposed against a phosphoimager screen for 48–72 h and developed using a phosphoimager (Fuji BAS2500). The images were acquired and quantified as described previously. Data are presented as the integrated density (I.D.) for each band in arbitrary units (A.U.) in each fraction of a representative experiment (from $n = 4$); values were not standardized between different sub-cellular fractions. To confirm band identity, immunoblotting against NTS3 was performed on these same nitrocellulose membranes.

2.7. Immunofluorescence labeling

To assess the presence of NTS3 receptors on the cell surface after exposure to NT, HT29 cells were grown on 12 mm coverslips in DMEM supplemented with 10% FBS. These cells were pre-incubated for 10 min at 37 °C in Earle's buffer, pH 7.4, containing 25 mM HEPES, 140 mM NaCl, 5 mM KCl, 1.8 mM $CaCl_2$, 3.6 mM $MgCl_2$, 0.9 g/L glucose, and 0.8 mM 1,10-phenanthroline. They were then incubated in the same buffer in the presence of 10 nM NT for 40 min at 37 °C. After a rapid wash with PBS, cells were fixed with 3% paraformaldehyde (PFA) in PBS for 20 min at 4 °C. They were then rinsed twice with PBS and incubated with 50 mM NH_4Cl in PBS for 10 min to quench excess free aldehyde groups. After blocking for 20 min in PBS containing 10% horse serum (HS), cells were incubated for 30 min at room temperature with rabbit NTS3 receptor antibody (1:300) in PBS containing 5% HS. They were then rinsed three times in PBS and incubated for 30 min at room temperature with a Texas Red-conjugated donkey anti-rabbit antibody (1:600) in PBS containing 5% HS. After two washes with PBS and one with water, cell-bearing coverslips were mounted on glass slides with Mowiol for confocal microscopic examination.

To monitor the intracellular trafficking of NTS3 receptors after ligand binding, HT29 cells were grown in serum free medium at 37 °C for 1 h and incubated at 4 °C with rabbit NTS3 receptor antibody (1:100) in PBS containing 10% HS for 2 h. They were then washed three times with PBS and once with Earle's buffer and subsequently exposed to 10 nM NT at 37 °C for 40 min in Earle's buffer to promote internalization of receptor–ligand complexes. After three washes in PBS, cells were permeabilized with 0.1% Triton X-100 and fixed with 3% PFA at room temperature as described above, rinsed three times in PBS buffer, and incubated at room temperature with a FITC-conjugated donkey anti-rabbit antibody (1:600) in PBS containing 5% HS for 30 min. For dual detection of labeled NTS3 receptors and intracellular compartment markers, cells were incubated, after fixation and permeabilization, with mouse monoclonal anti-Lamp-1 antibody (1:1000), mouse monoclonal anti-Giantin antibody (1:500), or mouse monoclonal anti-syntaxin-6 antibody (3 μg/mL) for 30 min at room temperature. Secondary antibodies [FITC-conjugated donkey anti-rabbit antibody for NTS3 and Cy5-conjugated donkey anti-mouse antibody (1:600 for cell compartment markers)] were then jointly applied in PBS containing 5% HS for 30 min. After two washes with PBS and one with water, cells were mounted on glass slides with Mowiol and examined by confocal microscopy.

To determine whether NT-induced NTS3 internalization proceeded through classical endosomal pathways, HT29 cells were serum deprived at 37 °C for 1 h and incubated with rabbit anti-NTS3 receptor antibody (1:100) in PBS containing 1% BSA at 4 °C for 2 h. After three washes in PBS, cells were co-incubated for 15 and 40 min with 10 nM NT and 50 μg/mL iron-saturated human Alexa 568-transferrin at 37 °C in serum free medium containing 1% BSA. They were then washed three times with ice cold PBS, fixed with 3% PFA for 20 min at 4 °C and processed for NTS3 immunodetection as above.

2.8. Fluorescent ligand labeling

To monitor the fate of internalized NT, HT29 cells were plated on 12 mm coverslips in DMEM supplemented with 10% FBS, pre-incubated for 10 min at 37 °C in Earle's buffer, and incubated in the same buffer with 10 nM *N*α-Bodipy-NT (fluo-NT) at 37 °C for a further 40 min. To determine non-specific labeling, 1 μM of unlabeled NT was added to the incubation medium. After two washes in Earle's buffer and one in ice cold PBS, cells were fixed in 3% PFA in PBS for 20 min at 4 °C and mounted on glass slides with Mowiol for confocal microscopic examination.

To monitor in parallel the fate of internalized ligand and receptor in HT29 cells, cells were pre-incubated at 4 °C with the anti-NTS3 receptor antibody (1:100) in PBS containing 10% HS for 2 h. After three washes with PBS and one with Earle's buffer, cells were incubated for 40 min at 37 °C with 10 nM fluo-NT in Earle's buffer. They were then washed twice with Earle's buffer and twice with ice cold PBS, fixed with 3% PFA for 20 min at 4 °C, and permeabilized in PBS containing 10% HS and 0.1% Triton X-100 for 20 min at 4 °C. They were then immunoreacted for NTS3 as described above, using a FITC-conjugated donkey anti-rabbit antibody (1:600).

2.9. Confocal microscopy

Labeled cells were examined with a Leica laser scanning confocal microscope (TCS-SP) equipped with a DM-IRBE inverted microscope and an argon–krypton laser. Samples were scanned under either 488 nm (for FITC-conjugated donkey anti-rabbit), 568 nm (fluo-NT or Alexa 568-transferrin) or 647 nm (for Cy5-conjugated donkey anti-mouse antibody) wavelength excitation. Images were acquired as single transcellular optical sections and averaged over 32 scans/frame and processed using Adobe Photoshop 4.0.1.

2.10. Electron microscopy

For electron microscopic localization of NTS3 receptors, HT29 cells were incubated at 37 °C with or without 10 nM NT for 10 or 40 min. They were then washed in 0.1 M phosphate buffer (PB) and fixed with a mixture of 2% acrolein/2% PFA in PB for 20 min, followed by 2% PFA for 20 min, at room temperature. After thorough washes with 0.1 M TBS, they were incubated with 3% normal goat serum (NGS) in 0.1 M TBS for 30 min at room temperature, followed by NTS3 antibody (1:300) in 0.1 M TBS along with 0.05% Triton X-100 and 0.5% NGS for 24 h at 4 °C. Following incubation with the primary antibody, cells were repeatedly washed with 0.01 M PBS and non-specific binding sites were blocked using 0.1% gelatin and 0.1% BSA diluted in 0.01 M PBS. Cells were then incubated with a 1:50 dilution of goat anti-rabbit IgG-gold at room temperature for 2 h. After thorough washing, cells were fixed with 2% glutaraldehyde for 10 min at room temperature and immunogold deposits enhanced by incubation with ionic silver in citrate buffer. Subsequent to reaction amplification, cells were rinsed in buffer, post-fixed with 2% OsO_4, dehydrated in graded alcohols, embedded in Epon, and sectioned at 80 nm thickness on an ultramicrotome. Sections were stained with uranyl acetate and lead citrate and examined with a JEOL 100CX transmission electron microscope (JEOL USA, Inc., Peabody, MA, USA). Negatives were scanned and images were processed using Adobe Photoshop 4.0.1.

For immunogold particle quantification, cells were pooled from three independent experiments. Gold particles were classified as plasma membrane-associated, nuclear membrane-associated, nuclear or cytoplasmic. The total surface area and total perimeter as well as the nuclear surface area and nuclear perimeter of each immunolabeled HT29 cell were measured by computer-assisted morphometry (BioCom, Les Ulis, France). To calculate compartment percentages, the sum of immunoreactive gold particles in each compartment was divided by the sum of gold particles in all compartments for a given experiment. The density of immunoreactive NTS3 receptors per unit length of plasma or nuclear membrane was calculated by dividing the number of gold particles detected at the surface of each of these membranes by its respective perimeter. The number of NTS3 receptors per unit area (μm^2) of cytoplasm or nucleus was calculated by dividing the total number of gold particles detected by the surface area of these compartments (as measured by computer-assisted morphometry). Cal-

culations and statistical analysis (Kruskal–Wallis test) were performed using Excel 97 and Prism 3.02. Values are presented as the mean ± the standard error of the mean (S.E.M.).

3. Results

3.1. Sub-cellular distribution of NTS3 receptors in HT29 cells at steady state

3.1.1. Sub-cellular fractionation studies

Western blot analysis of whole cell lysates prepared from non-stimulated HT29 cells revealed the presence of an intense NTS3-immunoreactive band at an apparent molecular weight of 105 kDa (Fig. 1A). In addition, in some, but not all preparations, a weakly immunoreactive band was detected at an apparent molecular weight of 135 kDa (Fig. 1A). This second band, which was previously shown to correspond to a differentially glycosylated form of NTS3/sortilin (Martin et al., 2002), accounted for approximately 7% of total NTS3 immunoreactivity. Not surprisingly, therefore, only the 105 kDa band was readily apparent and quantifiable in Western blots prepared from sub-cellular fractions.

As illustrated in Fig. 1B, the highest proportion of 105 kDa NTS3-immunoreactive receptor proteins was associated with the LDM fraction. A smaller percentage was observed in association with the HDM fraction (Fig. 1B). Only an exceedingly small proportion of immunoreactive NTS3 was associated with the plasma membrane (Fig. 1B). Surprisingly, a significant proportion (~20%) of immunoreactive NTS3 was present in the nuclear (N + M) fraction (Fig. 1B). No immunoreactivity was detected in the cytosolic fraction (results not shown).

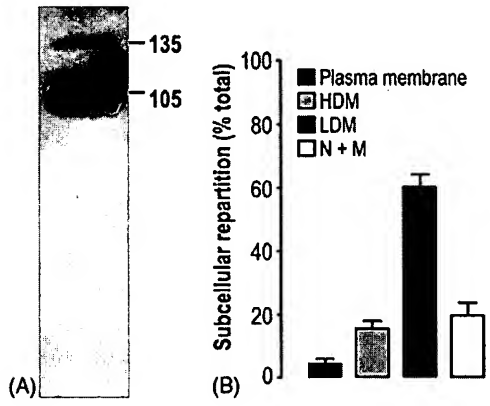

Fig. 1. Characterization and sub-cellular distribution of NTS3 receptors in HT29 cells at steady state. (A) Immunoblotting of whole cell lysates from HT29 cells with the anti-NTS3 antibody reveals the presence of two immunoreactive bands. The band at an apparent weight of 105 kDa represents the major immunoreactive species while the band at around 135 kDa, accounts for only about 7% of NTS3 immunoreactivity. (B) Sub-cellular fractionation reveals the presence of the 105 kDa band in the membrane, HDM, LDM and N + M fractions, with the highest concentration present in the LDM fraction. The repartition percentage was calculated by multiplying the I.D./μg protein loaded for each fraction by the weight of that fraction (μg) and dividing the resulting value by the sum of all fractions for each experiment ($n = 3$, expressed as a percentage). Values are presented as mean ± standard error of the mean (S.E.M.).

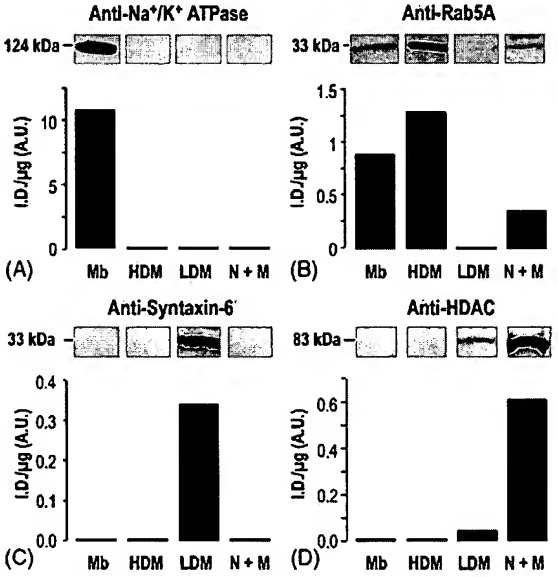

Fig. 2. Identification of sub-cellular fractions by immunoblotting. Sub-cellular fractions from unstimulated HT29 cells were resolved using 10% acrylamide gels and subsequently immunoblotted using compartment-specific sub-cellular markers. As expected, (A) the Mb fraction is enriched in the plasma membrane marker Na/K ATPase. (B) Rab5A, a marker of early endosomes, is found in association with the HDM fraction and, to a lesser extent, with the Mb and N + M fractions. (C) Syntaxin-6, a marker of the Trans-Golgi Network (TGN), is detected exclusively in the LDM. (D) Histone deacetylase-1 (HDAC-1), a protein usually present in the nucleus, is highly enriched in the N + M fraction. Immunoblots are representative of three independent experiments. Each bar in the graphs represents the I.D. of each immunoreactive band divided by the μg of protein loaded for each fraction (I.D./μg).

Immunoblotting of the same fractions with specific sub-cellular compartment markers confirmed that the plasma membrane fraction was enriched in the plasma membrane-associated protein Na^+/K^+-ATPase (Fig. 2A). HDM, and to a lesser extent plasma membrane and N + M fractions, were enriched in the early endosome marker Rab5A, whereas this protein was absent from the LDM fraction (Fig. 2B). Conversely, the recycling endosome/TGN marker syntaxin-6 was selectively detected in the LDM fraction (Fig. 2C). Finally, the N + M fraction was markedly and selectively enriched in histone deacetylase-1 (HDAC-1) immunoreactivity, confirming that it contained nuclear components (Fig. 2D).

3.2. Electron microscopy

In conformity with the results of sub-cellular fractionation studies, the bulk of NTS3 immunoreactivity detected by electron microscopy was intracellular (Fig. 3). Only a small proportion of the total number of immunogold particles detected per cell was associated with the plasma membrane (Fig. 3). The major fraction was observed in association with the membrane of vesicular and endosomal organelles of various sizes and shapes (Fig. 3), as well as with cisterns of smooth endoplasmic reticulum and Golgi saccules (Fig. 3A and B). Congruent with the results of sub-cellular fractionation studies, a sizeable proportion of im-

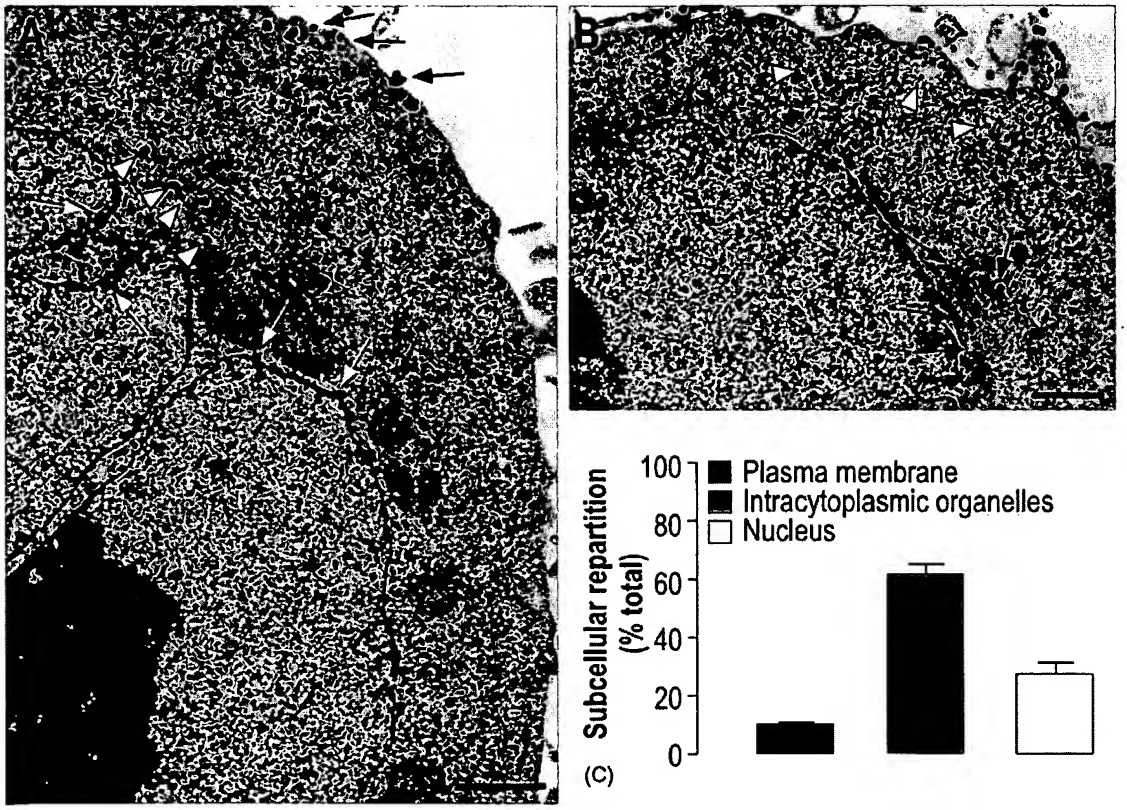

Fig. 3. Electron microscopic localization of NTS3 in HT29 cells. (A) and (B) The bulk of NTS3 immunoreactivity is located intracellularly. Only a few immunogold particles are detected over the plasma membrane (A, denoted by black arrows). Within the cytoplasm, gold particles are found in association with the membranes of the endoplasmic reticulum (A, arrowheads), endosomes (B, arrowheads), nucleus (A, white arrows) and Golgi cisterns (B, black arrows). Numerous immunogold particles are also observed in the nucleus (A) and (B). (A) and (B) scale bar: 1.0 μm. (C) Sub-cellular repartition of NTS3 in unstimulated HT29 cells. Gold particles were classified as plasma membrane-associated, nuclear or intracytoplasmic. To calculate compartment percentages, the sum of immunoreactive gold particles in each compartment was divided by the sum of gold particles in all compartments in each experiment. Each bar represents the mean ± the standard error of the mean (S.E.M.; $n = 6$).

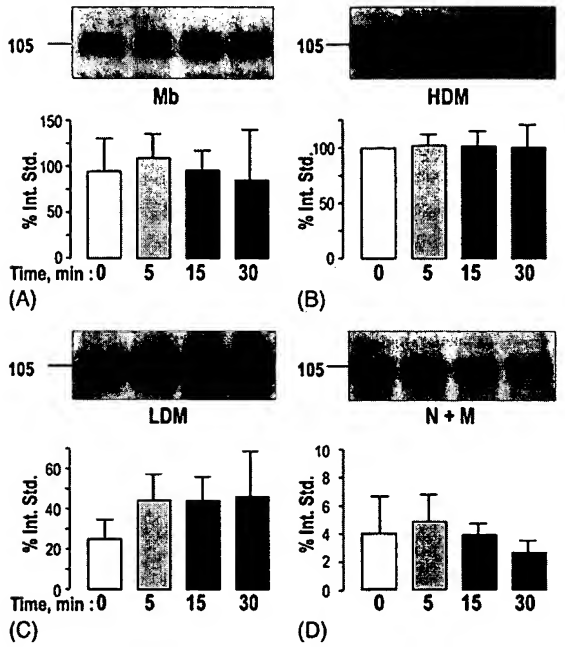

Fig. 4. Immunoblotting of sub-cellular fractions against NTS3. HT29 cells were stimulated, or not, with 0.3 nM azido-^{125}I-NT for 5–30 min prior to photoirradiation and sub-cellular fractionation. Fractions were resolved on Tris-glycine gels and probed with the anti-NTS3 antibody. NTS3 immunoreactivity was assessed over time (0, 5, 15, 30 min) in the Mb (A), HDM (B), LDM (C) and N + M (D) fractions. Immunoblots were scanned and digital images were quantified using computer-assisted densitometry. Graphs represent NTS3 immunoreactivity within individual fractions over time. Values from 3–4 independent experiments were pooled and expressed as a percentage of the I.D./μg of an internal standard (the steady-state HDM fraction of one experiment, which was loaded on all gels). No statistically significant difference was found in NTS3 immunoreactivity in any fraction at any timepoint. Error bars correspond to the S.E.M of 3–4 independent experiments.

munoreactive NTS3 was detected inside the nucleus (Fig. 3).

3.3. Traffic of NTS3 receptors in HT29 cells following stimulation with NT

3.3.1. Sub-cellular fractionation studies

In order to determine whether agonist exposure modified the sub-cellular distribution of NTS3 in HT29 cells, cells were subjected to 5–30 min stimulation with 0.3 nM ^{125}I-azido-NT and the distribution of immunoreactive NTS3 was analyzed by Western blotting in the same sub-cellular fractions as characterized above. As can be seen in Fig. 4A, stimulation with NT did not significantly modify the density of the 105 kDa NTS3-immunoreactive band detected in the plasma membrane fraction following 5, 15, or 30 min of stimulation with NT, when compared with non-stimulated controls. Similarly, no significant changes were detected at these time points in the intensity of immunoreactive NTS3 in HDM (Fig. 4B), LDM (Fig. 4C), or N + M fractions (Fig. 4D).

To follow the fate of ligand-NTS3 complexes following stimulation with NT, HT29 cells were incubated for 5–30 min at 37 °C with 0.3 nM azido-^{125}I-NT, after which the ligand was cross-linked to the receptor by photoirradiation and the distribution of radiolabeled NTS3 was assessed by autoradiography. Incubation of HT29 cells with azido-^{125}I-NT at 37 °C in the presence of 1 μM unlabeled NT completely abolished NTS3-radiolabeling (results not shown). In addition, incubation of azido-^{125}I-NT in

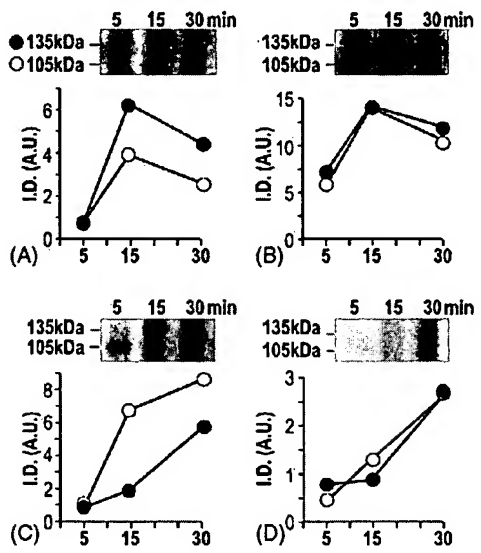

Fig. 5. Photoaffinity-labeled NTS3-NT complexes accumulate over time within intracellular compartments. HT29 cells were incubated with 0.3 nM azido-^{125}I-NT for 5, 15 or 30 min prior to irradiation, sub-cellular fractionation, and resolution by SDS–PAGE (8% acrylamide gel). The autoradiograms reveal the association of NT with bands of approximate molecular weights of 105 and 135 kDa in: (A) the membrane, (B) HDM, (C) LDM and (D) N + M fractions. Data are presented as the integrated density (I.D.) for each band in arbitrary units (A.U.) in each fraction of a representative experiment (from $n = 4$); values were not standardized between different sub-cellular fractions.

the presence of 0.45 M sucrose for 30 min prevented the intracellular accumulation of azido-^{125}I-NT (results not shown). In all sub-cellular fractions examined, two radiolabeled bands were observed at the 105 and 135 kDa molecular weight marks (Fig. 5), corresponding to the size of NTS3-immunoreactive bands detected by Western blot (Fig. 1A). However, the respective intensity of these two bands varied between fractions. Indeed, at all time intervals, the intensity of the 135 kDa band was greater than that of the 105 kDa band in the Mb fraction (Fig. 5A). Conversely, in the LDM fraction, the density of the 105 kDa band was higher than that of the 135 kDa form (Fig. 5C). In HDM and N + M fractions, 105 and 135 kDa bands were of approximately equal densities at all times (Fig. 5B and D).

In the plasma membrane fraction, the intensity of both 105 and 135 kDa bands increased markedly between 5 and 15 min and decreased slightly thereafter (Fig. 5A). The same temporal pattern was observed in the HDM fraction (Fig. 5B). In the LDM fraction, an increase in intensity with time was noted for both bands. However, this increase was more rapid and more pronounced for the 105 than the 135 kDa band and only peaked at 30 min (Fig. 5C). Finally, in the N + M fraction, an increase in the amount of ligand cross-linked to either form of the receptor was detected between 5 and 30 min of ligand exposure (Fig. 5D).

3.4. Confocal microscopy

Confocal microscopic examination of HT29 cells stimulated or not with 10 nM NT for 40 min at 37 °C, rinsed, fixed, and immunolabeled with anti-NTS3 without cell permeabilization revealed no obvious difference in the density of NTS3 receptors at the cell surface. Both before and after (Fig. 6A) NT stimulation, a thin ring of immunoreactivity was evident along the plasma membrane, in accordance with the results of sub-cellular fractionation studies.

To visualize the fate of cell surface receptors following binding of the agonist, cells were labeled with NTS3 antibodies at 4 °C, stimulated with 10 nM NT for 40 min at 37 °C, fixed with paraformaldehyde, and permeabilized to allow for secondary antibody penetration. Under these conditions, surface-labeled immunoreactive NTS3 receptors were found to undergo a massive translocation from the plasma membrane to the cytoplasm of the cells, in which they formed small, endosome-like, fluorescent clusters (Fig. 6B).

To determine the extent to which NTS3-bound ligand remained associated with the receptor following endocytosis, visualization of surface-labeled NTS3 receptors was combined with that of fluo-NT. As can be seen in Fig. 7A, B and C, immunoreactive receptors showed partial co-localization with fluorescent ligand molecules up to 40 min of incubation with the

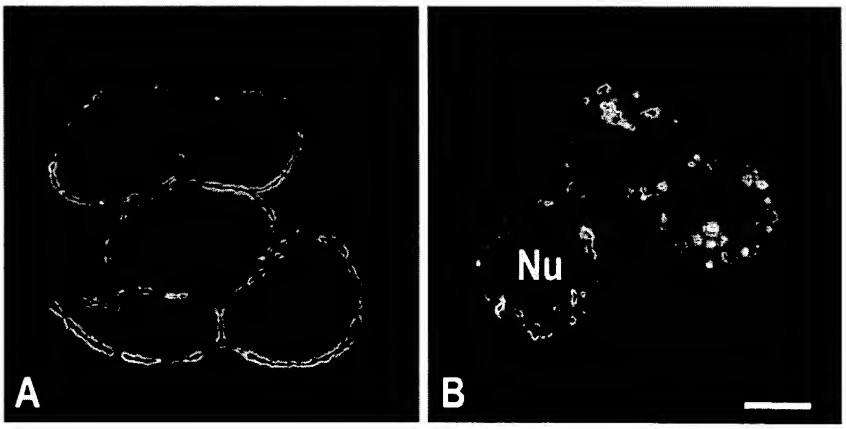

Fig. 6. Confocal microscopic tracking of receptor–ligand internalization in HT29 cells. (A) Cells stimulated with 10 nM NT for 40 min at 37 °C and immunolabeled with anti-NTS3 without permeabilization. Immunolabeled receptors are still visible at the cell surface, in the form of a fluorescent ring. (B) Cells immunolabeled at 4 °C with the anti-NTS3 antibody, stimulated for 40 min with 10 nM NT to promote internalization, and fixed and permeabilized to allow for the penetration of a fluorophore-linked secondary antibody. Immunolabeled NTS3 receptors are detected throughout the cytoplasm in the form of small fluorescent clusters. Nu, nucleus. Scale bar: 10 μm.

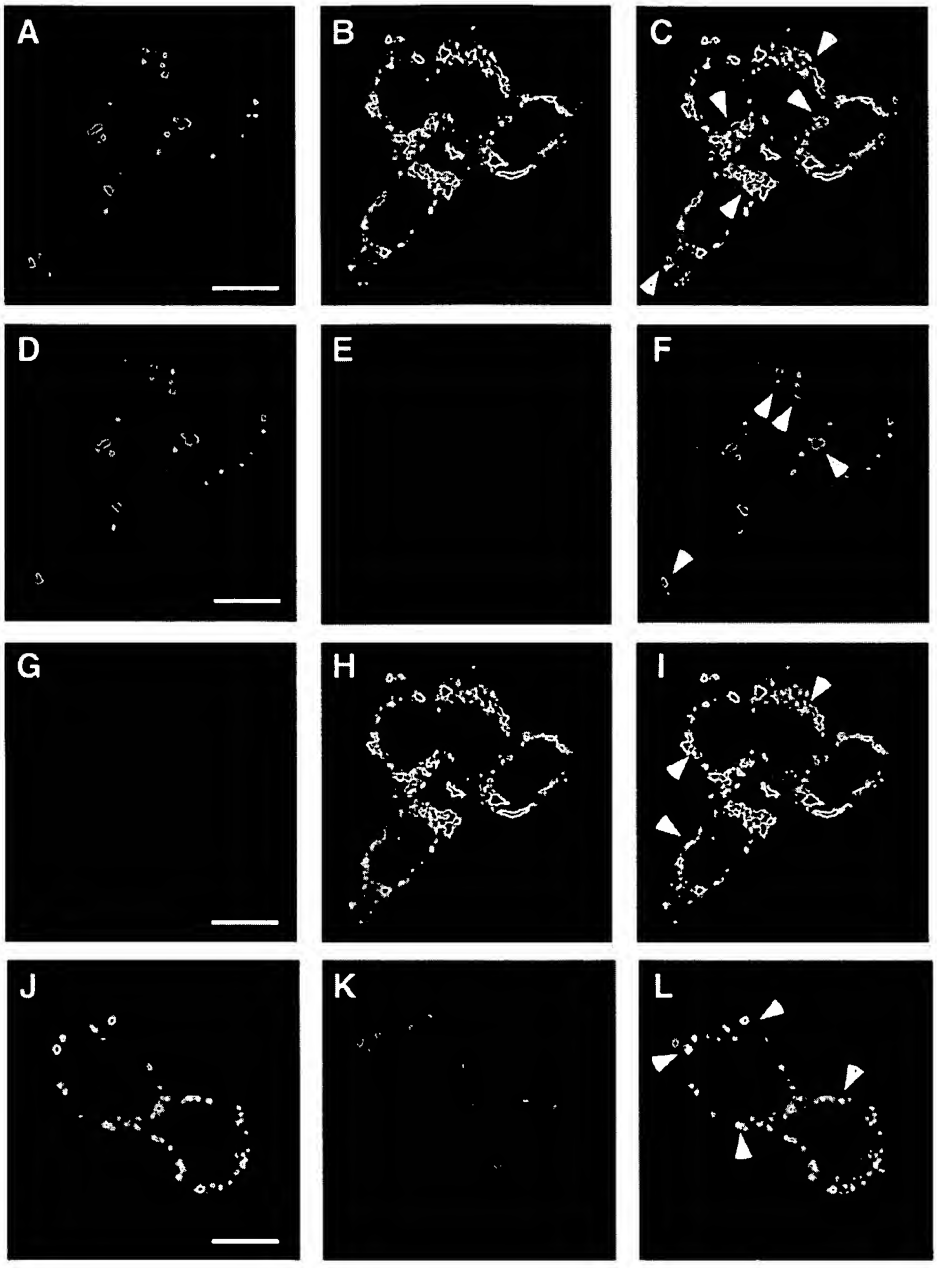

Fig. 7. Co-localization of internalized NTS3 receptors and fluo-NT, syntaxin-6, and transferrin in HT29 cells. (A), (B) and (C) Cell surface NTS3 receptors were immunolabeled at 4 °C and stimulated with 10 nM fluo-NT for 40 min at 37 °C. Internalized cell surface-labeled NTS3 (A, shown in red) and fluo-NT (B, shown in green) are partly co-localized within intra-cytoplasmic endosomes (arrowheads in (C)). (D), (E) and (F) Cell-surface NTS3 were immunolabeled at 4 °C, stimulated with 10 nM fluo-NT for 40 min, permeabilized, and immunolabeled with an anti-syntaxin-6 antibody. Internalized cell-surface labeled NTS3 (D, shown in red) shows partial overlap (arrowheads in F, magenta) with syntaxin-6 immunoreactivity (E, shown in blue). (G), (H) and (I) Internalized fluo-NT from the same experiment (shown in green) is also co-localized with syntaxin-6 (shown in blue), this is visualized in cyan in I (arrowheads). Cell-surface NTS3 receptors were immunolabeled at 4 °C and co-incubated at 37 °C for 15 min with 10 nM unlabeled NT and 50 μg/mL Alexa 568-transferrin. Note the extensive overlap (arrowheads) between internalized NTS3 (E, shown in green) and transferrin (F, shown in red). Images are presented in pseudocolor. Single trans-nuclear optical sections. Scale bar: 10 μM.

agonist. The fraction of internalized fluorescent ligand that did not co-localize with NTS3 might have internalized via NTS1, which is also expressed in this cell line (Fig. 7C). At 40 min, internalized receptors also partially overlapped with the TGN/central endosome marker syntaxin-6 (Fig. 7D, E and F). Likewise, internalized fluo-NT showed overlap with syntaxin-6 at the 40 min time point (Fig. 7G, H and I). Neither the Golgi marker Giantin nor the endosome marker Lamp-1 co-localized with internalized NTS3 (not shown).

To determine whether NT-induced internalization of NTS3 receptors proceeded through the classical endosomal pathway, the internalization of antibody-labeled cell surface receptors was monitored in parallel with that of Alexa 568-tagged transferrin. At both time points examined (15 and 40 min), substantial overlap was noted between NTS3- and Alexa 568-transferrin-labeled endosomes (Fig. 7J, K and L).

Quantification of the electron microscopic distribution of NTS3 immunoreactivity in HT29 cells before and after stimulation with 10 nM NT for either 10 or 40 min showed no significant difference in the density of gold particles in all of the compartments examined including membrane fraction, HDM and LDM fractions, and M + N fraction (not shown).

4. Discussion

The present study demonstrates that the neuropeptide, NT is internalized after binding to NTS3/sortilin receptors on the surface of HT29 cells. It also shows that internalized NT molecules are trafficked via different molecular forms of NTS3 from the cell surface to early endosomes and from early endosomes to the TGN/pericentriolar recycling endosome.

4.1. Sub-cellular distribution of NTS3 receptors in HT29 cells at steady state

Western blotting analysis of unstimulated whole cell lysates revealed the expression of two NTS3-immunoreactive proteins of molecular weight 105 and 135 kDa in HT29 cells. These results conform to those of earlier photoaffinity labeling experiments on these same cells in which α-azidobenzoyl-^{125}I-Tyr$_3$-NT was shown to label three specific bands of 50, 105, and 135 kDa (Martin et al., 2002). These proteins were found to correspond to NTS1 (50 kDa) and NTS3 (105 and 135 kDa) receptors by Western blotting using specific antibodies (Martin et al., 2002). Moreover, the 105 and 135 kDa forms of the NTS3 receptor were identified as two differentially glycosylated forms of the same receptor by virtue of the fact that tunicamicyn treatment generated the 105 kDa band at the expense of the other (Martin et al., 2002).

At steady state, only the largely predominant 105 kDa form (>90%) was consistently detected here by Western blot in sub-cellular fractions. However, the 135 kDa form was more heavily labeled than the 105 kDa one in photoaffinity labeling experiments, suggesting that the highly glycosylated form of the protein has a greater affinity for NT and may therefore correspond to the functional cell surface receptor.

Western blotting and electron microscopic data concurred in demonstrating a predominant intracellular localization of NTS3 in HT29 cells, both before and after stimulation with NT. Similarly, the bulk of NTS3/sortilin endogenously expressed in rat adipocytes (Morris et al., 1998) or heterologously expressed in COS-7 cells (Navarro et al., 2001; Petersen et al., 1997), was detected intracellularly. In HT29 cells, NTS3 was found by immunoblotting to predominate in the low-density microsomal fraction (LDM), which was selectively labeled here with the TGN/pericentriolar recycling endosome marker syntaxin-6 (Bock, Klumperman, Davanger, & Scheller, 1997). The LDM fraction also contains vesicles arising from the Golgi and the endoplasmic reticulum (Morris et al., 1998), consistent with the detection of NTS3 immunoreactivity in the Golgi apparatus and smooth endoplasmic reticulum by electron microscopy. NTS3/sortilin was previously shown to segregate with both LDM (Morris et al., 1998) and syntaxin-6-positive (Hashiramoto & James, 2000) fractions in rat and/or 3T3-L1 adipocytes. Within these cells, a high proportion of LDM-associated sortilin was found in vesicles containing the glucose transporter GLUT-4, which may account for the insulin-mediated recruitment of sortilin to the plasma membrane of these cells (Hashiramoto & James, 2000; Kandror & Pilch, 1998;Lin et al., 1997; Morris et al., 1998).

A smaller fraction of NTS3 immunoreactivity was detected in the high-density microsomal fraction

(HDM), which contains a variety of vesicular elements, including early endosomes, as attested here by its enrichment in the small GTPase Rab5A (Bucci et al., 1992; Chavrier, Parton, Hauri, Simons, & Zerial, 1990; Gorvel, Chavrier, Zerial, & Gruenberg, 1991). Accordingly, NTS3 immunoreactivity was found to decorate the membrane of endosomes by electron microscopy. These findings are congruent with the results of sub-cellular fractionation studies in adipocytes, which similarly found sortilin to be concentrated in the HDM fraction (Morris et al., 1998).

Only a small proportion of NTS3-immunoreactive receptors was detected here in association with the plasma membrane of HT29 cells by either Western blotting or electron microscopy. Similarly, only a limited fraction of the cells' provision of NTS3/sortilin was found at the plasma membrane in NTS3-transfected CHO (Nielsen et al., 1999) or COS-7 cells (Navarro et al., 2001) as well as in cell types endogenously expressing NTS3/sortilin, such as adipocytes (Morris et al., 1998). Nonetheless, studies in transfected CHO cells suggest that such low density of cell surface receptors is sufficient to ensure transduction of the effects of NT (Dal Farra et al., 2001).

A surprising finding was the presence of a relatively high concentration of NTS3/sortilin in Western blots of the N + M fraction. A similar association of NTS3 immunoreactivity with the N + M fraction was previously observed in transfected COS-7 cells (Navarro et al., 2001). This fraction contains mitochondrial, but also nuclear elements, as demonstrated by its high content in HDAC-1 immunoreactivity. Given that an important fraction of NTS3 immunoreactivity was also detected inside the nucleus by electron microscopy, it can be surmised that at least a fraction of receptor proteins detected in the N + M fraction by Western blot is associated with the nucleus as opposed to mitochondria or to other cross-contaminants. Nonetheless, this nuclear localization is puzzling since NTS3 is a transmembrane protein and since it possesses no recognized nuclear localization signal (Petersen et al., 1997). Furthermore, nuclei from adipocytes (Morris et al., 1998), microgial cells (Martin et al., 2003) and central neurons (Sarret et al., 2003) were devoid of nuclear labeling following immunostaining with the same antibody as used here. Thus, it would appear that the present nuclear labeling is specific, but may be a feature of tumoral cells.

4.2. Traffic of NTS3 receptors in HT29 cells following stimulation with NT

Stimulation of HT29 cells with NT resulted in ligand-induced internalization of NTS3/NT complexes as jointly demonstrated by photoaffinity labeling and confocal microscopic experiments. These results conformed to those of earlier photoaffinity labeling studies which had shown ^{125}I-azido-NT to internalize via both NTS1 and NTS3 receptors in these cells (Martin et al., 2002). In fact, these biochemical studies had suggested that the contribution of NTS3 might be more important than that of NTS1 in this process. Indeed, after acid wash of photoaffinity-labeled cells, bands corresponding to the NTS3 were more intensely labeled than the one corresponding to the NTS1 receptor (Martin et al., 2002). It was impossible in either these earlier or the present experiments to inhibit NT binding to NTS1 receptors using the NT antagonist SR48692 to selectively demonstrate ligand internalization via NTS3 receptors since this drug also recognizes the NTS3 (Martin et al., 2003). However, studies in COS-7 and CHO cells transfected with either human (not shown) or mouse NTS3 receptor have shown that cell surface NTS3 receptors could bind and mediate endocytosis of NT and LpL, respectively (Navarro et al., 2001; Nielsen et al., 1999).

As previously observed in transfected cells (Navarro et al., 2001), ligand-induced internalization of NTS3 caused no detectable decrease in the density of cell surface receptors, as assessed by Western blotting, as well as by confocal and electron microscopic immunocytochemistry. Using cell surface labeling and immunoprecipitation techniques on HT29 cells, we previously showed that NTS1, but not NTS3 receptors decrease from the plasma membrane upon stimulation with NT (Martin et al., 2002). This selective decrease in NTS1 likely accounts for the down regulation of NT binding sites observed after prolonged exposure to high concentrations of NT (Turner et al., 1990). On the contrary, photoaffinity-labeling experiments suggested that, if anything, the amount of NTS3 receptors available for NT binding might have been slightly increased after 15–30 min of ligand exposure. Two com-

plimentary mechanisms could account for this cell surface up-regulation. First, internalized NTS3 receptors might recycle to the cell surface as previously demonstrated in transfected cells (Navarro et al., 2001). Second, reserve intracellular receptors may be recruited to the plasma membrane from intracellular stores. As with other Type I receptors (e.g. CI-M6PR), NTS3 was shown to be translocated to the plasma membrane upon cell surface receptor stimulation (Chabry et al., 1993; Hashiramoto & James, 2000; Morris et al., 1998). In HT29 cells, translocation of NTS3 receptors to the plasma membrane could account for the reported rapid return of [^{125}I]-NT cell surface binding to control levels observed upon agonist removal (Turner et al., 1990).

The NT-induced internalization of NTS3 proceeded via the classical endosomal endocytic pathway, as attested by the increased photolabeling with time of receptors in HDM and LDM fractions and the co-localization of internalized receptors with fluorescent transferrin. The increase in the concentration of covalently bound NT in HDM and LDM compartments was not matched by an augmentation in the whole protein content of these fractions as measured by Western blot, suggesting that labeled receptors represent only a small proportion of the total. Also, the increase in NT-labeled NTS3 was tardier in the LDM than in the HDM fraction, which is consistent with traffic of internalized receptors from early endosomes (in the HDM) to late endosomes and/or to the pericentriolar recycling endosome and thereby to the TGN (Gruenberg & Maxfield, 1995; Mallet & Maxfield, 1999). Accordingly, confocal microscopic tracking of surface-labeled NTS3 receptors demonstrated that internalized NTS3 remained co-localized with transferrin over time, while becoming increasingly co-localized with the TGN marker syntaxin-6. Several endogenous proteins have been shown to travel from endosomes to the TGN, including CI-M6PR, TGN38, and furin (reviewed in Johannes & Goud, 1998). Targeting of internalized NTS3 receptors to the TGN is in keeping with the recent report that internalized chimeric receptors bearing the C-terminal tail of sortilin are trafficked to a TGN38-positive juxta-nuclear structure in transfected CHO cells (Nielsen et al., 2001).

The fact that azido-^{125}I-NT could still be covalently cross-linked to NTS3 receptors within the TGN was surprising given that NT/NTS3 complexes normally should have dissociated in the acidic environment of early endosomes. Furthermore, whereas the major form of NTS3 affinity-labeled at the cell surface was the heavily glycosylated 135 kDa protein, the one that showed the higher levels of increased radiolabeling within the LDM fraction with time was the low molecular weight one. A possible explanation for these findings could be that the ligand internalizes via cell surface NTS1 and/or 135 kDa NTS3 receptors, dissociates in early endosomes, and is then sorted from early endosomes to the TGN via the 105 kDa NTS3/sortilin (NTS1 receptors being targeted to lysosomes) (Vandenbulcke, Nouel, Vincent, Mazella, & Beaudet, 2000). Another possibility would be that the 135 kDa form of the receptor is either deglycosylated or degraded to a 105 kDa protein after internalization.

The fate of internalized NT once it has reached the TGN is unclear. One possibility is that it is sorted back to the plasma membrane and thereby cleared from its target cell. Indeed, other peptide ligands are reportedly released back into the extracellular space following internalization in epithelial cells (Koenig, Kaur, Dodgeon, Edwardson, & Humphrey, 1998). A second possibility is that internalized NT is sorted to lysosomes for degradation. This hypothesis appears unlikely, however, given that fluo-NT was never found to co-localize with lysosomal markers. Interestingly, cross-linked NTS3-ligand complexes were detected in the N + M fraction 30 min after ligand exposure in our sub-cellular fractionation studies. Admittedly, this fraction was not purified and its labeling could be due to cross-contamination with non-nuclear elements. Nonetheless, in view of the electron microscopic detection of NTS3 in the nucleus, the possibility that internalized NT or NT/NTS3 complexes are actually targeted to the nucleus cannot be readily excluded. Such nuclear targeting could account for the internalization-induced transcriptional changes (Souaze, Rostène, & Forgez, 1997) and induction of the primary response gene *Krox-24* (Poinot-Chazel et al., 1996) demonstrated in HT29 cells following stimulation with NT.

The present results demonstrate that NT binds to, and internalizes with, a large molecular form of NTS3 on the surface of HT29 cells. Once internalized, both ligand and receptor are trafficked to the TGN via the classical endosomal pathway. However, within the

TGN, NT is bound to a lower molecular form of the receptor than on the cell surface or in early endocytic compartments. These results suggest that either signaling and transport functions of NTS3/sortilin are mediated through different molecular forms of the protein, or that the receptor undergoes metabolic changes in the course of intra-cellular trafficking. In any event, the present results are consistent with NTS3 playing a receptor role for NT in HT29 cells.

Acknowledgements

This work was supported by the Centre National de la Recherche Scientifique (CNRS) Grant PICS No. 2051, by Grant MT-7366 from the Canadian Institutes for Health Research (CIHR) to A. Beaudet, and by a France-Québec exchange program from the Fonds de la Recherche en Santé du Québec to A. Beaudet and J. Mazella. A. Morinville and S. Martin are the recipients of fellowships from the Natural Sciences and Engineering Research Council of Canada (NSERC) and the Association Pour la Recherche sur le Cancer (ARC), respectively. The authors wish to thank N. Takeda for administrative assistance. The authors would also like to acknowledge Dr. C.M. Petersen for his generous gift of the NTS3 antibody as well as Drs. H. Nuthall and S. Stefani for providing the anti-HDAC-1 antibody.

References

Bock, J. B., Klumperman, J., Davanger, S., & Scheller, R. H. (1997). Syntaxin 6 functions in trans-Golgi network vesicle trafficking. *Molecular Biology of the Cell, 8*, 1261–1271.

Bradford, M. M. (1976). A rapid and sensitive method for the quantitation of microgram quantities of protein utilizing the principle of protein–dye binding. *Analytical Biochemistry, 72*, 248–254.

Bucci, C., Parton, R. G., Mather, I. H., Stunnenberg, H., Simons, K., & Hoflack, B. et al., (1992). The small GTPase *rab5* functions as a regulatory factor in the early endocytic pathway. *Cell, 70*, 715–728.

Chabry, J., Gaudriault, G., Vincent, J. P., & Mazella, J. (1993). Implication of various forms of neurotensin receptors in the mechanism of internalization of neurotensin in cerebral neurons. *Journal of Biological Chemistry, 268*, 17138–17144.

Chavrier, P., Parton, R. G., Hauri, H. P., Simons, K., & Zerial, M. (1990). Localization of low molecular weight GTP binding proteins to exocytic and endocytic compartments. *Cell, 62*, 317–329.

Clancy, M., & Czech, M. P. (1990). Hexose transport stimulation and membrane redistribution of glucose transporter isoforms in response to cholera toxin, dibutyryl cyclic AMP, and insulin in 3T3-L1 adipocytes. *Journal of Biological Chemistry, 265*, 12434–12443.

Dal Farra, C., Sarret, P., Navarro, V., Botto, J. M., Mazella, J., & Vincent, J. P. (2001). Involvement of the neurotensin receptor subtype NTR3 in the growth effect of neurotensin on cancer cell lines. *International Journal of Cancer, 92*, 503–509.

Faure, M. P., Alonso, A., Nouel, D., Gaudriault, G., Dennis, M., & Vincent, J. P. et al., (1995). Somatodendritic internalization and perinuclear targeting of neurotensin in the mammalian brain. *Journal of Neuroscience, 15*, 4140–4147.

Gorvel, J. P., Chavrier, P., Zerial, M., & Gruenberg, J. (1991). *rab5* controls early endosome fusion in vitro. *Cell, 64*, 915–925.

Gruenberg, J., & Maxfield, F. R. (1995). Membrane transport in the endocytic pathway. *Current Opinion on Cell Biology, 7*, 552–563.

Hampe, W., Rezgaoui, M., Hermans-Borgmeyer, I., & Schaller, H. C. (2001). The genes for the human *VPS10* domain-containing receptors are large and contain many small exons. *Human Genetics, 108*, 529–536.

Hashiramoto, M., & James, D. E. (2000). Characterization of insulin-responsive GLUT4 storage vesicles isolated from 3T3-L1 adipocytes. *Molecular and Cellular Biology, 20*, 416–427.

Iwase, K., Evers, B. M., Hellmich, M. R., Kim, H. J., Higashide, S., & Gully, D. et al., (1996). Indirect inhibitory effect of a neurotensin receptor antagonist on human colon cancer (LoVo) growth. *Surgical Oncology, 5*, 245–251.

Johannes, L., & Goud, B. (1998). Surfing on a retrograde wave: how does Shiga toxin reach the endoplasmic reticulum? *Trends in Cell Biology, 8*, 158–162.

Kandror, K. V., & Pilch, P. F. (1998). Multiple endosomal recycling pathways in rat adipose cells. *Biochemical Journal, 331*, 829–835.

Khatib, A. M., Siegfried, G., Prat, A., Luis, J., Chretien, M., & Metrakos, P. (2001). Inhibition of proprotein convertases is associated with loss of growth and tumorigenicity of HT-29 human colon carcinoma cells: importance of insulin-like growth factor-1 (IGF-1) receptor processing in IGF-1 mediated functions. *Journal of Biological Chemistry, 276*, 30686–30693.

Koenig, J. A., Kaur, R., Dodgeon, I., Edwardson, J. M., & Humphrey, P. P. (1998). Fates of endocytosed somatostatin sst2 receptors and associated agonists. *Biochemical Journal, 336*, 291–298.

Lin, B. Z., Pilch, P. F., & Kandror, K. V. (1997). Sortilin is a major protein component of Glut4-containing vesicles. *Journal of Biological Chemistry, 272*, 24145–24147.

Mallet, W. G., & Maxfield, F. R. (1999). Chimeric forms of furin and TGN38 are transported with the plasma membrane in the trans-Golgi network via distinct endosomal pathways. *Journal of Cell Biology, 146*, 345–359.

Maoret, J. J., Pospai, D., Rouyer-Fessard, C., Couvineau, A., Laboisse, C., & Voisin, T. et al., (1994). Neurotensin receptor and its mRNA are expressed in many human colon cancer cell lines but not in normal colonic epithelium: binding studies and

RT-PCR experiments. *Biochemical and Biophysical Research Communication, 203*, 465–471.

Marcusson, E. G., Horazdovsky, B. F., Cereghino, J. L., Gharakhanian, E., & Emr, S. D. (1994). The sorting receptor for yeast vacuolar carboxypeptidase Y is encoded by the *VPS10* gene. *Cell, 77*, 579–586.

Martin, S., Navarro, V., Vincent, J. P., & Mazella, J. (2002). Neurotensin receptor-1 and -3 complex modulates the cellular signaling of neurotensin in the HT29 cell line. *Gastroenterology, 123*, 1135–1143.

Martin, S., Vincent, J. P., & Mazella, J. (2003). Involvement of the neurotensin receptor-3 in the neurotensin-induced migration of human microglia. *Journal of Neuroscience, 23*, 1198–1205.

Mazella, J., Zsurger, N., Navarro, V., Chabry, J., Kaghad, M., & Caput, D. et al., (1998). The 100-kDa neurotensin receptor is gp95/sortilin a non-G-protein- coupled receptor. *Journal of Biological Chemistry, 273*, 26273–26276.

Mazella, J. (2001). Sortilin/neurotensin receptor-3: a new tool to investigate neurotensin signaling and cellular trafficking? *Cell Signal, 13*, 1–6.

Mazella, J., Kitabgi, P., & Vincent, J. P. (1985). Molecular properties of neurotensin receptors in rat brain Identification of subunits by covalent labeling. *Journal of Biological Chemistry, 260*, 508–514.

Morris, N. J., Ross, S. A., Lane, W. S., Moestrup, S. K., Petersen, C. M., & Keller, S. R. et al., (1998). Sortilin is the major 110-kDa protein in GLUT4 vesicles from adipocytes. *Journal of Biological Chemistry, 273*, 3582–3587.

Navarro, V., Martin, S., Sarret, P., Nielsen, M. S., Petersen, C. M., & Vincent, J. P. et al., (2001). Pharmacological properties of the mouse neurotensin receptor 3 Maintenance of cell surface receptor during internalization of neurotensin. *FEBS Letters, 495*, 100–105.

Nielsen, M. S., Madsen, P., Christensen, E. I., Nykjaer, A., Gliemann, J., & Kasper, D. et al., (2001). The sortilin cytoplasmic tail conveys Golgi-endosome transport and binds the VHS domain of the GGA2 sorting protein. *EMBO Journal, 20*, 2180–2190.

Nielsen, M. S., Jacobsen, C., Olivecrona, G., Gliemann, J., & Petersen, C. M. (1999). Sortilin/neurotensin receptor-3 binds and mediates degradation of lipoprotein lipase. *Journal of Biological Chemistry, 27*, 8832–8836.

Petersen, C. M., Nielsen, M. S., Nykjaer, A., Jacobsen, L., Tommerup, N., & Rasmussen, H. H. et al., (1997). Molecular identification of a novel candidate sorting receptor purified from human brain by receptor-associated protein affinity chromatography. *Journal of Biological Chemistry, 272*, 3599–3605.

Petersen, C. M., Nielsen, M. S., Jacobsen, C., Tauris, J., Jacobsen, L., & Gliemann, J. et al., (1999). Propeptide cleavage conditions sortilin/neurotensin receptor-3 for ligand binding. *EMBO Journal, 18*, 595–604.

Poinot-Chazel, C., Portier, M., Bouaboula, M., Vita, N., Pecceu, F., & Gully, D. et al., (1996). Activation of mitogen-activated protein kinase couples neurotensin receptor stimulation to induction of the primary response gene Krox-24a. *Biochemical Journal, 320*, 145–151.

Rostène, W. H., & Alexander, M. J. (1997). Neurotensin and neuroendocrine regulation. *Frontiers in Neuroendocrinology, 18*, 115–173.

Sadoul, J. L., Mazella, J., Amar, S., Kitabgi, P., & Vincent, J. P. (1984). Preparation of neurotensin selectively iodinated on the tyrosine 3 residue Biological activity and binding properties on mammalian neurotensin receptors. *Biochemistry and Biophysical Research Communication, 120*, 812–819.

Sarret, P., Krzywkowski, P., Segal, L., Nielsen, M. S., Petersen, C. M., & Mazella, J. et al., (2003). Distribution of NTS3 Receptor/Sortilin mRNA and Protein in the Rat Central Nervous System. *Journal of Comparative Neurology, 461*, 483–505.

Seethalakshmi, L., Mitra, S. P., Dobner, P. R., Menon, M., & Carraway, R. E. (1997). Neurotensin receptor expression in prostate cancer cell line and growth effect of NT at physiological concentrations. *Prostate, 31*, 183–192.

Souaze, F., Rostène, W., & Forgez, P. (1997). Neurotensin agonist induces differential regulation of neurotensin receptor mRNA. Identification of distinct transcriptional and post-transcriptional mechanisms. *Journal of Biological Chemistry, 272*, 10087–10094.

Tauris, J., Ellgaard, L., Jacobsen, C., Nielsen, M. S., Madsen, P., & Thogersen, H. C. et al., (1998). The carboxy-terminal domain of the receptor-associated protein binds to the Vps10p domain of sortilin. *FEBS Letters, 429*, 27–30.

Turner, J. T., James-Kracke, M. R., & Camden, J. M. (1990). Regulation of the neurotensin receptor and intracellular calcium mobilization in HT29 cells. *Journal of Pharmacology and Experimental Therapeutics, 253*, 1049–1056.

Vandenbulcke, F., Nouel, D., Vincent, J. P., Mazella, J., & Beaudet, A. (2000). Ligand-induced internalization of neurotensin in transfected COS-7 cells: differential intracellular trafficking of ligand and receptor. *Journal of Cell Science, 113*, 2963–2975.

Vincent, J. P., Mazella, J., & Kitabgi, P. (1999). Neurotensin and neurotensin receptors. *Trends in Pharmacological Sciences, 20*, 302–309.

Vita, N., Laurent, P., Lefort, S., Chalon, P., Dumont, X., & Kaghad, M. et al., (1993). Cloning and expression of a complementary DNA encoding a high affinity human neurotensin receptor. *FEBS Letters, 317*, 139–142.

THE JOURNAL OF BIOLOGICAL CHEMISTRY
Vol. 274, No. 13, Issue of Maarch 26, pp. 8832–8836, 1999
Printed in U.S.A.

Sortilin/Neurotensin Receptor-3 Binds and Mediates Degradation of Lipoprotein Lipase*

(Received for publication, December 21, 1998)

Morten S. Nielsen‡§, Christian Jacobsen‡, Gunilla Olivecrona¶, Jørgen Gliemann‡§, and Claus M. Petersen‡

From the ‡Department of Medical Biochemistry, University of Aarhus, 8000 Aarhus C, Denmark and ¶Department of Medical Biochemistry and Biophysics, Umeå University, S-901 87 Umeå, Sweden

Lipoprotein lipase and the receptor-associated protein (RAP) bind to overlapping sites on the low density lipoprotein receptor-related protein/α_2-macroglobulin receptor (LRP). We have investigated if lipoprotein lipase interacts with the RAP binding but structurally distinct receptor sortilin/neurotensin receptor-3. We show, by chemical cross-linking and surface plasmon resonance analysis, that soluble sortilin binds lipoprotein lipase with an affinity similar to that of LRP. The binding was inhibited by heparin and RAP and by the newly discovered sortilin ligand neurotensin. In ^{35}S-labeled 3T3-L1 adipocytes treated with the cross-linker dithiobis(succinimidyl propionate), lipoprotein lipase-containing complexes were isolated by anti-sortilin antibodies. To elucidate function in cells, sortilin-negative Chinese hamster ovary cells were transfected with full-length sortilin and shown to express about 8% of the receptors on the cell surface. These cells degraded ^{125}I-labeled lipoprotein lipase much faster than the wild-type cells. The degradation was inhibited by unlabeled lipoprotein lipase, indicating a saturable pathway, and by RAP and heparin. Moreover, inhibition by the weak base chloroquine suggested that degradation occurs in an acidic vesicle compartment. The results demonstrate that sortilin is a multifunctional receptor that binds lipoprotein lipase and, when expressed on the cell surface, mediates its endocytosis and degradation.

Lipoprotein lipase (LpL)[1] is rate-limiting in hydrolysis of triglycerides in circulating lipoproteins, and reduced levels or activity of the active dimeric species therefore lead to increased triglyceride levels. Even small changes in LpL function in man may have important consequences. Thus, common mutations in the LpL gene with marginal effects on the activity are associated with dyslipidemias (1, 2) and may enhance the development of atherosclerosis (3).

The mechanisms for synthesis, folding, and secretion of LpL to the lumenal side of the vascular epithelium are not known in detail. A large part of the synthesized LpL is normally degraded within the cell (4, 5), and trimming of sugar residues from oligosaccharide chains of LpL appears necessary for proper folding and expression of LpL activity (6). Moreover, dimerization is important for regulation of catalytic activity (7). At the endothelium, LpL is bound to heparan sulfate proteoglycans. LpL easily dissociates from these sites (8) and reassociates to other sites, including receptors that mediate its uptake into cells. Clearance occurs via multifunctional endocytic receptors of the LDL receptor family, notably LDL receptor-related protein/α_2-macroglobulin receptor (LRP) (9, 10), aided by accumulation of LpL on cell surface proteoglycans (10, 11) as well as directly via transmembrane proteoglycans (12–15).

Sortilin is a ~95-kDa type-I receptor first isolated from human brain (16) and recently shown to be identical with the neurotensin receptor-3 (17). It consists of a lumenal domain homologous to yeast vacuolar protein-sorting 10 protein, a single transmembrane domain, and a short cytoplasmic tail with a C terminus strongly homologous to that of the mannose 6-phosphate/insulin-like growth factor-II (IGF-II) receptor (16). In mature sortilin, an N-terminal 44-residue propeptide has been cleaved off, and recent results show that furin-mediated propeptide cleavage conditions sortilin for ligand binding (18). Besides in neurones, sortilin is abundant in several cell types including skeletal muscle, heart, and adipocytes (16, 19). Although sortilin, like the IGF-II receptor, is mainly located in the Golgi compartment and vesicles (16, 17), it is also expressed on the cell surface. In differentiated 3T3-L1 adipocytes, sortilin colocalizes with the IGF-II receptor, and insulin causes a ~2-fold increase in the expression of both receptors on the plasma membrane (19). Thus, like the IGF-II receptor, sortilin has the potential of functioning both as a sorting receptor in the Golgi compartment and as a clearance receptor on the cell surface.

Mature sortilin binds the receptor-associated protein, RAP (16), a specialized chaperone that interacts with LDL receptor family members, notably the multifunctional receptors LRP, megalin, and the very low density lipoprotein receptor (for reviews, see Refs. 20–22). RAP consists of three homologous domains of which domain D3 binds to sortilin (23). We have previously shown that LpL and segments of RAP containing D3 cross-compete for binding to LRP, and these ligands are therefore thought to bind to the same or overlapping sites on the receptor (24). As an approach to elucidate the function of sortilin as a putative endocytic and sorting receptor, we therefore investigated whether sortilin binds LpL. We show that the soluble lumenal domain of mature sortilin (s-sortilin) binds LpL with an affinity comparable with that of LRP and that the binding is inhibited by RAP and by neurotensin. Moreover, LpL is associated with sortilin in 3T3 adipocytes and is specifically

* This work was supported by The Danish Medical Research Council, Danish Biotechnology Program, and a grant from the Commission of the European Communities, Science, Research, and Development Section. The costs of publication of this article were defrayed in part by the payment of page charges. This article must therefore be hereby marked "*advertisement*" in accordance with 18 U.S.C. Section 1734 solely to indicate this fact.

§ To whom correspondence should be addressed: Dept. of Medical Biochemistry, University of Aarhus, Ole Worms Allé, Bldg. 170, DK-8000, Denmark. Tel.: +45-89-422880; Fax: +45-86-131160; E-mail: mn@biokemi.au.dk.

[1] The abbreviations used are: LpL, bovine lipoprotein lipase (dimeric); LDL, low density lipoprotein; LRP, LDL receptor-related protein/α_2-macroglobulin receptor; IGF-II, insulin-like growth factor-II; PAGE, polyacrylamide gel electrophoresis; RAP, receptor-associated protein; s-sortilin, soluble sortilin/neurotensin receptor-3; CHO, Chinese hamster ovary; CMV, cytomegalovirus; RU, response units; D23, domains 2 and 3.

degraded in stably transfected CHO cells that express mature full-length sortilin on the cell surface. We propose that sortilin, in addition to performing not yet elucidated sorting functions in the Golgi compartment, scavenges a diverse set of extracellular ligands such as LpL and neurotensin.

MATERIALS AND METHODS

Sortilin, LpL, and RAP—The extracellular domain of mature sortilin (s-sortilin), comprising residues 45–725 of full-length sortilin, was expressed in stably transfected Chinese hamster ovary (CHO-K1) cells and purified from the culture medium by RAP affinity chromatography as described (23). The propeptide (residues 1–44) was expressed in *Escherichia coli* BL21(DE3) cells as a glutathione *S*-transferase fusion protein using the pGEX4T vector (Amersham Pharmacia Biotech) and purified on a glutathione-agarose column (18). Full-length sortilin was subcloned from the cloning pBK-CMV vector (16) into the pCDNA3.1/Zeo(−) vector using *Xba*I and *Sma*I restriction enzymes and transfected into CHO-K1 cells (18). LpL was purified from bovine milk as the enzymatically active dimeric enzyme (~600 units/mg) as described previously (25). LpL and s-sortilin were ^{125}I-iodinated to specific activities of about 0.5 mol of ^{125}I/mol of protein using chloramine T as the oxidizing agent. The iodinated LpL preparation was applied to a Sepharose C16B column (Amersham Pharmacia Biotech). Labeled material that eluted at 0.9 M NaCl was discarded, and the fraction that eluted at 1.5 M NaCl, representing the dimeric form of the lipase, was used for experiments. In some cases, LpL was made monomeric by incubation with 1 M guanidinium hydrochloride for 3 h at 20 °C and dialyzed immediately before use (26). The construct LpL-(347–389/394–448 was produced in *E. coli* as described (27). The construct consists of the hexahistidine-Factor X substrate sequence Met-Gly-Ser-$(His)_6$-Ser-Ile-Glu-Gly-Arg and amino acid residues 347–389 and 394–448 of human LpL. Deletion of the sequence Trp^{390}-Ser-Asp-Trp^{393} from the construct LpL-(347–448) increases the solubility of the peptide. The construct contains the sites for binding to LRP and has about the same affinity as the uninterrupted stretch LpL-(347–448) and LpL-(313–448), which constitutes the C-terminal folding domain of LpL (27). Human RAP and RAP constructs containing domain D1 (residues 18–112) or domains 2 and 3 (D23) (residues 113–323) were produced in *E. coli* as hexahistidine-tagged peptides (28).

Antibodies—Rabbit anti-s-sortilin IgG used for immunoprecipitation of sortilin and for Western blotting and rabbit antiserum against a synthetic peptide containing residues Pro^{15}-Arg^{28} of the sortilin propeptide have been described (18). For detection of LpL in mouse 3T3-L1 adipocytes, we used IgG isolated from egg yolk of chickens immunized with bovine LpL (29).

Cross-linking of Soluble Components and Solid Phase Assay—^{125}I-Labeled s-sortilin (~10^5 cpm) was incubated with LpL in 140 mM NaCl, 10 mM $CaCl_2$, 10 mM Hepes, pH 7.8, for 16 h at 4 °C followed by incubation with the bifunctional reagent BS^3 (Pierce) at a final concentration of 100 μM for 30 min at 20 °C. The reaction was quenched by the addition of SDS sample buffer with 20 mM Tris followed by SDS-PAGE and autoradiography. For solid phase assay, LpL was immobilized in Polysorp microtiter wells (NUNC, Denmark), the wells were blocked with 2% Tween 20 for 2 h at 20 °C (24), and incubations with ^{125}I-s-sortilin were in the above buffer. After 16 h at 4 °C, the wells were washed, and bound radioactivity was eluted with 10% SDS and counted.

Surface Plasmon Resonance Analysis—All measurements were performed on a BIAcore 2000 instrument (Biosensor, Uppsala, Sweden) equipped with CM5 sensor chips. The carboxylated dextran matrix of the sensor chip (flow cells 1 and 2) was activated by the injection of 240 μl of solution containing 0.2 M *N*-ethyl-*N*′-(3-dimethylaminopropyl)carbodiimide and 0.05 M *N*-hydroxysuccimide in water, and s-sortilin was immobilized to an estimated density of 64 fmol/mm^2. Samples for binding (40 μl) were injected at 5 μl/min (4 °C) in 10 mM Hepes, 150 mM NaCl, 1.5 mM $CaCl_2$, 1 mM EGTA, 0.005% Tween 20, pH 7.4 (running buffer), and binding was expressed in terms of relative response units (RU), *e.g.* the response obtained from the flow cell with immobilized sortilin minus the response obtained using an activated but uncoupled flow cell. Regeneration of the chip was performed by injecting 20 μl of 10 mM Tris, 50 mM NaCl, 4 M urea, 0.005% Tween 20, pH 8.0. Kinetic parameters were determined using the BIAevaluation 3.0 software. The number of LpL molecules bound/mol of immobilized sortilin was estimated by dividing the ratio $RU_{ligand}/mass_{ligand}$ with $RU_{sortilin}/mass_{sortilin}$.

Culture and Incubation of Cells—3T3-L1 fibroblasts were grown in Dulbecco's modified Eagle's medium/F-12 (1:1 mix; Bio-Wittaker, Belgium), 10% donor calf serum, and 50 μg/ml gentamycin. To induce their differentiation to adipocytes, donor calf serum was replaced with fetal calf serum, and the medium was supplemented with 10 μM dexamethasone for 48 h and subsequently with insulin (10 μg/ml) for 8 days. Wild-type CHO-K1 cells and cells stably transfected with sortilin (18) were grown to near confluency in HyQ-CCM5 medium (HyClone, Utah; about 3 × 10^5 cells/well). Degradation of ^{125}I-LpL at was measured as 12% trichloroacetic acid-soluble radioactivity in the medium.

Metabolic Labeling—3T3-L1 adipocytes were washed, preincubated for 10 min in cysteine- and methionine-free modified Eagle's medium (Sigma) before overnight incubation in the same medium supplemented with 200 μCi/ml [^{35}S]cysteine and [^{35}S]methionine (pro-mix, Amersham Pharmacia Biotech), 5% full medium, and 10 μg/ml insulin. For identification of LpL-sortilin complexes, labeled 3T3-L1 cells were incubated with 1 mM cell-permeable and reducible cross-linker dithiobis(succinimidyl propionate) (Pierce). After 30 min at 4 °C, the reaction was quenched in 20 mM Tris, and following washes, the cells were lysed in 400 μl of 1.0% Triton X-100 containing 20 mM Tris and proteinase inhibitors (Complete Mini, Boehringer Mannheim). After centrifugation, the lysate supernatant was diluted in 2 ml of a Tris-balanced salt solution and incubated with Sepharose-coupled anti-s-sortilin IgG for 16 h at 4 °C. The beads were washed, and bound material was eluted in 300 μl of 100 mM glycine, pH 2.7, neutralized with Tris buffer and subjected to reducing SDS-PAGE either before or after an additional step of precipitation using chicken anti-LpL IgG. Diphenyloxazole-fluorographed gels were exposed at −70 °C.

Quantitation of Cell Surface-expressed Sortilin—The transfected CHO cells were washed three times in ice-cold phosphate-buffered saline, pH 8.0, and incubated with 0.5 mg/ml membrane-impermeable reagent sulfo-*N*-hydroxysuccinimidobiotin (Pierce, IL) for 90 min at 4 °C. After washes in phosphate-buffered saline with 50 mM Tris to quench any unreacted reagent, the cells were lysed for 10 min at 4 °C in 1% Triton X-100, 20 mM Tris, 10 mM EDTA, 150 mM NaCl, pH 8.0, with protease inhibitors, and biotinylated proteins were precipitated with streptavidin-coupled Sepharose 4B beads (Zymed Laboratories Inc., CA). The fractions of streptavidin-bound (*i.e.* surface-biotinylated) and unbound sortilin were detected by Western blotting using horseradish peroxidase-conjugated swine anti-rabbit IgG as secondary antibody (Dako, Denmark) and enhanced chemiluminescence (ECL; Amersham Pharmacia Biotech). Quantitation was performed by laser scanning densitometry using a 2202 Ultroscan instrument (LKB, Sweden).

RESULTS

Soluble Sortilin Binds LpL—To test for binding, we first incubated LpL with ^{125}I-labeled s-sortilin followed by the addition of the cross-linker BS^3. As shown in Fig. 1*A*, a complex was formed when the labeled receptor was incubated with 125 nM LpL (*lane 2*) but not without LpL (*lane 1*). The labeled complex was increased by unlabeled soluble sortilin at low concentration (9 nM) (*lane 3*). However, the formation of complex was inhibited by 180–540 nM unlabeled soluble sortilin (*lanes 4* and *5*) and by heparin (*lane 6*). In addition, 500 nM LRP or megalin, which are both known to bind LpL (10, 11, 30), abolished the formation of complex between sortilin and LpL (not shown).

We next examined if RAP inhibits the binding. Because the cross-linked complex with RAP is not easily distinguished from that with LpL (Fig. 1*B*, *lanes 3 versus* 2), we used the smaller construct comprising RAP D23, which binds to sortilin (23) and shares binding sites with LpL on LRP (24). At 5 μM, D23 markedly inhibited sortilin-LpL complex and caused the formation of a smaller complex (*lane 4*), whereas 125 nM D23 caused partial inhibition (*lane 5*). To further analyze the inhibition, ^{125}I-sortilin was incubated with LpL immobilized in microtiter wells. Fig. 2 shows that RAP and RAP D23, but not D1, inhibited the binding reaction. This agrees with the previous result that sortilin binds RAP D3 and D23 but not the individual domains D1 or D2 (23).

The binding of LpL was further substantiated by plasmon resonance analysis using s-sortilin immobilized on the sensor chip. Fig. 3*A* shows that LpL binds readily and demonstrates a marked decrease in binding when LpL was made monomeric by treatment with guanidinium hydrochloride. The calculated capacity was about 0.4 mol of LpL/mol of s-sortilin, suggesting

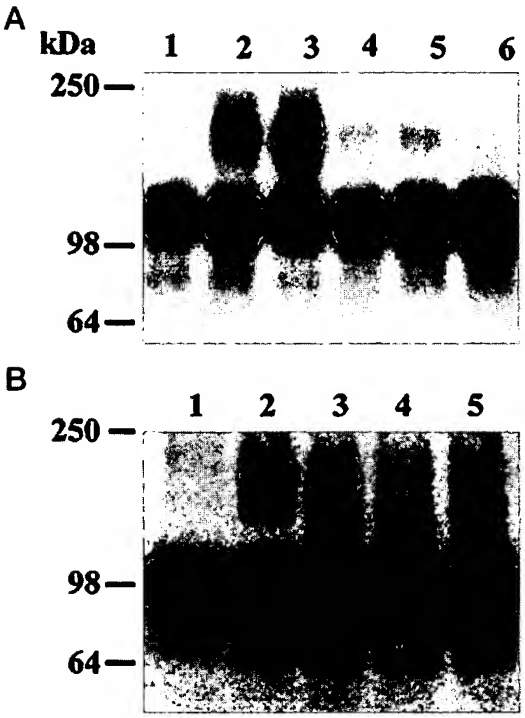

FIG. 1. **Cross-linking of sortilin to LpL.** *A*, ^{125}I-labeled s-sortilin (100 pM, ~10^5 cpm) was incubated for 16 h at 4 °C without additions (*lane 1*) or with 125 nM LpL in the absence (*lane 2*) or presence of 9, 180, or 540 nM unlabeled sortilin (*lanes 3–5*), or heparin (100 units/ml) (*lane 6*), followed by incubation with the cross-linker BS^3 for 30 min. The reaction was then quenched, and the samples were applied to reducing SDS-PAGE (4–16%). *B*, incubation was with ^{125}I-s-sortilin without additions (*lane 1*), with 125 nM LpL alone (*lane 2*), or with 125 nM LpL plus 5 μM RAP (*lane 3*), 5 μM RAP D23 (*lane 4*), or 125 nM RAP D23 (*lane 5*), followed by cross-linking and SDS-PAGE. The *bands* were visualized by autoradiography.

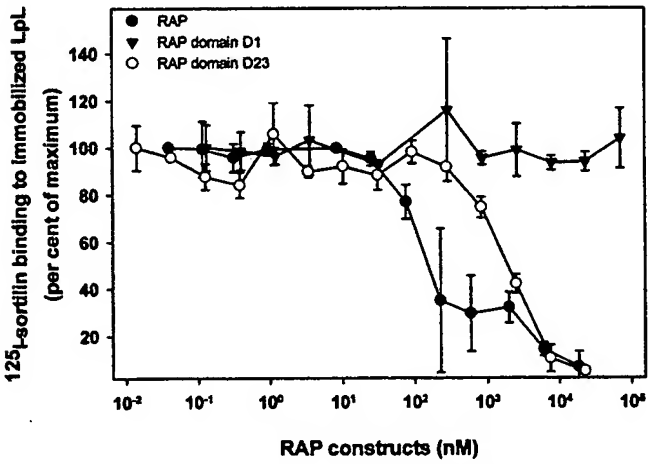

FIG. 2. **Inhibition of sortilin binding to LpL by RAP constructs.** ^{125}I-s-sortilin (~100 pM) was incubated in microtiter wells with immobilized LpL in the presence of RAP, RAP D1, or RAP D23 as indicated. The results are the mean values ±1 S.D. of three replicate values. The binding of ^{125}I-sortilin in the absence of inhibitors was approximately 5% that of the added tracer and was normalized to 100%. The background values for binding (about 0.5% of the added tracer) have been subtracted.

that the binding stoichiometry might be 1:1. The K_d for binding of LpL to s-sortilin was calculated at about 26 nM from these and a series of similar curves obtained at LpL concentrations ranging from 9 nM to 454 nM. The affinity for binding of monomeric LpL was about 100-fold lower. For comparison, LpL binding was also analyzed using LRP immobilized to the chip. The K_d value was calculated at about 11 nM for binding of LpL

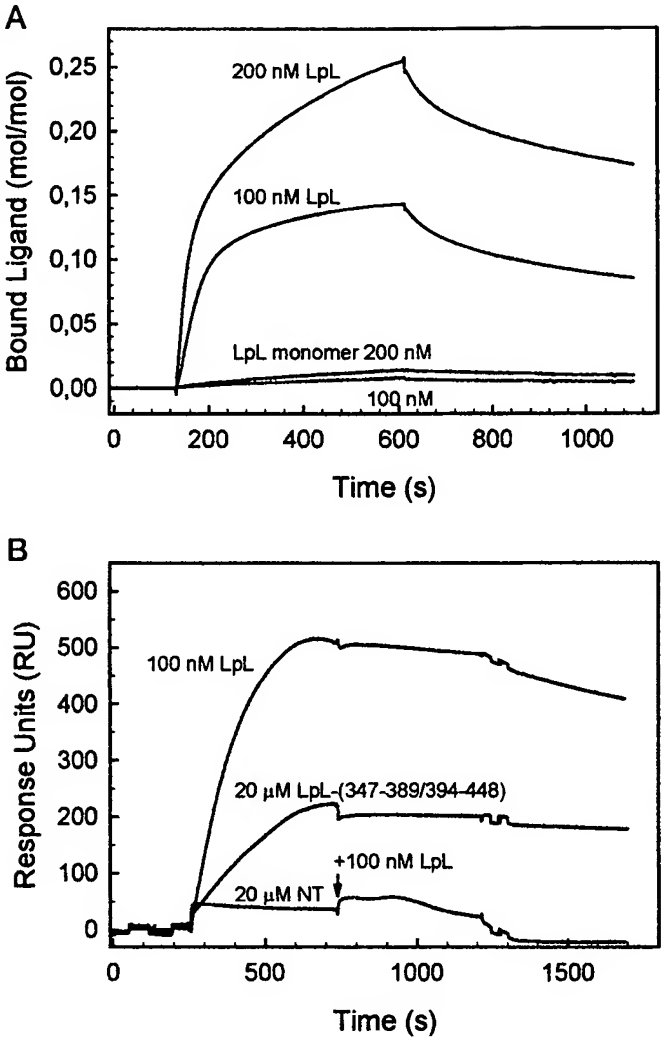

FIG. 3. **Surface plasmon resonance analysis of LpL binding to sortilin.** *A*, the sensor chip was coupled covalently with s-sortilin and perfused with LpL at the concentrations indicated or with LpL made monomeric by treatment with guanidinium hydrochloride. The perfusion was shifted to buffer alone at 700 s. *B*, the chip was perfused with 100 nM LpL or 20 μM of the peptide LpL-(347–389/394–448). Perfusion was also performed with 20 μM neurotensin (*NT*), which itself gives a minor signal because of its small size, and 100 nM LpL was added at 740 s (*arrow*).

to LRP and was in the micromolar range when LpL had been made monomeric (not shown), which is in broad agreement with previous observations using LRP immobilized in microtiter wells (11). To further test the specificity of LpL binding, the chip with immobilized sortilin was perfused with the fragment LpL-(347–389/394–448), which contains the two LRP binding segments in the C-terminal folding domain of human LpL (27). Fig. 3*B* shows that this peptide (20 μM) binds to sortilin, suggesting that the same segments in LpL are required for interaction with the two receptors. We also probed whether the 13-residue neuropeptide neurotensin, recently identified as a sortilin ligand (17), interferes with LpL binding. As shown in Fig. 3*B*, neurotensin at 20 μM essentially abolished the binding of LpL, suggesting that the two ligands bind to overlapping sites on sortilin. Finally, we tested the sortilin propeptide (as glutathione *S*-transferase fusion protein), which binds to s-sortilin as well as to mature full-length sortilin and inhibits binding of RAP and neurotensin (18). The results demonstrated that s-sortilin, when first incubated with LpL at a near-saturating concentration (200 nM, cf. *panel A*), was unable to bind propeptide (not shown).

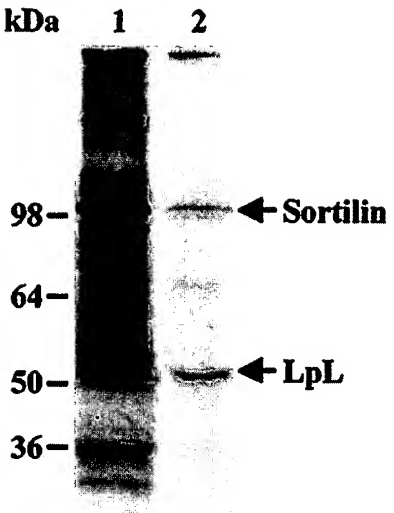

FIG. 4. **Binding of LpL to sortilin in 3T3-L1 adipocytes.** ^{35}S-Labeled 3T3 cells were treated with the cell-permeable and thiol-cleavable cross-linker, dithiobis(succinimidyl propionate). After quenching of the reaction, the cells were lysed followed by incubation with Sepharose-coupled anti-sortilin. *Lane 1* shows SDS-PAGE (8–16%) followed by autoradiography of acid-eluted labeled proteins after cleavage of the cross-linker by reduction. Some of the eluted material (before reduction) was immunoprecipitated with chicken anti-LpL. *Lane 2* shows the precipitated labeled proteins after cleavage of the cross-linker. The bands were visualized by autoradiography of 2,5-diphenyloxazole-impregnated gels.

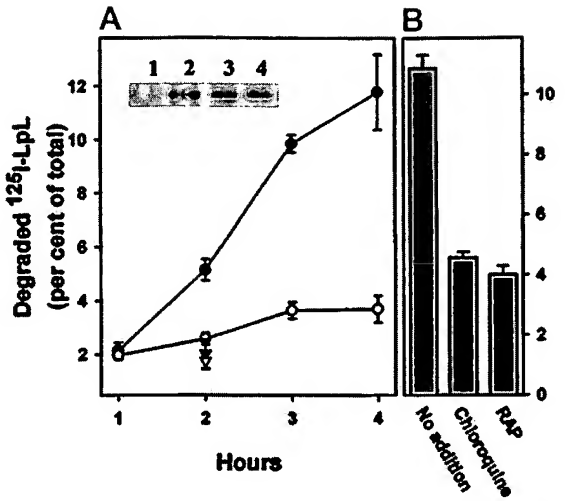

FIG. 5. **Degradation of LpL in sortilin-transfected CHO cells.** *A*, the cells (1×10^5/well) were incubated at 37 °C in 300 μl of medium with ^{125}I-LpL (1.5×10^4 cpm/ml). The *ordinate* shows the percent of the added tracer soluble in trichloroacetic acid. *A*, the *filled symbols* represent sortilin transfectants, and the *open symbols* represent wild-type cells without (*circles*) and with (*triangles*) 500 nM unlabeled LpL. The *inset* shows Western blots of total lysates of wild-type (*lane 1*) and transfected cells (*lane 2*). *Lane 3* shows the Western blot of biotinylated sortilin recovered on streptavidin-Sepharose from the lysate of surface-biotinylated cells. *Lane 4* shows Western blot of the remaining nonbiotinylated sortilin in the same lysate. The band shown in *lane 3* represents lysate from 11 times more cells than the band shown in *lane 4*. *B*, degradation of ^{125}I-LpL by the transfected cells incubated for 3 h without additions, with RAP (6 μM), or with chloroquine (100 μM). All values are means of triplicate determinations ±1 S.D.

Thus, LpL binds to soluble sortilin with an affinity comparable with that for binding to LRP, presumably via its C-terminal folding domain. Moreover, the binding is competed for by the sortilin ligands, RAP (via D3) and neurotensin and by the sortilin propeptide.

Binding of LpL to Sortilin in 3T3-L1 Cells—To elucidate interaction in cells, we used 3T3-L1 adipocytes because they express LpL as well as sortilin (31, 19). Initially we observed coexpression of LpL and sortilin upon differentiation, *i.e.* after 3–4 days in culture (not shown). Fully differentiated ^{35}S-labeled 3T3-L1 adipocytes were incubated with the permeable and thiol-cleavable cross-linker dithiobis(succinimidyl propionate) and lysed, followed by incubation with Sepharose-coupled rabbit anti-sortilin IgG. Complexes were then released from the Sepharose beads and subjected to reducing SDS-PAGE. As shown in Fig. 4, *lane 1*, a dominating band corresponds to sortilin itself, and a marked band is compatible with LpL. Other labeled peptides may represent nonspecific binding reactions. To confirm the presence of LpL, we immunoprecipitated the complexes released from the anti-sortilin Sepharose beads using chicken anti-LpL IgG. Fig. 4, *lane 2*, shows that reducing SDS-PAGE identified labeled peptides compatible with LpL and sortilin. Thus, a fraction of LpL appears associated with sortilin in the 3T3-L1 cells.

Sortilin Can Mediate LpL Degradation—We used stably transfected CHO cells to elucidate functional consequences of LpL binding to sortilin. The transfectants expressed sortilin in contrast to the wild-type cells as seen from Western blotting of total lysates (Fig. 5*A*, *inset*, *lane 2 versus lane 1*). The receptor was predominantly in the mature form because no reaction was observed when using anti-serum directed against the N-terminal propeptide (not shown). This is in agreement with the results of pulse-chase experiments, demonstrating that all newly synthesized sortilin is cleaved (18). To assess the fraction of sortilin expressed on the cell surface, the transfectants were treated with the nonpermeable reagent sulfo-*N*-hydroxysuccinimidobiotin at 4 °C and lysed, and biotinylated proteins were recovered on streptavidin-Sepharose beads. Sortilin was then detected by SDS-PAGE followed by Western blotting of the bound material as compared with the sortilin content in the fraction of the lysate not bound to streptavidin-Sepharose. Fig. 5, *inset*, shows that biotinylated (*lane 3*) as well as nonbiotinylated sortilin (*lane 4*) were readily detected. Scanning densitometry of the Western blots (*cf.* legend to Fig. 5) revealed that about 8% sortilin in the transfected cells had been accessible to biotinylation and, thus, represents the fraction expressed on the cell surface.

We next aimed at determining LpL binding to the cell surface expressed sortilin. However, ^{125}I-labeled LpL bound readily and equally well to wild-type and transfected CHO cells (not shown), presumably to cell surface proteoglycans as shown previously (12). Experiments were therefore performed to determine whether sortilin mediates uptake and subsequent degradation of the surface-associated LpL. As shown in Fig. 5*A*, the transfected cells degraded ^{125}I-LpL much faster than wild-type cells. The cell-mediated degradation was inhibited by 100 units/ml heparin (not shown) and by 500 nM unlabeled LpL, indicating a saturable mechanism. As shown in Fig. 5*B*, the degradation of LpL in sortilin transfectants was inhibited by RAP and by the weak base chloroquine that raises pH in intracellular compartments. We conclude that sortilin expressed on the cell surface can interact with LpL and mediate its degradation.

DISCUSSION

The results show that sortilin is multifunctional because it binds LpL in addition to neurotensin, and they establish sortilin as an endocytic receptor on the cell surface because it can mediate LpL degradation. The affinity of LpL for binding to sortilin is similar to that for binding to LRP. As also shown for LRP (11), the LpL monomer has markedly reduced affinity, possibly because the dimeric state provides the right conforma-

tion for receptor binding segments in the C-terminal folding domain. Alternatively, it cannot be excluded that the LpL dimer can interact with two sortilin molecules. We consistently observed that small amounts of unlabeled s-sortilin facilitated cross-linking of labeled sortilin to LpL (Fig. 1). Although this phenomenon remains unexplained, it is possible that sortilin, like heparin, can help stabilizing LpL in the dimeric form.

Sortilin is mainly located intracellularly in several cell types. In transiently transfected COS-1 cells, full-length sortilin is mainly in the Golgi compartment, and chimeric receptors consisting of the C-terminal cytoplasmic tail of sortilin and the lumenal domain of the interleukin-2 receptor colocalize with the IGF-II receptor (16). The molecular basis for the predominant retrieval of sortilin to the Golgi compartment is most likely the acidic cluster at the C terminus, because an identical cluster in the IGF-II receptor, containing a phosphorylatable serine residue, is important for the retrieval via interaction with the newly identified protein PACS-1 (32). In neurons, however, sortilin is up-regulated on the cell membrane following neurotensin-induced sequestration of the neurotensin receptor-1 (17, 33), and in rat adipocytes and 3T3-L1-cultured adipocytes, the fraction of sortilin expressed on the surface is increased 1.7-fold by insulin (19). Interestingly, both the localization and the insulin responsiveness of sortilin in adipocytes resembles that of the IGF-II receptor, presumably because of the homology of important signal sequences in their cytoplasmic tails (16). The two receptors are therefore likely to be similar in terms of cycling among the Golgi, endosomal, and plasma membrane compartments. The transfected CHO cells described in this report express about 8% of sortilin on the cell surface, in broad agreement with the fractional surface expressions of sortilin and IGF-II receptors in adipocytes and of IGF-II receptors in normal rat kidney cells (19, 34).

LpL is taken up by members of the LDL receptor family, particularly LRP (9, 11), through contacts in the the C-terminal folding domain of the LpL (27). The molecular basis for the interaction with sortilin appears to be similar because a construct of LpL containing the segments important for binding to LRP also bound to sortilin. In addition, RAP domains D23 and LpL cross-compete for binding to sortilin, indicating that the two ligands have the same or overlapping sites for binding like on LRP (24). Previous studies using cultured cells have shown that LpL, independent of its catalytic activity, can enhance lipoprotein uptake by providing a bridge between lipoproteins and endocytic receptors of the LDL receptor family (Refs. 11, 35, and 36; for review, see Ref. 22), and LpL-facilitated lipoprotein uptake has recently been confirmed *in vivo* (37). Future studies should show whether sortilin, via interaction with LpL, participates in receptor-mediated lipoprotein uptake.

The result that cell surface-expressed sortilin can mediate degradation of LpL may apply to other ligands, *e.g.* neurotensin (17, 33). However sortilin may also exhibit important functions in the Golgi compartment in analogy with the established dual functions of the IGF-II receptor as an endocytic and a sorting receptor. Because sortilin is abundantly expressed in cell types that secrete LpL, future studies should elucidate whether it is involved in sorting of newly synthesized LpL to specialized compartments.

In conclusion, we find that sortilin binds LpL with an affinity comparable with that of LRP and that the receptor can mediate uptake and degradation of the ligand when expressed on the cell surface.

Acknowledgment—We thank Dr. M. Etzerodt, Laboratory of Gene Expression, University of Aarhus, for providing recombinant RAP domains.

REFERENCES

1. Gerdes, C., Fischer, R. M., Nicaud, V., Boer, J., Humphries, S. E., Talmud, P. J., and Færgeman, O. (1997) *Circulation* **95,** 733–740
2. Wittrup, H. H., Tybjærg-Hansen, A., Abildgaard, S., Steffensen, R., Schnohr, P., and Nordestgaard, B. G. (1997) *J. Clin. Invest.* **99,** 1606–1613
3. Jukema, J. W., van Boven, A. J., Groenemeijer, B., Zwinderman, A. H., Reiber, J. H., Bruschke, A. V., Henneman, J. A., Molhoek, G. P., Bruin, T., Jansen, H., Gagne, E., Hayden, M. R., and Kastelein, J. J. (1996) *Circulation* **94,** 1913–1918
4. Semb, H., and Olivecrona, T. (1987) *Biochim. Biophys. Acta* **921,** 104–115
5. Doolittle, M. H., Ben Zeev, O., Elovson, J., Martin, D., and Kirchgessner, T. G. (1990) *J. Biol. Chem.* **265,** 4570–4577
6. Masuno, H., Blanchette-Mackie, E. J., Schultz, C. J., Spaeth, A. E., Scow, R. O., and Okuda, H. (1992) *J. Lipid Res.* **33,** 1343–1349
7. Bergö, M., Olivecrona G., and Olivecrona T. (1996) *Biochem. J.* **313,** 893–898
8. Lookene, A., Savonen, R., and Olivecrona, G. (1997) *Biochemistry* **36,** 5267–5275
9. Chappell, D. A., Fry, G. L., Waknitz, M. A., Iverius, P. H., Williams, S. E., and Strickland, D. K. (1992) *J. Biol. Chem.* **267,** 25764–25767
10. Nykjær, A., Bengtsson-Olivecrona, G., Lookene, A., Moestrup, S. K., Petersen, C. M., Weber, W., Beisiegel, U., and Gliemann, J. (1993) *J. Biol. Chem.* **268,** 15048–15055
11. Nykjær, A., Nielsen, M., Lookene, A., Meyer, N., Røigaard, H., Etzerodt, M., Beisiegel, U., Olivecrona, G., and Gliemann, J. (1994) *J. Biol. Chem.* **269,** 31747–31755
12. Berryman, D. E., and Bensadoun, A. (1995) *J. Biol. Chem.* **270,** 24525–24531
13. Weaver, A. M., Lysiak, J. J., and Gonias, S. L. (1997) *J. Lipid Res.* **38,** 1841–1850
14. Fuki, I. V., Kuhn, K. M., Lomazov, I. R., Rothman, V. L., Tuszynski, G. P., Iozzo, R. V., Swenson, T. L., Fischer, E. A., and Williams, K. J. (1997) *J. Clin. Invest.* **100,** 1611–1622
15. Fernandez-Borja, M., Bellido, D., Vilella, E., Olivecrona, G., and Vilaro, S. (1996) *J. Lipid Res.* **37,** 464–481
16. Petersen, C. M., Nielsen, M. S., Nykjær, A., Jacobsen, L., Tommerup, N., Rasmussen, H. H., Røigaard, H., Gliemann, J., Madsen, P., and Moestrup, S. K. (1997) *J. Biol. Chem.* **272,** 3599–3605
17. Mazella, J., Zsürger, N., Navarro, V., Chabry, J., Kaghad, M., Caput, D., Ferrara, P., Vita, N., Gully, D., Maffrand, J. P., and Vincent, J.-P. (1998) *J. Biol. Chem.* **273,** 26273–26276
18. Petersen C. M., Nielsen, M. S., Jacobsen, C., Tauris, J., Jacobsen, L., Gliemann, J., Moestrup, S. K., and Madsen, P. (1999) *EMBO J.* **18,** 595–604
19. Morris, N. J., Ross, S. A., Lane, W. S., Moestrup, S. K., Petersen, C. M., Keller, S. R., and Lienhard, G. E. (1998) *J. Biol. Chem.* **273,** 3582–3587
20. Bu, G., and Schwartz, A. L. (1998) *Trends Cell Biol.* **8,** 272–276
21. Willnow, T. E. (1998) *Biol. Chem. Hoppe-Seyler* **379,** 1025–1032
22. Gliemann, J. (1998) *Biol. Chem. Hoppe-Seyler* **379,** 951–964
23. Tauris, J., Ellgaard, L., Jacobsen, C., Nielsen, M. S., Madsen, P., Thøgersen, H. C., Gliemann, J., Petersen, C. M., and Moestrup, S. K. (1998) *FEBS Lett.* **429,** 27–30
24. Nielsen, M. S., Nykjær, A., Warshawsky, I., Schwartz, A. L., and Gliemann, J. (1995) *J. Biol. Chem.* **270,** 23713–23719
25. Bengtsson-Olivecrona, G., and Olivecrona, T. (1991) *Methods Enzymol.* **197,** 345–356
26. Osborne, J. C., Jr., Bengtsson-Olivecrona, G., Lee, N. S., and Olivecrona, T. (1985) *Biochemistry* **24,** 5606–5611
27. Nielsen, M. S., Brejning, J., García, R., Zhang, H., Hayden, M. R., Vilaró, S., and Gliemann, J. (1997) *J. Biol. Chem.* **272,** 5821–5827
28. Ellgaard, L., Holtet, T. L., Nielsen, P. R., Etzerodt, M., Gliemann, J., and Thøgersen, H. C. (1997) *Eur. J. Biochem.* **244,** 544–551
29. Vilella, E., Joven, J., Fernandez, M., Vilaro, S., Brunzell, J. D., Olivecrona, T., and Bengtsson-Olivecrona, G. (1993) *J. Lipid Res.* **34,** 1555–1564
30. Kounnas, M. Z., Chappell, D. A., Strickland, D. K., and Argraves, W. S. (1993) *J. Biol. Chem.* **268,** 14176–14181
31. Olivecrona, T., Chernick, S. S., Bengtsson-Olivecrona, G., Garrison, M., and Scow, R. O. (1987) *J. Biol. Chem.* **262,** 10748–10759
32. Wan, L., Molloy, S. S., Thomas, L., Liu, G., Xiang, Y., Rybak, S. L., and Thomas, G. (1998) *Cell* **94,** 205–216
33. Chabry J., Gaudriault, G., Vincent, J.-P., and Mazella, J. (1993) *J. Biol. Chem.* **268,** 17138–17144
34. Griffiths, G., Matteoni, R., Back, R., and Hoflack, B. (1990) *J. Cell Sci.* **95,** 441–461
35. Beisiegel, U., Weber, W., and Bengtsson-Olivecrona, G. (1991) *Proc. Natl. Acad. Sci. U. S. A.* **88,** 8342–8346
36. Chappell, D. A., Inoue, I., Fry, G. L., Pladet, M. W., Bowen, S. L., Iverius, P. H., Lalouel, J. M., and Strickland, D. K. (1994) *J. Biol. Chem.* **269,** 18001–18006
37. Merkel, M., Kako, Y., Radner, H., Cho, I. S., Ramasamy, R., Brunzell, J. D., Goldberg, I. J., and Breslow J. L. (1998) *Proc. Natl. Acad. Sci. U. S. A.* **95,** 13841–13846

Regulation of Cell Survival by Secreted Proneurotrophins
Ramee Lee, *et al.*
Science **294**, 1945 (2001);
DOI: 10.1126/science.1065057

Science (print ISSN 0036-8075; online ISSN 1095-9203) is published weekly, except the last week in December, by the American Association for the Advancement of Science, 1200 New York Avenue NW, Washington, DC 20005.

way. To confirm PA's specific involvement in the mTOR pathway, we used an S6K1 mutant ($\Delta N_{23}\Delta C_{104}$), the activity of which is resistant to rapamycin and sensitive to wortmannin (*27*). When transiently expressed in HEK293 cells, the rapamycin-resistant $\Delta N_{23}\Delta C_{104}$ mutant S6K1 activity was insensitive to butanol, whereas the recombinant wild-type S6K1 activity was inhibited by 1- and 2-butanol (Fig. 4A) to a similar extent as was the endogenous kinase (Fig. 2B). These observations support the hypothesis that PA signaling to S6K1 specifically goes through mTOR and not through PI3K . However, the specific PI3K inhibitor wortmannin abolished PA-stimulated S6K1 activation and 4E-BP1 phosphorylation (*26*), implying that PI3K is indispensable for the downstream response to PA. Based on the collective evidence, we propose a mechanism by which amino acid sufficiency sensed by the mTOR pathway, mitogenic stimulation of the mTOR pathway mediated by PA, and mitogenic stimulation of the PI3K pathway independent of PA are all required for full activation of S6K1 and 4E-BP1 (Fig. 4B). The observed PA stimulatory effect on these downstream effectors is likely dependent on the basal activity of PI3K in the absence of serum, which may also explain the fact that PA had a less potent stimulatory effect than did serum (Fig. 1).

Our findings reveal a mitogenic pathway upstream of S6K1 and 4E-BP1, which involves PA and probably its direct interaction with mTOR. The data suggest that rapamycin's inhibitory effect may derive from its competition with PA for binding to the FRB domain, preventing mTOR from activating downstream effectors but without inhibiting mTOR's catalytic activity. Another PIKK family member, DNA-PK, binds to inositol hexakisphosphate (IP_6), and its function in DNA double-strand break repair is regulated by IP_6 (*28*). The modulation of mTOR signaling by PA, together with DNA-PK stimulation by IP_6, may reveal a common theme of lipidlike molecules participating in regulation of PIKK proteins.

References and Notes

1. E. J. Brown *et al.*, *Nature* **369**, 756 (1994).
2. D. M. Sabatini, H. Erdjument-Bromage, M. Lui, P. Tempst, S. H. Snyder, *Cell* **78**, 35 (1994).
3. C. J. Sabers *et al.*, *J. Biol. Chem.* **270**, 815 (1995).
4. C. T. Keith, S. L. Schreiber, *Science* **270**, 50 (1995).
5. T. Schmelzle, M. N. Hall, *Cell* **103**, 253 (2000).
6. F. G. Kuruvilla, S. L. Schreiber, *Chem. Biol.* **6**, R129 (1999).
7. A. C. Gingras, B. Raught, N. Sonenberg, *Genes Dev.* **15**, 807 (2001).
8. A. C. Gingras, B. Raught, N. Sonenberg, *Annu. Rev. Biochem.* **68**, 913 (1999).
9. S. Fumagalli, G. Thomas, in *Translational Control of Gene Expression*, N. Sonenberg, J. W. B. Hershey, M. B. Mathews, Eds. (Cold Spring Harbor Laboratory Press, Cold Spring Harbor, NY, 2000), pp. 695–718.
10. E. J. Brown *et al.*, *Nature* **377**, 441 (1995).
11. G. J. Brunn *et al.*, *Science* **277**, 99 (1997).
12. P. E. Burnett, R. K. Barrow, N. A. Cohen, S. H. Snyder, D. M. Sabatini, *Proc. Natl. Acad. Sci. U.S.A.* **95**, 1432 (1998).
13. P. H. Scott, G. J. Brunn, A. D. Kohn, R. A. Roth, J. C. Lawrence Jr., *Proc. Natl. Acad. Sci. U.S.A.* **95**, 7772 (1998).
14. D. English, Y. Cui, R. A. Siddiqui, *Chem. Phys. Lipids* **80**, 117 (1996).
15. A. G. Buckland, D. C. Wilton, *Biochim. Biophys. Acta* **1483**, 199 (2000).
16. K. Fukami, T. Takenawa, *J. Biol. Chem.* **267**, 10988 (1992).
17. H. L. Reeves, M. G. Thompson, C. L. Dack, A. D. Burt, C. P. Day, *Hepatology* **31**, 95 (2000).
18. S. F. Yang, S. Freer, A. A. Benson, *J. Biol. Chem.* **242**, 477 (1967).
19. M. J. Cross *et al.*, *Curr. Biol.* **6**, 588 (1996).
20. M. Vilella-Bach, P. Nuzzi, Y. Fang, J. Chen, *J. Biol. Chem.* **274**, 4266 (1999).
21. J. Chen, X. F. Zheng, E. J. Brown, S. L. Schreiber, *Proc. Natl. Acad. Sci. U.S.A.* **92**, 4947 (1995).
22. J. Choi, J. Chen, S. L. Schreiber, J. Clardy, *Science* **273**, 239 (1996).
23. J. P. Segrest *et al.*, *J. Lipid Res.* **33**, 141 (1992).
24. Y. Barenholz *et al.*, *Biochemistry* **16**, 2806 (1977).
25. Y. Fang, M. Vilella-Bach, J. Chen, unpublished data.
26. Supplementary Web material is available on *Science* Online at www.sciencemag.org/cgi/content/full/294/5548/1942/DC1.
27. Q. P. Weng, K. Andrabi, M. T. Kozlowski, J. R. Grove, J. Avruch, *Mol. Cell. Biol.* **15**, 2333 (1995).
28. L. A. Hanakahi, M. Bartlet-Jones, C. Chappell, D. Pappin, S. C. West, *Cell* **102**, 721 (2000).
29. J. E. Kim, J. Chen, *Proc. Natl. Acad. Sci. U.S.A.* **97**, 14340 (2000).
30. HEK293 cells were maintained in Dulbecco's modified Eagle medium (DMEM) containing 10% fetal bovine serum (FBS) at 37°C with 5% CO_2. Serum starvation of cells was carried out in serum-free DMEM for 24 hours. For amino acid deprivation, the cells were incubated in Dulbecco's phosphate-buffered solution containing 10% dialyzed FBS for 2 hours. Transient transfections were performed with SuperFect or PolyFect (Qiagen, Valencia, CA). The amount of plasmid DNA transfected per well in six-well plates was 1 μg of mTOR, 1 μg of S6K1, and 0.4 μg of 4E-BP1.
31. All bacterial expression plasmids were constructed in pGEX-2T (Pharmacia), and all mammalian expression plasmids were constructed in pCDNA3 (Invitrogen). pCDNA-FLAG-mTOR/S2035T, pCDNA-FLAG-mTOR/S2035T/D2357E (kinase-dead), pCDNA-Myc-S6K1 (p70s6k), pCDNA-FLAG-4E-BP1, pGEX-FRB (wild type), and pGEX-FRB/S2035I were previously described (*20*, *29*). $\Delta N_{23}\Delta C_{104}$ S6K1 (amino acids 24 to 398) cDNA was amplified by polymerase chain reaction (PCR) and inserted into pCDNA-Myc via Not I and Xba I sites. All point mutations were generated by nested PCR using Bam HI and Eco RI as the flanking sites for pGEX-FRB constructs and Kpn I and Hpa I for pCDNA-FLAG-mTOR constructs. Glutathione *S*-transferase (GST)–FKBP12 and various FRB proteins were expressed and purified from *Escherichia coli* strain BL21, as described previously (*20*).

32. We thank J. George for technical guidance with the lipid binding assays, J. Clardy for suggestions regarding the FRB structure, and Z. Liu for discussions about the manuscript. Supported by NIH R01 grant GM58064 and American Heart Association Midwest Affiliate grant 9951123Z.

5 September 2001; accepted 23 October 2001

Regulation of Cell Survival by Secreted Proneurotrophins

Ramee Lee, Pouneh Kermani, Kenneth K. Teng, Barbara L. Hempstead*

Neurotrophins are growth factors that promote cell survival, differentiation, and cell death. They are synthesized as proforms that can be cleaved intracellularly to release mature, secreted ligands. Although proneurotrophins have been considered inactive precursors, we show here that the proforms of nerve growth factor (NGF) and the proforms of brain derived neurotrophic factor (BDNF) are secreted and cleaved extracellularly by the serine protease plasmin and by selective matrix metalloproteinases (MMPs). ProNGF is a high-affinity ligand for $p75^{NTR}$ with high affinity and induced $p75^{NTR}$-dependent apoptosis in cultured neurons with minimal activation of TrkA-mediated differentiation or survival. The biological action of neurotrophins is thus regulated by proteolytic cleavage, with proforms preferentially activating $p75^{NTR}$ to mediate apoptosis and mature forms activating Trk receptors to promote survival.

The neurotrophin family of growth factors, including NGF, BDNF, and neurotrophins-3 and -4 (NT-3, NT-4) regulates neuronal survival and synaptic plasticity (*1*). They are synthesized as precursors (proneurotrophins) that are proteolytically cleaved to mature, biologically active neurotrophins (*2*). Because neurotrophins are normally expressed at low levels, little is known about their processing and secretion by neurons and non-neuronal cells in vivo. However, when expressed in heterologous cells, proneurotrophins are secreted as well as cleaved intracellularly by furin or proconvertases at a highly conserved dibasic amino acid cleavage site for secretion as stable, noncovalent dimers (*3*, *4*). Mature neurotrophins selectively bind to members of the Trk family of receptor tyrosine kinases, but they also interact with low affinity to a structurally distinct receptor, $p75^{NTR}$. Although $p75^{NTR}$ can increase the affinity and specificity of Trk-neurotrophin

Division of Hematology, Department of Medicine, Weill Medical College of Cornell University, 1300 York Avenue, New York, NY 10021, USA.

*To whom correspondence should be addressed: E-mail: blhempst@med.cornell.edu

interactions, $p75^{NTR}$ can also induce apoptosis in oligodendrocytes, neurons, and vascular smooth muscle cells when Trk activation is reduced or absent (*5*). High doses of neurotrophin elicit cell death through $p75^{NTR}$, indicating that $p75^{NTR}$ signaling is relatively limited in comparison to that of other receptors of the tumor necrosis factor (TNF) receptor superfamily (*5*).

Defined functions for the neurotrophin prodomains have been limited to promoting the folding of the mature domain (*6–8*) and to sorting neurotrophins to either constitutive or regulated secretory pathways (*9*). However, sequence comparison of proneurotrophins revealed regions of the prodomain that are highly conserved across species, suggesting that they may mediate additional biological actions (*10*). To assess this possibility, the expression of proNGF and proBDNF in adult mouse tissues was determined (*11*). Using antibodies specific for the mature domains of NGF or BDNF (*11*), immunoreactive proteins with molecular masses of 18 to 30 kD were detected, in addition to the 13.5-kD mature forms of NGF and BDNF (*11*, *12*). This suggested that tissue-specific proteolytic processing of proneurotrophins occurs in vivo.

Because proneurotrophins are secreted by cells (*4*, *11*, *12*) and contain consensus sites for cleavage by plasmin and by MMP-3 and MMP-7 (*13*), we considered whether secreted proneurotrophins could be cleaved extracellularly by such proteases. Both plasmin and MMPs exhibit expression patterns consistent with neurotrophin action: at the synapse, where mature BDNF can activate presynaptic and postsynaptic TrkB receptors (*14*), and on endothelial cell surfaces, where mature BDNF promotes TrkB-mediated endothelial cell survival (*15*).

BDNF was harvested from the media of 293 or endothelial cells that were infected with recombinant adenovirus encoding BDNF (*16*). In addition to 13.5-kD mature BDNF, proBDNF forms of molecular mass 30, 28, and 24 kD, and those of mass 28 kD, were detected by a BDNF-specific antibody in the media of 293 cells and endothelial cells, respectively (Fig. 1, A and B). Addition of plasmin, MMP-3, or MMP-7 to the harvested media reduced the amount of the 30-kD proBDNF (Fig. 1A). The 28-kD proBDNF from endothelial cell media was also cleaved by plasmin and MMP-7 but not MMP-3, possibly reflecting differences in expression of tissue inhibitors of metalloproteinases by endothelial and 293 cells (Fig. 1B). MMP-7 treatment of secreted proBDNF from 293 or endothelial cells yielded a 17-kD proBDNF form, suggesting that cleavage occurred approximately 90 amino acids from the NH_2-terminus (*11*). Incubation of plasmin or MMP-7 with specific inhibitors verified the specificity of these proteolytic events.

To confirm the extracellular cleavage of proBDNF, endothelial cells expressing BDNF were incubated with plasmin before media collection (Fig. 1C). Inhibition of plasmin activity by the cell-impermeable inhibitor aprotinin reduced cleavage of proBDNF, suggesting that these higher molecular weight forms are released from cells and then cleaved by plasmin at the cell surface. Thus, in addition to furin, cleavage of proneurotrophins can be regulated selectively by plasmin and MMPs.

To analyze the cleavage of secreted proNGF, a point mutation in the dibasic site used by furin was generated to impair intracellular proteolysis (*17*). Furin-resistant proNGF was expressed in 293 cells (Fig. 1D), and, when secreted, was cleaved by plasmin to a 13-kD form (Fig. 1E). In addition, incubation with MMP-7 but not MMP-2, -3, or -9 resulted in cleavage of the 30-kD proNGF to the 17-kD form (Fig. 1E).

To evaluate whether proneurotrophins selectively bind and activate Trk and $p75^{NTR}$ receptors, furin-resistant proNGF and mature NGF were purified from the media of transfected 293 cells (Fig. 1D), and their ability to bind TrkA or $p75^{NTR}$ was determined (Fig. 2) (*18*). Cells expressing either TrkA or $p75^{NTR}$ were treated with radiolabeled mature NGF and either unlabeled proNGF or unlabeled mature NGF. Unlabeled mature NGF displaced binding of radiolabeled mature NGF from TrkA expressing cells with an IC_{50} (concentration of inhibitor that reduced binding by 50%) of 1.2 nM, in agreement with equilibrium binding studies [dissociation constant (K_d) = 1 nM] (*19*, *20*). However, furin-resistant proNGF was ineffective in displacing mature NGF bound to TrkA, with an IC_{50} of greater than 5 nM. Mature NGF also

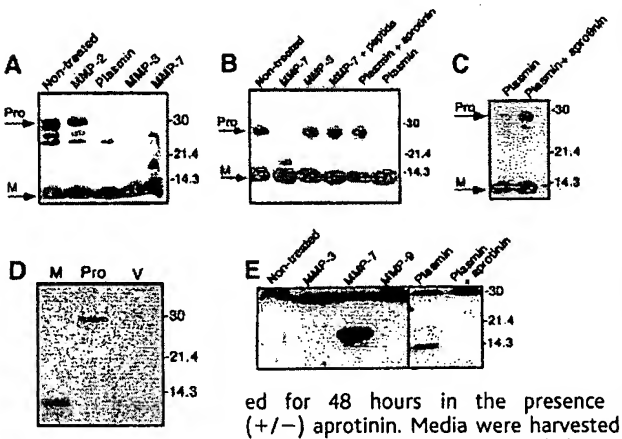

Fig. 1. Cleavage of secreted proBDNF and proNGF by candidate proteinases. Harvested media of BDNF-expressing 293 cells (**A**), or murine endothelial cells (**B**) was incubated with the indicated proteinases, and cleavage products were probed in Western blot analysis with antibody to BDNF (*16*). To confirm enzymatic specificity, plasmin was incubated with the inhibitor aprotinin or MMPs were incubated with a peptide inhibitor. (**C**) Endothelial cells expressing BDNF were incubated for 48 hours in the presence of plasmin with or without (+/−) aprotinin. Media were harvested and analyzed by Western blot. (**D**) Purification of mature NGF (M) and cleavage-resistant proNGF (Pro) from media from 293 cells stably expressing native NGF, of a furin-resistant form of NGF with a His tag at the COOH-terminus, or of the vector alone (V) with the use of Ni-column chromatography (*17*). Proteins eluted with imidazole were analyzed by SDS–polyacrylamide gel electrophoresis (SDS-PAGE) and silver staining. (**E**) Purified furin-resistant proNGF was incubated with the indicated proteinases with or without (+/−) inhibitors and proteolytic products were detected by Western blot analysis with antibody to NGF. The inability of MMP-3 to cleave proNGF, as compared to proBDNF, may reflect sequence differences at the putative MMP site.

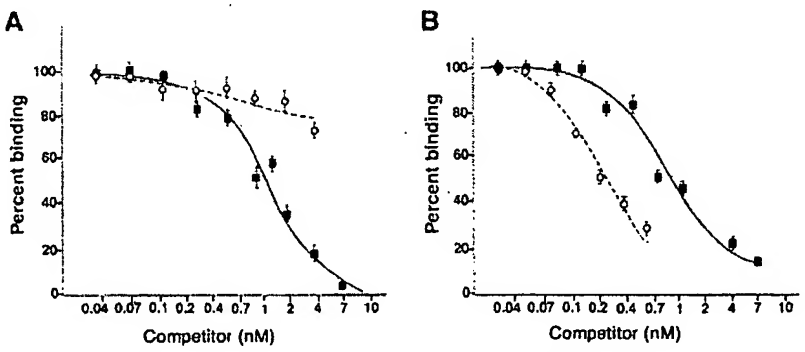

Fig. 2. Binding analysis of mature and cleavage-resistant proNGF to TrkA or $p75^{NTR}$ receptors. Dilutions of purified furin-resistant proNGF (Fig. 1D), or commercial mature NGF were assayed for their ability to displace ^{125}I-radiolabeled commercial mature NGF (1 nM) from 293 cells expressing TrkA (**A**) or from A875 cells expressing $p75^{NTR}$ (**B**) (*28*). Squares, commercial mature NGF; open circles, cleavage resistant proNGF. Competition with purified mature NGF yielded results that were comparable to those obtained with commercial NGF (*18*).

displaced radiolabeled mature NGF bound to $p75^{NTR}$ with an IC_{50} of 1.0 nM, consistent with equilibrium binding studies (K_d = 1.3 nM) (*19*). However, furin-resistant proNGF bound to $p75^{NTR}$ with five times greater affinity than mature NGF, with an IC_{50} of 0.2 nM. These results demonstrate that proNGF is the preferred ligand for $p75^{NTR}$ but not TrkA, and they suggest that $p75^{NTR}$-dependent cellular processes might be more efficiently induced by proNGF than by mature NGF.

To determine whether the higher affinity binding of proNGF to $p75^{NTR}$ resulted in enhanced $p75^{NTR}$-mediated apoptosis, we used a vascular smooth muscle cell line expressing $p75^{NTR}$ but not Trk receptors, which exhibits dose-dependent apoptosis upon addition of NGF (*21*). Cells were exposed to purified mature NGF or furin-resistant proNGF (*22*). Treatment of cells with mature NGF from commercial sources (predominantly mature NGF) induced apoptosis in 20% of the cells at 2 nM concentration (~50 ng/ml) (*5*, *21*) (Fig. 3A). In contrast, treatment of cells with proNGF was at least 10 times more potent than mature NGF in inducing apoptosis in 18% of cells at 0.1 nM. This result, together with the binding data (Fig. 2B), suggests that occupancy of less than 30% of $p75^{NTR}$ receptors with furin-resistant proNGF can induce apoptosis.

To determine the relative activities of mature NGF and furin-resistant proNGF in activating Trk-mediated cellular responses, we assessed TrkA autophosphorylation in dose-response studies (*22*) (Fig. 3B). Mature NGF and commercial NGF induced TrkA autophosphorylation at a concentration of 0.2 nM. However, furin-resistant proNGF did not induce TrkA phosphorylation even at concentrations of 1 nM, consistent with the observed reduction in TrkA binding (Fig. 2A). To assess the functional consequences of proNGF-TrkA interactions, TrkA-expressing PC12 cells and dissociated superior cervical ganglia (SCG) neurons were used in neurite outgrowth assays (Fig. 3, C and D). Treatment of PC12 cells with purified mature NGF or commercial NGF induced neurite elongation at 0.2 to 0.4 nM concentration. However, reduced neurite outgrowth was observed in PC12 cells or SCG neurons that were treated with the furin-resistant proNGF at concentrations of 0.2 to 0.8 nM, consistent with prior reports that proneurotrophins are less active than the mature forms in promoting Trk-mediated neuronal survival (*6*) and in activating Trk receptors (*3*). Treatment of SCG neurons, which coexpress both $p75^{NTR}$ and TrkA (*23*), with proNGF resulted in cell death (Fig. 3D). Taken together, these results suggest that the cleavage-resistant proform of NGF is a high-affinity, functional ligand for the pro-apoptotic $p75^{NTR}$ receptor, whereas the proteolytically cleaved mature NGF is the preferred ligand for TrkA.

These studies shed light on the often-conflicting roles for $p75^{NTR}$ in mediating apoptosis (*23–25*) and in augmenting Trk-induced survival and differentiation (*5*). The selectivity of proNGF for $p75^{NTR}$ suggests that its local secretion may determine whether apoptotic or survival actions predominate. Thus, despite widespread $p75^{NTR}$ expression, an evaluation of proneurotrophin expression should clarify the spatial and temporal restriction of apoptosis in injured neuronal tissues (after seizures, inflammation, or degeneration) and in injured blood vessels where neurotrophins, $p75^{NTR}$, and Trk receptors are coexpressed (*1*, *26*). The regulated activity of proteases such as plasmin and selective MMPs may further define these proapoptotic or prosurvival effects of neurotrophins. Examination of potential biological activities for the precursor forms of other growth factors, such as glial derived neurotrophic factor and neuregulins, whose cleaved forms bind to multicomponent receptors, may uncover differential activation of individual receptor components.

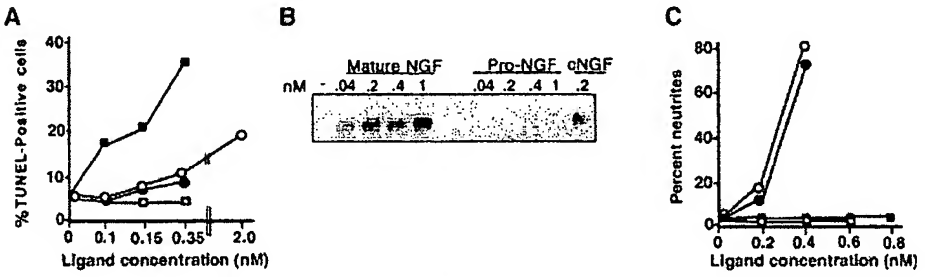

Fig. 3. Distinct biological activities are elicited by mature and cleavage-resistant proNGF. (**A**) Induction of apoptosis in $p75^{NTR}$-expressing smooth muscle cells (p75Ts-Tag-SMC) (*21*) by mature NGF and furin-resistant proNGF. Cells were cultured at 39.5°C for 96 hours to permit differentiation and were then incubated with the indicated concentration of commercial mature NGF (open circles), purified mature NGF (solid circles), purified furin-resistant proNGF (solid squares), or column eluates from vector transfected cells (open squares). After 18 hours, cells were stained with 4′,6′-diamidino-2-phenylindole (DAPI) to visualize nuclei, were fixed, and were subjected to TUNEL analysis (Roche Molecular Biochemicals, Indianapolis, Indiana). At least 400 cells per condition were counted, and the result is representative of two independent experiments with different preparations of NGFs. (**B**) Mature NGF is more active than proNGF in inducing TrkA phosphorylation. TrkA-expressing 293 cells were cultured in reduced serum for 18 hours, followed by either the addition of diluent (–) or of mature NGF, proNGF, or commercial NGF (cNGF) at the indicated concentrations for 10 min. Immunoprecipitations using antibody to Trk were analyzed by Western blot with antibody to phosphotyrosine. (**C** and **D**) Effects of mature and cleavage resistant proNGF on neuritogenesis using PC12 cells (C) or SCG neurons (D). Cells were treated with mature NGF (solid circles), cleavage-resistant proNGF (solid squares), or commerical mature NGF (open circles) at the indicated concentration or with the control column eluates from vector-transfected cells (open squares) for 48 hours in serum-free media, and cells were evaluated for neurite processes greater than one cell body in length. SCG neurons were treated with 0.4 nM mature or proNGF for 36 hours and were fixed. Trk was detected using rhodamine-conjugated antibody to Trk, TUNEL analysis performed with fluorescein isothiocyanate–deoxyuridine 5′-triphosphate (FITC-dUTP), and nuclei were detected by DAPI staining. The percentage of neurite-expressing cells (white typeface) and apoptotic cells (green typeface) is indicated. Cells treated with diluent alone yielded 30 ± 10% apoptosis. Scale bar, 30 μm. At least 200 cells per condition were scored, and results are representative of three independent experiments using different preparations of NGFs.

References and Notes

1. A. Patapoutian, L. F. Reichardt, *Curr. Opin. Neurobiol.* **11**, 272 (2001).
2. R. H. Edwards, M. J. Selby, P. D. Garcia, W. J. Rutter, *J. Biol. Chem.* **263**, 6810 (1988).
3. S. J. Mowla *et al.*, *J. Biol. Chem.* **276**, 12660 (2001).
4. J. V. Heymach, E. M. Shooter, *J. Biol. Chem.* **270**, 12297 (1995).
5. F. S. Lee, A. H. Kim, G. Khursigara, M. V. Chao, *Curr. Opin. Neurobiol.* **11**, 281 (2001).
6. U. Suter, J. V. Heymach, E. M. Shooter, *EMBO J.* **10**, 2395 (1991).
7. A. Rattenholl *et al.*, *J. Mol. Biol.* **305**, 523 (2001).
8. R. Kolbeck, S. Jungbluth, Y.-A. Barde, *Eur. J. Biochem.* **225**, 995 (1994).
9. H. W. Farhadi *et al.*, *J. Neurosci.* **20**, 4059 (2000).
10. G. Heinrich, T. Lum, *Int. J. Dev. Neurosci.* **18**, 1 (2000).
11. Web figure 1 is available at *Science* Online at www.sciencemag.org/cgi/content/full/294/5548/1945/DC1.
12. M. Fahnestock *et al.*, *Mol. Cell. Neurosci.* **18**, 210 (2001).

13. M. M. Smith, L. Shi, M. Navre, *J. Biol. Chem.* **270**, 6440 (1995).
14. M. M. Poo, *Nature Rev. Neurosci.* **2**, 24 (2001).
15. M. Donovan *et al.*, *Development* **127**, 4531 (2000).
16. Recombinant adenovirus encoding rat BDNF (*27*) was used to infect 293 cells or a temperature-sensitive SV40 T antigen transformed murine cardiac microvascular endothelial cell line at a multiplicity of infection of 100 or 200, respectively. Forty-eight-hours after infection, BDNF in the media was harvested and incubated with plasmin (3 μg/ml; American Diagnostics, Greenwich, CT) with or without (+/−) aproptinin (3 μl/ml; Sigma, St. Louis, MO), MMP-2, -3, -7 (10 μl/ml; Calbiochem, San Diego, CA) or harvested and incubated with MMP-9 (10 μl/ml; Oncogene, Cambridge, MA) with or without (+/−) MMP inhibitor (5 μl/ml, Calbiochem) for 1 hour at 37°C. Purified proNGF (0.8 μg/ml) (*17*) was used for proteolytic digestion in parallel samples. Cleavage products were detected by Western blot analysis using antibody specific for mature BDNF or mature NGF.
17. The cDNA encoding mouse NGF was amplified by reverse transcriptase–polymerase chain reaction (RT-PCR) and was bidirectionally sequenced. To improve translation initiation, 11 bases from mouse 5′ untranslated region (UTR) of mouse NT-3 including the Kozak consensus were exchanged for the mouse NGF sequence [GenBank M35075, base pairs (bp) 84 to 95] immediately 5′ of the initiating methionine. Using PCR-based mutagenesis, six histidine (His) residues were added at the COOH-terminus, and residues RR (bp 1008 to 1013) near the COOH-terminus were mutated to AA to prevent cleavage of the His-tag. To generate proNGF with impaired furin-cleavage, residues RR (bp 531 to 536) were mutated to AA using PCR. After bidirectional sequencing, constructs were subcloned into the expression vector pCDNA and stably transfected 293 cells were isolated after selection in G418 containing medium. Cells were incubated in serum-depleted media for 18 hours, and the media was collected and depleted of cells by centrifugation. His-tagged mature or furin-resistant proNGF was purified using Ni-bead chromatography (Xpress System Protein Purification; Invitrogen, Carlsbad, CA) per manufacturer's methods with the use of 350 mM imidazole for elution. Medium from 293 cells stably transfected with vector alone was harvested in parallel.
18. Mouse NGF (Harlan, Indianapolis, IN) was radioiodinated using lactoperoxidase and hydrogen peroxide as described (*28*) to an average specific activity of 3000 disintegrations per minute (dpm)/fmol and was used within 2 weeks. Competition analysis of equilibrium binding was performed using a whole-cell assay. A875 melanoma cells expressing $p75^{NTR}$ but not Trk receptors or 293 cells stably transfected with pCDNA-rat TrkA (*17*) were resuspended at 0.75 × 10^6 cells/ml final concentration. Cells were incubated with 1 nM radioiodinated NGF in the presence or absence of unlabeled mature NGF or unlabeled proNGF from 0.005 to 7 nM concentration and binding proceeded for 1 hour at 0.4°C. Cell-bound NGF was separated from free NGF by centrifuging through calf serum. Each condition was assessed in quadruplicate. Nonspecific binding measured in parallel incubation with 500-fold excess mature NGF was less than 10% of total binding. Results corrected for this nonspecific binding were expressed as the mean ± standard deviation. The PRISM program was used to generate the IC_{50} with the use of linear regression.
19. B. L. Hempstead *et al.*, *Nature* **350**, 678 (1991).
20. A. Schropel, D. von Schack, G. Dechant, Y. A. Barde, *Mol. Cell. Neurosci.* **6**, 544 (1995).
21. S. Wang *et al.*, *Am. J. Pathol.* **157**, 1247 (2000).
22. 293 cells expressing TrkA were serum-starved for 18 hours and then neurotrophins were added for 10 min before cell harvest. TrkA was immunoprecipitated with pan-Trk antibody (*19*), and Western blots probed with antibody to phosphotyrosine. TrkA-expressing PC12 cells (*29*) were used for neuritogenesis assays, and freshly isolated SCG from P0 rat pups were used on collagen substrate.
23. S. X. Bamji *et al.* *J. Cell Biol.* **140**, 911 (1998).
24. J. M. Frade, A. Rodriguez-Tebar, Y.-A. Barde, *Nature* **383**, 166 (1996).
25. P. Cassacia-Bonnefils, B. D. Carter, R. T. Dobrowski, M. V. Chao, *Nature* **383**, 716 (1996).
26. M. J. Donovan *et al.*, *Am. J. Pathol.* **147**, 309 (1995)
27. E. Benraiss *et al.*, *J. Neurosci.* **21**, 6718 (2001).
28. D. Mahadeo *et al.*, *J. Biol. Chem.* **269**, 6884 (1994).
29. B. L. Hempstead *et al.*, *Neuron* **9**, 883 (1992).
30. Supported by NIH grant NS30687, the Burroughs Wellcome Fund and the American Heart Association (to B.L.H.), and NIH grant T32 EY07138. We thank M. Chao, J. Salzer, D. Falcone, I. Feit, K. Hajjar, and S. Rafii for comments; C. Cummins and M. Kobi for technical assistance; and C. Wieland for manuscript preparation. Adenoviral vectors were kindly provided by S. Goldman, and murine endothelial cells were provided by B. Weksler and D. Poulan.

3 August 2001; accepted 25 October 2001

Lobster Sniffing: Antennule Design and Hydrodynamic Filtering of Information in an Odor Plume

M. A. R. Koehl,[1]* Jeffrey R. Koseff,[2] John P. Crimaldi,[2]† Michael G. McCay,[1] Tim Cooper,[1] Megan B. Wiley,[2] Paul A. Moore[3]

The first step in processing olfactory information, before neural filtering, is the physical capture of odor molecules from the surrounding fluid. Many animals capture odors from turbulent water currents or wind using antennae that bear chemosensory hairs. We used planar laser–induced fluorescence to reveal how lobster olfactory antennules hydrodynamically alter the spatiotemporal patterns of concentration in turbulent odor plumes. As antennules flick, water penetrates their chemosensory hair array during the fast downstroke, carrying fine-scale patterns of concentration into the receptor area. This spatial pattern, blurred by flow along the antennule during the downstroke, is retained during the slower return stroke and is not shed until the next flick.

Many animals use chemical cues in the water or air around them to detect mates, competitors, food, predators, and suitable habitats (*1–3*). Large-scale turbulent flow in the environment carries odorants from a source to an animal's olfactory organ (such as an antenna or nose), while small-scale laminar flow near the organ's surface and molecular diffusion transport odorants to the receptors (*2*, *4*). Turbulent fluid motion on a scale of meters to millimeters (*5*) determines the patchy intermittent structure of odor plumes in the environment (*6*); hence, chemical signals monitored at a point downstream from an odor source fluctuate in terrestrial (*7*, *8*) and aquatic (*9*, *10*) habitats and in laboratory flumes (*11–12*). Recent attention has focused on the relation between the neural output of antennae and of the brain antennal lobe of moths in odor plumes (*13*) and on the neural processing of odorant pulses (*14*). We used lateral antennules of spiny lobsters, *Panulirus argus*, to analyze the critical first step in determining the spatial and temporal patterns of odor pulses arriving at receptors: the physical interaction of the olfactory organ with an odor plume. *P. argus* lateral antennules (Fig. 1A) bear rows of aesthetascs (hairs containing hundreds of chemoreceptor cells) flanked by larger guard hairs (*15*) and thus provide a system for investigating the design of hair-bearing olfactory antennae (*16*, *17*).

Fluid flow around a hair in an array depends on the relative importance of inertial and viscous forces, as represented by the Reynolds number (Re) (*18*). Because the fluid in contact with the surface of a moving object does not slip relative to the object, a velocity gradient develops in the flow around the object. The smaller or slower the object (that is, the lower its Re), the thicker this boundary layer of sheared fluid is relative to the size of the object. If the boundary layers around the hairs in an array are thick relative to the gaps between hairs, then little fluid leaks through the array. Hair arrays undergo a transition between nonleaky paddlelike behavior and leaky sievelike behavior as Re is increased (*19–21*). Although flow velocity has only a small effect on the rate of molecule

[1]Department of Integrative Biology, University of California, Berkeley, CA 94720–3140, USA. [2]Environmental Fluid Mechanics Laboratory, Department of Civil and Environmental Engineering, Stanford University, Stanford, CA 94305–4020, USA. [3]Department of Biological Sciences and the J. P. Scott Center for Neuroscience, Mind, and Behavior, Bowling Green State University, Bowling Green, OH 43403, USA.

*To whom correspondence should be addressed. E-mail: cnidaria@socrates.berkeley.edu

†Present address: Department of Civil, Environmental, and Architectural Engineering, University of Colorado, Boulder, CO 80309–0428, USA.

not observed for the mature form, and that proHB-EGF may act as a tumor survival factor in hepatoma cells.

Hepatomas at the earliest stage do not always need rapid growth, but it is necessary for escape from various immune systems. Resistance against several factors may play a role in the early progression of hepatomas. A hepatoma overexposing proHB-EGF showed strong resistance to several factors. Although the mechanism underlying resistance to TGFβ-induced apoptosis remain unknown, the resistance to serum-starved treatment is thought to be due to G1 arrest induced by up-regulation of p21. In some cases, cells under G1 arrest undergo apoptosis. However, pHB-AH cells showed slow growth with a high percentage of the G1 phase in the cell cycle. Thus, proHB-EGF specifically may act as a cell survival factor in liver tissues.

6. Apoptosis in Neurodegenerative Disorders

Yoshikuni MIZUNO, Hideki MOCHIZUKI, Yukihiro SUGITA and Keigo GOTO

The Department of Neurology, Juntendo University School of Medicine, Tokyo

Key words: Parkinson's disease, neuronal death, apoptosis, Alzheimer's disease, Huntington's disease

Apoptosis has been implicated as a mechanism of neuronal degeneration in many neurodegenerative disorders. We report recent progress in apoptosis in Parkinson's disease (PD) and other major neurodegenerative disorders. We studied autopsied midbrains from 11 patients with Parkinson's disease and 6 control patients who died from various causes but not from neurodegenerative disorders; the details have been reported elsewhere (1). Four out of the 11 PD patients were of young onset PD (onset before 40 years of the age) and the remaining 7 were late onset sporadic patients. We used the standard TUNEL method to detect apoptosis. None of the control and young onset PD patients showed TUNEL positive neurons in the substantia nigra. Four of the 7 late onset PD patients had TUNEL-positive neurons in the substantia nigra. Counting the TUNEL-positive neurons in one of the midbrain sections revealed that 0.6 to 4.8% (mean 2.1%) of the remaining nigral neurons were TUNEL positive in those 4 patients. Although the percentages were low, we believe that apoptosis is involved in nigral cell death in PD. The low percentage is understandable considering that fragmented nuclei are quickly phagocytosed by glia cells, and the chance is small that fragmented DNA can be picked up by the TUNEL method. TUNEL-positive astrocytic and oligodendrocytic nuclei were also seen in some patients; 6 out of 7 late onset PD patients, 2 out of 4 young onset PD patients, and 1 out of 6 control patients had TUNEL positive glia cells. The reason why glia cells were more TUNEL positive may be due to the fact that glia cells have to be removed from the tissue when their roles are over.

According to the literature, Dragunow et al (2) studied 3 patients with PD, but they could not detect TUNEL-positive neurons. Anglade et al (3) studied 3 PD patients, and Tompkins and Hill (4) studied 28 patients with Lewy body diseases including PD, and both groups found evidence of apoptosis in all of the patients studied. It has been claimed that TUNEL does not discriminate apoptosis from necrosis (5), but another report stated that TUNEL stained more apoptosis than necrosis, although TUNEL is not 100% specific for apoptosis (6).

Although histochemical evidence of apoptosis in PD is not sufficient, there is biochemical evidence which supports the presence of apoptosis in PD. It has been well known that in PD, mitochondrial complex I and α-ketoglutarate dehydrogenase complex are decreased in the substantia nigra (7–9); therefore, mitochondrial respiration is impaired in PD, which causes an increase in the formation of oxygen free radical species, because of incomplete reduction of oxygen to water. There is ample evidence to indicate oxidative stress in PD (10, 11).

According to the recent progress in the study of the mechanism of apoptosis, loss of mitochondrial inner membrane potential ($\Delta\Psi m$) has been found to be one of the major triggers of apoptosis (12). This membrane potential is achieved by electron transport in which protons are expelled from the matrix space to the intermembrane space; thus the matrix side becomes negatively charged. Induction of apoptosis by mitochondrial respiratory toxins have been described (13, 14). Recently, Susin et al (15) have shown that a 50-kDa protein is released from the mitochondrial intermembrane space to cytoplasm, and this protein induces nuclear fragmentation and apoptosis when applied to the nucleus. Further, opening of permeability transi-

Reprint requests should be addressed to Dr. Yoshikuni Mizuno, the Department of Neurology, Juntendo University School of Medicine, 2-1-1 Hongo, Bunkyo-ku, Tokyo 113-8421

tion pores which are present in the inner membrane of mitochondria has been recently postulated as the initial mediator of loss of mitochondrial membrane potential (16, 17) which ultimately induces apoptosis. Opening of the permeability transition pores increases the permeability of the inner mitochondrial membrane and thus dissipates the membrane potential. Interestingly, oxygen free radicals are able to open these permeability transition pores (18). When we review the recent progress in the study of the role of mitochondria in the induction of apoptosis, early observation of loss of complex I in PD is a very important step to elucidate the pathogenesis of PD. We believe that there is ample evidence to believe that apoptosis plays a very important role in the nigral cell death in PD.

In Alzheimer's disease, Su et al (19) and Lassmann et al (20) observed many TUNEL-positive cortical neurons. Recently, Wolozin et al (21) reported that presenilin 2 has a facilitatory action on apoptosis in cultured cells; mutation of presenilin 2-gene is responsible for one type of autosomal dominant familial Alzheimer's disease. In Huntington's disease, TUNEL-positive neurons have been found in the striatum (22). Further, abnormally elongated polyglutamine stretch appears to enhance apoptosis (23).

Thus the accumulating evidence indicates the involvement of apoptosis in various neurodegenerative disorders. Under the supposition that apoptosis is an important mechanism of neuronal death, it may become possible to stop or retard the degenerative process by interrupting apoptosis in the future. Further studies on apoptosis in neurodegenerative disorders are very important from the therapeutic aspect.

References

1) Mochizuki H, et al. Histochemical detection of apoptosis in Parkinson's disease. J Neurol Sci **137:** 120, 1996.
2) Dragunow M, et al. In situ evidence for DNA fragmentation in Huntington's disease striatum and Alzheimer's disease temporal lobes. Neuro Report **6:** 1053, 1995.
3) Anglade P, et al. Apoptosis and autophagy in nigral neurons of patients with Parkinson's disease. Histology Histopathol **12:** 25, 1997.
4) Tompkins MM, Hill WD. Apoptotic-like changes in human substantia nigra. Society for Neuroscience Abstract **21** (Part 1): 1273, 1995.
5) Grasl-Kraupp B, et al. In situ detection of fragmented DNA (TUNEL assay) fails to discriminate among apoptosis, necrosis, and autolytic cell death: a cautionary note. Hepatology **21:** 1465, 1995.
6) Gold R, et al. Differentiation between cellular apoptosis and necrosis by the combined use of in situ tailing and nick translation techniques. Lab Invest **71:** 219, 1994.
7) Schapira AHV, et al. Mitochondrial Complex I deficiency in Parkinson's disease. J Neurochem **54:** 823, 1990.
8) Hattori N, et al. Immunohistochemical studies on Complexes I, II, III, and IV of mitochondria in Parkinson's disease. Ann Neurol **30:** 563, 1991.
9) Mizuno Y, et al. An immunohistochemical study on a-ketoglutarate dehydrogenase complex in Parkinson's disease. Ann Neurol **35:** 204, 1994.
10) Jenner P, et al. Oxidative stress as a cause of nigral cell death in Parkinson's disease and incidental Lewy body disease. Ann Neurol **32:** S82, 1992.
11) Youdim MBH, et al. Review: The possible role of iron in the ethipathology of Parkinson's disease. Mov Dis **8:** 1, 1993.
12) Shimizu S, et al. Bcl-2 blocks loss of mitochondrial membrane potential while ICE inhibitors act at a different step during inhibition of death induced by respiratory chain inhibitors. Oncogene **13:** 21, 1996.
13) Mochizuki H, et al. Apoptosis is induced by 1-methyl-4-phenylpyridinium ion (MPP+) in a ventral mesencephalic-striatal co-culture. Neurosci Lett **170:** 191, 1994.
14) Dipasquale B, et al. Apoptosis and DNA degradation by 1-methyl-4-phenylpyridinium in neurons. Biochem Biophys Res Commun **181:** 1442, 1991.
15) Susin SA, et al. Bcl-2 inhibits the mitochondrial release of an apoptogenic protease. J Exp Med **184:** 1331, 1996.
16) Marchetti P, et al. Mitochondrial permeability transition triggers lymphocyte apoptosis. J Immunol **157:** 4830, 1996.
17) Zamzami N, et al. Inhibitors of permeability transition interfere with the disruption of the mitochondrial transmembrane potential during apoptosis. FEBS Lett **384:** 53, 1996.
18) Skulachev VP. Why are mitochondria involved in apoptosis? Permeability transition pores and apoptosis as selective mechanisms to eliminate superoxide-producing mitochondria and cell. FEBS Lett **397:** 7, 1996.
19) Su JH, et al. Immunohistochemical evidence for apoptosis in Alzheimer's disease. Neuro Report **5:** 2529, 1994.
20) Lassmann H, et al. Cell death in Alzheimer's disease evaluated by DNA fragmentation in situ. Acta Neuropathol (Berl) **89:** 35, 1995.
21) Wolozin B, et al. Participation of presenilin 2 in apoptosis: enhanced basal activity conferred by an Alzheimer mutation. Science **274:** 1710, 1996.
22) Portera-Cailliau C, et al. Evidence for apoptotic cell death in Huntington disease and excitotoxic animal models. J Neurosci **15:** 3775, 1995.
23) Nasir J, et al. Huntington disease: new insights into the relationship between CAG expansion and disease. Hum Mole Genet **5** Spec No: 1431, 1996.

Eur Respir J, 1996, 9, 1293–1305
DOI: 10.1183/09031936.96.09061293
Printed in UK - all rights reserved

European Respiratory Journal
ISSN 0903 - 1936

REVIEW

The role of apoptosis in the pathogenesis and treatment of diseases

E. Solary, L. Dubrez, B. Eymin

The role of apoptosis in the pathogenesis and treatment of diseases. E. Solary, L. Dubrez, B. Eymin. ©ERS Journals Ltd 1996.

ABSTRACT: In adult multicellular organisms, homeostasis is determined in each cell lineage by a balance between cell death and cell growth. Dysregulation of cell death mechanisms is involved in the pathogenesis of an increasing number of diseases. Defective apoptosis can participate in malignant transformation, viral latency and autoimmune diseases. Excessive apoptotic cell death is involved in CD4+ T-cell depletion observed in acquired immune deficiency syndrome, in fulminant hepatitis associated with infection by hepatitis B and C viruses, in some neurodegenerative disorders and haematological diseases, in polycystic kidney disease and ischaemia.

Three steps can be distinguished in the pathway that leads to cell death. The first step involves interactions between the extracellular and intracellular signals that decide whether a cell should live or die. When death is chosen, a common pathway that involves at least the Bcl-2- family of proteins and the interleukin-1β (IL-1β)-converting enzyme-related cysteine proteases confirms whether or not the cell should die. Finally, if death is allowed to occur, the apoptotic process itself is characterized by deoxyribonucleic acid (DNA) fragmentation, proteolysis and morphological changes that precede the engulfment of apoptotic cells by neighbouring cells and phagocytes.

Several inducers and inhibitors of apoptosis acting on one or several of these three steps that characterize the apoptotic process have been identified *in vitro*. Their potential usefulness in improving the current therapeutic strategies and designing new strategies in several different diseases is discussed.

Eur Respir J., 1996, 9, 1293–1305

Laboratory of Oncohematology and Pharmacology, Faculty of Medicine, Dijon, France.

Correspondence: E. Solary
Laboratory of Oncohematology and Pharmacology
Faculty of Medicine
7 boulevard Jeanne d'Arc
21033 Dijon Cedex
France

Keywords: Apoptosis
diseases
pathogenesis
treatment

Received: October 5 1995
Accepted after revision February 8 1996

In a famous French play by Molière, the prominent character, Monsieur Jourdain, realizes that he has been speaking in prose for a long time without even knowing it. Similarly, the recent interest in cell death mechanisms has revealed that we have been using induction or inhibition of apoptosis for a long time for the treatment of some diseases without knowing it. For instance, chemotherapeutic drugs and radiations induce apoptosis of tumour cells [1] and haematopoietic growth factors act by preventing apoptosis of haematopoietic progenitors [2]. A better understanding of the mechanisms that regulate cell death pathways might make it possible to improve the current therapeutic strategies and to define new strategies in several different diseases.

To live or to die?

In adult multicellular organisms, different cell types vary widely in the mechanisms by which they maintain themselves throughout life. Red blood cells undergo constant renewal from haematopoietic progenitor cells, whereas neural cells have no or limited capacity for self-renewal. Between these extremes, lymphocytes and cells from reproductive organs undergo cyclical expansions and contractions as they participate in host defence and reproduction, respectively. Within all of these cell lineages, the control of cell number is determined by a balance between cell proliferation and cell death. Recent studies suggest that the mechanisms that control cell proliferation and cell death could share several factors. Growth factors can either stimulate cell growth or prevent cell death [2–4]. Antigenic stimulation of the T-cell receptor first triggers the proliferation of mature peripheral T-cells, which are later eliminated by Fas-mediated apoptosis [5]. Proto-oncogenes associated with cell proliferation, such as *c-myc;* are capable of inducing apoptosis when they are aberrantly expressed [6]. Tumour suppressor genes, such as *p53*, are involved into checkpoints that decide whether a cell progresses in cell cycle or dies by apoptosis in response to deoxyribonucleic acid (DNA) damage [7]. Therefore, a given signal will induce a cell either to live or to die, depending on the cell type and its level of differentiation [8]. Cell survival could depend upon the constant supply of survival factors provided by neighbouring cells and extracellular matrix [9–11].

To die or not to die?

Beyond different signalling pathways that ultimately converge to activate a cell death signal, apoptosis appears to involve a common final pathway that has been, at least partially, conserved throughout animal evolution (fig. 1).

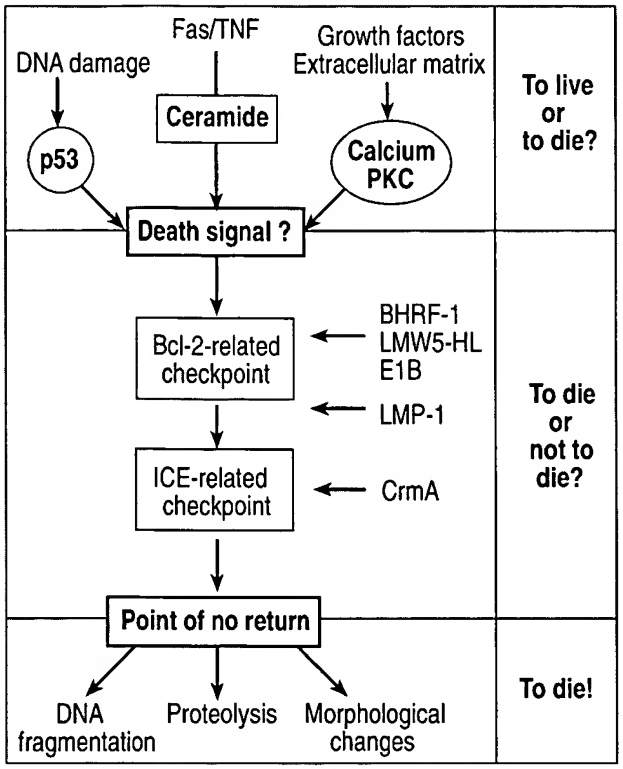

Fig. 1. – The three steps of the apoptotic process. During the first step, intracellular and extracellular signals activate specific pathways that will determine whether a cell should live or die. The tumour suppressor gene *p53* is involved in a checkpoint that decides whether a cell progresses in the cell cycle or dies by apoptosis in response to deoxyribonucleic acid (DNA) damage. Interaction of Fas ligand or tumour necrosis factor (TNF) with their membrane receptor increases intracellular ceramide level. Growth factors or interactions with extracellular matrix increase intracellular calcium and activate the protein kinase C (PKC). The second step involves two checkpoints that could regulate the final cell death pathway. One checkpoint is controlled by proteins from the Bcl-2 family. Bcl-2 expression can be increased by interaction with viral proteins (BHRF-1 from Epstein-Barr virus, LMW5-HL from the swine fever virus, and E1B from adenovirus) or mimicked by LMP-1 from Epstein-Barr virus. The other checkpoint could be determined by the cysteine proteases related to interleukin-1β (IL-1β) converting enzyme (ICE) that is inhibited by the CrmA protein from cowpox virus. The cell death pathway then reaches a point of no return, and apoptosis is associated with internucleosomal DNA fragmentation, proteolysis of several nuclear and cytosolic proteins, and characteristic morphological changes.

Much of our knowledge about the specific steps that regulate this cell death pathway has been derived from genetic studies of the nematode *Caenorhabditis elegans* [12]. Among the 14 genes whose mutation affects the various steps of programmed cell death in this nematode, three genes affect the death process itself, namely *ced-3* and *ced-4*, that are required for cells that must die to undergo programmed cell death, and *ced-9* that is required to protect cells that should live from undergoing apoptosis. The *ced-3* gene encodes a protein that is similar to the family of cysteine proteases, which includes interleukin-1β-converting enzyme (ICE), Nedd2/Ich-1, CPP32/Yama, Tx/Ich-2 and Mch2 (for review see [13]). These proteases share a pentameric peptide, QACRG, surrounding a putative activated site Cys. Accordingly, overexpression of these proteases in mammalian cells causes apoptosis, and the cowpox virus *crmA* gene product, that inhibits some ICE-like proteases, can protect mammalian cells against apoptosis induced by growth factor withdrawal [14]. By contrast, the protein encoded by the *ced-4* gene has no similarity with other known proteins. The protein encoded by *ced-9* is homologous to the Bcl-2 family of cell death regulators identified in mammalian cells, and the expression of the human Bcl-2 in nematodes partially substitutes for the loss of *ced-9* function [15]. Studies performed on the role of cysteine proteases and Bcl-2-related proteins suggest that these two components define two checkpoints in the final common pathway that decides whether or not a cell should die.

To die!

When the final common pathway has allowed the execution of the cell suicide programme, characteristic morphological changes of the dying cell [16] precede the production of apoptotic bodies, membrane-enclosed particles containing intracellular material (fig. 1). These particles are rapidly engulfed and digested by neighbouring cells and phagocytes to prevent any release of intracellular material that would otherwise trigger an inflammatory response, as observed during necrosis. Apoptosis is usually associated with the activation of one or several nucleases that degrade nuclear DNA first into large and subsequently into very small fragments [17, 18]. One of the consequences of DNA fragmentation is the irreversible degradation of viral or mutated cellular DNA. Proteolytic cleavage of several nuclear proteins by an activity similar to but distinct from ICE is another biochemical marker of apoptotic cell death [19–21].

Apoptosis and the pathogenesis of disease

Diseases due to defective cell death

The failure of cells to undergo apoptosis might be involved in the pathogenesis of several human proliferative disorders characterized by the accumulation of cells, including cancer, autoimmune diseases and certain viral infections (fig. 2).

Apoptosis and cancer. Cancer is usually envisaged as a disease of excessive cellular proliferation. Recently, genetic alterations that dysregulate the physiological cell death process appeared to contribute to the clonal expansion of malignant cells. Accordingly, a number of oncogenes and anti-oncogenes have been found to regulate apoptotic cell death. Oncogenes that promote cell proliferation and those that inhibit cell death could co-operate to induce a neoplastic lesion. Genetic alterations that induce cell proliferation, such as dysregulation of either *myc* or *ras* proto-oncogenes, would lead to the induction of apoptosis [6, 22], unless simultaneous expression of an oncogene, such as *bcl-2*, that inhibits this apoptotic response allows the cell transformation to occur [23]. The best example of these oncogenes is *bcl-2*, identified at the site of a chromosomal translocation between chromosomes 14 and 18, present in most human follicular lymphomas, (for review, see [24]). Upregulation of *bcl-2* oncogene expression specifically inhibits apoptosis induced by a

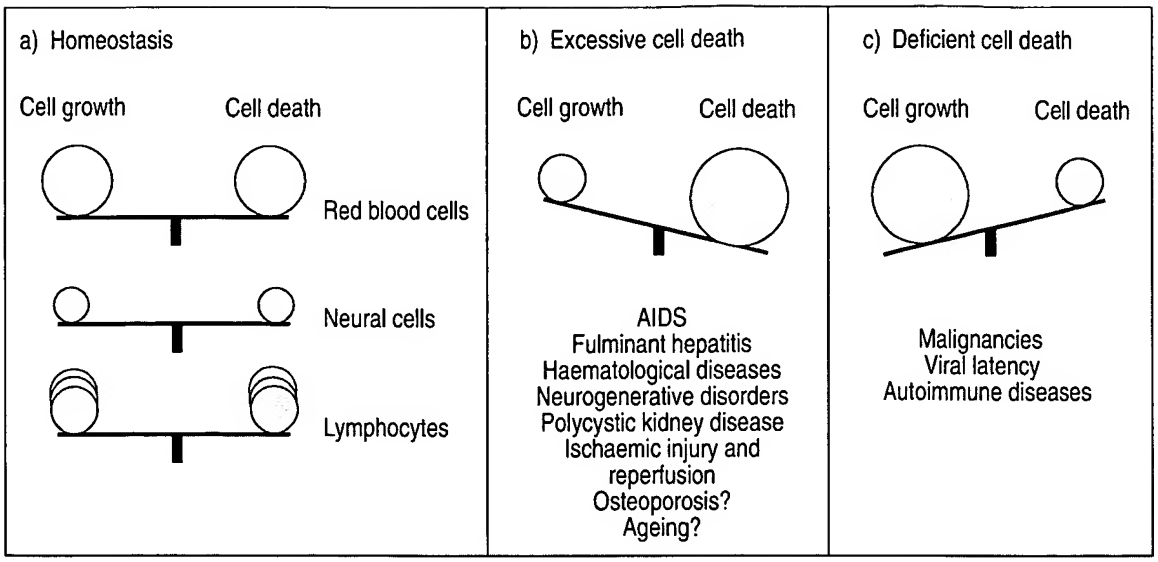

Fig. 2. – a) The level of cell death and cell growth varies widely from one cell lineage to another. b) Excessive; or c) deficient apoptosis are suspected to be involved in the pathogenesis of various diseases. AIDS: acquired immune deficiency syndrome.

wide range of insults and stimuli such as growth factor deprivation, loss of contact with extracellular matrix, cytotoxic T-cells, cytotoxic lymphokines, chemotherapeutic drugs and radiations [24–27]. As indicated previously, human *bcl-2* can promote cell survival in lower organisms, such as nematodes, and substitute for the loss of function of *ced-9* [15]. An elevated level and aberrant pattern of Bcl-2 protein expression have been found in a wide variety of human cancers, including lymphomas, leukaemias, adenocarcinomas, neuroblastomas, renal and lung cancers and melanomas [24]. In most of these tumours, dysregulation of *bcl-2* gene expression is not the consequence of the t(14;18) chromosomal translocation. Structural alterations of the *bcl-2* gene are not detected in most leukaemias and solid tumours, suggesting that transregulatory rather than cis-regulatory mechanisms account for overexpression of Bcl-2. This overexpression can represent either an early or a late event in the tumour progression. For example, disturbances in the pattern of *bcl-2* expression represent an early event in colorectal cancers, whereas it occurs later in prostate cancer, in which elevation of Bcl-2 protein level is associated with acquisition of a metastatic and androgen-independent phenotype [24].

One of the potential transregulators of *bcl-2* that can become altered in cancer is the tumour suppressor *p53*, which represses *bcl-2* gene expression [28]. Germ-line *p53* mutations predispose individuals with Li-Fraumeni cancer syndrome to the development of tumours, and the *p53* gene becomes inactivated in over half of all human tumours [29]. The wild-type p53 protein binds DNA and functions, at least in part, as a transcriptional regulator, activating or repressing the expression of various target genes involved in DNA replication and repair. Wild-type p53 functions primarily to suppress neoplastic growth by inducing apoptosis [30], and contributes to tumour suppression by inducing cell cycle arrest at the G1/S checkpoint in response to DNA damage, in order to facilitate DNA repair [31]. The p53 is also an inducer of apoptosis in certain normal tissues, such as myeloid progenitors and epithelial stem cells [32]. Its presence or absence is an important determinant of the relative sensitivity of normal and tumour cells to apoptosis induced by DNA damaging therapeutic agents [7, 30].

In addition to repressing *bcl-2* gene expression, *p53* transactivates the expression of a homologue of *bcl-2* termed *bax* [28, 33]. In contrast to Bcl-2, the protein encoded by *bax* functions as a promoter of cell death. Bax and Bcl-2 are members of a larger family of proteins that can either promote or repress apoptosis [34], including Bcl-x, mcl-1, A1, BAK, Bad, and BAG-1 [35–40]. These proteins can interact through heterodimerization [41]. The functional significance of these interactions remains unknown. Bcl-x can be expressed under two different isoforms, resulting from alternative splicing of *bcl-x* messenger ribonucleic acid (mRNA) [35]. Bcl-xl, that functions as a death inhibitor, is markedly elevated in several tumours, whereas Bcl-xs could promote cell death by sequestering Bcl-2 so that it cannot interact with Bax and other proteins. Other oncogenes, such as *c-abl*, are potent inhibitors of apoptosis by a mechanism that seems to be independent of Bcl-2 and Bcl-2-related proteins but remains unexplained [42, 43]. Interestingly, neither mutations of ICE and ICE-related proteases nor their inhibition by viral products, such as CrmA, have so far been implicated in oncogenesis.

Apoptosis and viral latency. Cells infected with a virus can undergo apoptosis as a defence mechanism to prevent viral infection. Infected cells can also express viral peptides in association with cell surface major histocompatibility class I molecules, in order to be recognized and killed by cytotoxic T-cells. T-cells will induce apoptosis, either by using perforin to introduce proteases into the target cell [44], or by activation of the Fas receptor on its surface (see below). A number of viruses disrupt the normal regulation of apoptosis within infected cells to circumvent the host defences. To reach this goal, viral genes encode inhibitory proteins, most of which target one of the two main checkpoints of the final common pathway that leads to apoptosis. The cowpox virus gene, *crmA* [14, 45], encodes a protease inhibitor that prevents

apoptotic cell death by specifically inhibiting ICE, a key protease in the final pathway of Fas- and tumour necrosis factor-α- mediated cell death [46, 47]. Other viral genes encode a protein with structural and functional similarities with Bcl-2: they include the *BHRF-1* gene of Epstein-Barr virus, the *LMW5-HL* gene of African swine fever virus, and the *E1B* gene of adenovirus [24, 48, 49]. The product of some viral genes, such as LMP-1 from Epstein-Barr virus, can upregulate Bcl-2 to allow the establishment of viral latency [50]. The mechanism by which the *p35* gene, identified in baculovirus as a potent inhibitor of apoptosis, inhibits cell death in infected cells is still not understood. Interestingly, another baculovirus gene that inhibits apoptosis, namely inhibitor of apoptosis protein (*IAP*), is analogous to a gene recently involved in the pathogenesis of a recessive neurodegenerative disorder observed in children [51]. Although biochemical mechanisms by which viral proteins inhibit cell death remain poorly explained, nitric oxide produced by human B-lymphocytes was recently reported to contribute to the maintenance of viral latency in downregulating the expression of an Epstein Barr virus early antigen [52].

Apoptosis and autoimmune diseases. Several recent studies have implicated apoptosis in the pathogenesis of autoimmune diseases. The human organism protects itself from autoimmune reactions by clonal deletion of autoreactive T-cells, a process called negative selection. One mechanism by which negative selection takes place is apoptosis. Alterations in the susceptibility of lymphocytes to die by apoptosis *in vitro* have been reported in several autoimmune diseases, such as systemic lupus erythematosus, rheumatoid arthritis, autoimmune diabetes mellitus or inflammatory bowel disease [53]. Serum proteins could also be involved: serum from patients with type 1 diabetes mellitus, an autoimmune disease associated with the destruction of pancreatic beta cells, was shown to contain a factor that promotes Ca^{2+}-mediated apoptosis in beta cells [54].

Animal model systems have provided new information about the potential role of dysregulated apoptosis in autoimmune diseases. Linkage analysis has established an association between the *bcl-2* locus and autoimmune diabetes in nonobese diabetic mice [55]. A lupus-like autoimmune disease has been reported in transgenic mice constitutively expressing Bcl-2 in their B-lymphocytes [56]. The most informative observations to date were performed in the MRL mouse strain. Spontaneous autosomal recessive mutation on either chromosome 19 (locus *lpr* for lymphoproliferative disease) or chromosome 1 (locus *gld* for generalized lymphoproliferative disease) were observed to accelerate the occurrence of a spontaneous autoimmune disease observed in these mice [57, 58]. Both MRL *lpr/lpr* and MRL *gld/gld* mouse strains show a similar phenotype. Mice develop lymphadenopathy and splenomegaly, produce large amounts of anti-DNA and rheumatoid factor autoantibodies, and die of nephritis or arthritis at approximately 5 months of age. Both *lpr* and *gld* were shown to be loss-of-function mutations that affect genes encoding a pair of interacting proteins: *lpr* mutation affects a cell surface protein named Fas (or APO-1 or CD95); whereas, *gld* affects a soluble or membrane-bound cytokine, which is called Fas ligand (for review see [59]). Molecular and cellular characterization of Fas and Fas ligand in animals and humans revealed their homology with members of the tumour necrosis factor (TNF) receptor family and TNF family, respectively [60, 61]. Fas ligand binds to its receptor Fas, thus inducing apoptosis of the Fas-bearing target cell. Triggering of this apoptotic pathway requires the cross-linking of Fas with either purified Fas ligand, or cells expressing Fas ligand or antibodies to Fas [59]. It has recently been demonstrated that activated Fas interacts with several cellular proteins [62–65], and activates a sphingomyelinase-dependent pathway [66]. Fas-mediated apoptosis is triggered by ICE or ICE-like proteases [46, 47].

Fas is abundantly expressed in activated lymphocytes and in the primary cells from various other tissues, such as liver, heart, lung and ovary. Fas ligand is expressed predominantly in activated CD4+ and CD8+ T-cells and natural killer (NK) cells. The Fas/Fas ligand system is involved in the clonal deletion of autoreactive T-cells in the periphery, not in the thymus. The system is also involved in the deletion of T-cell receptor (TCR)-activated mature T-cells that is necessary to limit every immune response [67, 68], and in the mechanisms that cytotoxic T-cells use to kill infected target cells, a pathway distinct from the perforin-mediated pathway (for review see [69]). Genes other than Fas or Fas ligand are probably involved in Fas-related pathology, because *lpr* mutations induce nephritis or arthritis in MRL mice but not in C3H mice [70].

In humans, two recent studies identified Fas gene mutations in children who developed a rare autoimmune lymphoproliferative disorder, characterized by massive nonmalignant lymphadenopathy, autoimmune phenomena and expanded populations of immature lymphocytes [71–73]. An elevated level of the soluble form of Fas was detected in the serum of some patients with systemic lupus erythematosus. It was suggested that the soluble form of Fas could inhibit Fas-mediated elimination of autoreactive lymphocytes [74]. A soluble form of Fas ligand was also identified as an homotrimer in the culture medium of activated human T lymphocytes. If such a molecule is produced *in vivo*, it may work as an agent that causes systemic tissue damage [75]. The primary cells from several tissues are sensitive to Fas-mediated apoptosis, suggesting that the Fas system may be involved in cytotoxic T-lymphocyte (CTL)-mediated diseases in these tissues [59]. Bone marrow transplantation performed between *lpr* mutant and wild-type MRL mice have suggested that Fas system may be involved in the graft-*versus*-host disease induced by allogenic bone marrow transplantation in humans [59].

Diseases related to excessive cell death

Fas-mediated diseases. A variety of diseases characterized by excessive cell loss may result from accelerated rates of cell death. Besides defective Fas-signalling involved in lymphoproliferative disorders, Fas-related diseases may be caused by excessive activity of the Fas system. Abnormal activation of Fas ligand expressed on cytotoxic T-cells could be involved in human fulminant hepatitis. Intraperitoneal injection of a cytotoxic monoclonal antibody generated against mouse Fas has been shown to kill wild-type mice by inducing fulminant hepatitis. Two hours after

injection, the serum level of glutamate oxaloacetate transaminase (GOT) and glutamate pyruvate transaminase (GPT) increased rapidly and reached about 200 and 1,000 fold above basal level, respectively. Histochemical analysis showed massive haemorrhagic necrosis in the entire liver, and electron microscopy of the affected hepatocytes revealed condensed and fragmented nuclei, an aspect characteristic of apoptosis. It was concluded that the anti-Fas antibody had caused the hepatocytes to die. It was suggested that rapid and widespread cell death had not allowed the macrophages to remove the apoptotic cells, resulting in secondary necrosis and release of lethal toxic components. Anti-Fas antibody injection did not kill MRL *lpr/lpr* mice [76]. Primary hepatocytes are sensitive to Fas-mediated apoptosis *in vitro*. Fas is overexpressed in hepatocytes transformed by human hepatitis C virus. Injection of CTLs specific for the human hepatitis B virus in transgenic mice carrying the virus induced fulminant hepatitis [77–79]. These observations are consistent with the hypothesis of involvement of Fas system in the occurrence of fulminant hepatitis when hepatocytes are infected with hepatitis B or C viruses. The process may normally occur to remove virus-infected cells but, when exaggerated, could lead to fulminant hepatitis. Similarly, Fas system may be involved in other CTL-mediated autoimmune diseases, such as chronic thyroiditis [6, 59].

Acquired immune deficiency syndrome. AIDS is characterized by a progressive and selective depletion of the CD4+ population of T-lymphocytes. The exact mechanisms by which the human immunodeficiency virus-1 (HIV-1) kills immune cells is not understood. Most T-cells that die during HIV infection do not appear to be infected with the virus, and the number of apoptotic T-cells does not correlate with progression of disease [80]. Nevertheless, a growing body of experimental evidence suggests a role for apoptosis in CD4+ T-cell depletion. Enhanced apoptosis has been observed in primate models of lentiviral infections, as well as in lymphocytes and lymph nodes from AIDS patients. Picomolar concentrations of the soluble viral product, gp120, were reported to prime human CD4+ T-cells for activation-induced cell death [81]. More recently, HIV-1 Tat protein was shown to induce cell death by apoptosis in a T-cell line and in mononuclear peripheral blood cells from uninfected donors [82]. Tat protein was shown to induce in T-cells a premature activation of cyclin-dependent kinases, an event that has been associated with apoptosis induction in several other cell systems. Tat-activated T-cells would then be depleted when either the T-cell receptor is activated by an antigen or when gp120 binds to CD4 receptor. Fas could be involved in the death of CD4+ T-cells during the course of an HIV infection [83]. Human T-cell lines, transformed with HIV, are more sensitive to Fas-mediated apoptosis than the parental cells. Fas is highly expressed on T-cells of mice with retrovirus-induced immunodeficiency syndrome and on T-lymphocytes of HIV-infected children. The current hypothesis is that HIV-1 Tat and gp120 accelerate Fas-mediated, activation-induced T-cell apoptosis, therefore contributing to CD4+ T-cell depletion during the course of AIDS [82] (fig. 3). Viral replication itself may not be limited by CD4+ T-cells death because CD4 receptor is downregulated on infected cells, which could prevent both viral reinfection and CD4-mediated apoptosis. Lymphocyte apoptosis has also recently been involved in the pathogenesis of the leukaemia-like disease induced by the human T-lymphocyte virus-1 (HTLV-1) infected T-cells [84], and virally-induced abortive activation of T-cells may be a response to several other viral infections in mammals [85].

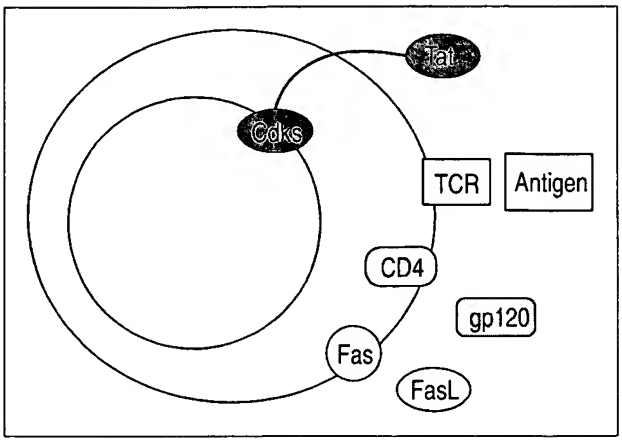

Fig. 3. – Factors of the CD4+ T-cell depletion in acquired immune deficiency syndrome. The current hypothesis is that two viral proteins produced by human immune deficiency virus-1 (HIV-1)-infected cells, namely Tat and gp120, prime activated CD4+ T-cells for apoptosis mediated by the Fas system (interaction of a soluble ligand and a membrane receptor). T-cell activation is triggered by an interaction between an antigen and the T-cell receptor (TCR). The soluble viral product, gp120, binds to CD4 receptor. The viral protein tat induces a premature activation of cyclin-dependent kinases (Cdks), an event that has been associated with induction of apoptosis in several other cell systems. The membrane receptor Fas is highly expressed on retrovirally-infected T-cells.

Haematological diseases. Haematopoietic growth factors, including stem cell factor, colony-stimulating factors, erythropoietin and thrombopoietin, play a key role in the regulation of haematopoiesis. These factors were demonstrated to act, in part, by promoting the survival of progenitor cells, by suppressing apoptosis during the differentiation of intrinsically committed progenitors [2, 4]. Overexpression of Bcl-2 prevents apoptosis of haematopoietic cells induced by growth factor withdrawal [86]. Bone marrow-derived stromal cells also prevent apoptotic death of normal and malignant haematopoietic cells [11]. Haematological diseases, such as myelodysplastic syndromes, aplastic anaemia, chronic neutropenia or severe β-thalassaemia are associated with increased apoptotic cell death within the bone marrow [87–89]. The mechanisms by which increased apoptotic cell death is involved in the aetiology of these diseases remains unexplained and could involve stroma cell deficiencies, gene deregulation and direct effects of toxins or mediators of the immune response.

Neurodegenerative disorders. The same mechanisms could apply for the increased apoptosis of specific sets of neural cells described in several neurological diseases such as Alzheimer's and Parkinson's diseases, or cerebellar degeneration [90–91]. Like haematopoietic growth factors and bone marrow stromal cells, several specific and less specific growth factors and extracellular matrix prevent

neural cell apoptosis, an effect that can be mimicked by overexpressing Bcl-2 in the neural cells [92–94]. Several gene mutations that lead to increased apoptotic cell death were identified in neurodegenerative disorders. Mutations in a superoxide dismutase gene were identified in patients with autosomal dominant amyotrophic lateral sclerosis [95]. These mutations decrease the ability of motor neurons to detoxify oxygen-free radicals. Mutations in any of the three photoreceptor-specific genes lead to photoreceptor apoptosis and retinal degeneration observed in patients with retinal pigmentosa [96]. Either dysfunction of the mutated protein or its accumulation could be responsible for increased apoptosis. Mutations in the neuronal apoptosis inhibitory protein (NAIP) gene, a gene homologous to IAP from baculovirus, have been identified in spinal muscular atrophy and may decrease the apoptotic threshold of spinal cord neurons [51].

Other diseases. Although apoptotic cells are phagocytosed within a few hours by neighbouring cells, apoptosis has been demonstrated histologically and histochemically to occur in several disease. Apoptosis is a pathological feature of polycystic kidney disease [97], and toxic-induced liver diseases [98], and may be central to the pathogenesis of these diseases. Ischaemic injury, such as myocardial infarction or stroke, induces the rapid death of cells within the central area of ischaemia by necrosis. Outside the central ischaemic zone, cells die over a more protracted time period by apoptosis. Rapid reperfusion of acutely occluded blood vessels induces an increase in free radical production and in intracellular calcium level, which both trigger apoptosis of cardiac myocytes [99]. Apoptosis has recently been described in atheroma, in which its pathogenic role remains to be explained [100, 101]. Degenerative disorders of the musculoskeletal system, including arthritis and osteoporosis, could also be the consequence of increased apoptosis of chondrocytes and osteocytes, respectively. Lastly, tissue homeostatic control is altered during the course of ageing, and the equilibrium is shifted toward cell death. The true nature of this age-related cell deletion phenomenon could be apoptosis [102], as a consequence of diminished synthesis of various growth factors, transmembrane signalling defects, inability to cope with oxidative stress, or abnormal cell cycle regulation [103]. Conversely, senescence can be associated with defective apoptosis: Fas expression and Fas ligand-induced apoptosis are decreased in T-cells from old mice compared to young mice [104]. T-cells from old mice also demonstrate a markedly decreased response to anti-CD3 stimulation [104, 105].

Other relationships between apoptosis and diseases

Another relationship between autoimmune diseases and apoptosis was suggested by the recent observation of ultra violet (UV)-irradiated cultured human keratinocytes. Systemic lupus erythematosus (SLE) is often regarded as the prototypic systemic autoimmune disease. This disease is characterized by an autoantibody response directed against selected intracellular antigens. The skin plays an important role in the disease, that can appear after extended exposure to sunlight. UV-induced apoptosis of the keratinocytes is associated with the clustering of potentially immunogenic cellular components in apoptotic blebs, a process that might participate to the induction of autoantibodies directed at multiple antigens [106]. A similar phenomenon could be involved in the development of an immune response to cancer cells, as suggested by recent observations in a regressive/progressive model of rat colon carcinoma cells (F. Martin, personal communication).

Identification of apoptosis is suggested to be a useful criterion in the assessment of response to various treatments, such as hormonal treatment of prostate cancer [107], and radiotherapy of cervical carcinoma [108]. Excessive toxicity of some treatments could also involve induction of apoptosis; toxicity of L-DOPA for the treatment of Parkinson's disease was recently related to the induction of apoptosis in target cells, suggesting that modulation of this phenomenon could prevent the acceleration of neuronal damage in this disease [109].

Apoptosis and the treatment of diseases

Based on the observation of the role of deficient or excessive cell death in the pathogenesis of several diseases, new therapeutic strategies could be designed to enhance or decrease the susceptibility of individual cell types to undergo apoptosis. Treatments that restore the ability of target cells to properly undergo apoptosis in response to a given signal could be of benefit in diseases with deficient cell death, such as malignancies. Conversely, treatments that increase the apoptotic threshold may be of benefit in disorders associated with cell loss, such as degenerative disorders. During the past 5 yrs, studies performed *in vitro* and sometimes *in vivo* have identified a large number of agents that either inhibit or induce apoptosis.

Therapeutic strategies targeting the nucleus

Nuclear changes and internucleolytic cleavage of nuclear DNA are observed at an early stage of apoptosis in many cell systems [18]. Therefore, endogenous activation of an endonuclease activity was suspected to be an essential step in the apoptotic process. Chromatin structure plays a determinant role in DNA fragmentation, that will take place only when linker regions separating nucleosomes are made accessible by a decondensation or local reduction in histone-DNA interaction. Spermine, a polyamine that modifies the degree of chromatin accessibility, can prevent DNA fragmentation in several cell systems [110]. Zinc and aurintricarboxylic acid inhibit oligonucleosomal DNA fragmentation associated with apoptosis in several cell systems [110]. Accordingly, zinc depletion can induce cell death by itself. The effect of zinc has been attributed to a direct inhibition of the putative endonuclease [18]. Zinc could have other cellular effects, since it is a cofactor of several enzymes, such as poly-(ADP)polymerase or the nuclear DNA topoisomerase I that could be involved in apoptosis. Zinc may also stabilize the association of protein-DNA complexes, which in turn may act on chromatin structure. However, both purpose and mechanisms of DNA fragmentation in apoptotic cells remain unclear. Recent studies have demonstrated

that internucleosomal DNA fragmentation is preceded by, and sometimes limited to, the formation of high molecular weight DNA fragments, referred to as "domain" cleavages [111]. This fragmentation is not inhibited by zinc, and may be due to topoisomerase II. Whether inhibitors of topoisomerase II that do not stabilize cleavable complexes could be good therapeutic tools to prevent this fragmentation remains to be determined. Cells without a nucleus can be induced to undergo the characteristic cytoplasmic changes of apoptosis [112, 113] while oligonucleosomal DNA fragmentation can be induced in isolated nuclei [8, 18, 19, 114], suggesting that structural and biochemical changes of each cellular compartment occur independently. For all these reasons, therapeutic strategies designed to prevent nuclear changes will not inhibit the whole process [115], and internucleosomal DNA fragmentation is an event that probably occurs too late to be a good therapeutic target.

Therapeutic strategies targeting the final common pathway

A more convincing target for the treatment of diseases is the final common pathway that involves the products of the Bcl-2 family and ICE-related cysteine proteases. Several lines of evidence indicate that these central components of the cell death machinery are most likely to be localized to the cytosol. This pathway is regulated by a balance between the opposing activities of proteins that promote and those that inhibit cell death. Several pairs of inducers and repressors such as Bcl-xl/Bcl-xs [35] and Ichll/Ichls [116], are issued from the same gene by alternative splicing. At least five isoforms of ICE have recently been identified as resulting from alternative splicing, some inducing and others repressing cell death [117]. The functional role of these numerous members of Bcl-2 and ICE family remains unknown at present. How could the recent and still incomplete knowledge of the checkpoints that regulate the final common pathway of apoptosis be used to improve the treatment of diseases?

The involvement of Bcl-2 overexpression in the resistance to essentially all cytotoxic anticancer drugs suggests that inhibition of the protein expression or activity could make it possible to increase the sensitivity of tumour cells to chemotherapeutic agents. Schematically, three main levels of cellular resistance to cytotoxic drugs have been identified: the first level includes the mechanisms that prevent the drug from reaching its target, most often localized in the nucleus. The most studied of these mechanisms is P-glycoprotein mediated drug efflux. The second level concerns the interactions between the drug and its intracellular target, whose quantitative or qualitative changes can prevent the drug from inducing specific damage. More recently, a third level was identified that is independent of the drug and concerns the ability of the cell to trigger its apoptotic machinery in response to specific damage induced by the drug [118–120]. Therefore, the intrinsic killing power of a drug could be less important than the ability to induce the tumour cells into killing themselves. In cells overproducing Bcl-2 due to gene transfer manipulations, the drug enters the cell at a normal rate and induces specific molecular damage [24]. Bcl-2 increases the threshold of specific molecular damage that is necessary to generate the biochemical events that will lead to apoptotic cell death, for example activation of cysteine proteases and endonucleases [27]. Upon removal of the drug, Bcl-2-protected cells can repair drug-induced damage and resume their proliferation. These unique functional properties of Bcl-2 presumably account for the poor clinical outcome associated with *bcl-2* overexpression in some series of patients with low grade follicular non-Hodgkin's lymphoma, acute myeloblastic leukaemia and solid tumour [121].

The inhibitory properties of Bcl-2 could be used to protect normal cells from chemotherapy-induced cell death. Enforced expression of *bcl-2* gene in bone marrow cells, using retroviral gene transfer techniques, was demonstrated to rescue these cells from apoptosis induced by topoisomerase inhibitors [122]. Conversely, specific strategies that will decrease Bcl-2 expression in tumour cells that overexpress the protein could increase their sensitivity to chemotherapeutic drugs and radiation. Antisense oligonucleotides have been successfully tested to specifically decrease *bcl-2* expression *in vitro*, and this inhibition increases leukaemic cell sensitivity to cytotoxic agents [123]. These short stretches of synthetic single-strand DNA enter the cell, bind to specific messenger ribonucleic acid (mRNA) sequences and prevent the expression of the corresponding protein. A similar strategy was also tested in a cell line derived from a patient with chronic myeloid leukaemia, a disease in which a t(9;22) chromosomal translocation generates a chimeric bcr-abl protein with constitutive c-abl kinase activity [44]. Increased abl kinase activity induces a high level of cellular resistance to induction of apoptosis by a variety of stimuli, including chemotherapeutic drugs [42]. Again, antisense oligonucleotides, corresponding to bcr-abl, have proved efficient at increasing the sensitivity of the bcr-abl positive cell line to cytotoxic agents [43]. In some cell lines with either *bcl-2* overexpression or *bcr-abl* rearrangement, specific antisense oligonucleotides can inhibit cell growth and induce apoptosis without additional treatment [124].

Although such antisense intervention might have potential clinical application, the therapeutic use of oligonucleotides has been shown to be problematical for a variety of reasons. A better strategy would be to identify agents that specifically interfere with the biochemical mechanisms by which either Bcl-2 or bcr-abl inhibit the apoptotic process. Unfortunately, these biochemical mechanisms have not yet been clearly identified.

Inhibition of the expression or function of Bcl-2, a protein involved in the final pathway that seems to be common to numerous forms of apoptosis, could not be specific enough to be a good therapeutic strategy. Recent data analysing a Bcl-2 loss of function murine model suggest that the function of Bcl-2 is absolutely necessary only in a limited number of normal cell types or, alternatively, there is a redundancy within the Bcl-2 family such that specific loss of Bcl-2 is relatively well-tolerated [125]. Therefore, short-term treatment with the antisense oligonucleotide anti-*bcl-2* may not be as toxic as might initially have been expected. Targeting Bcl-x, a Bcl-2 related protein whose isoform Bcl-xL also inhibits drug-induced apoptosis, could be more toxic, since Bcl-x deficient mice demonstrated extensive apoptotic cell death of neurons and haematopoietic progenitors [126].

Bcl-2 overexpression has not been associated with poor clinical outcome in all types of malignant tumours. Recent reports suggest a better prognosis in some tumours with increased Bcl-2 expression. This clinical observation could have several explanations. Firstly, growth factors were demonstrated to modulate the expression [127, 128], and to induce post-transcriptional modifications of the protein [24] that could modulate its activity. Better understanding of this regulation could suggest therapeutic use of this modulating activity. Secondly, Bcl-2 activity is modulated by heterodimerization with several other proteins from the Bcl-2 family, for example Bax [41]. Bax functions as a promoter rather than a repressor of cell death [33]. Relationships between the two proteins is enforced by the observation that p53, both represses *bcl-2* expression and promotes Bax expression [28]. A cell with low Bax expression would require only low levels of Bcl-2 to reach the critical stoichiometry at which Bcl-2/Bax dimer form, and reprieve from death is assured. Conversely, high Bax levels could render the cell more sensitive to death and more difficult to rescue. Accordingly, several tumours demonstrated marked reduction in Bax expression, sometimes associated with p53 mutations and/or drug resistance. Finally, interactions of Bcl-2 with other proteins from the Bcl-2 family could induce the specific inhibition of some apoptotic pathways. For example, Bcl-2 needs to interact with BAG-1 to efficiently prevent apoptosis induced by the Fas signalling pathway [40]. Therefore, modulation of Bcl-2 activity may require pharmacological agents that mimic or prevent specific interactions between proteins of the Bcl-2 family in order to be more specific with regard to the cell type and the stimuli.

Proteases involved in the final common pathway that leads to apoptosis, mainly ICE and ICE-related protein family, constitute another potential therapeutic target. Again, alternative spliced forms of members of ICE family, such as Ich1l and Ich1s, can have opposite effects [116]. This suggests that cysteine protease inhibitors that are specific for each member of the family, and pharmacological agents that modulate interactions between these members, may be developed [129–131]. These agents exist in nature: granzyme A and B, synthesized by cytotoxic T-cells, are ICE-related proteases that directly activate the apoptotic machinery in the target cell [132]. Conver-sely, several viruses synthesize proteins that either mim-ic Bcl-2 (BHRF1 from EBV, E1B from adenovirus, and LMW5-HL of African swine fever virus) or stimulate Bcl-2 expression (LMP-1 from EBV) or inhibit ICE (CrmA from cowpox virus) [49, 50]. Generation of attenuated viruses that do not express the genes which allow them to establish latent infection could be used for vaccination.

Therapeutic strategies targeting more specific pathways

Other targets for the therapeutic modulation of apoptosis are the different signalling pathways that activate the central cell death machinery. Most inducers of apoptosis use a specific signalling pathway. DNA damaging agents use a p53-dependent pathway. In leukaemic cells, activation of Fas and TNF receptors induces sphingomyelin hydrolysis and ceramide production. In thymocytes, interaction of cytokines and growth factors with their membrane receptors activates a calcium-dependent pathway. Only cytotoxic T-cells induce apoptosis by delivering in the target cells several proteases (or granzymes), some of them mimicking the activity of ICE. It is very important to understand how early steps of apoptosis are activated through the cell, because this may make it possible to define successful strategies. Nitric oxide (NO) synthase expression and NO production are increased in MRL *lpr/lpr* mice, and spontaneous glomerulonephritis and arthritis can be reduced by oral administration of N-mono-methyl-arginine, which inhibits NO production [59]. Early HIV infection is associated with reduced glutathione levels in blood cells. The pro-oxidant state associated with HIV infection may result in perturbations of activation-induced signal transduction in T-lymphocytes, which may be related to the enhanced tendency of these cells to undergo apoptosis [133]. Beneficial effects could be obtained by treatment of HIV-infected individuals with antioxidants, such as N-acetylcysteine [134].

Again, malignant cells provide a good example for testing this strategy. Mutations of *p53* were suggested to reduce the efficacy of DNA damaging agents in human tumours [7]. The protein p53 is not an element of the final common pathway, since cells lacking p53 can still undergo apoptosis, although some apoptotic stimuli do not function. The protein is an important trigger for apoptosis induced by DNA damage. Two mechanisms were proposed to explain the involvement of p53 in induction of apoptosis in response to DNA damage. A "clash" mechanism suggest's that p53-mediated cell cycle arrest conflicts with oncoprotein driven cell cycle progression stimulus, leading to apoptosis. The "dual pathway" mechanism suggests that the outcome of p53-mediated G1 arrest depends on the cell genotype, *i.e.* the expression of adenovirus E1A protein [135]. Whatever the true mechanism, *p53* mutations have been related to radioresistance, and reintroduction of wild-type *p53* was shown to restore cisplatin-induced apoptosis into p53-deficient lung carcinoma cells. Several clinical studies also suggest that the presence of *p53* mutations is associated with poor prognosis [136], and sometimes with drug resistance [137], in various cancers. Based on this observation, the identification of *p53* mutations in certain tumour types may become an important factor in treatment decision. The use of drugs or gene vectors that restore p53 activity may increase the therapeutic efficacy of DNA damaging agents. Alternatively, identification of *p53* mutations should lead to the use of molecules that induce tumour cell apoptosis independently of p53, such as Taxol [138].

A paradox of the immune response leading to T- or B-cell apoptosis could be use for the treatment of autoimmune diseases. Despite the role of acquired immunity in the defence against infectious agents, very high doses of antigen, or prolonged exposure to antigen can suppress T- and B-cell mediated immune response in adult animals. For example, large numbers of viruses produce antigenic loads that induce the deletion of cytotoxic T-cells and eliminate a recall response. T-cell death was demonstrated to be a physiological response to interleukin-2-mediated cell cycle stimulation and T-cell receptor re-engagement at high antigen doses [139]. On the other hand, hypermutation of immunoglobulin genes in B-cells proliferating within germinal centres during an

immune response generates variant antibodies that react with higher affinity against either foreign or self antigens. Recent studies have shown that administration of soluble antigen induces the rapid apoptosis of antigen-specific germinal centre B-cells, a mechanism that could cope with affinity maturation of autoantibodies to systemic autoantigens and induce tolerance [140, 141]. This mechanism could have failed in patients with rheumatoid arthritis, who develop antibodies that react with their own immunoglobulin [142]. Specific deletion of lymphocytes by repetitive treatment with a disease-associated autoantigen has been shown to be effective in the treatment of experimental autoimmune encephalitis in mice [139]. Similar treatment strategies may prove effective in human autoimmune disease, if the specific antigens involved in the autoimmune reaction can be identified. A better understanding of the tolerance induced by high doses of antigen could also help immunologists to improve their protocols for inducing specific tolerance to transplantation antigens. Another apoptosis-related strategy for the immunotherapy of autoimmune diseases *in vivo* would be to deliver an antigen-specific signal to the T-cells in the absence of the second co-stimulatory signal; a strategy that was recently shown to induce specific apoptosis of autoreactive T-cells [143].

If the role of the Fas/Fas ligand system is confirmed in diseases, such as chronic thyroiditis or fulminant hepatitis, induced by hepatitis B or hepatitis C viruses, the soluble form of Fas as well as neutralizing antibodies to Fas or Fas ligand could prove clinically useful. Fas-based reagents (such as activating anti-Fas or FasL) were also considered for the treatment of AIDS, in combination with 3'azido-3'-deoxythymidine, since anti-Fas monoclonal antibodies are cytotoxic to the HIV-infected cells, without increasing HIV infection [144]. These antibodies were also demonstrated to induce apoptosis of leukaemia cells, suggesting they could be used for the treatment of adult T-cell leukaemia [145]. Moreover, anti-Fas antibodies were shown to synergize with toxins and chemotherapeutic drugs to overcome TNF and drug resistance in various human tumour cell lines [146].

Increased expression of Fas in cisplatin- and gamma interferon-treated colon carcinoma cells could make it possible to obtain a synergistic effect of cytotoxic drugs and anti-Fas antibodies (M.T. Dimanche-Boitrel and O. Michaux, personal communication). However, it would be necessary to find a method to accurately target the reagents to the target cells *in vivo*, in order to avoid the potential risk of these reagents for normal tissues [76]. Targeted gene transfer techniques could resolve this obstacle: CD2-Fas transgene was recently reported to allow the maintenance of Fas apoptosis function and T-cell function in aged mice at a level comparable to that of young mice [104].

The use of cell surface receptors and second messenger systems to regulate cell death responses *in vivo* may have pleiotropic effects. For example, interleukin-12 (IL-12) treatment *in vivo* has recently been shown to protect bone marrow from gamma irradiation-induced apoptosis; whereas, it potentiates cell death within the gastrointe stinal tract in response to the same stimulus [147]. Haematopoietic growth factors prevent apoptosis of haematopoietic cells that express membrane receptors for these factors and are already in therapeutic use to prevent excessive cell death in patients treated with chemotherapeutic agents [148]. Protection of malignant cells from the cytotoxic effect of the therapeutic compounds suggests that the clinical use of these cytokines in combination with cytotoxic drugs should be carefully timed [149]. Accordingly, a clinical trial that combined granulocyte/macrophage colony-stimulating factor (GM-CSF) and standard induction cytotoxic therapy for the treatment of acute myeloblastic leukaemias suggested a negative effects of the growth factor on the response rate [150]. However, several other trials combining either granulocyte colony stimulating factor (G-CSF) or GM-CSF with chemotherapy did not confirm the negative impact of growth factors; and additional randomized studies will be necessary to determine whether growth factors improve or decrease the response rate of acute myeloblastic leukaemias to chemotherapy [148].

Hormones can prevent apoptosis induced by their deprivation [151]. Conversely, the β-chain of human chorionic gonadotrophin (β-HCG), a pregnancy hormone, was shown to induce *in vitro* and *in vivo* cell death, supposed to be apoptosis, in a neoplastic Kaposi's sarcoma cell line [152]. It was proposed that the low rate of Kaposi's sarcoma in women could be due to the interplay of hormones in the regulation of vascular proliferation. HIV-1-associated Kaposi's sarcoma has a high incidence among homosexual men. The antitumour properties of β-HCG could offer a new strategy for the treatment of this disease.

In conclusion, there is no doubt that apoptosis is an important factor in the pathogenesis and treatment of numerous diseases. It must be emphasized that apoptosis can certainly not explain all death phenomena observed in human diseases. Nevertheless, the notion that many diseases are related to deregulated cell death, and that new therapeutic strategies can derive from these observations, probably explains the enormous enthusiasm for this area of research.

Acknowledgements: The authors are grateful to F. Martin for his pertinent advice on the manuscript. L.D. is a PhD student receiving fellowship support from the Ligue Nationale Contre le Cancer in France.

References

1. Lennon SV, Martin SJ, Cotter TG. Dose-dependent induction of apoptosis in human tumour cell lines by widely divergent stimuli. *Cell Prolif* 1991; 24: 203–214.
2. Williams GT, Smith CA, Spooncer E, Dexter TM, Taylor DR. Haematopoietic colony-stimulating factors promote cell survival by suppressing apoptosis. *Nature* 1990; 343: 76–79.
3. Crompton T. IL-3-dependent cells die by apoptosis on removal of their growth factor. *Growth Factors* 1991; 4: 109–116.
4. Koury MJ, Bondurant MC. Erythropoietin retards DNA breakdown and prevents programmed cell death in erythroid progenitor cells. *Science* 1990; 248: 371–378.
5. Strasser A. Death of a T-cell. *Nature* 1995; 373: 385–386.
6. Evan GI, Wyllie AH, Gilbert CS, *et al.* Induction of apoptosis in fibroblasts by c-myc protein. *Cell* 1992; 69: 119–128.
7. Lowe SW, Bodis S, McClatchey A, *et al.* p53 status

and the efficacy of cancer therapy *in vivo*. *Science* 1994; 266: 807–810.
8. Solary E, Bertrand R, Pommier Y. Differential induction of apoptosis in undifferentiated and differentiated HL-60 cells by DNA topoisomerase I and II inhibitors. *Blood* 1993; 81: 1359–1368.
9. Raff MC. Social controls on cell survival and cell death. *Nature* 1992; 356: 397–400.
10. Boudreau N, Sympson CJ, Werb Z, Bissell MJ. Suppression of ICE and apoptosis in mammary epithelial cells by extracellular matrix. *Science* 1995; 267: 891–893.
11. Manabe A, Coustan-Smith E, Behm FG, Raimondi SC, Campana D. Bone marrow-derived stromal cells prevent apoptotic cell death in B-lineage acute lymphoblastic leukemia. *Blood* 1992; 79: 2370–2377.
12. Hengartner MO, Horvitz HR. Programmed cell death in *Caenorhabditis elegans*. *Curr Opin Gen Dev* 1994; 4: 581–586.
13. Martin SJ, Green DR. Protease activation during apoptosis: death by a thousand cuts. *Cell* 1995; 82: 349–352.
14. Gagliardini V, Fernandez PA, Lee RKK, *et al* Prevention of vertebrate neuronal death by the *crmA* gene. *Science* 1994; 263: 826.
15. Hengartner MO, Horvitz HR. *C. elegans* cell survival gene *ced-9* encodes a functional homolog of the mammalian proto-oncogene *bcl-2*. *Cell* 1994; 76: 665–676.
16. Arends MJ, Wyllie AH. Apoptosis: mechanisms and roles in pathology. *Int Rev Exp Pathol* 1991; 32: 223–254.
17. Zhivotovski B, Wade D, Nicotera P, Orrenius S. Role of nucleases in apoptosis. *Int Arch Allergy Appl Immunol* 1994; 105: 333–338.
18. Earnshaw WC. Nuclear changes in apoptosis. *Curr Opin Cell Biol* 1995; 7: 337–343.
19. Lazebnik YA, Kaufmann SH, Desnoyers S, Poirier GG, Earnshaw WC. Cleavage of poly(ADP-ribose)polymerase by a proteinase with properties like ICE. *Nature* 1994; 371: 346–347.
20. Li CJ, Friedman DJ, Wang C, Metelev V, Pardee AB. Induction of apoptosis in uninfected lymphocytes by HIV-1 tat protein. *Science* 1995; 268: 429–431.
21. Jensen PH, Cressey LI, Gjertsen BT, *et al*. Cleaved intracellular plasminogen activator inhibitor 2 in human myeloleukaemia cells is a marker of apoptosis. *Br J Cancer* 1994; 70: 834–840.
22. Wyllie AH, Rose KA, Morris RG, Stell CM, Forster E, Spandidis DA. Rodent fibroblast tumors expressing human *myc* and *ras* genes: growth, metastasis and endogenous oncogene expression. *Br J Cancer* 1987; 56: 251–259.
23. Vaux DL, Cory S, Adams JM. *Bcl-2* gene promotes hematopoietic cell survival and co-operates with *c-myc* to immortalize pre-B cells. *Nature* 1992; 335: 440–442.
24. Reed JC. Bcl-2 and the regulation of cell death. *J Cell Biol* 1994; 124: 1–6.
25. Allsopp TE, Wyatt S, Paterson HF, Davies AM. The proto-oncogene *bcl-2* can selectively rescue neurotrophic factor-dependent neurons from apoptosis. *Cell* 1993; 73: 295–307.
26. Levine B, Huang Q, Isaacs JT, Reed JC, Griffin DE, Hardwick JM. Conversion of lytic to persistent alphavirus infection by the *bcl-2* cellular oncogene. *Nature* 1993; 361: 739–742.
27. Miyashita T, Reed JC. Bcl-2 oncoprotein blocks chemotherapy-induced apoptosis in a human leukemia cell line. *Blood* 1993; 81: 151–157.
28. Miyashita T, Krajewski S, Krajewska M, *et al*. Tumor suppressor p53 is a regulator of *bcl-2* and *bax* in gene expression *in vitro* and *in vivo*. *Oncogene* 1994; 9: 1799–1805.
29. Harris CC, Hollstein M. Clinical implications of the *p53* tumor suppressor gene. *N Engl J Med* 1993; 329: 1318–1327.
30. Kamb A. Sun protection factor *p53*. *Nature* 1994; 372: 730–731.
31. Kastan MB, Zhan Q, el-Deiry WS, *et al*. A mammalian cell cycle checkpoint pathway utilizing p53 and GADD45 is defective in ataxia telangectasia. *Cell* 1992; 71: 587–597.
32. Ziegler A, Jonason AS, Leffel DJ, *et al*. Sunburn and p53 in the onset of skin cancer. *Nature* 1994; 372: 773–776.
33. Oltvai ZN, Milliman CL, Korsmeyer SJ. Bcl-2 heterodimerizes *in vivo* with a conserved homolog, Bax, that accelerates programed cell death. *Cell* 1993; 74: 609–619.
34. Wyllie AH. Death gets a brake. *Nature* 1994; 369: 272–273.
35. Boise LH, Gonzales-Garcia M, Postema CE, *et al*. *bcl-x*, a *bcl-2*-related gene that functions as a dominant regulator of apoptotic cell death. *Cell* 1993; 74: 597–608.
36. Kozopas KM, Yang T, Buchan HL, Zhou P, Craig RW. *MCL-1*, a gene expressed in programed myeloid cell differentiation, has sequence similarity to *Bcl-2*. *Proc Natl Acad Sci USA* 1993; 90: 3516–3520.
37. Kiefer MC, Brauer MJ, Powers VC, *et al*. Modulation of apoptosis by the widely distributed Bcl-2 homolog Bak. *Nature* 1995; 374: 736–739.
38. Chittenden T, Harrington EA, O'Connor R, *et al*. Induction of apoptosis by the Bcl-2 homolog Bak. *Nature* 1995; 374: 733–736.
39. Yang E, Zha J, Jockel J, Boise LH, Thompson CB, Korsmeyer SJ. Bad, a heterodimeric partner for Bcl-XL and Bcl-2, displaces Bax and promotes cell death. *Cell* 1995; 80: 285–291.
40. Takayama S, Sato T, Krajewski S, *et al*. Cloning and functional analysis of BAG-1: a novel Bcl-2 binding protein with anti-cell death activity. *Cell* 1995; 80: 279–284.
41. Sato T, Hanada M, Bodrug S, *et al*. Interactions among members of the Bcl-2 protein family analyzed with a two-yeast hybrid system. *Proc Natl Acad Sci USA* 1994; 91: 9238–9242.
42. Evans CA, Owen-Lynch PJ, Whetton AD, Dive C. Activation of the Abelson tyrosine kinase activity is associated with suppression of apoptosis in hemopoietic cells. *Cancer Res* 1993; 53: 1735–1738.
43. McGahon AR, Bissonnette R, Schmitt M, Cotter KM, Green DR, Cotter TG. BCR-ABL maintains resistance of chronic myelogenous leukemia cells to apoptotic cell death. *Blood* 1994; 83: 1179–1187.
44. Kagi D, Ledermann B, Bürki K, *et al*. Cytotoxicity mediated by T-cells and natural killer cells is greatly impaired in perforin-deficient mice. *Nature* 1994; 369: 31–37.
45. Ray CA, Black RA, Kronheim SR, *et al*. Viral inhibition of inflammation: cowpox virus encodes an inhibitor of the interleukin-1β converting enzyme. *Cell* 1992; 69: 597–604.
46. Enari M, Hug H, Nagata S. Involvement of an ICE-like protease in Fas-mediated apoptosis. *Nature* 1995; 375: 78–81.
47. Los M, Van de Craen M, Penning LC, *et al*. Requirement of an ICE/CED-3 protease for Fas/APO-1-mediated apoptosis. *Nature* 1995; 375: 81–83.
48. Rao L, Debbas M, Sabbatini P, Hockenbery D, Korsmeyer S, White E. The adenovirus E1A proteins induce apoptosis which is inhibited by the E1B 19K and Bcl-2 proteins. *Proc Natl Acad Sci USA* 1992; 89: 7742–7746.

49. Henderson S, Huen D, Rowe M, Dawson C, Johnson G, Rickinson A. Epstein-Barr virus-coded BHRF1 protein, a viral homolog of Bcl-2, protects human B-cells from programmed cell death. *Proc Natl Acad Sci USA* 1993; 90: 8479–8483.
50. Henderson S, Rowe M, Gregory C, *et al.* Induction of *bcl-2* expression by Epstein-Barr virus latent membrane protein 1 protects B cells from programmed cell death. *Cell* 1991; 65: 1107–1115.
51. Roy N, Mahadevan MS, McLean M, *et al.* The gene for neuronal apoptosis inhibitory protein is partially deleted in individuals with spinal muscular atrophy. *Cell* 1995; 80: 167–178.
52. Mannick JB, Asano K, Izumi K, Kieff E, Stamler JS. Nitric oxide produced by human B-lymphocytes inhibits apoptosis and Epstein-Barr virus reactivation. *Cell* 1994; 79: 1137–1146.
53. Emlen W, Niebur J, Kadera R. Accelerated *in vitro* apoptosis of lymphocytes from patients with systemic lupus erythematosus. *J Immunol* 1994; 152: 3685–3692.
54. Juntti-Berggren L, Larsson O, Rorsman P, *et al.* Increased activity of L-type Ca^{2+} channels exposed to serum from patients with type I diabetes. *Science* 1993; 261: 86–90.
55. Garchon HJ, Luan JJ, Eloy L, Bedossa P, Bach JF. Genetic analysis of immune dysfunction in nonobese diabetic (NOD) mice: mapping of a susceptibility locus close to the Bcl-2 gene correlates with increased resistance of NOD T-cells to apoptosis induction. *Eur J Immunol* 1994; 24: 380–384.
56. Strasser A, Whittingham S, Vaux DL, *et al.* Enforced Bcl-2 expression in B-lymphoid cells prolongs antibody responses and elicits autoimmune disease. *Proc Natl Acad Sci USA* 1991; 88: 8661–8665.
57. Watanabe-Fukunaga R, Brannan CI, Copeland NG, Jenkins NA, Nagata S. Lymphoproliferation disorder in mice explained by defects in Fas antigen that mediates apoptosis. *Nature* 1992; 356: 314–317.
58. Roths JB, Murphy ED, Eicher EM. A new mutation, gld, that produces lymphoproliferation and autoimmunity in C3H/HeJ mice. *J Exp Med* 1984; 159: 1–20.
59. Nagata S, Goldstein P. The Fas death factor. *Science* 1995; 267: 1449–1456.
60. Suda T, Takahashi T, Goldstein P, Nagata S. Molecular cloning and expression of the Fas ligand, a novel member of the tumor necrosis factor family. *Cell* 1993; 75: 1169–1178.
61. Itoh N, Yonehara S, Ishii A, *et al.* The polypeptide encoded by the cDNA for human cell surface antigen Fas can mediate apoptosis. *Cell* 1991; 66: 233–243
62. Sato T, Irie S, Kitida S, Reed JC. FAP-1: a protein tyrosine phosphatase that associates with Fas. *Science* 1995; 168: 411–415.
63. Chinnaiyan AM, O'Rourke K, Tewari M, Dixit VML. FADD, a novel death domain-containing protein, interacts with the death domain of Fas and initiates apoptosis. *Cell* 1995; 81: 505–512.
64. Stanger BZ, Leder P, Lee TH, Kim E, Seed B. RIP: a novel protein containing a death domain that interacts with Fas/APO-1 (CD95) in yeast and causes cell death. *Cell* 1995; 81: 513–523.
65. Boldin MP, Varfolomeev EE, Pancer Z, Mett L, Camonis JH, Wallach D. A novel protein that interacts with the death domain of Fas/APO1 contains a sequence motif related to death domain. *J Biol Chem* 1995; 270: 7795–7798.
66. Cifone MG, De Maria R, Roncaioli P, *et al.* Apoptotic signaling through CD95 (Fas/APO-1) activates an acidic sphingomyelinase. *J Exp Med* 1994; 180: 1547–1552.
67. Dhein J, Walczak H, Baümler C, Debatin KM, Krammer PH. Autocrine T-cell suicide mediated by APO-1/(Fas/CD95). *Nature* 1995; 373: 438–441.
68. Ju ST, Panka DJ, Cui H, *et al.* Fas(CD95)/FasL interactions required for programmed cell death after T-cell activation. *Nature* 1995; 373: 444–448.
69. Berke G. The CTL's kiss of death. *Cell* 1995; 81: 9–12.
70. Watson M, Roa JK, Gilkeson GS, *et al.* Genetic analysis of MRL-lpr mice: relationship of the Fas apoptosis gene to disease manifestations and renal disease-modifying loci. *J Exp Med* 1992; 176: 1645–1656.
71. Fischer GH, Rosenberg FJ, Straus SE, *et al.* Crosslinking CD4 by human immunodeficiency virus gp120 primes T-cells for activation-induced apoptosis. *J Exp Med* 1992; 176: 1099–1106.
72. Rieux-Laucat F, Le Deist F, Hivroz C, *et al.* Mutations in Fas associated with human lymphoproliferative syndrome and autoimmunity. *Science* 1995; 268: 1347–1349.
73. Lenardo MJ, Puck JM. Dominant interfering Fas gene mutations impair apoptosis in a human autoimmune lymphoproliferative syndrome. *Cell* 1995; 81: 935–936.
74. Cheng J, Zhou T, Liu C, *et al.* Protection from Fas-mediated apoptosis by a soluble form of the Fas molecule. *Science* 1994; 263: 1759–1762.
75. Tanaka M, Suda T, Takahashi T, Nagata S. Expression of the functional soluble form of human Fas ligand in activated lymphocytes. *EMBO J* 1995; 14: 1129–1135.
76. Ogasawara J, Watanabe-Fukunaga R, Adachi M, *et al.* Lethal effect of the anti-Fas antibody in mice. *Nature* 1993; 364: 806–809.
77. Ando S, Hirabayashi Y, Kon K, Inagaki F, Tate S, Whittaker VP. A trisialoganglioside containing a sialyl alpha 2-6 N-acetylgalactosamine residue is a cholinergic-specific antigen, Chol-1 alpha. *J Biochem* 1992; 111: 287–290.
78. Ni R, Tomita Y, Matsuda K, *et al.* Fas-mediated apoptosis in primary cultured mouse hepatocytes. *Exp Cell Res* 1994; 215: 332–337.
79. Hiramatsu N, Hayashi N, Katayama K, *et al.* Immunohistochemical detection of Fas antigen in liver tissue of patients with chronic hepatitis C. *Hepatology* 1994; 19: 1354–1359.
80. Meyaard L, Otto SA, Keet IP, Roos MT, Miedema F. Programmed death of T-cells in human immunodeficiency virus infection: no correlation with progression to disease. *J Clin Invest* 1994; 93: 982–988.
81. Banda NK, Bernier J, Kurahara DK, *et al.* Crosslinking CD4 by human immunodeficiency virus gp120 primes T-cells for activation-induced apoptosis. *J Exp Med* 1992; 176: 1099–1106.
82. Westendorp MO, Frank R, Ochsenbauer C, *et al.* Sensitization of T-cells to CD95-mediated apoptosis by HIV-1 tat and gp120. *Nature* 1995; 375: 497–500.
83. Katsikis PD, Wunderlich ES, Smith CA, Herzenberg LA. Fas antigen stimulation induces marked apoptosis of T-lymphocytes in human immunodeficiency virus-infected individuals. *J Exp Med* 1995; 181: 2029–2036.
84. Leno M, Simpson RM, Bowers FS, Kindt TJ. Human T-lymphocyte virus I from a leukemogenic cell line mediates *in vivo* and *in vitro* lymphocyte apoptosis. *J Exp Med* 1995; 181: 1575–1580.
85. Cohen DA, Fitzpatrick EA, Barve SS, *et al.* Activation dependent apoptosis in CD4+ T-cells during murine AIDS. *Cell Immunol* 1993; 151: 392–402.
86. Nunez G, London L, Hockenbery D, Alexander M, McKearn JP, Korsmeyer SJ. Deregulated Bcl-2 gene

expression selectively prolongs survival of growth factor-deprived hemopoietic cell lines. *J Immunol* 1990; 144: 3602–3610.
87. Yoshida Y. Hypothesis: apoptosis may be the mechanism responsible for the premature intramedullary cell death in the myelodysplastic syndrome. *Leukemia* 1993; 7: 144–146.
88. Clark DM, Lampert IA. Apoptosis is a common histopathological finding in myelodysplastic syndrome: the correlate of ineffective hemopoiesis. *Leuk Lymphoma* 1990; 2: 415–418.
89. Yuan J, Angelucci E, Lucarelli G, *et al.* Accelerated programmed cell death (apoptosis) in erythroid precursors of patients with severe β-thalassemia (Cooley's anemia). *Blood* 1993; 82: 374–377.
90. Choi DW. Excitotoxic cell death. *J Neurobiol* 1992; 23: 1261–1276.
91. Loo DT, Copani A, Pike CJ, Whittemore ER, Walencewicz AJ, Cotman CW. Apoptosis is induced by beta-amyloid in cultured central nervous system neurons. *Proc Natl Acad Sci USA* 1993; 90: 7951–7955.
92. Edwards SN, Buckmaster AE, Tolkovsky AM. The death program in cultured sympathetic neurones can be suppressed at the post-translational level by nerve growth factor, cyclic AMP, and depolarization. *J Neurochem* 1991; 57: 2140–2143.
93. Barres BA, Hart IK, Coles HSR, *et al.* Cell death and control of cell survival in the oligodendrocyte lineage. *Cell* 1992; 70: 31–46.
94. Arenas E, Persson H. Neurotrophin-3 prevents the death of adult central noradrenergic neurons *in vivo*. *Nature* 1994; 367: 368–371.
95. Rosen DR, Siddique T, Patterson D, *et al.* Mutations in Cu/Zn superoxide dismutase gene are associated with familial amyotrophic lateral sclerosis. *Nature* 1993; 362: 59–62.
96. Rao VR, Cohen GB, Oprian DD. Rhodopsin mutation G90D and a molecular mechanism for congenital night-blindness. *Nature* 1994; 367: 639–642.
97. Woo D. Apoptosis and loss of renal tissue in polycystic kidney diseases. *New Engl J Med* 1995; 333: 18–25.
98. Goldin RD, Hunt NC, Clark J, Wickramassinghe SN. Apoptotic bodies in a murine model of alcoholic liver disease: reversibility of ethanol-induced changes. *J Pathol* 1993; 171: 73–76.
99. Gottlieb RA, Burleson KO, Kloner RA, Babior BM, Engler RL. Reperfusion injury induces apoptosis in rabbit cardiomyocytes. *J Clin Invest* 1994; 94: 1621–1628.
100. Han DKM, Haudenschild CC, Hong MK, Tinkle BT, Leon MB, Liau G. Evidence for apoptosis in human atherogenesis and in rat vascular injury model. *Am J Pathol* 1995; 147: 267–277.
101. Geng YJ, Libby P. Evidence for apoptosis in advanced human atheroma: co-localization with interleukin-1β converting enzyme. *Am J Pathol* 1995; 147: 251–266.
102. Whyte MKB, Meagher LC, MacDermot J, Haslett C. Impairment of function in aging neutrophils is associated with apoptosis. *J Immunol* 1993; 150: 5124–5134.
103. Lockshin RA, Zackeri ZF. Programmed cell death: new thoughts and relevance to aging. *J Gerontol* 1990; 45: 135–140.
104. Zhou T, Edwards CK 3rd, Mountz JD. Prevention of age-related T-cell apoptosis defect in CD2-Fas-transgenic mice. *J Exp Med* 1995; 182: 129–137.
105. Hodes RJ. Molecular alterations in the aging immune system. *J Exp Med* 1995; 182: 1–3.
106. Casciola-Rosen LA, Anhalt G, Rosen A. Autoantigens targeted in systemic lupus erythematosus are clustered in two populations of surface blebs on apoptotic keratinocytes. *J Exp Med* 1994; 179: 1317–1330.
107. Szende B, Romics I, Vass L. Apoptosis in prostate cancer after hormonal treatment. *Lancet* 1993; 342: 1422.
108. Levine EL, Davidson SE, Roberts SA, Chadwick CA, Potten CS, West CM. Apoptosis as predictor to radiotherapy in cervical carcinoma. *Lancet* 1994; 344: 472.
109. Walkinshaw G, Waters CM. Induction of apoptosis in catecholaminergic PC12 cells by L-DOPA: implications for the treatment of Parkinson's disease. *J Clin Invest* 1995; 95: 2458–2464.
110. Bertrand R, Solary E, Jenkins J, Pommier Y. Apoptosis and its modulation in human promyelocytic HL-60 cells treated with topoisomerase I and II inhibitors. *Exp Cell Res* 1993; 207: 388–397.
111. Brown DG, Sun XM, Cohen GM. Dexamethasone-induced apoptosis involves cleavage of DNA to large fragments prior to internucleosomal fragmentation. *J Biol Chem* 1993; 268: 3037–3039.
112. Jacobson MD, Burne JF, Raff MC. Programmed cell death and Bcl-2 protection in the absence of a nucleus. *EMBO J* 1994; 13: 1899–1910.
113. Nakajima H, Goldstein P, Henkart PA. The target cell nucleus is not required for cell-mediated granzyme- or Fas-based cytotoxicity. *J Exp Med* 1995; 181: 1905–1909.
114. Bertrand B, Kohn KW, Solary E, Pommier Y. Detection of apoptosis-associated DNA fragmentation using a rapid and quantitative filter binding assay. *Drug Dev Res* 1995; 34: 138–144.
115. McGowan AJ, Fernandes RS, Verhaegen S, Cotter TG. Zinc inhibits UV radiation-induced apoptosis but fails to prevent subsequent cell death. *Int J Rad Biol* 1994; 66: 343–349.
116. Wang L, Miura M, Bergeron L, Zhu H, Yuan J. Ich-1, an ICE/ced-3-related gene, encodes both positive and negative regulators of programmed cell death. *Cell* 1994; 78: 739–750.
117. Alnemri ES, Fernandez-Alnemri T, Litwack G. Cloning and expression of four novel isoforms of human interleukin-1 beta converting enzyme with different apoptotic activities. *J Biol Chem* 1995; 270: 4312–4317.
118. Dubrez L, Goldwasser F, Genne P, Pommier Y, Solary E. The role of cell cycle regulation and apoptosis triggering in determining the sensitivity of leukemic cells to topoisomerase I and II inhibitors. *Leukemia* 1995; 9: 1013–1024.
119. Pommier Y, Leteurtre F, Fesen M, *et al.* Cellular determinants of sensitivity and resistance to DNA topoisomerase inhibitors. *Cancer Invest* 1994; 12: 530–542.
120. Kamesaki S, Kamesaki H, Jorgensen TJ, Tanizawa A, Pommier Y, Cossman J. Bcl-2 protein inhibits etoposide-induced apoptosis through its effects on events subsequent to topoisomerase II-induced DNA strand breaks ant their repair. *Cancer Res* 1993; 53: 4251.
121. Campos L, Rouault JP, Sabido O, *et al.* High expression of Bcl-2 protein in acute myeloblastic leukemia cells is associated with poor response to chemotherapy. *Blood* 1993; 81: 3091–3096.
122. Kondo S, Yin D, Takeuchi J, Morimura T, Oda Y, Kikuchi H. *bcl-2* gene enables rescue from *in vitro* myelosuppression (bone marrow cell death) induced by chemotherapy. *Br J Cancer* 1994; 70: 421–426.
123. Campos L, Sabido O, Rouault JP, Guyotat D. Effects of Bcl-2 antisense oligonucleotides on *in vitro* proliferation and survival of normal bone marrow progenitors and leukemic cells. *Blood* 1994; 84: 595–600.

124. de Fabritiis P, Amadori S, Calabretta B, Mandelli F. Elimination of clonogenic Philadelphia positive cells using BCR-ABL antisense oligonucleotides. *Bone Marrow Transpl* 1993; 12: 261–265.
125. Veis DJ, Sorenson CM, Shutter JR, Korsmeyer SJ. Bcl-2-deficient mice demonstrate fulminant lymphoid apoptosis, polycystic kidneys, and hypopigmented hair. *Cell* 1993; 75: 229–240.
126. Motoyama N, Wang F, Roth KA, *et al.* Massive cell death of immature hematopoietic cells and neurons in Bcl-x-deficient mice. *Science* 1995; 267: 1506–1510.
127. Levy Y, Brouet JC. Interleukin-10 prevents spontaneous death of germinal center B-cells by induction of the Bcl-2 protein. *J Clin Invest* 1994; 93: 424–428.
128. Dancescu M, Rubio-Trujillo M, Biron G, Bron D, Delespesse G, Sarfati M. Interleukin-4 protects chronic lymphocytic leukemic B-cells from death by apoptosis and upregulates Bcl-2 expression. *J Exp Med* 1992; 176: 1319–1326.
129. Sarin A, Clerici M, Blatt SP, Hendrix CW, Shearer GM, Henkart PA. Inhibition of activation-induced programmed cell death and restoration of defective immune responses of HIV+ donors by cysteine protease inhibitors. *J Immunol* 1994; 153: 862–872.
130. Squier MKT, Miller ACK, Malkinson AM, Cohen JJ. Calpain activation in apoptosis. *J Cell Physiol* 1994; 159: 229–237.
131. Wright SC, Wei QS, Zhong J, Zheng H, Kinder DH, Larrick JW. Purification of a 24 kD protease from apoptotic tumor cells that activate DNA fragmentation. *J Exp Med* 1994; 180: 2113–2123.
132. Irmler M, Hertig S, MacDonald HR, *et al.* Granzyme A is an interleukin-1 beta converting enzyme. *J Exp Med* 1995; 181: 1917–1922.
133. Staal FJT, Anderson MT, Staal GEJ, Herzenberg LA, Gitler C, Herzenberg LA. Redox regulation of signal transduction: tyrosine phosphorylation and calcium influx. *Proc Natl Acad Sci USA* 1994; 91: 3169–3122.
134. Dröge W, Eck HP, Mihm S. HIV-induced cysteine deficiency and T-cell dysfunction: a rationale for treatment with N-acetylcysteine. *Immunol Today* 1992; 13: 211–214.
135. Fisher DE. Apoptosis in cancer therapy: crossing the threshold. *Cell* 1994; 78: 539–542.
136. Horio Y, Takahashi T, Kuroishi T, *et al.* Prognostic significance of *p53* deletions in primary resected non-small cell lung cancer. *Cancer Res* 1993; 53: 1–4.
137. Elrouby S, Thomas A, Costin D, *et al.* *p53* gene mutation in B-cell chronic lymphocytic leukemia is associated with drug resistance and is independent of *mdr1/mdr3* gene expression. *Blood* 1993; 82: 3452–3459.
138. Lowe SC, Bodis S, McClatchey, *et al.* P53 status and the efficacy of cancer therapy *in vivo*. *Science* 1994; 266: 807–810.
139. Critchfield JM, Racke MK, Zuniga-Pflücker JC, *et al.* T-cell deletion in high antigen dose therapy of autoimmune encephalitis. *Science* 1994; 263: 1139–1143.
140. Pulendran B, Kannourakis G, Nouri S, Smith KGC, Nossal GJV. Soluble antigen can cause enhanced apoptosis of germinal-centre B-cells. *Nature* 1995; 375: 331–334.
141. Shokat KM, Goodnow CC. Antigen-induced B-cell death and elimination during germinal centre immune response. *Nature* 1995; 375: 334–338.
142. Deftos M, Olee T, Carson DA, Chen PP. Defining the genetic origins of three rheumatoid synovium-derived IgG rheumatoid factors. *J Clin Invest* 1994; 93: 2525–2553.
143. Nicolle NW, Nag B, Sharma SD, *et al.* Specific tolerance to an acetylcholine receptor epitope induced *in vitro* in myasthenia gravis CD4+ lymphocytes by soluble major histocompatibility complex class II-peptide complexes. *J Clin Invest* 1994; 93: 1361–1369.
144. Kobayashi N, Hamamoto Y, Yamùamoto N, Ishii A, Yonehara M, Yonehara S. Anti-Fas monoclonal antibody is cytocidal to human immunodeficiency virus-infected cells without augmenting viral replication. *Proc Natl Acad Sci USA* 1990; 87: 9620–9624.
145. Debatin KM, Goldman CK, Waldmann TA, Krammer PH. APO-1 induced apoptosis of leukemia cells from patients with adult T-cell leukemia. *Blood* 1993; 81: 2972–2977.
146. Morimoto H, Yonehara S, Bonavida B. Overcoming tumor necrosis factor and drug resistance of human tumor cell lines by combination treatment with anti-Fas antibody and drugs or toxins. *Cancer Res* 1993; 53: 2591–2596.
147. Neta R, Stiefel SM, Finkelman F, Herrmann S, Ali N. IL-12 protects bone marrow from and sensitizes intestinal tract to ionizing radiations. *J Immunol* 1994; 153: 4230–4237.
148. Löwenberg B, Touw P. Hematopoietic growth factors and their receptors in acute leukemia. *Blood* 1993; 81: 281–292.
149. Lotem J, Sachs L. Hematopoietic cytokines inhibit apoptosis induced by transforming growth factor-β and cancer chemotherapy compounds in myeloid leukemic cells. *Blood* 1992; 80: 1750–1757.
150. Estey E, Thall PF, Kantarjian H, *et al.* Treatment of newly diagnosed acute myelognous leukemia with granulocyte-macrophage colony-stimulating factor (GM-CSF) before and during continuous-infusion high dose ara-C + daunorubicin: comparison to patients treated without GM-CSF. *Blood* 1992; 79: 2246–2255.
151. Colombel M, Olsson CA. Hormone-regulated apoptosis results from re-entry of differentiated prostate cells onto a defective cell cycle. *Cancer Res* 1992; 52: 4313–4319.
152. Lunardi-Iskandar Y, Bryant JL, Zeman RA, *et al.* Tumorigenesis and metastasis of neoplastic Kaposi's sarcoma cell line in immunodeficient mice blocked by a human pregnancy hormone. *Nature* 1995; 375: 64–68.

The Journal of Neuroscience, June 15, 1999, 19(12):4828–4838

Nerve Growth Factor Signaling through p75 Induces Apoptosis in Schwann Cells via a Bcl-2-Independent Pathway

Merja Soilu-Hänninen,[1] Paul Ekert,[1] Tamara Bucci,[1] Daniel Syroid,[2] Perry F. Bartlett,[1] and Trevor J. Kilpatrick[1]

[1]The Walter and Eliza Hall Institute of Medical Research, The Royal Melbourne Hospital, Parkville Victoria 3050, Australia, and [2]The Salk Institute for Biological Studies, La Jolla, California 92186-5800

Apoptosis is involved in the regulation of Schwann cell numbers during normal development and after axonal damage, but the molecular regulation of Schwann cell death remains unknown. We have used stably transfected rat Schwann cell lines to study the potential roles of nerve growth factor (NGF), the antiapoptotic protein Bcl-2 and the cytokine response modifier A (CrmA) in modulating Schwann cell death *in vitro*. Bcl-2 inhibited Schwann cell apoptosis induced by survival factor withdrawal, whereas CrmA did not. In contrast, Bcl-2-transfected Schwann cells were susceptible to apoptosis in response to exogenous NGF, whereas CrmA-expressing cell lines were resistant. Demonstration of high levels of the low-affinity neurotrophin receptor p75 but not the high-affinity TrkA receptor on the Bcl-2-transfected cell lines suggested that the NGF-induced killing was mediated by p75. This was confirmed by resistance of Schwann cells isolated from p75 knockout mice to the NGF-induced cell death. Nerve growth factor also promoted the death of wild-type mouse and rat Schwann cells in the absence of survival factor withdrawal. Endogenous Bcl-2 mRNA was expressed by wild-type Schwann cells in all conditions that promoted survival but was downregulated to undetectable levels after survival factor withdrawal. In conclusion, our results demonstrate the existence of two separate pathways that expedite apoptosis in Schwann cells: a Bcl-2-blockable pathway initiated on loss of trophic support, and a Bcl-2-independent, CrmA-blockable pathway mediated via the p75 receptor.

Key words: apoptosis; neurotrophins; Schwann cells; nerve growth factor; Bcl-2; low-affinity neurotrophin receptor

The number of Schwann cells in peripheral nerve is tightly regulated, and programmed cell death, or apoptosis, has been implicated in this process (Syroid et al., 1996; Trachtenberg and Thompson, 1996). Axonally derived neuregulins prevent Schwann cell apoptosis, suggesting that Schwann cell numbers are controlled by competition for axonally derived trophic support (Grinspan et al., 1996). However, the molecules involved in mediating Schwann cell apoptosis are unknown.

Apoptosis involves activation of a cascade of proteolytic enzymes called caspases (Nicholson and Thornberry, 1997). Members of the Bcl-2 protein family are key regulators of apoptosis and are categorized according to their ability to promote (e.g., Bak, Bax, Bik) or inhibit (e.g., Bcl-2, Bcl-xL, Bcl-w) apoptosis (Newton and Strasser, 1998). The mechanism of the anti-apoptotic function of Bcl-2 is uncertain, but Bcl-2 proteins regulate the activation of key caspases (Adams and Cory, 1998; Newton and Strasser, 1998). Recently, it was suggested that Bcl-2 could also serve as a caspase substrate, such that activation of the cell surface receptor Fas (Itoh et al., 1991) leads to cleavage of Bcl-2, which then accelerates rather than inhibits apoptosis (Cheng et al., 1997).

Schwann cells express high levels of the low-affinity neurotrophin receptor p75 (Lemke and Chao, 1988), which has sequence similarity to the tumor necrosis factor receptor (TNFR) $p55^{TNFR}$ and to Fas (Meakin and Shooter, 1992). Ligand binding to Fas or $p55^{TNFR}$ initiates programmed cell death via activation of caspase 8, which can cleave other caspases. This caspase 8-mediated pathway cannot be blocked by Bcl-2 but is inhibitable by a poxvirus caspase inhibitor, cytokine response modifier A (CrmA) (Chinnaiyan et al., 1995; Strasser et al., 1995; Cohen, 1997). A role for p75 in signaling the death of neural cells has also been established (Rabizadeh et al., 1993; Barrett and Bartlett, 1994; Frade et al., 1996; Frade and Barde, 1998), but the role of ligand binding in p75 activation is uncertain. In some systems, p75 induces cell death constitutively (Rabizadeh et al., 1993), whereas cell death can also be induced by p75 activation through ligand binding (Casaccia-Bonnefil et al., 1996; Frade et al., 1996). The intracellular death pathway initiated by p75 signaling is unknown.

The neurotrophins not only bind to p75 but also bind with high affinity to receptor tyrosine kinases known as Trks, comprising Trk-A, -B, and -C (Kaplan et al., 1991; Kaplan and Miller, 1997). Potential mechanisms by which the prototypic neurotrophin, nerve growth factor (NGF), signals were recently assessed in oligodendrocytes; it was suggested that activation of Trk-A promoted survival via activation of NF-kB and via suppression of a death signal delivered by p75, acting through c-jun kinase (Yoon et al., 1998). It is of note that Schwann cells express only low levels of the Trk receptors (Yamamoto et al., 1993).

The role of p75 in Schwann cells is obscure. Schwann cells could possibly bind and present NGF to regenerating neurons

Received Dec. 14, 1998; revised March 8, 1999; accepted April 7, 1999.

This work was supported by the National Health and Medical Research Council (NH&MRC) of Australia and the Sylvia and Viertel Charitable Foundation. M.S.-H. was supported by grants from the Finnish Multiple Sclerosis Society, the Finnish Cultural Foundation, the Academy of Finland, and the Maud Kuistila Foundation. P.E. was supported by a NH&MRC postgraduate scholarship. We thank Dr. Duanzhi Wen (Amgen Inc.) for the neuregulin-β and Dr. Greg Lemke (Salk Institute) for the P_0 probe. We also thank Dr. David Vaux and the members of his laboratory for helpful discussions, for their kind gifts of CrmA and Bcl-2 plasmids, and for critical reading of this manuscript. Mrs. Radmilla Milekic is acknowledged for secretarial assistance in the preparation of this manuscript.

Correspondence should be addressed to Trevor J. Kilpatrick, The Walter and Eliza Hall Institute of Medical Research, Post Office The Royal Melbourne Hospital, Parkville Victoria 3050, Australia.

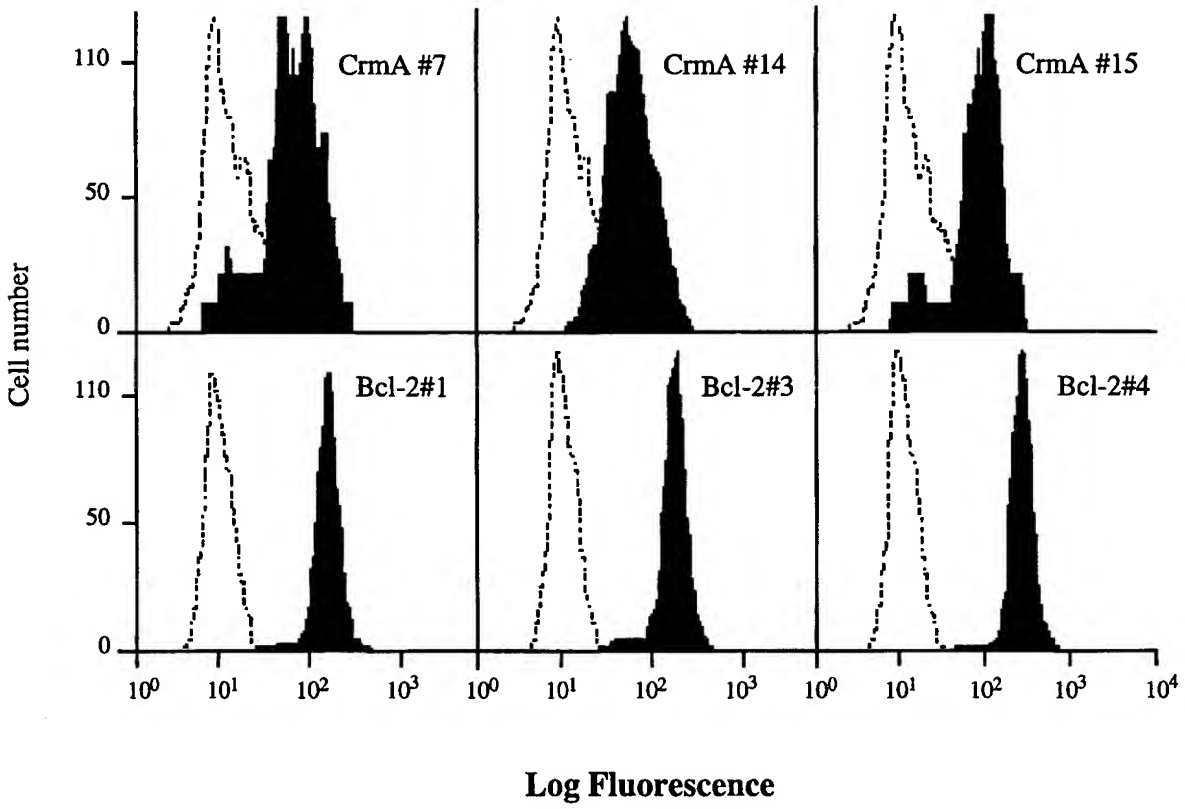

Figure 1. Intracellular expression of the human Bcl-2 protein and the poxvirus caspase inhibitor CrmA in the transfected rat Schwann cell lines Bcl-2#1, -#3, -#4, and CrmA#7, #14, and #15. Immunofluorescence staining was performed with the mouse mAb Bcl-2–100 against the human Bcl-2 (for the Bcl-2 cell lines) or with mouse anti-Flag mAb (for the CrmA cell lines), and binding of primary antibody was detected with FITC-conjugated sheep anti-mouse IgG. As negative controls, rat Schwann cells transfected with the empty expression plasmid pEF were similarly stained (indicated in the histograms with a *dashed line*).

after peripheral axotomy (Heumann et al., 1987), and it has been suggested that NGF could support Schwann cell migration (Anton et al., 1994). There is no compelling evidence, however, to indicate a role for NGF as a Schwann cell survival factor, although NGF can activate NF-kB through p75 (Carter et al., 1996). To date, cell death signaling through p75 has not been demonstrated in Schwann cells.

In this study, using stably transfected Schwann cell lines, we found that Bcl-2, but not CrmA, protects Schwann cells from apoptosis induced by survival factor withdrawal. In contrast, Schwann cells transfected with Bcl-2 were sensitive to apoptosis in response to exogenous NGF, whereas CrmA-transfected Schwann cells were resistant. Lack of TrkA expression in the Bcl-2-transfected cell lines and resistance of p75-deficient Schwann cells to NGF-induced killing suggested that the NGF-induced death response was mediated via the p75 receptor.

MATERIALS AND METHODS

Cell culture and transfections. Cultures of rat Schwann cells were prepared from postnatal day 3 sciatic nerve and purified to >99.5% homogeneity as described previously (Brockes et al., 1979). Cells were plated on poly-L-lysine-coated (100 μg/ml; Sigma, St. Louis, MO) 10 cm tissue culture Petri dishes or 6-well plates (Falcon) and maintained in DMEM (Life Technologies, Gaithersburg, MD), 10% fetal calf serum (FCS) (HyClone, Logan, UT), 2 μm forskolin (Sigma), and 10 ng/ml recombinant human neuregulin-β (Amgen, Thousand Oaks, CA). Subconfluent cultures that had been passaged 5–10 times were transfected either by using the transfection reagent LipofectAMINE (Life Technologies) according to the manufacturer's instructions or by electroporation of 2×10^7 Schwann cells suspended in 500 μl of PBS, at 270 V and 960 μFD, with 10 μg of plasmid cDNA containing either full-length human Bcl-2 or poxvirus CrmA cloned into the pEF FLAGpGKpuro (pEF) mammalian expression vector (Huang et al., 1997). This vector contains sequences encoding a Flag-tag and puromycin resistance. Both the Bcl-2 and CrmA plasmid cDNAs were kind gifts from Dr. David Vaux (The Walter and Eliza Hall Institute of Medical Research). Puromycin (Sigma) was added to facilitate positive selection at 2 μg/ml 48 hr after transfection.

Mouse Schwann cells were isolated from postnatal day 2 sciatic nerves of BALB/c mice and homozygous mutant mice deficient for p75 (Lee et al., 1992) backcrossed onto the BALB/c and 129 genetic background. Briefly, nerves were digested for 30 min at 37°C by incubation with 0.25% trypsin (Sigma) and 0.02% collagenase (Sigma) in HBSS. Digestion was terminated by addition of 10% ice-cold FCS. Single-cell suspensions were subsequently prepared by passage of the cells through 18, 21, and 23 gauge needles fitted to a 1 ml syringe. Cells were then pelleted, washed once with DMEM/10% FCS, and plated on 96-well plate wells in DMEM containing 10% FCS and 10 ng/ml of neuregulin-β. Cells were expanded for 5–7 d and then sorted using rat anti-mouse Thy 1.2 antibody (Ab) (10× concentrated supernatant of hybridoma 30H12) and rabbit complement (Life Technologies) to remove contaminating fibroblasts. Sorted cells were washed and plated on poly-L-lysine-coated 24-well plate wells and then subsequently dissociated on the following day to set up viability assays (see below). The percentage of Schwann cells in both the wild-type and knockout cultures was determined after sorting by S-100 staining of cells plated on 8-well chamber slides. A total of 500 cells/culture were counted from six to seven separate fields at 40× magnification, yielding purities of 94 ± 2% for the wild-type cultures and 96 ± 3% for the p75 knockout cultures.

Growth factors. The β-form of recombinant human neuregulin was obtained from Amgen. Nerve growth factor, purified from male mouse submaxillary glands (mNGF 2.5S; Alomone Labs), was purchased from Sapphire Bioscience (Alexandria, NSW, Australia). Recombinant human insulin-like growth factor (IGF-1) was purchased from Boehringer Mannheim.

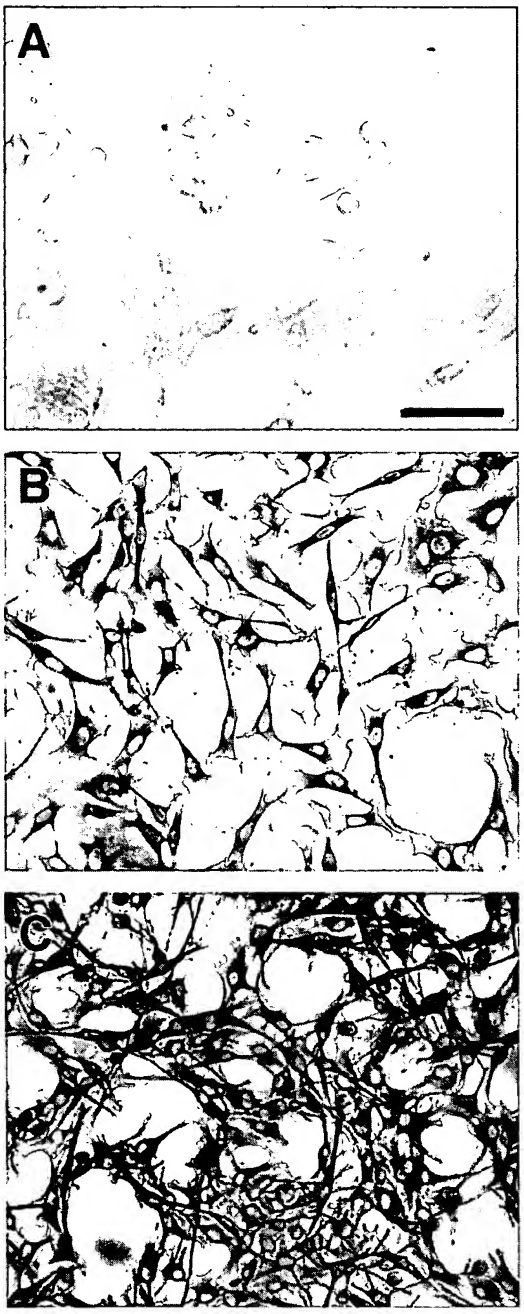

Figure 2. The transfected Schwann cells express the astroglial protein S-100. Immunoperoxidase staining of Bcl-2#1 cells (*B*) and CrmA#14-cells (*C*) with rabbit anti-cow-S-100 protein is shown. As negative controls, the same cell lines were stained with secondary antibody only, as shown for the Bcl-2#1 cell line in *A*. Scale bar (shown in *A*): *A*, *B*, 50 μm; *C*, 100 μm.

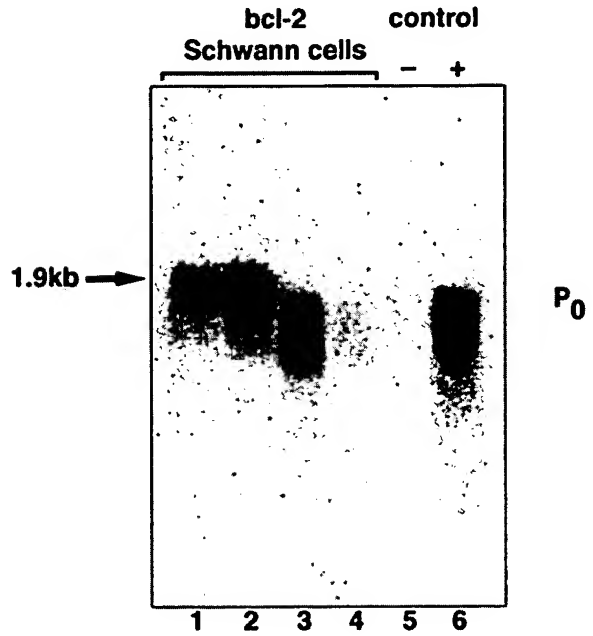

Figure 3. Northern blot analysis confirms that the Bcl-2-transfected cell lines express transcripts of the Schwann cell-specific P_0 gene. Shown is P_0 expression of the three Bcl-2-transfected cell lines cultured in either high (20 μM, *lanes 1–3*) or low concentration of forskolin (2 μM, Bcl-2#1 cell line, *lane 4*). *Lane 5* contains fibroblast RNA as a negative control, and *lane 6* contains wild-type rat Schwann cell RNA as a positive control.

Antibodies and flow cytometry reagents. Monoclonal antibody to the low-affinity nerve growth factor receptor of rat (clone MC192) and a monoclonal antibody to mouse nerve growth factor (clone 27/21, which also reacts with NGF from rat) were purchased from Boehringer Mannheim. Anti-Flag Ab (clone M_2) was from Sigma (NSW, Australia). Anti-human Bcl-2 Ab that was used for flow cytometry (DAKO-Bcl-2, clone 124) and rabbit anti-cow-S-100 antibody were from Dako Corporation (Carpinteria, CA). Anti-human Bcl-2 Ab [Bcl-2–100 (Pezzella et al., 1990)] that was used for Western blotting was a kind gift from Dr. David Huang (The Walter and Eliza Hall Institute of Medical Research). Anti-human CD40L monoclonal antibody (mAb; isotype control for the MC192 mAb) was from PharMingen (San Diego, CA). FITC-conjugated sheep anti-mouse IgG and FITC-conjugated goat anti-mouse IgG (Southern Biotechnology Associates, Birmingham, AL) were purchased from Silenius Laboratories (Victoria, Australia). Annexin-V-Fluos reagent, a fluorescence-conjugated anticoagulant for the detection of phosphatidylserine on the outer leaflet of apoptotic cells, was purchased from Boehringer Mannheim.

3-[4,5-Dimethylthiazol-2-yl]-2,5-diphenyltetrazolium bromide survival assay. To assess the survival kinetics of the various transfected rat Schwann cell lines, the cells were first trypsinized and washed three times with ice-cold DMEM. Washed cells were then plated at 4×10^4 cells/ml in either DMEM without serum and without growth factors or with DMEM together with either 1, 10, or 100 ng/ml NGF, with 500 ng/ml anti-mouse NGF antibody, or 10 ng/ml NGF together with 500 ng/ml anti-NGF. Assays were performed over a 72 hr period in multiple Terasaki microwell plates, such that numbers of viable 3-[4,5-dimethylthiazol-2-yl]-2,5-diphenyltetrazolium bromide (MTT)-positive cells were counted at 0, 24, 48, and 72 hr. Six wells for each time point and each condition were assessed. Cells exhibiting a blue granular reaction product 1 hr after addition of 0.5 mg/ml MTT were counted as positive. The percentage of surviving cells was then determined as a fraction of the baseline cell count for each experimental condition. Wild-type rat and mouse Schwann cells were similarly assessed, in either DMEM alone, DMEM together with 10 ng/ml NGF and, in a subset of experiments, 100 ng/ml IGF-1 and 50 ng/ml neuregulin-β with or without 10 ng/ml NGF. Because of the limited numbers of mouse Schwann cells, only baseline and 48 hr time points were included.

Statistics. Statistical significance of the differences in survival between Bcl-2 and CrmA-transfected and control cell lines for each of the culture conditions tested was assessed using unpaired Student's *t* test, with the aid of Microsoft Excel Version 4.0 computer software and the Student Distribution from Geigy Scientific Tables. p values <0.05 were taken as statistically significant.

S-100 immunohistochemistry. To analyze for expression of the glial protein S-100, Schwann cells were cultured on 8-well Chamber slides (Nunc, Roskilde, Denmark). The cultures were then fixed with 4% paraformaldehyde and stained with rabbit anti-cow S-100 antibody at 1:200 dilution. Binding of the primary antibody was detected using a Vectastain peroxidase anti-rabbit IgG kit according to the manufacturer's instructions. A chromogenic reaction was developed with DAB, and the slides were mounted in Gurr's Aquamount (BDH Laboratory Sup-

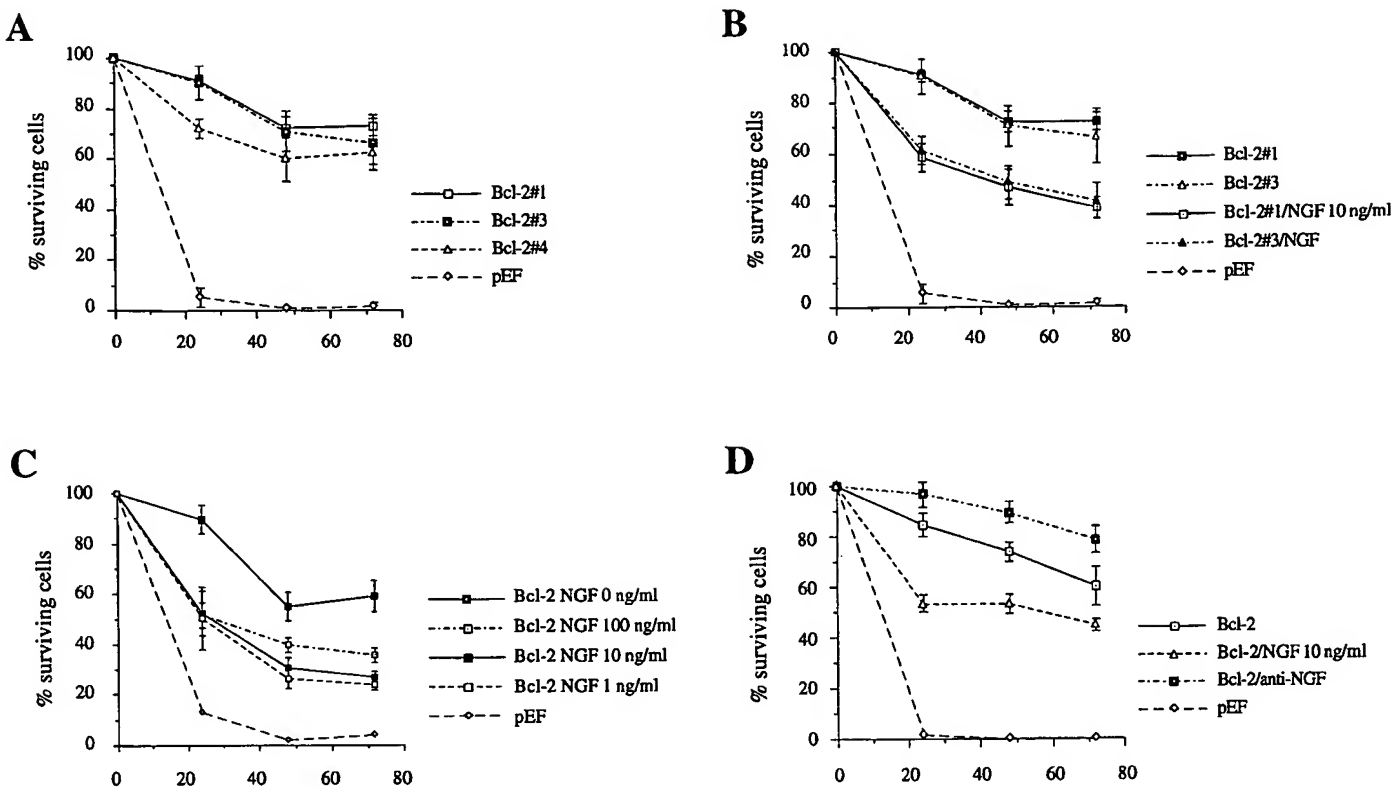

Figure 4. Survival of Bcl-2-transfected rat Schwann cells *in vitro* after survival factor withdrawal or treatment with either exogenous NGF or anti-NGF antibodies. The control cells were transfected with the empty mammalian expression vector pEF. Cells were cultured in multiple microwell plates in (*A*) DMEM only or (*B*, *C*) DMEM containing exogenous NGF or (*D*) anti-NGF antibody. The numbers of viable cells were assessed daily over a 3 d period. *A*, Bcl-2 protects Schwann cells from apoptosis induced by survival factor withdrawal. The data shown represent means ± SEM of three independent experiments comparing the survival of three separate Bcl-2-transfected Schwann cell lines (*Bcl-2#1*, *Bcl-2-#3*, and *Bcl-2#4*) with the survival of a control cell line, *pEF*. All three Bcl-2-transfected cell lines exhibited a significant survival advantage at 24, 48, and 72 hr (p values from 0.005 to <0.0005). *B*, Nerve growth factor at 10 ng/ml significantly reduces the survival of Bcl-2-transfected Schwann cells. Means ± SEM of three independent experiments with Bcl-2#1 and -#3 cell lines and the control cell line pEF#1 are shown. p values are 0.001, 0.01, and 0.0025 for the Bcl-2#1 cell line and 0.025, 0.001, and 0.1 (NS) for the Bcl-2#3 cell line at 24, 48, and 72 hr, respectively. *C*, Dose–response study of the effect of NGF on the survival of Bcl-2-transfected Schwann cells. Shown are mean viabilities ±SEM of Bcl-2#1, Bcl-2#3, and Bcl-2#4 cell lines assayed in one survival experiment. Culture conditions were either DMEM alone or DMEM with 1, 10, or 100 ng/ml of NGF. All three concentrations of NGF significantly reduced the survival of the Bcl-2-transfected cell lines, the lower concentrations slightly but not significantly ($p > 0.05$) more than 100 ng/ml. *D*, Anti-NGF antibody increases the survival of Bcl-2-transfected Schwann cells. Shown are the means ± SEM, comparing the viability of three separate Bcl-2-transfected cell lines assayed in one survival experiment. Culture conditions were DMEM only, DMEM + 10 ng/ml NGF, or DMEM + 500 ng/ml anti-NGF antibody. The difference in survival between DMEM only and anti-NGF conditions was significant at 48 hr ($p = 0.025$), and the difference between NGF-neutralized (anti-NGF) and NGF-added conditions was significant at all time points (p values from 0.001 to 0.005).

plies, Poole, UK), coverslipped, and photographed using Ektachrome 200 ASA color slide film.

Flow cytometry. To determine whether the transfected Schwann cell lines expressed the human Bcl-2 protein intracellularly, the cells were stained with anti-human Bcl-2 Ab as described previously (Strasser et al., 1995). Intracellular expression of CrmA protein from the CrmA plasmid was indirectly assessed by staining transfected cells with anti-Flag antibodies, using a similar protocol. Cell surface expression of p75 was determined by incubating the cells for 30 min on ice with 1 μg/ml mouse mAb clone 192 against rat p75, or with isotype-matched control mAb (anti-human CD40L). The cells were then washed twice with PBS containing 2% FCS and 0.1% sodium azide, incubated for an additional 30 min with FITC-conjugated sheep anti-mouse IgG, washed twice, and analyzed using a FACScan flow cytometer (Becton Dickinson, Mountain View, CA).

To distinguish between apoptosis and necrosis, the pEF-1 and the Bcl-2#1 transfected Schwann cell lines were cultured on 6-well plates in DMEM or DMEM containing 10 ng/ml NGF for 48 hr. The cells were then trypsinized and washed once with DMEM/10% FCS and twice with MT-PBS containing 2% FCS. A total of 10^6 cells were incubated in 100 μl of solution containing 20 μl of Annexin-V-Fluos labeling reagent and 20 μl of 50 μg/ml propidium iodide solution in 1 ml of incubation buffer (10 mM HEPES/NaOH, pH 7.4, 140 mM NaCl, 5 mM $CaCl_2$). After 15 min of incubation, 200 μl of a HEPES and phosphate-buffered balanced salt solution containing 5% FCS was added per tube, and the cells were immediately analyzed on a flow cytometer for fluorescein and propidium iodide detection.

Northern blotting. To confirm that the transfected clones were Schwann cells, transcripts of the Schwann cell glycoprotein P_0 gene in untransfected and transfected Schwann cells were analyzed by Northern blotting, using a 1.85 kb probe that recognizes the Schwann cell-specific P_0 RNA. The pSN63 plasmid containing the P_0 cDNA insert was a gift from G. Lemke (The Salk Institute, La Jolla, CA). Briefly, the P_0 fragment was cut from the SN63 vector with *Eco*RI digestion, gel-purified using a QIAEX II gel extraction kit, and labeled with ^{32}P using a NeBlot kit (New England Biolabs, Beverly, MA). The labeled probe was hybridized overnight at 68°C with Schwann cell mRNA previously transferred to a Hybond-N membrane (Amersham). Images were developed after a 4 hr exposure using a Phosphoimager (Molecular Dynamics, Sunnyvale, CA). In addition, Northern blotting was used to determine expression of the high-affinity NGF receptor Trk-A on the Bcl-2-transfected Schwann cell lines. A 398 bp fragment of Trk-A cDNA, cloned into the pBSKS(−)

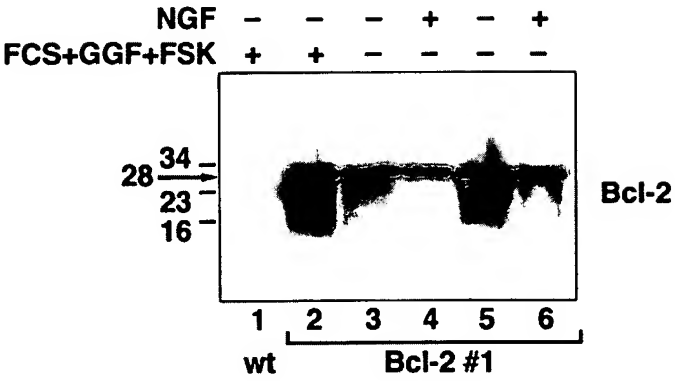

Figure 5. Nerve growth factor does not induce cleavage of Bcl-2. Western blotting of Bcl-2-transfected and control Schwann cells was performed to determine whether NGF induces cleavage of Bcl-2. *Lane 1*, Wild-type rat Schwann cells; *lane 2*, Bcl-2-transfected Schwann cells in serum, neuregulin-β, and forskolin; *lanes 3* and *4*, survival factor-deprived condition for 24 hr; *lanes 5* and *6*, survival factor-deprived condition for 72 hr. No cleavage product was detected when 10 ng/ml NGF was present in the survival factor-deprived conditions (*lanes 4* and *6*).

vector was a gift from Dr. R. Klein (EMBL, Heidelberg, Germany). The fragment was cut from the expression vector with *Eco*RI and *Xba*I digestion and gel-purified using a QIAquick gel extraction kit. A total of 50 ng of purified DNA was labeled with ^{32}P as described above and hybridized overnight at 68°C with 0.5 μg of mRNA isolated from Bcl-2#1 cells and with 10 μg of total RNA from PC12 neuronal cells as a positive control. Images were developed after a 72 hr exposure using a Phosphoimager. To assess the amount of RNA loaded, the membrane was further hybridized with a 280 bp G3PD (GAPDH)-probe, cut with *Pst*I–*Hin*dIII digestion from a pGEM3Z plasmid.

Western blotting. Reduced and denatured protein samples from control and Bcl-2-transfected Schwann cells were run on a 4–15% SDS Tris-HCl gel (Bio-Rad, Richmond, CA), transferred to a polyvinylidene difluoride membrane, and blotted with Bcl-2–100 mAb. Bound antibodies were detected with HRP-conjugated sheep anti-mouse IgG (Silenius) and enhanced using chemiluminescence (Amersham).

RT-PCR. Degenerate primers amplifying a 549 bp fragment from the coding region of exon 1 of the *Rattus norvegicus* Bcl-2 cDNA were designed with the aid of NCBI's Blast 2.0 sequence similarity search program. The upper primer was 5′-CGCAAGCCGGGAGAACAGGGTA-3′, and the lower primer was 5′-AGGTGTGCAGATGCCGGTTCAGGT-3′. These primers were designed to maximize amplification of sequences similar in the rat, mouse, and human Bcl-2 genes, with minimal homology to other Bcl family members, and were synthesized by Beckman Oligonucleotide Synthesis Service (Gladesville, NSW, Australia). As a positive control, a 760 bp fragment of rat β-actin was amplified using 5′-CTGAAGTACCCCATTGAACACGGC-3′ as the upper primer and 5′-CAGGGCAGTAATCTCCTTCTGCAT-3′ as the lower primer. The β-actin oligonucleotides were also designed using the Blast 2.0 computer program, and they were synthesized by Pacific Oligos (Southern Cross University Lismore, NSW, Australia).

To synthesize first-strand DNA for RT-PCR, total RNA (1 μg) or mRNA (50 ng) isolated from wild-type rat Schwann cells was reverse-transcribed using Superscript II RNase H⁻ Reverse Transcriptase (Life Technologies) in a 20 μl reaction volume at 42°C. The various culture conditions from which RNA had been prepared were as follows: (1) DMEM containing 10% FCS, 10 ng/ml neuregulin-β, and 2 μM forskolin, (2) DMEM containing IGF-1 for either 4 or 16 hr, (3) DMEM containing NGF for 4 hr, (4) DMEM only for 1, 2, 4, 8, or 24 hr. For RT-PCR, 5% (1 μl) of the first-strand reaction was amplified in a reaction containing 0.4 μl of 10 mM dNTP mixture (Life Technologies), 1 μl of each primer at 20 μM, 1 μl of 50 mM $MgCl_2$, 5 μl of 10× PCR buffer (Life Technologies), and 0.5 μl (2.5 U) of AmpliTag (Perkin-Elmer, Emeryville, CA) to a total volume of 50 μl. A total of 30 cycles of PCR amplification was performed on a Perkin-Elmer Cetus 480 thermal cycler (Perkin-Elmer) at 94° for 1 min, 58° for 1 min, and 72° for 2 min. Reaction products were electrophoretically separated on a 2% DNA grade agarose gel containing 5 μg/ml ethidium bromide stain to facilitate visualization of the bands under UV illumination.

RESULTS

Generation and characterization of Bcl-2- and CrmA-expressing Schwann cell lines

To assess the effect of Bcl-2 and CrmA on Schwann cell survival we transfected primary rat Schwann cells with puromycin-selectable constructs containing sequences encoding FLAG epitope-tagged human Bcl-2 or FLAG-tagged CrmA. Expression of the constructs in the stable puromycin-resistant rat Schwann cell lines that were generated was demonstrated by intracellular immunofluorescence staining with anti-human Bcl-2 antibodies or, in the case of the CrmA transfected cells, with anti-Flag-antibodies. Three Bcl-2-transfected and three CrmA-transfected cell lines that expressed high and similar levels of Bcl-2 and CrmA, respectively, were chosen for further experiments (Fig. 1).

To confirm that the transfected cell lines had retained Schwann cell characteristics, all cell lines were assessed by immunohistochemistry for expression of the glial protein S-100. All of the transfected cell lines that were used in subsequent experiments expressed S-100. Bcl-2#1 and CrmA#14 cell lines staining positively for S-100 are shown in Figure 2. Northern blotting was used to confirm expression of the Schwann cell-specific P_0 gene (Lemke and Axel, 1985). P_0 was expressed in all three Bcl-2-transfected cell lines that were studied as well as in wild-type rat Schwann cells but not in rat fibroblasts that were included as a negative control (Fig. 3).

Bcl-2 rescues Schwann cells from apoptosis triggered by withdrawal of survival factors but fails to rescue these cells from killing by NGF

To elucidate the potential role of Bcl-2 in Schwann cell apoptosis, we assessed the viability of three separate Bcl-2-transfected rat Schwann cell lines in comparison with rat Schwann cell lines transfected with the empty mammalian expression plasmid pEF FLAGpGKpuro (pEF). The first death stimulus that was assessed was withdrawal of serum, neuregulin-β, and forskolin. All three Bcl-2-transfected cell lines exhibited significant survival advantage at 24, 48, and 72 hr after factor deprivation in comparison with the pEF#1 control cell line (Fig. 4*A*). Survival of the pEF#1 and pEF#2 control cell lines used in this study did not significantly differ from wild-type Schwann cells (data not shown).

The survival factor-starved Bcl-2-transfected cells were also cultured with NGF at the time of plating. Addition of NGF at 10 ng/ml to the cultures reduced the viability of all three Bcl-2-transfected cell lines throughout the 72 hr observation period (Fig. 4*B*). There was a trend toward more cell death at the lower concentrations of NGF (1 and 10 ng/ml) than at 100 ng/ml, but

Table 1. Bcl-2-transfected Schwann cells are resistant to apoptosis induced by survival factor deprivation but undergo apoptosis in response to NGF

		PI− (%)	PI+ (%)	Annexin+ (%)
pEF	− NGF	1	98	98
pEF	+ NGF	7	92	96
Bcl-2#1	− NGF	92	7	13
Bcl-2#1	+ NGF	67	32	33

Control (pEF) and Bcl-2-transfected Schwann cells were deprived of serum, neuregulin-β, and forskolin for 48 hr. NGF (10 ng/ml) was added to half of the cultures. To determine the proportions of viable and apoptotic cells in each condition, the cells were detached and stained at 48 hr with propidium iodide (PI) and Annexin-V-Fluos solution and analyzed by flow cytometry. Viable cells exclude propidium iodide and appear in the table as PI−. The data are generated from a single experiment.

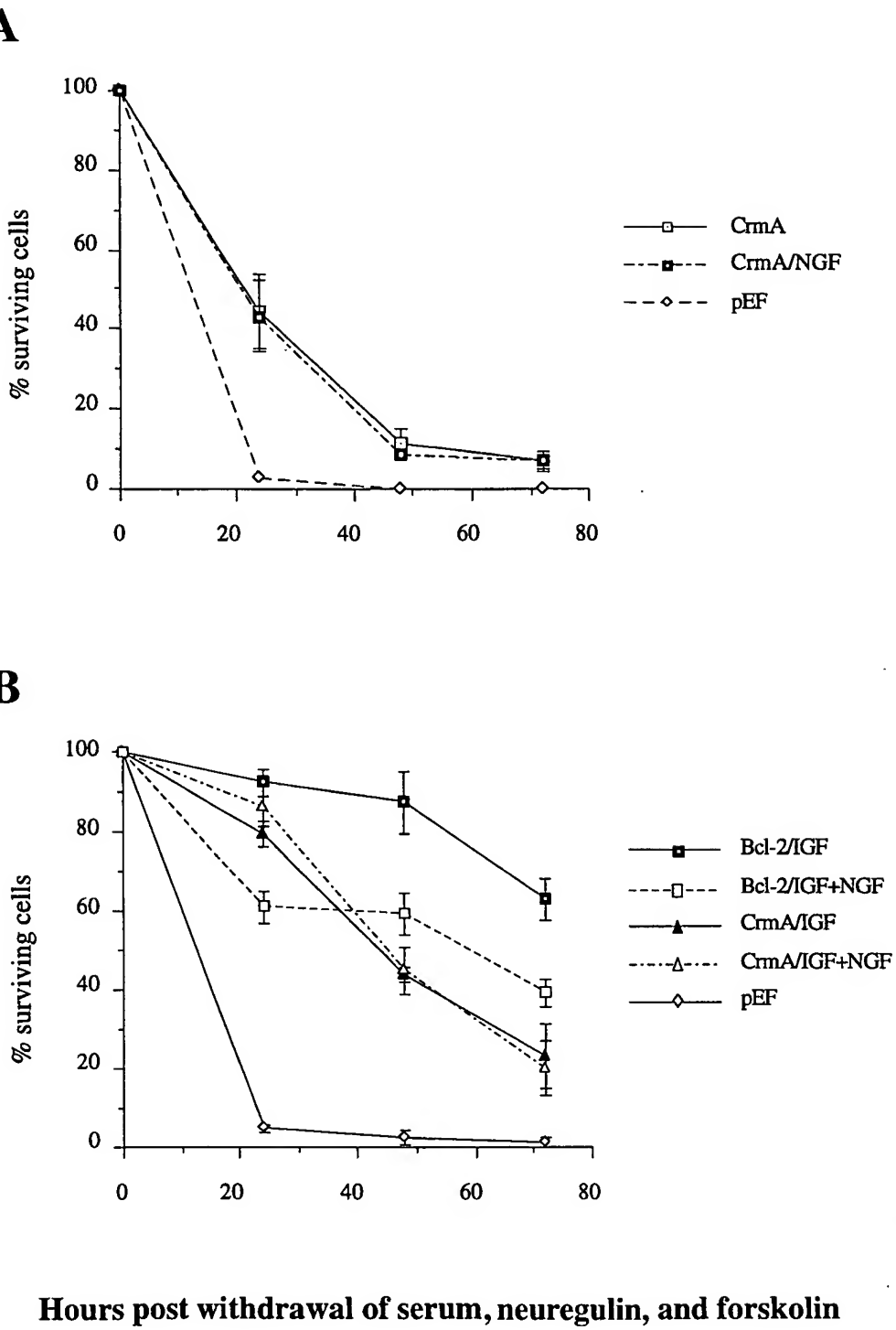

Figure 6. Survival analysis of CrmA-transfected rat Schwann cells *in vitro* after survival factor withdrawal or treatment with exogenous NGF. *A*, CrmA-transfected cells show delayed but retained susceptibility to survival factor deprivation but are protected against NGF killing. Shown are the mean viabilities ±SEM of three separate CrmA-transfected Schwann cell lines (CrmA#7, #14, and #15) in comparison with the pEF#1 control cell line, as assessed in one of two similar survival experiments. Cell lines were cultured either in DMEM only or in DMEM containing 10 ng/ml NGF. Control pEF cells died rapidly in both conditions (only DMEM is shown). CrmA-transfected cells showed some abrogated death at 24 hr ($p = 0.025$), but by 72 hr both the CrmA and control cells showed a similar death profile (p values 0.1 at 48 hr and 0.15 at 72 hr; NS). *B*, CrmA-transfected cells are resistant to NGF killing in the presence of IGF-1, whereas Bcl-2-transfected Schwann cells remain susceptible to NGF under these conditions. Shown are means ± SEM of three separate experiments using the cell lines Bcl-2#1 and CrmA#7. The cells were cultured in either DMEM containing 100 ng/ml IGF-1 or DMEM containing 100 ng/ml IGF-1 and 10 ng/ml NGF. The difference in survival between the two culture conditions was significant for the Bcl-2#1 cell line (p values from 0.025 to 0.005), but not for the CrmA#7 cell line ($p > 0.05$).

the differences in viability between the various concentrations were not statistically significant (Fig. 4*C*). Viability of the vector-only pEF#1 cells was not significantly affected by the addition of NGF under conditions of survival factor deprivation, presumably because these cells were dying so rapidly (data not shown).

To quantitate viability, the survival factor-deprived and the NGF-treated Schwann cells were stained with Annexin, which labels apoptotic cells, and the cells were analyzed by flow cytometry (Table 1). After withdrawal of survival factors, most (98%) of the control cells were Annexin positive at 48 hr, whereas only 13% of the Bcl-2#1 Schwann cells were Annexin positive. However, 33% of the survival factor-deprived Bcl-2#1 Schwann cells cultured with NGF were Annexin positive at 48 hr (Table 1). This correlated well with the survival advantage conferred by Bcl-2 and with the killing observed by NGF in the context of Bcl-2 expression, as assessed in the MTT assays.

Because Schwann cells have been reported to secrete low levels of NGF (Yamamoto et al., 1993), we next assessed the effect of neutralizing anti-NGF antibodies on the survival of the Bcl-2-transfected Schwann cells. Previously, it had been established that exogenous NGF and anti-NGF antibodies have no effect on the viability of wild-type Schwann cells in basal conditions after

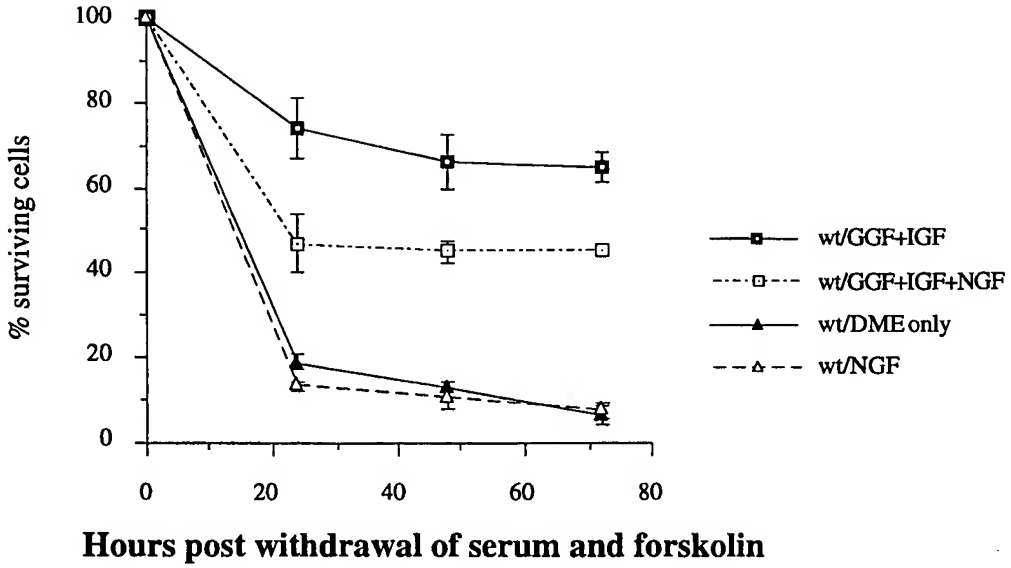

Figure 7. Wild-type rat Schwann cells undergo apoptosis after survival factor deprivation, with no significant difference in viability with or without NGF ($p > 0.05$). However, 10 ng/ml NGF significantly decreases Schwann cell viability when the cells are cocultured with IGF-1 and neuregulin-β. Means ± SEM of three separate experiments are shown. The differences in survival between IGF-1+GGF and IGF-1+GGF+NGF conditions were significant at all time points assessed (p values 0.05, 0.025, and 0.005 at 24, 48, and 72 hr, respectively).

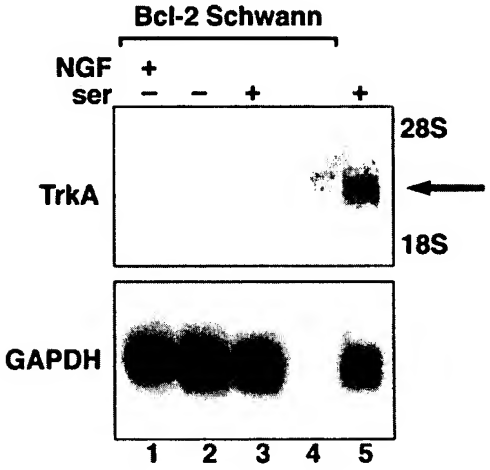

Figure 8. Transcripts of the high-affinity NGF receptor TrkA are not detectable in the Bcl-2-transfected Schwann cells. Northern blots were prepared using mRNA (~0.5 μg/lane) isolated from Bcl-2#1 Schwann cells cultured in DMEM containing 10 ng/ml NGF for 4 hr (*lane 1*) or on survival factor withdrawal for 4 hr (*lane 2*) or in DMEM containing serum, neuregulin-β, and forskolin (*lane 3*). Approximately 10 μg of total RNA isolated from PC12 neuronal cells was loaded as a positive control in *lane 5*. The *arrow* indicates the TrkA transcript between the 28S and 18S ribosomal RNA bands that was detected in RNA isolated from the PC12 cells.

growth factor withdrawal (T. J. Kilpatrick, unpublished observation). We found that blocking the NGF activity increased the survival of all three growth factor-deprived Bcl-2-transfected cell lines by 20–25% (Fig. 4*D*). At 48 hr the survival of Bcl-2-transfected Schwann cells that were treated with anti-NGF antibodies was almost 100% and significantly higher than the survival of untreated cells. The difference in survival between cultures treated with exogenous NGF and those in which endogenous NGF activity was neutralized was ~50% (Fig. 4*D*).

NGF does not lead to cleavage of Bcl-2 in Schwann cells

To determine whether cleavage of Bcl-2 could be involved in the NGF-induced killing of the Bcl-2-expressing Schwann cells, we prepared Western blots of Bcl-2-transfected Schwann cells. The Schwann cells were cultured with either serum, neuregulin-B, and forskolin or, alternatively, without these additives, either with or without NGF, for 24 or 48 hr. We used the same anti-human Bcl-2 100 antibody that was used for recognition of the cleaved 23 kDa fragment by Cheng et al. (1997). The antibody specifically recognized the 28 kDa noncleaved human Bcl-2 protein in the Bcl-2-transfected cells but, as expected, not endogenous Bcl-2 in the wild-type rat Schwann cells (Fig. 5). No cleavage of Bcl-2 was demonstrated (Fig. 5, *lanes 4* and *6*).

CrmA delays but does not inhibit apoptosis triggered by survival factor withdrawal but protects against killing by NGF

The effects of growth factor withdrawal and of exogenous NGF on the viability of CrmA-transfected Schwann cells were also assessed. The CrmA-transfected cell lines showed some potentiated survival in comparison to control cells at 24 hr after withdrawal of survival factors, but by 72 hr they showed a proportion of cell death similar to that of control cultures (Fig. 6*A*). Nerve growth factor did not decrease the survival of the growth factor-deprived CrmA-transfected Schwann cells (Fig. 6*A*). To exclude the possibility that the death signal induced by survival factor withdrawal masked killing of the CrmA-transfected Schwann cells triggered by NGF, assays were also performed in the presence of IGF-1 to potentiate the baseline survival of the CrmA-transfected population. CrmA-transfected cells were also protected against NGF killing in these conditions (Fig. 6*B*), whereas Bcl-2-transfected cells remained susceptible to NGF in the presence of IGF-1 (Fig. 6*B*).

Wild-type Schwann cells are susceptible to killing by NGF in the presence of survival factors

Survival factor-deprived wild-type rat Schwann cells died rapidly, and their survival was not significantly affected by NGF (Fig. 7). Because a death signal induced by NGF could not be assessed in cells that were already dying, we established conditions in which wild-type Schwann cells survived, but did not proliferate, by culturing them with IGF-1 and neuregulin-β. In these conditions, addition of 10 ng/ml exogenous NGF decreased the viability of wild-type Schwann cells by ~30% (Fig. 7). Thus, the susceptibil-

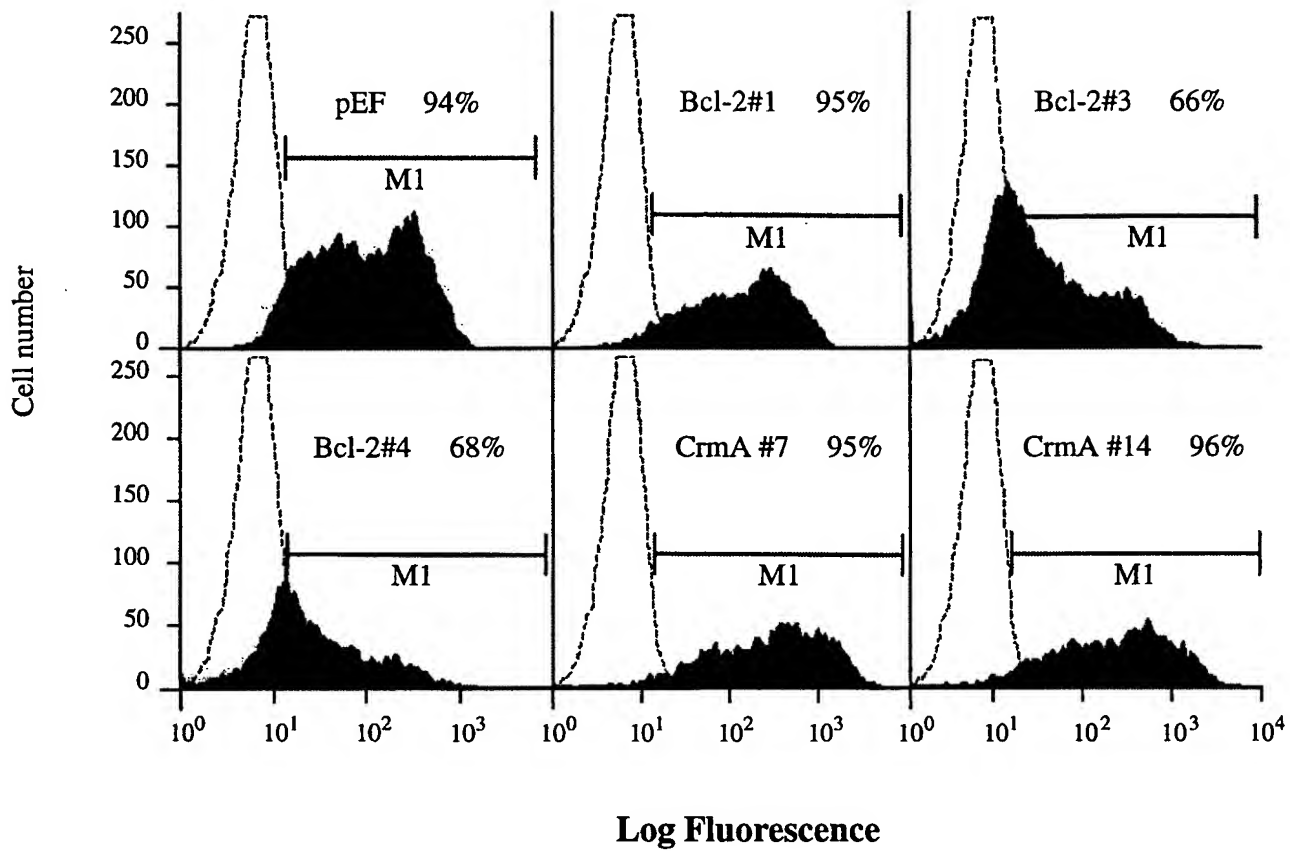

Figure 9. Bcl-2-transfected, CrmA-transfected, and control rat Schwann cells express the low-affinity NGF receptor p75 on the cell surface. Approximately 10^6 pEF, Bcl-2#1, Bcl-2#3, Bcl-2#4, CrmA#7, or CrmA#14 cells were stained with mAb MC192 against the rat p75 receptor or with mouse IgG1 control mAb, followed by FITC-conjugated sheep anti-mouse IgG. Fluorescence was measured using a flow cytometer. The background fluorescence obtained with the isotype-matched control mAb (*dotted lines*) was subtracted from the total pool to enable calculation of the percentages of cells from each cell line that expressed p75 (labeled as the *M1* population).

ity of wild-type Schwann cells to NGF was similar to the susceptibility of the Bcl-2-transfected Schwann cells, once no other interfering death stimuli were operative.

Expression of NGF receptors by the transfected Schwann cell lines

The induction of wild-type Schwann cell death by NGF was likely to have been mediated by p75, because these cells have not been shown to express TrkA but they express high levels of p75 (Lemke and Chao, 1988; Yamamoto et al., 1993). To determine whether the NGF-mediated effects in the Bcl-2-transfected rat Schwann cell lines were mediated by p75, we assessed expression of TrkA by these cells by Northern blotting. No TrkA message was detectable in Bcl-2-transfected Schwann cells cultured for 4 hr in DMEM containing serum, neuregulin-β, and forskolin, in DMEM alone, or in DMEM containing 10 ng/ml of NGF (Fig. 8). Expression of p75 was assessed by indirect immunofluorescence staining and flow cytometry. All of the cell lines expressed p75, with the CrmA lines appearing to express the receptor at the highest level (Fig. 9).

p75-deficient Schwann cells are resistant to killing by NGF

To establish whether NGF-mediated Schwann cell death required p75, we generated Schwann cell cultures from mice homozygous for a deletion in the p75 gene and from wild-type control mice. Unlike the wild-type rat Schwann cells that had been passaged several times *in vitro*, ~25% of the wild-type mouse Schwann cells (second to third passage) survived 48 hr without serum or neuregulin-β, and their survival was significantly decreased by NGF added at the time of plating (Fig. 10) ($p < 0.0005$). In contrast, the Schwann cells isolated from p75 knockout mice were completely resistant to NGF killing (Fig. 10). As we have shown before (our unpublished results), the p75-deficient Schwann cells also exhibited a survival advantage in comparison with the wild-type mouse Schwann cells on survival factor deprivation (Fig. 10).

Expression of the Bcl-2 gene is regulated by wild-type Schwann cells

Regulation of Bcl-2 expression in wild-type rat Schwann cells was studied using RT-PCR. Bcl-2 mRNA was expressed in all culture conditions that promoted survival, including IGF-1 alone, throughout the 16 hr assay period (Fig. 11). In contrast, after 2 hr of serum, neuregulin-β, and forskolin withdrawal, Bcl-2 mRNA expression was downregulated to an undetectable level (Fig. 11). However, when NGF was present in the media, after the withdrawal of serum and other survival factors, Bcl-2 could be still detected at 4 hr, suggesting that NGF, at least in the short term, maintained Bcl-2 expression (Fig. 11).

DISCUSSION

Rat Schwann cell lines that stably express either human Bcl-2 or a poxvirus caspase inhibitor, CrmA, were used to investigate the

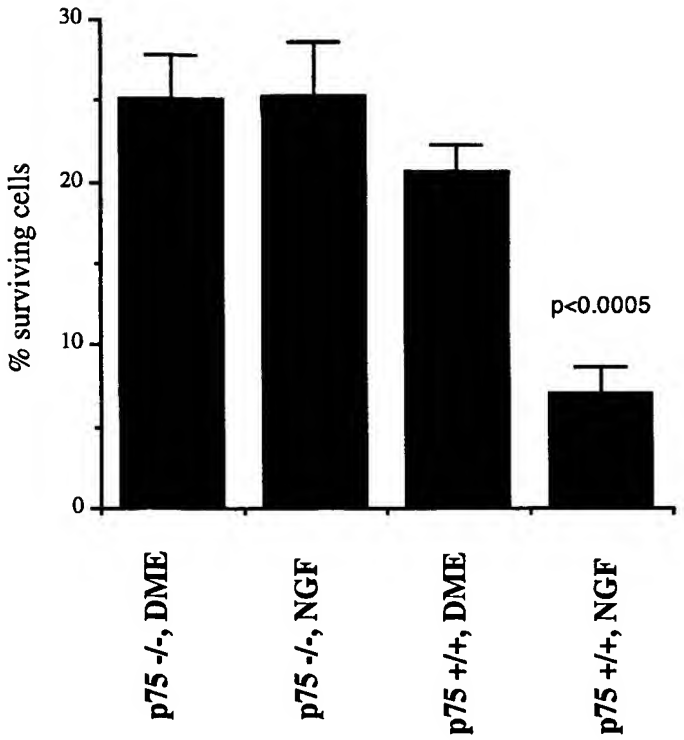

Figure 10. Schwann cells isolated from p75 knockout mice are resistant to NGF killing, whereas wild-type mouse Schwann cells are susceptible. The viability of Thy-1.2-sorted, $p75^{-/-}$ and $p75^{+/+}$ Schwann cells was assessed at 48 hr after FCS and neuregulin-β withdrawal, with or without 10 ng/ml NGF. Shown is the mean viability ±SEM of cells cultured in six parallel wells for each condition as assessed in one of two survival experiments, each with similar results.

mechanisms that effect Schwann cell survival in response to different death stimuli, either survival factor deprivation or a stimulus initiated by NGF, signaling through its low-affinity receptor p75. The results indicated that Bcl-2 protected Schwann cells from apoptosis induced by survival factor deprivation, whereas CrmA did not. This is consistent with previously established differential roles for Bcl-2 and CrmA as inhibitors of apoptosis: Bcl-2 blocks apoptosis induced by a wide variety of insults, apparently acting by inhibiting adaptors required for activation of certain caspases such as caspase 9 (Strasser et al., 1995; Adams and Cory, 1998), whereas CrmA appears to be more effective in blocking TNF family receptor-mediated apoptosis, by inhibiting caspase 8 (Smith et al., 1996; Ashkenazi and Dixit, 1998). Our results confirm a functional dichotomy in the regulation of Schwann cell death into Bcl-2 inhibitable and CrmA-inhibitable death pathways, although the death of neurons after deprivation of NGF is blockable by either Bcl-2 (Park et al., 1996) or CrmA (Gagliardini et al., 1994). It is thus possible that the pathways of cell death initiated by loss of trophic support are different in Schwann cells and neurons. This is consistent with emerging *in vivo* data that suggest coexistence of several different, not only stimulus-specific but also cell type-specific, apoptotic pathways in mammalian cells (Hakem et al., 1998).

Several neuronal cell types die in response to NGF, including sensory dorsal root ganglion neurons (Barrett and Bartlett, 1994), neuronal precursors in embryonic chicken retina (Frade et al., 1996), and cholinergic forebrain neurons (Van der Zee et al., 1996). In at least three instances, this mechanism has been demonstrated to contribute to developmentally regulated death of neurons *in vivo* (Frade et al., 1996; Van der Zee et al., 1996; Bamji et al., 1998). In addition, mature oligodendrocytes that express p75, but not TrkA, are susceptible to NGF-induced cell death, whereas oligodendrocyte precursors and astrocytes are resistant (Casaccia-Bonnefil et al., 1996). Similarly, the Bcl-2-transfected Schwann cell lines that we have analyzed did not express TrkA mRNA (Fig. 8), whereas p75 was expressed at high levels (Fig. 9). The effect of p75 activation, however, is almost certainly contextural, as demonstrated by the resistance of the CrmA-transfected Schwann cells to killing by NGF (Fig. 6*A*). CrmA is quite selective in its ability to inhibit caspases, showing the highest affinities to caspase 1 (interleukin-1β converting enzyme) and caspase 8 (Zhou et al., 1997; Garcia-Calvo et al., 1998). Therefore, activation of caspase 1 or caspase 8 or both, in addition to expression of p75 in the absence of TrkA, is likely to be necessary for induction of cell death by NGF. High levels of the Bcl-2 transgene expressed in Schwann cells, or alternatively, culture of wild-type Schwann cells in conditions that maintained their viability and Bcl-2 expression, were permissive for killing induced by exogenous NGF, suggesting that NGF was killing via a Bcl-2-independent pathway. Schwann cells isolated from mice lacking a functional p75 receptor were resistant to the NGF-induced cell death, corroborating that the NGF killing was mediated by p75.

Schwann cells secrete NGF (Lindholm et al., 1987), and we found that inhibition of endogenous NGF activity resulted in a significant increase in the viability of survival factor-deprived Bcl-2-transfected Schwann cells. This suggests that incomplete protection of the Bcl-2-transfected Schwann cells against survival factor deprivation was caused by death induced by endogenous NGF. Death-inducing activity of endogenous NGF could also explain the observed inferior survival of wild-type mouse Schwann cells in comparison with the p75-deficient mouse Schwann cells after survival factor deprivation (Fig. 10). Moreover, our results argue against a role for constitutive death-inducing activity of p75 in the absence of ligand binding (Rabizadeh et al., 1993) in this lineage, because prevention of ligand binding increased survival rather than induced death.

The Bcl-2 family is regulated by cytokines and other death/survival signals (Adams and Cory, 1998). Using RT-PCR we confirmed that wild-type Schwann cells express Bcl-2 mRNA. We also demonstrated early downregulation of Bcl-2 transcript expression in Schwann cells after survival factor deprivation (Fig. 11). This supports a role for Bcl-2 in the maintenance of Schwann cell viability induced by survival factors. Detailed analysis of the nervous systems of $Bcl\text{-}2^{-/-}$ mice has indicated progressive loss of neurons during early postnatal development, but the effects on Schwann cell numbers ensheathing surviving neurons or the effects on Schwann cell survival after axotomy remain unexplored (Michaelidis et al., 1996). Preliminary experiments using ribonuclease protection assays have suggested that Bcl-2 is indeed expressed by postnatal Schwann cells in wild-type animals both in the quiescent state and after axotomy (D. Syroid and G. Lemke, unpublished observations). Further analyses of these expression patterns will form the basis for understanding the potential physiological relevance of Bcl-2 as a modulator of Schwann cell survival.

Previously, it has been established that axotomy leads to potentiated apoptosis among Schwann cells deprived of axonal contact (Grinspan et al., 1996; Syroid et al., 1996). If Bcl-2 were upregulated after nerve injury in response to cytokines released at the lesion site (Creange et al., 1997), this would facilitate the survival of Schwann cells in the distal stump. Downregulation of

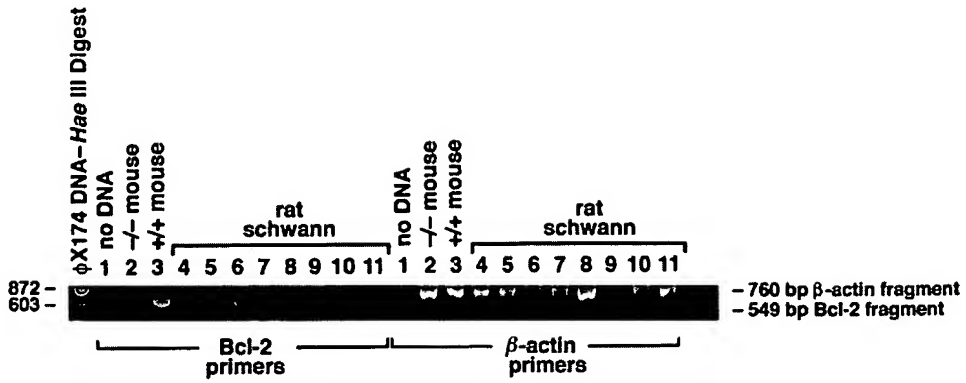

Figure 11. Regulation of Bcl-2 expression in wild-type rat Schwann cells as studied by RT-PCR. Bcl-2 expression was detected in cells cultured in IGF-1 for 4 hr (*lane 4*), IGF-1 for 16 hr (*lane 5*), NGF for 4 hr (*lane 6*), and after withdrawal of FCS, neuregulin-β, and forskolin for 1 hr (*lane 7*) or 2 hr (*lane 8*). Bcl-2 was downregulated to undetectable levels after 4, 8, and 24 hr of survival factor deprivation (*lanes 9–11*). Rat β-actin was amplified as control to verify the fidelity of the cDNA. A φX174–*Hae*III digest in *lane 0* served as a molecular weight marker. Negative controls included no DNA in *lane 1* and tail DNA from a Bcl-2 knockout mouse (Bcl-2$^{-/-}$) in *lane 2*. Tail DNA from a Bcl-2 wild-type littermate of the Bcl-2$^{-/-}$ mouse served as a positive control (*lane 3*, Bcl-2$^{+/+}$).

Bcl-2 expression by Schwann cells that completely lose access to axonally derived neuregulins (Grinspan et al., 1996) and IGF-1 (Syroid et al., 1999) would increase their susceptibility to apoptosis.

Our results also suggest an alternative mechanism by which the cells could die. Schwann cells upregulate their p75 expression and production of NGF after axotomy (Lindholm et al., 1987; Lemke and Chao, 1988; Taniuchi et al., 1988). This could facilitate the presentation of NGF to regenerating axons (Taniuchi et al., 1988). In this context, Schwann cells that fail to make a viable contact with the regenerating axons and subsequently fail to present NGF to them could be eliminated via continued activation of p75, even if Bcl-2 expression is maintained. Early and robust invasion of macrophages is also a feature in peripheral nerve injury and has been hypothesized to contribute to peripheral nerve degeneration (Franzen et al., 1998). Macrophages, like Schwann cells, can release NGF, and it is of note that microglia-derived NGF induces apoptosis in embryonic chick retinal neurons (Frade et al., 1996; Frade and Barde, 1998). Thus it is possible that infiltrating macrophages contribute to the induction of Schwann cell death. This could be useful in the killing of supernumerary Schwann cells, but if unchecked could lead to excessive cell death and thus limit peripheral nerve repair. A potential role of NGF in mediating Schwann cell death could have important implications for the ongoing clinical trials in which NGF is being assessed as a potential therapeutic agent for peripheral neuropathies (Rogers, 1996; Apfel et al., 1998).

Little is known about the intracellular pathways that mediate p75-induced apoptosis, although the molecular events that signal downstream of the related molecule TNFR have been investigated extensively (Ashkenazi and Dixit, 1998). Regulation of transcription factor expression is likely to be implicated, because inhibition of both NF-κB and JNK/AP1 pathways sensitizes cells to apoptosis induced by TNF (Beg and Baltimore, 1996; Roulston et al., 1998). Moreover, aspartyl-glutamyl-valyl-aspartyl (DEVD)-specific caspases appear to participate in TNF-mediated apoptosis only when NF-κB is inhibited (Wang et al., 1998). Overexpression of Bcl-2 in PC12 neuronal cells has been shown to block JNK activation caused by growth factor withdrawal (Park et al., 1996). It remains to be investigated whether blockade of JNK (or NF-κB) also occurs in Bcl-2-expressing Schwann cells and whether this inhibition increases the susceptibility to p75-mediated cell death.

REFERENCES

Adams JM, Cory S (1998) The Bcl-2 protein family: arbiters of cell survival. Science 281:1322–1326.

Anton ES, Weskamp G, Reichardt LF, Matthew WD (1994) Nerve growth factor and its low-affinity receptor promote Schwann cell migration. Proc Natl Acad Sci USA 91:2795–2799.

Apfel SC, Kessler JA, Adornato BT, Litchy WJ, Sanders C, Rask CA (1998) Recombinant human nerve growth factor in the treatment of diabetic polyneuropathy. NGF Study Group. Neurology 51:695–702.

Ashkenazi A, Dixit VM (1998) Death receptors: signaling and modulation. Science 281:1305–1308.

Bamji SX, Majdan M, Pozniak CD, Belliveau DJ, Aloyz R, Kohn J, Causing CG, Miller FD (1998) The p75 neurotrophin receptor mediates neuronal apoptosis and is essential for naturally occurring sympathetic neuron death. J Cell Biol 140:911–923.

Barrett GL, Bartlett PF (1994) The p75 nerve growth factor receptor mediates survival or death depending on the stage of sensory neuron development. Proc Natl Acad Sci USA 91:6501–6505.

Beg AA, Baltimore D (1996) An essential role for NF-kappaB in preventing TNF-alpha-induced cell death. Science 274:782–784.

Brockes JP, Fields KL, Raff MC (1979) Studies on cultured rat Schwann cells. I. Establishment of purified populations from cultures of peripheral nerve. Brain Res 165:105–118.

Carter BD, Kaltschmidt C, Kaltchhmidt B, Offenhauser N, Bohm-Matthaei R, Baeuerle PA, Barde YA (1996) Selective activation of the NF-kB by nerve growth factor through the neurotrophin receptor p75. Science 272:542–545.

Casaccia-Bonnefil P, Carter BD, Dobrowsky RT, Chao MV (1996) Death of oligodendrocytes mediated by the interaction of nerve growth factor with its receptor p75. Nature 383:716–719.

Cheng EHY, Kirsch DG, Clem RJ, Ravi R, Kastan MB, Bedi A, Ueno K, Hardwick JM (1997) Conversion of Bcl-2 to a Bax-like death effector by caspases. Science 278:1966–1968.

Chinnaiyan AM, O'Rourke K, Tewari M, Dixit VM (1995) FADD, a novel death domain-containing protein, interacts with the death domain of Fas and initiates apoptosis. Cell 81:505–512.

Cohen GM (1997) Caspases: the executioners of apoptosis. Biochem J 326:1–16.

Creange A, Barlovatz-Meimon G, Gherardi RK (1997) Cytokines and peripheral nerve disorders. Eur Cytokine Netw 8:145–151.

Frade JM, Barde YA (1998) Microglia-derived nerve growth factor causes cell death in the developing retina. Neuron 20:35–41.

Frade JM, Rodriguez-Tebar A, Barde YA (1996) Induction of cell death by endogenous nerve growth factor through its p75 receptor. Nature 383:166–168.

Franzen R, Schoenen J, Leprince P, Joosten E, Moonen G, Martin D

(1998) Effects of macrophage transplantation in the injured adult rat spinal cord: a combined immunocytochemical and biochemical study. J Neurosci Res 51:316–327.

Gagliardini V, Fernandez P-A, Lee RKK, Drexler HCA, Rotello RJ, Fishman MC, Yan J (1994) Prevention of vertebrate neuronal death by the crmA gene. Science 263:824–828.

Garcia-Calvo M, Peterson EP, Leiting B, Ruel R, Nicholson DW, Thornberry NA (1998) Inhibition of human caspases by peptide-based and macromolecular inhibitors. J Biol Chem 273:32608–32613.

Grinspan JB, Marchionni MA, Reeves M, Coulaloglou M, Scherer SS (1996) Axonal interactions regulate Schwann cell apoptosis in developing peripheral nerve: neuregulin receptors and the role of neuregulin. J Neurosci 16:6107–6118.

Hakem R, Hakem A, Duncan GS, Henderson JT, Woo M, Soengas M, Elia A, la Pompa JL, Kagi D, Khoo W, Potter J, Yoshida R, Kaufman SA, Lowe SW, Penninger JM, Mak TW (1998) Differential requirement for caspase 9 in apoptotic pathways in vivo. Cell 94:339–352.

Heumann R, Lindholm D, Bandtlow C, Meyer M, Radeke MJ, Misko TP, Shooter E, Thoenen H (1987) Differential regulation of mRNA encoding nerve growth factor and its receptor in rat sciatic nerve during development, degeneration and regeneration: role of macrophages. Proc Natl Acad Sci USA 84:8735–8739.

Huang DC, Cory S, Strasser A (1997) Bcl-2, Bcl-XL and adenovirus protein E1B19kD are functionally equivalent in their ability to inhibit cell death. Oncogene 14:405–414.

Itoh N, Yonehara S, Ishii A, Yonehara M, Mizushima S, Sameshima M, Hase A, Seto Y, Nagata S (1991) The polypeptide encoded by the cDNA for human cell surface antigen Fas can mediate apoptosis. Cell 66:233–243.

Kaplan D, Hempstead B, Martin-Zanca D, Chao M, Parada L (1991) The trk proto-oncogene product: a signal transducing receptor for nerve growth factor. Science 252:554–558.

Kaplan DR, Miller FD (1997) Signal transduction by the neurotrophin receptors. Curr Opin Cell Biol 9:213–221.

Lee KF, Bachman K, Landis S, Jaenisch R (1992) Dependence on p75 for innervation of some sympathetic targets. Science 263:1447–1449.

Lemke G, Axel R (1985) Isolation and sequence of a cDNA encoding the major structural protein of peripheral myelin. Cell 40:501–508.

Lemke G, Chao M (1988) Axons regulate Schwann cell expression of the major myelin and NGF receptor genes. Development 102:499–504.

Lindholm D, Heumann R, Meyer M, Thoenen H (1987) Interleukin-1 regulates synthesis of nerve growth factor in non-neuronal cells of rat sciatic nerve. Nature 330:658–659.

Meakin SO, Shooter EM (1992) The nerve growth factor family of receptors. Trends Neurosci 15:323–331.

Michaelidis TM, Sendtner M, Cooper JD, Airaksinen MS, Holtmann B, Meyer M, Thoenen H (1996) Inactivation of bcl-2 results in progressive degeneration of motoneurons, sympathetic and sensory neurons during early postnatal development. Neuron 17:75–89.

Newton K, Strasser A (1998) The Bcl-2 family and cell death regulation. Curr Opin Genet Dev 8:68–75.

Nicholson DW, Thornberry NA (1997) Caspases: killer proteases. Trends Biochem Sci 22:299–306.

Park DS, Stefanis L, Yan CYI, Farinelli SE, Greene LA (1996) Ordering the cell death pathway. J Biol Chem 271:21898–21905.

Pezzella F, Tse AG, Cordell JL, Pulford KA, Gatter KC, Mason DY (1990) Expression of the bcl-2 oncogene protein is not specific for the 14;18 chromosomal translocation. Am J Pathol 137:225–232.

Rabizadeh S, Oh J, Zhong L, Yang J, Bitler CM, Butcher LL, Bredesen DE (1993) Induction of apoptosis by the low-affinity NGF receptor. Science 261:345–348.

Rogers BC (1996) Development of recombinant human nerve growth factor (rhNGF) as a treatment for peripheral neuropathic disease. Neurotoxicology 17:865–870.

Roulston A, Reinhard C, Amiri P, Williams LT (1998) Early activation of c-Jun N-terminal kinase and p38 kinase regulate cell survival in response to tumor necrosis factor a. J Biol Chem 273:10232–10239.

Smith KG, Strasser A, Vaux DL (1996) CrmA expression in T lymphocytes of transgenic mice inhibits CD95 (Fas/APO-1)-transduced apoptosis, but does not cause lymphadenopathy or autoimmune disease. EMBO J 15:5167–5176.

Strasser A, Harris A, Huang DC, Krammer PH, Cory S (1995) Bcl-2 and Fas.APO-1 regulate distinct pathways to lymphocyte apoptosis. EMBO J 14:6136–6147.

Syroid DE, Maycox PR, Burrola PG, Liu N, Wen D, Lee KF, Lemke G, Kilpatrick TJ (1996) Cell death in the Schwann cell lineage and its regulation by neuregulin. Proc Natl Acad Sci USA 93:9229–9234.

Syroid DE, Zorick TS, Arbet-Engels C, Kilpatrick TJ, Eckhart W, Lemke G (1999) A role for insulin-like growth factor-1 in the regulation of Schwann cell survival. J Neurosci 19:2059–2068.

Taniuchi M, Clark HB, Schweitzer JB, Johnson EMJ (1988) Expression of nerve growth factor receptors by Schwann cells of axotomized peripheral nerves: ultrastructural location, suppression by axonal contact, and binding properties. J Neurosci 8:664–681.

Trachtenberg JT, Thompson WJ (1996) Schwann cell apoptosis at developing neuromuscular junctions is regulated by glial growth factor. Nature 379:174–177.

Van der Zee CE, Ross GM, Riopelle RJ, Hagg T (1996) Survival of cholinergic forebrain neurons in developing p75NGFR-deficient mice. Science 274:1729–1732.

Wang C-Y, Mayo MW, Korneluk RG, Goeddel DV, Baldwin Jr AS (1998) NF-kB antiapoptosis: induction of TRAF1 and TRAF2 and c-IAP1 and c-IAP2 to suppress caspase-8 activation. Science 281:1680–1683.

Yamamoto M, Sobue G, Li M, Arakawa Y, Mitsumata T, Kimata K (1993) Nerve growth factor (NGF), brain-derived neurotrophic factor (BDNF) and low-affinity nerve growth factor receptor (LNGFR) mRNA levels in cultured rat Schwann cells: differential time- and dose-dependent regulation by cAMP. Neurosci Lett 152:37–40.

Yoon SO, Casaccia-Bonnefil P, Carter B, Chao MV (1998) Competitive signaling between TrkA and p75 nerve growth factor receptors determines cell survival. J Neurosci 18:3273–3281.

Zhou Q, Snipas S, Orth K, Muzio M, Dixit VM, Salvesen GS (1997) Target protease specificity of the viral serpin CrmA. Analysis of five caspases. J Biol Chem 272:7797–7800.

Neuron, Vol. 36, 375–386, October 24, 2002, Copyright ©2002 by Cell Press

ProNGF Induces p75-Mediated Death of Oligodendrocytes following Spinal Cord Injury

Michael S. Beattie,[3,8] Anthony W. Harrington,[1,4,8] Ramee Lee,[5] Ju Young Kim,[2,4] Sheri L. Boyce,[3] Frank M. Longo,[6] Jacqueline C. Bresnahan,[3] Barbara L. Hempstead,[5] and Sung Ok Yoon [3,4,7]
[1]Biochemistry Program
[2]Molecular, Cellular, and Developmental Biology Program
[3]Department of Neuroscience
The Ohio State University
Columbus, Ohio 43210
[4]Neurobiotechnology Center
The Ohio State University Medical Center
Columbus, Ohio 43210
[5]Department of Medicine
Weill Medical College of Cornell University
1300 York Avenue
New York, NY 10021
[6]Department of Neurology
VA Medical Center and
University of California, San Francisco
San Francisco, California 94143

Summary

The neurotrophin receptor p75 is induced by various injuries to the nervous system, but its role after injury has remained unclear. Here, we report that p75 is required for the death of oligodendrocytes following spinal cord injury, and its action is mediated mainly by proNGF. Oligodendrocytes undergoing apoptosis expressed p75, and the absence of p75 resulted in a decrease in the number of apoptotic oligodendrocytes and increased survival of oligodendrocytes. ProNGF is likely responsible for activating p75 in vivo, since the proNGF from the injured spinal cord induced apoptosis among $p75^{+/+}$, but not among $p75^{-/-}$, oligodendrocytes in culture, and its action was blocked by proNGF-specific antibody. Together, these data suggest that the role of proNGF is to eliminate damaged cells by activating the apoptotic machinery of p75 after injury.

Introduction

It has been recently discovered that unprocessed NGF precursor, proNGF, binds p75 preferentially over TrkA, and this selective binding of proNGF to p75 leads to apoptotic death of cells that express both TrkA and p75 (Lee et al., 2001). Mature NGF, on the other hand, binds and activates both receptors, which results in promotion of cell survival due to the TrkA-mediated survival signal overriding p75-mediated apoptotic signal (Yoon et al., 1998; Friedman, 2000; Harrington et al., 2002). Before the discovery of an independent function for proNGF, p75 was thought to activate its apoptotic program when TrkA was not expressed in a cell. With the finding that proNGF can activate p75 regardless of the presence of TrkA, the ratio of proNGF to mature NGF now emerges as a critical regulatory factor for the maintenance of the balance between survival and death (Chao and Bothwell, 2002).

In vivo, p75 is often induced by an injury or a disease state among neurons, oligodendrocytes, or Schwann cells. p75 expression was induced in dying neurons following seizure (Roux et al., 1999), ischemia (Park et al., 2000), excitotoxic agents (Oh et al., 2000), axotomy (Giehl et al., 2001), and in cortical neurons following experimental allergic encephalomyelitis (Calza et al., 1997; Nataf et al., 1998). In the white matter plaques of multiple sclerosis patients, p75 induction was also observed among oligodendrocytes and their precursors (Chang et al., 2000; Dowling et al., 1999). In neonatal Schwann cells, p75 has been shown to play a death-inducing role following axotomy (Syroid et al., 2000). In the CNS, however, the consequence of this induced p75 expression has been unclear. Induction of p75 could be one of the first steps that initiate the apoptotic cascade after injury, or it may signify regenerative responses undertaken by the injured system, perhaps in cooperation with resident Trks.

It is well established in the literature that neurotrophins are induced or their level is greatly increased by pathological conditions that are known to cause induction of p75 (Bengzon et al., 1992; Donovan et al., 1995; Heumann et al., 1987; Widenfalk et al., 2001). The recent discovery of the functionality of proNGF leads to the prediction that the presence or absence of pro neurotrophins under injury conditions will determine whether activation of p75 induction will lead to a proapoptotic or anti-apoptotic response. For instance, in Alzheimer's patients, the level of proNGF is increased (Fahnestock et al., 2001), suggesting a possible role for p75 in Alzheimer's disease. Induction of p75 among cortical neurons in Alzheimer's patients has been reported (Mufson and Kordower, 1992).

In this report, we investigated whether expression of p75 and proNGF is responsible for injury-mediated apoptosis of oligodendrocytes in vivo, using spinal cord injury as an injury model. As one of the secondary events triggered by the initial spinal cord injury, oligodendrocytes undergo apoptosis (Crowe et al., 1997), and the presence of apoptotic oligodendrocytes was shown to correlate closely with lesion extension along fiber tracts undergoing Wallerian degeneration after spinal cord injury (Shuman et al., 1997). The death of oligodendrocytes might contribute to chronic demyelination, resulting in spinal cord dysfunction (Beattie et al., 2000; Blight, 1993; Crowe et al., 1997; Li et al., 1996; Liu et al., 1997; Shuman et al., 1997; Warden et al., 2001). Although the temporal and spatial patterns of oligodendrocyte death have been well characterized in a number of studies (reviewed in Beattie et al., 2000; Warden et al., 2001), the mechanisms by which oligodendrocytes die during Wallerian degeneration is unknown.

Here, we report that p75 and proNGF are both induced

[7]Correspondence: yoon.84@osu.edu
[8]M.S.B. and A.W.H. contributed equally to this work.

following spinal cord injury. p75 expression was specifically induced among oligodendrocytes, and the majority of p75$^+$ cells was positive for cleaved caspase 3, suggesting that they were undergoing apoptosis. Corollary to these data, the number of cleaved caspase 3$^+$ oligodendrocytes was reduced after spinal cord injury in the absence of p75. Likewise, the absence of p75 permitted survival of oligodendrocytes under conditions that would otherwise lead to apoptosis both in vivo and in vitro. In addition, we demonstrate that proNGF present in the extracts from the injured spinal cord is active in inducing apoptosis among oligodendrocytes, while its action can be blocked by a proNGF-specific, but not proBDNF-specific, antibody. Together, these results support the hypothesis that a consequence of p75 expression after injury is, in part, to eliminate damaged cells in the CNS, and its activation is mediated predominantly by proNGF.

Results

Temporal and Spatial Correlation between Apoptotic Profile and Actual Loss of Oligodendrocytes after Spinal Cord Injury

Although the presence of apoptotic oligodendrocytes has been documented after spinal cord injury (Crowe et al., 1997), it has not been determined whether this results in significant cell loss, which could potentially contribute to eventual demyelination. To address this question, we performed thoracic spinal cord contusion lesions on rats and assessed the changes in the number of oligodendrocytes in regions rostral and caudal to the lesion center at 5, 8, 21, and 42 days after the injury. The oligodendrocytes were identified by CC1/APC immunoreactivity (Bhat et al., 1996; Crowe et al., 1997; Rosenberg et al., 1999). At the fifth day postinjury, there was a small reduction in the number of oligodendrocytes in the dorsal columns, but by the eighth day postinjury, the extent of reduction reached 30%–50% throughout the four sampled regions (Figure 1). The greatest reduction, which was approximately 50%, was found in the dorsal columns rostral to the injury center. Previously, the number of apoptotic cells was found to be highest in this region (Crowe et al., 1997), indicating a spatial correlation between the number of apoptotic cells and the loss of oligodendrocytes. Temporally, the greatest loss in oligodendrocytes was found at the eighth day postinjury, which also coincides with the time when the number of apoptotic cells reached its peak (Crowe et al., 1997). This temporal and spatial correlation between the extent of apoptosis and actual cell loss indicates that apoptosis in oligodendrocytes after spinal cord injury leads to the eventual loss of oligodendrocytes.

Spinal Cord Injury-Specific Induction of p75 among Oligodendrocytes

It has been shown that the presence of p75 is required for the NGF-dependent death of oligodendrocytes in culture (Harrington et al., 2002). In addition, p75 expression has been observed in the white matter plaques of multiple sclerosis patients (Chang et al., 2000; Dowling et al., 1999) and near the lesion epicenter following spinal cord injury (Brandoli et al., 2001; Casha et al., 2001;

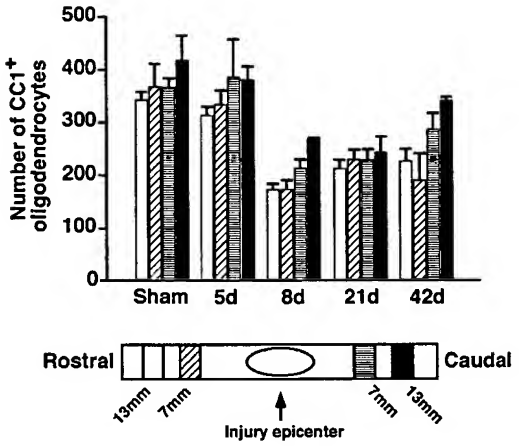

Figure 1. Spinal Cord Injury Leads to a Loss of Oligodendrocytes

Contusion injury in rats leads to a loss of oligodendrocytes. Estimated total number of oligodendrocytes within the confines of the rat dorsal columns at 7 and 13 mm rostral and 7 and 13 mm caudal to a contusion lesion at spinal level T10 (25 mm, NYU device). Counts were made using a stereology program (see Experimental Procedures). An approximate 50% reduction in numbers was seen after 8 and 21 days with significant reductions continuing to 42 days ($p < 0.05$). Similar results were obtained when measuring the density (number per mm^3).

Reynolds et al., 1991). We asked whether spinal cord injury induces p75 expression among oligodendrocytes and whether its expression correlates with the observed pattern of cell loss in the dorsal columns after spinal cord injury. Contusion injuries were performed on rats, and the presence of p75 was determined at various time points after spinal cord injury by performing Western analyses using 5 mm spinal cord blocks taken from the lesion centers, as well as from regions rostral and caudal to the central samples. p75 expression was not detected in sham-operated animals, but first observed at 5 days postinjury, continuing to 8 days postinjury (Figure 2A). This temporal expression pattern of p75 correlates closely to the actual loss of oligodendrocytes (compare with Figure 1). It should be noted that there was very little p75 protein detected in sham-operated animals, although sensory neuron projections into the spinal cord are known to contain p75 in their terminals (Richardson and Riopelle, 1984). This may be due to a low level of p75 present in these fibers. Taniuchi et al. (1988) have reported that ^{125}I-NGF binding in the spinal cord was less than 5% of the level found in the periphery. Our Western data agree with this observation and also with a report that demonstrated low levels of p75 in the adult spinal cord, except among motor neurons during development or after axotomy (Ernfors et al., 1989).

Since p75 expression correlates with oligodendrocyte loss temporally, we tested whether oligodendrocytes express p75 upon spinal cord injury by performing immunohistochemistry. Similarly to the Western data, p75$^+$ cells were mainly found at 8 days postinjury in the dorsal funiculus, although we also observed some positive cells at 48 hr postinjury (data not shown). These p75$^+$ cells were positive for CC1/APC, indicating that oligodendrocytes in the dorsal funiculus expressed p75 (Figure 2B). p75 expression was not observed in sham-

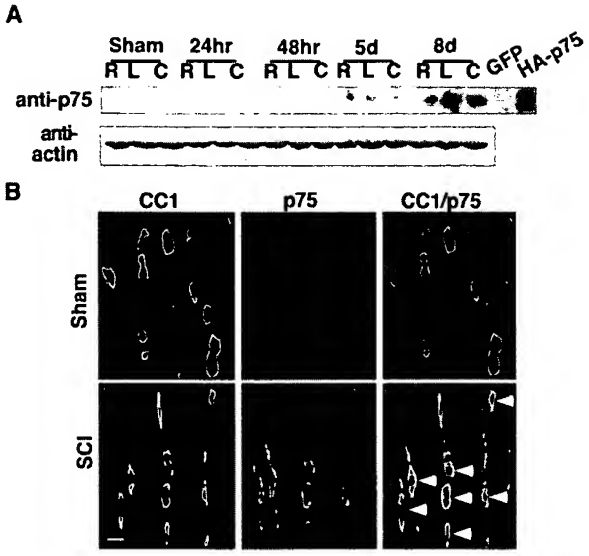

Figure 2. Spinal Cord Injury-Specific Induction of p75 among Oligodendrocytes

(A) Injury-specific induction of p75 in rats after contusion injury. A 5 mm spinal cord block was taken from rostral (R), caudal (C), as well as from the injury epicenter (L) at the indicated times after initial injury and processed for anti-p75 Western. The data are from a representative Western blot, and the same pattern was observed from five independent sets of samples. The lysates from 293 cells transfected with vector (GFP) or rat-p75 cDNA (HA-p75) were used as a negative or positive control, respectively. The same blot was reprobed for actin as a negative control.

(B) Oligodendrocytes express p75 after spinal cord injury. Colocalization of CC1 and p75 in the dorsal column region 13 mm rostral to the injury epicenter and 8 days after the lesion. The arrows point to $CC1^+/p75^+$ cells. Scale bar, 12.5 μm.

operated animals, as was also the case with Western analyses (Figure 2A). Together, these results indicate that p75 expression is induced among oligodendrocytes in a manner specific to spinal cord injury, and its temporalexpression profile correlates with actual loss of oligodendrocytes.

Majority of $p75^+$ Oligodendrocytes Are Apoptotic

The temporal course of p75 expression correlated with the loss of oligodendrocytes and the apoptotic profile previously reported after spinal cord injury (Crowe et al., 1997). We therefore tested whether $p75^+$ cells were undergoing apoptosis by measuring caspase 3 activation. For this, the sections taken from 8 days postinjury were processed for double immunohistochemistry for p75 and active caspase 3. In injured animals, the majority of $p75^+$ cells were also positively stained with active, cleaved caspase 3 antibody (Figure 3A). In sham-operated animals, the number of cells positive for active caspase 3 was much smaller than in injured animals, and no cells double-positive for p75 and active caspase 3 were observed.

A spinal cord injury-mediated increase in caspase 3 activity in oligodendrocytes has been reported, but only up to 2 days postinjury (Springer et al., 1999). Since the greatest loss of oligodendrocytes is observed from 5 days postinjury, we asked whether caspase 3 was still activated among oligodendrocytes at 8 days postinjury. If so, this would suggest that the induction of apoptosis among oligodendrocytes is continuous, rather than initiated at a given point and then ceasing. As shown in Figure 3B, the majority of oligodendrocytes in the dorsal funiculus was positive for active caspase 3 stain, even at 8 days postinjury. The number of oligodendrocytes positive for active caspase 3 was much reduced in sham-operated animals. Together with the data for p75 and active caspase 3, these results suggest that $p75^+$ oligodendrocytes undergo apoptosis continuously after spinal cord injury.

p75 Is Required for the Apoptosis of Spinal Cord Oligodendrocytes in Culture

We next tested whether ligand-dependent activation of p75 is necessary for apoptosis of spinal cord oligodendrocytes. As the first step, we investigated whether the absence of p75 would render spinal cord oligodendrocytes resistant to NGF-dependent apoptosis by culturing the spinal oligodendrocytes from $p75^{+/+}$ and $p75^{-/-}$ mice. In culture, spinal cord oligodendrocytes taken from postnatal day (P)12–14 pups expressed p75, as did their cortical counterparts (data not shown; Harrington et al., 2002). When NGF purified from the submaxillary gland (Harlan Bioproducts for Science) was added to $p75^{+/+}$ oligodendrocytes at 100 ng/ml for 4–48hr, the proportion of $TUNEL^+$ and MBP^+ cells increased to 24% from a basal level of 2% (Figure 4B). Among $p75^{-/-}$ oligodendrocytes, however, for the entire period of NGF treatment, the proportion of $TUNEL^+$ and MBP^+ cells remained the same as for those left untreated. A representative picture is shown in Figure 4A. These data therefore indicate that p75 is required for NGF-dependent apoptosis in spinal cord oligodendrocytes in culture.

p75 Plays a Critical Role for Apoptosis of Oligodendrocytes after Spinal Cord Injury

As the second step, we investigated whether p75 is required for apoptosis of oligodendrocytes in vivo by injuring the spinal cord in $p75^{+/+}$ and $p75^{-/-}$ mice. After spinal cord injury, mouse oligodendrocytes express p75 in the dorsal column, as their rat counterparts do (Figure 5A, left). For spinal cord injury in mice, dorsal hemisection was chosen as our method instead of contusion, since hemisection also induces axon degeneration and subsequent oligodendrocyte death without the potential complications associated with a temporally expanding contusion injury in the small mouse spinal cord. Two different approaches were taken to assess the role of p75 following spinal cord hemisection. One was to measure the extent of oligodendrocyte survival (Figure 5B), and the other was to measure the extent of oligodendrocyte apoptosis (Figure 5C) in the absence of p75. The extent of oligodendrocyte survival was first determined by estimating the density of the $CC1^+$ cells per mm^3, using sections taken from 1.8 mm and 1.2 mm rostral and 1.2 mm and 1.8 mm caudal to the injury epicenter on the eighth day following spinal cord injury (Figure 5B). Following hemisection, the density of oligodendrocytes in the dorsal columns dropped 51% from 39,600 to 19,500 per mm^3 in $p75^{+/+}$ mice, while it dropped 36%

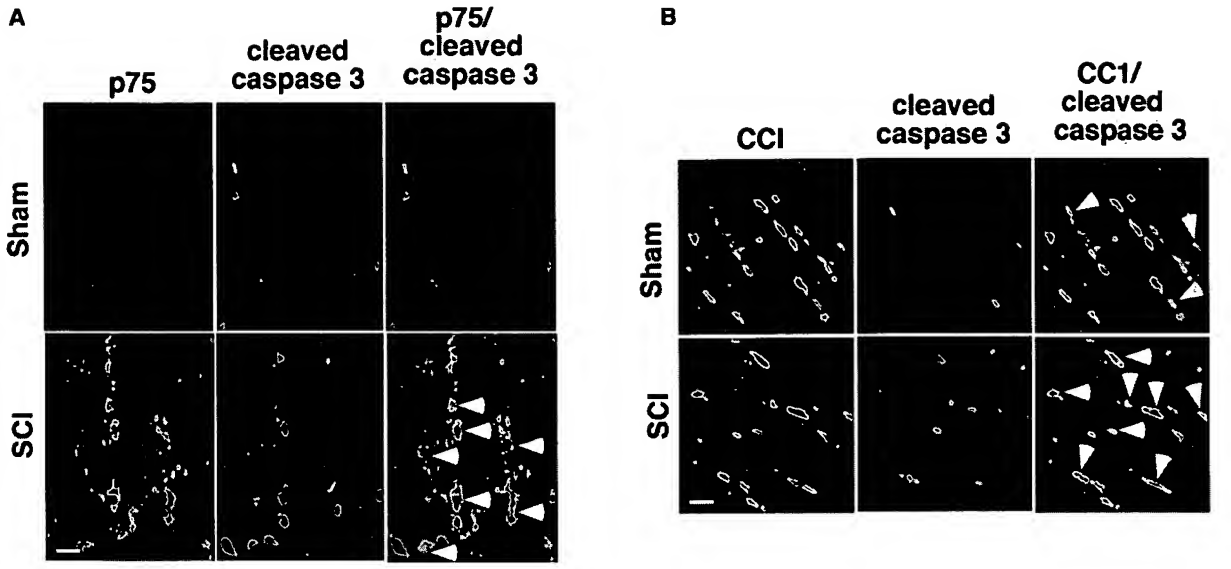

Figure 3. p75$^+$ Oligodendrocytes Are Positive for Active Caspase 3

(A) Colocalization of p75$^+$ and active caspase 3 in the rostral region at 8 days after spinal cord injury. The arrows point to cells that are positive for both.

(B) Colocalization of CC1$^+$ and active caspase 3 in the rostral region at 8 days after spinal cord injury. The arrows point to cells that are positive for both. Scale bar, 12.5 μm.

from 42,600 to 27,100 per mm^3 in p75$^{-/-}$ mice. This result indicates that the lack of p75 resulted in a 15% increase in oligodendrocyte survival.

As the CC1$^+$ cell counts include mainly the healthy surviving cells, it is likely that the density estimation does not fully represent the extent of protection in the absence of p75. For this reason, we examined the number of apoptotic oligodendrocytes in p75$^{+/+}$ and p75$^{-/-}$ mice at 5 days postinjury. As a marker for apoptosis, we stained sections with cleaved caspase 3 in addition to CC1. A representative picture is shown in Figure 5A (right). The average number of CC1$^+$/cleaved caspase 3$^+$ cells in the dorsal columns was 229 per section in p75$^{+/+}$ mice, while it was 155 in p75$^{-/-}$ mice, representing a 32% reduction in the number of apoptotic oligodendrocytes in the absence of p75 (Figure 5C). The extent of protection assessed by cleaved caspase 3 is higher than the estimation of surviving oligodendrocytes, since the staining of cleaved caspase 3 allows detection of oligodendrocytes that are at an early stage in the apoptotic process. Together, these data indicate that p75 is one of the critical components for inducing apoptosis of oligodendrocytes following spinal cord injury.

Spinal Cord Injury-Mediated Production of ProNGF Is Responsible for the Death of Oligodendrocytes

What is activating p75 to elicit apoptotic programs in vivo? It has been known that NGF expression is strongly induced among astrocytes, activated microglia, and meningeal cells in the spinal cord by spinal cord injury in the rat (Krenz and Weaver, 2000; Widenfalk et al., 2001). Since neurotrophins are known to be present in pro forms in many brain tissues (Chao and Bothwell, 2002) and in the case of proNGF its expression is increased in Alzheimer's patients (Fahnestock et al., 2001), we decided to examine the profiles of neurotrophin expression in our spinal cord injury paradigm. BDNF and NT3 were present in pro forms as reported (Lee et al., 2001), based on the predicted size, but no significant increase was detected in the amount of pro or mature forms of BDNF or NT3 produced after spinal cord injury (Figure 6A). The lack of induction of BDNF was further confirmed using proBDNF-specific antibody, which produced similar results to those shown in Figure 6A (data not shown). In contrast, NGF expression was strongly induced in a manner specific to spinal cord injury based on Western analyses, using an anti-mature-NGF antibody (Figure 6A). The size of induced proteins that are detected with anti-mature-NGF antibody (14 kDa, 24–32 kDa) suggests that both mature and proNGF are induced in rats, but the extent of induction of proNGF is greater than that observed with mature NGF (Figure 6A). Interestingly, only proNGF and not mature NGF was induced following spinal cord injury in mice (Figure 6A). This may be due to species differences, or it may represent the difference in the type of injury inflicted, that is, contusion lesion in rats versus hemisection in mice.

To confirm that the high-molecular weight bands are indeed proNGF, we utilized proNGF-specific antibody. ProNGF antibody was generated using a 51 amino acid sequence present in the pro domain of NGF (See Experimental Procedures for details). The specificity of this proNGF antibody was tested both in biochemical and biological assays. In Western analyses and in immunodepletion assays, the proNGF antibody detects only recombinant, cleavage-resistant proNGF, and not recombinant mature NGF (Figures 6C and 6D). In a functional assay using oligodendrocytes, the antibody blocks the apoptotic action of recombinant proNGF, but not that of recombinant mature NGF (Figure 7D). These results

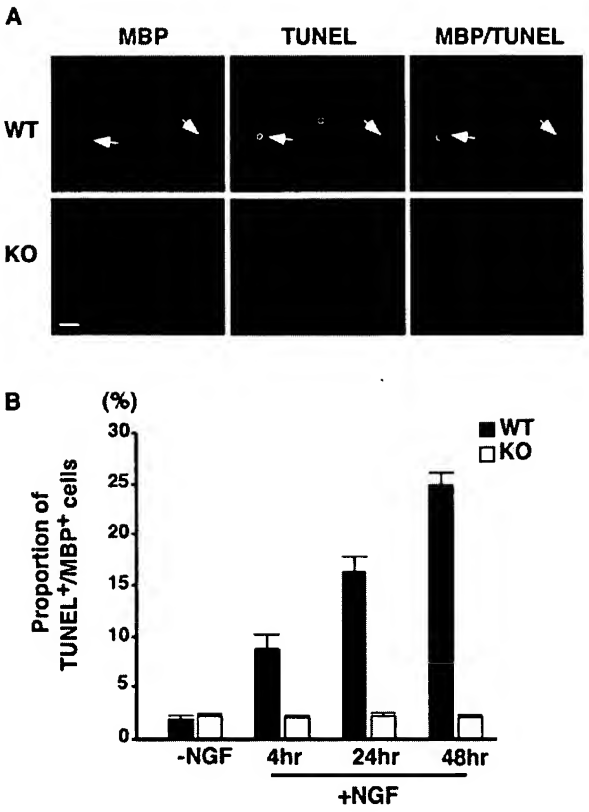

Figure 4. Mouse Oligodendrocytes Fail to Die in Culture in the Absence of p75

(A) A representative picture of MBP^+ cells counted for data in Figure 4B. After 6 days in culture, cells were treated with purified mature NGF at 100 ng/ml. At the amounts of time indicated in Figure 4B, cells were fixed, stained for TUNEL, then subsequently for MBP. The arrows point to $TUNEL^+$ cells in the field. Scale bar, 20 μm.

(B) Quantification of $TUNEL^+$ MBP^+ cells following purified NGF treatment at 100 ng/ml. The quantification data are from six independent experiments, with 80–120 cells counted in each experiment, for a total of 480–720 cells counted.

confirm that the proNGF antibody specifically detects and binds proNGF, but not mature NGF. When the rat lysates containing both proNGF and mature NGF were subjected to immunoprecipitation using this proNGF-specific antibody, only high-molecular weight bands of 26–32 kDa were detected and not the band of 14 kDa (Figure 6B, top). Similar data were obtained with mouse lysates as well (Figure 6B, bottom). In addition, when both the rat and mouse lysates were subjected to immunodepletion using the proNGF antibody, these high-molecular weight bands were no longer detected, while the undepleted samples demonstrated immunoreactive species of 26–32 kDa in Western analyses (Figure 6B). These data therefore confirm that the high-molecular weight bands of 26–32 kDa are proNGF.

We next investigated whether proNGF present in the spinal cord extracts activates p75. Since only proNGF and not mature NGF was induced in mice after spinal cord injury, we used mouse extracts obtained after spinal cord injury as a source of proNGF in functional assays using $p75^{+/+}$ and $p75^{-/-}$ mouse oligodendrocytes. When the spinal cord injury extracts were added at 0.14 μl (350 ng total protein added in 1 ml media) to $p75^{+/+}$ mouse oligodendrocytes for 24 hr, the proportion of $TUNEL^+$ and MBP^+ cells reached 17%, while it remained at 4% with extracts from sham-operated mice. With $p75^{-/-}$ mouse oligodendrocytes, the proportion of $TUNEL^+$ and MBP^+ cells remained below 4% (Figure 7A). This 17% value is very close to that obtained on $p75^{+/+}$ mouse oligodendrocytes using 100 ng/ml (4 nM) of NGF purified from submaxillary gland (Figure 4B). Based on estimation using purified mature NGF as a control in Western analysis, 0.14 μl of mouse extracts contains approximately 10–20 ng of proNGF (0.15–0.30 nM) in proNGF concentration. This represents approximately a 13- to 26-fold increase in the action of proNGF on p75 compared to mature NGF, which is comparable to that reported for smooth muscle cells (Lee et al., 2001).

We next compared the activity of proNGF in the spinal cord extracts to that of recombinant proNGF and recombinant mature NGF in oligodendrocytes. Generation and purification of recombinant, cleavage-resistant proNGF and comparably purified mature NGF were previously described (Lee et al., 2001). Within an estimated concentration range from 0.05 nM to 0.5 nM, proNGF in the spinal cord extracts induced apoptosis comparably to recombinant proNGF and more effectively than that observed with recombinant mature NGF (Figure 7B). These results therefore suggest that the apoptotic factor present in the injured spinal cord acts via p75, and its dose response suggests that the activity reflects a proneurotrophin.

In order to confirm that the activity was due to proNGF, we preincubated the injured spinal cord extracts with preimmune serum, anti-mature-NGF antibody, proNGF-specific antibody, or proBDNF-specific antibody before they were added to oligodendrocytes. The specificity of proNGF antibody was discussed earlier. ProBDNF-specific antibody was generated using peptide sequences present in the pro domain of BDNF in a manner similar to proNGF antibody (see Experimental Procedures for detail). In Western analyses, proBDNF antibody detects only proBDNF and not mature BDNF (Figure 6C). As a negative control, parallel cultures were treated with extracts from sham-operated mice, while cells treated with purified NGF from the submaxillary gland (Harlan Bioproducts for Science) were used as a positive control for the antibody action. The extent of apoptosis was assessed after 24 hr and is expressed in terms of the fold increase observed in $TUNEL^+$ and MBP^+ cells over that observed with samples treated with the individual antibody alone (Figure 7C). The extent of apoptosis in cells treated with spinal cord injury extracts was significantly attenuated with proNGF-specific antibody as well as anti-mature-NGF antibody. Preimmune serum or proBDNF-specific antibody did not have any effect.

ProNGF-specific antibody was also effective in attenuating the extent of apoptosis of cells treated with purified NGF. NGF purified from the submaxillary gland has been reported to contain proNGF, which we confirmed (Reinshagen et al., 2000; Figure 7C, bottom). The extent of apoptosis mediated by submaxillary gland derived NGF typically ranges from 5- to 7-fold above control in oligodendrocytes (Figure 4; Harrington et al., 2002). In

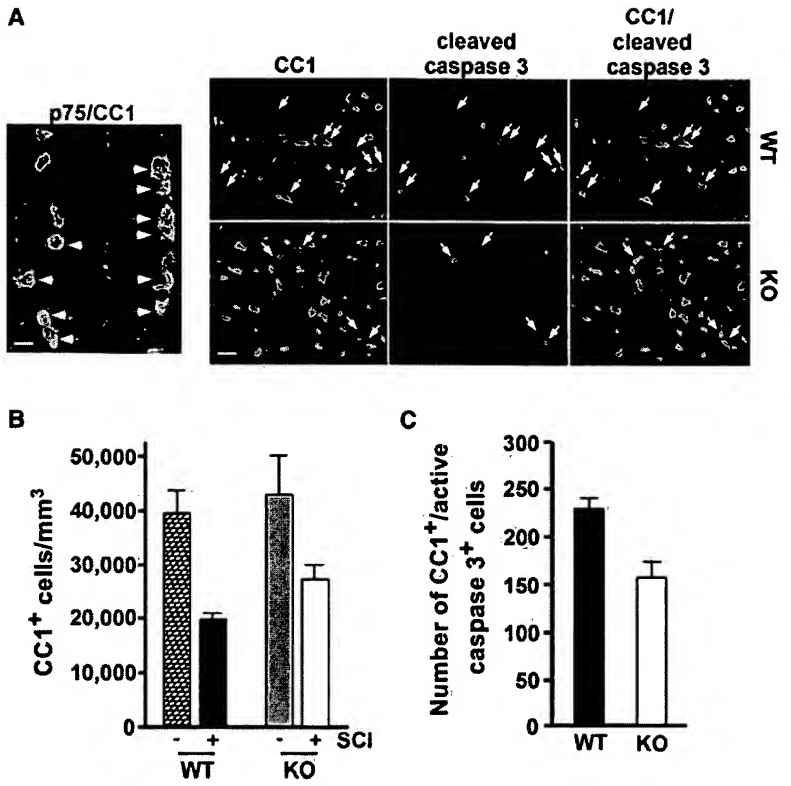

Figure 5. Increased Survival and Decreased Apoptosis of Oligodendrocytes after Spinal Cord Injury in $p75^{-/-}$ Mice

(A) Left: induction of p75 among oligodendrocytes in mice after hemisection. Scale bar, 12.5 μm. Right: representative pictures of cells stained for cleaved caspase 3 and CC1 at 5 days postinjury. The arrows point to cells that are stained for both antibodies. Note the decrease in the number of $CC1^+$/cleaved caspase 3^+ cells in $p75^{-/-}$ mice. Scale bar, 20 μm.

(B) The loss of oligodendrocytes is attenuated in the dorsal funiculus of $p75^{-/-}$ mice after dorsal hemisection ($p < 0.05$). The number is presented as the density of oligodendrocytes per mm^3. Counts were made using a stereology program.

(C) Reduction in the number of oligodendrocytes expressing active caspase 3 in $p75^{-/-}$ mice after dorsal hemisection ($p < 0.01$). The number represents average cell counts in the dorsal columns per coronal section of the spinal cord.

the presence of proNGF antibody, the extent of apoptosis was reduced to 2-fold above control (Figure 7C). This result suggests that proNGF present in submaxillary gland preparations is largely responsible for its apoptotic action, although it comprises only 2%–6% of total NGF. To directly compare the effects of mature NGF and proNGF, recombinant preparations were utilized (Lee et al., 2001) where the mature NGF preparations contained less than 2% proNGF. Utilizing these reagents, mature NGF can induce apoptosis of oligodendrocytes but less effectively than proNGF: 0.5 ng/ml of recombinant proNGF yielded 23% apoptosis, whereas 50 ng/ml recombinant mature NGF yielded 17% apoptosis (Figure 7D). These results, together with the observed inability of proNGF antisera to reduce the apoptosis induced by mature NGF (Figure 7D), suggest that although both proNGF and mature NGF are each capable of inducing apoptosis, proNGF is more active than mature NGF in inducing oligodendrocyte cell death. Together, these results indicate that proNGF present in the spinal cord injury extracts was largely responsible for inducing apoptosis in oligodendrocytes in culture. In addition, these data strongly suggest that proNGF is most likely a factor responsible for inducing apoptosis in vivo after spinal cord injury.

Discussion

In this report, we present data that support a physiological role of proNGF in p75-mediated apoptosis after spinal cord injury. The temporal induction of p75 correlates with the loss of oligodendrocytes following spinal cord injury. Consistent with these observations, in $p75^{-/-}$ mice after spinal cord injury, there is both a reduction in the number of cleaved caspase 3^+ oligodendrocytes and an increase in the number of surviving oligodendrocytes, indicating a predominantly proapoptotic role for p75 activation following injury. We further demonstrated that this apoptotic action of p75 is likely to be mediated by proNGF in vivo by showing that proNGF in extracts from the injured spinal cord induces apoptosis of oligodendrocytes in culture at an affinity comparable to that exhibited by purified, recombinant, cleavage-resistant proNGF. Together, these data provide strong evidence for the apoptotic role of p75 and proNGF after injury to the spinal cord.

Proapoptotic Role of p75 following Injury In Vivo

Injury-mediated induction of p75 in the CNS has been well documented in the literature (Calza et al., 1997; Koliatsos et al., 1991; Nataf et al., 1998; Park et al., 2000; Reynolds et al., 1991; Roux et al., 1999). The role of p75 under these circumstances, however, had not yet been clearly determined in vivo. The present report provides direct evidence that p75 plays a proapoptotic role in oligodendrocyte cell death after spinal cord injury. Oligodendrocytes in the spinal cord express significant levels of p75 in response to spinal cord injury and, in $p75^{-/-}$ mice, their apoptosis is attenuated while their survival is enhanced.

The proapoptotic role of p75 in oligodendrocytes in vivo was further supported by our spinal cord oligodendrocyte culture data. Like their cortical counterparts, spinal cord oligodendrocytes express p75 in culture,

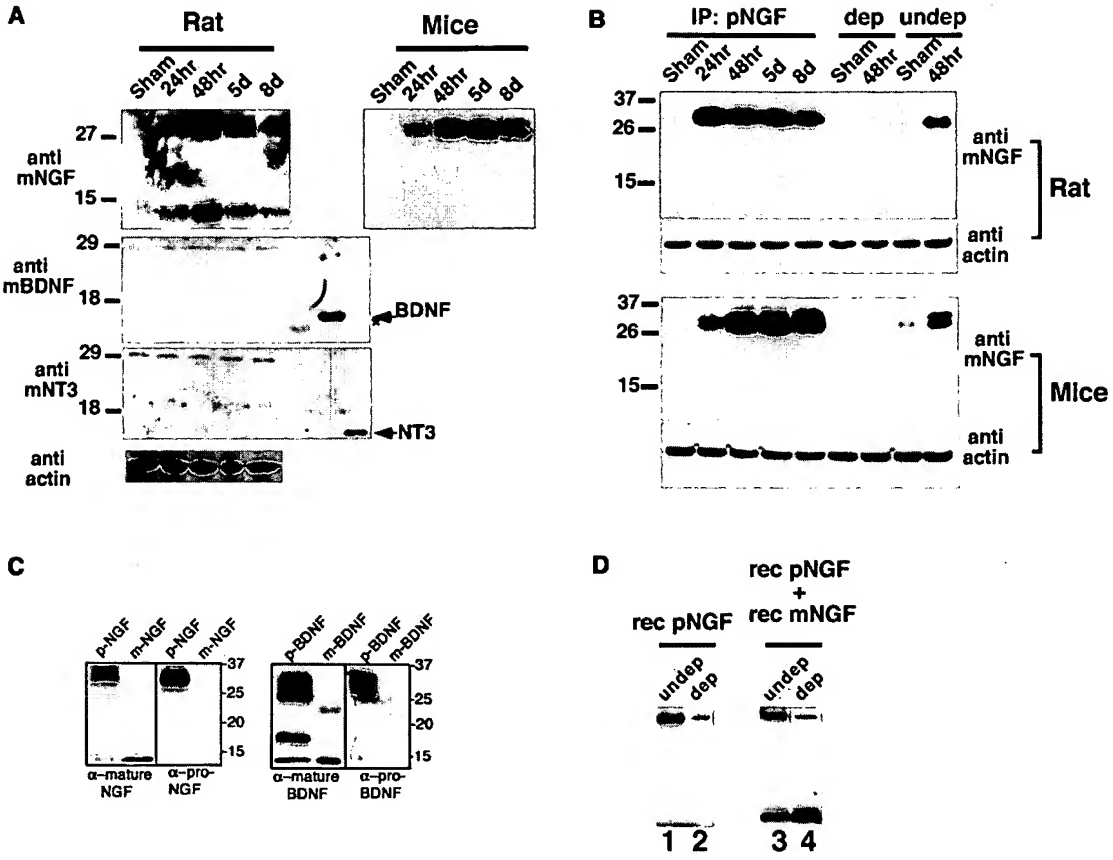

Figure 6. Spinal Cord Injury-Specific Induction of ProNGF

(A) High-molecular weight NGF is predominantly induced after spinal cord injury. 30 μg of extracts were analyzed at each time point in Western analyses for NGF (Chemicon), BDNF (Promega), and NT3 (Promega). The extracts were prepared from rostral 5 mm (rats) or 3 mm (mice) blocks from the lesion center, but the pattern of NGF expression did not vary whether the sample was taken caudally or from the lesion center. The arrow indicates the position of recombinant BDNF and NT3, which were used at 250 ng as a control for antibody specificity. The star points to purified NGF being weakly recognized by anti-BDNF antibody.

(B) The high-molecular weight NGF is proNGF. 350 μg of lysates was immunoprecipitated with proNGF antibody, and probed with anti-mature-NGF antibody (Chemicon). The bands at 26–32 KDa disappear almost completely following depletion with proNGF antibody, indicating that these bands are proNGF (compare lanes dep and undep). Although not shown, mature NGF is present in undepleted rat samples in longer exposure.

(C) Specificity of proNGF and proBDNF antibodies. Western blot of 50 ng of mature NGF (Harlan Bioproducts for Science), 50 ng of mature BDNF (Promega), 50 μg of lysate from 293 cells stably expressing cleavage resistant proNGF, and 250 ng of supernatant from 293 cells infected with cleavage-resistant adenoviral proBDNF. A set of pro and mature NGF was probed with anti-pro/mature NGF antibody (Cedarlane) and proNGF antibody, and a set of pro and mature BDNF was probed with anti-mature-BDNF (Santa Cruz) and anti-proBDNF antibody.

(D) ProNGF antibody depletes proNGF, but not mature NGF. Recombinant proNGF (lanes 1 and 2) or recombinant pro and mature NGF (lanes 3 and 4) were subjected to immunodepletion using proNGF antibody. Note that proNGF antibody depletes only proNGF, but not mature NGF (compare lanes 3 and 4).

and NGF binding to p75 leads to apoptosis in the absence of TrkA. Spinal cord oligodendrocytes do not express TrkA either in culture or in vivo (data not shown). Although it is not clear whether p75 is expressed in cortical oligodendrocytes in vivo, it has been argued that culture conditions represent a stress situation that models in vivo injury. In support of this contention, p75 was shown to activate an injury-specific JNK3 in cortical oligodendrocyte cultures (Harrington et al., 2002). Our current finding, that injury induces p75 among oligodendrocytes in the spinal cord and that these cells also express p75 in culture and die upon binding NGF, provides in vivo evidence in support of this contention.

Although the absence of p75 was fully protective of spinal cord oligodendrocytes in culture, its effect in vivo was not complete. These observations suggest that p75 is but one contributing factor in vivo where other factors and molecules are also involved. Likely candidates include cytokines, such as TNFα, and excitatory amino acids (Beattie et al., 2000; McDonald et al., 1998). The analyses of TNF receptor knockout mice suggest that TNFα plays a protective role by activating NF-κB pathways after spinal cord injury (Kim et al., 2001). This result differs from previous reports where TNFα induced apoptosis of oligodendrocytes in culture (Hisahara et al., 1997; Ladiwala et al., 1998; Louis et al., 1993). When TNFα was applied to dorsal columns, it failed to induce apoptosis among oligodendrocytes (Schnell et al., 1999). When applied together with sublethal doses of kainic acid, however, TNFα induced rapid, massive cell

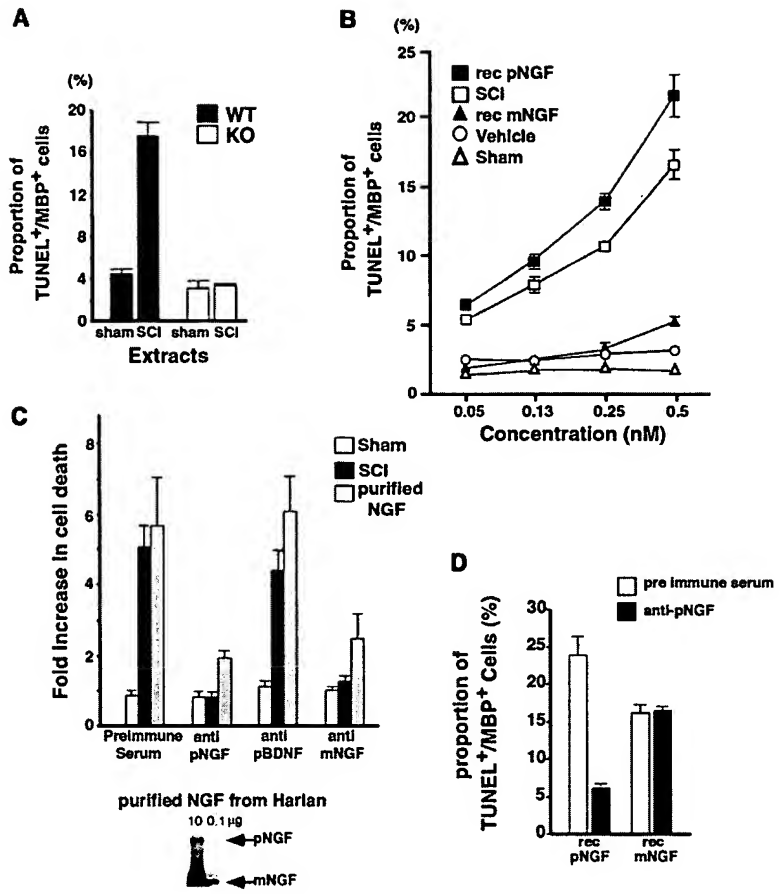

Figure 7. ProNGF Present in Injured Mouse Spinal Cord Extracts Is Active in p75-Mediated Apoptosis of Oligodendrocytes in Culture

(A) p75 is required for apoptosis mediated by the injured spinal cord extracts. Extracts from sham-operated or injured mouse spinal cord extracts were added to either $p75^{+/+}$ or $p75^{-/-}$ mouse oligodendrocytes. After 24 hr, cells were processed for TUNEL/MBP stain as described. For quantification of apoptotic cells, 150–200 cells were counted in each of two to four independent experiments to yield the total cell count of 300–800.

(B) ProNGF in the injured spinal cord extracts behaves similarly to recombinant, cleavage-resistant proNGF in its affinity to induce apoptosis of oligodendrocytes. The concentration of proNGF in the extracts was estimated when added to 1 ml media. After 24 hr, cells were processed for TUNEL/MBP staining as described. For quantification of apoptotic cells, 250–350 cells were counted in each of three independent experiments to yield the total cell count of 750–1050. Abbreviations: rec pNGF, recombinant, cleavage-resistant proNGF; SCI, spinal cord injury extracts; rec mNGF, recombinant mature NGF.

(C) ProNGF present in the spinal cord injury extracts is responsible for apoptosis of oligodendrocytes. Top: the data are represented in terms of the fold increase in the proportion of $TUNEL^+$ MBP^+ cells compared to that with the samples treated with individual antibody. The death mediated by the spinal cord injury extract is significantly attenuated with Chemicon anti-NGF and proNGF antibodies, but not by preimmune serum or proBDNF antibody. The cells treated with purified NGF (Harlan Bioproducts for Science) were used as a positive control. For quantification of apoptotic cells, 250–350 cells were counted in each of three independent experiments to yield the total cell count of 750–1050. Bottom: purified NGF from Harlan contains proNGF.

(D) Functional specificity of proNGF antibody. Rat oligodendrocytes were treated with 50 ng/ml of purified, recombinant mature NGF or 0.5 ng/ml of purified, recombinant, cleavage-resistant proNGF in the presence of either preimmune serum or anti-proNGF antibody. After 24 hr, cells were processed for TUNEL/MBP staining as described. For quantification of apoptotic cells, 200–300 cells were counted in each of three independent experiments to yield the total cell count of 600–900. Note that both proNGF and mature NGF can induce apoptosis, but proNGF is at least 50-fold more active than mature NGF.

death in the spinal cord gray matter (Hermann et al., 2001). These results suggest that induction of secondary injury is likely to involve interactions among multiple pathways. In this report, we identify the p75 neurotrophin receptor as a key player in the downstream apoptotic cascade that could lead to functional loss following spinal cord injury.

In culture, $p75^{-/-}$ mouse oligodendrocytes were resistant to the cell killing effect of the injured spinal cord extracts. This seems surprising, since spinal cord injury induces expression of an array of potential apoptotic agents that act on receptors other than p75, as was discussed previously. A possible explanation may be that our culture conditions provide compensatory mechanisms that result in overall protection against such insults. One potential protective reagent is insulin present in our serum-free media. Expression of the IGF family of factors has been reported to be induced among reactive astrocytes after spinal cord injury (Hammarberg et al., 1998; Yao et al., 1995a). Administration of these factors at the time of demyelinating injuries was known to exert a protective and regenerative effect (Pulford et al., 1999; Sharma et al., 1997; Yao et al., 1995b).

Selective Upregulation of NGF and ProNGF upon Injury

In brain extracts, NGF and BDNF were reported present predominantly as pro forms (Fahnestock et al., 2001; Lee et al., 2001). In the spinal cord, NT3 also exists mainly as 30 kDa proNT3 (Figure 6). Of the three neurotrophins, only NGF was induced after spinal cord injury. When comparing NGF and proNGF induced in rats after spinal cord injury, the level of proNGF is at least equivalent to or higher than the level of mature NGF. The significance of this preferential induction of proNGF as compared to mature NGF is not clear with regard to oligodendrocyte survival, as significant levels of TrkA are not expressed either before or after spinal cord injury (data not shown). In the absence of TrkA, either form of NGF should be capable of activating p75 to induce apoptosis, albeit at a different affinity (Figure 7D). Perhaps a different population of cells express proNGF or

mature NGF, or the secretion mechanism or the site of release for the two forms may differ (Farhadi et al., 2000). These different factors are likely to affect the accessibility of mature NGF/proNGF to $p75^+$ oligodendrocytes.

The NGF level has been shown to increase both in meningeal layer (Widenfalk et al., 2001) and also among astrocytes and activated microglia (Krenz and Weaver, 2000) after spinal cord injury. Activated microglia are often found juxtaposed to apoptotic oligodendrocytes during Wallerian degeneration (Shuman et al., 1997), suggesting that NGF produced by microglia may activate p75 expressed among adjacent oligodendrocytes. Although it is not yet known which cell types express proNGF after spinal cord injury, a scenario analogous to what was reported in the developing retina where NGF secreted by microglia promoted apoptotic actions of p75 (Frade and Barde, 1998) may apply as well.

In hippocampal cultures, the release of BDNF and NT3 required stimuli such as depolarization (Farhadi et al., 2000). NGF, on the other hand, was constitutively released both in a 32 kDa precursor form as well as a 14 kDa mature form when expressed in hippocampal neurons (Mowla et al., 1999). Following injury, a 32 kDa precursor was the predominant form of NGF present in the spinal cord, at least after hemisection in mice. Since a 32 kDa precursor can be released from the cell, at least in culture, this result suggests that proteolytic processing that cleaves proNGF to mature NGF may be a critical step in determining the extent of oligodendrocyte death. In culture, proNGF is significantly more potent than mature NGF in inducing apoptosis of oligodendrocytes, suggesting that inhibition of the protease activity responsible for the conversion of proNGF to mature NGF can provide a potential therapeutic means following spinal cord injury. Lee et al. (2001) have identified matrix metalloproteinase (MMP) 3 and plasmin as a protease that can cleave proNGF and proBDNF in vitro. MMP 2 and 9 expression increases following spinal cord injury (de Castro et al., 2000), however, proNGF was not cleaved by MMP 2 or 9 in vitro (Lee et al., 2001). It is plausible that as yet unidentified MMPs or other proteases regulate the proteolytic processing of proNGF once it is released from the cell.

In conclusion, we report that proNGF is induced by spinal cord injury, and it is likely to play a role in inducing apoptosis in vivo by activating p75. Activation of p75 contributes to the demise of oligodendrocytes. The p75 neurotrophin receptor is therefore identified as a key player in the downstream apoptotic cascade in secondary degeneration following spinal cord injury and other CNS injuries.

Experimental Procedures

Animals Used in the Study

Mice: two groups of $p75^{+/+}$ and $p75^{-/-}$ mice were used for the study. For the injury study, a congenic C57/BL6 line that carries a mutation in exon 3 of the p75 gene (Lee et al., 1992) was purchased from the Jackson Laboratory (Bar Harbor, ME). For the culture study, the $p75^{-/-}$ and $p75^{+/+}$ mice were obtained from heterozygote mating as littermates. Their genotype was determined by PCR analyses of tail DNA according to Bentley and Lee (Bentley and Lee, 2000).

Rats: adult female Long-Evans hooded rats were obtained from Simonsen Labs (Los Angeles, CA).

Spinal Cord Injuries

Mice were anesthetized with isoflurane and the spinal cord was exposed at T10. A Beaver blade was used to produce a dorsal hemisection of the cord, including the dorsal columns and the dorsal part of the lateral funiculus. Contusion injuries in rats were made using the NYU device (Gruner, 1992). Under pentobarbital anesthesia, the spinal cord was exposed at T10 and a 10g weight was dropped from 25 mm onto the dural surface as previously described (Basso et al., 1996). All procedures were approved by the Institutional Laboratory Animal Care and Use Committee and followed the NIH Guidelines for the proper use and care of laboratory animals.

Perfusion

Under deep anesthesia (80 mg/kg ketamine, Fort Dodge Animal Health, Fort Dodge, IA; 10 mg/kg xylazine, Vedco, Inc., St. Joseph, MO), rats and mice were transcardially perfused with 0.9% saline followed by 4% paraformaldehyde fixative. The spinal cords were removed, and three adjacent blocks were cut from the cords, each being either 3 mm long for the mouse cords or 5 mm long for the rat cords. In each case, one block was centered on the lesion, and the others were rostral and caudal to that block. The blocks were sectioned at 20 μm thickness on a cryostat.

Immunohistochemistry

Sections were incubated in blocking solution containing 10% goat serum, 10% horse serum, 1% BSA, and 0.3% Triton X-100 in 0.1M PB for 2 hr at room temperature. For double-staining for p75 and oligodendrocyte cell bodies, the sections were incubated simultaneously with an anti-p75 antibody, 9651 (Huber and Chao, 1995), and CC1 antibody (Bhat et al., 1996; Crowe et al., 1997) in 5% goat serum, 5% horse serum, and 0.1% BSA in 0.1M PB at room temperature overnight. 9651 recognizes the extracellular domain of p75. CC1 antibody recognizes the APC gene product, which is expressed in rat oligodendrocyte somata and proximal processes (Bhat et al., 1996). Although CC1 antibody can detect $GFAP^+$ astrocytes, less than 0.5% of cells were positive for both CC1 and GFAP in our rat and mouse spinal cord tissue. Sections were then incubated with biotinylated anti-rabbit antibody (Vectorlabs) for p75 stain and an anti-mouse antibody conjugated to Alexa 488 (Molecular Probes) for CC1. P75 staining was visualized using Extravidin Cy3 (Sigma). For double-staining for p75 and active caspase 3, 192 anti-mouse anti-p75 antibody was used simultaneously with active caspase 3 anti-rabbit antibody (Cell Signaling, Beverly, MA). For 192 immunostaining, a biotinylated anti-mouse secondary and an anti-mouse antibody conjugated to Alexa 488 (Molecular Probes) was used, and for active caspase 3, an anti-rabbit secondary conjugated to Cy3 (Jackson ImmunoResearch, West Grove, PA) was used. For double-staining for CC1 and active caspase 3, a biotinylated anti-mouse secondary and an anti-mouse antibody conjugated to Alexa 488 (Molecular Probes) was used for CC1. Active caspase 3 was detected with anti-rabbit secondary conjugated to Cy3 (Jackson ImmunoResearch, West Grove, PA). The sections were mounted with Vectashield containing DAPI to label the nuclei (Vector Labs). For confocal microscopy, BioRad MRC 1024 attached to a Nikon Optiphot-2 was used.

For cell counts shown in Figures 1 and 5A, CC1 staining of rat and mouse tissues were done in the same way as the fluorescence staining, except that the positive staining was visualized using DAB and the Vectastain ABC kit (Vector Labs).

Cell Counts

All the counts were done blind to mouse genotype or lesion condition. Cell counts were made on rat and mouse coronal sections at a series of rostral and caudal locations relative to the contusion or hemisection lesions. Counts and reference volumes were estimated using procedures specified in the Stereologer ™ program (Systems Planning and Associates, Inc., Alexandria, VA). For rat contusion injuries, three sections were randomly sampled from 1 mm blocks taken from 13 and 7 mm rostral and 7 and 13 mm caudal to the lesion epicenter. A pilot study was run to determine the optimal disector size and spacing to allow for counts of at least 100 cells per block. CC1 positive cells were only counted when the cell body and proximal processes were darkly labeled and were within the

inclusive zone of each disector frame. Results are reported as total number of oligodendrocytes and as density (number per mm^3). Data were gathered from rats with 25 mm spinal cord injury surviving for 5 or 8 days (n = 4/time point) or 3 or 6 weeks (n = 3/time point), and control uninjured rats (n = 3). Mouse $CC1^+$ cells were counted in a similar fashion at 8 days postinjury, except that the distance from the lesion center sampled was 1.2 mm and 1.8 mm rostral (R1 and R2) and 1.2 mm and 1.8 mm caudal (C1 and C2). The number of mice analyzed was n = 6 for $p75^{+/+}$ and n = 5 for $p75^{-/-}$. For quantification of $CC1^+$/active caspase 3^+ cells in Figure 5B, $p75^{+/+}$ (n = 5) and $p75^{-/-}$ (n = 5) mice were analyzed at 5 days postinjury, using rostral 4 mm blocks.

Primary Oligodendrocyte Cultures

The p75 knockout and the wild-type mice were obtained from heterozygote mating as littermates. For spinal cord oligodendrocytes (Figure 4), mouse pups at postnatal days 12–14 and for cortical oligodendrocytes (Figure 7), mouse pups at postnatal days 15–16 were used. Cell suspension obtained from the triturated tissues was loaded onto a 36% Percoll gradient, and oligodendrocytes were isolated following centrifugation at 10,000 g (Fuss et al., 2000; Lubetzki et al., 1991). Isolated oligodendrocytes were resuspended in 10% FBS in DMEM and plated onto poly-D-Lysine coated 4-well slide dishes at 0.1×10^6 per well. The following day, the medium was changed to a differentiation medium with no serum, as previously described (Yoon et al., 1998). The culture was kept for 4 days before NGF was added at 100 ng/ml for the indicated amount of time. Rat oligodendrocytes were cultured as described (Harrington et al., 2002).

Quantification of Apoptotic Oligodendrocytes in Culture

For quantification of apoptotic mouse oligodendrocytes, cells were fixed at indicated times after NGF treatment and incubated with anti-myelin basic protein (MBP) antibody (Boehringer-Mannheim). Cells were then stained for TUNEL and processed for visualization of MBP stain using an anti-mouse secondary antibody conjugated to Alexa 488 (Molecular Probes, Eugene, OR).

Western Analyses

The spinal cords were homogenized in a lysis buffer containing 1% Nonidet P-40, 20 mM Tris (pH 8.0), 137 mM NaCl, 0.5 mM EDTA, 10% glycerol, 10 mM $Na_2P_2O_7$, 10 mM NaF, 1 μg/ml aprotinin, 10 μg/ml leupeptin, 1 mM vanadate, and 1 mM phenylmethylfulfonyl fluoride. Induction of p75 by spinal cord injury was detected on Western analyses using an anti-rabbit, anti-p75 antibody from Covance (Berkeley, CA). For detection of proNGF and mature NGF, anti-mouse anti-NGF from Chemicon International (Temecula, CA) was used, but the same data were obtained with anti-rabbit anti-NGF from Cedarlane (Hornby, Ontario). The samples for neurotrophin Western analyses were prepared in Laemli buffer that was supplemented with 20 mM DTT and 100 mM iodoacetamide to prevent any potential dimeric interaction between mature NGFs. BDNF and NT3 antibodies were from Promega (Madison, WI).

Immunodepletion

The lysates were subjected to two rounds of immunoprecipitation using proNGF antiserum. The supernatants resulting from immunoprecipitation were analyzed in Western analyses with NGF antibody (Chemicon International, Temecular, CA) to assess the extent of depletion. The lysates taken before immunodepletion was used as undepleted controls in Figure 6B.

Generation of Recombinant ProNGF and Mature NGF

The cDNA of murine NGF was amplified by RT-PCR and sequenced in both directions for any errors. To improve translation initiation, 11 bases from the mouse untranslated region of murine NT-3, including the Kozak consensus site, was exchanged for the murine NGF sequence. PCR-mutagenesis was performed to add six histidine (His) residues at the C terminus, and residues RR (bp 1008–1013) near the C terminus were mutated to AA to impair cleavage of the His tag. To generate proNGF with impaired furin cleavage (proNGF), the KR (bp 651–657) was mutated AA. After bidirectional sequencing, the constructs were cloned into pcDNA, and stable 293 transfectants expressing pcDNA, pcDNA-proNGF, and pcDNA-mature-NGF were isolated following G418 treatment. For purification, cells were cultured for 18 hr in serum-free media, and the resulting media were collected after removing cells by centrifugation. His-tagged mature or cleavage resistant proNGF was purified using Ni-bead chromatography (Xpress System Protein purification, Invitrogen) as per the manufacturer's instructions using imidazole (350 mM) for elution. Medium from cells stably transfected with pcDNA vector alone was harvested and purified in parallel. The concentration of proNGF or mature NGF was estimated by silver stain, using known concentrations of mature NGF (Harlan Bioproducts for science) in parallel.

Generation of ProNGF- and ProBDNF-Specific Antibodies

GST fusion proteins encoding amino acids 23–81 (asp23 to arg81) of human proNGF or amino acids 25–90 (asn25 to asp90) of human proBDNF were generated in bacteria and purified by chromatography with glutathione-sepharose. Rabbits (using GST-proNGF) or chickens (using GST-proBDNF) were immunized to generate antisera. Specific antisera were purified by first incubating whole serum with GST to adsorb GST-specific immunoreactivity and then by adsorption to and elution from a glutathione column to which GST-proBDNF or GST-proNGF had been irreversibly coupled.

Antibody Blocking Experiments Using Injured Spinal Cord Extracts

The extracts from injured spinal cord were added at 0.14 μl in volume, which was estimated to give a final proNGF concentration of 14 ng/ml based on Western analyses. Extracts from sham-operated spinal cord were used at the same volume. For the dose curves in Figure 7B, rat oligodendrocytes were treated with column-purified recombinant proNGF, column-purified recombinant mature NGF, injured spinal cord extracts from mice, sham extracts, or vehicle at the indicated concentrations. For the vehicle control for the recombinant NGFs, the elution buffer containing 350 mM imidazole was used. The final concentration of imidazole therefore ranged from 250 μM to 5 mM. Following a 24 hr incubation period, samples were processed for TUNEL and MBP staining as described. For antibody blocking experiments, either the injured or sham extracts (0.14 μl) were preincubated with mature NGF (5 μl; Chemicon), proNGF (5 μl), proBDNF (10 μl) antibodies, or pre-immune serum (10 μl) for 2 hr at 4°C. The extract and antibody mix was then added to oligodendrocytes for 24 hr before they were processed for TUNEL and MBP stain.

Statistical Methods

A two-way ANOVA (site × time) was used for the cell counts in the rat and a Student's t test in the mice to evaluate the number of surviving and apoptotic oligodendrocytes.

Acknowledgments

We thank Drs. Pilar Perez, Bruce Carter, John Oberdick, Tsonwin Hai, and Moses Chao for discussion. We especially thank Dr. Juan C. Arevalo for the help with antibody production and Dr. Paul Worley for an insightful suggestion. Dr. Stan Baldwin helped establish stereological methods. John Komon, Amy Tovar, and Tina van Meter provided excellent technical assistance for the in vivo studies. This project was supported by grants to S.O.Y. from Whitehall Foundation, ACS, and NIH (RO1: NS39472); to J.C.B. and M.S.B. from NIH (RO1: NS 38079) and the Spinal Cord Research Foundation (SCRF 1734); to F.M.L. from NIH (R01 AG09873) and the Veterans Administration; and to B.L.H. from NIH (RO1: NS30687).

Received: April 3, 2002
Revised: September 27, 2002

References

Basso, D.M., Beattie, M.S., and Bresnahan, J.C. (1996). Graded histological and locomotor outcomes after spinal cord contusion using the NYU weight-drop device versus transection. Exp. Neurol. *139*, 244–256.

Beattie, M.S., Farooqui, A.A., and Bresnahan, J.C. (2000). Review

of current evidence for apoptosis after spinal cord injury. J. Neurotrauma *17*, 915–925.

Bengzon, J., Soderstrom, S., Kokaia, Z., Kokaia, M., Ernfors, P., Persson, H., Ebendal, T., and Lindvall, O. (1992). Widespread increase of nerve growth factor protein in the rat forebrain after kindling-induced seizures. Brain Res. *587*, 338–342.

Bentley, C.A., and Lee, K.F. (2000). p75 is important for axon growth and schwann cell migration during development. J. Neurosci. *20*, 7706–7715.

Bhat, R.V., Axt, K.J., Fosnaugh, J.S., Smith, K.J., Johnson, K.A., Hill, D.E., Kinzler, K.W., and Baraban, J.M. (1996). Expression of the APC tumor suppressor protein in oligodendroglia. Glia *17*, 169–174.

Blight, A.R. (1993). Remyelination, revascularization, and recovery of function in experimental spinal cord injury. Adv. Neurol. *59*, 91–104.

Brandoli, C., Shi, B., Pflug, B., Andrews, P., Wrathall, J.R., and Mocchetti, I. (2001). Dexamethasone reduces the expression of p75 neurotrophin receptor and apoptosis in contused spinal cord. Brain Res. Mol. Brain Res. *87*, 61–70.

Calza, L., Giardino, L., Pozza, M., Micera, A., and Aloe, L. (1997). Time-course changes of nerve growth factor, corticotropin-releasing hormone, and nitric oxide synthase isoforms and their possible role in the development of inflammatory response in experimental allergic encephalomyelitis. Proc. Natl. Acad. Sci. USA *94*, 3368–3373.

Casha, S., Yu, W.R., and Fehlings, M.G. (2001). Oligodendroglial apoptosis occurs along degenerating axons and is associated with FAS and p75 expression following spinal cord injury in the rat. Neuroscience *103*, 203–218.

Chang, A., Nishiyama, A., Peterson, J., Prineas, J., and Trapp, B.D. (2000). NG2-positive oligodendrocyte progenitor cells in adult human brain and multiple sclerosis lesions. J. Neurosci. *20*, 6404–6412.

Chao, M.V., and Bothwell, M. (2002). Neurotrophins. To cleave or not to cleave. Neuron *33*, 9–12.

Crowe, M.J., Bresnahan, J.C., Shuman, S.L., Masters, J.N., and Beattie, M.S. (1997). Apoptosis and delayed degeneration after spinal cord injury in rats and monkeys. Nat. Med. *3*, 73–76.

de Castro, R.C., Jr., Burns, C.L., McAdoo, D.J., and Romanic, A.M. (2000). Metalloproteinase increases in the injured rat spinal cord. Neuroreport *11*, 3551–3554.

Donovan, M.J., Miranda, R.C., Kraemer, R., McCaffrey, T.A., Tessarollo, L., Mahadeo, D., Sharif, S., Kaplan, D.R., Tsoulfas, P., Parada, L., et al. (1995). Neurotrophin and neurotrophin receptors in vascular smooth muscle cells. Regulation of expression in response to injury. Am. J. Pathol. *147*, 309–324.

Dowling, P., Ming, X., Raval, S., Husar, W., Casaccia-Bonnefil, P., Chao, M., Cook, S., and Blumberg, B. (1999). Up-regulated p75NTR neurotrophin receptor on glial cells in MS plaques. Neurology *53*, 1676–1682.

Ernfors, P., Henschen, A., Olson, L., and Persson, H. (1989). Expression of nerve growth factor receptor mRNA is developmentally regulated and increased after axotomy in rat spinal cord motoneurons. Neuron *2*, 1605–1613.

Fahnestock, M., Michalski, B., Xu, B., and Coughlin, M.D. (2001). The precursor pro-nerve growth factor is the predominant form of nerve growth factor in brain and is increased in Alzheimer's disease. Mol. Cell. Neurosci. *18*, 210–220.

Farhadi, H.F., Mowla, S.J., Petrecca, K., Morris, S.J., Seidah, N.G., and Murphy, R.A. (2000). Neurotrophin-3 sorts to the constitutive secretory pathway of hippocampal neurons and is diverted to the regulated secretory pathway by coexpression with brain-derived neurotrophic factor. J. Neurosci. *20*, 4059–4068.

Frade, J.M., and Barde, Y.A. (1998). Microglia-derived nerve growth factor causes cell death in the developing retina. Neuron *20*, 35–41.

Friedman, W.J. (2000). Neurotrophins induce death of hippocampal neurons via the p75 receptor. J. Neurosci. *20*, 6340–6346.

Fuss, B., Mallon, B., Phan, T., Ohlemeyer, C., Kirchhoff, F., Nishiyama, A., and Macklin, W.B. (2000). Purification and analysis of in vivo-differentiated oligodendrocytes expressing the green fluorescent protein. Dev. Biol. *218*, 259–274.

Giehl, K.M., Rohrig, S., Bonatz, H., Gutjahr, M., Leiner, B., Bartke, I., Yan, Q., Reichardt, L.F., Backus, C., Welcher, A.A., et al. (2001). Endogenous brain-derived neurotrophic factor and neurotrophin-3 antagonistically regulate survival of axotomized corticospinal neurons in vivo. J. Neurosci. *21*, 3492–3502.

Gruner, J.A. (1992). A monitored contusion model of spinal cord injury in the rat. J. Neurotrauma *9*, 123–126; discussion 126–128.

Hammarberg, H., Risling, M., Hokfelt, T., Cullheim, S., and Piehl, F. (1998). Expression of insulin-like growth factors and corresponding binding proteins (IGFBP 1-6) in rat spinal cord and peripheral nerve after axonal injuries. J. Comp. Neurol. *400*, 57–72.

Harrington, A.W., Kim, J.Y., and Yoon, S.O. (2002). Activation of Rac GTPase by p75 is necessary for c-jun n-terminal kinase-mediated apoptosis. J. Neurosci. *22*, 156–166.

Hermann, G.E., Rogers, R.C., Bresnahan, J.C., and Beattie, M.S. (2001). Tumor necrosis factor-alpha induces cFOS and strongly potentiates glutamate-mediated cell death in the rat spinal cord. Neurobiol. Dis. *8*, 590–599.

Heumann, R., Korsching, S., Bandtlow, C., and Thoenen, H. (1987). Changes of nerve growth factor synthesis in nonneuronal cells in response to sciatic nerve transection. J. Cell Biol. *104*, 1623–1631.

Hisahara, S., Shoji, S., Okano, H., and Miura, M. (1997). ICE/CED-3 family executes oligodendrocyte apoptosis by tumor necrosis factor. J. Neurochem. *69*, 10–20.

Huber, L.J., and Chao, M.V. (1995). Mesenchymal and neuronal cell expression of the p75 neurotrophin receptor gene occur by different mechanisms. Dev. Biol. *167*, 227–238.

Kim, G.M., Xu, J., Song, S.K., Yan, P., Ku, G., Xu, X.M., and Hsu, C.Y. (2001). Tumor necrosis factor receptor deletion reduces nuclear factor-kappaB activation, cellular inhibitor of apoptosis protein 2 expression, and functional recovery after traumatic spinal cord injury. J. Neurosci. *21*, 6617–6625.

Koliatsos, V.E., Crawford, T.O., and Price, D.L. (1991). Axotomy induces nerve growth factor receptor immunoreactivity in spinal motor neurons. Brain Res. *549*, 297–304.

Krenz, N.R., and Weaver, L.C. (2000). Nerve growth factor in glia and inflammatory cells of the injured rat spinal cord. J. Neurochem. *74*, 730–739.

Ladiwala, U., Lachance, C., Simoneau, S.J., Bhakar, A., Barker, P.A., and Antel, J.P. (1998). p75 neurotrophin receptor expression on adult human oligodendrocytes: signaling without cell death in response to NGF. J. Neurosci. *18*, 1297–1304.

Lee, K.F., Li, E., Huber, L.J., Landis, S.C., Sharpe, A.H., Chao, M.V., and Jaenisch, R. (1992). Targeted mutation of the gene encoding the low affinity NGF receptor p75 leads to deficits in the peripheral sensory nervous system. Cell *69*, 737–749.

Lee, R., Kermani, P., Teng, K.K., and Hempstead, B.L. (2001). Regulation of cell survival by secreted proneurotrophins. Science *294*, 1945–1948.

Li, G.L., Brodin, G., Farooque, M., Funa, K., Holtz, A., Wang, W.L., and Olsson, Y. (1996). Apoptosis and expression of Bcl-2 after compression trauma to rat spinal cord. J. Neuropathol. Exp. Neurol. *55*, 280–289.

Liu, X.Z., Xu, X.M., Hu, R., Du, C., Zhang, S.X., McDonald, J.W., Dong, H.X., Wu, Y.J., Fan, G.S., Jacquin, M.F., et al. (1997). Neuronal and glial apoptosis after traumatic spinal cord injury. J. Neurosci. *17*, 5395–5406.

Louis, J.C., Magal, E., Takayama, S., and Varon, S. (1993). CNTF protection of oligodendrocytes against natural and tumor necrosis factor-induced death. Science *259*, 689–692.

Lubetzki, C., Goujet-Zalc, C., Gansmuller, A., Monge, M., Brillat, A., and Zalc, B. (1991). Morphological, biochemical, and functional characterization of bulk isolated glial progenitor cells. J. Neurochem. *56*, 671–680.

McDonald, J.W., Althomsons, S.P., Hyrc, K.L., Choi, D.W., and Goldberg, M.P. (1998). Oligodendrocytes from forebrain are highly vulnerable to AMPA/kainate receptor-mediated excitotoxicity. Nat. Med. *4*, 291–297.

Mowla, S.J., Pareek, S., Farhadi, H.F., Petrecca, K., Fawcett, J.P.,

Seidah, N.G., Morris, S.J., Sossin, W.S., and Murphy, R.A. (1999). Differential sorting of nerve growth factor and brain-derived neurotrophic factor in hippocampal neurons. J. Neurosci. *19*, 2069–2080.

Mufson, E.J., and Kordower, J.H. (1992). Cortical neurons express nerve growth factor receptors in advanced age and Alzheimer disease. Proc. Natl. Acad. Sci. USA *89*, 569–573.

Nataf, S., Naveilhan, P., Sindji, L., Darcy, F., Brachet, P., and Montero-Menei, C.N. (1998). Low affinity NGF receptor expression in the central nervous system during experimental allergic encephalomyelitis. J. Neurosci. Res. *52*, 83–92.

Oh, J.D., Chartisathian, K., Chase, T.N., and Butcher, L.L. (2000). Overexpression of neurotrophin receptor p75 contributes to the excitotoxin-induced cholinergic neuronal death in rat basal forebrain. Brain Res. *853*, 174–185.

Park, J.A., Lee, J.Y., Sato, T.A., and Koh, J.Y. (2000). Co-induction of p75NTR and p75NTR-associated death executor in neurons after zinc exposure in cortical culture or transient ischemia in the Rat. J. Neurosci. *20*, 9096–9103.

Pulford, B.E., Whalen, L.R., and Ishii, D.N. (1999). Peripherally administered insulin-like growth factor-I preserves hindlimb reflex and spinal cord noradrenergic circuitry following a central nervous system lesion in rats. Exp. Neurol. *159*, 114–123.

Reinshagen, M., Geerling, I., Eysselein, V.E., Adler, G., Huff, K.R., Moore, G.P., and Lakshmanan, J. (2000). Commercial recombinant human beta-nerve growth factor and adult rat dorsal root ganglia contain an identical molecular species of nerve growth factor prohormone. J. Neurochem. *74*, 2127–2133.

Reynolds, M.E., Brunello, N., Mocchetti, I., and Wrathall, J.R. (1991). Localization of nerve growth factor receptor mRNA in contused rat spinal cord by in situ hybridization. Brain Res. *559*, 149–153.

Richardson, P.M., and Riopelle, R.J. (1984). Uptake of nerve growth factor along peripheral and spinal axons of primary sensory neurons. J. Neurosci. *4*, 1683–1689.

Rosenberg, L.J., Teng, Y.D., and Wrathall, J.R. (1999). 2,3-Dihydroxy-6-nitro-7-sulfamoyl-benzo(f)quinoxaline reduces glial loss and acute white matter pathology after experimental spinal cord contusion. J. Neurosci. *19*, 464–475.

Roux, P.P., Colicos, M.A., Barker, P.A., and Kennedy, T.E. (1999). p75 neurotrophin receptor expression is induced in apoptotic neurons after seizure. J. Neurosci. *19*, 6887–6896.

Schnell, L., Fearn, S., Schwab, M.E., Perry, V.H., and Anthony, D.C. (1999). Cytokine-induced acute inflammation in the brain and spinal cord. J. Neuropathol. Exp. Neurol. *58*, 245–254.

Sharma, H.S., Nyberg, F., Gordh, T., Alm, P., and Westman, J. (1997). Topical application of insulin like growth factor-1 reduces edema and upregulation of neuronal nitric oxide synthase following trauma to the rat spinal cord. Acta Neurochir. Suppl. *70*, 130–133.

Shuman, S.L., Bresnahan, J.C., and Beattie, M.S. (1997). Apoptosis of microglia and oligodendrocytes after spinal cord contusion in rats. J. Neurosci. Res. *50*, 798–808.

Springer, J.E., Azbill, R.D., and Knapp, P.E. (1999). Activation of the caspase-3 apoptotic cascade in traumatic spinal cord injury. Nat. Med. *5*, 943–946.

Syroid, D.E., Maycox, P.J., Soilu-Hanninen, M., Petratos, S., Bucci, T., Burrola, P., Murray, S., Cheema, S., Lee, K.F., Lemke, G., and Kilpatrick, T.J. (2000). Induction of postnatal schwann cell death by the low-affinity neurotrophin receptor in vitro and after axotomy. J. Neurosci. *20*, 5741–5747.

Taniuchi, M., Clark, H.B., Schweitzer, J.B., and Johnson, E.M., Jr. (1988). Expression of nerve growth factor receptors by Schwann cells of axotomized peripheral nerves: ultrastructural location, suppression by axonal contact, and binding properties. J. Neurosci. *8*, 664–681.

Warden, P., Bamber, N.I., Li, H., Esposito, A., Ahmad, K.A., Hsu, C.Y., and Xu, X.M. (2001). Delayed glial cell death following wallerian degeneration in white matter tracts after spinal cord dorsal column cordotomy in adult rats. Exp. Neurol. *168*, 213–224.

Widenfalk, J., Lundstromer, K., Jubran, M., Brene, S., and Olson, L. (2001). Neurotrophic factors and receptors in the immature and adult spinal cord after mechanical injury or kainic acid. J. Neurosci. *21*, 3457–3475.

Yao, D.L., West, N.R., Bondy, C.A., Brenner, M., Hudson, L.D., Zhou, J., Collins, G.H., and Webster, H.D. (1995a). Cryogenic spinal cord injury induces astrocytic gene expression of insulin-like growth factor I and insulin-like growth factor binding protein 2 during myelin regeneration. J. Neurosci. Res. *40*, 647–659.

Yao, D.L., Liu, X., Hudson, L.D., and Webster, H.D. (1995b). Insulin-like growth factor I treatment reduces demyelination and up-regulates gene expression of myelin-related proteins in experimental autoimmune encephalomyelitis. Proc. Natl. Acad. Sci. USA *92*, 6190–6194.

Yoon, S.O., Casaccia-Bonnefil, P., Carter, B.D., and Chao, M.V. (1998). Competitive signaling between TrkA and p75 determines cell survival. J. Neurosci. *18*, 3273–3281.

Proc. Natl. Acad. Sci. USA
Vol. 88, pp. 4771–4775, June 1991
Medical Sciences

Anti-transferrin receptor antibody and antibody-drug conjugates cross the blood–brain barrier

(drug delivery/methotrexate)

PHILLIP M. FRIDEN*, LEE R. WALUS, GARY F. MUSSO, MARJORIE A. TAYLOR, BERNARD MALFROY, AND RUTH M. STARZYK

Alkermes, Inc., 26 Landsdowne Street, Cambridge, MA 02139

Communicated by Hilary Koprowski, February 19, 1991

ABSTRACT **Delivery of nonlipophilic drugs to the brain is hindered by the tightly apposed capillary endothelial cells that make up the blood–brain barrier. We have examined the ability of a monoclonal antibody (OX-26), which recognizes the rat transferrin receptor, to function as a carrier for the delivery of drugs across the blood–brain barrier. This antibody, which was previously shown to bind preferentially to capillary endothelial cells in the brain after intravenous administration (Jefferies, W. A., Brandon, M. R., Hunt, S. V., Williams, A. F., Gatter, K. C. & Mason, D. Y. (1984) *Nature (London)* 312, 162–163), labels the entire cerebrovascular bed in a dose-dependent manner. The initially uniform labeling of brain capillaries becomes extremely punctate ≈4 hr after injection, suggesting a time-dependent sequestering of the antibody. Capillary-depletion experiments, in which the brain is separated into capillary and parenchymal fractions, show a time-dependent migration of radiolabeled antibody from the capillaries into the brain parenchyma, which is consistent with the transcytosis of compounds across the blood–brain barrier. Antibody-methotrexate conjugates were tested *in vivo* to assess the carrier ability of this antibody. Immunohistochemical staining for either component of an OX-26-methotrexate conjugate revealed patterns of cerebrovascular labeling identical to those observed with the unaltered antibody. Accumulation of radiolabeled methotrexate in the brain parenchyma is greatly enhanced when the drug is conjugated to OX-26.**

The levels of various substances in the blood, such as hormones, amino acids, and ions, undergo frequent small fluctuations that can be brought about by activities such as eating and exercise (1). If the brain were not protected from these variations in serum composition, the result could be uncontrolled neural activity. The blood–brain barrier (BBB) functions to ensure that the homeostasis of the brain is maintained. Specialized characteristics of the endothelial cells that form brain capillaries are responsible for this barrier (1, 2). Brain capillary endothelial cells are joined together by tight intercellular junctions that form a continuous wall against the passive movement of substances from the blood to the brain (3, 4). These cells lack continuous gaps or channels connecting the luminal and abluminal membranes, which, in other endothelial cells, allow relatively unrestricted passage of blood-borne molecules into tissue.

The isolation of the brain from the bloodstream is not complete; were this the case, the brain would be unable to function properly due to a lack of nutrients and because of the need to exchange hormones and other compounds with the rest of the body. The presence of specific transport systems within the capillary endothelial cells, such as those for amino acids, transferrin, glucose, and insulin (2, 5–8), assures that the brain receives, in a controlled manner, all of the compounds required for normal growth and function. For the transferrin receptor, it has been reported (9) that brain endothelial cells are selectively labeled by anti-receptor antibodies in the rat after *in vivo* administration, presumably due to a high density of transferrin receptors on the surface of brain capillary endothelial cells.

A problem posed by the BBB is that, in the process of protecting the brain, it also excludes many potentially useful therapeutic agents. Currently, only substances that are sufficiently lipophilic or are recognized by an existing transport system can readily penetrate the BBB (1, 2). The lipidization of drugs to enhance brain uptake is very nonspecific, in that it will increase the ability of the particular compound to cross all cellular membranes, and is not possible for many compounds. A carrier system that has some degree of organ selectivity and that could be used for a wide range of compounds would have a significant advantage over current methods for circumventing the BBB. Such a carrier system could be developed by exploiting a transport system known to deliver compounds across the BBB, such as that for transferrin.

We report experimental results that suggest that anti-transferrin receptor antibodies may have utility as drug delivery carriers for the brain. This delivery system takes advantage of the high density of transferrin receptors on brain endothelial cells as well as the ability of these receptors to shuttle molecules across the BBB. Both qualitative and quantitative experiments show that, in the rat, the anti-transferrin receptor antibody OX-26 and antibody-methotrexate (MTX) conjugates bind to capillary endothelial cells in the brain in a dose- and time-dependent manner. In addition, we present data that indicate that this antibody and antibody-drug conjugates cross the BBB.

MATERIALS AND METHODS

Preparation of Antibody and Antibody Conjugates. OX-26 antibodies were purified from supernatants harvested from cultures of the OX-26 hybridoma cell line [provided by Alan F. Williams, Medical Research Council, Oxford, U.K. (10)] by using protein A-Sepharose column chromatography. The control IgG2a antibody (UPC10) was purchased from Sigma.

A hydrazone-linked conjugate between MTX and OX-26 was synthesized by incubating MTX γ-hydrazide with antibody that had been oxidized with sodium periodate to form aldehydes from the carbohydrate groups located on the Fc portion of the protein (G.F.M., S. Abelliera, and A. Morrow, unpublished data and ref. 11). The conjugate, which consisted of approximately six MTX molecules per antibody, was analyzed as described (12). The same procedure was

The publication costs of this article were defrayed in part by page charge payment. This article must therefore be hereby marked "*advertisement*" in accordance with 18 U.S.C. §1734 solely to indicate this fact.

Abbreviations: BBB, blood–brain barrier; MTX, methotrexate.
*To whom reprint requests should be addressed.

followed for synthesizing [^{3}H]MTX-OX-26 conjugates, using [3',5',7-^{3}H]MTX (Amersham).

Immunohistochemistry. Female Sprague–Dawley rats (100–125 g) were anesthetized with halothane for tail vein injections. At sacrifice, the animals were perfused with phosphate-buffered saline (PBS) to remove blood from the vasculature. The brains were frozen in liquid nitrogen for cryostat sectioning. Sections (≈30 μm) were fixed in acetone at room temperature and stored at −20°C. Immunolocalization of injected OX-26 in the brain sections was performed using a horse anti-mouse IgG Vectastain ABC kit from Vector Laboratories by following the manufacturer's protocol. MTX was detected using a rabbit anti-MTX antisera from Western Chemical Research and a biotinylated goat anti-rabbit IgG antisera from Vector Laboratories. All sections were counterstained with methyl green (0.05% in PBS).

Capillary Depletion. Antibodies were labeled with either [^{14}C]acetic anhydride or [^{3}H]succinimidyl propionate (Amersham) essentially as described (13, 14). For ^{14}C, the number of acetyl groups per antibody was in the range of 5 to 10; for ^{3}H, less than one propionyl group was added per antibody. Average specific activities were ≈10 Ci/mmol and 280 mCi/mmol (1 Ci = 37 GBq) for ^{3}H and ^{14}C, respectively. Routinely, 1×10^6 dpm of ^{3}H and 5×10^5 dpm of ^{14}C were injected per animal. For all experiments, the radiolabeled compounds were injected as a 400-μl bolus into the tail vein of female Sprague–Dawley rats (100–125 g) under halothane anesthesia and the animals were sacrificed at the appropriate time after injection using a lethal dose of anesthetic. A radiolabeled IgG2a control antibody (^{14}C for ^{3}H-labeled OX-26, or vice versa) was co-injected with the labeled OX-26 to serve as a control for nonspecific radioactivity in the brain due to residual blood.

Capillary depletion experiments were performed essentially as described by Triguero *et al.* (15). This method removes >90% of the vasculature from the brain homogenate. The entire capillary pellet and samples of the homogenate and supernatant were solubilized overnight with 2 ml of Soluene 350 (Packard) prior to liquid scintillation counting. All data were collected as dpm by using a Beckman model TD5000 liquid scintillation counter. Data are expressed as percent of the injected dose per brain of the antibody in either the parenchyma or capillary fractions. Blood samples were centrifuged to pellet erythrocytes (which did not display significant binding of radiolabeled materials) and the radioactivity in a sample of serum was determined using liquid scintillation counting.

RESULTS

Dose- and Time-Dependent Localization of an Anti-Transferrin Receptor Antibody to Brain Capillaries *in Vivo*. Immunohistochemistry was used to localize the anti-transferrin receptor antibody OX-26 in the rat brain vasculature after intravenous injection by the tail vein as shown by Jefferies *et al.* (9). One hour after injection of 0.5 mg of purified antibody, uniform intense staining of the capillaries was observed throughout the brain (Fig. 1*A*). Larger blood vessels as well as capillaries showed the presence of bound antibody. This staining of the brain vasculature was clearly detected at doses as low as 50 μg per rat and appeared to saturate at a dose of ≈0.5 mg per rat (data not shown). As reported by Jefferies *et al.* (9), specific staining of capillaries was not observed in any of the other organs that were examined (data not shown).

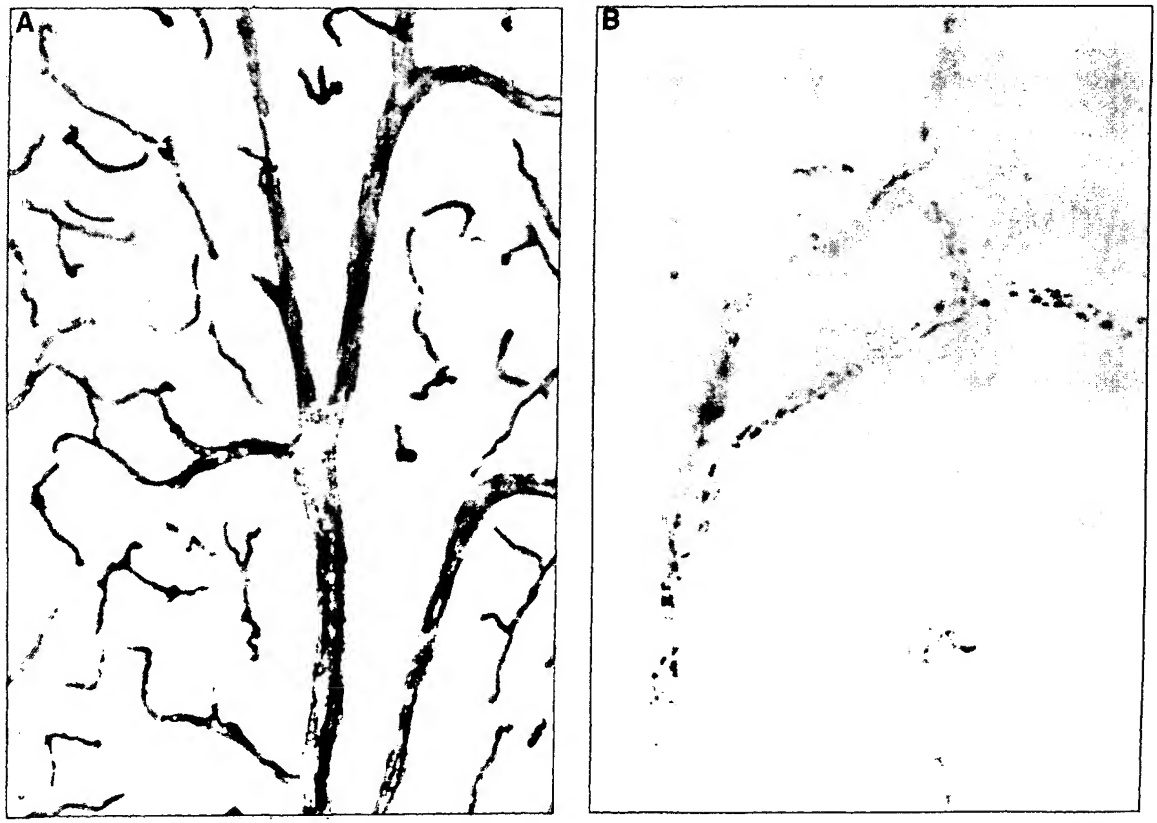

FIG. 1. Immunohistochemical detection of OX-26 in brain sections. Sections were cut from brains taken from rats sacrificed 1 hr (*A*) and 4 hr (*B*) after injection of 0.5 mg of OX-26 into the tail vein. The tissue sections were stained with horse anti-mouse IgG. The brown reaction product outlines the cerebral vasculature. The punctate staining pattern is clearly visible 4 hr after injection (*B*). A methyl green counterstain was used to label cell nuclei. (*A*, ×100; *B*, ×400.)

To determine how early after injection the anti-transferrin receptor antibody could be detected in the brain capillaries as well as how long it persisted, a time course experiment was performed. Rats were injected with 0.5 mg of OX-26 per animal and sacrificed at various times after the injection. Antibody was detected immunohistochemically within the brain capillaries as early as 5 min after injection (data not shown). The staining observed at this time was uniformly distributed along the capillary endothelium. By 1 hr after injection, the observed staining for antibody along the brain capillaries had become more intense (Fig. 1*A*) and, as for the 5-min time point, was quite uniform. By ≈4 hr after injection, the staining pattern of OX-26 in the brain vasculature changed dramatically and became very punctate (Fig. 1*B*), suggesting sequestration of the antibody in some manner. The pattern of localization was still punctate 8 hr after injection but returned to a uniform, fainter staining by 24 hr after injection (data not shown).

To ensure that the observed staining was unique to the OX-26 antibody, a control antibody (UPC10) of the same subclass (IgG2a) was injected into rats for immunohistochemical localization. No staining of brain vasculature was observed with the control IgG2a at doses and times comparable to those used with OX-26 (data not shown).

Distribution of OX-26 in Brain Parenchyma and Capillaries. The above results show qualitatively that the anti-transferrin receptor antibody OX-26 is present in the brain vasculature after i.v. administration. To demonstrate quantitatively that the anti-transferrin receptor antibody accumulates in the brain parenchyma, homogenates of brains taken from animals injected with radiolabeled OX-26 were depleted of capillaries by centrifugation through dextran to yield a brain tissue supernatant and a capillary pellet. A comparison of the relative amounts of radioactivity in the different brain fractions as a function of time should indicate whether the labeled monoclonal antibody has crossed the BBB. Because the vasculature remains intact during the capillary depletion procedure, the antibody that reaches the parenchyma has traversed the basement membrane and perivascular cells associated with the capillaries. As a control for nonspecific association with the brain due to residual blood contamination, a ^{14}C-labeled IgG2a control antibody was co-injected with the ^{3}H-labeled OX-26.

The amounts of OX-26 in the brain parenchyma fraction and in the brain capillary fraction plotted as a function of time after injection are shown in Fig. 2. Initially, the amount of OX-26 associated with the brain capillaries rises sharply, reaching a level of ≈0.6% of the injected dose by 1 hr after injection. This level then decreases over time, dropping to 0.13% of the injected dose by 24 hr after injection. As the amount of antibody associated with the capillaries decreases, the amount associated with the brain parenchyma increases, reaching a value of 0.44% of the injected dose by 24 hr after injection. This redistribution of the radiolabeled OX-26 from the capillary fraction to the parenchyma fraction is consistent with the time-dependent migration of the anti-transferrin receptor antibody across the BBB.

To address the question of stability of the radiolabeled carrier in the circulation, total IgG was extracted from serum followed by polyacrylamide gel electrophoresis and autoradiography. This analysis did not reveal detectable levels of OX-26 degradation as late as 48 hr after injection (data not shown).

Localization of OX-26-MTX Conjugates in the Brain Vasculature. If an anti-transferrin receptor antibody is to function as a drug carrier, it must retain its ability to bind to and be internalized by brain capillary endothelial cells after conjugation with drug. To test for targeting and binding to brain capillaries *in vivo*, an OX-26-MTX conjugate (≈6 MTX per 1 antibody) was prepared using a hydrazone linkage. One hour after its injection into the rat tail vein, the brain was removed and sectioned for immunohistochemistry as for the studies described above. Both the antibody carrier and the MTX "passenger" were visualized in the brain using either anti-mouse IgG or anti-MTX antisera.

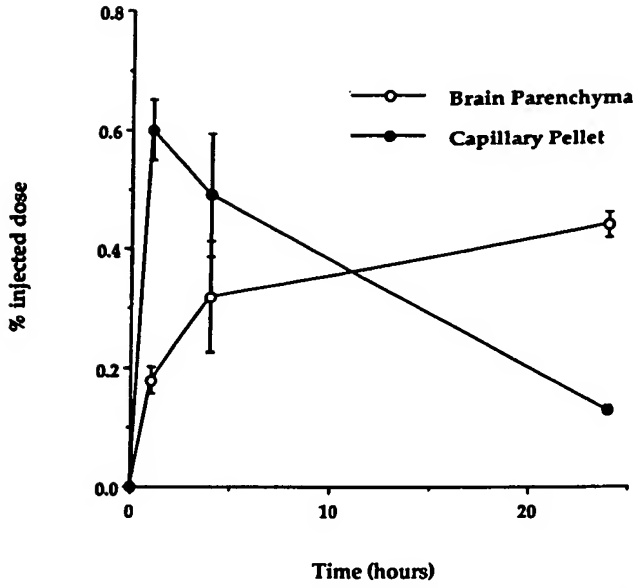

FIG. 2. Time-dependent changes in the disposition of ^{3}H-labeled OX-26 between brain parenchyma and vasculature. Capillary depletion was performed on homogenates prepared from brains taken from animals 1, 4, and 24 hr after injection of radiolabeled OX-26. The percent injected dose of antibody per brain in the parenchyma fraction (○) and vascular pellet (●) are shown. Similar results were obtained using ^{14}C-labeled OX-26 (data not shown). The values shown are mean ± SEM (n = 3 rats per time point). These results are representative of other studies that have been done.

A staining pattern similar to that seen with OX-26 alone was revealed when sections from the conjugate-injected animals were stained for the carrier antibody (Fig. 3*A*). A similar pattern was seen when these sections were stained with anti-MTX antisera (Fig. 3*B*), indicating colocalization of OX-26 and MTX in the brain vasculature.

When equivalent amounts of free MTX were injected into rats, no staining of the brain vasculature was observed using the anti-MTX antisera, indicating that localization of the drug to the brain capillaries is dependent on OX-26 (data not shown). Also, no staining was observed when the anti-MTX antiserum was used on sections containing only OX-26.

Distribution of the OX-26-MTX Conjugate in Brain Parenchyma and Capillaries. Capillary-depletion studies identical to those described above for OX-26 were performed with an OX-26-MTX conjugate in which the MTX moiety was labeled with ^{3}H at the 3′, 5′, and 7 positions. As with unconjugated antibody, the amount of label in the capillary fraction at an early time after injection (30 min for these experiments) was greater than that in the parenchyma fraction (Fig. 4). This distribution changed over time such that by 24 hr after injection, ≈5-fold more of the labeled MTX was in the brain parenchyma than was in the capillaries. These results are consistent with those obtained with unconjugated antibody and suggest that the OX-26-MTX conjugate crosses the BBB.

To ensure that these results were not due to contaminating amounts of free [^{3}H]MTX or [^{3}H]MTX that had been cleaved from the conjugate after injection, a mixture of labeled drug and antibody was injected into rats and a capillary-depletion experiment was performed. The amount of [^{3}H]MTX in the different brain fractions was significantly lower for the mixture as compared to the conjugate (as much as 47-fold in the capillary fraction 30 min after injection; Fig. 4). The

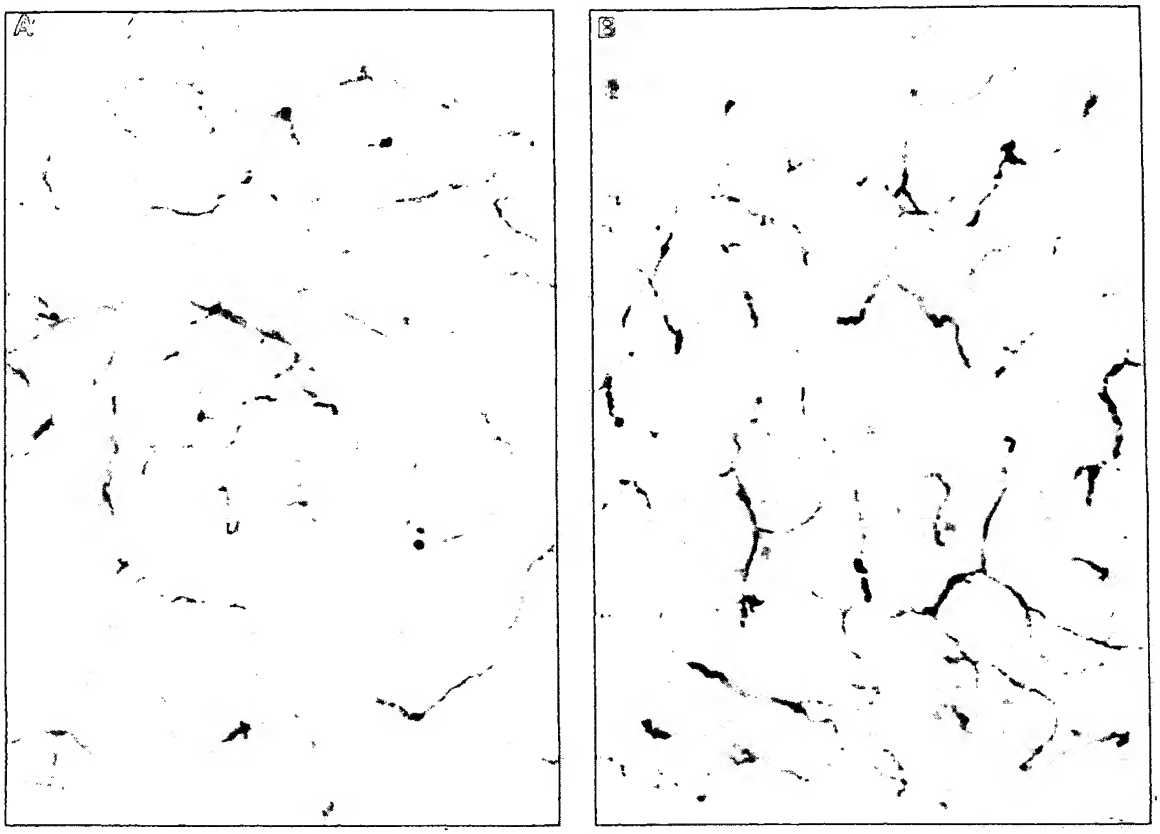

FIG. 3. Immunohistochemical detection of an OX-26-MTX conjugate in brain sections. Horse anti-mouse IgG (*A*) and rabbit anti-MTX (*B*) antisera were used to detect the carrier antibody and the passenger drug, respectively, in the brain vasculature after i.v. administration of 0.2 mg of OX-26-MTX conjugate. Immunohistochemistry was as described in Fig. 1. (×100.)

[^{3}H]MTX in the mixture also did not show the change in distribution of the label between the various brain fractions over time as was seen with the antibody-MTX conjugate or antibody alone (Figs. 2 and 4).

DISCUSSION

The results presented herein indicate that an antibody which recognizes an extracellular epitope of the transferrin receptor crosses the BBB and can be used to deliver the chemotherapeutic drug MTX to the brain after intravenous administration. Initially, immunohistochemistry was used to corroborate and elaborate on earlier studies by Jefferies *et al.* (9) demonstrating that anti-transferrin receptor antibodies bind preferentially to vascular endothelial cells within the brain. This phenomenon is most likely attributable to a higher density of these receptors on the endothelial cells that make up the BBB as compared to those in other capillary beds. Physiologically, this is consistent with the fact that the primary, if not only, pathway for iron to enter the brain is by the transcytosis of iron-loaded transferrin across the BBB (2, 7, 8).

Immunohistochemical staining of brain sections taken from animals sacrificed at various times after injection shows that the localization of OX-26 in the brain vasculature changes with time. A very punctate pattern of staining is observed from ≈2 to 4 hr to ≈8 to 16 hr after injection as compared to the more uniform pattern observed before and after this period. This most likely represents endocytosis and concentration of the antibody in an intracellular compartment followed by eventual exocytosis. One hour after injection by the carotid artery, ferrotransferrin–horseradish peroxidase conjugates have been observed to label perivascular clefts and cells, apparently as a result of crossing the endothelial cell layer (16). The time frame in which the OX-26 punctate staining occurs is consistent with uptake by perivascular cells, indicating BBB penetration.

Although suggestive, the above results do not demonstrate that the antibody crosses the BBB as opposed to simply

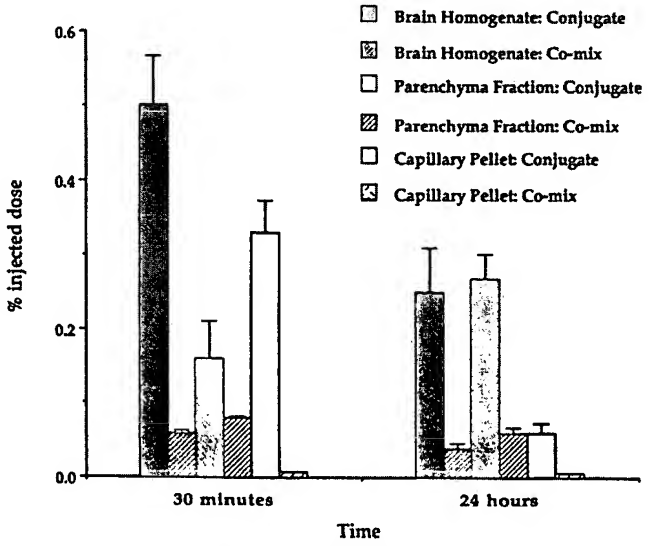

FIG. 4. Enhanced delivery of MTX across the BBB using OX-26 as a drug carrier. Capillary depletion experiments were used to compare the distribution of an OX-26-MTX conjugate to that of a mixture of antibody and drug. The data are expressed as percent of the injected dose of ^{3}H-labeled MTX per brain in unfractionated homogenate, the parenchyma fraction, and the capillary fraction. The values shown are mean ± SEM (n = 3 rats per time point). These results are representative of other studies that have been done.

binding to the luminal surface of the capillary endothelial cells. To address these concerns as well as to obtain more quantitative data, OX-26 was radioactively labeled and its distribution within the brain was determined using the technique of capillary depletion as developed by Triguero *et al.* (15). The time-dependent changes that were observed in the distribution of radiolabeled OX-26 within the vascular and parenchymal fractions of the brain are consistent with models for the transcytosis of blood-borne proteins across the BBB (2, 17). This pathway consists of (*i*) binding of the blood-borne compound to a receptor on the luminal side of the capillary endothelial cell, (*ii*) engulfment of occupied receptors into endocytic vesicles and transport of the vesicular contents to the abluminal surface of the cell, and (*iii*) exocytosis of the internalized materials on the abluminal surface. There is precedence for the binding of anti-transferrin receptor antibodies to the receptor on the cell surface with subsequent internalization of the antibody–receptor complex (18), suggesting that steps *i* and *ii* of the transcytosis pathway described above can occur. With regard to the release of the antibody on the abluminal surface of endothelial cells, it has been demonstrated that certain antibodies to the low density lipoprotein receptor-related protein undergo internalization, escape degradation in the lysosome, and recycle to the cell surface where they dissociate from the receptor in an acid-precipitable form (19). A similar pathway may be followed by the anti-transferrin receptor antibodies in traversing the brain capillary endothelial cells.

The use of radiolabeled antibody in the capillary depletion experiments also allows the quantitation of the amount of carrier in the different brain fractions at specific times. However, because the brain is a dynamic system with uptake from the blood and clearance to the cerebrospinal fluid and the blood occurring concurrently, these calculations most likely underestimate the total amount of antibody that reaches the brain parenchyma from the circulation.

Conjugates of OX-26 and MTX were synthesized and tested *in vivo* to examine the ability of this antibody to deliver drugs to the brain. The results presented suggest that the targeting of OX-26 to brain capillary endothelial cells is not markedly affected by the attachment of "passenger" drug molecules. However, although we have clearly demonstrated enhanced delivery of MTX to the brain by using OX-26 as a carrier, the amount that reaches the brain parenchyma is lower than that of antibody alone (0.27 and 0.44% of the injected dose, respectively, 24 hr after injection). It appears that this difference may be a reflection of the physical-chemical properties of the passenger compound, as we have found that some conjugates of OX-26 exhibit enhanced uptake into the brain parenchyma relative to antibody alone (L.R.W. and P.M.F., unpublished data). The use of radiolabeled MTX in the capillary depletion experiments clearly demonstrates that it is the drug which is delivered to the brain parenchyma.

The results presented demonstrate the feasibility of delivering drugs across the BBB by using an anti-transferrin receptor antibody as a carrier. Although the present study establishes delivery of a small drug molecule, neuroactive peptides and neurotrophic factors whose effective brain concentrations are in the nanomolar range (or lower) are also potential candidates for delivery using this system. OX-26 has been shown to deliver proteins as large as 40 kDa to the brain and to achieve concentrations in the brain estimated to be in the 10–100 nM range (L.R.W., P.M.F. and M.A.T., unpublished data). Thus, therapeutic levels of neuroactive compounds may be achieved in the brain using an anti-transferrin receptor antibody.

We thank Biba Tehrani, Joseph Eckman, Susan Abelleira, and Anne Morrow for their excellent technical support. We also thank Floyd Bloom, Timothy Curran, John Kozarich, Paul Schimmel, and Michael Wall for their support and insightful comments. We appreciate the many helpful comments made by our colleagues at Alkermes, Inc.

1. Goldstein, G. W. & Betz, A. L. (1986) *Sci. Am.* **255**, 74–83.
2. Pardridge, W. M. (1986) *Endocr. Rev.* **7**, 314–330.
3. Brightman, M. W. (1977) *Exp. Eye Res.* **25**, 1–25.
4. Reese, T. S. & Karnovsky, M. J. (1967) *J. Cell Biol.* **34**, 207–217.
5. Pardridge, W. M. (1983) *Physiol. Rev.* **63**, 1481–1535.
6. Pardridge, W. M., Eisenberg, J. & Yang, J. (1985) *J. Neurochem.* **44**, 1771–1778.
7. Fishman, J. B., Rubin, J. B., Handrahan, J. V., Connor, J. R. & Fine, R. E. (1987) *J. Neurosci. Res.* **18**, 299–304.
8. Pardridge, W. M., Eisenberg, J. & Yang, J. (1987) *Metabolism* **36**, 892–895.
9. Jefferies, W. A., Brandon, M. R., Hunt, S. V., Williams, A. F., Gatter, K. C. & Mason, D. Y. (1984) *Nature (London)* **312**, 162–163.
10. Jefferies, W. A., Brandon, M. R., Williams, A. F. & Hunt, S. V. (1985) *Immunology* **54**, 333–341.
11. Kralovec, J., Spencer, G., Blair, A. H., Mammen, M., Singh, M. & Ghose, T. (1989) *J. Med. Chem.* **32**, 2426–2431.
12. Endo, N., Takeda, Y., Umemoto, N., Kishida, K., Watanabe, K., Saito, M., Kato, Y. & Hara, T. (1988) *Cancer Res.* **48**, 3330–3335.
13. Kummer, U. (1986) *Methods Enzymol.* **121**, 670–678.
14. Montelaro, R. C. & Rueckert, R. R. (1975) *J. Biol. Chem.* **250**, 1413–1421.
15. Triguero, D., Buciak, J. & Pardridge, W. M. (1990) *J. Neurochem.* **54**, 1882–1888.
16. Broadwell, R. D. (1989) *Acta Neuropathol.* **79**, 117–128.
17. Broadwell, R. D., Balin, B. J. & Salcman, M. (1988) *Proc. Natl. Acad. Sci. USA* **85**, 632–636.
18. Lesley, J., Schulte, R. & Woods, J. (1989) *Exp. Cell Res.* **182**, 215–233.
19. Herz, J., Kowal, R. C., Ho, Y. K., Brown, M. S. & Goldstein, J. L. (1990) *J. Biol. Chem.* **265**, 21355–21362.

Annu. Rev. Neurosci. 1999. 22:11–28

THE CELL BIOLOGY OF THE BLOOD-BRAIN BARRIER

L. L. Rubin
Ontogeny, Inc., Cambridge, Massachusetts 02138-1118; e-mail: lrubin@ontogeny.com

J. M. Staddon
Eisai London Research Laboratories Ltd., University College London, London WC1E 6BT, United Kingdom; e-mail: jstaddon@elrl.co.uk

KEY WORDS: phosphorylation, endothelial cells, tight junction, adherens junction

ABSTRACT

The blood-brain barrier (BBB) is formed by brain capillary endothelial cells (ECs). In the late embryonic and early postnatal period, these cells respond to inducing factors found in the brain environment by adopting a set of defined characteristics, including high-electrical-resistance tight junctions. Although the factors have not been identified definitively, a great deal of information about brain ECs has been obtained, especially recently. This review concentrates on a cell biological analysis of the BBB, with an emphasis on regulation of the specialized intercellular junctions. The development of these junctions seems to depend on two primary processes: the appearance of high levels of the tight junction protein occludin and intracellular signaling processes that control the state of phosphorylation of junctional proteins. Recent studies have revealed that the BBB can be modulated in an ongoing way to respond to environmental stimuli.

INTRODUCTION

The existence of the blood-brain barrier (BBB) has been recognized for more than 100 years, having been demonstrated first by the German microbiologist Ehrlich. Although most neuroscientists are generally familiar with the idea that the BBB acts to keep toxic substances out of the brain, they are poorly informed about its underlying biology, and until recently, few studies applied detailed cellular and molecular biology to this problem. Although specialized

0147-006X/99/0301-0011$08.00

endothelial cells (ECs) constitute the BBB, neuroscientists do not generally concern themselves with ECs, and those cell biologists who are interested in ECs generally work with cells that are easier to obtain in large numbers, such as those from the aorta. This review describes the basic properties of the BBB and how it develops. A detailed molecular analysis of the BBB is presented first, with emphasis on the junctions that couple neighboring ECs. The final sections analyze the ways in which the properties of the BBB can be regulated and suggest when such regulation may occur.

WHAT IS THE BBB?

Ultrastructure

Early electron microscopic studies using electron-dense tracers revealed that the BBB is an endothelial barrier present in capillaries that course through the brain (Reese & Karnovsky 1967). Astrocytes that contact and influence EC properties do not form a true barrier in vertebrates, although they do in invertebrates (Abbott & Pichon 1987). Ultrastructural studies also pointed out two ways in which ECs in brain differ fundamentally from those in most peripheral tissues. First, they have very few endocytotic vesicles, thereby limiting the amount of transcellular flux. Second, they are coupled by tight junctions, severely restricting the amount of paracellular flux. This combination of features constitutes the BBB (see Figure 1).

Permeability Properties

The BBB significantly impedes entry from blood to brain of virtually all molecules, except those that are small and lipophilic. There are, however, sets of small and large hydrophilic molecules that can enter the brain, and they do so by active transport (Rowland et al 1992). For essential nutrients, such as glucose and certain amino acids (or related molecules, including L-DOPA), specific membrane transporting proteins are present in relatively high concentrations in brain ECs. There also seem to be systems, at least some of which are receptor mediated, capable of shuttling macromolecules into the brain. The best known of these is the transferrin receptor (reviewed in Pardridge 1997), but evidence indicates that other growth factors and cytokines have a limited ability to cross the BBB (McLay et al 1997).

One of the more important transporters is P-glycoprotein, also present in relatively high concentrations on brain capillaries. This transporter works in an opposite direction to those described above. That is, it generally transports back into the blood a variety of lipophilic molecules that enter ECs or penetrate into the brain. This membrane protein is a functional part of the barrier, since P-glycoprotein knock-out mice show enhanced sensitivity to circulating drugs

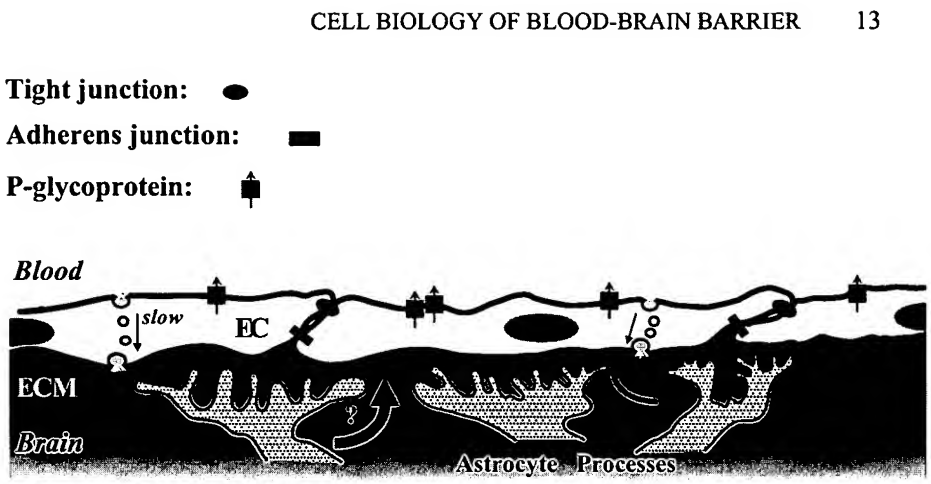

Figure 1 Essential features of the blood-brain barrier. Brain capillary ECs are coupled by adherens and tight junctions, the latter limiting paracellular flux. P-glycoprotein is expressed in the apical membrane of the ECs and actively ejects certain undesired substances from the central nervous system (CNS). Transcytosis across brain ECs occurs slowly, minimizing transcellular movement into the CNS. Astrocyte processes ensheath the ECs, although an extracellular matrix (ECM) is interposed and may release molecules that influence their phenotype. Not shown are the transporters for essential nutrients, such as glucose and certain amino acids, and for macromolecules such as transferrin.

and potential toxins that accumulate in the brain at higher-than-normal levels (Schinkel et al 1994, 1996).

Intercellular Junctions

The permeability properties of the BBB reflect, to a major degree, the tightness of the intercellular junctions. Moreover, as is described below, the junctions are the part of the BBB most likely to be modified in physiological and pathological situations. Therefore, the cell biology of brain EC tight junctions is a major topic in this review.

DEVELOPMENT OF THE BBB

The BBB reflects the combination of low rates of endocytosis and the impermeability of intercellular junctions. These properties are potentially subject to independent regulation. Rates of endocytosis can be determined by measuring the rate at which a marker such as horseradish peroxidase is taken up by the cells. The tightness of junctions, however, is best reflected by their electrical resistance. Unfortunately, there is no direct way of measuring the electrical resistance of capillaries within the brain parenchyma. Instead, direct

electrical resistance measurements have been made on capillaries within the pia mater on the surface of the brain (Butt et al 1990). These junctions do have high resistance, and it is tempting to think of them as being equivalent in all ways to parenchymal capillaries. How true this is remains somewhat unclear.

When blood vessels first enter the brain in rodents, they are discontinuous, much like capillaries in certain peripheral tissues (Kniesel et al 1996). The first known marker of brain ECs appears at E10.5 in mouse, even before astrocytes are present (Qin & Sato 1995). Surprisingly, however, the time of actual barrier formation is somewhat controversial (Saunders et al 1991). In part, this uncertainty relates to the difficulty of assessing barrier function. In adult animals, such an assessment is readily accomplished by introducing dyes or enzymatic tracers into the circulation. In embryonic or neonatal animals, however, the addition of such tracers may actually disrupt the barrier by significantly increasing either the volume of blood or its oncotic pressure.

More important, it now seems unlikely that all of the properties of the BBB are acquired simultaneously. For example, serum proteins are excluded from the brain even at relatively early times in rodent embryos, indicating that a protein barrier is present early in development (Saunders et al 1991). However, the full ionic barrier may not develop until later. Pial vessel resistance measurements, for example, suggest the acquisition sometime after birth of a significant ion barrier with resistance greater than 1000–2000 ohm-cm^2, compared with the 10 ohm-cm^2 characteristic of peripheral capillaries (Butt et al 1990).

INDUCTIVE EVENTS IN BBB FORMATION

The Role of Microenvironment

The BBB forms as brain capillary ECs adopt a phenotype that is distinctly different from that of peripheral capillaries. Stewart & Wiley (1981) examined this process using the classical technique of tissue transplantation between quail and chick embryos. To assess capillary permeability, they injected embryos with one of several cationic dyes that bind tightly to serum albumin and can be used to assess that protein's entry into tissue. They found that gut tissue transplanted to brain was vascularized by ECs from brain that became leaky in their new location. On the other hand, brain tissue transplanted to gut became vascularized by gut ECs that gained the capacity to exclude macromolecules.

Hence, the final microenvironment, rather than the source, of ECs appears to be of prime importance in specifying at least certain cellular properties. That environment is significant is supported by the finding that there is a leaky barrier between the circulation and brain tumors, even though the tumors are vascularized by ECs of brain origin. However, there is a limitation, often overlooked, on the interpretation of transplantation experiments—namely, there

is no way to determine the electrical resistance of EC junctions in the newly vascularized tissue. Therefore, it is not certain that a true high-resistance barrier was formed under these circumstances.

The Role of Astrocytes

Of utmost interest after Stewart & Wiley's work was the determination of the cellular source of factors stimulating partial or complete BBB formation. Structurally, the cell closest to brain capillary ECs is the astrocyte, whose endfeet cover much of the capillary's basal surface. For that reason, Janzer & Raff (1987) investigated the notion that astrocytes might induce ECs to adopt a brain phenotype. They purified and cultured astrocytes from neonatal rat brain and transplanted them onto the chick chorioallantoic membranes and into the rat eye. As before, they assessed barrier properties with the aid of a cationic dye (Evan's blue) that marks albumin flux. Their experiments established that rat astrocytes, in the absence of other cell types, are capable of causing even chick peripheral ECs to become less leaky to large molecules. The reservations pointed out for the chick-quail transplantation experiments apply to these as well. That is, although these experiments are widely quoted as demonstrating that astrocytes induce BBB formation—including high-resistance tight junctions—they do not actually show that.

There are other limitations to reaching this simple conclusion. Holash and associates (1993) were seemingly unable to replicate Janzer & Raff's results, although technical differences between the two sets of experiments may account for this difficulty. Another consideration is that pial vessels, which do have high electrical resistance, are not contacted in the same uniform way by astrocytic endfeet (Allt & Lawrenson 1997; see Cassella et al 1997 for an interesting discussion of potentially variable influences of astrocytes on pial vessels). Also, as mentioned above, at least one differentiated property of brain ECs, the accumulation of P-glycoprotein, appears to be acquired prior to contact with astrocytes. Finally, since the full brain EC phenotype appears likely to be acquired over a period of days to weeks, several different factors, possibly from cells other than astrocytes, might influence EC properties. As to what other cells might be involved, different kinds of nerve endings are found in the vicinity of brain capillaries (Cohen et al 1997), and they could easily be the source of differentiating factors.

CELL CULTURE MODELS OF THE BBB

Early Approaches

There has been considerable interest in establishing BBB cell culture models for two reasons. The first and original reason was to set up an assay system to predict

how well drug candidates would penetrate across the BBB. Such predictions are not easy to make in vivo. Generally, these models have used primary cultures or cell lines established from ECs isolated from bovine, porcine, or rodent brain capillaries (Audus et al 1996). In most cases, the ECs were grown in standard culture conditions—that is, in the presence of high percentages of fetal calf or calf serum. In reality, these cells were thereby removed from the central nervous system (CNS) environment. Virtually uniformly, these cultures did form junctional complexes, but they were not very brain-like, having trans-monolayer resistances of 10 ohm-cm^2 or so, similar to what would be seen with ECs derived from aorta. In view of the experiments described above, this result is not surprising. However, the cells did seem to retain some transport properties similar to those found in vivo (reviewed in Audus et al 1996).

The second major reason for resorting to cell culture models has been to try to understand, in a carefully controlled experimental situation, more about how phenotypic characteristics of capillary ECs are modulated. In culture, numerous properties of ECs, including tight junction resistance, rate of endocytosis, and the presence of specific transporters, can be assayed. In this context, the major goal has been to derive cultures that are quite brain-like. These models have used ECs derived from bovine, porcine, rodent, and even human brain microvessels, with different types of peripheral ECs and with some brain and non-brain EC lines.

Use of Astrocyte-Derived Factors

A frequent strategy has been to use astrocytes to make the culture environment more CNS-like. Clear predictions are difficult, however, since the exact effect of astrocytes is still uncertain. For instance, the ability of astrocytes to induce EC tight junctions of high electrical resistance is not guaranteed by in vivo studies. Also uncertain is the molecular mechanism of astrocyte signaling to ECs. In that regard, the following possibilities must be considered: direct membrane-membrane interactions (probably unlikely); secreted factors that are freely diffusible; secreted factors that are short range, because of either inherent instability (e.g. nitric oxide) or particular molecular characteristics (such as cholesterol addition to the active form of the inducing protein sonic hedgehog, which restricts its diffusion; Porter et al 1996); and secreted factors that localize in the extracellular matrix that separates astrocytes from ECs.

Studies in this area are somewhat compromised in that not all groups report resistance values for their cultures. Rather, they report relative changes in EC permeabilities to small and large tracers, and these results are difficult to compare with brain ECs in situ. Since high-resistance tight junctions are the hallmark of the BBB, it is somewhat surprising that these measurements are not carried out more routinely. This hesitation aside, the greatest degree of success has been achieved with adult brain ECs and astrocytes co-cultured on opposite

sides of porous filters. In this system, astrocyte processes can extend through the pores and terminate close to ECs. Different degrees of induction have been reported, including the achievement of relatively high-resistance monolayers starting with rat brain astrocytes and either bovine brain or bovine aortic ECs (Dehouck et al 1990, Isobe et al 1996, Hayashi et al 1997). In another approach, ECs co-cultured in this manner with astrocytes, but grown in permeable tubes and placed in a flow situation, were reported to achieve remarkably high resistances (Stanness et al 1997).

Numerous studies have utilized conditioned medium generated from cultures of rat brain astrocytes or of C6 glioma cells (Rubin et al 1991, Hurst & Fritz 1996, Raub 1996, Rist et al 1997; reviewed in Cancilla et al 1993). It is somewhat difficult to understand the use of C6 cells given that there is a leaky barrier between blood and glial tumors. In general, the results have been disappointing: High-resistance monolayers of ECs have been achieved only rarely, whether peripheral or brain ECs were used. In most cases, there was either a marginal increase in resistance or resistance results were not reported at all. However, in several cases, significant effects were observed on gross trans-monolayer tracer permeability or on other properties of ECs.

How should these results be interpreted? It may be that very close contact between astrocytes and ECs is required before induction of brain-like endothelial properties can be achieved, and there are other examples of cell-derived inducing molecules that act within only a few cell diameters of their source (Tanabe & Jessell 1996). Little is known about factors made by astrocytes that might have such inducing effects, although astrocytes make numerous signaling molecules, including cytokines of different types and neurotrophins (Ridet et al 1997). Also, the matrix between brain ECs and astrocyte endfeet has at least two potentially important components—an agrin isoform (Barber & Lieth 1997) and $\beta 2$ laminin (Hunter et al 1992)—that are also localized in the extracellular matrix at the neuromuscular junction.

However, even though astrocytes do play a role in BBB induction, they may not be the sole inducers of high-resistance tight junction formation. This possibility would still be consistent with the transplantation experiments, since these measured only decreased albumin flux, which can be obtained with much lower resistance junctions than those present at the BBB. So, it still seems possible that the bulk of the in vitro experiments simply reflect the true situation—that factors from non-astrocyte sources are also significant in regulating tight junction formation.

Other Approaches to Achieving High-Resistance Junctions

Rubin and coworkers (1991) described another method of achieving high-resistance monolayers. They found that elevating cyclic AMP levels in brain ECs pretreated with astrocyte-derived conditioned medium produced a striking

increase in tight junction resistance and structural changes consistent with induction of high-resistance junctional complexes. Since that time, this observation has been repeated in several laboratories (Deli et al 1995, Raub 1996, Rist et al 1997).

This result suggests that it is possible to make ECs more brain-like by bypassing normal inducers of EC differentiation through direct activation of intracellular signaling systems. In the next section, we begin a discussion of the structure of the junctional complex that couples neighboring ECs in both peripheral and brain capillaries. We then return to the issue of how intracellular signaling systems control the structure and function of cellular junctions.

THE JUNCTIONAL COMPLEX: ADHERENS AND TIGHT JUNCTIONS

Because tight junctions probably represent the major functional component of the BBB, the remaining sections of this review focus on their structure and regulation. Until recently, much more was known about epithelial than endothelial junctions because a variety of epithelial cell lines form elaborate junctional complexes that can be investigated easily. Fortunately, recent experiments have shown brain ECs to be very epithelial-like, at least in certain respects.

Numerous studies have demonstrated conclusively that tight junctions depend very much on adherens junctions, where the cell-cell adhesion molecules are found. For example, experiments by Gumbiner & Simons (1986) revealed that antibodies against E-cadherin, the Ca^{2+}-dependent epithelial cell adhesion molecule, block tight junction formation. The presumption, then, is that the normal course of events after cell contact is cadherin-dependent cell adhesion followed by tight junction assembly. Even later, however, tight junction integrity depends on having intact adherens junctions. Thus, perturbations that influence the strength of intercellular adhesion could also affect the "tightness" of tight junctions. Since tight and adherens junctions are spatially and biochemically distinct, adherens junction proteins must indirectly affect tight junction proteins. This must involve cytoplasmic or cytoskeletal components that interconnect the two arrays of junctional molecules.

Tight Junction Proteins

The tight junction is the most apical section of the junctional complex and is clearly separated from the adherens junction in epithelial cells such as MDCK cells (reviewed in Staddon & Rubin 1996). In other types of cells, including brain ECs, there may be some intermixing of adherens and tight junctional complexes in the paracellular cleft (Schulze & Firth 1993). One of the major problems in identifying tight junction components was that it had to be done in the

absence of any known biochemical properties. This problem was solved in part by generating monoclonal antibodies against junctional membrane fractions. The first tight-junction–associated protein to be identified was the 220-kDa protein ZO-1 (Stevenson et al 1986), which is present in both epithelial cells (Stevenson et al 1986) and ECs (Rubin et al 1991, Hirase et al 1997). Cloning and sequencing of the cDNA encoding ZO-1 (Itoh et al 1993, Willott et al 1993) revealed it to be a member of the MAGUK (membrane-associated guanylate kinase) protein family (Anderson 1996), suggesting that it may act in intracellular signaling. Immunoprecipitation experiments on cell extracts then revealed a ZO-1-associated 160-kDa protein, termed ZO-2 (Gumbiner et al 1991), that was found to be related to ZO-1 (Jesaitis & Goodenough 1994). Immunocytochemical experiments have shown that ZO-2 also is present at tight junctions in brain ECs (Schulze et al 1997). The 7H6 antigen (Zhong et al 1993) and cingulin (Citi et al 1988) are additional tight-junction–associated proteins that have yet to be cloned and sequenced. All of the molecules described thus far, although present in the vicinity of tight junctions, are cytoplasmic and could not function as the permeability barrier per se.

More recently, the same general approach led to a significant breakthrough in the identification of the tight junction protein occludin, a four-pass transmembrane protein similar to gap junction connexins (Furuse et al 1993). Although occludin was identified initially in chickens, mammalian homologs were discovered subsequently (Ando-Akatsuka et al 1996). A picture of a complex of proteins at tight junctions is now emerging in which the C-terminal cytoplasmic tail of occludin directly forms a complex with ZO-1 (Furuse et al 1994), which in turn associates with ZO-2. However, even though progress in identifying tight junction components has been significant, the exact role of these proteins in permeability control has yet to be established.

Adherens Junction Proteins

Cell-cell adhesion is dependent on a class of membrane proteins termed cadherins. The classical cadherins, such as E, P, and N, are single-pass transmembrane glycoproteins that interact homotypically in the presence of Ca^{2+} (Takeichi 1995). Peripheral ECs express a more recently discovered cadherin termed VE-cadherin or cadherin-5, which appears to be the major cell-cell adhesion molecule (Lampugnani et al 1995), but it remains unclear which cadherins are expressed in brain ECs (see Liaw et al 1990).

The extracellular binding domain of cadherins is itself insufficient to promote junction formation. Also required is their cytoplasmic tail, which associates with a group of proteins termed catenins (Gumbiner 1996). Initially, three catenins were identified in epithelial cells: α, β, and γ. α-Catenin is a vinculin homolog that binds to β-catenin and probably links cadherins to the actin-based

cytoskeleton. β-Catenin possesses multiple copies of a motif originally identified in the segment polarity gene product Armadillo and binds directly to cadherin. γ-Catenin is related to β-catenin and can substitute for it in the cadherin-catenin complex. Another catenin, p120, is described in more detail below. The catenins link the cadherins to the cytoskeleton and to other signaling components. They are, thereby, part of the system by which adherens and tight junctions communicate. All of them are expressed and localized to junctions in brain ECs as well (Staddon et al 1995a, Schulze et al 1997).

Junctional Proteins and the BBB

How does this structural information contribute to an understanding of BBB formation? It might be expected that tight and adherens junctions between ECs in brain would be distinct in composition from those in the periphery. However, for the most part, this does not appear to be the case. ZO-1 and ZO-2 levels are similar in brain and peripheral ECs, although ZO-1 distribution is continuous in brain ECs but discontinuous in peripheral ECs (Hirase et al 1997). Likewise, α- and β-catenin levels are similar (Hirase et al 1997). Because comparisons of cadherin expression have yet to be carried out, it is still possible that a unique cell adhesion molecule exists in brain ECs.

The one major difference in junction composition between the two types of cells rests in occludin, which is much more strongly expressed in brain ECs (Hirase et al 1997). This difference in expression was seen by immunocytochemical examination of capillaries in tissue sections prepared from peripheral and nervous tissues. A similar difference was observed when ECs cultured from peripheral and brain tissues were compared. Occludin expression in brain ECs was much higher than that in peripheral ECs and more like that in epithelial cells, which have well-developed tight junctions. Large differences were also seen at the mRNA level, suggesting that transcriptional control is involved.

Hirase and coworkers (1997) studied the appearance of occludin at the developing rodent BBB. They found that substantial levels of occludin appeared in brain capillaries only after the first postnatal week in rat. Thus, its appearance correlates with the time of complete development of the BBB. However, the observation that a substantial barrier to serum proteins exists at earlier times in development raises the issue of whether a functional equivalent of occludin exists at these earlier stages.

SIGNALING AND TIGHT JUNCTIONS

At first glance, it might be expected that differences in occludin levels would completely account for differences between central and peripheral capillaries, at least in terms of tight junction permeability. However, this does not appear to

be true. Although high levels of occludin seem to be required to generate fully developed tight junctions (high resistance to ion flux), such high levels are not sufficient to ensure high-resistance junctions. As mentioned previously, when brain ECs are cultured in normal cell culture medium, they have relatively low resistance in spite of having high occludin levels. These observations require that there be another level of control important in determining junctional properties. A large amount of data suggests that the state of phosphorylation of junctional proteins is also centrally involved.

cAMP, the Cytoskeleton, and Junctional Regulation

Mentioned previously was the observation that brain ECs are very sensitive to cAMP elevation. This perturbation in cells derived from bovine, porcine, human, and rodent brains produces an almost immediate elevation of tight junction resistance and a slower reorganization of the actin cytoskeleton (Rubin et al 1991). Untreated cultures contain actin stress fibers throughout their cytoplasm, but after cAMP treatment these stress fibers become less abundant, focal contacts (between cells and substrate) become less pronounced, and the belt of filamentous actin at sites of cell junctions becomes more apparent. Effects on resistance are readily reversible—as cAMP levels return to normal, resistance decreases rapidly. Thus, effects of cAMP on resistance seem likely to be independent of new gene transcription.

The rate of resistance modulation by cAMP suggests the existence of one or more proteins, capable of being phosphorylated by protein kinase A, whose state of phosphorylation controls permeability. These phosphoproteins may either directly regulate tight junction properties or control the strength of cell-cell adhesion. Another possibility is that such phosphoproteins regulate interactions between the membrane and the cytoskeleton. This is supported to some degree by studies on the effects of lysophosphatidic acid. This agent, released from platelets during clotting (Moolenaar 1995) and during other circumstances of cell damage, including stroke, has an effect opposite to that of elevated cAMP (Schulze et al 1997). Lysophosphatidic acid has been suggested to signal by activating rho, a small GTP-binding protein that appears to function in control of stress fiber formation and myosin light chain phosphorylation (Narumiya et al 1997, Hall 1998). cAMP is known to affect myosin light chain phosphorylation and might allow relaxation of the actin-based cytoskeleton, which, because of its linkage to the adherens and tight junctions, could result in strengthened cell-cell contacts and increased tight junction permeability (see Goeckeler & Wysolmerski 1995).

Tyrosine Phosphorylation

A variety of observations indicate that tyrosine phosphorylation of proteins at cell-cell junctions is involved in junctional regulation. Maher & Pasquale

(1988) suggested that decreased tyrosine phosphorylation of proteins at cell-cell contacts during development may correlate with the acquisition of barrier function. Tyrosine kinases of the src family are localized at epithelial cell adherens junctions (Tsukita et al 1991), and β-catenin is one of the proteins that is most highly phosphorylated in src transfected cells (Matsuyoshi et al 1992, Behrens et al 1993, Hamaguchi et al 1993; but see Takeda et al 1995). Furthermore, some evidence, although controversial (Zondag et al 1996), indicates that receptor protein tyrosine phosphatases are associated with the cadherin-catenin complex (Brady-Kalnay et al 1995, Balsamo et al 1996, Fuchs et al 1996, Kypta et al 1996). Thus, cell-cell junctions seem to possess the requisite proteins for signaling via tyrosine phosphorylation. In addition, evidence indicates that inhibition of protein tyrosine phosphatase in epithelial cells increases the degree of tyrosine phosphorylation of junctional proteins and weakens cell adhesion. However, functional evidence that increased tyrosine phosphorylation affected tight junction resistance was not provided until recently.

Such evidence was provided in studies using cultured epithelial and brain ECs treated with tyrosine phosphatase inhibitors (Staddon et al 1995a). This approach resulted in enhanced tyrosine phosphorylation of junctional proteins in both cell types, seen by immunocytochemical and biochemical analysis, and a rapid decrease in tight junction resistance. A more detailed analysis of epithelial cells demonstrated that both β-catenin and ZO-1 were tyrosine phosphorylated (Staddon et al 1995a), suggesting that adherens and tight junction proteins are targets for tyrosine kinases. However, the true physiological significance of this observation remains to be established, and detailed information on situations in which junctional kinases and phosphatases might be activated also is needed. Recent evidence has suggested, however, that the degree of tyrosine phosphorylation of junctional proteins decreases following endothelial cell-cell contact and maturation of junctions (Lampugnani et al 1997).

p120 and Regulation of Junctional Permeability

Another set of observations linking signaling and the regulation of cell junctions derives from experiments analyzing a new cadherin-associated protein, p120, initially discovered as a src substrate phosphorylated during cell transformation (see Daniel & Reynolds 1997). Sequence analysis of p120 revealed the presence of Armadillo repeats similar to those found in β-catenin, but the function of p120 was not clear. Subsequently, several groups realized that a significant portion of p120 and a related protein, p100, were associated with the cadherin/catenin complex (Reynolds et al 1994, Kinch et al 1995, Shibamoto et al 1995, Staddon et al 1995b). This association was seen in both epithelial cells and ECs (Staddon et al 1995b), suggesting that it could play a key role in mediating the effects on cell junctions of phosphorylation by junctional src-like tyrosine

kinases. In later experiments, the state of phosphorylation of p120 and p100, not only on tyrosine but on serine and threonine residues as well, was broadly sensitive to a variety of stimuli that affect tight junction permeability (Ratcliffe et al 1997). However, much remains to be established about p120 signaling pathways before its role in junctional control can be understood.

Occludin Phosphorylation

The preceding discussion focused primarily on changes in cell adhesion produced by phosphorylation of adherens junction proteins and their indirect impact on tight junctions. However, there is also a strong possibility that tight junction proteins, including occludin itself, are phosphorylated (Sakakibara et al 1997). Recent preliminary experiments in our lab suggest that occludin is more highly phosphorylated in cultured brain ECs than in peripheral ECs. However, these studies also suggest that some agents that affect resistance, such as cAMP derivatives and lysophosphatidic acid, do not have obvious effects on occludin phosphorylation. Nonetheless, occludin phosphorylation may be involved in tight junction control under some circumstances.

PHYSIOLOGICAL AND PATHOLOGICAL REGULATION OF BBB PERMEABILITY

One question that becomes immediately relevant is the degree to which observations made on cultured cells apply to understanding control of EC permeability in vivo. Thus far, there does seem to be some predictability. For example, elevation of cAMP levels decreases permeability in both rat pial vessels (Easton et al 1997) and frog peripheral capillaries (He & Curry 1993). Elevated cAMP also seems to lessen the increase in BBB permeability observed after cerebral ischemia (Belayev et al 1997). Finally, the same tyrosine phosphatase inhibitors that so dramatically decrease resistance in cultured ECs and epithelial cells also do so in frog peripheral capillaries (Adamson 1996).

Since tight junctions in culture seem to respond readily to an array of physiological and pharmacological agents, another important question arises: Are there conditions in which BBB permeability, particularly tight junction permeability, is modulated in vivo? It is now agreed that some lesions of the BBB, visible by gadolinium-enhanced magnetic resonance imaging (MRI), are associated with the progression of multiple sclerosis. In this case, gross misregulation of BBB permeability appears to be associated with worsening of the disease and with the sometimes observed brain edema but not with its initial onset (see below, though). Obvious disruption of the BBB can be a relatively major part of the pathology following cerebral ischemia. There is little disagreement over whether a change in permeability occurs, although the timing

and causes have been debated (see Albayrak et al 1997, Belayev et al 1997, Gartshore et al 1997; reviewed in Betz 1996). Different investigators have supported EC damage, increased fluid-phase endocytosis, and modulation of tight junction permeability as being causative. Our position is that altered tight junction permeability is likely to be involved in an essential way.

Another situation in which the BBB is central is that of cell trafficking from blood to brain, a process that takes place under normal and pathological situations. Activated lymphocytes, macrophages, and certain types of metastatic cells can cross the intact BBB. These cells must share an ability to recognize and bind to brain ECs and then initiate junction-opening mechanisms. For lymphocytes, binding has been studied in some detail because even though normal entry and exit of these cells occurs as part of ongoing immune surveillance of the CNS, entry and proliferation of myelin-reactive lymphocytes is thought to be the cause of multiple sclerosis.

What is less clear in these cases is the mechanism of cell entry. Some investigators have claimed that it occurs transcellularly (through brain ECs), while others have claimed paracellular movement (between ECs, by opening junctions). The latter option seems to us to be more likely and more consistent with observations made in instances of cell trafficking across epithelial and peripheral ECs. It has been proposed (Del Maschio et al 1996, Allport et al 1997) that this process can result in destruction of the cadherin/catenin complex, at least when neutrophils and peripheral ECs are involved, although recent evidence favors dissociation rather than destruction (Sandig et al 1997). We favor this latter mechanism, since the process appears to be reversible. In addition, recent data point to technical problems leading to a false conclusion of junction dissolution (Moll et al 1998).

How can cells have the ability to traverse the BBB where small molecules do not? Based on the extensive discussion above, we think it likely that cells traverse the BBB by activating intracellular signaling systems involved in junctional control. For example, bound leukocytes might activate the junctional src-like tyrosine kinases already mentioned. This could happen as a result of leukocytes binding to brain ECs and directly activating intracellular signaling systems or via secretion of cytokine-like molecules by the bound cells. Neutrophils clearly trigger adhesion-dependent EC calcium fluxes that seem to be necessary for transmigration (Huang et al 1993). Transmigration and signaling will undoubtedly be a topic of future investigation.

ONGOING LOCAL REGULATION OF BBB PERMEABILITY

The hallmark of the BBB is its impermeability, but we have already seen instances in which this feature is violated. Also, there are areas of the brain,

such as the circumventricular organs, in which there is no BBB, so it seems as if there can be regional regulation of brain capillary permeability. Recent evidence indicates that capillary permeability is also subject to regulation by conditions such as stress (Friedman et al 1996). In fact, it has been claimed that such effects were involved in enhanced susceptibility to acetylcholinesterase inhibitors used in the Gulf War. As a result of these observations, an interesting possibility may be raised. Can other physiological events, such as increased neural activity, alter BBB permeability? This might promote rapid egress of accumulated ions, neurotransmitters, or other neuroactive agents. If alterations in BBB permeability occur, our prediction is that it will be found to occur by activation of EC junctional kinases and phosphatases.

ACKNOWLEDGMENTS

The authors would like to thank Anne Leeds and Kaye Ferguson for editorial assistance.

Literature Cited

Abbott NJ, Pichon Y. 1987. The glial blood-brain barrier of crustacea and cephalopods: a review. *J. Physiol. (Paris)* 82:304–13

Adamson RH. 1996. Protein tyrosine phosphorylation modulates microvessel permeability in frog mesentery. *Microcirculation* 3:245–47

Albayrak S, Zhao Q, Siesjo BK, Smith ML. 1997. Effect of transient focal ischemia on blood-brain barrier permeability in the rat: correlation to cell injury. *Acta Neuropathol.* 94:158–63

Allport JR, Ding H, Collins T, Gerritsen ME, Luscinskas FW. 1997. Endothelial-dependent mechanisms regulate leukocyte transmigration: a process involving the proteasome and disruption of the vascular endothelial-cadherin complex at endothelial cell-to-cell junctions. *J. Exp. Med.* 186:517–27

Allt G, Lawrenson JG. 1997. Is the pial microvessel a good model for blood-brain barrier studies? *Brain Res. Rev.* 24:67–76

Anderson JM. 1996. Cell signalling: MAGUK magic. *Curr. Biol.* 6:382–84

Ando-Akatsuka Y, Saitou M, Hirase T, Kishi M, Sakakibara A, et al. 1996. Interspecies diversity of the occludin sequence: cDNA cloning of human, mouse, dog and rat-kangaroo homologues. *J. Cell Biol.* 133:43–47

Audus KL, Ng L, Wang W, Borchardt RT. 1996. Brain microvessel endothelial cell culture systems. In *Models for Assessing Drug Absorption and Metabolism*, ed. RT Borchardt, PI Smith, G Wilson, 13:239–58. New York: Plenum

Balsamo J, Leung TC, Ernst H, Zanin MKB, Hoffman S, Lilien J. 1996. Regulated binding of a PTP 1B-like phosphatase to N-cadherin: control of N-cadherin-mediated adhesion by dephosphorylation of β-catenin. *J. Cell Biol.* 134:801–13

Barber AJ, Lieth E. 1997. Agrin accumulates in the brain microvascular basal lamina during development of the blood-brain barrier. *Dev. Dyn.* 208:62–74

Behrens J, Vakaet L, Friis R, Winterhager E, Van Roy F, et al. 1993. Loss of epithelial differentiation and gain of invasiveness correlates with tyrosine phosphorylation of the E-cadherin/beta-catenin complex in cells transformed with a temperature-sensitive v-SRC gene. *J. Cell Biol.* 120:757–66

Belayev L, Busto R, Ikeda M, Rubin LL, Ginsberg MD. 1997. Postischemic administration of BBB022, a cyclic AMP-selective phosphodiesterase inhibitor, protects against blood-brain barrier disruption in focal cerebral ischemia. *Soc. Neurosci.* 23:1377 (Abstract)

Betz AL. 1996. Alterations in cerebral endothelial cell function in ischemia. In *Advances in Neurobiology, Cellular and Molecular Mechanisms of Ischemic Brain Damage*, ed. BK Kiesjo, T Wieloch, pp. 301–13. Philadelphia: Lippincott-Raven

Brady-Kalnay SM, Rimm DL, Tonks NK. 1995. Receptor protein tyrosine phosphatase PTPμ associates with cadherins and catenins in vivo. *J. Cell Biol.* 130:977–86

Butt AM, Jones HC, Abbott NJ. 1990. Electrical resistance across the blood-brain barrier in anaesthetized rats: a developmental study. *J. Physiol. (London)* 429:47–62

Cancilla PA, Bready J, Berliner J. 1993. Astrocyte-endothelial cell interactions. In *Astrocytes: Pharmacology and Function*, ed. S Murphy, 16:383–97. San Diego: Academic

Cassella JP, Lawrenson JG, Firth JA. 1997. Development of endothelial paracellular clefts and their tight junctions in the pial microvessels of the rat. *J. Neurocytol.* 26:567–75

Citi S, Sabanay H, Jales R, Geiger B, Kendrick-Jones J. 1988. Cingulin, a new peripheral component of tight junctions. *Nature* 333: 272–76

Cohen Z, Molinatti G, Hamel E. 1997. Astroglial and vascular interactions of noradrenaline terminals in the rat cerebral cortex. *J. Cereb. Blood Flow Metab.* 17:894–904

Daniel JM, Reynolds AB. 1997. Tyrosine phosphorylation and cadgerin/catenin function. *BioEssays* 19:883–91

Dehouck MP, Meresse S, Delorme P, Fruchart JC, Cecchelli R. 1990. An easier, reproducible, and mass-production method to study the blood-brain barrier in vitro. *J. Neurochem.* 54:1798–801

Deli MA, Dehouck MP, Abraham CS, Cecchelli R, Joo F. 1995. Penetration of small molecular weight substances through cultured bovine brain capillary endothelial cell monolayers: the early effects of cyclic adenosine 3′,5′-monophosphate. *Exp. Physiol.* 80:675–78

Del Maschio A, Zanetti A, Corada M, Rival Y, Ruco L, et al. 1996. Polymorphonuclear leukocyte adhesion triggers the disorganization of endothelial cell-to-cell adherens junctions. *J. Cell Biol.* 135:497–510

Easton AS, Sarker MH, Fraser PA. 1997. Two components of blood-brain barrier disruption in the rat. *J. Physiol.* 503:613–23

Friedman A, Kaufer D, Shemer J, Hendler I, Soreq H, Tur-Kaspa I. 1996. Pyridostigmine brain penetration under stress enhances neuronal excitability and induces early immediate transcriptional response. *Nat. Med.* 2:1382–85

Fuchs M, Muller T, Lerch MM, Ullrich A. 1996. Association of human protein tyrosine phosphatase k with members of the Armadillo family. *J. Biol. Chem.* 271:16712–19

Furuse M, Hirase T, Itoh M, Nagafuchi A, Yonemura S, et al. 1993. Occludin: a novel integral membrane protein localizing at tight junctions. *J. Cell Biol.* 123:1777–88

Furuse M, Itoh M, Hirase T, Nagafuchi A, Yonemura S, et al. 1994. Direct association of occludin with ZO-1 and its possible involvement in the localization of occludin at tight junctions. *J. Cell Biol.* 127:1617–26

Gartshore G, Patterson J, Macrae IM. 1997. Influence of ischemia and reperfusion on the course of brain tissue swelling and blood-brain barrier permeability in a rodent model of transient focal cerebral ischemia. *Exp. Neurol.* 147:353–60

Goeckeler ZM, Wysolmerski RB. 1995. Myosin light chain kinase-regulated endothelial contraction: the relationship between isometric tension, actin polymerization and myosin phosphorylation. *J. Cell Biol.* 130:613–27

Gumbiner BM. 1996. Cell adhesion: the molecular basis of tissue architecture and morphogenesis. *Cell* 84:345–57

Gumbiner BM, Lowenkopf T, Apatira D. 1991. Identification of a 160 kDa polypeptide that binds to the tight junction protein ZO-1. *Proc. Natl. Acad. Sci. USA* 88:3460–64

Gumbiner BM, Simons K. 1986. A functional assay for proteins involved in establishing an epithelial occluding barrier: identification of a uvomorulin-like polypeptide. *J. Cell Biol.* 102:457–68

Hall A. 1998. Rho GTPases and the actin cytoskeleton. *Science* 279:509–14

Hamaguchi M, Matsuyoshi N, Ohnishi Y, Gotoh B, Takeichi M, Nagai Y. 1993. $p60^{v\text{-}src}$ causes tyrosine phosphorylation and inactivation of the N-cadherin-catenin cell adhesion system. *EMBO J.* 12:307–14

Hayashi Y, Nomura M, Yamagishi S-I, Harada S-I, Yamashita J, Yamamoto H. 1997. Induction of various blood-brain barrier properties in non-neural endothelial cells by close apposition to co-cultured astrocytes. *Glia* 19:13–26

He P, Curry FE. 1993. Differential actions of cAMP on endothelial $[Ca^{2+}]$i and permeability in microvessels exposed to ATP. *Am. J. Physiol.* 265:H1019–23

Hirase T, Staddon JM, Saitou M, Ando-Akatsuka Y, Itoh M, Furuse et al. 1997. Occludin as a possible determinant of tight junction permeability in endothelial cells. *J. Cell Sci.* 110:1603–13

Holash HA, Noden DM, Stewart PA. 1993. Re-evaluating the role of astrocytes in blood-brain barrier induction. *Dev. Dyn.* 197:14–25

Huang A, Manning TM, Bandak MC, Ratau KR, Hanser KR, Silverstein SC. 1993.

Endothelial cell cytosolic free calcium regulates neutrophil migration across monolayers of endothelial cells. *J. Cell Biol.* 120:1371–80

Hunter DD, Llinas R, Ard M, Merlie JP, Sanes JR. 1992. Expression of s-laminin and laminin in the developing rat central nervous system. *J. Comp. Neurol.* 323:238–51

Hurst RD, Fritz IB. 1996. Properties of an immortalised vascular endothelial/glioma cell co-culture model of the blood-brain barrier. *J. Cell. Physiol.* 167:81–88

Isobe I, Watanabe T, Yotsuyanagi T, Hazemoto N, Yamagata K, et al. 1996. Astrocytic contributions to blood-brain barrier (BBB) formation by endothelial cells: a possible use of aortic endothelial cell for *in vitro* BBB model. *Neurochem. Int.* 5:523–33

Itoh M, Nagafuchi A, Yonemura S, Kitani-Yasuda T, Tsukita S, Tsukita S. 1993. The 220-kD protein colocalizing with cadherins in non-epithelial cells is identical to ZO-1, a tight junction–associated protein in epithelial cells: cDNA cloning and immunoelectron microscopy. *J. Cell Biol.* 121:491–502

Janzer RC, Raff MC. 1987. Astrocytes induce blood-brain barrier properties in endothelial cells. *Nature* 325:253–57

Jesaitis LA, Goodenough DA. 1994. Molecular characterization and tissue distribution of ZO-2, a tight junction protein homologous to ZO-1 and the Drosophila discs-large tumor suppressor protein. *J. Cell Biol.* 124:949–61

Kinch MS, Clark GJ, Der CJ, Burridge K. 1995. Tyrosine phosphorylation regulates the adhesions of ras-transformed breast epithelia. *J. Cell Biol.* 130:461–71

Kniesel U, Risau W, Wolburg H. 1996. Development of blood-brain barrier tight junctions in the rat cortex. *Dev. Brain Res.* 96:229–40

Kypta RM, Su H, Reichardt LF. 1996. Association between a transmembrane protein tyrosine phosphatase and the cadherin-catenin complex. *J. Cell Biol.* 134:1519–29

Lampugnani MG, Corada M, Cavead L, Breviario F, Ayalon O, et al. 1995. The molecular organization of endothelial cell to cell junctions: differential association of plakoglobin, β-catenin, and α-catenin with vascular endothelial cadherin (VE-cadherin). *J. Cell Biol.* 129:203–17

Lampugnani MG, Corada M, Andriopoulou P, Esser S, Risau W, Dejana E. 1997. Cell confluence regulates tyrosine phosphorylation of adherens junction components in endothelial cells. *J. Cell Sci.* 110:2065–77

Liaw CW, Cannon C, Power MD, Kiboneka PK, Rubin LL. 1990. Identification and cloning of two species of cadherins in bovine endothelial cells. *EMBO J.* 9:2701–8

Maher PA, Pasquale EB. 1988. Tyrosine phosphorylated proteins in different tissue during chick embryo development. *J. Cell Biol.* 106:1747–55

McLay RN, Kimura M, Banks WA, Kastin AJ. 1997. Granulocyte-macrophage colony stimulating factor crosses the blood-brain and blood-spinal cord barriers. *Brain* 120:2083–91

Matsuyoshi N, Hamaguchi M, Taniguchi S, Nagafuchi A, Tsukita S, Takeichi M. 1992. Cadherin-mediated cell-cell adhesion is perturbed by v-src tyrosine phosphorylation in metastatic fibroblasts. *J. Cell Biol.* 118:703–14

Moll T, Dejana E, Vestweber D. 1998. In vitro degradation of endothelial catenins by a neutrophil protease. *J. Cell Biol.* 140:403–7

Moolenaar WH. 1995. Lysophosphatidic acid, a multifunctional phospholipid messenger. *J. Biol. Chem.* 270:12949–52

Narumiya S, Ishizaki T, Watanabe N. 1997. Rho effectors and reorganization of the actin cytoskeleton. *FEBS Lett.* 410:68–72

Pardridge WM. 1997. Drug delivery to the brain. *J. Cereb. Blood Flow Metab.* 17:713–31

Porter JA, Young KE, Beachy PA. 1996. Cholesterol modification of hedgehog signaling proteins in animal development. *Science* 274:255–59

Qin Y, Sato TN. 1995. Mouse multidrug resistance 1a/3 gene is the earliest known endothelial cell differentiation marker during blood-brain barrier development. *Dev. Dyn.* 202:172–80

Ratcliffe MJ, Rubin LL, Staddon JM. 1997. Dephosphorylation of the cadherin-associated p100/p120 proteins in response to activation of protein kinase C in epithelial cells. *J. Biol. Chem.* 272:1–8

Raub TJ. 1996. Signal transduction and glial cell modulation of cultured brain microvessel endothelial cell tight junctions. *Am. Physiol. Soc.* C495–C503

Reese TS, Karnovsky MJ. 1967. Fine structural localization of a blood-brain barrier to exogenous peroxidase. *J. Cell Biol.* 34:207–17

Reynolds AB, Daniel J, McCrea P, Wheelock MJ, Wu J, Zhang Z. 1994. Identification of a new catenin: the tyrosine kinase substrate $p120^{cas}$ associates with E-cadherin complexes. *Mol. Cell Biol.* 14:8333–42

Ridet JL, Malhotra SK, Privat A, Gage FH. 1997. Reactive astrocytes: cellular and molecular cues to biological function. *Trends Neurosci.* 20:570–77

Rist RJ, Romero IA, Chan MWK, Couraud P-O, Roux F, Abbott NJ. 1997. F-actin cytoskeleton and sucrose permeability of immortalised rat brain microvascular endothelial cell monolayers: effects of cyclic AMP

and astrocytic factors. *Brain Res.* 768:10–18

Rowland LP, Fink ME, Rubin LL. 1992. Cerebrospinal fluid: blood-brain barrier, brain oedema and hydocephalus. In *Principles of Neural Science*, ed. ER Kandel, JH Schwartz, T Jessell, pp. 1050–60. New York: Elsevier

Rubin LL, Hall DE, Porter S, Barbu K, Cannon C, et al. 1991. A cell culture model of the blood-brain barrier. *J. Cell Biol.* 115:1725–35

Sakakibara A, Furuse M, Ando-Akatsuka Y, Tsukita S. 1997. Possible involvement of phosphorylation of occludin in tight junction formation. *J. Cell Biol.* 137:1393–401

Sandig M, Negrou E, Rogers KA. 1997. Changes in the distribution of LFA-1, catenins, and F-actin during transendothelial migration of monocytes in culture. *J. Cell Sci.* 110:2807–18

Saunders NR, Dziegielewska KM, Mollgard K. 1991. The importance of the blood-brain barrier in fetuses and embryos. *Trends Neurosci.* 14:14–15

Schinkel AH, Smit JJ, van Tellingen O, Beijnen JH, Wagenaar E, et al. 1994. Disruption of the mouse mdr1a P-glycoprotein gene leads to a deficiency in the blood-brain barrier and to increased sensitivity to drugs. *Cell* 77:491–502

Schinkel AH, Wagenaar E, Mol CAAM, van Deemter L. 1996. P-glycoprotein in the blood-brain barrier of mice influences the brain penetration and pharmacological activity of many drugs. *J. Clin. Invest.* 97:2517–24

Schulze C, Firth JA. 1993. Immunohistochemical localization of adherens junction components in blood-brain barrier microvessels of the rat. *J. Cell Sci.* 104:773–82

Schulze C, Smales C, Rubin LL, Staddon JM. 1997. Lysophosphatidic acid increases tight junction permeability in cultured brain endothelial cells. *J. Neurochem.* 86:991–1000

Shibamoto S, Hayakawa M, Takeuchi K, Hori T, Miyazawa K, et al. 1995. Association of p120, a tyrosine kinase substrate, with E-cadherin/catenin complexes. *J. Cell Biol.* 128:949–57

Staddon JM, Herrenknecht K, Smales C, Rubin LL. 1995a. Evidence that tyrosine phosphorylation may increase tight junction permeability. *J. Cell Sci.* 108:609–19

Staddon JM, Rubin LL. 1996. Cell adhesion, cell junctions and the blood-brain barrier. *Curr. Opin. Neurobiol.* 6:622–27

Staddon JM, Smales C, Schulze C, Esch FS, Rubin LL. 1995b. p120, a p120-related protein (p100) and the cadherin/catenin complex. *J. Cell Biol.* 130:369–81

Stanness KA, Westrum LE, Fornaciari E, Mascagni P, Nelson JA, et al. 1997. Morphological and functional characterization of an in vitro blood-brain barrier model. *Brain Res.* 771:329–42

Stevenson BR, Siciliano JD, Mooseker MS, Goodenough DA. 1986. Identification of ZO-1: a high molecular weight polypeptide associated with the tight junction (zonula occludens) in a variety of epithelia. *J. Cell Biol.* 103:755–66

Stewart PA, Wiley MJ. 1981. Developing nervous tissue induces formation of blood-brain barrier characteristics in invading endothelial cells: a study using quail-chick transplantation chimeras. *Dev. Biol.* 84:183–92

Takeda H, Nagafuchi A, Yonemura S, Tsukita SA, Behrens J, et al. 1995. V-src kinase shifts the cadherin-based cell adhesion from the strong to the weak state and beta catenin is not required for the shift. *J. Cell Biol.* 131:1839–47

Takeichi M. 1995. Morphogenetic roles of classic cadherins. *Curr. Biol.* 7:619–27

Tanabe Y, Jessell TM. 1996. Diversity and pattern in the developing spinal cord. *Science* 274:1115–23

Tsukita S, Oishi K, Akiyama T, Tamanishi Y, Yamamoto T, et al. 1991. Specific proto-oncogenic tyrosine kinases of the src family are enriched in cell-to-cell adherens junction where the level of tyrosine phosphorylation is elevated. *J. Cell Biol.* 113:867–79

Willott E, Balda MS, Fanning AS, Jameson B, Van Itallie C, Anderson JM. 1993. The tight junction protein ZO-1 is homologous to the Drosophila discs-large tumor suppressor protein of septate junctions. *Proc. Natl. Acad. Sci. USA* 90:7834–38

Zhong Y, Saitoh T, Minase T, Sawada N, Enomoto K, Mori M. 1993. Monoclonal antibody 7H6 reacts with a novel tight junction associated protein distinct from ZO-1, cingulin and ZO-2. *J. Cell Biol.* 120:477–83

Zondag GCM, Moolenaar WH, Gebbink MFBG. 1996. Lack of association between receptor protein tyrosine phosphase RPTPμ and cadherins. *J. Cell Biol.* 134:1513–17

Annual Review of Neuroscience
Volume 22, 1999

CONTENTS

J Neural Transm (2006) 113: 1697–1707
DOI 10.1007/s00702-006-0524-4

Journal of Neural Transmission
Printed in Austria

Review

Alzheimer's disease, brain immune privilege and memory: a hypothesis

Y. I. Arshavsky

Institute for Nonlinear Science, University of California San Diego, La Jolla, CA, USA

Received: February 8, 2006 / Accepted: April 28, 2006 / Published online: August 24, 2006

Summary The most distinctive feature of Alzheimer's disease (AD) is the specific degeneration of the neurons involved in memory consolidation, storage, and retrieval. Patients suffering from AD forget basic information about their past, loose linguistic and calculative abilities and communication skills. Thus, understanding the etiology of AD may provide insights into the mechanisms of memory and *vice versa*. The brain is an immunologically privileged site protected from the organism's immune reactions by the blood–brain barrier (BBB). All risk factors for AD (both cardiovascular and genetic) lead to destruction of the BBB. Evidence emerging from recent literature indicates that AD may have an autoimmune nature associated with BBB impairments. This hypothesis suggests that the process of memory consolidation involves the synthesis of novel macromolecules recognized by the immune system as "non-self" antigens. The objective of this paper is to stimulate new approaches to studies of neural mechanisms underpinning memory consolidation and its breakdown during AD. If the hypothesis on the autoimmune nature of AD is correct, the identification of the putative antigenic macromolecules might be critical to understanding the etiology and prevention of AD, as well as for elucidating cellular mechanisms of learning and memory.

Keywords: Alzheimer's disease, immune privilege, blood–brain barrier, autoimmunity, declarative memory

Introduction

The brain is one of the immune privileged sites of the body. This follows from the fact that heterologous tissues implanted in the brain are less susceptible to rejection than the tissues transplanted to other organs (Barker and Billingham, 1977; Ferguson et al., 2002; Pachter et al., 2003; Ransohoff et al., 2003). The important role in maintaining brain immune privilege belongs to the blood–brain barrier (BBB). The detailed description of the BBB is out of the scope of this paper. Here the BBB is regarded as the structural and functional mechanism that protects the brain from the entry of macromolecules, including immunoglobulins (Igs), and restricts the penetration of immunocompetent cells (see below). The functional role of the brain's immune privilege is not entirely understood. A common viewpoint is that immune privilege limits the spread of inflammation in the brain (Ferguson et al., 2002). However, it is possible that immune privilege plays additional roles related to the brain's function of information processing and storage (Peña de Ortiz and Arshavsky, 2001; Arshavsky, 2003a; Peña De Ortiz et al., 2004). This idea is based on a comparison of the brain with other immune privileged organs.

Among other immune privileged organs are the retina, testis, ovary, and fetoplacental unit in the pregnant uterus (Barker and Billingham, 1977; Streilein, 1995; Ferguson et al., 2002). For some of them, the role of immune privilege is well explained. For example, the placental barrier protects the fetus from the mother's immune system. Another example is the testis. The adaptive immune system sorts "self" from "non-self" at the embryonic and neonatal periods, while the maturation of spermatozoa occurs at puberty and an array of new surface molecules is expressed on the differentiating germ cells. These spermatozoon-specific proteins are recognized by the adaptive immune system as non-self antigens (Flickinger et al., 1997; Raghupathy et al., 1989; Filippini et al., 2001). However, the immune reaction against one's own spermatozoa is normally prevented by the blood-testis barrier. A damage of the blood-testis barrier leads to the autoimmune response that eventually results in male sterilization.

Correspondence: Yuri I. Arshavsky, Institute for Nonlinear Science, UCSD, La Jolla, CA 92093-0402, USA
e-mail: yarshavs@ucsd.edu

Based on these comparisons, it is plausible to propose that neurons also produce certain proteins only post-natally, after the maturation of the immune system, and that one of the functions of the brain's immune privilege is to prevent autoimmune responses against these proteins. Recent studies suggest that Alzheimer's disease (AD), characterized by selective neuronal death in the cortical areas responsible for learning and memory, is an autoimmune disorder resulting from BBB disruption (see below). This provokes the idea that processes of memorization involve the synthesis of macromolecules that are absent from the brain at the developmental stages when its immune privilege is formed. In this review, I will discuss the implications of this idea to the existing theories of memory.

Alzheimer's disease and cerebrovascular pathology

AD is a neurodegenerative disease characterized by the formation of amyloid plaques and neurofibrillary tangles. The neuron degeneration in AD brains is area-specific. A massive neural loss occurs primarily in cerebral regions related to the acquisition and storage of declarative memory (the hippocampus and entorhinal cortex, amygdala, and association cortices), but not in primary sensory and motor cortices (Price, 2000; Hof and Mobbs, 2001; Selkoe, 2001; Walsh and Selkoe, 2004). Within the memory-related regions, specific neuronal populations are preferentially vulnerable, whereas other neurons are spared. The main symptom of AD is the impairment and subsequent loss of declarative memory. As was emphasized in a recent review: "Alzheimer's disease characteristically produces a remarkably pure impairment of declarative memory in its earliest stages" (Walsh and Selkoe, 2004). In contrast, other cognitive functions are impaired only in later studies of AD. Therefore, it is very likely that the process of degeneration *specifically* affects those neurons, which serve as the carriers of memory traces. Revealing the mechanism underlying this specificity appears to be crucial in understanding the etiology of AD.

As was highlighted by many authors, the etiology of the severe degeneration of cerebral neurons during AD remains an enigma and this limits the development of therapeutic approaches. The growing bulk of evidence suggests that the development of AD might be related with impairments of the barrier function of the BBB and, therefore, with the abolition of the brain immune privilege. There are two groups of risk factors for AD, cardiovascular (atherosclerosis, hypertension, stroke, traumatic brain injuries, etc.) and genetic. It has been shown that among the effects the cardiovascular factors leading to AD is the interruption of the BBB (reviewed by Sparks, 1997; Kalaria, 1999, 2003; de la Torre, 2002, 2004; Jellinger, 2002; Iadecola, 2004; Sadowski et al., 2004; Jellinger and Attems, 2005; Szczygielski et al., 2005; Zlokovic, 2005). Below I will argue that genetic factors for AD lead to the BBB injuries as well.

AD is characterized by accumulation of the amyloid β peptide (Aβ) in the brain. Aβ is cleaved from the amyloid precursor protein (APP), a transmembrane glycoprotein that is present in most cells. There are various forms of Aβ: the predominant, soluble form of 40 amino acids in length (Aβ1–40) and insoluble form (Aβ1–42). One of the genetic risk factors for AD is the mutation of the *APP* gene leading to the overproduction of Aβ, including its insoluble form. This results in an increased Aβ accumulation in the brain, the formation of amyloid plaques, and eventually AD (Yankner, 1996; Hardy, 1997; Mattson, 1997; Price, 2000; Hof and Mobbs, 2001; Selkoe, 2001; Walsh and Selkoe, 2004). The critical role of Aβ1–42 for the *in vivo* formation of amyloid deposits was recently proved experimentally on transgenic mice that selectively overexpressed either Aβ1–40 or Aβ1–42 (McGowan et al., 2005).

Many studies on AD patients demonstrated that the mutation of the *APP* gene leading to Aβ overproduction results in amyloid accumulation not only in the brain, but also in the walls of cerebral blood vessels (cerebral amyloid angiopathy, CAA) with subsequent BBB impairments (reviewed by Kalaria, 1999, 2003; Jellinger, 2002; Iadecola, 2004; Sadowski et al., 2004; Jellinger and Attems, 2005; Zlokovic, 2005). This was confirmed experimentally on transgenic mice expressing human mutant APP. Just as an AD-like phenotype, CAA developed in transgenic mice overexpressing Aβ1–42, but not in mice overexpressing Aβ1–40 (McGowan et al., 2005). Experimental evidence has been presented that suggests that neuron pathology might be more closely associated with CAA than with accumulation of amyloid plaques within the brain. Intracarotid infusion of Aβ(1–42) rapidly (within 60 min) affects endothelial cells and impairs the BBB in rats (Jancso et al., 1998). In experiments on transgenic mice developing an AD-like phenotype, it was found that memory deficits emerged prior the amyloid plaque formation (Dodart et al., 1999; Moechars et al., 1999; Dewachter et al., 2001; Ujiie et al., 2003; although see Ashe, 2001 for the opposite viewpoint). In addition, it was shown that, in transgenic mice, abnormalities in the BBB permeability preceded cerebral amyloid plaque formation (3–4 months and 9–12 months, respectively). The memory impairments in these mice developed around the age of 6–10 months, when the BBB was severely damaged but the plaques were

not yet formed (Ujiie et al., 2003). All these results suggest that AD neuron pathology and memory deficit resulting from the mutation of the *APP* gene may be more closely related to a faulty BBB than to accumulation of Aβ in the brain.

Other genetic risk factors for AD are the inheritance of the *E4* allele of the *apolipoprotein E* gene that produces a type of lipoprotein (ApoE) participating in a metabolism of cholesterol and other lipids and mutations in the *presenilin 1* and *2* genes that that produce components of secretase complex responsible for the processing of APP. In many studies it was shown that all these factors facilitate not only the accumulation of amyloid plaques in the brain (Strittmatter and Roses, 1996; Yankner, 1996; Price, 2000; Methia et al., 2001; Selkoe, 2001; Walsh and Selkoe, 2004), but also the development of premature atherosclerosis and CAA accompanied by BBB impairments (Sparks, 1997; Kalaria, 1999, 2003; Zarow et al., 1999; Olichney et al., 2000; Methia et al., 2001; Jellinger, 2002; Sadowski et al., 2004; Jellinger and Attems, 2005; Zlokovic, 2005). Moreover, in postmortem studies it was found that the inheritance of the ApoE4 isoform favors intravascular over parenchymal accumulation of Aβ in AD brains (Chalmers et al., 2003).

Degenerative changes of the cerebral vessels and BBB in AD patients were directly shown in autopsies and biopsies (Joachim et al., 1988; Arai et al., 1989; Stewart et al., 1992; Perlmutter, 1994; Vinters et al., 1994; Claudio, 1996; Farkas et al., 2000; Aliev et al., 2003; Jellinger and Attems, 2005; Zlokovic, 2005). As was concluded by Joachim et al. (1988) who studied results of autopsy in the 150 cases, amyloid angiopathy was a constant accompaniment of AD. These findings, as well as results obtained on transgenic mice led some investigators to the suggestion that the primary cause for the onset of AD (caused both cardiovascular disorders and genetic factors) is cerebral vascular pathology leading to the impairment of the barrier function of the BBB (Jancso et al., 1998; Kalaria, 1999, 2003; Miyakawa et al., 2000; de la Torre, 2002, 2004; Aliev et al., 2003; Kumar-Singh et al., 2005). In the next section I will discuss putative mechanisms underlying the connection between a brain immune privilege impairment and AD.

Alzheimer's disease may have autoimmune etiology

At present, many authors accept that the immune system is involved in the etiology of AD. An essential part of AD pathogenesis is the inflammatory process contributing to neurodegeneration (McGeer et al., 1989; McGeer and Rogers, 1992; Singh, 1997; Matyszak, 1998; Gahtan and Overmier, 1999; Gonzalez-Scarano and Baltuch, 1999; Halliday et al., 2000; Akiyama et al., 2000; McGeer and McGeer, 2001; Weninger and Yankner, 2001; Aisen, 2002; Eikelenboom and van Gool, 2004).[1] According to the most common viewpoint, amyloid deposition is the primary factor, which triggers local inflammation involving intracerebral microglia (and probably astroglia) that produce a broad spectrum of inflammatory factors. However, in contrast to this viewpoint, some findings suggest that conversion of soluble Aβ into its fibrillar neurotoxic form is an offshoot of the more fundamental degenerative process initiated by inflammation (see Ringheim and Conant, 2004 for review).

Independent of the cause/effect relationships between the formation of amyloid plaques and brain inflammation,

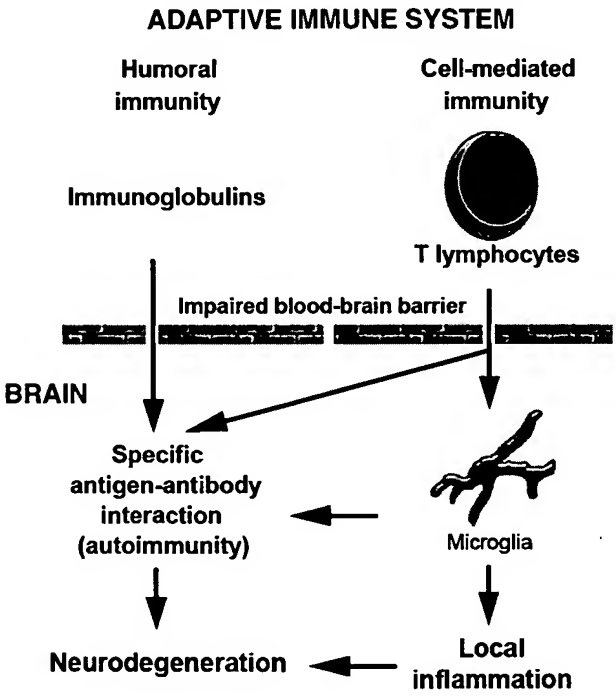

Fig. 1. The illustration of the autoimmune hypothesis for AD. Immunoglobulins and T cells penetrate the impaired BBB and produce an autoimmune reaction leading to specific degeneration of the neurons involved in memory storage and retrieval. In addition, T cells activate microglia that induce local inflammation. Activated microglia may perform the function of antigen-presenting cells (see text for further explanations)

[1] These findings have led to an idea of using anti-inflammatory agents to prevent or alleviate AD symptoms. However clinical trials gave discrepant results (see Akiyama et al., 2000 for review). According to some authors anti-inflammatory drugs inhibit the progress of AD (McGeer and Rogers, 1992; Breitner et al., 1995; Rich et al., 1995; Stewart et al., 1997), whereas others did not confirm this conclusion on a beneficial effect of anti-inflammatory therapy (Aisen, 2002; Wolfson et al., 2002; Eikelenboom and van Gool, 2004).

the concept that the pathogenesis of AD is solely connected with the intracerebral innate immune system resulting in an inflammatory process in the brain has at least two serious limitations. It does not accommodate for the tight connection between BBB dysfunction and the development of AD. More importantly, this concept does not explain the reason for *specific* degeneration of neurons involved in memory storage and retrieval since it is reasonable to expect that an inflammatory process have to lead to non-specific degeneration of all neurons.

The alternative concept suggests that AD is an autoimmune disease and that the adaptive immune system plays a significant role in its pathogenesis (Fig. 1). This concept is based on the results obtained in postmortem immunostaining studies of AD brains and "control" brains taken from individuals of a similar age. These studies have revealed significant penetration of blood proteins, including Igs, into the brain parenchyma of AD patients (Ishii and Haga, 1976; Mann et al., 1982; Licandro et al., 1983). Strong immunostaining by the anti-immunoglobulin serum was observed in those cortical areas that contained numerous amyloid plaques, whereas only minor staining was observed in the areas where few plaques were found. The authors suggested that autoimmune factors could be involved in AD neurodegeneration. However, others argued that Igs are not prominent in AD brains, which led them to conclude that classical autoimmunity is not primary involved in AD (Watts et al., 1981).

The detailed study of a link between a faulty BBB and neuron death in AD patients was recently performed by D'Andrea (2003). The author analyzed postmortem hippocampal and entorhinal tissues from AD patients by using polyclonal anti-Ig antibodies, which recognized all major classes of Igs. As compared to the age-matched controls, a significant increase in Ig staining was detected in both parenchyma and individual neurons of AD tissue (35–40% of neurons in AD brains *versus* <5% in control tissue). Most of the Ig^+ neurons were undergoing degeneration typical of AD. The Ig^+ neurons were intermixed with non-degenerating Ig^- neurons. This is consistent with data showing that only specific neurons are vulnerable to AD (see above).

D'Andrea discussed two hypotheses regarding the cause/effect relationship between Ig positivity in neurons and their degeneration. The autoimmune hypothesis suggests that the immune system attacks neurons after a BBB impairment. In this case, Igs binding to autoantigens exposed on specific neurons, which are involved in the memory storage (see above), leads to their degeneration and death. The alternative hypothesis suggests that the neurons undergoing degeneration during AD express "stress" proteins serving as targets for Igs. In this case, the Ig positivity of neurons is the secondary effect of AD but not its cause. D'Andrea advocates the first hypothesis because, in addition to the neurons showing signs of degeneration, some seemingly healthy neurons were Ig positive as well. This implies that Ig binding precedes morphological degeneration. If the alternative hypothesis were correct, one could expect that Ig binding would appear either simultaneously or after degeneration, and that some Ig^- neurons would have morphological signs of degeneration. Yet neither of these expectations was confirmed in the postmortem immunostaining study (D'Andrea, 2003). Later, additional evidence to support the autoimmune hypothesis of AD was obtained (D'Andrea, 2005). It was found that the Ig^+ neurons were destroyed via the classical pathway of the complement system activated by antigen-antibody complexes and that microglia, performing a phagocytic function in the brain (see Kim and de Vellis, 2005 for a recent review), are more associated with the Ig^+ neurons than the Ig^- neurons.

The hypothesis on the role of humoral immunity in AD was recently reviewed by Bouras et al. (2005). These authors also concluded that Igs penetrate into the brain after an impairment of the BBB and their effects on neuronal pathology can occur at the very early stages of the degenerative process prior to formation of neurofibrillary tangles.

Additional support for the autoimmune hypothesis of AD was obtained in studies of the potential role of T lymphocytes in AD pathology. Although lymphocytes are generally able to penetrate the BBB, only a few T lymphocytes are present within the normal brain. In contrast, significant numbers of both CD4 and CD8 T cells are present in the hippocampus and temporal cortex obtained from the AD patients (Itagaki et al., 1988; Rogers et al., 1988; McGeer et al., 1989; Singh, 1997; Neumann, 2001; Togo et al., 2002). This finding was confirmed in experiments on rats. It was shown that intracarotid injection of Aβ leading to BBB disruption enhanced T lymphocytes migration toward the brain (Farkas et al., 2003). T cell penetration in the brain is accompanied by a markedly increased expression of major histocompatibility complex (MHC) classes I and II molecules, which are necessary for antigen presentation and binding to T cells. MHC molecules are mainly produced by microglia concentrated in areas showing hallmark AD pathology (Itagaki et al., 1988, 1989; Rogers et al., 1988; McGeer et al., 1989; Mattiace et al., 1990; Gonzalez-Scarano and Baltuch, 1999; Szpak et al., 2001; Perlmutter et al., 1992; Kim and de Vellis, 2005; Walker and Lue,

2005). In AD cases, neocortical microglia have the morphology of so-called "activated microglia", with plump somas and thickened processes (Perlmutter et al., 1992). Activated microglia surrounding degenerating neurons were also found in the neocortex and hippocampus of transgenic mice expressing human mutant APP (Stalder et al., 1999; Wegiel et al., 2004; Simard et al., 2006). This suggests that the microglial cells, which are able to phagocytose and display antigen fragments associated with MHC molecules on their surface, may mediate the function of antigen-presenting cells (see Kim and de Vellis, 2005).

Although most authors emphasize that the significance of T cells in the pathogenesis of AD remains unclear, one can hypothesize that the increased migration of T lymphocytes into the specific areas of the brain occurs as a result of a BBB impairment and that it is one of the manifestations of an autoimmune reaction against one's own neurons involved in learning and memory. This hypothesis was distinctly formulated by Singh (1997) as follows: "AD ... may be a cell-mediated neuroautoimmune disease perhaps initiated by the activation of the CD8+ arm of the immunoregulatory network; CD4+ T cells ... may also be involved."

It should be stressed that the autoimmune basis of neuron degeneration during AD does not contradict an involvement of the inflammatory process mediated by the intracerebral innate immune system (see above). Igs and T lymphocytes permeating the BBB and bending antigen-bearing neurons will induce inflammation through the activation of microglia (Fig. 1; see also Singh, 1997; D'Andrea, 2005; Kim and de Vellis, 2005). Such an inflammatory process would be localized in the vicinity of neurons primarily attacked by the adaptive immune system. As most other autoimmune diseases (Abbas and Lichtman, 2003), AD is chronic and slowly progressive.

Autoimmune hypothesis of AD and theories of declarative memory

The idea that AD results from a subtle, permanent autoimmune reaction against specific antigens, exposed by the neurons responsible for memory storage, raises the question of the origin and nature of these antigens. It is plausible to suggest that the origin of these antigens is directly related to the function of these neurons to carry memory traces. Therefore, identification of the specific antigens would be crucial to understanding the neural mechanisms of memory. This brings us to the discussion of how the hypothesis that new antigens are produced by the memory-related neurons after the formation of the brain immune privilege fits with the existing theories of learning and memory.

A key characteristic of declarative memory is its potential permanency. As everybody knows from personal experience, we can recall facts and events that occurred in childhood and have not been recalled in many years. Special psycho-physiological studies indicate that people can store large amounts of information over the entire lifespan, even if this information is useless or never used. For example, in the study of elderly individuals who had taken a Spanish course in school but never used Spanish later, it was found that large portions of the originally acquired knowledge remained accessible for over 50 years (Bahrick, 1984). A similar result was obtained in a study of memory for the names and faces of high school classmates. The participants were able to recognize about 90% of portraits of their classmates 35 years after graduation (Bahrick et al., 1975). The inability to recall certain memories does not necessarily mean that the traces of information are deleted from the brain. The fact and events that seem to be completely forgotten may be revived in a hypnotic state (Luria, 1976) or in response to electrical stimulation of the temporal lobe during brain surgery (Penfield, 1958).

The synaptic plasticity hypothesis of memory

Memorizing new facts and events means that certain physical changes occur within the brain. The lifetime persistence of declarative memory suggests that these changes are extremely stable. The prevailing hypothesis of long-term memory, the synaptic plasticity hypothesis, assumes that traces of memory are stored through the structural modifications of synaptic connections resulting in changes in synaptic efficiency and, therefore, in formations of new patterns of neural activity. These structural modifications require intensive protein synthesis and, indeed, it is well established that inhibition of protein synthesis precludes the consolidation of long-term memory (see Davis and Squire, 1984 for a review). According to the synaptic plasticity hypothesis, input signals act on the glutamatergic receptors of the targeted hippocampal neurons resulting in Ca^{2+} influx. Ca^{2+} initiates an intracellular signaling cascade: the activation of the Ca^{2+}-binding protein calmodulin and adenylyl cyclase, the increased synthesis of cAMP, and the activation of several protein kinases. Activated kinases are translocated to the cell nucleus, where they phosphorylate the cAMP response element-binding protein (CREB). CREB binds to the cAMP-response elements (CRE) of the promoter regions of its target genes and stimulates their transcription. The products of these genes

are transcription factors themselves, and regulate the transcription of the downstream genes. The final step of this cascade is the activation of the genes responsible for the synthesis of the structural proteins involved both in the modification of preexisting synapses and in the formation of new ones (reviewed by Kandel, 2001; Silva, 2003; Lamprecht and LeDoux, 2004; Thomas and Huganir, 2004).

Which of the molecules involved in synaptic rearrangements could be recognized as non-self antigens? Only those molecules that would appear after the brain immune privilege is formed. Brain capillaries start to differentiate into the BBB during the late embryogenesis and the formation of the BBB is completed shortly after birth (Leibowitz and Hughes, 1983; Vorbrodt et al., 2001; Schulze and Firth, 1992; Stonestreet et al., 1996; Lossinsky and Wisniewski, 1998). By that time, most synaptic connections have already been formed and all proteins involved in synaptic transmission are present in the brain. Modifications of the existing synaptic connections do not require synthesis of novel proteins, but rather an enhanced synthesis of already existing proteins. Therefore, proteins synthesized to establish new synaptic connections in the process of memory formation are unlikely to be recognized by the immune system as non-self antigens. It is more plausible to suggest that immunogenic proteins may be produced to mark the distinction between naïve plastic synaptic connections and those formed in the process of memory consolidation.

The permanency of declarative memory means that its consolidation includes not only changes in the strength of synaptic connections, but also an irreversible transfer of the synapses into a rigid state protected from any further changes. As was highlighted by Bailey et al. (2004), "... the structural change once initiated is not sufficient as a maintenance mechanism for long-term memory. The structural change itself must be actively maintained." Different intraneural mechanisms contributing to the local stabilization of learning-related synaptic modifications has been suggested (Bailey et al., 2004; Kelleher et al., 2004; Routtenberg and Rekart, 2005). In particular, it has been hypothesized that the conversion of the neuron-specific isoform of cytoplasmic polyadenelation element binding protein (CPEB) to its self-perpetuating prione state helps to maintain long-term synaptic changes (Bailey et al., 2004; Si et al., 2003a, b). It is possible that the mechanism maintaining the stability of learning-related synaptic modifications includes the production of novel, non-preexisted macromolecules that might be recognized by the immune system as immunogenic.

The genomic hypothesis of memory

An alternative, genomic hypothesis of declarative memory suggests that acquired information is stored within individual neurons through modifications of DNA molecules, and that these modifications serve as the carriers of elementary memory traces. This hypothesis was distinctly formulated by Crick (1984) and Davis and Squire (1984) in their attempt to explain the permanency of memory. Later, the genomic hypothesis was supported by several other authors (Holliday, 1999; De Fonzo et al., 2000; Dietrich and Been, 2001; Peña de Ortiz and Arshavsky, 2001; Arshavsky, 2003a, b; Peña de Ortiz et al., 2004; Levenson and Sweatt, 2005). Peña de Ortiz and Arshavsky further developed the genomic hypothesis of memory (Peña de Ortiz and Arshavsky, 2001; Arshavsky, 2003a, b; Peña de Ortiz et al., 2004) by proposing that permanent memory storage occurs via a mechanism of somatic DNA recombination similar (although not identical) to DNA recombination in the cells of the immune system. Because DNA changes resulting from somatic recombination cannot be reversed or altered (Hochedlinger and Jaenisch, 2002), the recombinant genes would provide a stable basis for the storage of memory. Memory traces coded by recombinant DNA can be deleted from the brain only with the death of proper neurons.

Experimental data, supporting the hypothesis that somatic recombination occurs in postnatal neurons and may be involved in long-term memory, have been obtained. As shown in Fig. 2, the process of DNA recombination is initiated by RAG1 and RAG2. It was found that the process of object recognition learning was impaired in *RAG1* knockout mice (McGowan et al., 2004). Furthermore, DNA recombination critically depends on NHEJ factors responsible for the DNA double strand break repair (Box 1). It has been shown that the level of NHEJ activity in adult rodents is higher in the brain, including the neocortex and hippocampus, than in other tissues (Ren and Peña de Ortiz, 2002). In rats, intracerebroventricular infusion of the DNA ligase inhibitor blocked long-term memory of conditioned taste aversion (Wang et al., 2003) and context fear conditioning (Colón-Cesario et al., 2006) without affecting short-term memory. One of the enzymes participating in DNA recombination is TdT (Box 1). To determine whether the product of the *tdt* gene is related to learning and memory, the expression of the *tdt* gene was studied in mice reared within standard and enriched environments (Peña de Ortiz et al., 2003). Obviously, mice reared in enriched conditions had more possibilities for experience-dependent learning. Experiments were performed on C57Bl/6 and

Box 1. *Mechanism of somatic DNA recombination in the immune system*

V(D)J recombination is of fundamental importance to the production of the antigen-recognizing immunoglobulins and T-cell receptors (Abbas and Lichtman, 2003). Briefly, the antigen-binding molecules include a variable region generated by a combination of noncontiguous V (variable), D (diversity) and J (joining) genes. Their exons consist of a set of non-identical segments. The number of V, D, and J segments is approximately equal to 1000, 15 and 4, respectively (*Germline DNA* in Fig. 2). The joined V and J or V, D, and J gene segments create a single coding unit (*Rearranged VDJ gene*). The

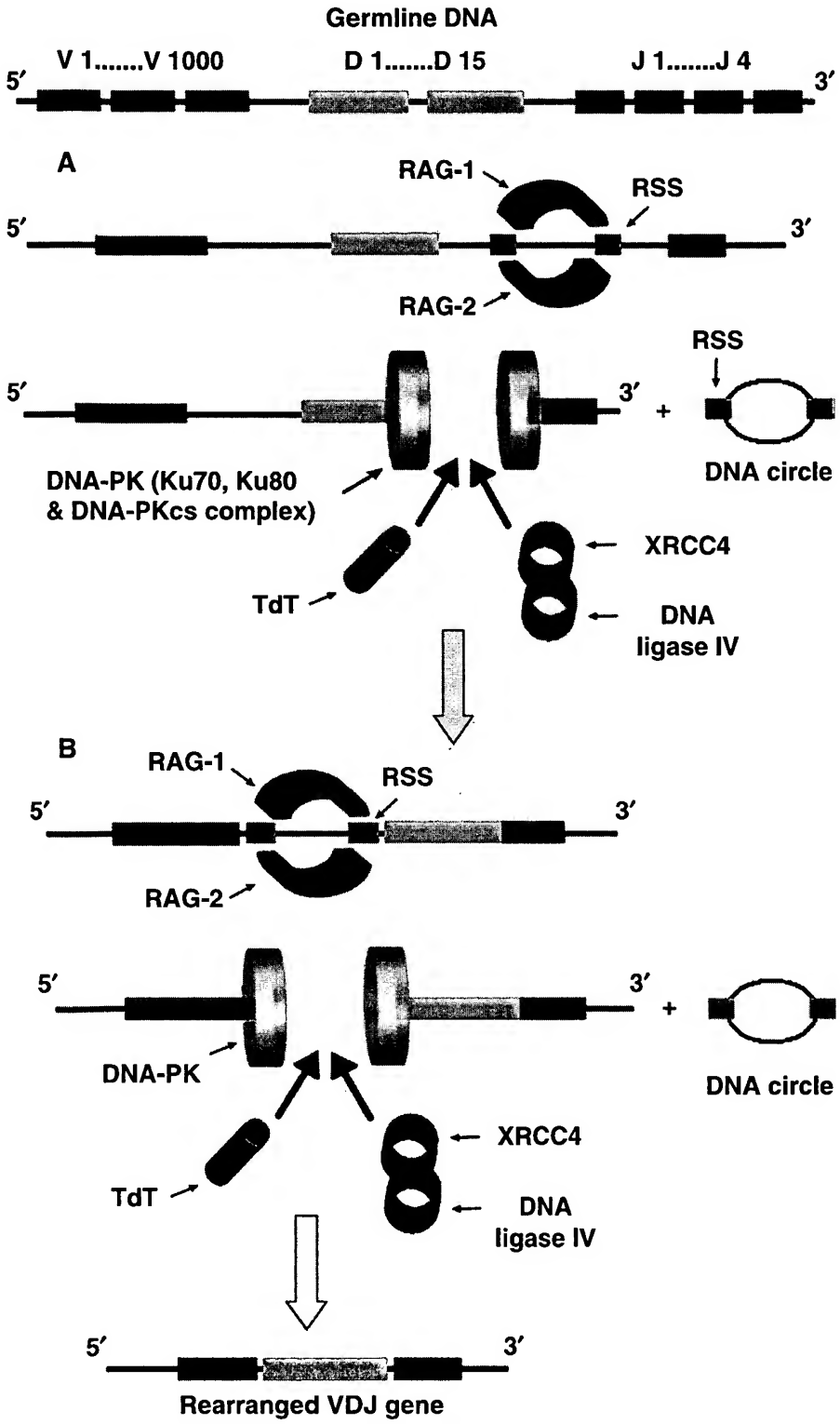

Fig. 2. A scheme of V(D)J recombination. *Germline DNA*: Hypothetical germal DNA containing variable (*V*), diversity (*D*) and joining (*J*) segments of genes to be rearranged. (A) Somatic recombination of D and J segments. RAG-1 and RAG-2 randomly bind to RSSs, flanking both segments, and introduce the double-strand breaks. The deleted portion of a chromosome between two segments forms circular DNA. The non-homologous DNA end joining reaction is performed by the NHEJ machinery, which includes the Ku70, Ku80 and DNA-PKcs complex (*DNA-PK*), the XRCC4/DNA ligase IV heterodimer and TdT (see text for explanation). (B) Somatic recombination of V and D segments. V gene segments are joined to rearranged D-J segments. At the end of the reaction, a *Rearranged V(D)J gene* is produced, which encodes the variable portion of immunoglobulins or T-cell receptors

Box 1 (continued)

random nature of recombination makes a contribution in high diversity of antigen receptors with a relatively modest investment of genetic material.

Figure 2 illustrates the main factors involved in the process of the V(D)J recombination. It is initiated by specific endonucleases (RAG1 and RAG2) which bind to recombination signal sequences (RSS) flanking germal V, D, and J gene segments. RAG1 and RAG2 introduce double-strand breaks between gene segments and RSSs. The ends of the broken DNA molecules are recombined by a non-homologous end joining (NHEJ) mechanism. This phase of V(D)J recombination depends on end-joining enzymes including the Ku70 and Ku80 proteins, DNA-dependent protein kinase catalytic subunit (DNA-PKcs), X-ray cross-complementation factor 4 (XRCC4) and DNA ligase IV. DNA-PKcs, Ku70 and Ku80 are three subunits of the DNA-activated protein kinase (DNA-PK), which initiate the NHEJ reaction. Activated DNA-PK phosphorylates XRCC4, which forms a complex with DNA ligase IV. The DNA ligase IV/XRCC4 heterodimer completes the ligation of DNA double-strand breaks.

The mechanism of junctions between gene segments includes an additional source of diversity. This source is the insertion of template-independent nucleotides (N nucleotides) to exposed 3′ segment termini in the course of V(D)J recombination. N-region diversity results from the activity of a unique DNA polymerase, terminal deoxynucleotidyl transferase (TdT), which lacks template direction. The function of TdT is to add 1–20 random nucleotides to the 3′ ends of double strand breaks of V, D, and J segments in the process of their joining.

DBA/2 inbred mice known as good and poor learners, repectively. The level of *tdt* expression was found to be significantly higher within the hippocampus, cerebellum and neocortex of C57Bl/6 mice reared in enriched conditions. Control experiments on DBA/2 mice showed no increase in *tdt* expression in response to enriched rearing. An involvement of TdT in the process of memory storage was also demonstrated on *tdt* knockout mice tested in a hippocampus-dependent spatial discrimination task. In contrast to wild type animals, knockout mice learned rather poorly and lost traces of memory after an interruption in training. Although the results described in this paragraph are not sufficient to prove the genomic mechanism of memory, they may stimulate further investigation in this direction.

The genomic hypothesis of memory storage is well consistent with the existence of brain immune privilege (Peña de Ortiz and Arshavsky, 2001; Arshavsky, 2003a; Peña de Ortiz et al., 2004). Recombinant genes responsible for carrying traces of permanent memory have to code entirely novel proteins that had not existed at the time when the immune system sorted between self and non-self. Upon the disruption of the BBB, the immune system would be expected to recognize these *de novo* synthesized proteins as non-self antigens. The presence of these proteins might serve as a source of autoimmunity during AD. Thus, the genomic hypothesis brings together the mechanism of memory permanency, the role of brain immune privilege, and the etiology of AD.

Since the genomic hypothesis of memory suggests that recombinant genes serve as permanent templates for novel protein products, the most intriguing issue would be how the brain uses these putative proteins. Different hypothetical scenarios are possible. One of them suggests that modified DNA determines the permanency in changes of synaptic connections (Hilschmann et al., 2001; Frank and Kemler, 2002). Another possibility is that modified genes determine changes of intrinsic neuron properties, such as an excitability and response patterns to income signals (Zhang and Linden, 2003) or some unknown properties that render cortical neurons to be carriers of *consciously-retrieved* traces of memory (Arshavsky, 2003a).

Conclusion

Recent findings strongly suggest that AD is an autoimmune disease resulting from a breakdown of the BBB and brain immune privilege. The autoimmune response targets specific classes of neurons responsible for learning and memory. This line of logic provokes a hypothesis that these neurons contain antigens, which appear postnatally in the process of memory acquisition and consolidation. While still speculative, this hypothesis might stimulate new approaches to studies of neural mechanisms underpinning memory consolidation and its breakdown during AD. According to this hypothesis, identification of the putative antigens causing the autoimmune response during AD may be essential for understanding the etiology and prevention of AD, as well as for elucidating molecular and cellular mechanisms underlying the permanent memory storage.

Acknowledgments

I thank Drs. Sandra Peña De Ortiz and Melissa Colón for valuable discussions of the genomic hypothesis of memory and their help in preparing one of the Figs. I thank Dr. Alexander Chervonsky for helpful discussion of immunological aspects of the paper.

References

Abbas AK, Lichtman AH (2003) Cellular and molecular immunology, 6th edn. Saunders, Philadelphia

Aisen PS (2002) The potential of anti-inflammatory drugs for the treatment of Alzheimer's disease. Lancet Neurol 1: 279–284

Akiyama H, Barger S, Barnum S, Bradt B, Bauer J et al. (2000) Inflammation and Alzheimer's disease. Neurobiol Aging 21: 383–421

Aliev G, Seyidova D, Lamb BT, Obrenovich ME, Siedlak SL, Vinters HV, Friedland RP, LaManna JC, Smith MA, Perry G (2003) Mitochondria and vascular lesions as a central target for the development of Alzheimer's disease and Alzheimer disease-like pathology in transgenic mice. Neurol Res 25: 665–674

Arai H, Sagi N, Noguchi I, Haga S, Ishii T, Makino Y, Kosaka K (1989) An immunohistochemical study of beta-protein in Alzheimer-type dementia brains. J Neurol 236: 214–217

Arshavsky YI (2003a) Cellular and network properties in the functioning of the nervous system: from central pattern generators to cognition. Brain Res Rev 41: 229–267

Arshavsky YI (2003b) Long-term memory: does it have a structural or chemical basis? Trends Neurosci 26: 465–466

Ashe KH (2001) Learning and memory in transgenic mice modeling Alzheimer's disease. Learn Mem 8: 301–308

Bahrick HP (1984) Semantic memory content in permastore: fifty years of memory for Spanish learned in school. J Exp Psychol Gen 113: 1–29

Bahrick HP, Bahrick PO, Wittlinger RP (1975) Fifty years of memories for names and faces. J Exp Psychol Gen 104: 54–75

Bailey CH, Kandel ER, Si K (2004) The persistence of long-term memory; a molecular approach to self-sustaining changes in learning-induced synaptic growth. Neuron 44: 49–57

Barker CF, Billingham RE (1977) Immunologically privileged sites. Adv Immunol 25: 1–54

Bouras C, Riederer BM, Kovari E, Hof PR, Giannakopoulos P (2005) Humoral immunity in brain aging and Alzheimer's disease. Brain Res Rev 48: 477–487

Breitner JC, Welsh KA, Helms MJ, Gaskell PC, Gau BA, Roses AD, Pericak-Vance MA, Saunders AM (1995) Delayed onset of Alzheimer's disease with nonsteroidal antiinflammatory and histamine H2 blocking drugs. Neurobiol Aging 16: 523–530

Chalmers K, Wilcock GK, Love S (2003) APOE epsilon 4 influences the pathological phenotype of Alzheimer's disease by favouring cerebrovascular over parenchymal accumulation of Aβ protein. Neuropathol Appl Neurobiol 29: 231–238

Claudio L (1996) Ultrastructural features of the blood–brain barrier in biopsy tissue from Alzheimer's disease patients. Acta Neuropathol (Berl) 91: 6–14

Colón-Cesario M, Wang J, Ramos X, García HG, Dávila JJ, Laguna J, Rosado G, Peña de Ortiz S (2006) An inhibitor of DNA recombination blocks memory consolidation, but not reconsolidation, in context fear conditioning. J Neurosci 26: 5524–5533

Crick F (1984) Memory and molecular turnover. Nature 312: 101

D'Andrea MR (2003) Evidence linking neuronal cell death to autoimmunity in Alzheimer's disease. Brain Res 982: 19–30

D'Andrea MR (2005) Evidence that immunoglobulin-positive neurons in Alzheimer's disease are dying via the classical antibody-dependent complement pathway. Am J Alzheimers Dis Other Demen 20: 144–150

Davis HP, Squire LR (1984) Protein synthesis and memory: a review. Psychol Bull 96: 518–559

De Fonzo V, Bersani E, Aluffi-Pentini F, Parisi V (2000) A new look at the challenging world of tandem repeats. Med Hypoth 54: 750–760

de la Torre JC (2002) Alzheimer's disease: how does it start? J Alzheimer's Dis 4: 497–512

de la Torre JC (2004) Alzheimer's disease is a vasocognopathy: a new term to describe its nature. Neurol Res 26: 517–524

Dewachter I, Moechars D, van Dorpe J, Tesseur I, Van den Haute C, Spittaels K, Van Leuven F (2001) Modelling Alzheimer's disease in multiple transgenic mice. Biochem Soc Symp 67: 203–210

Dietrich A, Been W (2001) Memory and DNA. J Theor Biol 208: 145–149

Dodart JC, Meziane H, Mathis C, Bales KR, Paul SM, Ungerer A (1999) Behavioral disturbances in transgenic mice overexpressing the V717F beta-amyloid precursor protein. Behav Neurosci 113: 982–990

Eikelenboom P, van Gool WA (2004) Neuroinflammatory perspectives on the two faces of Alzheimer's disease. J Neur Transmiss 111: 281–294

Farkas E, De Jong GI, de Vos RA, Jansen-Steur EN, Luiten PG (2000) Pathological features of cerebral cortical capillaries are doubled in Alzheimer's disease and Parkinson's disease. Acta Neuropath (Berl) 100: 395–402

Farkas IG, Czigner A, Farkas E, Dobo E, Soos K, Penke B, Endresz V, Mihaly A (2003) Beta-amyloid peptide-induced blood–brain barrier disruption facilitates T-cell entry into the rat brain. Acta Histoch 105: 115–125

Ferguson TA, Green DR, Griffith TS (2002) Cell death and immune privilege. Int Rev Immunol 21: 153–172

Filippini A, Riccioli A, Padula F, Lauretti P, D'Alessio A, De Cesaris P, Gandini L, Lenzi A, Ziparo E (2001) Control and impairment of immune privilege in the testis and in semen. Human Reprod Update 7: 444–449

Flickinger CJ, Howards SS, Baran ML, Pessoa N, Herr JC (1997) Appearance of 'natural' antisperm autoantibodies after sexual maturation of normal Lewis rats. J Reprod Immunol 33: 127–145

Frank M, Kemler R (2002) Protocadherins. Curr Opin Cell Biol 14: 557–562

Gahtan E, Overmier JB (1999) Inflammatory pathogenesis in Alzheimer's disease: biological mechanisms and cognitive sequeli. Neurosci Biobehav Rev 23: 615–633

Gonzalez-Scarano F, Baltuch G (1999) Microglia as mediators of inflammatory and degenerative diseases. Annu Rev Neurosci 22: 219–240

Halliday G, Robinson SR, Shepherd C, Kril J (2000) Alzheimer's disease and inflammation: a review of cellular and therapeutic mechanisms. Clin Exp Pharmacol Physiol 27: 1–8

Hardy J (1997) Amyloid, the preselins and Alzheimer's disease. Trends Neurosci 20: 154–159

Hilschmann N, Barnikol HU, Barnikol-Watanabe S, Gotz H, Kratzin H, Thinnes FP (2001) The immunoglobulin-like genetic predetermination of the brain: the protocadherins, blueprint of the neuronal network. Naturwissenschaften 88: 2–12

Hochedlinger K, Jaenisch R (2002) Monoclonal mice generated by nuclear transfer from mature B and T donor cells. Nature 415: 1035–1038

Hof PR, Mobbs CV (2001) Functional neurobiology of aging. Academic Press, San Diego

Holliday R (1999) Is there an epigenetic component in long-term memory? J Theor Biol 200: 339–341

Iadecola C (2004) Neurovascular regulation in the normal brain and in Alzheimer's disease. Nat Rev Neurosci 5: 347–360

Ishii T, Haga S (1976) Immuno-electron microscopic localization of immunoglobulins in amyloid fibrils of senile plaques. Acta Neuropathol (Berl) 36: 243–249

Itagaki S, McGeer PL, Akiyama H (1988) Presence of T-cytotoxic suppressor and leucocyte common antigen positive cells in Alzheimer's disease brain tissue. Neurosci Lett 91: 259–264

Itagaki S, McGeer PL, Akiyama H, Zhu S, Selkoe D (1989) Relationship of microglia and astrocytes to amyloid deposits of Alzheimer's disease. J Neuroimmunol 24: 173–182

Jancso G, Domoki F, Santha P, Varga J, Fischer J, Orosz K, Penke B, Becskei A, Dux M, Toth L (1998) Beta-amyloid (1-42) peptide impairs blood–brain barrier function after intracarotid infusion in rats. Neurosci Lett 253: 139–141

Jellinger KA (2002) Alzheimer disease and cerebrovascular pathology: an update. J Neur Transmiss 109: 813–836

Jellinger KA, Attems J (2005) Prevalence and pathogenic role of cerebrovascular lesions in Alzheimer disease. J Neurol Sci 229–230: 37–41

Joachim CL, Morris JH, Selkoe DJ (1988) Clinically diagnosed Alzheimer's disease: autopsy results in 150 cases. Ann Neurol 24: 50–56

Kalaria RN (1999) The blood–brain barrier and cerebrovascular pathology in Alzheimer's disease. Ann N Y Acad Sci 893: 113–125

Kalaria RN (2003) Vascular factors in Alzheimer's disease. Int Psychogeriatr 15 [Suppl] 1: 47–52

Kandel ER (2001) The molecular biology of memory storage: a dialog between genes and synapses. Biosci Rep 21: 565–611

Kelleher RJ, Govindarajan A, Tonegawa S (2004) Translational regulatory mechanisms in persistent forms of synaptic plasticity. Neuron 44: 59–73

Kim SU, de Vellis J (2005) Microglia in health and disease. J Neurosci Res 81: 302–313

Kumar-Singh S, Pirici D, McGowan E, Serneels S, Ceuterick C, Hardy J, Duff K, Dickson D, Van Broeckhoven C (2005) Dense-core plaques in Tg2576 and PSAPP mouse models of Alzheimer's disease are centered on vessel walls. Am J Pathol 167: 527–543

Lamprecht R, LeDoux J (2004) Structural plasticity and memory. Nat Rev Neurosci 5: 45–54

Leibowitz S, Hughes RAC (1983) Immunology of the nervous system. Edward Arnold, London

Levenson JM, Sweatt JD (2005) Epigenetic mechanisms in memory formation. Nat Rev Neurosci 6: 108–118

Licandro A, Ferla S, Tavolato B (1983) Alzheimer's disease and senile brains: an immunofluorescence study. Rivis Patol Nerv Ment 104: 75–87

Lossinsky AS, Wisniewski HM (1998) Immunoultrastructural expression of ICAM-1 and PECAM-1 occurs prior to structural maturity of the murine blood–brain barrier. Develop Neurosci 20: 518–524

Luria AR (1976) The Neuropsychology of memory. Winston, New York

Mann DM, Davies JS, Hawkes J, Yates PO (1982) Immunohistochemical staining of senile plaques. Neuropathol Appl Neurobiol 8: 55–61

Mattiace LA, Davies P, Dickson DW (1990) Detection of HLA-DR on microglia in the human brain is a function of both clinical and technical factors. Am J Pathol 136: 101–114

Mattson MP (1997) Cellular actions of beta-amyloid precursor protein and its soluble and fibrillogenic derivatives. Physiol Rev 77: 1081–1132

Matyszak MK (1998) Inflammation in the CNS: balance between immunological privilege and immune responses. Progr Neurobiol 56: 19–35

McGeer PL, Akiyama H, Itagaki S, McGeer EG (1989) Immune system response in Alzheimer's disease. Canad J Neurol Sci [Suppl] 16: 516–527

McGeer PL, McGeer EG (2001) Inflammation, autotoxicity and Alzheimer disease. Neurobiol Aging 22: 799–809

McGeer PL, Rogers J (1992) Anti-inflammatory agents as a therapeutic approach to Alzheimer's disease. Neurology 42: 447–449

McGowan E, Pickford F, Kim J, Onstead L, Murphy MP, Beard J, Das P, Jansen K, DeLucia M, Lin WL, Dolios G, Wang R, Eckman CB, Dickson DW, Hutton M, Hardy J, Golde T (2005) Aβ42 is essential for parenchymal and vascular amyloid deposition in mice. Neuron 47: 191–199

McGowan PO, Hope T, Kelsoe GH, Meck WH, Williams CL (2004) Recombination activating gene 1 (RAG1) may have a novel function in brain. Soc Neurosci, 34th Annual Meeting, 32221

Methia N, Andre P, Hafezi-Moghadam A, Economopoulos M, Thomas KL, Wagner DD (2001) ApoE deficiency compromises the blood brain barrier especially after injury. Molec Med 7: 810–815

Miyakawa T, Kimura T, Hirata S, Fujise N, Ono T, Ishizuka K, Nakabayashi J (2000) Role of blood vessels in producing pathological changes in the brain with Alzheimer's disease. Ann N Y Acad Sci 903: 46–54

Moechars D, Dewachter I, Lorent K, Reverse D, Baekelandt V, Naidu A, Tesseur I, Spittaels K, Haute CV, Checler F, Godaux E, Cordell B, Van Leuven F (1999) Early phenotypic changes in transgenic mice that overexpress different mutants of amyloid precursor protein in brain. J Biol Chem 274: 6483–6492

Neumann H (2001) Control of glial immune function by neurons. Glia 36: 191–199

Olichney JM, Hansen LA, Lee JN, Hofstetter CR, Katzman R, Thal LJ (2000) Relationship between severe amyloid angiopathy, apolipoprotein E genotype, and vascular lesions in Alzheimer's disease. Ann NY Acad Sci 903: 138–143

Pachter JS, de Vries HE, Fabry Z (2003) The blood–brain barrier and its role in immune privilege in the central nervous system. J Neuropathol Exp Neurol 62: 593–604

Peña de Ortiz S, Arshavsky YI (2001) DNA recombination as a possible mechanism in declarative memory: a hypothesis. J Neurosci Res 63: 72–81

Peña de Ortiz S, Colón M, Arshavsky YI (2004) Genomic theory of declarative memory. In: Parisi V, De Fonzo V, Aluffi-Pentini F (eds) Dynamical genetics. Signpost, Kerala, pp 345–364

Peña de Ortiz S, Colón M, Carrasquillo Y, Ren K, Padilla B, Silva R, Arshavsky YI (2003) Experience-dependent expression of the gene encoding terminal deoxynucleotidyl transferase in the mouse brain. Neuroreport 14: 1141–1144

Penfield W (1958) Some mechanisms of consciousness discovered during electrical stimulation of the brain. Proc Nat Acad Sci USA 44: 51–66

Perlmutter LS (1994) Microvascular pathology and vascular basement membrane components in Alzheimer's disease. Mol Neurobiol 9: 33–40

Perlmutter LS, Scott SA, Barron E, Chui HC (1992) MHC class II-positive microglia in human brain: association with Alzheimer lesions. J Neurosci Res 33: 549–558

Price DL (2000) Aging of the brain and dementia of the Alzheimer type. In: Kandel ER, Schwartz JH, Jessell TM (eds) Principles of neural science, 4th edn. McGraw-Hill, New York, pp 1149–1161

Raghupathy R, Shaha C, Gupta SK (1989) Autoimmunity to sperm antigens. Curr Opin Immunol 2: 757–760

Ransohoff RM, Kivisakk P, Kidd G (2003) Three or more routes for leukocyte migration into the central nervous system. Nat Rev Immunol 3: 569–581

Ren K, Peña de Ortiz S (2002) Nonhomologous DNA end joining in the mature rat brain. J Neurochem 80: 949–959

Rich JB, Rasmusson DX, Folstein MF, Carson KA, Kawas C, Brandt J (1995) Nonsteroidal anti-inflammatory drugs in Alzheimer's disease. Neurology 45: 51–55

Ringheim GE, Conant K (2004) Neurodegenerative disease and the neuroimmune axis (Alzheimer's and Parkinson's disease, and viral infections). J Neuroimmunol 147: 43–49

Rogers J, Luber-Narod J, Styren SD, Civin WH (1988) Expression of immune system-associated antigens by cells of the human central nervous system: relationship to the pathology of Alzheimer's disease. Neurobiol Aging 9: 339–349

Routtenberg A, Rekart JL (2005) Post-translational protein modification as the substrate for long-lasting memory. Trends Neurosci 28: 12–19

Sadowski M, Pankiewicz J, Scholtzova H, Li YS, Quartermain D, Duff K, Wisniewski T (2004) Links between the pathology of Alzheimer's disease and vascular dementia. Neurochem Res 29: 1257–1266

Schulze C, Firth JA (1992) Interendothelial junctions during blood–brain barrier development in the rat: morphological changes at the level of individual tight junctional contacts. Develop Brain Res 69: 85–95

Selkoe DJ (2001) Alzheimer's disease: genes, proteins, and therapy. Physiol Rev 81: 741–766

Si K, Giustetto M, Etkin A, Hsu R, Janisiewicz AM, Miniaci MC, Kim JH, Zhu H, Kandel ER (2003a) A neuronal isoform of CPEB regulates local protein synthesis and stabilizes synapse-specific long-term facilitation in Aplysia. Cell 115: 893–904

Si K, Lindquist S, Kandel ER (2003b) A neuronal isoform of the aplysia CPEB has prion-like properties Cell 115: 879–891

Silva AJ (2003) Molecular and cellular cognitive studies of the role of synaptic plasticity in memory. J Neurobiol 54: 224–237

Simard AR, Soulet D, Gowing G, Julien JP, Rivest S (2006) Bone marrow-derived microglia play a critical role in restricting senile plaque formation in Alzheimer's disease. Neuron 49: 489–502

Singh VK (1997) Neuroautoimmunity: pathogenic implications for Alzheimer's disease. Gerontology 43: 79–94

Sparks DL (1997) Coronary artery disease, hypertension, ApoE, and cholesterol: a link to Alzheimer's disease? Ann N Y Acad Sci 826: 128–146

Stalder M, Phinney A, Probst A, Sommer B, Staufenbiel M, Jucker M (1999) Association of microglia with amyloid plaques in brains of APP23 transgenic mice. Am J Pathol 154: 1673–1684

Stewart PA, Hayakawa K, Akers MA, Vinters HV (1992) A morphometric study of the blood–brain barrier in Alzheimer's disease. Lab Invest 67: 734–742

Stewart WF, Kawas C, Corrada M, Metter EJ (1997) Risk of Alzheimer's disease and duration of NSAID use. Neurology 48: 626–632

Stonestreet BS, Patlak CS, Pettigrew KD, Reilly CB, Cserr HF (1996) Ontogeny of blood–brain barrier function in ovine fetuses, lambs, and adults. Am J Physiol 271: R1594–R1601

Streilein J (1995) Unraveling immune privilege. Science 270: 1158–1159

Strittmatter WJ, Roses AD (1996) Apolipoprotein E and Alzheimer's disease. Annu Rev Neurosci 19: 53–77

Szczygielski J, Mautes A, Steudel WI, Falkai P, Bayer TA, Wirths O (2005) Traumatic brain injury: cause or risk of Alzheimer's disease? A review of experimental studies. J Neural Transm 112: 1547–1564

Szpak GM, Lechowicz W, Lewandowska E, Bertrand E, Wierzba-Bobrowicz T, Gwiazda E, Schmidt-Sidor B, Dymecki J (2001) Neurones and microglia in central nervous system immune response to degenerative processes part 1: Alzheimer's disease and Lewy body variant of Alzheimer's disease. Quantitative study. Folia Neuropathol 39: 181–192

Thomas GM, Huganir RL (2004) MAPK cascade signaling and synaptic plasticity. Nat Rev Neurosci 5: 173–183

Togo T, Akiyama H, Iseki E, Kondo H, Ikeda K, Kato M, Oda T, Tsuchiya K, Kosaka K (2002) Occurrence of T cells in the brain of Alzheimer's disease and other neurological diseases. J Neuroimmunol 124: 83–92

Ujiie M, Dickstein DL, Carlow DA, Jefferies WA (2003) Blood–brain barrier permeability precedes senile plaque formation in an Alzheimer disease model. Microcirculation 10: 463–470

Vinters HV, Secor DL, Read SL, Frazee JG, Tomiyasu U, Stanley TM, Ferreiro JA, Akers MA (1994) Microvasculature in brain biopsy specimens from patients with Alzheimer's disease: an immunohistochemical and ultrastructural study. Ultrastruct Patholol 18: 333–348

Vorbrodt AW, Dobrogowska DH, Tarnawski M (2001) Immunogold study of interendothelial junction-associated and glucose transporter proteins during postnatal maturation of the mouse blood–brain barrier. J Neurocytol 30: 705–716

Walker DG, Lue LF (2005) Investigations with cultured human microglia on pathogenic mechanisms of Alzheimer's disease and other neurodegenerative diseases. J Neurosci Res 81: 412–425

Walsh DM, Selkoe DJ (2004) Deciphering the molecular basis of memory failure in Alzheimer's disease. Neuron 44: 181–193

Wang J, Ren K, Pérez J, Silva AJ, Peña de Ortiz S (2003) The antimetabolite ara-CTP blocks long-term memory of conditioned taste aversion. Learn Mem 10: 503–510

Watts H, Kennedy PG, Thomas M (1981) The significance of anti-neuronal antibodies in Alzheimer's disease J Neuroimmunol 1: 107–116

Wegiel J, Imaki H, Wang KC, Wegiel J, Rubenstein R (2004) Cells of monocyte/microglial lineage are involved in both microvessel amyloidosis and fibrillar plaque formation in APPsw tg mice. Brain Res 1022: 19–29

Weninger SC, Yankner BA (2001) Inflammation and Alzheimer disease: the good, the bad, and the ugly. Nat Med 7: 527–528

Wolfson C, Perrault A, Moride Y, Esdaile JM, Abenhaim L, Momoli F (2002) A case-control analysis of nonsteroidal anti-inflammatory drugs and Alzheimer's disease: are they protective? Neuroepidemiology 21: 81–86

Yankner BA (1996) Mechanisms of neuronal degeneration in Alzheimer's disease. Neuron 16: 921–932

Zarow C, Zaias B, Lyness SA, Chui H (1999) Cerebral amyloid angiopathy in Alzheimer disease is associated with apolipoprotein E4 and cortical neuron loss. Alzheimer Dis Assoc Disord 13: 1–8

Zhang W, Linden DJ (2003) The other side of the engram: experience-driven changes in neuronal intrinsic excitability. Nat Rev Neurosci 4: 885–900

Zlokovic BV (2005) Neurovascular mechanisms of Alzheimer's neurodegeneration. Trends Neurosci 28: 202–208

DOI 10.1007/s00702-005-0375-4
J Neural Transm (2006) 113: 455–462

Journal of Neural Transmission

Blood–brain barrier dysfunction and recovery

A. G. de Boer and **P. J. Gaillard**

Blood–Brain Barrier Research Group, Division of Pharmacology, Leiden/Amsterdam Center for Drug Research, University of Leiden, Gorlaeus Laboratories, Leiden, The Netherlands

Received June 10, 2005; accepted August 31, 2005

Summary. In this paper we discuss the importance of the blood–brain barrier (BBB) as an interface between blood and brain. Many (brain) diseases change the functionality and integrity of the BBB. Mostly this results in increased BBB permeability. Therefore we have studied de various signal transduction routes that are influenced by inflammatory stimuli. The radical scavenger N-acetylcysteine was able to protect the BBB against inflammatory stimuli. Similar results were found following application of glucocorticoids. In addition, it was observed that glucocorticoids and interferon-α,β increased the tightness of the *in vitro* BBB and when given together a potentiating effect was seen.

Keywords: *In vitro* blood–brain barrier, cell culture, permeability, inflammatory disease, gluocorticoids, interferon-α,β.

Introduction

The blood–brain barrier (BBB) is the interface between blood and brain. It protects the brain against undesirable penetration of compounds and cells. The BBB is localized in the capillary endothelial cells in the brain. The special properties of these cells are mainly induced by brain cells (e.g. astrocytes). Therefore, in this context, the BBB can be considered as an organ that protects and maintains the homeostasis of the brain. Many diseases with an inflammatory component like multiple sclerosis, meningitis, encephalitis, ischemic stroke, head trauma, neurodegenerative diseases like Parkinson's and Alzheimer, AIDS-related dementia, change the functionality and/or integrity of the BBB and thus brain homeostasis. In this paper we describe the effects of lipopolisaccharide (LPS) with and without the application of glucocorticoids and the radical scavenger N-acetylcysteine (NAC), and the interaction between glucocorticoids and type 1 interferons (INF-α,β) on the permeability of the *in vitro* BBB.

Barriers in the brain

Principally drug transport from blood to brain is limited by two barriers, the blood–brain barrier (BBB) and the blood–cerebrospinal fluid barrier (Fig. 1) (de Boer et al., 2003). The BBB is presented by the capillary endothelium in the brain, while the blood–cerebrospinal fluid barrier is presented by the epithelium of choroid plexi in the ventricles in the brain. A third barrier is presented by an epithelial cell layer (the ependyma) that limits the transport of drugs and cells from the

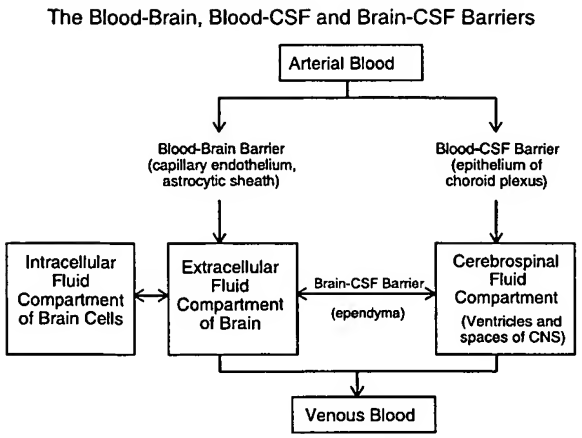

Fig. 1. An overview of the various barriers in the brain. Drugs can enter the brain via the BBB or the B–CSF barrier. The ependyma covers the brain tissue and presents a barrier for the transport between brain and the CSF (de Boer et al., 2003)

cerebrospinal fluid to the brain tissue and vice versa. Since the surface area of the BBB is about 1000 times larger than the area of the blood–cerebrospinal fluid barrier, it can be considered as the most important barrier for the transport of drugs to the brain. In addition, the BBB functions not only as a dynamical physical barrier but also as a metabolic and an immunological barrier to the brain. Its functionality is affected by physiological processes and diseases that subsequently may also influence the paracellular and transcellular transport of drugs.

Properties of the BBB

The capillary endothelium in the brain has special properties when compared to peripheral capillaries. It has narrow tight-junctions, no fenestrate, low pinocytotic activity and a continuous basement membrane. In addition, the endothelial cells have a negative surface charge that repulses negatively charged compounds. They have many mitochondria and

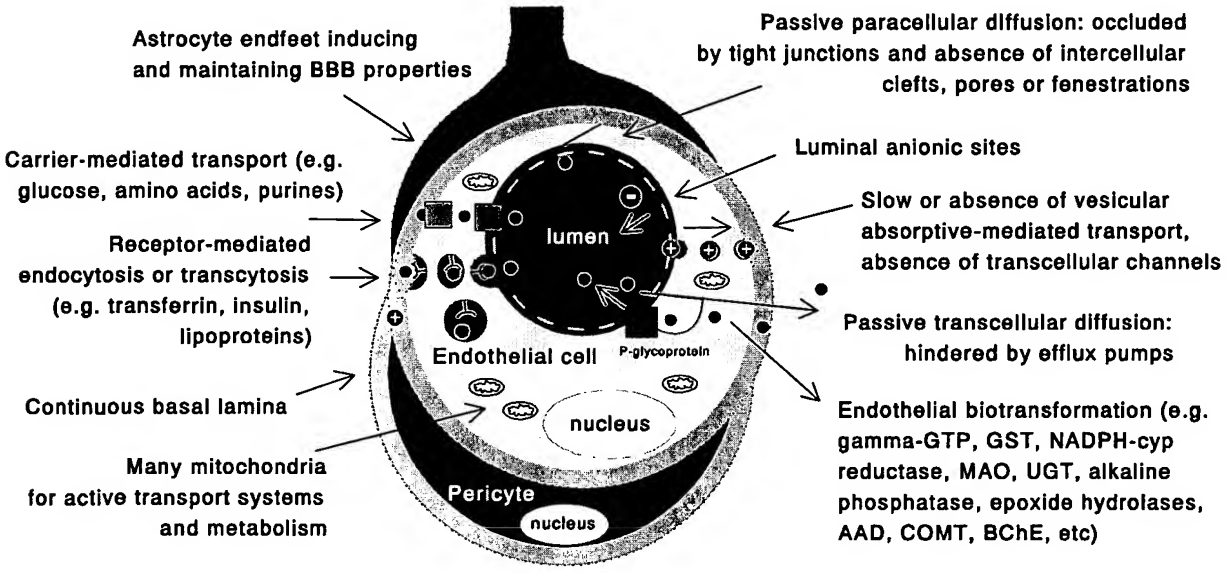

Fig. 2. The various properties of the BBB and the mechanisms for transport of drugs including the localization of the P-glycoprotein efflux system. Drugs may be transported by passive hydrophilic transport via the tight-junctions, passive lipophilic transcellular transport and adsorptive-, carrier-, and receptor-mediated transcytosis. Enzymatic breakdown may occur intra- and extra-cellularly while compounds may be effluxed by e.g. P-glycoprotein. Astrocytes induce the typical BBB properties. *Gamma-GTP* gamma-glutamyl-transpeptidase, *GST* glutathion S-transferase, *NADPH-cyp reductase* NADPH-cytochrome P450 reductase, *MAO* monoamine oxidase type A and B, *UGT* UDP-glucuronosyl transferase, *AAD* L-amino-acid decarboxylase, *COMT* catechol-O-methyl transferase, *BChE* butyryl-cholinesterase (modified from de Boer et al., 2003)

enzymes to break down compounds and various selective transport systems to actively transport nutrients and other compounds (e.g. drugs) into and out of the brain (Fig. 2) (de Boer et al., 2003). The narrow tight-junctions result in a high electrical resistance of 1500–2000 Ohm · cm^2 (Butt, 1995). In contrast, capillaries in the circum-ventricular organs like the area postrema or medial eminence are fenestrated and therefore more permeable for compounds from blood (Wilting and Christ, 1989; Wilting et al., 1995). The endothelium has the property to transdifferentiate from one phenotype to another and vice versa by environmental factors released by astrocytes in the brain which induce many properties in the capillary endothelium (Augustin et al., 1994; Janzer and Raff, 1987). The present understanding of the BBB is that it functions as a dynamically regulated organ, influenced by peripheral (e.g. cortisol, adrenaline) and local (e.g. cytokines, chemokines) hormones. In addition, several cells like pericytes, neurones and cells of the immune system, influence its properties (Ramsauer et al., 1998). Next to that, the endothelium is involved in other processes like coagulation, control of vasotonus, antigen-presentation and the control of the basement membrane by e.g. growth factors. Particularly, under pathological conditions like brain and cerebral inflammation, angiogenesis in brain tumours, the activated endothelium plays an important role (Pardridge, 1991).

Concluding one can say that physiological basis of the BBB is presented by the capillary endothelium together with the various surrounding cells and compounds present in these capillaries. Insight into the dynamics of these systems and knowledge of physico-chemical properties, pharmacokinetics and pharmacodynamics of drugs, gives the possibility to understand BBB functionality and to improve protection against and recovery from damage.

In vitro BBB co-culture model

Research on BBB functionality/recovery has been very much enhanced by the availability of *in vitro* BBB (co)-culture systems and many efforts have been made to develop such systems (Audus and Borchardt, 1986; de Boer and Sutanto, 1997; Dehouck et al., 1990; de Boer and Gaillard, 2002; Gumbleton and Audus, 2001). In addition, the use of such systems allows to study in detail BBB related phenomena at the (sub)-cellular level in the absence of feedback systems from the rest of the body. This makes it much easier to study *in vitro* BBB functionality and BBB (drug) transport by (pharmacological) intervention techniques like the application of receptor agonists and antagonists, blockers of transporters and enzymes, antisense and antigene approaches and the influence of disease. The culture of the *in vitro* BBB involves the isolation of capillaries and culture of BCEC alone or in combination with astrocytes or astrocyte conditioned medium. We have developed in our laboratory an *in vitro* BBB co-culture system comprising bovine brain capillary endothelial cells and new born rat astrocytes (Gaillard et al., 2001). This model has been well characterized and has a relatively high electrical resistance, a small paracellular permeability and expresses various transporters e.g. Pgp (Gaillard and de Boer, 2000).

BBB and (inflammatory) disease

The BBB is sensitive to the pharmacodynamic effects of (endogenous) compounds and disease mediators that may result in changed BBB functionality. Increased BBB permeability for blood compounds has been observed under the influence of diseases, like multiple sclerosis (Williams and Hickey, 1994), Alzheimer (Mattila et al., 1994), AIDS-related dementia (Poland et al., 1995), encephalitis and meningitis (Tunkel and Scheld, 1993), high blood pressure, seizures and by

psychiatric diseases (Black, 1995; Müller, 1995). Excessive amounts of neurotransmitters, cytokines, chemokines and peripheral hormones, can influence BBB functionality. Particularly, excitatory amino acids (Kustova et al., 1999), radical nitrogen (Merrill and Murphy, 1997) and oxygen (Lagrange et al., 1999) species, and pro-inflammatory cytokines (Tsao et al., 2001; Blamire et al., 2000) are able to change BBB functionality and permeability. Bacterial endotoxins like LPS, have shown to increase BBB permeability *in vitro* via several signal transduction routes (Fig. 3) (Boje, 1995; Gaillard et al., 2003). In addition, *in vivo* (rats) it was shown that an inflammatory stimulus at the level of the BBB, such as occur under inflammatory disease conditions (in experimental allergic encephalomyelitis: which is a model for multiple sclerosis), BBB functionality was changed while a systemically administered inflammatory stimulus (LPS) did not (de Vries et al., 1995).

To date, glucocorticoids (i.e. methylprednisolone and prednisone) are the most widely used drugs for the treatment of the acute exacerbations in multiple sclerosis (MS) because of their anti-inflammatory and immunomodulatory properties, but also for their beneficial effect on the BBB (Schluep and Gogousslavsky, 1997). In addition, recombinant human interferon-beta 1b (IFN-β) has been approved for treatment to prevent relapses and disease progression (IFNB Multiple Sclerosis Study Group, 1993; IFNB Multiple Sclerosis Study Group and University of British Columbia MS/MRI Analysis Group, 1995). We have studied therefore these compounds with respect to their effect on the integrity of the *in vitro* BBB.

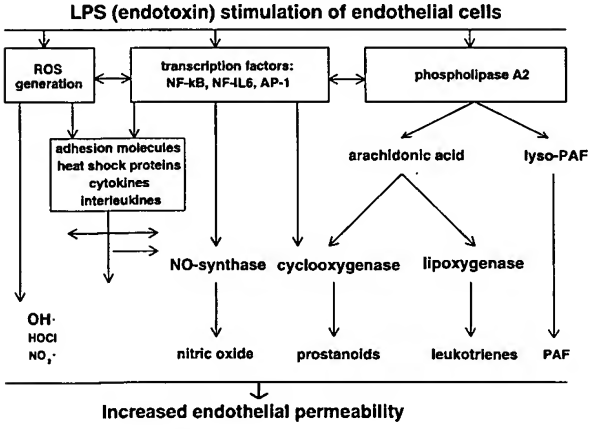

Fig. 3. The various endothelial signal transduction routes and intracellular intermediates that are involved in changed permeability of the *in vitro* BBB following exposure to lipopolysaccharide (LPS). *ROS* radical oxygen species, *NF-kB* nuclear factor-kappa-B, *NF-IL6* nuclear factor-interleukine-6, *AP-1* activation-factor-1, *PAF* platelet activating factor (modified from Gaillard et al., 2003)

Results and discussion

With the *in vitro* BBB co-culture system we have pharmacologically investigated the signal transduction routes that were involved in the change in BBB functionality/permeability following stimulation with LPS. The various routes have been indicated in Fig. 3. In addition, it can be seen that monolayers of endothelial cells were not able to recover from an inflammatory stimulus (Fig. 4). In contrast, co-cultures of endothelial cells and astrocytes showed resistance to and recovery from an inflammatory stimulus and dose dependent protection by glucocorticoids was found following stimulation with LPS (Gaillard et al., 2003). Glucocorticoids (e.g. dexamethason) inhibit e.g. phospholipase-A_2 and various genes but also activate genes that are involved in the cellular protection and recovery. Monolayers of BCEC were less resistant and recovery was less following stimulation with LPS than co-cultures with astrocytes. Moreover, glucocorticoids (dexamethason) were able to improve the recovery following an LPS stimulus (Fig. 4). Inhibition of signal transduction routes involving cyclo-oxygenase and lipoxygenase did not give any protection against an LPS stimulus. Therefore, it was con-

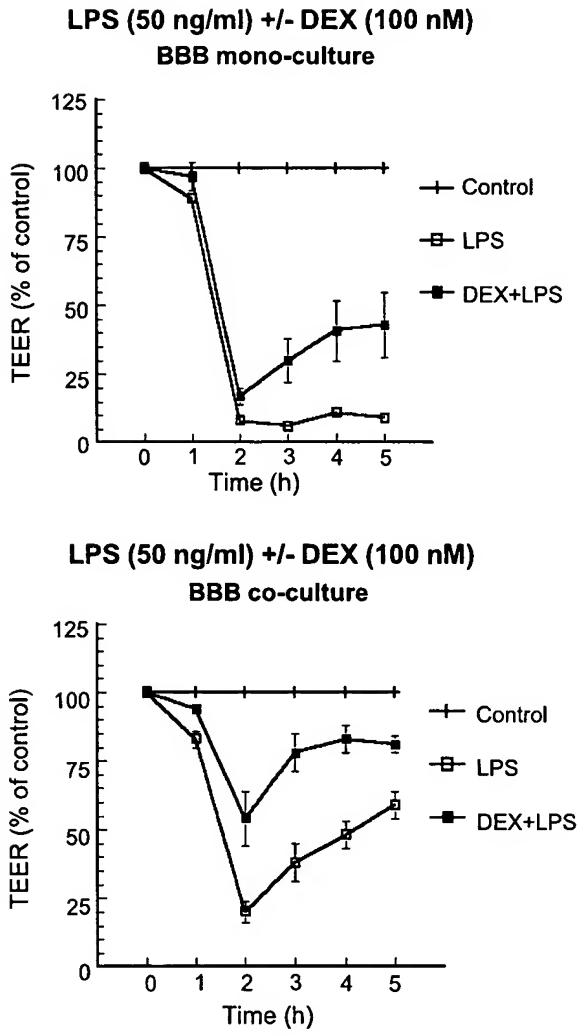

Fig. 4. An overnight 100 nM dexamethason (DEX) pretreatment protects against the 50 ng/ml LPS-induced disruption of BCEC monolayers (top panel) and BCEC + astrocyte co-cultures (bottom panel) and enhances recovery. *TEER* trans-endothelial-electrical-resistance (modified from Hoheisel et al., 1998)

cluded that other signal transduction routes were involved that played a more important role in the cellular damage following an LPS stimulus. For instance, following LPS treatment compounds like nitrogen monoxide (NO), superoxide anion ($O_2^{\bullet}$), hydroxyl radical ($OH^{\bullet}$) and hydrogen peroxide (H_2O_2) may be produced. Therefore, we applied single radical scavengers like uric acid (that binds peroxynitrite) and monomethyl-L-arginine acetate (NMMA; that inhibits NO-synthase) but these did not give any protection. In contrast, application of the multi radical scavenger N-acetylcysteine (NAC; that binds both NO and ($O_2^{\bullet}$)) gave a complete protection against an LPS stimulation (Gaillard et al., 2003).

In our *in vitro* model of the BBB it was found that both glucocorticoids and type 1 interferons (IFN-α,β) decreased the permeability of the BBB (i.e. increase of transendothelial electrical resistance (TEER)) in a dose- and time-dependent manner (Fig. 5) (Gaillard et al., 2001). In fact, the glucocorticoid receptor agonist RU28362 was found to be about 100 fold more potent than the endogenous ligand corticosterone, where IFN-α was found to be about 10 fold more potent than IFN-β. In these studies, however, no effect of human IFN-γ was observed, possibly because of species differences between human IFN-γ and bovine endothelial cells (Pestka and Meager, 1997). Species differences in the IFN-receptor may also explain the differences in potency found following

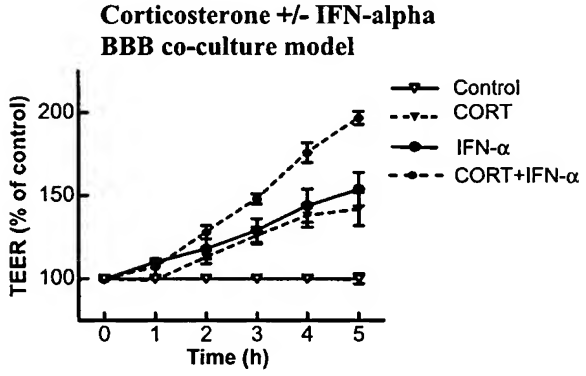

Fig. 5. Glucocorticoids and type 1 interferons have additive affects on the increase in TEER across BCEC + astrocyte co-cultures: Corticosterone (100 nM) gradually increased TEER across BCEC + astrocyte co-cultures, IFN-α (300 U/ml) also gradually increased TEER, where co-incubation of corticosterone and IFN-α increased TEER in an additive manner (modified from Gaillard et al., 2001)

administration of IFN-α and IFN-β (Gaillard et al., 2001) since we were using a xenogenic co-culture model. In addition, no data are available about the cross-reactivity of IFN-α in our cell culture experiments. Nevertheless, these findings may be relevant for the development of therapeutic strategies aimed to protect or restore the compromised integrity of the BBB associated with MS. Potentially also other BBB related diseases may benefit from such strategies. Furthermore, it was found that type 1 interferons highly potentiated the effect of glucocorticoids. This lead us to suggest that type 1 interferons may restore the dysfunctional T helper 1 (Th1)/Th2 balance associated with MS, by an increased sensitivity for glucocorticoids (Gaillard et al., 2001).

Conclusions

It can be concluded that the blood–brain barrier is a functional system that can be considered as an organ where various mechanisms and systems play an operational role, locally as well as in time. Therefore, the isolation and culture of brain capillary endothelial cells (BCEC) has tremendously enhanced research on BBB functionality and our understanding of drug transport across the BBB into the brain, particularly at the (sub)cellular level. The use of isolated systems, such as the BBB co-culture system, allows a detailed study of BBB related phenomena in the absence of feedback systems in the rest of the body. This makes it much easier to study *in vitro* BBB transport and BBB functionality by (pharmacological) intervention techniques.

With the BBB co-culture system, we were able to study the functionality and recovery of the BBB under disease (e.g. inflammation) conditions. It was shown that glucocorticoids were able to protect the *in vitro* BBB against an inflammatory stimulus and to increase its recovery. The inhibition/scavenging of various intracellular mediators was investigated but only the multi-radical scavenger NAC was able to protect the *in vitro* BBB against damage caused by inflammatory stimuli (Hoheisel et al., 1998).

Furthermore, it was shown that glucocorticoids and type 1 interferons were able to increase the electrical resistance (TEER) across the BBB endothelium (Gaillard et al., 2003) similar to type-I interferon experiments that showed an enhanced TEER across the blood–retina barrier (Gillies and Su, 1995). In addition, recently these observations were confirmed in-vitro in a human- and a bovine-blood–brain barrier cell culture system (Harzheim et al., 2004; Kraus et al., 2005). Furthermore, using our *in vitro* BBB co-culture system, we have demonstrated a potentiating effect of type-I interferons on the glucocorticoid effect at TEER (Gaillard et al., 2001).

References

Audus KL, Borchardt RT (1986) Characterization of an *in vitro* blood–brain barrier model system for studying drug transport and metabolism. Pharm Res 3: 81–87

Augustin HG, Kozian DH, Johnson RC (1994) Differentiation of endothelial cells: analysis of the constitutive and activated endothelial cell phenotypes. Bioessays 16(12): 901–906

Black KL (1995) Biochemical opening of the blood–brain barrier. Adv Drug Deliv Rev 15: 37–52

Blamire AM, Anthony DC, Rajagopalan B, Sibson NR, Perry VH, Styles P (2000) Interleukin-1beta-induced changes in blood–brain barrier permeability, apparent diffusion coefficient, and cerebral blood volume in the rat brain: a magnetic resonance study. J Neurosci 20(21): 8153–8159

Boje KM (1995) Cerebrovascular permeability changes during experimental meningitis in the rat. J Pharmacol Exp Ther 274: 1199–1203

Butt AM (1995) Effect of inflammatory agents on electrical resistance across the blood–brain barrier in pial microvessels of anaesthetized rats. Brain Res 696: 145–150

de Boer AG, Sutanto W (eds) (1997) Drug transport across the blood–brain barrier: new experimental strategies. Harwood Scientific Publisher, Amsterdam

de Boer AG, Gaillard PJ (2002) *In vitro* models of the blood–brain barrier: when to use which? Current Medicinal Chemistry – Central Nervous System Agents 2(3): 203–209

de Boer AG, van der Sandt ICJ, Gaillard PJ (2003) The role of drug transporters at the BBB. Ann Rev Pharmacol Tox 43: 629–656

de Vries HE, Eppens EF, Prins M, Kuiper J, Van Berkel ThJC, De Boer AG, Breimer DD (1995) Blood–brain barrier permeability during experimental allergic encephalomyelitis and acute septic shock. Pharm Res 12(12): 1932–1936

Dehouck M-P, Méresse S, Delorme P, Fruchart J-C, Cecchelli R (1990) An easier, reproducible, and mass-production method to study the blood–brain barrier *in vitro*. J Neurochem 54: 1798–1801

Gaillard PJ, De Boer AG (2000) Relationship between permeability status of the blood–brain barrier and *in vitro* permeability coefficient of a drug. Eur J Pharm Sci 12: 95–102

Gaillard PJ, De Boer AG, Breimer DD (2003) Pharmacological investigations on lipopolysaccharide-induced permeability changes in the blood–brain barrier *in vitro*. Microvasc Res 65(1): 24–31

Gaillard PJ, Voorwinden LH, Nielsen JL, Ivanov A, Atsumi R, Engman H, Ringbom C, De Boer AG, Breimer DD (2001) Establishment and functional characterization of an *in vitro* model of the blood–brain barrier, comprising a co-culture of brain capillary endothelial cells and astrocytes. Eur J Pharm Sci 12: 215–222

Gaillard PJ, Van Der Meide PH, De Boer AG, Breimer DD (2001) Glucocorticoid and type I interferon interactions at the blood–brain barrier: relevance for drug therapies for multiple sclerosis. Neuroreport 12(10): 2189–2193

Gillies MC, Su T (1995) Interferon-alpha 2b enhances barrier function of bovine retinal microvascular endothelium *in vitro*. Microvasc Res 49(3): 277–288

Gumbleton M, Audus KL (2001) Progress and limitations in the use of *in vitro* cell cultures to serve as a permeability screen for the blood–brain barrier. J Pharm Sci 90(11): 1681–1698

Harzheim M, Stepien-Mering M, Schroder R, Schmidt S (2004) The expression of microfilament-associated cell–cell contacts in brain endothelial cells is modified by IFN-beta1a (Rebif). J Interferon Cytokine Res 24(12): 711–716

Hoheisel D, Nitz T, Franke H, Wegener J, Hakvoort A, Tilling T, Galla HJ (1998) Hydrocortisone reinforces the blood–brain properties in a serum free cell culture system. Biochem Biophys Res Commun 247(2): 312–315

IFNB Multiple Sclerosis Study Group (1993) Interferon beta-1b is effective in relapsing-remitting multiple sclerosis. I. Clinical results of a multicenter, randomized, double-blind, placebo-controlled trial. Neurology 43: 655–661

IFNB Multiple Sclerosis Study Group and University of British Columbia MS/MRI Analysis Group (1995) Interferon beta-1b in the treatment of multiple sclerosis: final outcome of the randomized controlled trial. Neurology 45: 1277–1285

Janzer RC, Raff MC (1987) Astrocytes induce blood–brain barrier properties in endothelial cells. Nature 325: 253–257

Kraus J, Ling AK, Hamm S, Voigt K, Oschmann P, Engelhardt B (2005) Interferon-beta stabilizes barrier characteristics of brain endothelial cells in vitro. Ann Neurol 56(2): 192–205

Kustova Y, Grinberg A, Basile AS (1999) Increased blood–brain barrier permeability in lp-bm5 infected mice is mediated by neuroexcitatory mechanisms. Brain Res 839(1): 153–163

Lagrange P, Romero IA, Minn A, Revest PA (1999) Transendothelial permeability changes induced by free radicals in an *in vitro* model of the blood–brain barrier. Free Radic Biol Med 27(5–6): 667–672

Mattila KM, Pirtilä T, Blennow K, Wallin A, Vitanen M, Frey H (1994) Altered blood–brain barrier function in alzheimer's disease? Acta Neurol Scand 89: 192–198

Merrill JE, Murphy SP (1997) Inflammatory events at the blood brain barrier: regulation of adhesion molecules, cytokines, and chemokines by reactive nitrogen and oxygen species. Brain Behav Immun 11(4): 245–263

Müller N (1995) Psychoneuroimmunology: implications for the drug treatment of psychiatric disorders. CNS Drugs 4(2): 125–140

Pardridge WM (1991) Peptide drug delivery to the brain. Raven Press, New York

Poland SD, Rice GPA, Dekaban GA (1995) HIV-1 infection of human brain-derived microvascular endothelial cells *in vitro*. J Acquir Immune Defic Syndr Hum Retrovirol 8: 437–445

Ramsauer M, Kunz J, Krause D, Dermietzel R (1998) Regulation of a blood–brain barrier-specific enzyme expressed by cerebral pericytes (pericytic aminopeptidase) under cell culture

conditions. J Cereb Blood Flow Metab 18: 1270–1281

Schluep M, Bogousslavsky J (1997) Emerging treatments in multiple sclerosis. Eur Neurol 38: 216–221

Tsao N, Hsu HP, Wu CM, Liu CC, Lei HY (2001) Tumor necrosis factor-alpha causes an increase in blood–brain barrier permeability during sepsis. J Med Microbiol 50(9): 812–821

Tunkel A, Scheld WM (1993) Pathogenesis and pathophysiology of bacterial meningitis. Ann Rev Med 44: 103–120

Williams KC, Hickey WF (1994) Immunology of multiple sclerosis. Clin Neurosci 2: 229–245

Wilting J, Brand-Saberi B, Kurz H, Christ B (1995) Development of the embryonic vascular system. Cell Mol Biol Res 41(4): 219–232

Wilting J, Christ B (1989) An experimental and ultrastructural study on the development of the avian choroid plexus. Cell Tissue Res 255: 487–494

Authors' address: A. G. de Boer, Blood–Brain Barrier Research Group, Division of Pharmacology, Leiden/Amsterdam Center for Drug Research, University of Leiden, Gorlaeus Laboratories, P.O. Box 9502, 2300 RA Leiden, The Netherlands,
e-mail: B.Boer@LACDR.LeidenUniv.NL

Cellular and Molecular Neurobiology, Vol. 25, No. 1, February 2005 (©2005)
DOI: 10.1007/s10571-004-1377-8

Permeability Studies on In Vitro Blood–Brain Barrier Models: Physiology, Pathology, and Pharmacology

Mária A. Deli,[1,5] Csongor S. Ábrahám,[2] Yasufumi Kataoka,[3] and Masami Niwa[4]

Received October 23, 2003; accepted March 25, 2004

SUMMARY

1. The specifically regulated restrictive permeability barrier to cells and molecules is the most important feature of the blood–brain barrier (BBB). The aim of this review was to summarize permeability data obtained on in vitro BBB models by measurement of transendothelial electrical resistance and by calculation of permeability coefficients for paracellular or transendothelial tracers.

2. Results from primary cultures of cerebral microvascular endothelial cells or immortalized cell lines from bovine, human, porcine, and rodent origin are presented. Effects of coculture with astroglia, neurons, mesenchymal cells, blood cells, and conditioned media, as well as physiological influence of serum components, hormones, growth factors, lipids, and lipoproteins on the barrier function are discussed.

3. BBB permeability results gained on in vitro models of pathological conditions including hypoxia and reoxygenation, neurodegenerative diseases, or bacterial and viral infections have been reviewed. Effects of cytokines, vasoactive mediators, and other pathogenic factors on barrier integrity are also detailed.

4. Pharmacological treatments modulating intracellular cyclic nucleotide or calcium levels, and activity of protein kinases, protein tyrosine phosphatases, phospholipases, cyclooxygenases, or lipoxygenases able to change BBB integrity are outlined. Barrier regulation by drugs involved in the metabolism of nitric oxide and reactive oxygen species, as well as influence of miscellaneous treatments are also listed and evaluated.

5. Though recent advances resulted in development of improved in vitro BBB model systems to investigate disease modeling, drug screening, and testing vectors targeting the brain, there is a need for checking validity of permeability models and cautious interpretation of data.

KEY WORDS: blood–brain barrier; cerebral endothelial cells; coculture; in vitro model; permeability; transendothelial electrical resistance.

[1] Laboratory of Molecular Neurobiology, Institute of Biophysics, Biological Research Centre of the Hungarian Academy of Sciences, Temesvári körút 62, H-6726 Szeged, Hungary.
[2] N-Gene Research Laboratories, Csillagvirág utca 8, H-1106 Budapest, Hungary.
[3] Department of Pharmaceutical Care and Health Sciences, Faculty of Pharmaceutical Sciences, Fukuoka University, 8-19-1 Nanakuma, Fukuoka 814-0180, Japan.
[4] Department of Pharmacology 1, Nagasaki University School of Medicine, 1-12-4 Sakamoto, Nagasaki 852-8523, Japan.
[5] To whom correspondence should be addressed at Laboratory of Molecular Neurobiology, Institute of Biophysics, Biological Research Centre of the Hungarian Academy of Sciences, Temesvári körút 62, H-6726 Szeged, Hungary; e-mail: deli@nucleus.szbk.u-szeged.hu.

INTRODUCTION

Since the discovery of blood–brain barrier (BBB) more than 100 years ago, its permeability barrier function has been in the focus of several generations of researchers. BBB can be defined as a dynamic interaction between cerebral endothelial cells constituting the anatomical basis of the BBB and other neighboring cells, such as astroglia, pericytes, perivascular microglia, and neurons. The cross talk between these cells endow endothelial cells with a unique BBB phenotype comprising not only the morphological barrier of interendothelial tight junctions (TJ), but also the enzymic and metabolic barriers, and the uptake and efflux transport systems (Abbott, 2005).

There are two tightly controlled pathways for molecules and cells to cross the BBB, namely the paracellular (junctional) and the transendothelial routes. One of the hallmarks of the BBB-phenotype is the restrictive paracellular pathway, regulated by interendothelial TJ. The importance of endothelial TJ in permeability regulation was first observed in the tracer experiments of Reese and Karnovsky (1967), and Brightman and Reese (1969). TJ not only restricts paracellular flux, but also maintains polarity of enzymes and receptors on luminal and abluminal membrane domains. The most important integral membrane TJ proteins include occludin, claudin-1 and -5, and junctional adhesion molecules (JAMs) (for review, see Krizbai and Deli, 2003; Matter and Balda, 2003b; Wolburg and Lippoldt, 2002).

Expression level of a certain TJ protein does not necessarily reflects changes in TJ permeability. Brain endothelial cell monocultures expressing high levels of occludin may have low transendothelial electrical resistance (TEER) value (Rubin and Staddon, 1999). Another good example is that complete loss of claudin-5 in knockout mice results in a selective increase in paracellular permeability for small molecules (Nitta *et al.*, 2003). In agreement with these observations, modulation of junctional permeability in cultured cerebral endothelial cells does not correlate with a loss of TJ proteins from the cellular contacts (Hamm *et al.*, 2004). Therefore, indication of TEER value or permeability coefficient for a paracellular permeability marker should be a prerequisite in papers focusing on in vitro expression and functional organization of TJ proteins at the BBB.

Changes in the structure of TJ strands are also affecting BBB function. Redistribution of TJ particles in the internal/external membrane leaflets of brain endothelium results in disturbed fence function, that is, altered polarity of glucose transporter-1 (GLUT-1) in stroke-prone spontaneously hypertensive (SHRSP) rats with no change in occludin, claudin-1, -5, and zonula occludens protein-1 (ZO-1) expression (Lippoldt *et al.*, 2000). Paracellular permeability, however, is regulated by diverse signaling cascades (Krizbai and Deli, 2003; Rubin and Staddon, 1999).

The transendothelial pathways are also restricted at the brain microvasculature. In contrast to peripheral endothelium, the rate of pinocytosis is minimal, and free membrane diffusion applies mainly to small lipophilic molecules, for example, ethanol or nicotine (Pardridge, 2002). Active or catalyzed transport systems can be divided into three main groups. Carrier-mediated bidirectional transport is responsible for nutrient uptake in the brain, these transporters include among others glucose transporter GLUT-1, monocarboxylic acid transporter MCT1, large

neutral amino-acid transporter LAT1, or sodium-coupled nucleoside transporter CNT2 (Pardridge, 2002). Efflux transport is unidirectional and delivers metabolites and xenobiotics from brain to blood. P-Glycoprotein and MRP-1 multidrug resistance proteins, brain multidrug resistance protein (ABCG2/BCRP), or organic anion-transporting polypeptide OATP2 belong to the rapidly growing group of efflux transporters at the BBB (de Boer *et al.*, 2003; Kusuhara and Sugiyama, 2001a,b). Receptor mediated transport by endo- and transcytosis is important for the brain supply of peptides and proteins, such as low-density lipoproteins, transferrin, leptin, and insulin (Banks, 1999; Pardridge, 2002).

Specific enzymes expressed by brain endothelial cells (monoamine oxidases, epoxy hydrolase, endopeptidases, etc.) are important elements of the BBB phenotype constituting the so-called metabolic barrier, and participate in the regulation of brain penetration of drugs (Joó, 1993; Pardridge, 2002).

In vitro reconstituted models of the BBB from different mammalian species have been employed since the late 1970s. However, their comparison is difficult because of the different species and methods used for isolation, culture, coculture, and characterization of the models (de Boer *et al.*, 1999). The importance of the permeability properties of in vitro BBB models, our present topic, is emphasized by recent reviews (Gumbleton and Audus, 2001; Reichel *et al.*, 2003). A report (Lundquist *et al.*, 2002) confirmed that the epithelial cells might not represent a valid and reliable in vitro BBB model, because results obtained on epithelial monolayers correlated poorly with in vivo BBB permeability values. Permeability data of various in vitro BBB models using brain endothelial cells proved to be in strong correlation with in vivo cerebrovascular permeability coefficients (Cecchelli *et al.*, 1999; Dehouck *et al.*, 1992b; Gumbleton and Audus, 2001; Reichel *et al.*, 2003).

Though the number of published papers in the field of in vitro BBB permeability has been multiplied in recent years, to our knowledge no attempt has been made so far to collect data obtained on various models and systematically compare permeability properties published in the literature. This review aimed to summarize available permeability studies obtained on in vitro BBB models and compile data with relevance to BBB physiology, pathology, and pharmacology. Two basic measures were selected in our outline, TEER and endothelial permeability coefficient (P_e) for paracellular markers, to evaluate published in vitro BBB models.

METHODS TO MEASURE PARACELLULAR PERMEABILITY IN VITRO

TEER Measurements

Since BBB as a permeability barrier restricts even the movement of ions, the most straightforward method to assess the tightness of a permeability model is to measure TEER. On the basis of in vivo measurements by Crone and Olesen (1982) and others on pial microvessels, it is estimated that TEER of brain parenchymal microvessels exceeds 1000 Ω cm^2 (Gumbleton and Audus, 2001).

The first TEER measurements on cultured monolayers of brain endothelial cells were published in 1987 by the use of Ussing chamber setup (Hart *et al.*, 1987; Rutten *et al.*, 1987). The measurement technique became much easier by the availability of commercial equipments. For cultures grown on microporous filters or culture inserts most groups use Volt–Ohm resistance meters (World Precision Instruments, Millipore, etc.) equipped with "chopstick" or chamber type electrodes. The chamber gives lower background TEER values, while repeated and fast measurements of different treatment groups are easier by chopstick electrodes.

Data measured by custom devices are also available (Hoheisel *et al.*, 1998; Raub, 1996; Raub *et al.*, 1992; Stanness *et al.*, 1999; Tilling *et al.*, 1998; Nitz *et al.*, 2003). Although the use of such equipments can be justified by special culture or modeling requirements, for example, dynamic BBB model (Stanness *et al.*, 1999), it is difficult to compare or repeat the obtained results in other laboratories. For comparison, the Galla group (Münster, Germany) has published TEER values (400 Ω cm^2 for cells in serum and 700 Ω cm^2 for cells in serum-free condition) measured by Endohm chamber (Franke *et al.*, 1999), which are lower than data (1200–1800 Ω cm^2) measured by custom equipments in the same laboratory (Hoheisel *et al.*, 1998, Tilling *et al.*, 1998; Nitz *et al.*, 2003).

TEER is commonly expressed as resistance measured multiplied by the area of endothelial monolayer (Ω cm^2). The surface of filters vary considerably from type to type and range between 0.3 cm^2(24-well format), 1 cm^2 (12-well format), and 4.2 cm^2 (6-well format). The measured resistance value of 100 Ω in these three formats can be expressed as 33, 100, or 420 Ω cm^2, respectively, depending on the surface of the insert, therefore indication of the insert surface in published papers is useful.

Permeability Measurements and Coefficient Calculations

The most important criterion for a probe to measure paracellular or junctional permeability is that it should not be a ligand for uptake or efflux transporters, brain endothelial receptors, or a substrate for an endothelial enzyme (monoaminooxidase, endopeptidase, etc.).

Most tracers are labeled by a fluorescent dye or isotope that helps the quantification of the molecule. Fluorescent probes include sodium fluorescein (m.w.: 376 Da) and fluorescein isothiocyanate (FITC)-labeled various size dextrans (m.w.: 1–150 kDa). The first [^{14}C]sucrose (m.w.: 342 Da) flux measurement on brain endothelial monolayer was published by Bowman *et al.* (1983), and since then radiolabeled sucrose, inulin (m.w.: 5 kDa), or mannitol (m.w.: 182 Da) is among the most frequently used paracellular tracers. Albumin (m.w.: 67 kDa) is a marker of transendothelial permeability and it has been observed in endothelial vesicles (Plateel *et al.*, 1997). Evans blue dye–albumin complex (Deli *et al.*, 1995b, 2003), [^{3}H]albumin (Plateel *et al.*, 1997), or biotin–albumin (Annunziata *et al.*, 1998) can be equally used for quantification of serum protein permeability.

To calculate P_e endothelial permeability coefficient (Audus and Borchardt, 1986a; Dehouck *et al.*, 1992a,b), flux of the selected tracer across monolayers and cell-free inserts is measured. Transport is expressed as microliter of tracer diffusing

from luminal to abluminal compartments:

$$\text{Clearance}(\mu\text{L}) = [\text{concentration}_{\text{abluminal}}] \times [\text{volume}_{\text{abluminal}}] \times [\text{concentration}_{\text{luminal}}]^{-1}$$

The average volume cleared is plotted versus time, and permeability × surface area product value for endothelial monolayer (PS_e) is calculated by the following formula:

$$PS_{\text{endothelial}^{-1}} = PS_{\text{time-plotted}^{-1}} - PS_{\text{insert}^{-1}}$$

PS_e divided by the surface area generates the endothelial permeability coefficient [P_e (cm/s)]. Modifications have been suggested in the calculation of in vitro permeability coefficient to achieve accurate, permeability status independent estimation of P_{app} apparent permeability (Gaillard and de Boer, 2000; Youdim *et al.*, 2003).

In vivo measured sucrose permeability data vary between 0.03 and 0.1 × 10^{-6} cm/s in the rat (Gumbleton and Audus, 2001; Reichel *et al.*, 2003), while in vitro P_e values are between 1 and 30 × 10^{-6} cm/s (Reichel *et al.*, 2003), and 0.08 and 42 × 10^{-6} cm/s (Table I) for BBB models using primary cells of various mammalian species.

The relationship between electrical resistance and transport of solutes is nonlinear, because solute transport depends on the sum of transport across all junctional pathways, while TEER depends on areas with the lowest electrical resistance between single cells (Madara, 1998). A threshold TEER value of 131 Ω cm^2 has been determined on an in vitro BBB model, above which permeability coefficient for fluorescein remained independent of TEER status (Gaillard and de Boer, 2000). A consensus has been reached that reasonable information can be obtained on in vitro BBB models if the system shows a sufficiently high TEER of at least 150–200 Ω cm^2 (Gumbleton and Audus, 2001; Reichel *et al.*, 2003). It should be noted that on a reproducible porcine model with the highest TEER close to the estimated in vivo value, the lowest published sucrose permeability coefficient has been measured approaching in vivo data (Franke *et al.*, 1999; Hoheisel *et al.*, 1998; Tilling *et al.*, 1998) (Table I).

IN VITRO BLOOD–BRAIN BARRIER MODELS

By the successful isolation of viable microvessels, Ferenc Joó and his co-workers opened the era of in vitro studies of the BBB 30 years ago (Joó and Karnushina, 1973). Subsequent experiments on this model provided important data on cerebral endothelial receptors, transporters, and signaling mechanisms (for review see Joó, 1985, 1993). Just 5 years later, the first observation on brain microvessel endothelial cells in culture was published (Panula *et al.*, 1978), and in the following decade, several culture methods have been elaborated. The first in vitro BBB filter model, adaptation of a technique already used in epithelial cell biology, was introduced in the early 1980s (Bowman *et al.*, 1983). The insert was made by the researchers using nylon mesh and polycarbonate tubing, and bovine brain endothelial cells were seeded on it for studying the effect of calcium-free medium and osmotic shock on sucrose flux (Bowman *et al.*, 1983). Since then, a variety of chambers and inserts from different materials and with diverse pore sizes became commercially available.

Table I. Transendothelial Electrical Resistance and Permeability Data Obtained on In Vitro Blood–Brain Barrier Models with Primary Cells

Endothelial cells	Cocultured cells	Special treatment	TEER (Ω cm^2)	Tracer, P_e (10^{-6} cm/s)[a]	Reference
Bovine brain endothelial cells					
BBEC (P1)	–	10% Porcine PDS	N.I.	Sucrose: N.C.	Bowman *et al.* (1983)
BBEC (P1)	–	10% Horse PDS	N.I.	Sucrose: N.C.	Audus and Borchardt (1986a,b), Guillot and Audus (1991), Borges *et al.* (1994)
BBEC (P1)	–	Fibronectin-collagen	783 ± 7	Albumin: N.C.	Rutten *et al.* (1987)
BBEC (P1)	–	–	N.I.	Sucrose P_e: 0.08	Smith and Borchardt (1989)
BBEC (P1)	–	–	N.I.	NaFl: 67	van Bree *et al.* (1988, 1989)
BBEC (P1)	–	–	61 ± 2	Sucrose: N.C.	Rubin *et al.* (1991)
BBEC (P1)	Rat ACM	–	115 ± 11	Sucrose: N.C.	Rubin *et al.* (1991)
BBEC (P1)	–	cAMP↑	339 ± 107	Sucrose: N.C.	Rubin *et al.* (1991)
BBEC (P1)	Rat ACM	cAMP↑	625 ± 82	Sucrose: N.C.	Rubin *et al.* (1991)
BBEC (P1)	–	10% FCS	25	N.I.	Rubin *et al.* (1991)
BBEC (P1)	–	Specific ECM	50–130	Sucrose: 25	Raub *et al.* (1992), Raub (1996)
BBEC (P1)	Rat C6-CM	Specific ECM	160 ± 8	Sucrose: 24	Raub *et al.* (1992)
BBEC (P > 2)	–	Specific ECM	<9	Sucrose: 25	Raub *et al.* (1992)
BBEC (P1)	–	–	20	Inulin: N.C.	Wolburg *et al.* (1994)
BBEC (P1)	Rat ACM	–	120–800	Inulin: N.C.	Wolburg *et al.* (1994)
BBEC (P1)	–	cAMP↑	125	Inulin: N.C.	Wolburg *et al.* (1994)
BBEC (P1)	–	–	125[b]	Sucrose: N.C.	Pirro *et al.* (1994)
BBEC (P1)	Rat ACM	cAMP↑	225–600	Sucrose: N.C.	Staddon *et al.* (1995)
BBEC (P1)	Rat C6 glioma	Specific ECM	204 ± 5	Sucrose: 13	Raub (1996)
BBEC (P1)	–	10% HS	165	Sucrose: N.C.	Wang *et al.* (1996, 2001)
BBEC (P1)	–	10% Horse PDS	N.I.	Sucrose: 14–42	Eddy *et al.* (1997)
BBEC (P1)	–	–	N.I.	[D-Ala^2]deltorphin I: 38	Thomas *et al.* (1997)
BBEC (P1)	–	–	N.I.	NaFl: 29	Mark and Miller (1999)
BBEC (P1)	–	–	72–184	Morphine: 16	Letrent *et al.* (1999)
BBEC (P1)	–	–	200	Sucrose: 8–13	Abbruscato and Davis (1999a)
BBEC (P1)	Rat C6-CM	–	210	Sucrose: 8	Abbruscato and Davis (1999a)
BBEC (P1)	Rat C6 glioma	–	220	Sucrose: 11	Abbruscato and Davis (1999a)
BBEC (P1)	–	–	N.I.	L-glucose: 0.45	Sobue *et al.* (1999)
BBEC (P1)	Rat AC/ACM	–	98 ± 50	NaFl: 2.2	Gaillard *et al.* (2000, 2001, 2003)
BBEC (P1)	Rat AC	–	500–600	N.I.	Zysk *et al.* (2001)
BBEC (P1)	–	–	N.I.	Sucrose: 7.6	Brown *et al.* (2003)
BBEC (P1)	Rat ACM	–	N.I.	Sucrose: 6.7	Brown *et al.* (2003)
BBEC (P1)	Rat C6-CM	–	N.I.	Sucrose: 6.7	Brown *et al.* (2003)
BBEC (P1)	Rat AC	–	145 ± 16	N.I.	Schaddelee *et al.* (2003)

BBEC (P1)	–	–	1350	N.I.	Zenker *et al.* (2003)
BBEC (P1)	Human Mø	–	2100	N.I.	Zenker *et al.* (2003)
BBEC (P1)	Rat C6 glioma	–	2100	N.I.	Zenker *et al.* (2003)
Cloned bovine brain endothelial cells					
BcBEC (P < 10)	Rat AC	–	661 ± 48 (500–800)	Sucrose: 5.4–32	Dehouck *et al.* (1990, 1992a,b, 2002) Deli *et al.* (1995a,b,c), Plateel *et al.* (1995, 1997), Dehouck *et al.* (1997), Descamps *et al.* (1997, 2003), Chopineau *et al.* (1998), Leveugle *et al.* (1998), Fenart *et al.* (1998, 1999), Carpentier *et al.* (1999), Cecchelli *et al.* (1999), Fillebeen *et al.* (1999a,b), Girod *et al.* (1999), Trottein *et al.* (1999), Brillault *et al.* (2002), Demeule *et al.* (2002), Lundquist *et al.* (2002), Hamm *et al.* (2004)
BcBEC (P10)	–	–	25	N.I.	Rubin *et al.* (1991)
BcBEC (P10)	–	cAMP↑	100–225	N.I.	Rubin *et al.* (1991)
BcBEC (P10)	Rat ACM (in P1–10)	–	35	N.I.	Rubin *et al.* (1991)
BcBEC (P10)	Rat ACM (in P1–10)	cAMP↑	300	N.I.	Rubin *et al.* (1991)
BcBEC (P < 10)	–	–	416 ± 58	Sucrose: 11	Dehouck *et al.* (1992a), Ruchoux *et al.* (2002)
BcBEC (P < 10)	Bovine pericytes	–	>500	Sucrose: 27	Ruchoux *et al.* (2002)
Human brain endothelial cells					
HBEC (P1)	Human AC	10% FCS	297 ± 17	N.I.	Kása *et al.* (1991)
HBEC (P1)	Rat ACM	–	67 ± 12	Sucrose: N.C.	Rubin *et al.* (1991)
HBEC (P1)	Rat ACM	cAMP↑	339 ± 107	Sucrose: N.C.	Rubin *et al.* (1991)
HBEC (P1)	–	–	55–69[b]	NaFl: 53	Muruganandam *et al.* (1997, 2002)
HBEC (P0)	–	–	120–180	Inulin: 7.9	Mackic *et al.* (1999)
HBEC (P1–2)	–	–	33–53[b]	Inulin: N.C.	Stins *et al.* (2001)
HBEC (P8–10)	–	–	33[b]	Inulin: N.C.	Jong *et al.* (2001)
HBEC (P?)	Human ACM + MCM	–	N.I.	Albumin: N.C.	Prat *et al.* (2001)
HBEC (P1)	–	–	N.I.	Inulin: 3.6	Liu *et al.* (2002)
HBEC (P < 10)	–	–	N.I.	FD_{70}: N.C.	Collard *et al.* (2002)
HBEC (P3)	–	–	61 ± 2	Sucrose: 50	Megard *et al.* (2002), Didier *et al.* (2003)
HBEC (P3)	Human AC	–	260 ± 130	Sucrose: 17	Megard *et al.* (2002), Didier *et al.* (2002, 2003)

Table I. Continued

Endothelial cells	Cocultured cells	Special treatment	TEER (Ω cm^2)	Tracer P_e (10^{-6} cm/s)[a]	Reference
HBEC (P1)	–	–	200	N.I.	Zenker *et al.* (2003)
HBEC (P1)	Human Mø	–	500	N.I.	Zenker *et al.* (2003)
HBEC (P5–8)	Rat AC	–	N.I.	Sucrose: N.C.	Lee *et al.* (2003)
Mouse brain endothelial cells					
MBEC (P1)	–	10% FCS	N.I.	FD_4: N.C.	Sahagun *et al.* (1990)
MBEC (P1)	–	15% FCS	59 ± 4	N.I.	Imaizumi *et al.* (1996)
SOD Tg MBEC (P1)	–	15% FCS	61 ± 4	N.I.	Imaizumi *et al.* (1996)
MBEC (P1)	Rat hippocampal slice	–	N.I.	N.I.	Duport *et al.* (1998)
MBEC (P1)	Rat C6 glioma	cAMP↑	307 ± 15	NaFl: 30	Deli *et al.* (2003)
HDC$^{-/-}$ MBEC (P1)	Rat C6 glioma	cAMP↑	200–320	N.I.	Deli *et al.* (unpublished)
Porcine brain endothelial cells					
PBEC (P1)	Rat AC	–	358 ± 39	Sucrose: 7–33	Giese *et al.* (1995)
PBEC (P0)	–	20% (HS + FCS)	70–120	Sucrose: N.C.	Fischer *et al.* (1995, 1996, 1998, 1999a,b, 2000, 2001)
PBEC (P1)	–	cAMP↑; 5% PDS	350–600	Sucrose: N.C.	Schulze *et al.* (1997)
PBEC (P5–15)	–	–	N.I.	Inulin: N.C.	Gloor *et al.* (1997)
PBEC (P1)	–	Serum-free; HC	200–1800	Sucrose: 0.2–1.8	Hoheisel *et al.* (1998), Tilling *et al.* (1998); Franke *et al.* (1999), Nitz *et al.* (2003)
PBEC (P1)	–	–	75	Mannitol: N.C.	Igarashi *et al.* (1999)
PBEC (P1)	Rat AC	–	N.I.	Sucrose: 25	Schirmacher *et al.* (2000)
PBEC (P4–5)	–	FBS-free (3 d)	83 ± 8	N.I.	Yamagata *et al.* (2003)
PBEC (P1)	–	HC	800	Sucrose: 3.3	Omidi *et al.* (2003)
Rat brain endothelial cells					
RBEC (P1)	–	–	N.I.	Sucrose: 7.5	Grabb and Gilbert (1995)
RBEC (P1)	Rat C6 glioma	–	N.I.	Sucrose: 6.0	Grabb and Gilbert (1995)
RBEC (P1)	–	–	100–150	N.I.	De Vries *et al.* (1996b)
RBEC (P1)	Rat AC	–	φ[b]	N.I.	Kondo *et al.* (1996)
RBEC (P1)	–	–	N.I.	Mannitol: 52	Ichikawa *et al.* (1996)
RBEC (P0)	–	–	φ[b]	Albumin: N.C.	Annunziata *et al.* (1998)
RBEC (P1)	Rat hippocampal slice	–	N.I.	N.I.	Duport *et al.* (1998)
RBEC (P1)	Rat AC + neurons	3D dynamic model	50–420	Sucrose: 2.2	Stanness *et al.* (1999), Krizanac-Bengez *et al.* (2003), Parkinson *et al.* (2003)
RBEC (P1)	Rat AC	cAMP↑	350–500	NaFl: 4.2	Kis *et al.* (2001)
RBEC (P1)	Rat C6 glioma	–	17 ± 1	N.I.	Tan *et al.* (2001)

RBEC (P1)	Rat AC	–	N.I.	NaFl: 40	Blasig *et al.* (2001)
RBEC (P2)	–	ECGF + 20% PDS	50	N.I.	Demeuse *et al.* (2002)
RBEC (P2)	Rat AC <opp; 0.45>	ECGF + 20% PDS	130 ± 7	N.I.	Demeuse *et al.* (2002)
RBEC (P2)	Rat AC <opp; 1.0>	ECGF + 20% PDS	438 ± 75	N.I.	Demeuse *et al.* (2002)

Note. 3D = 3-Dimensional blood–brain barrier model, <opp; 0.45> = astrocytes seeded on the opposite side of insert with 0.45 μm pore size, <opp; 1.0> = astrocytes seeded on the opposite side of insert with 1.0 μm pore size, AC = astrocytes, ACM = astrocyte-conditioned medium, BBEC = bovine brain capillary endothelial cells, BcBEC = bovine cloned brain capillary endothelial cells, C6-CM = rat C6 glioma-conditioned medium, cAMP↑ = drug combination elevating intracellular adenosine 3′,5′-cyclic monophosphate level, d = day, Da = Dalton, EC = endothelial cells, ECGF = endothelial cell growth factor, ECM = extracellular matrix, FBS = fetal bovine serum, FCS = fetal calf serum, $FD_{m.w.}$ = fluorescein isothiocyanate-dextran (m.w. = molecular weight in kDa), h = hour, HBEC = human brain capillary endothelial cells, HC = hydrocortisone, $HDC^{-/-}$ = histidine decarboxylase deficient mice, HS = horse serum, kDa = kilodalton, MBEC = mouse brain capillary endothelial cells, MCM = microglia-conditioned medium, Mø = monocyte/macrophage, m.w. = molecular weight, NaFl = sodium fluorescein, N.C. = not comparable, N.I. = not indicated, P = passage number of endothelial cells, P? = passage number is not indicated, P0 = primary brain endothelial cells seeded directly on cell culture insert, PBEC = porcine brain capillary endothelial cells, PDS = platelet-derived serum, P_e = endothelial permeability coefficient, RBEC = rat brain capillary endothelial cells, SOD Tg = human CuZn-superoxide dismutase transgenic animal, TEER = transendothelial electrical resistance.

[a]Molecular weights of permeability tracers used are as follows, albumin: 67 kDa; [D-Ala^2]deltorphin I: 769 Da; FD_4: 4 kDa; FD_{70}: 70 kDa; inulin: 5 kDa; mannitol, 182 Da; morphine: 285 Da; L-glucose: 180 Da; NaFl: 376 Da; sucrose: 342 Da. This table contains representative P_e values of low m.w., paracellular tracers in order to compare the data. In some studies included such a tracer was not used, therefore permeability studies with albumin or FD_{70} are indicated, although the authors of original papers did not calculate P_e values.

[b]In some studies, TEER values were expressed as Ω/cm^2. In case surface area was given in the paper, comparable TEER value could be calculated.

However, the appropriate insert to use in permeability screens should be carefully selected, and permeability of cell-free inserts for each molecule tested has to be determined (Cecchelli *et al.*, 1999).

The cell culture insert/filter setup made it possible to use brain endothelial cells for coculture and permeability studies in vitro (Joó, 1992). The first studies used monocultures (Abbott *et al.*, 1992; Bowman *et al.*, 1981, 1983; Panula *et al.*, 1978; Rutten *et al.*, 1987; Table I), but it turned out very soon, that cultivation of brain endothelial cells alone leads to loss of phenotype, for example, a specific enzyme, γ-glutamyl transpeptidase, that can be restored by coculture with glial cells (DeBault and Cancilla, 1980). It has been demonstrated that astroglia induces the development of TJ in cerebral endothelial cells (for review see Abbott, 2002; Haseloff *et al.*, 2005). The intercommunication between astrocytes and brain endothelial cells, however, has mutual benefits, and endothelial cells also produce factors, including leukemia inhibitory factor, which facilitate astrocyte differentiation (Mi *et al.*, 2001). The results supported the use of brain endothelial cell–astroglia cocultures as in vitro reconstituted BBB models. Some systems use cells from different species in coculture, that is, bovine brain endothelial cells with rat astroglia (Dehouck *et al.*, 1990) others are syngeneic, using for example human cerebral endothelial cells and human astroglia (Kása *et al.*, 1991) (Tables I–III).

Other neighboring cells of endothelium in the brain microvasculature, such as neurons, pericytes, and monocytes/macrophages have also been tested in coculture with brain endothelial cells (Haseloff *et al.*, 2005; Tables I–III).

While all the above-mentioned BBB models are static, a new dynamic model has been recently developed by the group of Janigro (Krizanac-Bengez *et al.*, 2003; Parkinson *et al.*, 2003; Stanness *et al.*, 1999; Table I). This model has a 3-dimensional tube structure with a continuous flow of culture medium mimicking the physiological shear stress in blood vessels.

The fact that extracellular matrix is crucial in the culture of brain endothelial cells and in the local control of TJ biogenesis has long been known (Arthur *et al.*, 1987). Rat tail collagen gel has been found excellent to support monolayer formation of bovine brain endothelial cells, the basis of in vitro modeling, in contrast to laminin, matrigel, or extracellular matrix produced by MDCK cells (Raub *et al.*, 1992). Gelled rat tail collagen is also used in one of the most competent in vitro BBB model systems (Dehouck *et al.*, 1992a,b). Type IV collagen, fibronectin, and laminin either alone or in combination elevated drastically the TEER of low-resistance porcine brain endothelial monolayers (Tilling *et al.*, 1998).

In Vitro Reconstituted BBB Models Using Primary Cultures

Our list of BBB models covers bovine, human, porcine, and rodent (murine and rat) brain endothelial cell-based systems only (Table I). The reason is that although brain microvessel endothelial cells have been isolated from many other species, like monkey, dog, gerbil, and cat, well-characterized permeability models using them have not been described to our knowledge.

The first in vitro BBB model with measured permeability characteristics has been established from bovine brain gray matter (Bowman *et al.*, 1983; Table I).

Bovine systems provide high yield of brain endothelial cells sufficient for pharmacological screening, and they are widely used in basic as well as in applied research (Tables I–XIII). One of the best characterized bovine models developed in the laboratory of Cecchelli (Table I) is based on coculture of cloned and passaged bovine capillary endothelial cells and rat glia culture showing high TEER (500–800 Ω cm^2) and low P_e values. The highest TEER values measured on a bovine system exceed 2000 Ω cm^2, but no P_e values are available on this model (Zenker *et al.*, 2003).

Despite the ethical questions and difficulties to have access to human brain tissue (autopsy material, surgical specimen, and fetal tissue), human BBB models have been established for about 15 years (Table I; Reichel *et al.*, 2003). Other problems with human models are the low yield of cells, and whether the tissue, especially from autopsy or surgical material, can be regarded as "healthy." Human models published so far are less robust than bovine or porcine systems, and give lower resistance and permeability values. The highest published TEER is 500 Ω cm^2, the lowest P_e value for inulin is 3.6×10^{-6} cm/s (Table I).

Mouse brain yields the least endothelial cells compared to other species. No wonder that the fewest number of models can be found from mouse primary endothelial cells (Table I). The advantages of the murine system, however, include the availability of transgenic and gene-targeted animals, oligoprobes, and wide range of antibodies, therefore an expansion of mouse in vitro models is expected.

A high-resistance (1800 Ω cm^2) and low permeability (sucrose P_e is $0.2–1.8 \times 10^{-6}$ cm/s) porcine BBB model has been developed in the laboratory of Galla using serum-free culture condition and hydrocortisone treatment without coculture (Table I). Not all porcine BBB models reach this level of tightness, there is a considerable variation of TEER and P_e values published. The high yield of about 50 million endothelial cells per pig brain and some similarities between porcine and human vascular physiology make the porcine model suitable for high throughput drug screening.

Cultures of rat brain endothelial cells are available since the late 1970s; however, models with permeability measurements have been published only since the 1990s (Table I). Similarly to the mouse system the yield is low, only 1–2 million endothelial cells per rat brain can be isolated. Barrier properties are better than in the mouse models, but they do not reach the level of the best bovine or porcine monolayers. The advantage of the rat BBB model is that it can be easily compared to in vivo results, measurements, and it is simple to do syngeneic cultures.

All primary cultures have some disadvantages, they are expensive and time-consuming. Furthermore, it is difficult to ensure the purity and homogeneity of the cultures, since they are easily overgrown by contaminating cells like pericytes.

In Vitro Reconstituted BBB Models Using Cell Lines

In recent years, immortalized brain endothelial cell lines have been generated in growing number to overcome the above-mentioned difficulties and to establish easy, reproducible, and sufficiently tight in vitro BBB models. Until now, none of the available, more than 20 cell lines can fulfill all these criteria (Table II).

Table II. Transendothelial Electrical Resistance and Permeability Data Obtained on In Vitro Blood–Brain Barrier Models with Cell Lines

Endothelial cells	Cocultured cells	Special treatment	TEER (Ω cm^2)	Tracer P_e (10^{-6} cm/s)[a]	Reference
Bovine brain endothelial cell lines					
t-BBEC-117 (≤P50)	–	–	N.I.	L-glucose: 1.8	Sobue *et al.* (1999)
t-BBEC-117 (≤P50)	Rat ACM	–	N.I.	L-glucose: 1.2	Sobue *et al.* (1999)
Human brain endothelial cell lines					
SV-HCEC (P?)	–	–	55–69[b]	Sucrose: 4.7	Muruganandam *et al.* (1997)
Immortalized HCEC (P?)	–	–	40 ± 8	N.I.	Kannan *et al.* (2000)
Immortalized HCEC (P?)	Rat ACM	–	31 ± 10	N.I.	Kannan *et al.* (2000)
Immortalized HBMEC (P?)	Rat AC	20% NCS	60	N.I.	Zysk *et al.* (2001)
Transfected BEC (<P30)	–	–	33–53[b]	N.I.	Stins *et al.* (2001)
TERT-HBEC (P28)	–	–	18 ± 1	N.I.	Gu *et al.* (2003)
TERT-HBEC (P28)	Rat AC	–	36 ± 3	N.I.	Gu *et al.* (2003)
TERT-HBEC (P28)	Murine NIH-3T3	–	18	N.I.	Gu *et al.* (2003)
IHEC (P?)	–	–	61 ± 8[b]	N.I.	Sharp *et al.* (2003)
Other human cell lines used for permeability studies					
ECV304 (P?)	–	10% FBS	28–39	Sucrose: 9.7	Hurst and Fritz (1996), Hurst *et al.* (1998), Dobbie *et al.* (1999)
ECV304 (P?)	Rat C6 glioma <opp>	10% FBS	57 ± 2–94 ± 6	Sucrose: 5.3	Hurst and Fritz (1996), Hurst and Clark (1997, 1998), Hurst *et al.* (1998, 2001), Dobbie *et al.* (1999)
ECV304 (P?)	Rat C6 glioma	10% FBS	199 ± 30	Sucrose: 5.3	Hurst and Fritz (1996)
ECV304 (P?)	–	–	53 ± 7	Sucrose: 9.2	Scism *et al.* (1999)
ECV304 (P?)	Rat C6 glioma	–	86 ± 4	Sucrose: 6.2	Scism *et al.* (1999)
ECV304 (P?)	–	–	39 ± 6	N.I.	Tan *et al.* (2001)
ECV304 (P?)	Rat C6 glioma	–	80	N.I.	Tan *et al.* (2001)
ECV304 (P?)	Human 1321N1 astrocytoma	–	80	N.I.	Tan *et al.* (2001)
ECV304 (P?)	Rat AC	–	80	N.I.	Tan *et al.* (2001)
ECV304 (P?)	Rat ACM	10% FBS	N.I.	Sucrose: N.C.	Song *et al.* (2002)
ECV304 (P?)	–	10% FBS	75–80	N.I.	Easton and Abbott (2002)
ECV304 (P?)	Rat C6 glioma	10% FBS	120–221	Sucrose: 0.13	Easton and Abbott (2002), Youdim *et al.* (2003)

Mouse brain endothelial cell lines					
MB114 (P?)	–	–	12–44	FD_{20}: N.C.	Hart *et al.* (1987)
MBEC4 (P?)	–	–	N.I.	Sucrose: N.C.	Tatsuta *et al.* (1992), Kusuhara *et al.* (1998), Homma *et al.* (1999)
MBEC4 (P?)	–	–	N.I.	Sucrose: N.C.	Kochi *et al.* (1999)
MBEC4 (P?)	Rat C6 glioma	–	N.I.	NaFl: N.C.	Dohgu *et al.* (2000)
TM-BBB1-5 (P?)	–	–	105–118	Mannitol: 139	Hosoya *et al.* (2000)
b.End5 (P?)	–	–	7 ± 1	N.I.	Tan *et al.* (2001)
b.End5 (P?)	Rat C6 glioma	–	11 ± 1	N.I.	Tan *et al.* (2001)
b.End5 (P?)	–	10% FBS	N.I.	N.I.	Youdim *et al.* (2003)
b.End3 (P27–33)	–	10% FBS	40	Sucrose: 19	Omidi *et al.* (2003)
b.End3 (P27–33)	Rat C6 glioma	–	80	Sucrose: 19	Omidi *et al.* (2003)
b.End3 (P27–33)	Rat C6 glioma	cAMP↑	130	Sucrose: 16	Omidi *et al.* (2003)
Rat brain endothelial cell lines					
RBE4 (P20–60)	–	10% FCS	N.I.	Sucrose: 33–214	Rist *et al.* (1996, 1997), Romero *et al.* (1997a)
RBE4 (P20–60)	–	cAMP↑	N.I.	Sucrose: 103	Rist *et al.* (1997)
RBE4 (P20–60)	Rat AC	–	N.I.	Sucrose: 37	Rist *et al.* (1997)
RBE4 (P20–60)	Rat AC	cAMP↑	N.I.	Sucrose: 60	Rist *et al.* (1997)
RBE4 (P25–55)	Rat C6 glioma	–	N.I.	Sucrose: 68	Lagrange *et al.* (1999)
RBE4 (P?)	–	–	N.I.	Dopamine: N.C.	Cestelli *et al.* (2001)
RBE4 (P?)	Rat neurons	–	N.I.	Dopamine: N.C.	Cestelli *et al.* (2001)
RBE4 (P?)	–	–	N.I.	Sucrose: 35	Mertsch *et al.* (2001)
RBE4 (P?)	Rat AC	–	N.I.	Sucrose: 7.6	Mertsch *et al.* (2001)
RBE4 (P20–80)	–	–	N.I.	Chlorpyrifos: 400	Yang *et al.* (2001)
RBE4 (P20–80)	Rat ACM	–	N.I.	Chlorpyrifos: 100	Yang *et al.* (2001)
RBE4 (P?)	–	10% FBS	N.I.	Sucrose: 17	Blasig *et al.* (2002)
RBE4 (P?)	Rat AC	10% FBS	N.I.	Sucrose: 11	Blasig *et al.* (2002)
RBE4 (P?)	–	10% FBS	N.I.	N.I.	Youdim *et al.* (2003)
GPNT (P?)	–	–	66	Sucrose: 123	Romero *et al.* (2000, 2003)
RBEC1 (P?)	–	–	N.I.	N.I.	Tamai *et al.* (2000)
rBCEC1 (P22–23)	Rat AC	–	N.I.	NaFl: 22	Blasig *et al.* (2001)
rBCEC2 (P18–19)	Rat AC	–	N.I.	NaFl: 20	Blasig *et al.* (2001)
rBCEC3 (P22–23)	Rat AC	–	N.I.	NaFl: 21	Blasig *et al.* (2001)
rBCEC4 (P22–23)	Rat AC	–	N.I.	NaFl: 11	Blasig *et al.* (2001)
rBCEC5 (P22–23)	Rat AC	–	N.I.	NaFl: 24	Blasig *et al.* (2001)

Table II. Continued

Endothelial cells	Cocultured cells	Special treatment	TEER (Ω cm^2)	Tracer P_e (10^{-6} cm/s)[a]	Reference
rBCEC6 (P22–23)	Rat AC	–	N.I.	NaFl: 17	Blasig *et al.* (2001)
GP8 (P20–25)	Rat C6 glioma	–	22–26	NaFl: 182	Deli *et al.* (unpublished)

Note. AC = Astrocytes, ACM = astrocyte-conditioned medium, BEC = brain capillary endothelial cells, cAMP↑ = drug combination elevating intracellular adenosine 3′,5′-cyclic monophosphate level, d = day, Da = Dalton, EC = endothelial cells, FBS = fetal bovine serum, FCS = fetal calf serum, $FD_{m.w.}$ = fluorescein isothiocyanate-dextran (m.w. = molecular weight in kDa), h = hour, kDa = kilodalton, m.w. = molecular weight, NaFl, sodium fluorescein, N.C. = not comparable, NCS = newborn calf serum, N.I. = not indicated, <opp> = astrocytes cultured on the opposite side of cell culture inserts, P = passage number of endothelial cells, P? = passage number is not indicated, P_e = endothelial permeability coefficient, TEER = transendothelial electrical resistance. Abbreviated names of cell lines are used without definition as in original papers.

[a]Molecular weights of permeability tracers used are as follows, chlorpyrifos: 351 Da; dopamine: 190 Da; FD_{20}: 20 kDa; mannitol, 182 Da; L-glucose: 180 Da; NaFl: 376 Da; sucrose: 342 Da. This table contains representative P_e values of low m.w., paracellular tracers in order to compare the data.

[b]In some studies, TEER values were expressed as Ω/cm^2. In case surface area was given in the paper, comparable TEER value could be calculated.

Because of the availability of good bovine primary brain endothelial cell models (Table I), development of bovine cell lines is not a priority. The only bovine cell line published with comparable permeability data is t-BBEC-117 line, which has a permeability coefficient of 1.8×10^{-6} cm/s for L-glucose (Sobue *et al.*, 1999; Table II).

Human brain endothelial cell lines are widely used in infectological studies with human pathogens (Table VIII). The calculated resistance values are rather low, even compared to these in cell lines from other species. The only available permeability coefficient for sucrose is 4.6×10^{-6} cm/s in SV-HCEC line (Muruganandam *et al.*, 1997; Table II).

Although ECV304 proved to be a nonbrain and non-endothelial human cell line (Brown *et al.*, 2000), it expresses several endothelial features (Kiessling *et al.*, 1999; Suda *et al.*, 2001) and has been tested in permeability studies by several groups (reviewed in Gumbleton and Audus, 2001, Reichel *et al.*, 2003; Table II). There is a large variation in TEER, but values about 200 Ω cm^2 could be reached; and among the cell line models, the lowest permeability coefficient for sucrose, 0.13×10^{-6} cm/s, was published on ECV304 cells (Table II).

A spontaneously transformed MB114 mouse brain endothelial monolayer with a low TEER value was the first cell line used for in vitro BBB permeability studies (Hart *et al.*, 1987). Later, mouse brain endothelial cell lines became popular models in BBB transporter research (Kusuhara *et al.*, 1998; Kusuhara and Sugiyama, 2001a,b; Reichel *et al.*, 2003; Tamai *et al.*, 2000; Terasaki and Hosoya, 2001; Tsuji and Tamai, 1999). For permeability studies, the best characterized mouse lines are TM-BBB4 with a TEER of 105–118 Ω cm^2 (Hosoya *et al.*, 2000), and b.End3 with a basal TEER of 40 Ω cm^2 that can be enhanced to 130 Ω cm^2 by glial factors and treatment elevating intracellular level of adenosine 3′,5′-cyclic monophosphate (cAMP) level (Omidi *et al.*, 2003; Table II). Sucrose permeability of b.End3 monolayers is 16×10^{-6} cm/s reflecting a loose paracellular barrier.

Rat brain endothelial cell lines, especially RBE4, have been extensively studied in several areas of BBB research (reviewed in this issue by Roux and Couraud, 2005). The main problem with rat cell lines, similarly to all the above-mentioned ones, is that the monolayers are rather leaky. No TEER values are available in the published literature, but sucrose permeability values varying between 11 and 204×10^{-6} cm/s mirror this well. Data on GPNT cells (Romero *et al.*, 2000, 2003), a retransfected and cloned line of the parental GP8 cells (Greenwood *et al.*, 1996) falls in the same range (Table II).

USE OF BBB MODELS

In vitro reconstituted BBB models have been used for permeability studies for 20 years, and the number of publications in this field has been considerably increased recently. These studies, together with the results of in vivo observations, have contributed to the present knowledge about the structural and functional organization of the BBB under physiological and pathological conditions. Pharmacological studies on reliable and reproducible in vitro BBB models could accelerate the research and development of new drugs having better penetration into central nervous system.

PHYSIOLOGY

Regulation of Junctional Permeability by Coculture and Conditioned Media

The unique BBB phenotype of brain endothelial cells is the result of continuous influence from the surrounding nervous tissue, although the details of this induction are still unclear (Abbott, 2002; Bauer and Bauer, 2000; Haseloff *et al.*, 2005). Table III summarizes the in vitro effects of both neural and nonneural cells on resistance and permeability of brain endothelial cell monolayers.

The effect of astroglia, one of the most important cell types anatomically very close to cerebral capillaries, on endothelial characteristics and functions like permeability has been extensively studied (reviewed by Abbott, 2002; Haseloff *et al.*, 2005). It has been demonstrated in the 1980s by electronmicroscopic techniques that TJ structures, the main regulators of paracellular permeability, are deteriorated in subcultured brain endothelial cells, and coculture with astrocytes or astrocyte-produced factors re-enhance endothelial TJ in vitro (Arthur *et al.*, 1987; Tao-Cheng *et al.*, 1987). Resistance and permeability data measured on coculture models with bovine, human, mouse, porcine, and rat brain endothelial cells and immortalized cell lines strongly support these results (Tables I–III). In the majority of models using primary rat astroglial cells in a coculture setting, the paracellular barrier properties were increased (Table III). Even bovine aortic endothelial cells, which are of nonbrain origin, responded to this treatment (Yamagata *et al.*, 1997). Kása *et al.* (1991) found a similar induction of TEER by fetal human astroglia in human brain endothelial cell monolayers, although Fiala *et al.* (1997) failed to confirm this observation in their syngeneic model. It has been recently suggested that posthypoxic (Song *et al.*, 2002), or *src*-suppressed C-kinase substrate overexpressing (Lee *et al.*, 2003) astrocytes induce better TJ integrity than normal cells do; however, the validity of the BBB models used in these experiments was not confirmed by TEER or P_e measurements.

Glial cell lines gave similar results to cultured astroglia in permeability studies. The rat C6 glioma cell line, which has been widely tested, was also effective in tightening the interendothelial junctions when cocultured with bovine, mouse, and porcine brain endothelial cells or with human ECV304 cell line (Table III). In a comparative study, human and rat astroglia, and C6 glioma cells were equally effective in raising a very low basal TEER of ECV304 monolayers (Tan *et al.*, 2001; Table II). A recent paper reported that in vitro BBB models made from ECV304 and C6 cells purchased from two different commercial sources gave very different permeability results (Scism *et al.*, 1999). Human UC-11 MG astrocytoma elevated TEER in bovine endothelial cells (Raub *et al.*, 1992; Table III). Malignant glial cells, such as rat gliosarcoma (9L) or human glioblastoma (T98G), had an opposite, permeability increasing effect in rat brain endothelial monolayers (Grabb and Gilbert, 1995). Since brain tumors in vivo enhance BBB permeability by secreting angiogenic factors like vascular endothelial cell growth factor (VEGF), this seemingly contradictory result could be explained if mainly permeability increasing factors were released from these cell lines, while in C6 cells the balance would be shifted towards factors with barrier enhancing properties (Grabb and Gilbert, 1995).

Table III. Effect of Coculture with Cells or Conditioned Media on Permeability Data Obtained on In Vitro Blood–Brain Barrier Models

Cell type or cell product	Time	Endothelial cell type	TEER (Ω cm^2) [P_e (10^{-6} cm/s)][a]	Effect on permeability[a]	Reference
Astrocytes, microglial cells, and conditioned media					
Primary cells					
Rat AC	12 d	Bovine cBEC (P < 10)	416 ± 58	TEER↑ sucrose flux↓	Dehouck *et al.* (1990)
Human AC < opp>	5 d	Human BEC (P1)	67 ± 12	TEER↑	Kása *et al.* (1991)
Human AC	N.I.	Human BEC (P?)	N.I.	TEER≈	Fiala *et al.* (1997)
Rat AC	1 d	Rat RBE4 (P20–60)	[Sucrose P_e: 214]	Sucrose P_e ↓	Rist *et al.* (1997)
Rat AC (WKY)	4 d	Bovine aortic EC (P1)	75	TEER↑	Yamagata *et al.* (1997)
Rat AC (SPSHR)	4 d	Bovine aortic EC (P1)	75	TEER≈	Yamagata *et al.* (1997)
Rat AC	2–4 d	Porcine BEC (P0)	104 ± 7	TEER↑ inulin flux≈	Fischer *et al.* (2000)
Rat AC	4–6 d	Bovine BEC (P1)	92–124	TEER↑	Gaillard *et al.* (2001)
Rat AC < opp>	4–6 d	Bovine BEC (P1)	92–124	TEER↑	Gaillard *et al.* (2001)
Rat AC < opp>	6 d	Human ECV304 (P?)	39 ± 6	TEER↑	Tan *et al.* (2001)
Rat AC	12 d	Bovine cBEC (P < 10)	>500	Sucrose P_e ↓	Ruchoux *et al.* (2002)
Rat AC < opp>	4 d	Rat RBE4 (P?) + FBS	[Sucrose P_e: 17]	Sucrose P_e ↓ NaFl P_e ↓	Blasig *et al.* (2002)
Human AC < opp>	15 d	Human BEC (P3)	61±2	TEER↑ sucrose P_e ↓	Megard *et al.* (2002)
Rat AC < opp>	15–18 d	Rat BEC (P2)	50	TEER↑	Demeuse *et al.* (2002)
Rat AC	N.I.	Human BEC (P5–8)	N.I.	Sucrose flux↓	Lee *et al.* (2003)
Rat AC (SSeCKS-transf.)	N.I.	Human BEC (P5–8)	N.I.	Sucrose flux↓	Lee *et al.* (2003)
Rat AC	7 d	Human TERT-HBEC (P28)	18 ± 1	TEER↑	Gu *et al.* (2003)
Cell lines					
Human UC-11MG astrocyte	2 d	Bovine BEC (P1)	50	TEER↑	Raub *et al.* (1992)
Human T98G glioblastoma	3 d	Rat BEC (P1)	[Sucrose P_e: 7.5]	Sucrose P_e ↑	Grabb and Gilbert (1995)
Rat 9L gliosarcoma	3 d	Rat BEC (P1)	[Sucrose P_e: 7.5]	Sucrose P_e ↑	Grabb and Gilbert (1995)
Rat C6 glioma	2 d	Bovine BEC (P1)	50	TEER↑ sucrose P_e ↓ $FD_{70}P_e$ ↓	Raub *et al.* (1992)
Rat C6 glioma	3 d	Rat BEC (P1)	[Sucrose P_e: 7.5]	Sucrose P_e ↓	Grabb and Gilbert (1995)
Rat C6 glioma	1–2 d	Bovine BEC (P1)	91 ± 5	TEER↑	Raub (1996)
Rat C6 glioma	7 d	Human ECV304 (P?)	53 ± 7	TEER↑ sucrose P_e ↓	Scism *et al.* (1999)
Rat C6 glioma	1 d	Bovine BEC (P1)	200	Sucrose P_e ≈	Abbruscato and Davis (1999b)
Rat C6 glioma	2 d	Bovine BEC (P1)	190	TEER≈	Abbruscato and Davis (1999b)

Table III. Continued

Cell type or cell product	Time	Endothelial cell type	TEER (Ω cm^2) [P_e (10^{-6} cm/s)][a]	Effect on permeability[a]	Reference
Rat C6 glioma < opp>	2 d	Bovine BEC (P1)	190	TEER↑	Abbruscato and Davis (1999b)
Rat C6 glioma	2–4 d	Porcine BEC (P0)	104 ± 7	TEER↑ inulin flux≈	Fischer *et al.* (2000)
Rat C6 glioma	2 d	Mouse MBEC4	N.I.	NaFl flux↓	Dohgu *et al.* (2000)
Rat C6 glioma < opp>	6 d	Human ECV304 (P?)	39 ± 6	TEER↑	Tan *et al.* (2001)
Rat C6 glioma < opp>	6 d	Mouse b.End5 (P?)	7 ± 1	TEER↑	Tan *et al.* (2001)
Human 1321N1 astrocytoma < opp>	6 d	Human ECV304 (P?)	39 ± 6	TEER↑	Tan *et al.* (2001)
Rat C6 glioma	4–16 d	Bovine aortic EC (P6) 3D	530	N.I.	Cucullo *et al.* (2002)
Rat C6 glioma	4–8 d	Porcine BEC (P1) + HC + SF	N.I.	TEER↑ sucrose P_e ↓	Omidi *et al.* (2003)
Rat C6 glioma	4–8 d	Mouse b.End3 (P27–33)	40	TEER↑ sucrose P_e ≈	Omidi *et al.* (2003)
Rat C6 glioma	1–4 d	Bovine BEC (P1) + FCS	1400	TEER↑	Zenker *et al.* (2003)
Conditioned media					
Rat ACM	≤ 0.5h	Bovine BEC (P1)	61 ± 2	TEER↓	Rubin *et al.* (1991)
Rat ACM	1–72 h	Bovine BEC (P1)	61 ± 2	TEER↑	Rubin *et al.* (1991)
Rat ACM	2 d	Bovine BEC (P1)	35–45	TEER↑	Rubin *et al.* (1991)
Rat ACM + rat C6-CM	2 d	Bovine BEC (P1)	35–45	TEER↑	Rubin *et al.* (1991)
Rat ACM + human U-CM	2 d	Bovine BEC (P1)	35–45	TEER↑	Rubin *et al.* (1991)
Rat ACM + rat FB-CM	2 d	Bovine BEC (P1)	35–45	TEER≈	Rubin *et al.* (1991)
Rat C6-CM	2 d	Bovine BEC (P1)	50	TEER↑ sucrose P_e ↓ FD_{70} P_e ↓	Raub *et al.* (1992)
Rat C6-CM	2 d	Bovine BEC (P1)	15	TEER≈ inulin flux≈	Wolburg *et al.* (1994)
Rat C6-CM	2 d	Bovine BEC (P1) + cAMP?	26	TEER↑ inulin flux↓	Wolburg *et al.* (1994)

Human ACM	2 d	SV-HCEC (P?)	55–69[b]	TEER	Muruganandam *et al.* (1997)
Rat C6-CM	1 d	Bovine BEC (P1)	200	Sucrose $P_e \approx$	Abbruscato and Davis (1999a)
Rat C6-CM	2 d	Bovine BEC (P1)	190	TEER≈	Abbruscato and Davis (1999b)
Human ACM	18–72 h	Human HCEC (P?)	40 ± 8	TEER≈	Kannan *et al.* (2000)
Rat ACM	N.I.	Rat RBE4 (P20–80)	[CPI P_e: 400]	CPI $P_e \downarrow$	Yang *et al.* (2001)
Human ACM + human MCM	3 d	Human BEC (P?)	N.I.	Albumin flux↓	Prat *et al.* (2001)
Rat ACM	5 h	Human ECV304 (P?)	N.I.	Sucrose flux↓	Song *et al.* (2002)
Rat ACM (after H + R)	5 h	Human ECV304 (P?)	N.I.	Sucrose flux↓	Song *et al.* (2002)
Rat C6 CM	24 h	Bovine BEC (P1)	[Sucrose P_e: 7.6]	Sucrose $P_e \approx$	Brown *et al.* (2003)
Rat ACM	24 h	Bovine BEC (P1)	[Sucrose P_e: 7.6]	Sucrose $P_e \approx$	Brown *et al.* (2003)
Neurons					
Rat hippocampal slice	14 d	Rat BEC (P1)	N.I.	Dopamine flux↓	Duport *et al.* (1998)
Rat primary neurons	7 d	Rat RBE4 (P?)	N.I.	Dopamine flux↓	Cestelli *et al.* (2001)
Pericytes and conditioned media					
Mouse pericytoma	2 d	Bovine BEC (P1)	50	TEER≈	Raub *et al.* (1992)
Bovine retina pericyte CM	2 d	Bovine BEC (P1)	50	TEER↓	Raub *et al.* (1992)
Bovine pericytes	2 d	Bovine cBEC (P < 10)	[Sucrose P_e: 10.7]	Sucrose $P_e \uparrow$	Ruchoux *et al.* (2002)
Smooth muscle cells, fibroblast cells and conditioned media					
Bovine smooth muscle cells	2–4 d	Porcine BEC (P0)	104 ± 7	Inulin flux≈	Fischer *et al.* (2000)
Hamster CHO line	2 d	Bovine BEC (P1)	50	TEER↓	Raub *et al.* (1992)
Murine NIH-3T3 line	7 d	Human TERT-HBEC (P28)	18 ± 1	TEER≈	Gu *et al.* (2003)
Rat fibroblast CM	2 d	Bovine BEC (P1)	35–45	TEER↑	Rubin *et al.* (1991)
Lymphocytes and macrophages/monocytes					
Human T-ly	18 h	Rat GPNT (P?)	[FD_{70} P_e: 0.7]	FD_{70} $P_e \approx$	Romero *et al.* (2000)
Human Mø	1–4 d	Bovine BEC (P1) + FCS	1200–1400	TEER↑	Zenker *et al.* (2003)
Human Mø	2–6 d	Human BEC (P1) + FCS	250	TEER↑	Zenker *et al.* (2003)

Table III. Continued

Cell type or cell product	Time	Endothelial cell type	TEER (Ω cm^2) [P_e (10^{-6} cm/s)][a]	Effect on permeability[a]	Reference
Human Mø (LPS-stimulated)	1–3 d	Bovine BEC (P1) + FCS	1400	TEER↑	Zenker *et al.* (2003)
Human Mø (HIV-1-infected)	1–3 d	Bovine BEC (P1) + FCS	1400	TEER↑	Zenker *et al.* (2003)

Note. 3D = 3-Dimensional blood–brain barrier model, AC = astrocytes, ACM = astrocyte-conditioned medium, BEC = brain capillary endothelial cells, C6-CM = rat C6 glioma-conditioned medium, cAMP↑ = drug combination elevating intracellular adenosine 3′,5′-cyclic monophosphate level, cBEC = bovine cloned brain capillary endothelial cells, d = day, CM = conditioned medium, CPI = chlorpyrifos, Da = Dalton, FB-CM = fibroblast-conditioned medium, FBS = fetal bovine serum, FCS = fetal calf serum, $FD_{m.w.}$ = fluorescein isothiocyanate-dextran (m.w. = molecular weight in kDa), h = hour, HC = hydrocortisone, HIV-1 = human immunodeficiency virus type 1, H+ R = astrocytes underwent hypoxia (1% O_2; 48 h), kDa = kilodalton, LPS = lipopolysaccharide, MCM = microglia-conditioned medium, Mø = monocytes/macrophages, m.w. = molecular weight, NaFl = sodium fluorescein, N.C. = not comparable, N.I. = not indicated, P = passage number of endothelial cells, P? = passage number is not indicated, P0 = primary brain endothelial cells seeded directly on cell culture insert, P_e = endothelial permeability coefficient, SF = serum-free, SPSHR = stroke-prone spontaneously hypertensive rats, SSeCKS-transfected = cells transfected with Src suppressed C kinase substrate, TEER = transendothelial electrical resistance, T-ly = T-lymphocytes, U-CM = human U2-51 astrocytoma-conditioned medium, WKY = Wistar-Kyoto rats.

[a]Molecular weights of permeability tracers used are as follows, albumin: 67 kDa; chlorpyrifos: 351 Da; dopamine: 190 Da; FD_{70}: 70 kDa; inulin: 5 kDa; NaFl: 376 Da; sucrose: 342 Da. This table contains representative P_e values of low m.w., paracellular tracers in order to compare the data.

[b]In a study, TEER value was expressed as Ω/cm^2, however, surface area was given in the paper and comparable TEER value could be calculated.

The hypothesis that soluble factors released by glia or glioma cells participate in the induction of BBB phenotype is supported by a large number of studies with glia-conditioned media (Tables I–III). In most reports, barrier enhancing effects were found, however, at least 60 min incubation time was needed (Rubin *et al.*, 1991; Table III). The barrier tightening factors secreted by rat C6 glioma cells are unidentified, though a study indicates that nonprotein factors having molecular weight lower than 1000 Da are responsible for the effect (Ramsohoye and Fritz, 1998). A study trying to clarify the signaling pathways involved in barrier-enhancing effects of C6 cells suggests that the action is not mediated through cAMP, but rather by protein kinase C (PKC) activation via phospholipase D, independently of intracellular calcium increase (Raub, 1996).

All these results are verified by an opposite finding, that removal of astroglia from coculture with brain endothelial cells led to an increase in permeability for sucrose and peroxidase (Hamm *et al.*, 2004). However, the elevation of junctional permeability was not accompanied by any change in immunostaining of TJ proteins occludin, claudin-3 and -5, ZO-1, and ZO-2. This clearly indicates that loosening of TJ structure measured by paracellular markers does not mean a complete loss of TJ proteins. Indeed, previous observations on fast and reversible modulation of paracellular permeability in brain endothelial cells by osmotic shock (Bowman *et al.*, 1983; Dehouck *et al.*, 1990; Deli *et al.*, 1995c; Table XII) and by cAMP (Deli *et al.*, 1995a; Rubin *et al.*, 1991; Table X) raised an important role for TJ protein phosphorylation and dephosphorylation processes in permeability regulation (Rubin and Staddon, 1999).

Despite their localization close to capillaries, few data are available on the effect of neurons on BBB properties in general (Bauer and Bauer, 2000), and in particular on in vitro permeability (Table III). Coculture of RBE4 cells with rat primary neurons decreased transmonolayer dopamine flux (Cestelli *et al.*, 2001). In agreement with these data, organotypic brain slice culture induced differential permeability between L-Dopa and dopamine through rat brain endothelial cell monolayers with reduction of dopamine transport (Duport *et al.*, 1998). No glutamate transport was found in this coculture model compared to monocultures, which indicates the presence of glutamate efflux transporters found in vivo (Duport *et al.*, 1998).

Pericytes embedded in brain capillary basement membrane are the nearest neighbors of endothelial cells and they have a fundamental role in stabilizing brain capillary structure in vivo. Data are scarce, but the overall effect of pericytes in published papers seems to weaken the permeability barrier in vitro (Table III). Mouse pericytoma did not change, while bovine retina pericyte-conditioned medium decreased TEER of bovine cerebral endothelial cells (Raub *et al.*, 1992). Bovine pericytes also increased sucrose permeability (Ruchoux *et al.*, 2002).

Other cells of mesenchymal origin, smooth muscle cells, and fibroblasts exert contradictory effects (Table III). While bovine smooth muscle cells showed no specific action on bovine brain endothelial monolayers (Fischer *et al.*, 2000), rat fibroblast-conditioned medium increased TEER (Rubin *et al.*, 1991), a hamster fibroblast cell line decreased TEER (Raub *et al.*, 1992), whereas a murine fibroblast cell line had no effect on TEER (Gu *et al.*, 2003). The fibroblast cells were from

different species and organs with diverse characteristics, which could explain the dissimilar activity.

Blood cells continuously contact the luminal surface of capillaries, which is nonadherent physiologically. Human T-lymphocytes had no effect on FITC-labeled 70 kDa dextran permeability in GPNT cells (Romero *et al.*, 2000, Table III). Nontreated, bacterial lipopolysaccharide (LPS)-treated, or human immunodeficiency virus-1 (HIV-1) infected human macrophages all increased TEER of bovine brain endothelial monolayers to a similar extent that C6 glioma cells did (Zenker *et al.*, 2003). Human nontreated macrophages were also found to raise the resistance of human cerebral endothelial cells (Zenker *et al.*, 2003).

Regulation of Junctional Permeability by Physiological Factors

Since the earliest attempts to cultivate living cells serum and serum components have been used to provide cells with adhesion-promoting molecules, nutrients, trace minerals, transport proteins like transferrin and albumin, growth factors, and hormones. Several in vitro BBB models use serum containing media (Tables I and II). However, few studies examined systematically the effect of serum on permeability (Table IV). The ECV304/C6 model shows higher TEER value in the presence of fetal bovine serum, and reduction of serum content or serum-deprivation for 24 h led to decreased TEER even in the presence of C6 cells (Hurst and Fritz, 1996). Data from the laboratory of Galla demonstrate an opposite effect of serum on porcine brain endothelial monolayers (Tables I and IV). Bovine serum, ox serum, heat-inactivated ox serum, and human blood plasma all decreased TEER, and disturbed the correct localization of integral TJ proteins on their model (Franke *et al.*, 1999; Hoheisel *et al.*, 1998; Nitz *et al.*, 2003). Since fatty acid-free albumin was without effect (Nitz *et al.*, 2003), a variety of known and unidentified serum factors, among them lysophosphatidic acid (LPA), can be responsible for the phenomenon.

To promote the growth of endothelial cells in vitro, several growth factors are used. Basic and acidic fibroblast growth factors and heparin, which binds and stabilizes them, are devoid of any permeability effect (Raub *et al.*, 1992; Wang *et al.*, 1996; Table IV). The same applies for epidermal growth factor, platelet-derived growth factor, ciliary neurotrophic factor, and insulin-like growth factor-1 (Hoheisel *et al.*, 1998; Rubin *et al.*, 1991). Similar to these results, glial cell line-derived neurotrophic factor (GDNF) alone had no effect (Table IV). However, it had a dose-dependent barrier tightening action in porcine brain capillary endothelial cells, when applied together with intracellular cAMP elevating agents (Igarashi *et al.*, 1999). Although both GDNF and transforming growth factor-β1 (TGF-β1) belongs to the TGF-β family, TGF-β1 produced by pericytes shows a very different effect. TGF-β1 causes a time-dependent and polarized increase in permeability of bovine brain endothelial monolayers with a basolateral preference through a pertussis toxin-sensitive G-protein coupled pathway (Raub *et al.*, 1992; Raub, 1996). Atrial natriuretic factor, known for elevating guanosine 3′,5′-cyclic monophosphate (cGMP levels) in

Table IV. Effect of Physiological Factors on Permeability Data Obtained on In Vitro Blood–Brain Barrier Models

Drug (dose; time)	In vitro BBB model	TEER (Ω cm^2) [P_e (10^{-6} cm/s)][a]	Effect on permeability[a]	Reference
Serum and serum components				
FBS-free medium (1 d)	Human ECV304 (P?)	39 ± 6	TEER↓	Hurst and Fritz (1996)
FBS-free medium (1 d)	Human ECV304 (P?) + rat C6	92 ± 9	TEER↓	Hurst and Fritz (1996)
Reduction of FBS (10%→2%; 1 d)	Human ECV304 (P?) + rat C6	92 ± 9	TEER↓	Hurst and Fritz (1996)
Bovine serum (10%; 1 d)	Porcine BEC (P1)	1000	TEER↓ sucrose flux↑	Hoheisel *et al.* (1998)
Bovine serum (1%) + BSA (2.5%; 1 d)	Porcine BEC (P1)	300–500	Sucrose P_e ↑ retinol P_e ↓ RA P_e ↓	Franke *et al.* (1999)
Bovine serum (1–15%; 1–8 d)	Porcine BEC (P1)	1200–1800	TEER↓	Nitz *et al.* (2003)
Heat-inactivated bovine serum (10%; 3 d)	Porcine BEC (P1)	1200–1800	TEER↓	Nitz *et al.* (2003)
BSA isolated from serum (N.I.; 3 d)	Porcine BEC (P1)	1200–1800	TEER↓	Nitz *et al.* (2003)
Fatty-acid free BSA (N.I.; 3 d)	Porcine BEC (P1)	1200–1800	TEER≈	Nitz *et al.* (2003)
Human plasma (10%; 3 d)	Porcine BEC (P1)	1200–1800	TEER↓	Nitz *et al.* (2003)
Hormones and growth factors				
Adrenaline (0.1 μM; 30 min)	Bovine BEC (P1) + rat AC	N.I.	NaFl flux↑	Borges *et al.* (1994)
Adrenaline (1.0 μM; 30 min)	Bovine BEC (P1) + rat AC	N.I.	NaFl flux↓	Borges *et al.* (1994)
Adrenaline (10 μM; 5 h)	Bovine BEC (P1) + rat AC	98 ± 50	TEER↑	Gaillard and de Boer (2000)
Adrenomedullin (1 μM; 0.25–6 h)	Rat BEC (P1) + rat AC	350–500	TEER↑ NaFl P_e ≈ EBA P_e ≈	Kis *et al.* (2001)
Atrial natriuretic peptide (N.I; N.I.)	Bovine BEC (P1)	61 ± 2	TEER↓	Rubin *et al.* (1991)
Basic FGF (1–100 ng/mL; 2 d)	Bovine BEC (P1) + rat C6-CM	160 ± 18	TEER≈	Raub *et al.* (1992)
Basic FGF (50 ng/mL; 2 d)	Bovine BEC (P1)	N.I.	Sucrose flux≈	Wang *et al.* (1996)
Basic FGF (<abl>50 ng/mL; 2 d)	Bovine BEC (P1)	165	TEER≈ sucrose flux≈	Wang *et al.* (2001)
Calcitonin gene-related peptide (N.I; N.I.)	Bovine BEC (P1) + rat ACM	100	TEER↑	Rubin *et al.* (1991)
Ciliary neurotrophic factor (N.I; N.I.)	Bovine BEC (P1)	61 ± 2	TEER≈	Rubin *et al.* (1991)
Epidermal growth factor (2–8 nM; 1 d)	Porcine BEC (P1) + serum-free	1000	TEER≈	Hoheisel *et al.* (1998)
FGF (N.I; N.I.)	Bovine BEC (P1)	61 ± 2	TEER≈	Rubin *et al.* (1991)
GDNF (1 ng/mL; 1–15 h)	Porcine BEC (P1)	75	TEER≈	Igarashi *et al.* (1999)
GDNF (0.1–1.0 ng/mL; 1–15 h)	Porcine BEC (P1) + cAMP↑	75	TEER↑ mannitol flux↓	Igarashi *et al.* (1999)
Heparin (1–150 μg/mL; 2 d)	Bovine BEC (P1) + rat C6-CM	160 ± 18	TEER≈	Raub *et al.* (1992)
Hydrocortisone (70–550 nM; 1 d)	Porcine BEC (P1) + serum-free	1000	TEER↑ sucrose flux↓	Hoheisel *et al.* (1998)
Insulin (70–700 pM; 1 d)	Porcine BEC (P1) + serum-free	1000	TEER≈	Hoheisel *et al.* (1998)

Table IV. Continued

Drug (dose; time)	In vitro BBB model	TEER (Ω cm^2) [P_e (10^{-6} cm/s)][a]	Effect on permeability[a]	Reference
Insulin (70 μM; 1 d)	Porcine BEC (P1) + serum-free	1000	TEER↑	Hoheisel *et al.* (1998)
Insulin-like growth factor-1 (N.I; N.I.)	Bovine BEC (P1)	61 ± 2	TEER≈	Rubin *et al.* (1991)
Noradrenaline (0.1–1.0 μM; 30 min)	Bovine BEC (P1) + rat AC	N.I.	NaFl flux↑	Borges *et al.* (1994)
Noradrenaline (10 μM; 30 min)	Bovine BEC (P1) + rat AC	N.I.	NaFl flux≈	Borges *et al.* (1994)
Noradrenaline (100 μM; 5 h)	Bovine BEC (P1) + rat AC	98 ± 50	TEER↑	Gaillard and de Boer (2000)
TGF-β (≤0.5 ng/mL; N.I.)	Bovine BEC (P1)	50	TEER↓	Raub *et al.* (1992)
TGF-β1 (0.5 ng/mL; 1–2.5 h)	Bovine BEC (P1) + cAMP↑	163–179	TEER↓	Raub (1996)
Platelet-derived growth factor (N.I; N.I.)	Bovine BEC (P1)	61 ± 2	TEER≈	Rubin *et al.* (1991)
Lipids, lipid mediators, and lipoproteins				
Eicosapentaenoic acid (0.4–2.10 μM 4–48 h)	Porcine BEC (P4-5) + serum-free	83 ± 8	TEER↑	Yamagata *et al.* (2003)
γ-Linolenic acid (0.4–2.10 μM 4–48 h)	Porcine BEC (P4-5) + serum-free	83 ± 8	TEER↑	Yamagata *et al.* (2003)
Linoleic acid (0.4–2.10 μM; 4–48 h)	Porcine BEC (P4-5) + serum-free	83 ± 8	TEER≈	Yamagata *et al.* (2003)
Low-density lipoprotein (≤2 mg/mL; 8 h)	Bovine cBEC (P < 10) + rat AC	500–800	Sucrose P_e ≈	Dehouck B *et al.* (1997)
LPA (10–100 μM; 20 min–8 h)	Porcine BEC (P1) + PDS	308 ± 55	TEER↓ sucrose flux↑	Schulze *et al.* (1997)
LPA (10–100 μM; 20 min–8 h)	Porcine BEC(P1) + cAMP↑ + PDS	500–600	TEER↓ sucrose flux↑	Schulze *et al.* (1997)
LPA (0.1–1.0 μM; 20 min–6 h)	Porcine BEC (P1) + cAMP↑	350–900	TEER↓ sucrose flux↑	Schulze *et al.* (1997)
LPA (10 μM; 20 min–24 h)	Porcine BEC (P1)	1200–1800	TEER↓	Nitz *et al.* (2003)
Prostaglandin E_2 (10 ng/mL; 90 min)	Bovine BEC (P1)	N.I.	FD_3 flux↑	Mark *et al.* (2001)
Prostaglandin $F_{2\alpha}$ (10 ng/mL; 90 min)	Bovine BEC (P1)	N.I.	FD_3 flux↑	Mark *et al.* (2001)

Note. ↓ = Significant decrease. ≈ = no significant change. ↑ = significant increase. <abl> = abluminal application. AC = astrocytes. ACM = astrocyte-conditioned medium. BBB = blood–brain barrier. BEC = brain capillary endothelial cells. BSA = bovine serum albumin. C6-CM = rat C6 glioma-conditioned medium. cAMP↑ = drug combination elevating intracellular adenosine 3′,5′-cyclic monophosphate level. cBEC = bovine cloned brain capillary endothelial cells. CM = conditioned medium. d = day. Da = dalton. EBA = Evans blue-labeled albumin. FBS = fetal bovine serum. $FD_{m.w.}$ = fluorescein isothiocyanate-dextran (m.w. = molecular weight in kDa). FGF = fibroblast growth factor. GDNF = glial cell line-derived neurotrophic factor. h = hour. kDa = kilodalton. m.w. = molecular weight. LPA = lysophosphatidic acid. NaFl = sodium fluorescein. N.I. = not indicated. P = passage number of endothelial cells. P? = passage number is not indicated. PDS = platelet-derived serum. P_e = endothelial permeability coefficient. RA = retinoic acid. TEER = transendothelial electrical resistance. TGF-β = transforming growth factor-β.

[a] Molecular weights of permeability tracers used are as follows. EBA: 67 kDa; FD_3: 3 kDa; inulin: 5 kDa; mannitol: 182 Da; NaFl: 376 Da; RA, 300 Da; retinol: 286 Da; sucrose: 342 Da. This table contains representative P_e values of low m.w., paracellular tracers in order to compare data.

endothelium, decreased TEER in bovine brain endothelial monolayers (Rubin *et al.*, 1991).

The vasodilating, cAMP elevator peptide hormones adrenomedullin (Kis *et al.*, 2001) and calcitonin gene-related peptide (Rubin *et al.*, 1991) both decrease paracellular permeability. Physiological concentration of hydrocortisone, a glucocorticoid hormone, improves considerably the barrier properties of porcine cerebral endothelial cells in serum-free culture conditions, while insulin exerts a significant TJ tightening effect only at four magnitude higher concentrations than the physiological range (Hoheisel *et al.*, 1998; Table IV).

Endogenous catecholamines also influence BBB permeability (Table IV). Adrenaline (0.1 μM) and noradrenaline (0.1–1.0 μM) increase the sodium fluorescein flux through bovine brain endothelial monolayers, while adrenaline at 1 μM via β2 adrenoreceptors decreases permeability (Borges *et al.*, 1994). This TEER increasing effect of adrenaline or noradrenaline was also observed at 10 μM in another study (Gaillard and de Boer, 2000).

Fatty acids are major components of the cell membrane and are able to regulate junctional permeability (Table IV). Eicosapentaenoic acids and γ-linolenic acid, two polyunsaturated fatty acids supposed to be mediators in the cross talk between endothelial cells and astroglia, increased TEER of porcine brain endothelial cells after 3 days of serum starvation, whereas linoleic acid had no such effect (Yamagata *et al.*, 2003). The barrier tightening effect could be blocked by tyrosine kinase inhibitors or PKC inhibitors. The intracellular signaling molecule LPA, the simplest glycerophospholipid, strongly and reversibly reduced TEER and increased sucrose flux of porcine brain endothelial cells in a time- and dose-dependent manner independently of previous treatment with cAMP (Schulze *et al.*, 1997; Nitz *et al.*, 2003). LPA is more potent in serum-free conditions (Schulze *et al.*, 1997). Arachidonic acid enhanced the passage of trypan blue through brain endothelial cells cultured on dextran beads, in a system difficult to compare with present filter models (Kempski *et al.*, 1987; Villacara *et al.*, 1990). Lipid mediators of the cyclooxygenase pathway, prostaglandin E_2 and prostaglandin $F_{2\alpha}$ increased the permeability for 3 kDa dextran in bovine brain endothelial cells (Mark *et al.*, 2001).

Low-density lipoprotein, an important macromolecule responsible for the receptor-mediated transport of cholesterol from blood to brain, does not change the integrity of bovine brain endothelial monolayers measured by sucrose and inulin flux (Dehouck *et al.*, 1997).

PATHOLOGY

BBB permeability changes play a crucial role in brain edema formation and central nervous system injuries during human diseases, such as stroke, cerebral hypoxia-reoxygenation, head injuries, neurodegenerative diseases, and neurological infections including bacterial and viral meningitis, encephalitis, or HIV-1 infection. In vitro studies on reconstituted BBB models help to reveal the direct effects of pathological conditions on cerebral endothelium, and they can also unravel the contribution of cytokines, reactive oxygen species (ROS), nitric oxide (NO), vasoactive mediators, and other pathogenetic factors to the impairment of barrier integrity

(Deli and Joó, 1996). Investigations on these models of BBB pathology may offer a suitable tool for testing efficacy and brain penetration of new drugs.

Effects of Hypoxia and Reoxygenation on BBB Permeability In Vitro

Brain ischemia, a major neuropathological condition in humans, changes BBB permeability in vivo. To better understand the pathomechanism, several studies examined hypoxia and related factors on different in vitro BBB models (Table V). Susceptibility of brain endothelial cells to hypoxia differs significantly depending on time, culture and treatment conditions, and validity of the models used. Hypoxia (1.5–24 h) also induced a drop in TEER, and an increase in sucrose and inulin flux of porcine brain endothelial monolayers (Fischer *et al.*, 1996, 1998, 1999a,b, 2000, 2001). Hypothermia could effectively block the effect of hypoxia on inulin permeability (Fischer *et al.*, 1999b). In case of bovine cerebral endothelial cells, 24 h hypoxia (1% O_2) resulted in elevated sucrose flux (Brown *et al.*, 2003; Mark and Davis, 2002; Mark *et al.*, 2004). Interestingly, on the same model at 48 h, but not 24 h, hypoxia (0% O_2) augmented P_e of sucrose, while that of inulin was not affected (Abbruscato and Davis, 1999a).

Among the coculture models, 2 h hypoxia led to increased fluorescein flux in porcine brain endothelial cell–rat glia model (Giese *et al.*, 1995). In bovine brain endothelial cells cocultured with rat glia, 48 h hypoxia was needed to significantly raise sucrose and albumin P_e in endothelial monolayers in the absence of glial cells (Plateel *et al.*, 1995, 1997). The increase in albumin flux was abolished at 4°C, confirming that albumin transport is an active transendothelial process (Plateel *et al.*, 1997). On the same model system, 9 h hypoxia resulted in an enhanced endothelial monolayer permeability for inulin and NXY-059, a radical trapping neuroprotective agent (Dehouck *et al.*, 2002).

Hypoxia followed by reoxygenation led to increased permeability to ions and sucrose in porcine cerebral endothelial cells, which could be blocked by barbiturates (Fischer *et al.*, 1996). A similar barrier weakening effect could be demonstrated in rat brain endothelial cell/rat astroglia models (Kondo *et al.*, 1996; Utepbergenov *et al.*, 1998). In contrast, reoxygenation showed an attenuating effect compared to hypoxia-induced increased permeability on bovine brain endothelial monocultures (Mark and Davis, 2002; Mark *et al.*, 2004).

In all models tested, hypoxia combined with glucose deprivation resulted in a much faster (2–4 h) increase in endothelial permeability for sucrose, inulin, apotransferrin, and albumin than in hypoxia alone (Abbruscato and Davis, 1999a; Brillault *et al.*, 2002, Dehouck *et al.*, 2002). Interestingly, this was not accompanied by change in TEER suggesting that the permeability increase does not involve TJ disruption, but a temperature-sensitive transcellular transport for all the markers (Brillault *et al.*, 2002).

Importantly, hypercapnia, normoxic aglycemia, or hypoglycemia alone did not cause change in barrier tightness (Table V).

The role of glial factors in mediating the effect of hypoxia is controversial. Bovine brain endothelial permeability was significantly enhanced for sucrose, inulin,

Table V. Effects of Hypoxia, Ischemia, and Related Factors on Permeability Data Obtained on In Vitro Blood–Brain Barrier Models[a]

Insult (dose; time)	In vitro BBB model	TEER (Ω cm^2) [P_e (10^{-6} cm/s)][a]	Effect on permeability[a]	Reference
Hypoxia				
Hypoxia (0% O_2, 2 h)	Porcine BEC (P1) + rat AC	358 ± 39	NaFl P_e ↑	Giese *et al.* (1995)
Hypoxia (0% O_2; 12 h)	Bovine cBEC (P < 10) + rat AC	>500	Sucrose P_e ≈	Plateel *et al.* (1995)
Hypoxia (0% O_2; 24 h)	Bovine cBEC (P < 10) + rat AC	>500	Sucrose P_e ≈	Plateel *et al.* (1995)
Hypoxia (0% O_2; 48 h)	Bovine cBEC (P < 10) + rat AC	>500	Sucrose P_e ↑	Plateel *et al.* (1995)
Hypoxia (40 mmHg O_2, 1.5–6 h)	Porcine BEC (P0) + 15% HS + 5% FCS	80–120	TEER↓ sucrose flux↑	Fischer *et al.* (1996)
Hypoxia (0% O_2; 48 h)	Bovine cBEC (P < 10) + rat AC	>500	Sucrose P_e ↑ albumin P_e ↑	Plateel *et al.* (1997)
Hypoxia (0% O_2; 48 h; 4°C)	Bovine cBEC (P < 10) + rat AC	>500	Sucrose P_e↑ albumin P_e ≈	Plateel *et al.* (1997)
Hypoxia (4–5% O_2, 6 h)	Porcine BEC (P1)	100–120	Inulin flux↑	Fischer *et al.* (1998)
Hypoxia (0% O_2; 48 h)	Bovine BEC (P1)	200	Sucrose P_e ↑ insulin P_e ≈	Abbruscato and Davis (1999a)
Hypoxia (0% O_2;24 h)	Bovine BEC (P1)	200	Sucrose P_e ≈	Abbruscato and Davis (1999a)
Hypoxia (4–5% O_2, 3–24 h)	Porcine BEC (P1)	100–120	Inulin flux ↑	Fischer *et al.* (1999a)
Hypoxia (2% O_2, 6–24 h)	Porcine BEC (P1)	100–120	Inulin flux ↑	Fischer *et al.* (1999b, 2000, 2001)
Hypoxia (2% O_2, 6–24 h; 32°C)	Porcine BEC (P1)	100–120	Inulin flux≈	Fischer *et al.* (1999b)
Hypoxia (2% O_2, 6–24 h; 22°C)	Porcine BEC (P1)	100–120	Inulin flux≈	Fischer *et al.* (1999b)
Hypoxia (1% O_2; 24 h)	Bovine BEC (P1)	[Sucrose P_e: 8]	TEER ≈ sucrose P_e↑	Mark and Davis (2002), Mark *et al.* (2004)
Hypoxia (0% O_2; 4 h)	Bovine cBEC (P < 10) + rat AC	660 ± 50	Inulin P_e ≈	Brillault *et al.* (2002)
Hypoxia (0% O_2; 12 h)	Bovine cBEC (P < 10) + rat AC	660 ± 50	Sucrose P_e↑ inulin P_e ↑ albumin P_e↑	Brillault *et al.* (2002)
Hypoxia (0% O_2; 4 h) + OGD-ACM (2 h)	Bovine cBEC (P < 10) + rat AC	660 ± 50	Inulin P_e↑	Brillault *et al.* (2002)
Hypoxia (0% O_2; 4 h) + rat ACM (2 h)	Bovine cBEC (P < 10) + rat AC	660 ± 50	Inulin P_e↑	Brillault *et al.* (2002)
Hypoxia (0% O_2; 6 h)	Bovine cBEC (P < 10) + rat AC	>500	Inulin P_e↑ NXY-059 P_e↑	Dehouck *et al.* (2002)
Hypoxia (1% O_2; 24 h)	Bovine BEC (P1) + rat C6-CM	[Sucrose P_e: 7.6]	Sucrose P_e↑	Brown *et al.* (2003)
Hypoxia (1% O_2; 24 h)	Bovine BEC (P1) + rat ACM	[Sucrose P_e: 7.6]	Sucrose P_e↑	Brown *et al.* (2003)
Hypoxia (1% O_2; 24 h)	Bovine BEC (P1)	[Sucrose P_e: 7.6]	Sucrose P_e↑	Brown *et al.* (2003)

Table V. Continued

Insult (dose; time)	In vitro BBB model	TEER (Ω cm^2) [P_e (10^{-6} cm/s)][a]	Effect on permeability[a]	Reference
Hypoxia followed by reoxygenation				
Hypoxia (0% O_2; 4–8 h) + reox. (15 min)	Rat BEC (P1)	5.4[b]	TEER↓	Kondo *et al.* (1996)
Hypoxia (0% O_2; 4–8 h) + reox. (15 min)	Rat BEC (P1) + rat AC	9.1[b]	TEER↓	Kondo *et al.* (1996)
Hypoxia (40mmHg O_2; 6 h) + reox. (5 min)	Porcine BEC(P0) + 15% HS + 5% FCS	80–120	TEER≈	Fischer *et al.* (1996)
Hypoxia (0% O_2; 1 h) + reox. (95% O_2; 1 h)	Rat BEC (P1) + rat AC	[NaFl P_e = 13–33]	NaFl P_e↑	Utepbergenov *et al.* (1998)
Hypoxia (1% O_2;24 h) + reox. (2 h)	Bovine BEC (P1)	[Sucrose P_e: 8]	TEER ≈ sucrose P_e↑	Mark and Davis (2002), Mark *et al.* (2004)
Hypoxia combined with glucose deprivation				
Hypoxia + aglycemia (0% O_2;3–24 h)	Bovine BEC (P1)	200	Sucrose P_e ↑	Abbruscato and Davis (1999a)
Hypoxia + aglycemia (0% O_2;1 h)	Bovine BEC (P1)	200	Sucrose P_e ≈	Abbruscato and Davis (1999a)
Hypoxia + aglycemia (0% O_2;6 h)	Bovine BEC (P1) + rat C6-CM	200	Sucrose P_e↑	Abbruscato and Davis (1999a)
Hypoxia + aglycemia (0% O_2;6 h)	Bovine BEC (P1) + rat C6	200	Sucrose P_e↑	Abbruscato and Davis (1999a)
Hypoxia + aglycemia (0% O_2; 3–9 h)	Bovine cBEC (P < 10) + rat AC	>500	Inulin P_e↑ NXY-059 P_e ↑	Dehouck *et al.* (2002)
OGD (0% O_2; 0.2 g/L glucose; 2–4 h)	Bovine cBEC (P < 10) + rat AC	660 ± 50	TEER ≈ sucrose P_e ↑ albumin P_e↑ apoTF P_e ↑	Brillault *et al.* (2002)
OGD (0% O_2; 0.2 g/L glucose; 2–4 h; 4° C)	Bovine cBEC (P < 10) + rat AC	660 ± 50	Sucrose P_e ↑ inulin P_e↑ apoTF P_e ↑	Brillault *et al.* (2002)
Related factors without hypoxia				
Hypercapnia (10% CO_2, 24 h)	Porcine BEC (P0) + 15% HS + 5% FCS	100–120	TEER≈	Fischer *et al.* (1996)
Normoxia + aglycemia (21% O_2;6 h)	Bovine BEC (P1)	200	Sucrose P_e ≈	Abbruscato and Davis (1999a)
Hypoglycemia (0.2 g/L glucose; 4 h)	Bovine cBEC (P < 10) + rat AC	660 ± 50	Inulin P_e ≈	Brillault *et al.* (2002)

Note. ↓ = Significant decrease, ≈ = no significant change, ↑ = significant increase, AC = astrocytes, ACM = astrocyte-conditioned medium, apoTF = apotransferrin, BBB = blood–brain barrier, BEC = brain capillary endothelial cells, cBEC = bovine cloned brain capillary endothelial cells, C6 = rat C6 glioma cell line, C6-CM = rat C6 glioma cell line conditioned medium, Da = Dalton, FCS = fetal calf serum, h = hour, kDa = kilodalton, m.w. = molecular weight, NaFl = sodium fluorescein, N.C. = not comparable, N.I. = not indicated, OGD = oxygen-glucose deprivation (0% O_2 combined with 0.2 g/L glucose), OGD-ACM = conditioned medium from rat astrocytes underwent oxygen-glucose deprivation, P = passage number of endothelial cells, P0 = primary brain endothelial cells seeded directly on cell culture insert, P_e = endothelial permeability coefficient, reox. = reoxygenation, TEER = transendothelial electrical resistance.

[a]Molecular weights of permeability tracers used are as follows, apoTF: 80 kDa; albumin: 67 kDa; inulin: 5 kDa; NaFl: 376 Da; sucrose: 342 Da. This table contains a representative P_e value of a paracellular tracer if TEER value was not indicated in the paper.

[b]In a study, TEER value was expressed as Ω/cm^2. Because surface area (24-well format) was given in the paper, comparable TEER value could be calculated.

and albumin in the presence of glia when exposed to 12 h hypoxia (Brillault *et al.*, 2002).

Furthermore, while oxygen-glucose deprivation (OGD) for 4 h had no effect on endothelial cells alone, in the presence of glia or conditioned medium of OGD-treated glia cells a huge increase in inulin flux was seen in endothelial monolayers exposed to OGD suggesting that soluble glial factors can participate in the endothelial hyperpermeability (Brillault *et al.*, 2002). Other experiments argue, however, for a protective role of glia. On a rat BBB model, astroglia attenuated the increase in paracellular flux of brain endothelial monolayers following 4 h hypoxia and 15 min reoxygenation (Kondo *et al.*, 1996). Hypoxia-induced increase in inulin flux in porcine endothelial cells was decreased by coculture with glia or treatment with astrocyte-conditioned medium (Fischer *et al.*, 2000). Three-day culture of bovine cerebral endothelial cells in C6 glioma-conditioned medium protected against hypoxia-induced increase in permeability for sucrose, while astroglia- or C6 glioma-conditioned medium had no effect on basal permeability (Brown *et al.*, 2003). Finally, no effect of treatment by C6 glioma-conditioned medium or coculture with C6 glioma cells was seen in bovine endothelial cells subjected to OGD (Abbruscato and Davis, 1999a).

The following agents showed protective effects against hypoxia or OGD-induced brain endothelial hyperpermeability: *N*-methyl-D-aspartic acid (NMDA) receptor antagonist MK-801 and aminosteroid U83836E (Giese *et al.*, 1995), barbiturates methohexital and thiopental (Fischer *et al.*, 1996), NO and the NO donor *S*-nitroso-*N*-acetylpenicillamine (SNAP; Utepbergenov *et al.*, 1998), nonspecific cation channel blocker SKF 96365 and L-type calcium channel blocker nifedipine (Abbruscato and Davis, 1999a), dexamethasone (Fischer *et al.*, 2001), or NO synthase inhibitors Nω-nitro-L-arginine methyl ester (L-NAME) and 1400W (Mark *et al.*, 2004).

Regulation of In Vitro BBB Permeability by Cytokines

Interaction between proinflammatory or other cytokines and cells of the BBB is inevitable especially in inflammatory-, infectious-, or immune-mediated diseases. Human recombinant interferon-α2a, an anti-viral cytokine used in hepatitis C or antitumor therapies, elevated TEER in bovine brain endothelial cell-rat astroglia coculture, moreover, it reduced the LPS-induced damage to endothelial monolayer integrity (Gaillard *et al.*, 2003; Table VI). A similar effect was observed with interferon-β1b (Gaillard *et al.*, 2003). On the contrary, interferon-γ, a proinflammatory cytokine elevated albumin flux through rat brain endothelial monolayers (Annunziata *et al.*, 2002).

All proinflammatory interleukins tested so far affected brain endothelial paracellular permeability (Table VI). Interleukin-1α increased inulin flux through porcine cerebral endothelial monolayers (Gloor *et al.*, 1997), while interleukin-1β and interleukin-6 induced a decline in TEER of rat brain endothelial cells (de Vries *et al.*, 1996b). Although direct effect of interleukin-6 has not been tested on a dynamic 3-dimensional in vitro model of BBB, interleukin-6 production was a crucial

Table VI. Effects of Cytokines on Permeability Data Obtained on In Vitro Blood–Brain Barrier Models

Insult (dose; time)	In vitro BBB model	TEER (Ω cm^2) [P_e (10^{-6} cm/s)][a]	Effect on permeability[a]	Reference
Interferon-α2a (1–100 U/mL, 6 h)	Bovine BEC (P1) + rat AC	N.I.	TEER↑	Gaillard *et al.* (2003)
Interferon-β1b (1000 U/mL, 1 h-ON)	Bovine BEC (P1) + rat AC	N.I.	TEER↑	Gaillard *et al.* (2003)
Interferon-γ (10 IU/mL, 48 h)	Rat BEC (P1) + 30% FBS	9[b]	Biotin–albumin flux↑	Annunziata *et al.* (2002)
Interleukin-1α (1 ng/mL, 15–72 h)	Porcine BEC (P5–15)	N.I.	Inulin flux↑	Gloor *et al.* (1997)
Interleukin-1β (5–100 ng/mL, 1–4 h)	Rat BEC (P1) + rat ACM	100–150	TEER↓	de Vries *et al.* (1996)
Interleukin-6 (10–100 ng/mL, 1–5 h)	Rat BEC (P1) + rat ACM	100–150	TEER↓	de Vries *et al.* (1996)
TNF-α (50–500 U/mL; 4 h)	Bovine cBEC (P < 10) + rat AC	>500	Sucrose flux≈ inulin flux≈	Deli *et al.* (1995)
TNF-α (50–500 U/mL; 1 h + 16 h rat AC)	Bovine cBEC (P < 10) + rat AC	>500	Sucrose flux↑ inulin flux↑	Deli *et al.* (1995)
TNF-α (1–50 ng/mL, 1–4 h)	Rat BEC (P1) + rat ACM	100–150	TEER↓	de Vries *et al.* (1996)
TNF-α (50–500 U/mL; 36 h)	Bovine BEC (P?)	[Cisplatin P_e = 0.6]	Cisplatin P_e↑ FD_{70} P_e ≈	Anda *et al.* (1997)
TNF-α (250 U/mL; 4 h)	Bovine cBEC (P < 10) + rat AC	>500	Sucrose P_e ↑ inulin P_e ≈	Descamps *et al.* (1997)
TNF-α (250 U/mL; 4 h + 16 h rat AC)	Bovine cBEC (P < 10) + rat AC	>500	Sucrose P_e ≈ inulin P_e ≈	Descamps *et al.* (1997)
TNF-α (250 U/mL; 4 h)	Bovine cBEC (P < 10) + rat AC	>500	Sucrose P_e ≈ inulin P_e ≈	Fillebeen *et al.* (1999)
TNF-α (<abl>250 U/mL; 4 h)	Bovine cBEC (P < 10) + rat AC	>500	Sucrose P_e ≈ inulin P_e ≈	Fillebeen *et al.* (1999)
TNF-α (250 U/mL; 4 h, with rat AC)	Bovine cBEC (P < 10) + rat AC	>500	Sucrose P_e ≈ inulin P_e ≈	Fillebeen *et al.* (1999)
TNF-α (250 U/mL; 4 h + 20 h rat AC)	Bovine cBEC (P < 10) + rat AC	>500	Sucrose P_e ≈ inulin P_e ≈	Fillebeen *et al.* (1999)
TNF-α (110–11,000 U/mL, 2–12 h)	Bovine BEC (P1)	[NaFl P_e = 29]	NaFl P_e ↑ FD_4 P_e ↑ FD_{70} P_e ↑	Mark and Miller (1999)
TNF-α (200–400 ng/mL, 24 h)	Human ECV304 (P?) + rat C6	92 ± 9	TEER↓ sucrose flux↑	Hurst and Fritz (1996)

TNF-α (400 ng/mL, 18 h)	Human ECV304 (P?) + rat C6	77 ± 3	TEER↓	Hurst and Clark (1997)
TNF-α (400 ng/mL, 18 h)	Human ECV304 (P?) + rat C6	82 ± 3	TEER↓	Dobbie *et al.* (1999)
TNF-α (400 ng/mL, 18 h)	Human ECV304 (P?)	28 ± 1	TEER↓	Dobbie *et al.* (1999)
TNF-α (100 ng/mL, 6 h)	Bovine BEC (P1)	N.I.	NaFl flux↑ FD_3 flux↑	Mark *et al.* (2001)
TNF-α (10–100 IU/mL, 48 h)	Rat BEC (P1) + 30% FBS	9[b]	Biotin–albumin flux↑	Annunziata *et al.* (2002)
TNF-α (100–500 ng/mL, 24 h)	Human BEC (P3) + human AC	N.I.	Sucrose flux↑	Didier *et al.* (2003)
TNF-α (100–500 ng/mL, 24 h)	Human BEC (P3)	N.I.	Sucrose flux≈	Didier *et al.* (2003)

Note. ↓ = Significant decrease, ≈ = no significant change, ↑ = significant increase, AC = astrocytes, ACM = astrocyte-conditioned medium, BBB = blood–brain barrier, BEC = brain capillary endothelial cells, cBEC = bovine cloned brain capillary endothelial cells, Da = Dalton, $FD_{m.w.}$ = fluorescein isothiocyanate-dextran (m.w. = molecular weight in kDa), h = hour, m.w. = molecular weight, NaFl = sodium fluorescein, N.I. = not indicated, ON = overnight treatment, P = passage number of endothelial cells, P? = passage number is not indicated, P_e = endothelial permeability coefficient, TEER = transendothelial electrical resistance, TNF-α = tumor necrosis factor-α.

[a]Molecular weights of permeability tracers used are as follows, biotin–albumin: 67 kDa; cisplatin: 300 Da; FD_3: 3 kDa; FD_4: 4 kDa; FD_{70}: 70 kDa; inulin: 5 kDa; NaFl: 376 Da; sucrose: 342 Da. This table contains a representative P_e value of a paracellular tracer if TEER value was not indicated in the paper.

[b]In a study, TEER value was expressed as Ω/cm^2. Because surface area (24-well format) was given in the paper, comparable TEER value could be calculated.

component of a BBB protective mechanism triggered by normoxic, normoglycemic flow cessation and reperfusion (Krizanac-Bengez *et al.*, 2003).

The great majority of the studies on cytokines, investigated the effect of tumor necrosis factor-α (TNF-α), a prominent proinflammatory cytokine involved in many neuropathological conditions. In those experiments where no effect on permeability was seen, brain endothelial monolayers were incubated either for short period with TNF-α or without astroglia (Deli *et al.*, 1995c; Didier *et al.*, 2003). Importantly, even in those studies where no change in paracellular permeability was observed, TNF-α significantly elevated the specific transendothelial transcytosis of transport molecules LDL and lactoferrin (Descamps *et al.*, 1997; Fillebeen *et al.*, 1999a; Table VI). In the majority of studies, however, TNF-α increased paracellular or transcellular BBB permeability in vitro (Table VI). TNF-α decreased TEER of endothelial monolayers either in coculture with glia (de Vries *et al.*, 1996b; Dobbie *et al.*, 1999; Hurst and Clark, 1997; Hurst and Fritz, 1996) or in monoculture (Dobbie *et al.*, 1999). TNF-α also increased the flux of sucrose, sodium fluorescein, cisplatin, inulin, FITC-dextran with 3, 4, and 70 kDa m.w., and albumin (Table VI). The controversy of the results published might originate from differences between TNF-α doses used, application times, or barrier integrities of various in vitro BBB models.

Influence of Pathogenic Factors on In Vitro BBB Permeability

The role of vasoactive and inflammatory mediators in the modulation of BBB permeability has been in the focus of many studies and the topic was reviewed recently (Abbott, 2000). Studies on in vitro models avoid the problems of hemodynamic changes related to BBB permeability, and direct effects of mediators and signaling pathways involved can be examined in brain endothelium. All the mediators and pathogenetic factors listed in Table VII, except for adrenomedullin, dose-dependently increase in vitro BBB permeability on various models.

Bradykinin, an established mediator of vasogenic brain edema, decreases TEER in BBB models (Easton and Abbott, 2002; Gaillard and de Boer, 2000; Hurst and Clark, 1998). This effect mediated through B_2 bradykinin receptors has been exploited for reversible and temporal opening of the BBB by receptor agonist RMP-7 (Mackic *et al.*, 1999) and can be prevented by receptor antagonist HOE-140 (Easton and Abbott, 2002). Histamine, a mediator of brain edema (Joó, 1993), has a dual action on brain endothelial cells (Abbott, 2000). While low concentrations of this neurotransmitter vasogenic amine increase albumin permeability (Deli *et al.*, 1995b) and decrease TEER value (Hurst and Clark, 1998) via H_2 histamine receptor activation coupled to increased intracellular Ca^{2+} concentration, high concentrations increase TEER (Gaillard and de Boer, 2000) through H_1 receptor and elevation of cAMP level. Serotonin and adenosine triphosphate (ATP), both neurotransmitters and vasoactive molecules, also decreased TEER in a coculture model of ECV304 and C6 cell lines (Hurst and Clark, 1998).

The excitotoxic neurotransmitter glutamate is a key player in brain ischemic pathologies. While no permeability change was found in case of basolateral application on a bovine coculture model (Gaillard *et al.*, 1996), apical glutamate treatment

Table VII. Effects of Vasoactive Mediators and Other Pathogenic Factors on Permeability Data Obtained on In Vitro Blood–Brain Barrier Models

Mediator (dose; time)	In vitro BBB model	TEER (Ω cm^2) [P_e (10^{-6} cm/s)][a]	Effect on permeability[a]	Reference
Adrenomedullin (1 μM; 0.25–6 h)	Rat BEC (P1) + rat AC	350–500	TEER↑ NaFl P_e ≈ EBA P_e ≈	Kis *et al.* (2001)
Amyloid-β_{1-40} peptide (0.5–150 nM; 1 h)	Human BEC (P0)	N.I.	Inulin flux≈	Mackic *et al.* (1998)
Amyloid-β_{1-40} peptide (125 nM; 1 h)	Human BEC (P3–6)	11–16[b]	TEER≈ inulin flux≈ FD_{70} flux≈	Giri *et al.* (2000)
Amyloid-β_{25-35} peptide (100 μM; 24 h)	Rat BEC (P1) + rat AC	350–500	TEER↓	Deli *et al.* (unpublished)
Arachidonic acid (50–100 μM; 20 min)	Rat BEC (P1)	N.I.	TBA flux↑	Kempski *et al.* (1987), Villacara *et al.* (1990)
ATP (100 μM; 30 min)	Human ECV304 (P?) + rat C6	92 ± 4	TEER↓	Hurst and Clark (1998)
Atrial natriuretic peptide (N.I; N.I.)	Bovine BEC (P1)	61 ± 2	TEER↓	Rubin *et al.* (1991)
Bradykinin (100 μM, 30 min)	Human ECV304 (P?) + rat C6	106 ± 2	TEER↓	Hurst and Clark (1998)
Bradykinin (10 μM; 5 h)	Bovine BEC (P1) + rat AC	98 ± 50	TEER↓	Gaillard and de Boer (2000)
Bradykinin (1 μM, 2–20 min)	Human ECV304 (P?) + rat C6	144–221	TEER↓	Easton and Abbott (2002)
Endothelin-1 (0.1–1.0 μg/mL, 24 h)	Human BEC (P?) + human AC	N.I.	Sucrose flux↑	Didier *et al.* (2003)
Endothelin-1 (0.1–1.0 μg/mL, 24 h)	Human BEC (P?)	N.I.	Sucrose flux≈	Didier *et al.* (2003)
Glutamate (0.1–4.0 mM; 5 h)	Bovine BEC (P1) + rat AC	130	TEER≈ NaFl P_e ≈ FD_4 flux≈	Gaillard *et al.* (1996)
Glutamate (0.1–1.0 mM; 1 h)	Human BEC (P < 10)	N.I.	FD_{70} flux↑	Collard *et al.* (2002)
Glutamate (0.01–0.1 mM; 1–3 h)	Human IHEC (P?)	61 ± 8[b]	TEER≈	Sharp *et al.* (2003)
Glutamate (1.0 mM; 2–3 h)	Human IHEC (P?)	61 ± 8[b]	TEER↓	Sharp *et al.* (2003)
Histamine (1–10 μM; 1 h)	Bovine cBEC (P < 10) + rat AC	>500	Sucrose flux≈ inulin flux≈ EBA flux ↑	Deli *et al.* (1995)
Histamine (1 mM; 5 h)	Bovine BEC (P1) + rat AC	98 ± 50	TEER↑	Gaillard and de Boer (2000)
Histamine (100 μM, 30 min)	Human ECV304 (P?) + rat C6	106 ± 2	TEER↓	Hurst and Clark (1998)
Prostaglandin E_2 (10 ng/mL, 90 min)	Bovine BEC (P1)	N.I.	FD_3 flux↑	Mark *et al.* (2001)
Prostaglandin $F_{2\alpha}$ (10 ng/mL, 90 min)	Bovine BEC (P1)	N.I.	FD_3 flux↑	Mark *et al.* (2001)
PrP106–126 peptide (100 μM; 24 h)	Rat BEC (P1) + rat AC	300–500	TEER↓ NaFl P_e ↑ EBA P_e ↑	Deli *et al.* (unpublished)
Serotonin (100 μM, 30 min)	Human ECV304 (P?) + rat C6	106 ± 2	TEER↓	Hurst and Clark (1998)

Table VII. Continued

Mediator (dose; time)	In vitro BBB model	TEER (Ω cm^2) [P_e (10^{-6} cm/s)][a]	Effect on permeability[a]	Reference
VEGF (5 ng/mL; 6 h)	Porcine BEC (P0)	100–120	Inulin flux↑	Fischer *et al.* (1998, 1999a, 2001)
VEGF (<abl> 50–200 ng/mL; 10–48 h)	Bovine BEC (P1)	N.I.	TEER↓ sucrose flux↑	Wang *et al.* (1996, 2001)
VEGF (50–200 ng/mL; 24–48 h)	Bovine BEC (P1)	N.I.	Sucrose flux↑ albumin flux≈	Wang *et al.* (1996)
VEGF (50–200 ng/mL; 48 h)	Bovine BEC (P1)	165	TEER≈ sucrose flux≈	Wang *et al.* (2001)
VEGF (<abl> N.I.; 6–9 h)	Bovine cBEC (P < 10) + rat AC	500–800	P_e inulin↑	Ruchoux *et al.* (2002)
VEGF (5 ng/mL; 6 h) + α-LA (2 μM)	Porcine BEC (P0)	100–120	Inulin flux↑	Fischer *et al.* (1999b)
VEGF pAb (10 μg/mL)	Porcine BEC (P0)	100–120	Inulin flux≈	Fischer *et al.* (1998)

Note. ↓ = Significant decrease, ≈ = no significant change, ↑ = significant increase. AC = astrocytes, ACM = astrocyte-conditioned medium, ATP = adenosine triphosphate, BBB = blood–brain barrier, BEC = brain capillary endothelial cells, cBEC = bovine cloned brain capillary endothelial cells, Da = Dalton, EBA = Evans blue-labeled albumin, $FD_{m.w.}$ = fluorescein isothiocyanate-dextran (m.w. = molecular weight in kDa), h = hour, kDa = kilodalton, α-LA = α-lipoic acid, m.w. = molecular weight, NaFl = sodium fluorescein, N.I. = not indicated, P = passage number of endothelial cells, P? = passage number is not indicated, P0 = primary brain endothelial cells seeded directly on cell culture insert, pAb = polyclonal antibody, P_e = endothelial permeability coefficient, PGE_2 = prostaglandin E2, $PGF_{2\alpha}$ = prostaglandin F2α, RA = retinoic acid, TEER = transendothelial electrical resistance, VEGF = vascular endothelial growth factor.

[a]Molecular weights of permeability tracers used are as follows, albumin: 67 kDa; EBA: 67 kDa; FD_3: 3 kDa; FD_4: 4 kDa; FD_{70}: 70 kDa; inulin: 5 kDa; NaFl: 376 Da; sucrose: 342 Da.

[b]In some studies, TEER values were expressed as Ω/cm^2. In case surface area was given in the paper, comparable TEER value could be calculated.

increased the flux of 70 kDa FITC-dextran (Collard *et al.*, 2002) and decreased TEER (Sharp *et al.*, 2003) in human brain endothelial monolayers. These results support that brain endothelial cells express functional glutamate receptors (Krizbai *et al.*, 1998; Sharp *et al.*, 2003).

There are several pathogenic factors at the BBB, which are involved in the regulation of hypoxia-induced changes. Among hypoxia-inducible factor 1 regulated genes (Semenza, 2001), endothelin-1, inducible NO synthase (iNOS), TGF-β, and VEGF contribute to the damage of BBB integrity, whereas adrenomedullin reinforces the barrier function (Tables IV, VII, and X). VEGF stimulates endothelial cell growth, induces angiogenesis, and increases endothelial permeability both under in vivo conditions and in in vitro BBB models. VEGF increases sucrose and inulin flux, and decreases TEER (Table VII). It is more effective when applied at the abluminal side (Ruchoux *et al.*, 2002; Wang *et al.*, 1996, 2001) or when added in the presence of α-lipoic acid, an antioxidant (Fischer *et al.*, 1999a,b). This effect of VEGF can also be blocked by specific antibody (Fischer *et al.*, 1998). Endothelin-1 increases sucrose flux in the presence of astroglia in human brain endothelial cells (Didier *et al.*, 2003). Lipid mediators prostaglandin E_2 and prostaglandin $F_{2\alpha}$ increased in vitro BBB permeability and this effect can be involved in mediating action of TNF-α on brain endothelial cells (Mark *et al.*, 2001). Atrial natriuretic peptide decreases TEER acting through elevation of intraendothelial cGMP level (Rubin *et al.*, 1991).

Amyloid proteins are involved in the pathogenesis of fatal neurodegenerative diseases. Amyloid peptides, such as amyloid β 1–40 and 25–35 peptide fragments or prion peptide toxic fragment 106–126, are used for disease modeling. When tested on a syngeneic rat in vitro BBB coculture model for 24 h, they increased sucrose and albumin permeability and decreased TEER by exerting cytotoxic effect on brain endothelial cells (Deli *et al.*, unpublished). These changes could be prevented by pre-treatment with pentosan polysulfate, a semisynthetic polyanion. Incubation with low dose of amyloid β 1–40 peptide for 1 h, however, did not change TEER, and flux of inulin or 70 kDa FITC-dextran (Giri *et al.*, 2000; Mackic *et al.*, 1998).

Effects of Infectious Agents on In Vitro BBB Permeability

The interaction of infectious agents with brain endothelial cells is crucial in the pathogenesis of meningitis, encephalitis, and neurological symptoms of acquired immunodeficiency syndrome. Among Gram-negative bacteria causing neonatal meningitis, *Escherichia coli* and *Citrobacter freundii* are able to invade and transcytose human brain endothelial cells without affecting the integrity of the monolayer (Badger *et al.*, 1999; Stins *et al.*, 2001). Furthermore, *C. freundii* replicates within immortalized human brain endothelial cells, which can be related to its pathogenicity (Badger *et al.*, 1999). In contrast to these results, *Streptococcus pneumoniae*, possessing the cytotoxic virulence factor pneumolysin, dramatically decreases TEER of bovine brain endothelial cells (Zysk *et al.*, 2001). Pneumolysin-deficient or heat-killed bacteria show no effect (Table VIII).

Table VIII. Effects of Infectious Agents and Components on Permeability Data Obtained on In Vitro Blood–Brain Barrier Models

Infectious agent (number or dose; time)	In vitro BBB model	TEER (Ω cm^2) [P_e (10^{-6} cm/s)][a]	Effect on permeability[a]	Reference
Bacteria, and bacterial toxins				
Bacteria				
Citrobacter freundii (10^7; 2 h)	Transfected human BEC (<P30)	100[b]	TEER≈ inulin flux≈	Badger *et al.* (1999)
E. coli HB101 strain (10^7; 8 h)	Human BEC (P1–2)	33–55[b]	TEER≈ inulin flux↓	Stins *et al.* (2001)
E. coli HB101 strain (10^7; 8 h)	Transfected human BEC (<P30)	33–55[b]	TEER≈ inulin flux≈	Stins *et al.* (2001)
E. coli E44 strain (10^7; 8 h)	Human BEC (P1–2)	33–55[b]	TEER≈ inulin flux≈	Stins *et al.* (2001)
E. coli E44 strain (10^7; 8 h)	Transfected human BEC (<P30)	33–55[b]	TEER≈ inulin flux≈	Stins *et al.* (2001)
E. coli C5 strain (10^7; 8 h)	Human BEC (P1–2)	33–55[b]	TEER≈ inulin flux≈	Stins *et al.* (2001)
E. coli C5 strain (10^7; 8 h)	Transfected human BEC (<P30)	33–55[b]	TEER≈ inulin flux≈	Stins *et al.* (2001)
Str. pneumoniae D39 strain (10^7; 6–24 h)	Bovine BEC (P1) + rat AC	500–600	TEER↓	Zysk *et al.* (2001)
Str. pneumoniae (pneumolysin-deficient, 10^7; 1 d)	Bovine BEC (P1) + rat AC	500–600	TEER≈	Zysk *et al.* (2001)
Str. pneumoniae (heat-killed; 10^7; 1 d)	Bovine BEC (P1) + rat AC	500–600	TEER≈/↓	Zysk *et al.* (2001)
Lipopolysaccharides				
LPS (*H. influenzae* type B; 0.1–1 μg/mL; 4 h)	Bovine BEC (P1)	N.I.	Albumin flux↑	Tunkel *et al.* (1991)
LPS (*E. coli* O55:B5; 50–5000 ng/mL; 1–6 h)	Bovine (P1) + cAMP↑	250–300	TEER↓ NaFl flux↑ BSA flux↑	De Vries *et al.* (1996a)
LPS (type: N.I.; 50 ng/mL; 5 h)	Bovine BEC (P1) + rat AC	98 ± 50	TEER↓	Gaillard and de Boer (2000)
LPS (*E. coli* O55:B5; 1–100 ng/mL; 2–6 h)	Bovine cBEC (P~10) + rat AC	>500	Sucrose P_e ↑	Descamps *et al.* (2003)
LPS (*E. coli* O55:B5; 1–100 ng/mL; 2–5 h)	Bovine BEC (P1) + rat AC	N.I.	TEER↓	Gaillard *et al.* (2003)
Other bacterial toxins				
Cholera toxin (N.I.; N.I.)	Bovine BEC (P1) + rat ACM	100	TEER ↓	Rubin *et al.* (1991)
Cholera toxin (1000 ng/mL; 1–8 h)	Porcine BEC (P1) + HC + SF	200–1000	HRP flux≈	Bruckener *et al.* (2003)
Pertussis toxin (1 ng/mL; 1–2.5 h)	Bovine BEC (P1)	91 ± 5	TEER ↓	Raub (1996)
Pertussis toxin (0.1–1000 ng/mL; 1–8 h)	Porcine BEC (P1) + HC + SF	200–1000	TEER ↓ HRP flux ↑	Brückener *et al.* (2003)

Viruses, virus components, and virus-infected blood cells				
HIV-1_{LAI} strain (10^6; 24–48 h)	Human BEC (P1)	[Inulin P_e=3.65]	Inulin $P_e \approx$	Liu *et al.* (2002)
HIV-1_{ADA-M}-infected human Mø (2 /times 10^5; 4 d)	Bovine BEC (P1)	1304 ± 11	TEER↑	Zenker *et al.* (2003)
HIV-1_{D117IN}-infected human Mø (2 /times 10^5; 4 d)	Bovine BEC (P1)	1304 ± 11	TEER↑	Zenker *et al.* (2003)
HIV-1 gp120 (0.10–0.50 nM; 24 h)	Rat BEC (P1)	9[b]	Biotin–albumin flux↑	Annunziata *et al.* (1998)
HIV-1 gp120 (0.08–8.0 nM; 20–24 h)	Rat BEC (P1) + rat AC	350—500	TEER≈ NaFl $P_e \approx$ EBA $P_e \approx$	Deli *et al.* (unpublished)
HIV-1 ngp120 (0.08–8.0 nM; 20—24 h)	Rat BEC (P1) + rat AC	350—500	TEER≈ NaFl $P_e \approx$ EBA $P_e \approx$	Deli *et al.* (unpublished)
HTLV-1-infected human T-ly_{MT2} (N.C.; 18 h)	Rat GPNT (P?)	[$FD_{70}P_e$: 0.7]	$FD_{70}P_e$ ↑	Romero *et al.* (2000)
Measles virus NP (100–500 pM; 24 h)	Rat BEC (P1)	9[b]	Biotin–albumin flux↑	Annunziata *et al.* (1998)
Parasites and components				
S. mansoni schistosomula (10^4; 2-4–8 h)	Bovine cBEC (P2–4) + rat AC	>500	Inulin P_e ↓	Trottein *et al.* (1999)
S. mansoni E/S products (≤3 kDa; 5–30 min)	Bovine cBEC (P2–4) + rat AC	>500	Inulin P_e ↓	Trottein *et al.* (1999)
Fungal pathogens				
Candida albicans CAI4 strain (10^6; 6–24 h)	Human BEC (P8–10)	33[b]	TEER≈ inulin flux≈	Jong *et al.* (2001)

Note. ↓ = Significant decrease, ≈ = no significant change, ↑ = significant increase, AC = astrocytes, ACM = astrocyte-conditioned medium, BBB = blood–brain barrier, BEC = brain capillary endothelial cells, BSA = bovine serum albumin, cBEC = bovine cloned brain capillary endothelial cells, d = day, Da = Dalton, EBA = Evans blue-labeled albumin, *E. coli* = *Escherichia coli*, E/S = excretory/secretory, $FD_{m.w.}$ = fluorescein isothiocyanate-dextran (m.w., molecular weight in kDa), gp120 = glycoprotein viral coat of HIV-1, h = hour, HC = hydrocortisone, *H. influenzae* = *Haemophilus influenzae*, HIV-1 = human immunodeficiency virus type 1, HRP = horseradish peroxidase, HTLV-1 infected human T-ly_{MT2} = human T-cell leukemia virus type-1-producing MT2 human T-lymphocytes, kDa = kilodalton, Mø = monocytes/macrophages, m.w. = molecular weight, NaFl = sodium fluorescein, ngp120 = nonglycosylated gp120, N.I. = not indicated, NP = nucleoprotein, P = passage number of endothelial cells, P? = passage number is not indicated, P_e = endothelial permeability coefficient, SF = serum-free, *S. mansoni* = *Schistosoma mansoni*, TEER = transendothelial electrical resistance.

[a]Molecular weights of permeability tracers used are as follows: biotin–albumin, 67 kDa; EBA, 67 kDa; FD_{70}, 70 kDa; HRP, 40 kDa; inulin, 4–5 kDa; NaFl, 376 Da; sucrose, 342 Da. This table contains representative P_e values of permeability tracers if TEER value was not indicated in the paper.

[b]In some studies, TEER values were expressed as Ω/cm². In case surface area (or 24-well format) was given in the paper, comparable TEER value could be calculated.

Not just living bacteria but bacterial cell wall components and toxins can also cause severe BBB disturbances. LPS is the primary endotoxin involved in inflammatory processes, sepsis, and multiorgan failure caused by Gram-negative bacteria like *E. coli* or *Haemophilus influenzae*. In all the in vitro BBB models tested so far, LPS induced a concentration and time-dependent increase in monolayer permeability (Descamps *et al.*, 2003; de Vries *et al.*, 1996a; Gaillard and de Boer, 2000; Gaillard *et al.*, 2003; Tunkel *et al.*, 1991) (Table VIII). Interestingly, glial cells protected cerebral endothelial cells from LPS-mediated injury in a coculture model (Descamps *et al.*, 2003). Pertussis toxin, a virulence factor of *Bordetella pertussis*, severely compromises the integrity of brain endothelial monolayers in a dose- and time-dependent way (Brückener *et al.*, 2003; Raub, 1996). This effect is supposed to be mediated by the PKC pathway (Brückener *et al.*, 2003). Cholera toxin, an activator of protein kinase A (PKA), has a barrier tightening action similar to forskolin or cAMP treatment (Rubin *et al.*, 1991).

The BBB plays a decisive role in the penetration of HIV-1 to brain and development of neuroAIDS (Banks, 1999). Infectious HIV-1 penetrates human brain endothelial monolayer by macropinocytosis without changing its permeability for inulin (Liu *et al.*, 2002). In accordance with this result, HIV-1 envelope protein gp120, either in its infectious glycosylated or in nonglycosylated form, did not affect BBB integrity in a coculture model with high TEER (Deli *et al.*, unpublished observation), although gp120 was published to increase albumin flux in a rat brain endothelial cell monolayer through a substance P-mediated mechanism (Annunziata *et al.*, 1998). However, in the second in vitro model with low barrier characteristics, recombinant measles virus nucleoprotein could also elevate albumin permeability, which may suggest a nonspecific process (Annunziata *et al.*, 1998). Interestingly, even HIV-1 infection could not change the barrier enhancing inductive effect of blood-derived human macrophages in bovine brain endothelial monolayers (Zenker *et al.*, 2003) (Tables III and VIII).

Human T-cell leukemia virus type-1 (HTLV-1) infected human lymphocytes showed enhanced adhesion to and migration through rat GPNT cell line monolayers and induced a 2-fold increase in paracellular permeability (Romero *et al.*, 2000).

The helminth parasite *Schistosoma mansoni*, in its schistosomula stage, developed a special technique to evade from the host immune system. *S. mansoni* secretes factors elevating cAMP level in bovine brain endothelial cells that develop an anti-inflammatory phenotype and enhanced barrier properties (Trottein *et al.*, 1999).

Among fungal pathogens, only *Candida albicans* has been tested on BBB permeability in vitro (Table VIII) and no specific effect was seen in human brain endothelial monolayers (Jong *et al.*, 2001).

PHARMACOLOGY

In vitro models have been widely used in pharmacological research for screening drugs and drug candidate molecules for either modifying BBB permeability or investigating brain penetration. It is difficult to overestimate the importance of permeability screening during drug development in pharmaceutical industry, and it is assumed that the published reports are only the tip of the iceberg in this field (Cecchelli *et al.*, 1999; Eddy *et al.*, 1997; Gumbleton and Audus, 2001; Lundquist

et al., 2002; Pirro *et al.*, 1994; Thomas *et al.*, 1997). In this article, pharmacological treatments modulating signal transduction or cellular metabolism, and modification of physico-chemical properties of molecules to enhance their permeability are listed and evaluated.

Effects of Treatments Affecting Signal Transduction on In Vitro BBB Permeability

Elevation of Intraendothelial cAMP Level

The effect of intracellular cAMP increase is unequivocal, in all models tested until now cAMP elevation resulted in barrier tightening (Table IX). Elevation of intraendothelial cAMP by 8-(4-chlorophenylthio)-cAMP or dibutyryl-cAMP, both of them are cell-permeable cAMP analogues activating PKA, increases TEER, and decreases paracellular flux of sucrose, fluorescein, mannitol, and inulin (Table IX). Forskolin, a cell-permeable adenylate cyclase activator, has similar effect (Brückener *et al.*, 2003; Rubin *et al.*, 1991; Zenker *et al.*, 2003). Isoproterenol, a selective β-adrenergic agonist that stimulates adenylate cyclase activity and activates mitogen-activated protein kinases, also raised brain endothelial TEER (Rubin *et al.*, 1991). Calcitonin gene-related peptide and adrenomedullin clearly demonstrated a cAMP-like effect (Kis *et al.*, 2001; Rubin *et al.*, 1991; Tables IV and IX).

The permeability decreasing effect of cAMP analogues is more pronounced when phosphodiesterase blockers are used simultaneously to prevent the quick metabolization of cAMP. RO 20-1724, a selective inhibitor of cAMP-specific cGMP-independent phosphodiesterase-4 or 3-isobutyl-L-methylxanthine, a nonspecific inhibitor of cAMP and cGMP phosphodiesterases, are widely used for this purpose (Table IX). Moreover, treatment of brain endothelial cells with phosphodiesterase inhibitors alone was also able to strengthen monolayer integrity (Raub, 1996; Zenker *et al.*, 2003). Bovine brain endothelial cells reacted better to cAMP increasing treatment in the presence of glial induction by astrocyte-conditioned medium (Rubin *et al.*, 1991).

Cholera toxin, another strong elevator of intracellular cAMP level, also raised brain endothelial TEER (Rubin *et al.*, 1991; Tables VIII and IX). However, in porcine endothelial cells, cholera toxin and forskolin were ineffective in changing the flux of horseradish peroxidase, while strongly enhanced intracellular cAMP level (Brückener *et al.*, 2003). Since horseradish peroxidase is considered a transcellular permeability marker (Banks and Broadwell, 1994; Nag, 2003), these data clearly indicate a different regulation of junctional and transendothelial permeability in brain endothelial cells. Pertussis toxin, which barely elevates cAMP in brain endothelial cells, decreased TEER (Brückener *et al.*, 2003; Raub *et al.*, 1996), and at the same time, it elevated transendothelial horseradish peroxidase flux via the PKC pathway (Brückener *et al.*, 2003; Tables VIII–IX). This effect of pertussis toxin was completely abolished by concomitant cholera toxin or forskolin administration (Brückener *et al.*, 2003).

Modulation of intraendothelial cAMP concentration by adrenomedullin antisense mRNA probe decreased TEER (Kis *et al.*, 2001), while calmodulin antagonist

Table IX. Effects of Drugs Affecting Intracellular cAMP and Ca^{2+} Levels on Permeability Data Obtained on In Vitro Blood–Brain Barrier Models

Drug (dose; time)	In vitro BBB model	TEER (Ω cm^2) [P_e (10^{-6} cm/s)][a]	Effect on permeability[a]	Reference
Drugs affecting intracellular cyclic AMP level				
Adrenomedullin (1 μM; 0.25–6 h)	Rat BEC (P1) + rat AC	350–500	TEER↑ NaFl $P_e \approx$ EBA $P_e \approx$	Kis *et al.* (2001)
Adrenomedullin (1 μM; 0.25–6 h) + RO (17.5 μM)	Rat BEC (P1) + rat AC	350-500	TEER↑ NaFl P_e↓ EBA $P_e \approx$	Kis *et al.* (2001)
Adrenomedullin antisense (0.6 μg/mL; 3 d)	Rat BEC (P1) + rat AC	100	TEER↓	Kis *et al.* (2001)
Calcitonin gene-related peptide (N.I.; N.I.)	Bovine BEC (P1) + rat ACM	100	TEER↑	Rubin *et al.* (1991)
Cholera toxin (N.I.; N.I.)	Bovine BEC (P1) + rat ACM	100	TEER↑	Rubin *et al.* (1991)
Cholera toxin (1000 ng/mL; 1–8 h)	Porcine BEC (P1) + HC + SF	200–1000	HRP flux≈	Brückener *et al.* (2003)
Cpt-cAMP (250 μM; 72 h)	Bovine BEC (P1)	61 ± 2	TEER↑	Rubin *et al.* (1991)
Cpt-cAMP (250 μM; 3–20 h)	Bovine BEC (P1) + rat ACM	100	TEER↑	Rubin *et al.* (1991)
Cpt-cAMP (250 μM; 3–20 h)	Bovine cBEC (P10)	25	TEER↑	Rubin *et al.* (1991)
Cpt-cAMP (250 μM; 3–20 h)	Bovine cBEC (P10) + rat ACM	35	TEER↑	Rubin *et al.* (1991)
Cpt-cAMP (250 μM; 3–20 h) + RO (17.5 μM)	Bovine BEC (P1) + rat ACM	100	TEER↑	Rubin *et al.* (1991)
Cpt-cAMP (250 μM; 3–20 h) + RO (17.5 μM)	Bovine cBEC (P10)	25	TEER↑	Rubin *et al.* (1991)
Cpt-cAMP (250 μM; 1–4 h) + RO (17.5 μM)	Bovine cBEC (P < 10) + rat AC	>500	Sucrose flux↓ inulin flux↓	Deli *et al.* (1995a)
Cpt-cAMP (250 μM; 24 h) + RO (17.5 μM)	Rat RBE4 (P20–60)	[Sucrose P_e = 35]	Sucrose P_e ↓	Rist *et al.* (1997)
Cpt-cAMP (250 μM; 24 h) + RO (17.5 μM)	Rat RBE4 (P20–60) + rat AC	[Sucrose P_e = 214]	Sucrose $P_e \approx$	Rist *et al.* (1997)
Cpt-cAMP (125 μM; 1–15 h) + RO (17.5 μM)	Porcine BEC (P1)	75	TEER↑ mannitol flux↓	Igarashi *et al.* (1999)
Cpt-cAMP (250 μM; 0.25–6 h) + RO (17.5 μM)	Rat BEC (P1) + rat AC	350–500	TEER↑ NaFl P_e ↓ EBA $P_e \approx$	Kis *et al.* (2001)
Cpt-cAMP (312.5 μM; 2–3 d) + RO (17.5 μM)	Bovine BEC (P1)	92 ± 11	TEER↑	Gaillard *et al.* (2001)
Cpt-cAMP (250 μM; 24 h) + RO (20 μM)	Mouse b.End3 (P27–33) + rat C6	80	TEER↑ sucrose $P_e \approx$	Omidi *et al.* (2003)
Db-cAMP + IBMX (both 100 μM; 48 h)	Bovine BEC (P1)	91 ± 5	TEER↑	Raub (1996)
Forskolin (N.I., N.I.)	Bovine BEC (P1) + ACM	100	TEER↑	Rubin *et al.* (1991)
Forskolin (50 μM; 1–2 d)	Bovine BEC (P1) + rat C6 + FCS	1353 ± 39	TEER↑	Zenker *et al.* (2003)
Forskolin (50 μM; 1 – 2 d)	Bovine BEC (P1) + human Mø + FCS	1200–1400	TEER↑	Zenker *et al.* (2003)
Forskolin (50 μM; 1 – 8 h)	Porcine BEC (P1) + HC + SF	200–1000	HRP flux≈	Brückener *et al.* (2003)
Forskolin (1–250 μM; 1–2 d) + IBMX (100 μM)	Bovine BEC (P1)	91 ± 5	TEER↑	Raub (1996)

Forskolin + RO (both 50 μM; 2 d)	Bovine BEC (P1)	15	TEER↑ inulin flux↓	Wolburg *et al.* (1994)
Forskolin + RO (both 50 μM; 2 d)	Bovine BEC (P1) + rat ACM	20	TEER↑ inulin flux↓	Wolburg *et al.* (1994)
Forskolin + RO (both 20 μM; 24 h)	Human ECV304 (P?) + rat C6	92 ± 4	TEER↑	Hurst and Clark (1998)
IBMX (100 μM; 48 h)	Bovine BEC (P1)	91 ± 5	TEER↑ sucrose P_e ↓ FD_{70} P ↓	Raub (1996)
Isoproterenol (N.I.; N.I.)	Bovine BEC (P1) + rat ACM	100	TEER↑	Rubin *et al.* (1991)
Pertussis toxin (1 ng/mL; 1–2.5 h)	Bovine BEC (P1)	91 ± 5	TEER↓	Raub (1996)
Pertussis toxin (0.1–1000 ng/mL; 1–8 h)	Porcine BEC (P1) + HC + SF	200–1000	TEER↓ HRP flux↑	Brückener *et al.* (2003)
RO (50 μM, 1–2 d)	Bovine BEC (P1) + rat C6 + FCS	1353 ± 39	TEER↑	Zenker *et al.* (2003)
RO (50 μM, 1–2 d)	Bovine BEC (P1) + human Mø + FCS	1200–1400	TEER↑	Zenker *et al.* (2003)
SQ 22536 (100 mM, 1–2 d)	Bovine BEC (P1) + rat C6 + FCS	1353 ± 39	TEER≈	Zenker *et al.* (2003)
SQ 22536 (100 mM, 1–2 d)	Bovine BEC (P1) + human Mø + FCS	1200–1400	TEER≈	Zenker *et al.* (2003)
W-7 (50 μM, 1–2 d)	Bovine BEC (P1) + rat C6 + FCS	1353 ± 39	TEER≈	Zenker *et al.* (2003)
W-7 (50 μM, 1–2 d)	Bovine BEC (P1) + human Mø + FCS	1200–1400	TEER≈	Zenker *et al.* (2003)
Drugs affecting intracellular Ca^{2+} level and Ca^{2+} channels				
A23187 (1 μM; rapidly)	Bovine BEC (P1) + rat C6	91 ± 5	TEER↓	Raub (1996)
A23187 (10 μM; 30 min)	Human ECV304 (P?) + rat C6	92 ± 4	TEER↓	Hurst and Clark (1998)
BAPTA (4 mM; 10 min)	Porcine BEC (P1) + PDS	308 ± 55	Sucrose flux↑	Schulze *et al.* (1997)
BAPTA (4 mM; 10 min)	Porcine BEC(P1) + cAMP↑ + PDS	852 ± 67	Sucrose flux↑	Schulze *et al.* (1997)
Butyric acid (12.5–75 μM; 18 h)	Human ECV304 (P?) + rat C6	89 ± 6	TEER ↑	Hurst and clark (1999)
EGTA (2.5 mM; 10 min)	Bovine BEC (P1)	783 ± 7	TEER↓	Rutten *et al.* (1987)
EGTA (1 mM; 15 min)	Bovine BEC (P1)	50	TEER↓ sucrose P_e ↑	Raub *et al.* (1992)
EGTA (<abl>1 mM; 10 min)	Bovine BEC (P1)	165	TEER↓	Wang *et al.* (2001)
Ca^{2+}-free medium (5 min)	Rat BEC (P1)	N.I.	Sucrose flux↑	Bowman *et al.* (1983)
Ca^{2+}-free medium (10 min)	Bovine BEC (P1)	783 ± 7	TEER↓	Rutten *et al.* (1987)

Table IX. Continued

Drug (dose; time)	In vitro BBB model	TEER (Ω cm^2) [P_e (10^{-6} cm/s)][a]	Effect on permeability[a]	Reference
Ca^{2+}-free medium (1 h)	Porcine BEC (P0)	98 ± 2	TEER↓	Fischer *et al.* (1995)
Ionomycin (10 μM; 30 min)	Human ECV304 (P?) + rat C6	92 ± 4	TEER↓	Hurst and Clark (1998)
La^{3+} (10 μM; 10 min)	Human ECV304 (P?) + rat C6	144–221	TEER≈	Easton and Abbott (2002)
La^{3+} (10 μM; 10 min) + thapsigargin (1 μM)	Human ECV304 (P?) + rat C6	144–221	TEER≈	Easton and Abbott (2002)
Nifedipine (100 nM; 6 h)	Bovine BEC (P1)	200	Sucrose P_e≈	Abbruscato and Davis (1999a)
SKF 96365 (100 nM; 6 h)	Bovine BEC (P1)	200	Sucrose P_e≈	Abbruscato and Davis (1999a)
Thapsigargin (1 μM; 10 min)	Human ECV304 (P?) + rat C6	144–221	TEER↓	Easton and Abbott (2002)
Verapamil (20 μM; 1 h)	Rat RBE4 (P20–80)	[CP P_e = 400]	CP P_e ≈	Yang *et al.* (2001)
Verapamil (20 μM; 1 h)	Rat RBE4 (P20–80) + rat ACM	[CP P_e = 100]	CP P_e ≈	Yang *et al.* (2001)
Verapamil (100 μM; 4 h)	Bovine cBEC + rat AC	>500	Sucrose flux↑ cycloA flux↑	Carpentier *et al.* (1999)

Note. ↓ = Significant decrease, ≈ = no significant change, ↑ = significant increase, 3D = 3-dimensional blood–brain barrier model, A23187 = calmycin calcium ionophore, <abl> = abluminal application, AC = astrocytes, ACM = astrocyte-conditioned medium, BAPTA = 1,2-bis(2-aminophenoxy)ethane-*N*, *N*, *N*′, *N*′-tetraacetic acid, BBB = blood–brain barrier, BEC = brain endothelial cells, C6 = rat C6 glioma cell line, cAMP = adenosine 3′, 5′-cyclic monophosphate, cAMP↑ = drug combination elevating intracellular cAMP level, cBEC = cloned brain endothelial cells, CP = chlorpyrifos, cpt-cAMP = 8-(4-chlorophenylthio)-cAMP, cycloA = cyclosporin A, d = day, EBA = Evans blue-labeled albumin, EGTA = ethylene glycol-*bis*(2-aminoethylether)-*N*,*N*,*N*′,*N*′-tetraacetic acid, FCS = fetal calf serum, $FD_{m.w.}$ = fluorescein isothiocyanate-dextran (m.w. = molecular weight in kDa), h = hour, HC = hydrocortisone, HRP = horseradish peroxidase, IBMX = 3-isobutyl-1-methylxanthine, Mø = monocytes/macrophages, NaFl = sodium fluorescein, N.I. = not indicated, ON = overnight, P = passage number of endothelial cells, P? = passage number is not indicated, P0 = primary brain endothelial cells seeded directly on cell culture insert, PDS = platelet-derived serum, P_e = endothelial permeability coefficient, RO = 4-(3-butoxy-4-methoxybenzyl)-2-imidazolidinone (RO20–1724), SF = serum-free, SQ 22536 = 9-(tetrahydro-2′-furyl)adenine, TEER = transendothelial electrical resistance, W-7 = *N*-(6-aminohexyl)-5-chloro-1-naphtalenesulfonamide.

[a]Molecular weights of permeability tracers used are as follows: CP, 351 Da; cycloA, 1202 Da; EBA, 67 kDa; FD_3, 3 kDa; FD_4, 4 kDa; FD_{70}, 70 kDa; HRP, 40 kDa; inulin, 5 kDa; mannitol, 182 Da; NaFl, 376 Da; sucrose, 342 Da.

W7, or adenylate cyclase inhibitor SQ 22536 did not show any effect on permeability of in vitro models (Zenker *et al.*, 2003).

Changes in Intracellular Calcium Level

Calcium and other divalent cations are needed for the integrity of brain endothelial TJ structures, as discussed earlier. Removal of extracellular Ca^{2+} by using either Ca^{2+}-free medium or Ca^{2+} chelators, such as BAPTA or EGTA, results in a rapid opening of brain endothelial TJ, that is, decreased TEER and increased sucrose flux (Table IX).

Increasing intracellular Ca^{2+} levels by calcium ionophores calmycin (A23187) or ionomycin, rapidly decreases TEER in bovine and human cells (Raub, 1996; Hurst and Clark, 1998). Ca^{2+} channel blockers, such as ionic La^{2+}, SKF 96365, nifedipine, or verapamil, alone have no effect on brain endothelial monolayer integrity (Table IX). High concentration of verapamil, however, could elevate the flux of sucrose and cyclosporin A–cyclophilin B complex through the BBB in vitro (Carpentier *et al.*, 1999). Thapsigargin, used to deplete intracellular Ca^{2+} stores by blocking Ca^{2+} ATPase decreased (Easton and Abbott, 2002), while butyric acid interfering Ca^{2+} release from intracellular stores increased (Hurst and Clark, 1999) TEER values in human ECV304/rat C6 glioma coculture system.

Modulation of Protein Kinase and Protein Tyrosine Kinase Activity

Activation or inhibition of protein kinases could alter the paracellular and transcellular permeability of the BBB in various in vitro models. In bovine endothelial cells cocultured with rat C6 glioma cells, PKC activators, such as phorbol-12-myristate-13-acetate (PMA) or sn-1,2-dioctanoylglycerol (DiC8), could increase TEER (Raub, 1996). Specific PKC inhibitor calphostin C (Easton and Abbott, 2002) did not change, while selective PKA inhibitor H89 (Rubin *et al.*, 1991), or Ca^{2+}/calmodulin-dependent protein kinase II (CaM kinase II) inhibitor HA1004 (Raub, 1996) decreased TEER values in BBB in vitro models. The effect of broad-spectrum protein kinase inhibitors, such as H7, H8, K-252a, or staurosporine, on the barrier integrity depended on the dose-, time-, and in vitro BBB model used (Table X).

Protein tyrosine phosphatase inhibitors phenylarsine oxide and vanadate molecules decreased TEER value in a bovine (Staddon *et al.*, 1995) and increased inulin flux in a porcine (Gloor *et al.*, 1997) model of in vitro reconstituted BBB.

Transcellular permeability of horseradish peroxidase through monolayers of porcine brain endothelial cells did not change after treatment with PKC activators (DiC8, PMA), broad-spectrum protein kinase inhibitor staurosporine, or phosphatidylinositol 3-kinase inhibitors (wortmannin, LY294002) according to a recent paper (Brückener *et al.*, 2003).

Modulation of Phospholipase, Cyclooxygenase, and Lipoxygenase Activity

Similar to natural steroid hydrocortisone (Table IV), dexamethasone, an effective synthetic glucocorticoid hormone inhibiting phospholipase-2 (PLA_2) activity strengthened specific barrier properties, that is, increased TEER and decreased P_e

Table X. Effect of Drugs Affecting Signal Transduction on Permeability Data Obtained on In Vitro Blood–Brain Barrier Models

Drug (dose; time)	In vitro BBB model	TEER (Ω cm^2) [P_e (10^{-6} cm/s)][a]	Effect on permeability[a]	Reference
Drugs affecting protein kinases or tyrosine phosphatases				
DiC8 (100 μM; 1–2 d)	Bovine BEC (P1) + rat C6	91 ± 5	TEER↑	Raub (1996)
DiC8 (100 μg/mL; 5 h)	Porcine BEC (P1) + HC + SF	200–1000	HRP flux≈	Brückener *et al.* (2003)
H7 (50 μM; 1–2 d)	Bovine BEC (P1) + rat C6	91 ± 5	TEER↓	Raub (1996)
H7 (50 μM, 1–2 d)	Bovine BEC (P1) + rat C6 + FCS	1353 ± 39	TEER≈	Zenker *et al.* (2003)
H7 (50 μM, 1–2 d)	Bovine BEC (P1) + human Mø + FCS	1200–1400	TEER≈	Zenker *et al.* (2003)
H7 (50 μM; 5 h)	Porcine BEC (P1) + HC + SF	200–1000	HRP flux≈	Brückener *et al.* (2003)
H8 (≤50 μM; 1–2 d)	Bovine BEC (P1) + cAMP↑	91 ± 5	TEER≈	Raub (1996)
H8 (≤50 μM; 1–2 d)	Bovine BEC (P1) + rat C6	91 ± 5	TEER↑	Raub (1996)
H8 (50 μM, 1–2 d)	Bovine BEC (P1) + rat C6 + FCS	1353 ± 39	TEER≈	Zenker *et al.* (2003)
H8 (50 μM, 1–2 d)	Bovine BEC (P1) + human Mø + FCS	1200–1400	TEER≈	Zenker *et al.* (2003)
H-89 (25 μM; 1–18 h)	Bovine BEC (P1) + cAMP↑	100	TEER↓	Rubin *et al.* (1991)
HA1004 (100 μM; 1–2 d)	Bovine BEC (P1) + rat C6	91 ± 5	TEER↓	Raub (1996)
K-252a (N.I.; 1–18 h)	Bovine BEC (P1) + cAMP↑	100	TEER↓	Rubin *et al.* (1991)
LY294002 (10 μM; 5 h)	Porcine BEC (P1) + HC + SF	200–1000	HRP flux≈	Brückener *et al.* (2003)
PDBu (200 nM; 3 h)	Porcine BEC (P1) + cAMP↑ + PDS	500–600	TEER≈	Schulze *et al.* (1997)
PMA (16.2 nM; 2 d)	Bovine BEC (P1) + rat ACM	20	TEER≈ inulin flux≈	Wolburg *et al.* (1994)
PMA (500 nM; 1–2 d)	Bovine BEC (P1) + rat C6	91 ± 5	TEER↑	Raub (1996)
PMA (50 nM; 30 min)	Human ECV304 (P?) + rat C6	92 ± 4	TEER↓	Hurst and Clark (1998)
PMA (500 nM; 5 h)	Porcine BEC (P1) + HC + SF	200–1000	HRP flux≈	Brückener *et al.* (2003)
Pervanadate (1–100 μM; 10–60 min)	Bovine BEC (P1) + cAMP↑	225	TEER↓	Staddon *et al.* (1995)
Phenylarsine oxide (0.3–30 μM; 15–60 min)	Bovine BEC (P1) + cAMP↑	600	TEER↓	Staddon *et al.* (1995)
Retinoic acid (0.01–1.0 μM; 18 h)	Human ECV304 (P?) + rat C6	89 ± 6	TEER↓	Hurst and Clark (1999)
Staurosporine (100 nM; 1–18 h)	Bovine BEC (P1) + cAMP↑	100	TEER↓	Rubin *et al.* (1991)

Staurosporine (50 nM; 5 h)	Porcine BEC (P1) + HC + SF	200–1000	HRP flux≈	Brückener *et al.* (2003)
Vanadate (N.I.; 15–72 h)	Porcine BEC (P0)	N.I.	Inulin flux↑	Gloor *et al.* (1997)
Wortmannin (100 nM; 5 h)	Porcine BEC (P1) + HC + SF	200–1000	HRP flux≈	Brückener *et al.* (2003)
Drugs affecting phospholipases, cyclooxygenases, or lipoxygenases				
Aristolochic acid (0.5 mM; 10 min)	Human ECV304 (P?) + rat C6	144–221	TEER≈	Easton and Abbott (2002)
Bromophenacyl bromide (1 μM; 3 d)	RBEC (P1)	[Sucrose P_e: 7.5]	Sucrose P_e ≈	Grabb and Gilbert (1995)
Bromophenacyl bromide (1 μM; 3 d)	RBEC (P1) + rat C6	[Sucrose P_e: 6.0]	Sucrose P_e ≈	Grabb and Gilbert (1995)
Calphostin C (0.5 μM; 10 min)	Human ECV304 (P?) + rat C6	144–221	TEER≈	Easton and Abbott (2002)
Dexamethasone (0.1 μM; 3 d)	RBEC (P1)	[Sucrose P_e: 7.5]	Sucrose P_e ↓	Grabb and Gilbert (1995)
Dexamethasone (0.1 μM; 3 d)	RBEC (P1) + rat C6	[Sucrose P_e: 6.0]	Sucrose P_e ≈	Grabb and Gilbert (1995)
Dexamethasone (0.01–1.0 μM; 18 h)	Human ECV304 (P?) + rat C6	89 ± 6	TEER↑	Hurst and Clark (1999)
Dexamethasone (0.4–40 μM; 3–24 h)	Porcine BEC (P0)	70–120	Inulin flux≈	Fischer *et al.* (2001)
Dexamethasone (1 μM; from seeding)	Rat GPNT (P?)	66 ± 3	TEER≈ sucrose P_e ↓ $FD_{70}P_e$ ≈	Romero *et al.* (2003)
Dexamethasone (100 nM; ON)	Bovine BEC (P1)	N.I.	TEER↑	Gaillard *et al.* (2003)
Dexamethasone (100 nM; 6 h-ON)	Bovine BEC (P1) + rat AC	N.I.	TEER↑	Gaillard *et al.* (2003)
ET-18-OCH_3 (100 μM; 10 min)	Human ECV304 (P?) + rat C6	144–221	TEER↓	Easton and Abbott (2002)
Indomethacin (≤10 μM; 1–2 d)	Bovine BEC (P1) + rat C6	91 ± 5	TEER≈	Raub (1996)
Indomethacin (28 μM; 2 h)	Bovine BEC (P1)	N.I.	FD_3 flux≈	Mark *et al.* (2001)
Indomethacin (100 μM; 10 min)	Human ECV304 (P?) + rat C6	144–221	TEER≈	Easton and Abbott (2002)
Indomethacin (10 μM; ON)	Bovine BEC (P1) + rat AC	N.I.	TEER↑	Gaillard *et al.* (2003)
Mifepristone (RU486; 5 μM; 6 h)	Porcine BEC (P0)	70–120	inulin flux≈	Fischer *et al.* (2001)
Nordihydroguaiaretic acid (≤10 μM; 1–2 d)	Bovine BEC (P1) + rat C6	91 ± 5	TEER≈	Raub (1996)
Nordihydroguaiaretic acid (100 μM; 10 min)	Human ECV304 (P?) + rat C6	144–221	TEER≈	Easton and Abbott (2002)

Table X. Continued

Drug (dose; time)	In vitro BBB model	TEER (Ω cm^2) [P_e (10^{-6} cm/s)][a]	Effect on permeability[a]	Reference
Quinacrine (0.1–1.0 mM; 1–5 h)	Bovine BEC (P1) + rat AC	N.I.	TEER↓	Gaillard *et al.* (2003)
U73122 ($\leq$10 μM; 1–2 d)	Bovine BEC (P1) + rat C6	91 ± 5	TEER≈	Raub (1996)
U73122 (20 μM; 10 min)	Human ECV304 (P?) + rat C6	144–221	TEER↑	Easton and Abbott (2002)
U73122 (10 μM; 1–2 d)	Bovine BEC (P1) + rat C6 + FCS	1353 ± 39	TEER≈	Zenker *et al.* (2003)
U73122 (10 μM; 1–2 d)	Bovine BEC (P1) + human Mø + FCS	1200–1400	TEER≈	Zenker *et al.* (2003)

Note. ↓ = Significant decrease, ≈ = no significant change, ↑ = significant increase. AC = astrocytes, ACM = astrocyte-conditioned medium, ATP = adenosine triphosphate, BBB = blood–brain barrier, BEC = brain endothelial cells, C6 = rat C6 glioma cell line, cAMP↑ = drug combination elevating intracellular adenosine 3′,5′-cyclic monophosphate level, cBEC = cloned brain endothelial cells, d = day, DiC8 = sn-1,2-dioctanoylglycerol, ET-18-OCH_3 = 1-*O*-octadecyl-2-*O*-methyl-*rac*-glycero-3-phosphorylcholine=edelfosine, FCS = fetal calf serum, $FD_{m.w.}$ = fluorescein isothiocyanate-dextran (m.w., molecular weight in kDa), h = hour, H7 = 1-(5-isoquinolinesulfonyl)-2-methylpiperazine, H8 = *N*-[2-(methylamino)ethyl]-5-isoquinolinesulfonamide, H-89 = *N*-[2-(*p*-bromocinnamyl-amino)ethyl-5-isoquinolinesulfonamide, HA1004 = N-(2-guanidinoethyl)-5-isoquinolinesulfonamide hydrochloride, HC = hydrocortisone, HRP = horseradish peroxidase, LY294002 = 2-(4-morpholinyl)-8-phenyl-4H-1-benzopyran-4-one, Mø = monocytes/macrophages, NaFl = sodium fluorescein, NDGA = nordihydroguaiaretic acid, N.I. = not indicated, NO = nitric oxide, oligo = oligonucleotide, ON = overnight, P = passage number of endothelial cells, P? = passage number is not indicated, P0 = primary brain endthelial cells seeded directly on cell culture insert, PDBu = phorbol-12,13-dibutyrate, PDS = platelet-derived serum, P_e = endothelial permeability coefficient, PMA = phorbol-12-myristate-13-acetate, SF = serum-free, TEER = transendothelial electrical resistance, U73122 = 1-[6-((17β-3-methoxyestra-1,3,5(10)-trien-17-yl)amino)hexyl]-1H-pyrrole-2,5-dione.

[a]Molecular weights of permeability tracers used are as follows: FD_4, 3 kDa; FD_{70}, 70 kDa; HRP, 40 kDa; inulin, 5 kDa; sucrose, 342 Da.

for paracellular markers, in the majority of models (Table X), whereas mifepristone, a synthetic steroid receptor antagonist did not change inulin flux (Fischer *et al.*, 2001). Treatment with selective PLA_2 inhibitors, however, either did not result in significant change in case of bromophenacyl bromide (Grabb and Gilbert, 1995) and aristolochic acid (Easton and Abbott, 2002), or decreased TEER value, such as quinacrine did (Gaillard *et al.*, 2003).

Phospholipase C (PLC) inhibitor U73122 treatment resulted in a rapid increase in TEER in human ECV304/rat C6 coculture model (Easton and Abbott, 2002), but it was without long-term effect in bovine brain endothelial cell monolayers (Raub, 1996; Zenker *et al.*, 2003). Phosphatidylinositol-specific PLC inhibitor ET-18-OCH_3 (edelfosine), however, decreased TEER value (Easton and Abbott, 2002).

Nonsteroid anti-inlammatory drugs, such as indomethacin, a nonselective inhibitor of cycloxygenase-1 and -2 also affecting PLA_2, had limited effect on the regulation of BBB permeability in vitro, similar to nordihydroguaiaretic acid, a selective 5-lipoxygenase inhibitor (Easton and Abbott, 2002; Gaillard *et al.*, 2003; Mark *et al.*, 2001; Raub, 1996).

Drugs Affecting Metabolism of Nitric Oxide and Reactive Oxygen Species

The gaseous second messenger NO, involved in brain and BBB pathologies, can exert both damaging and protective effects on the barrier integrity (Table XI). NO, at lower concentration than 10 μM does not change in vitro permeability (Hurst and Clark, 1997; Utepbergenov *et al.*, 1998). Doses of NO higher than 20 μM induce a rapid drop in TEER and an increase in fluorescein flux (Hurst and Clark, 1997; Hurst *et al.*, 1998; Utepbergenov *et al.*, 1998). This threshold effect can be observed with NO donors, too. SNAP does not change the barrier integrity at 60 μM or below (Mark *et al.*, 2004; Raub, 1996; Utepbergenov *et al.*, 1998), but induces permeability increase at 150 μM (Utepbergenov *et al.*, 1998). For comparison, diethylenetriaamine NONOate, a longer acting NO donor, raises sucrose P_e above the dose of 10 μM (Mark *et al.*, 2004). Another NO donor, 3-morpholinosydnonimine is without effect on TEER (Raub, 1996), but sodium nitroprusside enhanced the permeability in all concentrations in all models (Table XI). $NaNO_2$ and $NaNO_3$, degradation products of NO, induced no barrier dysfunction (Hurst and Clark, 1997; Hurst *et al.*, 1998).

Nonselective blocker of NO synthases L-NAME, N^G-monomethyl-L-arginine (L-NMMA), or 1400W, a selective inhibitor of inducible NO synthase did not show a permeability modifying action (Table XI). On the dynamic in vitro BBB model, exposure to L-NAME during baseline flow with normal shear levels caused a rapid decrease in TEER arguing for protective actions by basal NO production, and that NO can be important in the maintenance of BBB functions (Krizanac-Bengez *et al.*, 2003).

NO activates the soluble guanylate cyclase signal transduction pathway and increases intracellular cGMP levels. Both exogenous 8-Br-cGMP and atrial natriuretic peptide impairs barrier functions (Rubin *et al.*, 1991; Fischer *et al.*, 1999a).

ROS has been proposed to participate in the pathomechanism of BBB disturbances in several brain diseases. In vitro data on BBB models support this hypothesis (Table XI). Hydrogen peroxide, added directly to rat brain endothelial

Table XI. Effects of Drugs Affecting NO or ROS Levels on Permeability Data Obtained on In Vitro Blood–Brain Barrier Models

Drug (dose; time)	In vitro BBB model	TEER (Ω cm^2) [P_e (10^{-6} cm/s)][a]	Effect on permeability[a]	Reference
Drugs affecting NO concentration and/or intracellular cGMP level				
1400W (100 nM; 24 h)	Bovine BEC (P1)	[Sucrose $P_e = 8$]	Sucrose $P_e \approx$	Mark *et al.* (2004)
Atrial natriuretic peptide (N.I.; 1–2 h)	Bovine BEC (P1)	61 ± 2	TEER↓	Rubin *et al.* (1991)
8-Br-cGMP (1 mM; 6 h)	Porcine BEC (P0)	100–120	Inulin flux↑	Fischer *et al.* (1999a)
DETA-NONOate (10–25 μM; 24 h)	Bovine BEC (P1)	[Sucrose $P_e = 8$]	Sucrose P_e ↑	Mark *et al.* (2004)
Gaseous NO (10 μM; 5–30 min)	Human ECV304 (P?) + rat C6	81 ± 7	TEER≈	Hurst and Clark (1997)
Gaseous NO (20 μM; 5–30 min)	Human ECV304 (P?) + rat C6	81 ± 7	TEER↓	Hurst and Clark (1997)
Gaseous NO (20 μM; 30 min)	Human ECV304 (P?) + rat C6	94 ± 6	TEER↓	Hurst *et al.* (1998)
Gaseous NO (20 μM; 30 min)	Human ECV304 (P?)	37 ± 1	TEER≈	Hurst *et al.* (1998)
Gaseous NO (6 μM; 90 min)	Rat RBE4 (P?) + rat C6	[NaFl P_e = 13–33]	NaFl $P_e \approx$	Utepbergenov *et al.* (1998)
Gaseous NO (25–50 μM; 90 min)	Rat RBE4 (P?) + rat C6	[NaFl P_e = 13–33]	NaFl P_e ↑	Utepbergenov *et al.* (1998)
L-NAME (1 mM, 10 min)	Human ECV304 (P?) + rat C6	144–221	TEER≈	Easton and Abbott (2002)
L-NAME (10 μM; 1 h)	Rat BEC (P1) + rat AC [3D]	320–450	TEER↓	Krizanac-Bengez *et al.* (2003)
L-NAME (100 nM; 24 h)	Bovine BEC (P1)	[Sucrose $P_e = 8$]	Sucrose $P_e \approx$	Mark *et al.* (2004)
L-NMMA (100 μM; 6 h)	Porcine BEC (P0)	100–120	Inulin flux≈	Fischer *et al.* (1999a)
$NaNO_2$ (60 μM; 30 min)	Human ECV304 (P?) + rat C6	81 ± 7	TEER≈	Hurst and Clark (1997)
$NaNO_2$ (60 μM; 30 min)	Human ECV304 (P?) + rat C6	94 ± 6	TEER≈	Hurst *et al.* (1998)
$NaNO_3$ (60 μM; 30 min)	Human ECV304 (P?) + rat C6	81 ± 7	TEER≈	Hurst and Clark (1997)
$NaNO_3$ (60 μM; 30 min)	Human ECV304 (P?) + rat C6	94 ± 6	TEER≈	Hurst *et al.* (1998)
SIN-1 (1–50 μM; 1 h)	Bovine BEC (P1)	91 ± 5	TEER≈	Raub (1996)
SNAP (1–50 μM; 1 h)	Bovine BEC (P1)	91 ± 5	TEER≈	Raub (1996)
SNAP (60 μM; 90 min)	Rat RBE4 (P?) + rat C6	[NaFl P_e = 13–33]	NaFl $P_e \approx$	Utepbergenov *et al.* (1998)
SNAP (150 μM; 90 min)	Rat RBE4 (P?) + rat C6	[NaFl P_e = 13–33]	NaFl P_e ↑	Utepbergenov *et al.* (1998)
SNAP (30 μM; 6–24 h)	Bovine BEC (P1)	[Sucrose $P_e = 8$]	Sucrose $P_e \approx$	Mark *et al.* (2004)
Sodium nitroprusside (0.1–100 μM; 1–2 h)	Bovine BEC (P1)	61 ± 2	TEER↓	Rubin *et al.* (1991)
Sodium nitroprusside (1 μM; 1 h)	Bovine BEC (P1)	91 ± 5	TEER↓	Raub (1996)
Sodium nitroprusside (1 μM; 6 h)	Porcine BEC (P0)	100–120	Inulin flux↑	Fischer *et al.* (1999a)

Sodium nitroprusside (100 μM; 1–5 h)	Bovine BEC (P1) + rat AC	98 ± 50	TEER↓	Gaillard and de Boer (2000)
Drugs affecting ROS level				
Benzylviologen (60 μM; 30 min)	Rat RBE4 (P25–55) + rat C6	[Sucrose P_e: 68]	Sucrose P_e ↑	Lagrange *et al.* (1999)
Buthionine sulfoximine (1 mM; 24 h)	Rat RBE4 (P?) + rat AC	[NaFl P_e = 11]	NaFl P_e ↑	Mertsch *et al.* (2001)
Desferrioxamine mesylate (27 μM; 1–24 h)	Mouse BEC (P1)	59 ± 4	TEER≈	Imaizumi *et al.* (1996)
Desferrioxamine mesylate (10 mM; 5 h)	Bovine BEC (P1) + rat AC	98 ± 50	TEER↑	Gaillard and de Boer (2000)
Desferrioxamine mesylate (1 mM; 3–5 h)	Bovine BEC (P1) + rat AC	N.I.	TEER↑	Gaillard *et al.* (2003)
Dimethyl sulfoxide (0.5%; 30 min)	Human ECV304 (P?) + rat C6	92 ± 4	TEER↑	Hurst and Clark (1998)
Dimethyl sulfoxide (0.05–1.0%; 18 h)	Human ECV304 (P?) + rat C6	89 ± 6	TEER↓	Hurst and Clark (1999)
Dimethyl sulfoxide (0.5%; 10 min)	Human ECV304 (P?) + rat C6	144–221	TEER≈	Easton and Abbott (2002)
Duroquinone (30 μM; 30 min)	Rat RBE4 (P25–55) + rat C6	[Sucrose P_e: 68]	Sucrose P_e ≈	Lagrange *et al.* (1999)
H_2O_2 (0.15–1.00 mM; 15 min)	Rat RBE4 (P?) + rat AC	[NaFl P_e = 7.5]	NaFl P_e ↑	Blasig *et al.* (2002)
α-Lipoic acid (2 μM, 6 h)	Porcine BEC (P0)	100–120	Inulin flux≈	Fischer *et al.* (1998, 1999a)
Menadione (350 μM; 30 min–24 h)	Mouse BEC (P1)	59 ± 4	TEER↓	Imaizumi *et al.* (1996)
Menadione (350 μM; 30 min–24 h)	Mouse SOD Tg BEC (P1)	61 ± 4	TEER↓	Imaizumi *et al.* (1996)
Menadione (10 μM; 30 min)	Rat RBE4 (P25–55) + rat C6	[Sucrose P_e: 68]	Sucrose P_e ≈	Lagrange *et al.* (1999)
Menadione (100 μM; 30 min)	Rat RBE4 (P25–55) + rat C6	[Sucrose P_e: 68]	Sucrose P_e ↑	Lagrange *et al.* (1999)
Methylviologen (0.16–1.25 mM; 1 h)	Mouse BEC (P1)	59 ± 4	TEER↓	Imaizumi *et al.* (1996)
Methylviologen (0.16–1.25 mM; 1 h)	Mouse SOD Tg BEC (P1)	61 ± 4	TEER↓	Imaizumi *et al.* (1996)
Methylviologen (0.4 mM; 30 min)	Rat RBE4 (P25–55) + rat C6	[Sucrose P_e: 68]	Sucrose P_e ≈	Lagrange *et al.* (1999)
N-Acetyl-cysteine (10 mM; 1 h)	Bovine BEC (P1) + rat AC	N.I.	TEER↓	Gaillard *et al.* (2003)
N-Acetyl-cysteine (10 mM; 2–5 h)	Bovine BEC (P1) + rat AC	N.I.	TEER≈	Gaillard *et al.* (2003)
N-Acetyl-cysteine (10 mM; ON)	Bovine BEC (P1) + rat AC	N.I.	TEER↑	Gaillard *et al.* (2003)
Nitrofurazone (730 μM; 30 min)	Rat RBE4 (P25–55) + rat C6	[Sucrose P_e: 68]	Sucrose P_e≈	Lagrange *et al.* (1999)
NXY-059 (100 μM; 1 h)	Bovine cBEC (P < 10) + rat AC	>500	Inulin P_e ≈	Dehouck *et al.* (2002)
4-OH-nonenal (100 μM; 20 min)	Rat RBE4 (P?) + rat AC	[NaFl P_e = 11]	NaFl P_e↑	Mertsch *et al.* (2001)
PBN (100 μM; 1 h)	Bovine cBEC (P < 10) + rat AC	>500	Inulin P_e ↓	Dehouck *et al.* (2002)

Table XI. Continued

Drug (dose; time)	In vitro BBB model	TEER (Ω cm^2) [P_e (10^{-6} cm/s)][a]	Effect on permeability[a]	Reference
S-PBN (100 μM; 1 h)	Bovine cBEC (P < 10) + rat AC	>500	Inulin P_e ↓	Dehouck *et al.* (2002)
SOD (6 U/mL; 30 min) + CAT (10 U/mL)	Rat RBE4 (P25–55) + rat C6	[Sucrose P_e: 68]	Sucrose P_e ≈	Lagrange *et al.* (1999)
SOD (60 U/mL; 30 min) + CAT (100 U/mL)	Rat RBE4 (P25–55) + rat C6	[Sucrose P_e: 68]	Sucrose P_e ≈	Lagrange *et al.* (1999)
Vitamin C and E (both 100 μM; 6 h)	Porcine BEC (P0)	100–120	Inulin flux≈	Fischer *et al.* (1999a)
Xanthine (5 μM; 1 h) + XO (7 nM; 1 h)	Mouse BEC (P1)	59 ± 4	TEER↓	Imaizumi *et al.* (1996)
Xanthine (5 μM; 1 h) + XO (7 nM; 1 h)	Mouse SOD Tg BEC (P1)	61 ± 4	TEER↓	Imaizumi *et al.* (1996)

Note. ↓ = Significant decrease, ≈ = no significant change, ↑ = significant increase, 3D = 3-dimensional blood–brain barrier model, 1400W = *N*-(3-aminomethyl)benzylacetamidine, AC = astrocytes, BBB = blood–brain barrier, BEC = brain endothelial cells, 8-Br-cGMP = 8-Br-guanosine 3′,5′-cyclic monophosphate, CAT = catalase, C6 = rat C6 glioma cell line, cBEC = cloned brain endothelial cells, cGMP = guanosine 3′,5′-cyclic monophosphate, d = day, DETA-NONOate = 2,2′-(hydroxynitrosohydrazino)-*bis*-ethanamine, h = hour, L-NAME = $N\omega$-nitro-L-arginine methyl ester, L-NMMA = N^G-monomethyl-L-arginine, NaFl = sodium fluorescein, N.I. = not indicated, NO = nitric oxide, NXY-059 = disodium-2,4-disulfophenyl-*N*-*tert*-butylnitrone, ON = overnight treatment (16 h), P = passage number of endothelial cells, P? = passage number is not indicated, P0 = primary brain endothelial cells seeded directly on cell culture insert, PBN = α-phenyl-*N*-*tert*-butylnitrone, P_e = endothelial permeability coefficient, ROS = reactive oxygen species, SIN-1 = 3-morpholinosydnonimine, SOD = superoxide dismutase, SOD Tg = human CuZn-superoxide dismutase transgenic animal, SNAP = *S*-nitroso-*N*-acetylpenicillamine, S-PBN = 2-sulfophenyl-*N*-*tert*-butylnitrone, TEER = transendothelial electrical resistance, XO = xanthine oxidase.

[a]Molecular weights of permeability tracers used are as follows: inulin, 5 kDa; NaFl, 376 Da; sucrose, 342 Da. This table contains representative P_e values of low m.w., paracellular tracers in order to compare data.

cells, increased permeability (Blasig *et al.*, 2002). Xenobiotics able to induce ROS production, such as benzylviologen, methylviologen, menadione, and nitrofurazone, all decreased barrier properties in a dose-dependent way (Table XI), and this observation further strengthens the hypothesis that oxidative stress damages barrier functions. Nitrofurazone and duroquinone in the applied concentration had no effect (Lagrange *et al.*, 1999). While methylviologen and exogenuos ROS-induction by xanthine/xanthine oxidase resulted in a similar decrease in TEER of monolayers from both wild-type and human CuZn-superoxide dismutase transgenic mice, menadione reduced TEER only in brain endothelial cells from the transgenic animals indicating the effect is mediated rather by hydroxyl radicals or peroxynitrite than by superoxide anion itself (Imaizumi *et al.*, 1996). Toxicity of ROS is partly mediated by lipid peroxidation products. 4-hydroxynonenal, produced by aldehydic lipid peroxidation, increased brain endothelial permeability (Mertsch *et al.*, 2001). The effect is supposed to be mediated by intracellular glutathione depletion, since reduction of glutathione level by buthionine sulfoximine also increased inulin flux on the same RBE4/C6 model (Mertsch *et al.*, 2001). Interestingly, buthionine sulfoximine treatment neither induced any change in EC304/C6 model, nor enhanced the susceptibility to NO-induced oxidative stress (Hurst *et al.*, 1998).

Brain endothelial cells possess highly active antioxidative defense mechanisms, but these can be damaged by aging and diseases. Several enzymes and compounds have been tested to prevent oxidative stress in brain endothelial cells (Table XI). Antioxidant enzymes superoxide dismutase and catalase alone did not change sucrose permeability of brain endothelial monolayers, but at higher concentration, they prevented the increase in sucrose permeability induced by menadione (Lagrange *et al.*, 1999). Antioxidative compound *N*-acetyl-cysteine showed a time-dependent effect. When added to brain endothelial cells, it had a TEER decreasing immediate effect, no change was seen with further incubation; finally, overnight treatment resulted in a TEER-enhancing protective effect (Gaillard *et al.*, 2003). Free-radical trapping nitrone compounds α-phenyl-*N*-*tert*-butylnitrone, 2-sulfophenyl-*N*-*tert*-butylnitrone and NXY-059 showed no significant effect on barrier integrity in normoxic or ischemic conditions (Dehouck *et al.*, 2002). Desferrioxamine mesylate, a Fe^{2+} chelator, dose-dependently increased TEER (Table XI). Vitamin C and E, and α-lipoic acid did not change inulin flux in porcine cerebral endothelial monolayers, while potentiated the effect of VEGF (Table VI). Free-radical scavenger dimethyl sulfoxide on ECV304/C6 model showed no effect at 10 min, it increased TEER at 30 min, but it resulted in a dose-dependent reduction in TEER after 18 h (Easton and Abbott, 2002; Hurst and Clark, 1998, 1999).

Effects of Miscellaneous Pharmacological Treatments

Effect of Drugs Affecting Vasoactive Mediators and Pathogenic Factors

Receptor agonists and antagonists of endogenous hormones (Table IV) and vasoactive mediators (Table VII) may have a therapeutical role in modulation of

BBB permeability with the aim either to prevent brain edema formation or to induce temporary BBB opening for a drug targeted to the brain.

Similar to the effect of endogenous catecholamines (Table IV), drugs acting on adrenoceptors may alter BBB permeability. Phenylephrine, an α-adrenoceptor agonist, increased, while β2 receptor agonist clenbuterol decreased fluorescein flux (Borges *et al.*, 1994), though propranolol, a blocker of β1 and β2 receptors, did not change the sucrose P_e in a bovine in vitro BBB model (Eddy *et al.*, 1997). Prazosin, an α-adrenoceptor antagonist could change the basal permeability-increasing effect of noradrenaline and treatment with this drug combination resulted in a decrease in fluorescein flux (Borges *et al.*, 1994).

Selective bradykinin B2 receptor agonist RMP-7, similarly to bradykinin, increased paracellular sucrose flux, while did not change 70 kDa FITC-dextran permeability through human endothelial cell monolayer (Mackic *et al.*, 1999). Bradykinin B2 receptor antagonist HOE 140 alone did not alter TEER in ECV304/C6 coculture model, but it protected against the bradykinin-induced decrease in barrier integrity (Easton and Abbott, 2002). Intracellular histamine-binding site antagonist *N,N*-diethyl-2-[4-(phenylmethyl)-phenoxy]ethanamine deteriorated barrier integrity in monolayers of mouse brain endothelial cells cocultured with rat C6 glioma cells (Deli *et al.*, 2003). Senktide, a selective neurokinin NK_3 receptor agonist peptide did not change sucrose P_e in a bovine model (Eddy *et al.*, 1997). Angiotensin II receptor antagonist sarathrin did not alter, while saralasin decreased barrier permeability through bovine brain endothelial monolayers (Guillot and Audus, 1991).

Adenosine, an endogenous neuromodulator activates A_1, A_{2A}, A_{2B}, and A_3 G-protein coupled receptors. Brain endothelial cells express adenosine receptor subtypes A_{2A}, and A_3, and es nucleoside transporter (Schaddelee *et al.*, 2003). Basolateral application of selective A_1 agonist cyclopentyladenosine, selective A_{2A} agonist CGS 21680, or A_1 and A_3 agonist 2-chloro-*N*-(3-iodobenzyl)adenosine-5′-*N*-ethyl-carboxamide (2-Cl-IB-MECA) did not change significantly TEEP or permeability for fluorescein or 4 kDa FITC dextran (Schaddelee *et al.*, 2003). However, apical application of high dose of 2-Cl-IB-MECA caused a temporary decrease in TEER (Schaddelee *et al.*, 2003). Nucleoside transporters at the BBB are involved in the regulation of brain extracellular adenosine level. BCX-34, a purine nucleoside phosphatase inhibitor, alone or in combination with dipyridamole, an inhibitor of nucleoside transport and selective inhibitor of cGMP dependent phosphodiesterase V, decreased BBB permeability both for purines and for permeability markers sucrose and FITC-albumin in a 3-dimensional rat BBB model (Parkinson *et al.*, 2003).

Effect of Glutamate Agonists and Antagonists

Excitatory neurotransmitter glutamate plays a crucial role in the pathology of ischemic brain injuries, and increases BBB permeability as it was demonstrated in Table VII. Glutamate receptor agonists and antagonists also alter barrier integrity and pharmacological studies may facilitate development of drugs effective in the prevention of postischemic brain edema. In a preliminary study, NMDA and kainic acid, two classical glutamate receptor agonists, were without significant effect on BBB

permeability (Gaillard *et al.*, 1996). However, NMDA or glutamate decreased TEER, whereas a specific metabotropic glutamate receptor (mGluR) agonist (*trans*-(±) 1-amino-1,3-cyclopentanedicarboxylic acid) could even temporarily increase barrier properties in a recent study in a model of human immortalized brain endothelial cells (Sharp *et al.*, 2003). NMDA antagonist MK-801, intracellular Ca^{2+} scavenger TMB-8 or antioxidant *N*-acetyl-L-cysteine could protect against glutamate-induced deterioration of barrier integrity in this model (Sharp *et al.*, 2003). Exogenous glutamate, as well as glutamate-containing fraction of supernatant produced by stimulated polymorphonuclear leukocytes, increases permeability for 70 kDa FITC-dextran in a model of human brain endothelial cells with high passage number (Collard *et al.*, 2002). This effect can be prevented by treatment of group I or group III mGluR receptor antagonists, while group I (3,5-dihydrophenyl-glycine) or group III (L-2-amino-4-phosphonobutyrate) mGluR receptor agonists had glutamate-like effect (Collard *et al.*, 2002; Table XII).

Effect of Sedatives

Barbiturates, such as methohexital or thiopental (Fischer *et al.*, 1995), benzodiazepines, such as diazepam or oxazapam (Eddy *et al.*, 1997), opiates, such as morphine (Letrent *et al.*, 1999) or fentanyl (Fischer *et al.*, 1995), or ethanol (Easton and Abbott, 2002; Hurst and Clark, 1999) had little, if any, effect on TEER or permeability for tracers used in reconstituted in vitro BBB models (Table XII).

Effect of Cytostatic and Immunosuppressant Drugs

Cycloheximide, an inhibitor of *de novo* protein synthesis, and vinblastine, an alkaloid affecting tubulin interactions, decreased TEER value (Gaillard and de Boer, 2000; Gaillard *et al.*, 2003), though vinblastine treatment did not alter sucrose P_e (Eddy *et al.*, 1997) in bovine brain endothelial cells. Immunosuppressant drugs cyclosporin A and tacrolimus increased the permeability for paracellular markers (Dohgu *et al.*, 2000; Kochi *et al.*, 1999). Complex of cyclosporin A with cyclophilin B, its binding protein located in endoplasmic reticulum, increased the permeability for cyclosporin A and sucrose through an in vitro reconstituted bovine BBB model (Carpentier *et al.*, 1999). Colchicine, which can disrupt microtubules, did not change P_e for retinol and retinoic acid (Franke *et al.*, 1999). Treatment with suramin, a drug having pleiotropic activity including anti-angiogenic effect, uncoupling of G-proteins, or PKC inhibition, caused a rapid decrease in TEER (Schulze *et al.*, 1997; Table XII).

Effect of Other Miscellaneous Compounds

Treatment with pyrithiamine, a competitive inhibitor of thiamine transport, in low thiamine medium significantly elevated P_e of sucrose, but not that of 4 kDa FITC-dextran, in monolayers of rat RBE4 cell line (Romero *et al.*, 1997a). Filipin III, a polyen macrolide binding to cholesterol in membranes, induced a huge increase in sucrose P_e after 30 min treatment, though no change was observed at

Table XII. Effect of Pharmacological Treatments on Permeability Data Obtained on In Vitro Blood–Brain Barrier Models

Drug (dose; time)	In vitro BBB model	TEER (Ω cm^2) [P_e (10^{-6} cm/s)][a]	Effect on permeability[a]	Reference
Miscellaneous drugs and chemicals				
L-AP4 (1 μM; 1 h)	Human BEC (P < 10)	N.I.	FD_{70} flux↑	Collard *et al.* (2002)
BCX-34 (10 μM; 2 h)	Rat BEC (P1) + rat AC [3D]	320–450	Sucrose flux↓ FITC-albumin flux↓	Parkinson *et al.* (2003)
BCX-34 + dipyridamole (both 10 μM; 2 h)	Rat BEC (P1) + rat AC [3D]	320–450	Sucrose flux↓ FITC-albumin flux↓	Parkinson *et al.* (2003)
Colchicine (1–10 μM; 2 h)	Porcine BEC (P1)	300–500	Retinol $P_e \approx$ RA $P_e \approx$	Franke *et al.* (1999)
CGS 21680 (0.5–50 μM; 5 h)	Bovine BEC (P1) + rat AC	145 ± 16	TEER≈ NaFl $P_e \approx$ FD_4flux≈	Schaddelee *et al.* (2003)
Clenbuterol (0.1 μM; 30 min)	Bovine BEC (P1) + rat AC	N.I.	NaFl flux↓	Borges *et al.* (1994)
2-Cl-IB-MECA (0.5–50 μM; 5 h)	Bovine BEC (P1) + rat AC	145 ± 16	TEER≈↓ NaFl$P_e \approx$ FD_4flux≈	Schaddelee *et al.* (2003)
CPA (0.5–50 μM; 5 h)	Bovine BEC (P1) + rat AC	145 ± 16	TEER≈ NaFl $P_e \approx$ FD_4 flux≈	Schaddelee *et al.* (2003)
Cycloheximide (10 μM; ON)	Bovine BEC (P1) + rat AC	N.I.	TEER↓	Gaillard *et al.* (2003)
Cyclophilin B (150 nM; 4 h)	Bovine cBEC (P < 10) + rat AC	>500	Sucrose P_e ↓ cycloA P_e↓	Carpentier *et al.* (1999)
Cyclophilin B (15 μM; 4 h)	Bovine cBEC (P < 10) + rat AC	>500	Sucrose P_e↑ cycloA P_e↑	Carpentier *et al.* (1999)
Cyclosporin A (5–10 μM; 24 h)	Mouse MBEC4 (P?)	N.I.	Sucrose flux↑	Kochi *et al.* (1999)
Cyclosporin A (10 μM; 4 h)	Mouse MBEC4 (P?)	N.I.	NaFl flux↑	Dohgu *et al.* (2000)
Diazepam (100–200 μM; 1 h)	Bovine BEC (P1)	[Sucrose P_e: 14–42]	Sucrose $P_e \approx$	Eddy *et al.* (1997)
DHPG (1 μM; 1 h)	Human BEC (P < 10)	N.I.	FD_{70} flux↑	Collard *et al.* (2002)
DPPE (100–200 μM; 60 min)	Mouse BEC (P1) + rat C6	307	TEER↓ NaFl $P_e \approx$ EBA P_e↑	Deli *et al.* (2003)
Ethanol (0.05%; 18 h)	Human ECV304 (P?) + rat C6	89 ± 6	TEER≈	Hurst and Clark (1999)
Ethanol (1%; 10 min)	Human ECV304 (P?) + rat C6	144–221	TEER≈	Easton and Abbott (2002)
Fentanyl (47–189 nM; 1.5–24 h)	Porcine BEC (P0)	98 ± 2	TEER≈ sucrose flux≈ EBA flux≈ AIB flux≈	Fischer *et al.* (1995)
Filipin (4.5 μM; ≥30 min)	Bovine cBEC (P < 10) + rat AC	500–800	Sucrose P_e↑	Dehouck B *et al.* (1997)
HOE 140 (1 μM; 10 min)	Human ECV304 (P?) + rat C6	144–221	TEER≈	Easton and Abbott (2002)

Kainic acid (100 μM; 5 h)	Bovine BEC (P1) + rat AC	130	TEER≈ NaFl P_e ≈ FD_4 flux≈	Gaillard *et al.* (1996)
Methohexital (84–352 μM; 1.5–24 h)	Porcine BEC (P0)	98 ± 2	TEER≈ sucrose flux≈ EBA flux≈ AIB flux≈	Fischer *et al.* (1995)
Morphine (50 μM; 2 h)	Bovine BEC (P1)	72–184	Sucrose P_e ≈	Letrent *et al.* (1999)
NMDA (100 μM; 5 h)	Bovine BEC (P1) + rat AC	130	TEER≈ NaFl P_e ≈ FD_4 flux≈	Gaillard *et al.* (1996)
NMDA (1.0 mM; 2–3 h)	Human IHEC (P?)	61 ± 8[b]	TEER↓	Sharp *et al.* (2003)
Oxazapam (100–200 μM; 1 h)	Bovine BEC (P1)	[Sucrose P_e: 14–42]	Sucrose P_e ≈	Eddy *et al.* (1997)
Pentosan (100 μM; 1–24 h)	Rat BEC (P1) + rat AC	320 ± 12	TEER≈ NaFl P_e ≈ EBA P_e ≈	Deli *et al.* (unpublished)
Phenylephrine (0.1 μM; 30 min)	Bovine BEC (P1) + rat AC	N.D.	NaFl flux↑	Borges *et al.* (1994)
Propranolol (100–200 μM; 1 h)	Bovine BEC (P1)	[Sucrose P_e: 14–42]	Sucrose P_e ≈	Eddy *et al.* (1997)
Pyrithiamine (60–120 μM; 3 d)	Rat RBE4 (P40–60) + FCS	[Sucrose P_e: 36]	Sucrose P_e ↑ FD_4 P_e ≈	Romero *et al.* (1997a)
RMP-7 (0.1–10 nM; 5–15 min)	Human BEC (P0)	120–180	Inulin flux↑ $dextran_{70}$flux≈	Mackic *et al.* (1999)
Saralasin (10–50 μM; 60 min)	Bovine BEC (P1)	N.I.	FD_4 flux↓ LY flux↓	Guillot and Audus (1991)
Sarathrin (10–50 μM; 60 min)	Bovine BEC (P1)	N.I.	FD_4 flux≈ LY flux≈	Guillot and Audus (1991)
Senktide (100–200 μM; 1 h)	Bovine BEC (P1)	[Sucrose P_e: 14–42]	Sucrose P_e ≈	Eddy *et al.* (1997)
Suramin (70–700 μM; rapidly)	Porcine BEC(P1) + cAMP↑ + PDS	500–600	TEER↓	Schulze *et al.* (1997)
*t*ACPD (1.0 mM; 1–3 h)	Human IHEC (P?)	61 ± 8[b]	TEER≈↑	Sharp *et al.* (2003)
Tacrolimus (10–40 μM; 24 h)	Mouse MBEC4	N.I.	Sucrose flux↑	Kochi *et al.* (1999)
Thiopental (103–512 μM; 1.5–24 h)	Porcine BEC (P0)	98 ± 2	TEER≈ sucrose flux≈ EBA flux≈ AIB flux↑	Fischer *et al.* (1995)
Vinblastine (100–200 μM; 1 h)	Bovine BEC (P1)	[Sucrose P_e: 14–42]	Sucrose P_e ≈	Eddy *et al.* (1997)
Vinblastine (100 nM; 1–5 h)	Bovine BEC (P1) + rat AC	98 ± 50	TEER↓	Gaillard and de Boer (2000)
Osmotic agents				
Arabinose (1.6 M; 5 min)	Rat BEC (P1)	N.I.	Sucrose flux↑	Bowman *et al.* (1983)
Arabinose (1.6 M; N.I.)	Bovine cBEC (P < 10) + rat AC	>500	Sucrose flux↑	Dehouck *et al.* (1990)
Arabinose (1.6 M; 1 h)	Porcine BEC (P0)	98 ± 2	TEER↓	Fischer *et al.* (1995)
Arabinose (1.6 M; 5 min)	Human ECV304 (P?)	39 ± 6	TEER↓	Hurst and Fritz (1996)
Arabinose (1.6 M; 5 min)	Human ECV304 (P?) + rat C6	92 ± 9	TEER↓	Hurst and Fritz (1996)

Table XII. Continued

Drug (dose; time)	In vitro BBB model	TEER (Ω cm^2) [P_e (10^{-6} cm/s)][a]	Effect on permeability[a]	Reference
Mannitol (27 mM, 0.5–6 min)	Mouse MB114	12–44	TEER↓	Hart *et al.* (1987)
Mannitol (1.4 M; 5 min)	Bovine cBEC (P < 10) + rat AC	>500	Sucrose flux↑ inulin flux↑	Deli *et al.* (1995c)
Mannitol (1.4 M; 4 h)	Bovine cBEC (P < 10) + rat AC	>500	Sucrose P_e↑ inulin P_e↑	Descamps *et al.* (1997), Fillebeen *et al.* (1999a)
Mannitol (1.4 M; 30 min)	Bovine cBEC (P < 10) + rat AC	>500	Sucrose P_e↑	Brillault *et al.* (2002)
Metabolic inhibitors				
α-Chlorohydrin (30 mM; 1 d)	Rat RBE4 (P40–60) + FCS	[Sucrose P_e: 33]	Sucrose $P_e \approx FD_4 P_e \approx$	Romero *et al.* (1997b)
2-Deoxyglucose (50 mM; 1 h)	Bovine BEC (P1)	N.I.	FD_4 flux↑ LY flux↑	Guillot and Audus (1991)
m-Dinitrobenzene (0.5 mM; 1 d)	Rat RBE4 (P40–60) + FCS	[Sucrose P_e: 33]	Sucrose P_e ↑ $FD_4 P_e$ ↑	Romero *et al.* (1997b)
Fluorocitrate (0.1–1.0 mM; 24 h)	Rat RBE4 (P30–60) + FCS	[Sucrose P_e: 33]	Sucrose $P_e \approx FD_4 P_e \approx$	Rist *et al.* (1996)
Iodoacetate (100 μM; 2–5 h)	Human ECV304 (P?) + rat C6	51 ± 3	TEER↓	Hurst *et al.* (2001)
KCN (50 μM; ≤30 min)	Human ECV304 (P?) + rat C6	106 ± 2	TEER≈	Hurst and Clark (1997)
KCN (100 μM; ≤5 h)	Human ECV304 (P?) + rat C6	51 ± 3	TEER≈	Hurst *et al.* (2001)
Myxothiazol (0.5 μM; ≤30 min)	Human ECV304 (P?) + rat C6	106 ± 2	TEER≈	Hurst and Clark (1997)

Note. ↓=Significant decrease, ≈ = no significant change, ↑ = significant increase. AC = astrocytes, AIB = α-aminoisobutyric acid, BBB = blood–brain barrier, BCX-34 = 9-(3-pyridylmethyl)-7H-9-deazaguanine (=peldesine), BEC = brain endothelial cells, C6 = rat C6 glioma cell line, cBEC = cloned brain endothelial cells, CGS 21680 = 2-*p*-(2-carboxyethyl)phenethyl amino-5′-*N*-ethylcarboxamidoadenosine hydrochloride, Cl-IB-MECA = 2-chloro-*N*-(3-iodobenzyl) adenosine-5′-*N*-ethylcarbox-amide, CPA = cyclopentyladenosine, cycloA = cyclosporin A, d = day, DHPG = 3,5-dihydrophenylglycine, DPPE = *N*,*N*-diethyl-2-[4-(phenylmethyl)phenoxy]ethanamine, EBA = Evans blue-labeled albumin, $FD_{m.w.}$ = fluorescein isothiocyanate-dextran (m.w., molecular weight in kDa), h = hour, HOE 140 = H$_2$N-D-Arg-Arg-Pro-Hyp-Gly-Thi-Ser-D-Tic-Oic-Arg, L-AP4 = L-2-amino-4-phosphonobutyrate, N.A. = not applicable, NaFl = sodium fluorescein, NBTI = *S*-(4-nitrobenzyl)-6-thioinosine, NECA = 5′-*N*-ethylcarboxamido-adenosine, N.I. = not indicated, NMDA = *N*-methyl-D-aspartic acid, ON = overnight, P = passage number of endothelial cells, P? = passage number is not indicated, PI = primary brain endothelial cells seeded directly on cell culture insert, P_e = endothelial permeability coefficient, RA = retinoic acid, RMP-7 = receptor mediated permeabilizer-7 = Cereport, *t*ACPD = *trans*-(±)1-amino-1,3-cyclopentanedicarboxylic acid, TEER = transendothelial electrical resistance.

[a]Molecular weights of permeability tracers used are as follows: AIB, 203 Da; chlorpyrifos, 351 Da; dopamine, 190 Da; EBA, 67 kDa; FITC-albumin, 67 kDa; FD_{20}, 20 kDa; mannitol, 182 Da; L-glucose, 180 Da; NaFl, 376 Da; sucrose, 342 Da. This table contains representative P_e values of low m.w., paracellular tracers in order to compare data.

[b]In some studies, TEER values were expressed as Ω/cm^2. In case surface area was given in the paper, comparable TEER value could be calculated.

20 min (Dehouck *et al.*, 1997). Pentosan polysulfate, a semisynthetic glucosaminoglycane, alone did not change barrier integrity, however, it could prevent increased BBB permeability induced by amyloid peptides (Deli *et al.*, unpublished; Table VII and XII).

Effect of Osmotic Agents

Osmotic stress induced by arabinose or mannitol induces a rapid and reversible decrease in TEER, and increases permeability for known paracellular markers sucrose and inulin through brain endothelial cell monolayers (Table XII).

Effect of Metabolic Inhibitors

Acute energy deprivation leads to a decrease in intracellular (ATP) concentration, which may be accompanied by changes in endothelial monolayer permeability. Although several compounds, such as 2-deoxyglucose, industrial toxicant *m*-dinitrobenzene, or iodoacetate damaged barrier integrity, other treatments such as α-chlorohydrin, mitochondrial aconitase inhibitor fluorocitrate, KCN, or myxithiazol did not alter BBB permeability in the models used (Table XII).

Effects of Other Miscellaneous Treatments

The luminal surface of brain endothelial cells contains glycocalyx residues that establish a negative charge, which contributes to the barrier phenotype. Negatively charged molecules, for example, FITC-dextrans or nanoparticles, crosses the barrier in significantly lower amount than neutral or cationic ones (Fenart *et al.*, 1999; Sahagun *et al.*, 1990). While nanoparticles did not change basal permeability of brain endothelial cells, their transport was enhanced by lipid coating.

As opposed to anionic charge, cationization of ferritin, albumin, or anti-tetanus immunoglobulin Fab'2 fragment all leads to better transcytosis of above-mentioned macromolecules without changing barrier integrity (Table XIII). Furthermore, albumin loaded in lipid coated cationic nanoparticles had a 27-fold enhanced transport (Fenart *et al.*, 1999). Neutralization of the brain endothelial luminal surface charge by cationic ferritin, as opposed to the treatment with neutral ferritin, resulted in increased transport of Evans blue dye, a small polar molecule, while TEER and permeability for 20 kDa m.w. FITC dextran was not changed (Hart *et al.*, 1987).

Glycosylation of albumin, similarly to cationization, also resulted in an 8-fold elevation of transendothelial transport (Smith and Borchardt, 1989).

Monoacylation of ribonuclease A facilitates the transport of the enzyme through the BBB: palmitoylated and stearoylated, but not myristoylated, derivatives show increased BBB transport without degradation of protein or modification of barrier permeability for sucrose or inulin (Chopineau *et al.*, 1998). It is suggested that a minimal length of 16 carbon atoms is required for a translocation of ribonuclease A across monolayers of bovine endothelial cells cocultured with rat astrocytes.

Table XIII. Effect of Miscellaneous Treatments and Temperature Changes on Permeability Data Obtained on In Vitro Blood–Brain Barrier Models

Drug (dose; time)	In vitro BBB model	TEER (Ω cm^2) [P_e (10^{-6} cm/s)][a]	Effect on permeability[a]	Reference
Miscellaneous treatments				
Anionic charge of FD_4 (N.A.)	Mouse BEC (P1)	N.I.	FD_4 flux↓ FD_{10} flux↓	Sahagun *et al.* (1990)
Anionic 60 nm nanoparticles (N.A.; 4 h)	Bovine cBEC (P < 10) + rat AC	500–800	Sucrose P_e ≈	Fenart *et al.* (1999)
Cationic ferritin (25–750 μg/mL, 1 h)	Mouse MB114 (P?)	12–44	TEER≈ EBD flux↑ FD_{20} flux≈	Hart *et al.* (1987)
Cationic 60 nm nanoparticles (N.A.; 4 h)	Bovine cBEC (P < 10) + rat AC	500–800	Sucrose P_e ≈ albumin P_e ↑	Fenart *et al.* (1999)
Cationization of anti-tetanus Fab'2 (N.A.)	Bovine BEC (P1)	>500	Fab' 2 flux ↑	Girod *et al.* (1999)
Cationization of BSA (N.A.)	Bovine BEC (P1)	[Sucrose P_e = 0.08]	BSA P_e↑	Smith and Borchardt (1989)
Cationized anti-tetanus Fab'2 (101 μg/mL; 3 h)	Bovine cBEC (P < 10) + rat AC	>500	Sucrose P_e ≈ inulin P_e ≈	Girod *et al.* (1999)
Electromagnetic fields (1.8 GHz; 2–4 d)	Porcine BEC (P1) + rat AC	[Sucrose P_e = 25]	Sucrose flux↑	Schirmacher *et al.* (2000)
Glycosylation of BSA (N.A.)	Bovine BEC (P1)	[Sucrose P_e = 0.08]	BSA P_e↑	Smith and Borchardt (1989)
Myristoylation of RNase A (100 μM; 2 h)	Bovine cBEC (P < 10) + rat AC	>500	Sucrose P_e ≈ inulin P_e ≈ RNaseA P_e ≈	Chopineau *et al.* (1998)
Native anti-tetanus Fab'2 (101 μg/mL; 3 h)	Bovine cBEC (P < 10) + rat AC	>500	Sucrose P_e ≈ inulin P_e ≈	Girod *et al.* (1999)
Native ferritin (500 μg/mL, 1 h)	Mouse MB114 (P?)	12–44	TEER≈ EBD flux↑ FD_{20} flux≈	Hart *et al.* (1987)
Native RNase A (100 μM; 2 h)	Bovine cBEC (P < 10) + rat AC	>500	Sucrose P_e ≈ inulin P_e ≈	Chopineau *et al.* (1998)
Neutral 60 nm nanoparticles (N.A.; 4 h)	Bovine cBEC (P < 10) + rat AC	500–800	Sucrose P_e ≈	Fenart *et al.* (1999)
Palmitoylation of RNase A (100 μM; 2 h)	Bovine cBEC (P < 10) + rat AC	>500	Sucrose P_e ≈ inulin P_e ≈ RNaseA P_e↑	Chopineau *et al.* (1998)
Single domain-BBB specific Ab (N.A.)	Human BCEC (P?)	[NaFl P_e: 53]	Ab flux↑	Muruganandam *et al.* (2002)
Stearoylation of RNase A (100 μM; 2 h)	Bovine cBEC (P < 10) + rat AC	>500	Sucrose P_e ≈ inulin P_e ≈ RNaseA P_e↑	Chopineau *et al.* (1998)
Temperature changes				
Cold (4 °C; 1 h)	Bovine BEC (P1) + horse PDS	N.I.	Sucrose flux≈	Audus and Borchardt (1986b)
Heat shock (43 °C for 2 h, after 24 h)	Bovine BEC (P1) + rat AC	N.I.	TEER≈	Gaillard *et al.* (2003)
Hypothermia (+ 22 °C; 6 h)	Porcine BEC (P1)	100–120	Inulin flux≈	Fischer *et al.* (1999b)
Hypothermia (+ 32 °C; 6 h)	Porcine BEC (P1)	100–120	Inulin flux≈	Fischer *et al.* (1999b)

Note. ↓ = Significant decrease, ≈ = no significant change, ↑ = significant increase, Ab = antibody, AC = astrocytes, BBB = blood–brain barrier, BEC = brain endothelial cells, BSA = bovine serum albumin, cBEC = cloned brain endothelial cells, d = day, EBD = Evans blue dye, Fab'2 = purified immunoglobulin fragment, $FD_{m.w.}$ = fluorescein isothiocyanate-dextran (m.w., molecular weight in kDa), h = hour, N.A. = not applicable, N.I. = not indicated, ON = overnight, P = passage number of endothelial cells, P_e = endothelial permeability coefficient, RNase A = ribonuclease A, TEER = transendothelial electrical resistance.

[a]Molecular weights of permeability tracers used are as follows: EBD, 960 Da; Fab'2, 100 kDa; FD_{20}, 20 kDa; inulin, 5 kDa; RNase A, 14 kDa; sucrose, 342 Da. This table contains representative P_e values of low m.w., paracellular tracers in order to compare data.

Using antibody phage display technology, single domain antibodies could be selected to effectively cross human in vitro BBB model and in vivo BBB with a potential to use in macromolecule delivery as brain targeting vector (Muruganandam *et al.*, 2002).

There is a debate on the effects of electromagnetic fields on biological systems, among them on the function of the BBB. Exposition to 1.8 GHz electromagnetic fields for 2–4 days significantly enhanced the permeability for sucrose in porcine brain endothelial monolayers (Schirmacher *et al.*, 2000).

Finally, temperature changes, either hypothermia (4, 22, or 32°C) measured by inulin flux, or heat stress (43°C) measured by TEER had no effect on brain endothelial barrier integrity (Table XIII). In contrast, in epithelial cells, temperature strongly affects TJ function, and higher TEER values are measured at ambient temperatures than at 37°C (Matter and Balda, 2003a).

CONCLUSIONS AND FUTURE PERSPECTIVES

In the third decade of in vitro BBB research, the number of permeability studies has been considerably expanded. Several excellent in vitro models have been developed, for example, of bovine and porcine origin, and they show highly restrictive paracellular permeability properties and BBB phenotype very close to the in vivo parameters (Table I). Despite efforts to critically compare in vitro models and transfer results between them with the purpose to establish an ideal model or reference system, no optimal in vitro BBB model exists and further diversification of BBB models is expected (Reichel *et al.*, 2003).

The number of published papers on in vitro BBB models modulating paracellular and transendothelial permeability by physiological, pathological, or pharmacological factors has been proliferated in the last 10 years. Although some of the original reports may be missing from the present review, the compiled data clearly show that in vitro models have significantly contributed to the better understanding of brain endothelial transport pathways and regulation. At the same time, these results may also point out a weakness of our knowledge acquired on in vitro BBB models till now, namely that many of the systems used are poorly characterized and comparable barrier permeability parameters, such as adequate TEER and P_e values, are missing.

Despite debates that there is no clear correlation between TEER and P_e, the presented data also demonstrate that the best models with highest TEER give the lowest P_e values. Because of the difficulties in obtaining models with sufficiently tight paracellular barrier from many species (e.g., rat, mouse, human) and because of the need to develop models for specific applications a compromise can be made. There is an agreement that models with minimal TEER of 150–200 Ω cm^2 give reasonable solute or drug permeability results (Gaillard and de Boer, 2000; Gumbleton and Audus, 2001; Reichel *et al.*, 2003).

Many models do not comply with the above-mentioned minimal criteria and results obtained on these systems should be critically evaluated and cautious interpretation of data is needed. This observation may also facilitate the repetition of pivotal experiments in valid and reproducible in vitro BBB models. However,

even results obtained on the best available models should be compared with in vivo measurements to reach a general conclusion about the effect of a physiological or pathological factor or a drug on the BBB function.

There is a need for better human in vitro BBB models, which can be probably achieved by development of human brain endothelial cell lines of high quality. Adaptation of techniques developed in epithelial cell biology to the brain endothelial monolayers may give a further impetus to in vitro BBB research and reveal specifics of brain endothelial TJ and regulation of BBB permeability.

Drug and gene targeting to central nervous system, as well as gene and protein profiling of brain endothelial cells under physiological and pathological conditions are two areas in which in vitro BBB model system can be successfully exploited and fascinating new results can be expected in the next decade of research.

ACKNOWLEDGMENTS

This work was supported by grants from the from the Hungarian Research Fund (OTKA T37834), the Hungarian Ministry of Public Health (296/2001), and Ministry of Education, Science, Sports, and Culture and the Ministry of Health and Welfare of Japan. Mária A. Deli is a recipient of János Bolyai Research Fellowship from the Hungarian Academy of Sciences.

REFERENCES

Abbott, N. J. (2000). Inflammatory mediators and modulation of blood–brain barrier permeability. *Cell. Mol. Neurobiol.* 20:131–147.

Abbott, N. J. (2002). Astrocyte-endothelial interactions and the blood–brain barrier permeability. *J. Anat.* 200:629–638.

Abbott N. J. (2005). Dynamics of CNS barriers: Evolution, differentiation and modulation. *Cell. Mol. Neurobiol.* 25:5–23.

Abbott, N. J., Hughes, C. C. W., Revest, P. A., and Greenwood, J. (1992). Development and characterisation of a rat brain capillary endothelial culture: Towards an in vitro blood–brain barrier. *J. Cell Sci.* 103:23–37.

Abbruscato, T. J., and Davis, T. P. (1999a). Combination of hypoxia/aglycemia compromises in vitro blood–brain barrier integrity. *J. Pharmacol. Exp. Ther.* 289:668–675.

Abbruscato, T. J., and Davis, T. P. (1999b). Protein expression of brain endothelial cell E-cadherin after hypoxia/aglycemia: Influence of astrocyte contact. *Brain Res.* 842:277–286.

Anda, T., Yamashita, H., Khalid, H., Tsutsumi, K., Fujita, H., Tokunaga, Y., and Shibata, S. (1997). Effect of tumor necrosis factor-alpha on the permeability of bovine brain microvessel endothelial cell monolayers. *Neurol. Res.* 19:369–376.

Annunziata, P., Cioni, C., Santonini, R., and Paccagnini, E. (2002). Substance P antagonist blocks leakage and reduces activation of cytokine-stimulated rat brain endothelium. *J. Neuroimmunol.* 131:41–49.

Annunziata, P., Cioni, C., Toneatto, S., and Paccagnini, E. (1998). HIV-1 gp120 increases the permeability of rat brain endothelium cultures by a mechanism involving substance P. *AIDS* 12:2377–2385.

Arthur, F. E., Shivers, R. R., and Bowman, P. D. (1987). Astrocyte-mediated induction of tight junctions in brain capillary endothelium: An efficient in vitro model. *Brain Res.* 433:155–159.

Audus, K. L., and Borchardt, R. T. (1986a). Characterization of an in vitro blood brain barrier model system for studying drug transport and metabolism. *Pharm. Res.* 3:81–87.

Audus, K. L., and Borchardt, R. T. (1986b). Characteristics of the large neutral amino acid transport system of bovine brain microvessel endothelial cell monolayers. *J. Neurochem.* 47:484–488.

Badger, J. L., Stins, M. F., and Kim, K. S. (1999). *Citrobacter freundii* invades and replicates in human brain microvascular endothelial cells. *Infect. Immun.* 67:4208–4215.

Banks, W. A. (1999). Physiology and pathology of the blood–brain barrier: Implications for microbial pathogenesis, drug delivery and neurodegenerative disorders. *J. Neurovirol.* **5**:538–555.

Banks, W. A., and Broadwell, R. D. (1994). Blood to brain and brain to blood passage of native horseradish peroxidase, wheat germ agglutinin, and albumin: Pharmacokinetic and morphological assessments. *J. Neurochem.* **62**:2404–2419.

Bauer, H. C., and Bauer, H. (2000). Neural induction of the blood–brain barrier: Still an enigma. *Cell. Mol. Neurobiol.* **20**:13–28.

Blasig, I. E., Giese, H., Schroeter, M. L., Sporbert, A., Utepbergenov, D. I., Buchwalow, I. B., Neubert, K., Schönfelder, G., Freyer, D., Schimke, I., Siems, W.-E., Paul, M., Haseloff, R. F., and Blasig, R. (2001). *NO and oxyradical metabolism in new cell lines of rat brain capillary endothelial cells forming the blood–brain barrier. *Microvasc. Res.* **62**:114–127.

Blasig, I. E., Mertsch, K., and Haseloff, R. F. (2002). Nitronyl nitroxides, a novel group of protective agents against oxidative stress in endothelial cells forming the blood–brain barrier. *Neuropharmacology* **43**:1006–1014.

Borges, N., Shi, F., Azevedo, I., and Audus, K. L. (1994). Changes in brain microvessel endothelial cell monolayer permeability induced by adrenergic drugs. *Eur. J. Pharmacol.* **269**:243–248.

Bowman, P. D., Betz, A. L., Wolinsky, J. S., Penny, J. B., Shivers, R. R., and Goldstein, G. W. (1981). Primary cultures of capillary endothelium from rat brain. *In Vitro* **17**:353–362.

Bowman, P. D., Ennis, S. R., Rarey, K. E., Betz, A. L., and Goldstein, G. W. (1983). Brain microvessel endothelial cells in tissue culture: A model for study of blood–brain barrier permeability. *Ann. Neurol.* **14**:396–402.

Brightman, M. W., and Reese, T. S. (1969). Junctions between intimately apposed cell membranes in the vertebrate brain *J. Cell Biol.* **40**:648–677.

Brillault, J., Berezowski, V., Cecchelli, R., and Dehouck, M.-P. (2002). Intercommunications between brain capillary endothelial cells and glial cells increase the transcellular permeability of the blood–brain barrier during ischaemia. *J. Neurochem.* **83**:807–817.

Brown, J., Reading, S. J., Jones, S., Fitchett, C. J., Howl, J., Martin, A., Longland, C. L., Michelangeli, F., Dubrova, Y. E., and Brown, C. A. (2000). Critical evaluation of ECV304 as a human endothelial cell model defined by genetic analysis and functional responses: A comparison with the human bladder cancer derived epithelial cell line T24/83. *Lab. Invest.* **80**:37–45.

Brown, R. C., Mark, K. S., Egleton, R. D., Huber, J. D., Burroughs, A. R., and Davis, T. P. (2003). Protection against hypoxia-induced increase in blood–brain barrier permeability: Role of tight junction proteins and NFκB. *J. Cell Sci.* **116**:693–700.

Brückener, K. E., el Bayâ, A., Galla, H.-J., and Schmidt, M. A. (2003). Permeabilization in a cerebral endothelial barrier model by pertussis toxin involves the PKC effector pathway and is abolished by elevated levels of cAMP. *J. Cell Sci.* **116**:1837–1846.

Carpentier, M., Descamps, L., Allain, F., Denys, A., Durieux, S., Fenart, L., Kieda, C., Cecchelli, R., and Spik, G. (1999). Receptor-mediated transcytosis of cyclophilin B through the blood–brain barrier. *J. Neurochem.* **73**:260–270.

Cecchelli, R., Dehouck, B., Descamps, L., Fenart, L., Buée-Scherrer, V., Duhem, C., Lundquist, S., Rentfel, M., Torpier, G., and Dehouck, M.-P. (1999). In vitro model for evaluating drug transport across the blood–brain barrier. *Adv. Drug Deliv. Rev.* **36**:165–178.

Cestelli, A., Catania, C., D'Agostino, S., Di Liegro, I., Licata, L., Schiera, G., Pitarresi, G. L., Savettieri, G., De Caro, V., Giandalia, G., and Giannola, L. I. (2001). Functional feature of a novel model of blood brain barrier: Studies on permeation of test compounds. *J. Control. Release* **76**:139–147.

Chopineau, J., Robert, S., Fénart, L., Cecchelli, R., Lagoutte, B., Paitier, S., Dehouck, M.-P., and Domurado, D. (1998). Monoacylation of ribonuclease A enables its transport across an in vitro model of the blood–brain barrier. *J. Control. Release* **56**:231–237.

Collard, C. D., Park, K. A., Montalto, M. C., Alapati, S., Buras, J. A., Stahl, G. L., and Colgan, S. P. (2002). Neutrophil-derived glutamate regulates vascular endothelial barrier function. *J. Biol. Chem.* **277**:14801–14811.

Crone, C., and Olesen, S. P. (1982). Electrical resistance of brain microvascular endothelium. *Brain Res.* **241**:49–55.

Cucullo, L., McAllister, M. S., Kight, K., Krizanac-Bengez, L., Marroni, M., Mayberg, M. R., Stanness, K. A., and Janigro, D. (2002). A new dynamic in vitro model for the multidimensional study of astrocyte-endothelial cell interactions at the blood–brain barrier. *Brain Res.* **951**:243–254.

DeBault, L. E., and Cancilla, P. A. (1980). Gamma-glutamyl transpeptidase in isolated brain endothelial cells: Induction by glial cells in vitro. *Science* **207**:653–655.

de Boer, A. G., Gaillard, P. J., and Breimer, D. D. (1999). The transference of results between blood–brain barrier cell culture systems. *Eur. J. Pharm. Sci.* **8**:1–4.

de Boer, A. G., van der Sandt, I. C. J., and Gaillard, P. J. (2003). The role of drug transporters at the blood–brain barrier. *Annu. Rev. Pharmacol. Toxicol.* 43:629–656.

Dehouck, B., Fenart, L., Dehouck, M.-P., Pierce, A., Torpier, G., and Cecchelli, R. (1997). A new function for the LDL receptor: Transcytosis across the blood–brain barrier. *J. Cell Biol.* 138:877–889.

Dehouck, M.-P., Cecchelli, R., Green, A. R., Renftel, M., and Lindquist, S. (2002). In vitro blood–brain barrier permeability and cerebral endothelial cell uptake of the neuroprotective nitrone compound NXY-059 in normoxic, hypoxic and ischemic conditions. *Brain Res.* 955:229–235.

Dehouck M.-P., Jolliet-Riant, P., Brée, F., Fruchart, J.-C., Cecchelli, R., and Tillement, J.-P. (1992b). Drug transfer across the blood–brain barrier: Correlation between in vitro and in vivo models. *J. Neurochem.* 58:1790–1797.

Dehouck, M.-P., Méresse, S., Dehouck, B., Fruchart, J. C., and Cecchelli, R. (1992a). In vitro reconstituted blood–brain barrier. *J. Control. Release* 21:81–92.

Dehouck, M.-P., Méresse, S., Delorme, P., Fruchart, J. C., and Cecchelli, R. (1990). An easier, reproducible, and mass-production method to study the blood–brain barrier in vitro. *J. Neurochem.* 54:1798–1801.

Deli, M. A., Ábrahám, C. S., Niwa, M., and Falus, A. (2003). *N,N*-diethyl-2-[4-(phenylmethyl)phenoxy]-ethanamide increases the permeability of primary mouse cerebral endothelial cell monolayers. *Inflamm. Res.* 52:S39–S40.

Deli, M. A., Dehouck, M.-P., Ábrahám, C. S., Cecchelli, R., and Joó, F. (1995a). Penetration of small molecular weight substances through cultured bovine brain capillary endothelial cells. The early effects of 3′,5′-cyclic adenosine monophosphate. *Exp. Physiol.* 80:675–678.

Deli, M. A., Dehouck, M.-P., Cecchelli, R., Ábrahám, C. S., and Joó, F. (1995b). Histamine induces a selective albumin permeation through the blood–brain barrier in vitro. *Inflamm. Res.* 44:S56–S57.

Deli, M. A., Descamps, L., Dehouck, M.-P., Cecchelli, R., Joó, F., Ábrahám, C. S., and Torpier, G. (1995c). Exposure of tumor necrosis factor α to the luminal membrane induces a delayed increase of permeability and formation of cytoplasmic actin stress fibers in brain capillary endothelial cells cocultured with astrocytes. *J. Neurosci. Res.* 41:717–726.

Deli, M. A., and Joó, F. (1996). Cultured vascular endothelial cells of the brain. *Keio J. Med.* 45:183–198.

Demeule, M., Poirier, J., Jodoin, J., Bertrand, Y., Desrosiers, R. R., Dagenais, C., Nguyen, T., Lanthier, J., Gabathuler, R., Kennard, M., Jefferies, W. A., Karkan, D., Tsai, S., Fenart, L., Cecchelli, R., and Beliveau, R. (2002). High transcytosis of melanotransferrin (P97) across the blood–brain barrier. *J. Neurochem.* 83:924–933.

Demeuse, P., Kerkhofs, A., Struys-Ponsar, C., Knoops, B., Remacle, C., and van den Bosch de Aguilar, P. (2002). Compartmentalized coculture of rat brain endothelial cells and astrocytes: A syngenic model to study the blood–brain barrier. *J. Neurosci. Methods* 121:21–31.

Descamps, L., Cecchelli, R., and Torpier, G. (1997). Effects of tumor necrosis factor on receptor-mediated endocytosis and barrier functions of bovine brain capillary endothelial cell monolayers. *J. Neuroimmunol.* 74:173–184.

Descamps, L., Coisne, C., Dehouck, B., Cecchelli, R., and Torpier, G. (2003). Protective effect of glial cells against lipopolysaccharide-mediated blood–brain barrier injury. *Glia* 42:46–58.

de Vries, H. E., Blom-Roosemalen, M. C., de Boer, A. G., van Berkel, T. J., Breimer, D. D., and Kuiper, J. (1996a). Effect of endotoxin on permeability of bovine cerebral endothelial cell layers in vitro. *J. Pharmacol. Exp. Ther.* 277:1418–1423.

de Vries, H. E., Blom-Roosemalen, M. C., van Oosten, M., de Boer, A. G., van Berkel, T. J., Breimer, D. D., and Kuiper, J. (1996b). The influence of cytokines on the integrity of the blood–brain barrier in vitro. *J. Neuroimmunol.* 64:37–43.

Didier, N., Banks W. A., Creminon, C., Dereuddre-Bosquet, N., and Mabondzo, A. (2002). HIV-1-induced production of endothelin-1 in an in vitro model of the human blood–brain barrier. *Neuroreport* 13:1179–1183.

Didier, N., Romero, I. A., Creminon, C., Wijkhuisen, A., Grassi, J., and Mabondzo, A. (2003). Secretion of interleukin-1β by astrocytes mediates endothelin-1 and tumour necrosis factor-α effects on human brain microvascular endothelial cell permeability. *J. Neurochem.* 86:246–254.

Dobbie, M. S., Hurst, R. D., Klein, N. J., and Surtees, R. A. H. (1999). Upregulation of intracellular adhesion molecule-1 expression on human endothelial cells by tumour necrosis factor-α in an in vitro model of the blood–brain barrier. *Brain Res.* 830:330–336.

Dohgu, S., Kataoka, Y., Ikesue, H., Naito, M., Tsuruo, T., Oishi, R., and Sawada, Y. (2000). Involvement of glial cells in cyclosporine-increased permeability of brain endothelial cells. *Cell Mol. Neurobiol.* 20:781–786.

Duport, S., Robert, F., Muller, D., Grau, G., Parisi, L., and Stoppini, L. (1998). An in vitro blood–brain barrier model: Cocultures between endothelial cells and organotypic brain slice cultures. *Proc. Natl Acad. Sci. USA* **95**:1840–1845.

Easton, A. S., and Abbott, J. N. (2002). Bradykinin increases permeability by calcium and 5-lipoxygenase in the ECV304/C6 cell culture model of the blood–brain barrier. *Brain Res.* **953**:157–169.

Eddy, E. P., Maleef, B. E., Hart, T. K., and Smith, P. L. (1997). In vitro models to predict blood–brain barrier. *Adv. Drug Delivery Rev.* **23**:185–198.

Fenart, L., Buee-Scherrer, V., Descamps, L., Duhem, C., Poullain, M. G., Cecchelli, R., and Dehouck, M. P. (1998). Inhibition of P-glycoprotein: Rapid assessment of its implication in blood–brain barrier integrity and drug transport to the brain by an in vitro model of the blood–brain barrier. *Pharm. Res.* **15**:993–1000.

Fenart, L., Casanova, A., Dehouck, B., Duhem, C., Slupek, S., Cecchelli, R., and Betbeder, D. (1999). Evaluation of effect of charge and lipid coating on ability of 60-nm nanoparticles to cross an in vitro model of the blood–brain barrier. *J. Pharmacol. Exp. Ther.* **291**:1017–1022.

Fiala, M., Looney, D. J., Stins, M., Way, D. D., Zhang, L., Gan, X., Chiappelli, F., Schweitzer, E. S., Shapshak, P., Weinand, M., Graves, M. C., Witte, M., and Kim, K. S. (1997). TNF-alpha opens a paracellular route for HIV-1 invasion across the blood–brain barrier. *Mol. Med.* **3**:553–564.

Fillebeen, C., Dehouck, B., Benaïssa, M., Dhennin-Duthille, I., Cecchelli, R., and Pierce, A. (1999a). Tumor necrosis factor-α increases lactoferrin transcytosis through the blood–brain barrier. *J. Neurochem.* **73**:2491–2500.

Fillebeen, C., Descamps, L., Dehouck, M. P., Fenart, L., Benaïssa, M., Spik, G., Cecchelli, R., and Pierce, A. (1999b). Receptor-mediated transcytosis of lactoferrin through the blood–brain barrier. *J. Biol. Chem.* **274**:7011–7017.

Fischer, S., Clauss, M., Wiesnet, M., Renz, D., Schaper, W., and Karliczek, G. F. (1999a). Hypoxia induces permeability in brain microvessel endothelial cells via VEGF and NO. *Am. J. Physiol. Cell Physiol.* **276**:C812–C820.

Fischer, S., Renz, D., Schaper, W., and Karliczek, G. F. (1995). In vitro effects of fentanyl, methohexital, and thiopental brain endothelial permeability. *Anesthesiology* **82**:451–458.

Fischer, S., Renz, D., Schaper, W., and Karliczek, G. F. (1996). Effects of barbiturates on hypoxic cultures of brain derived microvascular endothelial cells. *Brain Res.* **707**:47–53.

Fischer, S., Renz, D., Schaper, W., and Karliczek, G. F. (1998). Barbiturates decreases the expression of vascular endothelial growth factor in hypoxic cultures of porcine brain derived microvascular endothelial cells. *Mol. Brain Res.* **60**:89–97.

Fischer, S., Renz, D., Schaper, W., and Karliczek, G. F. (2001). In vitro effects of dexamethasone on hypoxia-induced hyperpermeability and expression of vascular endothelial growth factor. *Eur. J. Pharmacol.* **411**:231–243.

Fischer, S., Renz, D., Wiesnet, M., Schaper, W., and Karliczek, G. F. (1999b). Hypothermia abolishes hypoxia-induced hyperpermeability in brain microvessel endothelial cells. *Mol. Brain Res.* **74**:135–144.

Fischer, S., Wobben, M., Kleinstück, J., Renz, D., and Schaper, W. (2000). Effect of astroglial cells on hypoxia-induced permeability in PBMEC cells. *Am. J. Physiol. Cell Physiol.* **279**:C935–C944.

Franke, H., Galla, H.-J., and Beuckmann, C. T. (1999). An improved low-permeability in vitro-model of the blood–brain barrier: Transport studies on retinoids, sucrose, haloperidol, caffeine and mannitol. *Brain Res.* **818**:65–71.

Gaillard, P. J., and de Boer, A. G. (2000). Relationship between permeability status of the blood–brain barrier and in vitro permeability coefficient of a drug. *Eur. J. Pharm. Sci.* **12**:95–102.

Gaillard, P. J., de Boer, A. G., and Breimer, D. D. (1996). Blood–brain barrier permeability and stress: A study on excitotoxic stress and vasogenic edema. *Eur. J. Pharm. Sci.* **4**:S195.

Gaillard, P. J., de Boer, A. G., and Breimer, D. D. (2003). Pharmacological investigation on lipopolysaccharide-induced permeability changes in the blood–brain barrier in vitro. *Microvasc. Res.* **65**:24–31.

Gaillard, P. J., Voorwinden, H., Nielsen, J., Ivanov, A., Atsumi, R., Engman, H., Ringbom, C., de Boer, A. G., and Breimer, D. D. (2001). Establishment and functional characterization of an in vitro model of the blood–brain barrier, comprising a co-culture of brain capillary endothelial cells and astrocytes. *Eur. J. Pharm. Sci.* **13**:215–222.

Giese, H., Mertsch, K., and Blasig, I. E. (1995). Effect of MK-801 and U83836 on a porcine brain capillary endothelial cell barrier during hypoxia. *Neurosci. Lett.* **191**:169–172.

Giri, R., Shen, Y., Stins, M., Yan, S. D., Schmidt, A. M., Stern, D., Kim, K.-S., Zlokovic, B., and Kalra, V. K. (2000). β-Amyloid-induced migration of monocytes across human brain endothelial cells involve RAGE and PECAM-1. *Am. J. Physiol. Cell Physiol.* **279**:C1772–C1781.

Girod, J., Fenart, L., Régina, A., Dehouck, M.-P., Hong, G., Scherrmann, J.-M., Cecchelli, R., and Roux, F. (1999). Transport of cationized anti-tetanus Fab'2 fragments across an in vitro blood–brain barrier model: Involvement of the transcytosis pathway. *J. Neurochem.* 73:2002–2008.

Gloor, S. M., Weber, A., Adachi, N., and Frei, K. (1997). Interleukin-1 modulates protein tyrosine phosphatase activity and permeability of brain endothelial cells. *Biochem. Biophys. Res. Commun.* 239:804–809.

Grabb, P. A., and Gilbert, M. R. (1995). Neoplastic and pharmacological influence on the permeability of an in vitro blood–brain barrier. *J. Neurosurg.* 82:1053–1058.

Greenwood, J., Pryce, G., Devine, L., Male, D. K., dos Santos, W. L., Calder, V. L., and Adamson, P. (1996). SV40 large immortalised cell lines of the rat blood–brain and blood-retinal barriers retain their phenotypic and immunological characteristics. *J. Neuroimmunol.* 71:51–63.

Gu, X., Zhang, J., Brann, D. W., and Yu, F.-S. X. (2003). Brain and retinal vascular endothelial cells with extended life span established by ectopic expression of telomerase. *Invest. Ophthalmol. Vis. Sci.* 44:3219–3225.

Guillot, F. L., and Audus, K. L. (1991). Angiotensin peptide regulation of bovine brain microvessel endothelial cell monolayer permeability. *J. Cardiovasc. Pharmacol.* 18:212–218.

Gumbleton, M., and Audus, K. L. (2001). Progress and limitations in the use of in vitro cell cultures to serve as a permeability screen for the blood–brain barrier. *J. Pharm. Sci.* 90:1681–1698.

Hamm, S., Dehouck, B., Kraus, J., Wolburg-Buchholz, K., Wolburg, H., Risau, W., Cecchelli, R., Engelhardt, B., and Dehouck, M. P. (2004). Astrocyte mediated modulation of blood brain barrier permeability does not correlate with a loss of tight junction proteins from the cellular contacts. *Cell Tissue Res.* 315:157–166.

Hart, M. N., VanDyk, L. F., Moore, S. A., Shasby, D. M., and Cancilla, P. A. (1987). Differential opening of the brain endothelial barrier following neutralization of the endothelial luminal anionic charge in vitro. *J. Neuropathol. Exp. Neurol.* 46:141–153.

Haseloff, R. F., Blasig, I. E., Bauer, H.-C., and Bauer, H. (2005). In search of the astrocytic factor(s) modulating blood–brain barrier functions in brain capillary endothelial cells in vitro. *Cell. Mol. Neurobiol.* 25:25–39.

Hoheisel, D., Nitz, T., Franke, H., Wegener, J., Hakvoort, A., Tilling, T., and Galla, H.-J. (1998). Hydroocortisone reinforces the blood–brain barrier properties in a serum free cell culture system. *Biochem. Biophys. Res. Commun.* 247:312–315.

Homma, M., Suzuki, H., Kusuhara, H., Naito, M., Tsuruo, T., and Sugiyama, Y. (1999). High-affinity efflux transport system for glutathione conjugates on the luminal membrane of a mouse brain capillary endothelial cell line (MBEC4). *J. Pharmacol. Exp. Ther.* 288:198–203.

Hosoya, K., Tetsuka, K., Nagase, K., Tomi, M., Saeki, S., Ohtsuki, S., and Terasaki, T. (2000). Conditionally immortalized brain capillary endothelial cell lines established from a transgenic mouse harboring temperature-sensitive simian virus 40 large T-antigen gene. *AAPS PharmSci* 2(3):E27, 1–11. [http://www.pharmsci.org].

Hurst, R. D., Azam, S., Hurst, A., and Clark, J. B. (2001). Nitric-oxide-induced inhibition of glyceraldehyde-3-phosphate dehydrogenase may mediate reduced endothelial cell monolayer integrity in an in vitro model blood–brain barrier. *Brain Res.* 894:181–188.

Hurst, R. D., and Clark, J. B. (1997). Nitric oxide-induced blood–brain barrier dysfunction is not mediated by inhibition of mitochondrial respiratory chain activity and/or energy depletion. *Nitric Oxide* 1:121–129.

Hurst, R. D., and Clark, J. B. (1998). Alterations in transendothelial electrical resistance by vasoactive agonists and cyclic AMP in a blood–brain barrier model system. *Neurochem. Res.* 23:149–154.

Hurst, R. D., and Clark, J. B. (1999). Butyric acid mediated induction of enhanced transendothelial resistance in an in vitro model blood–brain barrier system. *Neurochem. Int.* 35:261–267.

Hurst, R. D., and Fritz, I. B. (1996). Properties of an immortalised vascular endothelial/glioma cell coculture model of the blood–brain barrier. *J. Cell. Physiol.* 167:81–88.

Hurst, R. D., Heales, S. J. R., Dobbie, M. S., Barker, J. E., and Clark, J. B. (1998). Decreased endothelial cell glutathione and increased sensitivity to oxidative stress in an in vitro blood–brain barrier model system. *Brain Res.* 802:232–240.

Ichikawa, N., Naora, K., Hirano, H., Hashimoto, M., Masumara, S., and Iwamoto K. (1996). Isolation and primary culture of rat cerebral microvascular endothelial cells for studying drug transport in vitro. *J. Pharmacol. Toxicol. Methods* 36:45–52.

Igarashi, Y., Utsumi, H., Chiba, H., Yamada-Sasamori, Y., Tobioka, H., Kamimura, Y., Furuuchi, K., Kokai, Y., Nakagawa, T., Mori, M., and Sawada, N. (1999). Glial cell-line-derived neurotrophic factor induces barrier function of endothelial cells forming the blood–brain barrier. *Biochem. Biophys. Res. Commun.* 261:108–112.

Imaizumi, S., Kondo, T., Deli, M. A., Gobbel, G., Joó, F., Epstein, C. J., Yoshimoto, T., and Chan, P. H. (1996). The influence of oxygen free radicals on the permeability of the monolayer of cultured brain endothelial cells. *Neurochem. Int.* 29:205–211.

Jong, A. Y., Stins, M. F., Huang, S.-H., Chen, S. H. M., and Kim, K. S. (2001). Traversal of *Candida albicans* across human blood–brain barrier in vitro. *Infect. Immun.* 69:4536–4544.

Joó, F. (1985). The blood–brain barrier in vitro: Ten years of research on microvessels isolated from the brain. *Neurochem. Int.* 7:1–25.

Joó, F. (1992). The cerebral microvessels in culture, an update. *J. Neurochem.* 58:1–17.

Joó, F. (1993). The blood–brain barrier in vitro: The second decade. *Neurochem. Int.* 23:499–521.

Joó, F., and Karnushina, I. (1973). A procedure for the isolation of capillaries from rat brain. *Cytobios* 8:41–48.

Kannan, R., Chakrabarti, R., Tang, D., Kim, K. J., and Kaplowitz, N. (2000). GSH transport in human cerebrovascular endothelial cells and human astrocytes: Evidence for luminal localization of Na^+-dependent GSH transport in HCEC. *Brain Res.* 852:374–382.

Kása, P., Pákáski, M., Joó, F., and Lajtha, A. (1991). Endothelial cells from human fetal brain microvessels may be cholinoceptive, but do not synthesize acetylcholine. *J. Neurochem.* 56:2143–2146.

Kempski, O., Villacara, A., Spatz, M., Dodson, R. F., Corn, C., Merkel, N., and Bembry, J. (1987). Cerebromicrovascular endothelial permeability. In-vitro studies. *Acta Neuropathol. (Berl).* 74:329–334.

Kiessling, F., Kartenbeck, J., and Haller, C. (1999). Cell–cell contacts in the human cell line ECV304 exhibit both endothelial and epithelial characteristics. *Cell Tissue Res.* 297:131–140.

Kis, B., Deli, M. A., Kobayashi, H., Ábrahám, C. S., Yanagita, T., Kaiya, H., Isse, T., Nishi, R., Gotoh, S., Kangawa, K., Wada, A., Greenwood, J., Niwa, M., Yamashita, H., and Ueta, Y. (2001). Adrenomedullin regulates blood–brain barrier functions in vitro. *Neuroreport* 12:4139–4142.

Kochi, S., Takanaga, H., Matsuo, H., Naito, M., Tsuruo, T., and Sawada, Y. (1999). Effect of cyclosporin A or tacrolimus on the function of blood–brain barrier cells. *Eur. J. Pharmacol.* 372:287–295.

Kondo, T., Kinouchi, H., Kawase, M., and Yoshimoto, T. (1996). Astroglial cells inhibit the increasing permeability of brain endothelial cell monolayer following hypoxia/reoxygenation. *Neurosci. Lett.* 208:101–104.

Krizanac-Bengez, L., Kapural, M., Parkinson, F., Cucullo, L., Hossain, M., Mayberg, M. R., and Janigro, D. (2003). Effects of transient loss of shear stress on blood–brain barrier endothelium: Role of nitric oxide and IL-6. *Brain Res.* 977:239–246.

Krizbai, I. A., and Deli, M. A. (2003). Signalling pathways regulating the tight junction permeability in the blood–brain barrier. *Cell Mol. Biol. (Noisy-le-grand).* 49:23–31.

Krizbai, I. A., Deli, M. A., Pestenácz, A., Siklós, L., Szabó, C. A., András, I., and Joó, F. (1998). Expression of glutamate receptors on cultured cerebral endothelial cells. *J. Neurosci. Res.* 54:814–819.

Kusuhara, H., and Sugiyama, Y. (2001a). Efflux transport systems for drugs at the blood–brain barrier and blood-cerebrospinal fluid barrier (Part 1). *Drug Discov. Today* 6:150–156.

Kusuhara, H., and Sugiyama, Y. (2001b). Efflux transport systems for drugs at the blood–brain barrier and blood-cerebrospinal fluid barrier (Part 2). *Drug Discov. Today* 6:206–212.

Kusuhara, H., Suzuki, H., Naito, M., Tsuruo, T., and Sugiyama, Y. (1998). Characterization of efflux transport of organic anions in a mouse brain capillary endothelial cell line. *J. Pharmacol. Exp. Ther.* 285:1260–1265.

Lagrange, P., Romero, I. A., Minn, A., and Revest, P. A. (1999). Transendothelial permeability changes induced by free radicals in an in vitro model of the blood–brain barrier. *Free Radic. Biol. Med.* 27:667–672.

Lee, S.-W., Kim, W. J., Choi, Y. K., Song, H. S., Son, M. J., Gelman, I. H., Kim, Y.-J., and Kim, K.-W. (2003). SSeCKS regulates angiogenesis and tight junction formation in blood–brain barrier. *Nat. Med.* 9:900–906.

Letrent, S. P., Polli, J. W., Humphreys, J. E., Pollack, G. M., Brouwer, K. R., and Brouwer, K. L. R. (1999). P-Glycoprotein-mediated transport of morphine in brain capillary endothelial cells. *Biochem. Pharmacol.* 58:951–957.

Leveugle, B., Ding, W., Fenart, L., Dehouck, M.-P., Scanameo, A., Cecchelli, R., and Fillit, H. (1998). Heparin oligosaccharides that pass the blood–brain barrier inhibit β-amyloid precursor protein secretion and heparin binding to β-amyloid peptides. *J. Neurochem.* 70:736–744.

Lippoldt, A., Kniesel, U., Liebner, S., Kalbacher, H., Kirsch, T., Wolburg, H., and Haller, H. (2000). Structural alterations of tight junctions are associated with loss of polarity in stroke-prone spontaneously hypertensive rat blood–brain barrier endothelial cells. *Brain Res.* 885:251–261.

Liu, N. Q., Lossinsky, A. S., Popik, W., Li, X., Gujuluva, C., Kriederman, B., Roberts, J., Pushkarsky, T., Bukrinsky, M., Witte, M., Weinand, M., and Fiala, M. (2002). Human immunodeficiency virus type 1 enters brain microvascular endothelia by macropinocytosis dependent on lipid rafts and the mitogen-activated protein kinase signaling pathway. *J. Virol.* 76:6689–6700.

Lundquist, S., Renftel, M., Brillault, J., Fenart, L., Cecchelli, R., and Dehouck, M. P. (2002). Prediction of drug transport through the blood–brain barrier in vivo: A comparison between two in vitro cell models. *Pharm. Res.* 19:976–981.

Mackic, J. B., Stins, M., Jovanovic, S., Kim, K. S., Bartus, R. T., and Zlokovic, B. V. (1999). Cereport (RMP-7) increases the permeability of human brain microvascular endothelial cell monolayers. *Pharm. Res.* 16:1360–1365.

Mackic, J. B., Stins, M., McComb, J. G., Calero, M., Ghiso, J., Kim, K. S., Yan, S. D., Stern, D., Schmidt, A. M., Frangione, B., and Zlokovic, B. V. (1998). Human blood–brain barrier receptors for Alzheimer's amyloid-beta 1–40. Asymmetrical binding, endocytosis, and transcytosis at the apical side of brain microvascular endothelial cell monolayer. *J. Clin. Invest.* 102:734–743.

Madara, J. L. (1998). Regulation of the movement of solutes across tight junctions. *Annu. Rev. Physiol.* 60:143–159.

Mark, K. S., Burroughs, A. R., Brown, R. C., Huber, J. D., and Davis, T. P. (2001). Nitric oxide mediates hypoxia-induced changes in paracellular permeability of cerebral microvasculature. *Am. J. Physiol. Heart Circ. Physiol.* 286:H174–H180.

Mark, K. S., and Davis, T. P. (2002). Cerebral microvascular changes in permeability and tight junctions induced by hypoxia-reoxygenation. *Am. J. Physiol. Heart Circ. Physiol.* 282:H1485–H1494.

Mark, K. S., and Miller, D. W. (1999). Increased permeability of primary cultured brain microvessel endothelial cell monolayers following TNF-α exposure. *Life Sci.* 64:1941–1953.

Mark, K. S., Trickler, W. J., and Miller, D. W. (2001). Tumor necrosis factor-α induces cyclooxygenase-2 expression and prostaglandin release in brain microvessel endothelial cells. *J. Pharmacol. Exp. Ther.* 297:1051–1058.

Matter, K., and Balda, M. (2003a). Functional analysis of tight junctions. *Methods* 30:228–234.

Matter, K., and Balda, M. (2003b). Holey barrier: Claudins and the regulation of brain endothelial permeability. *J. Cell. Biol.* 161:459–460.

Megard, I., Garrigues, A., Orlowski, S., Jorajuria, S., Clayette, P., Ezan, E., and Mabondzo, A. (2002). A co-culture-based model of human blood–brain barrier: Application to active transport of indinavir and in vivo-in vitro correlation. *Brain Res.* 927:153–167.

Mertsch, K., Blasig, I., and Grune, T. (2001). 4-Hydroxynonenal impairs the permeability of an in vitro rat blood–brain barrier. *Neurosci. Lett.* 314:135–138.

Mi, H., Haeberle, H., and Barres, B. A. (2001). Induction of astrocyte differentiation by endothelial cells. *J. Neurosci.* 21:1538–1547.

Muruganandam, A., Herx, L. M., Monette, R., Durkin, J. P., and Stanimirovic, D. (1997). Development of immortalized human cerebromicrovascular endothelial cell line as an in vitro model of the human blood–brain barrier. *FASEB J.* 11:1187–1197.

Muruganandam, A., Tanha, J., Narang, S., and Stanimirovic, D. (2002). Selection of phage-displayed llama single-domain antibodies that transmigrate across human blood–brain barrier endothelium. *FASEB J.* 16:240–242.

Nag, S. (2003). Blood–brain barrier permeability using tracers and immunohistochemistry. In Nag, S. (ed.), *The Blood–Brain Barrier: Biology and Research Protocols. Methods in Molecular Medicine, Vol. 89*, Humana Press, Totowa, NJ, pp. 133–144.

Neuhaus, J., Risau, W., and Wolburg, H. (1991). Induction of blood–brain barrier characteristics in bovine brain endothelial cells by rat astroglial cells in transfilter coculture. *Ann. N. Y. Acad. Sci.* 633:578–580.

Nitta, T., Hata, M., Gotoh, S., Seo, Y., Sasaki, H., Hashimoto, N., Furuse, M., and Tsukita, S. (2003). Size-selective loosening of the blood–brain barrier in claudin-5-deficient mice. *J. Cell. Biol.* 161:653–660.

Nitz, T., Eisenblatter, T., Psathaki, K., and Galla, H.-J. (2003). Serum-derived factors weaken the barrier properties of cultured porcine brain capillary endothelial cells in vitro. *Brain Res.* 981:30–40.

Omidi, Y., Campbell, L., Barar, J., Connell, D., Akhtar, S., and Gumbleton, M. (2003). Evaluation of the immortalised mouse brain capillary endothelial cell line, b.End3, as an in vitro blood–brain barrier model for drug uptake and transport studies. *Brain Res.* 990:95–122.

Panula, P., Joó, F., and Rechardt, L. (1978). Evidence for the presence of viable endothelial cells in cultures derived from dissociated rat brain. *Experientia* 34:95–97.

Pardridge, W. M. (2002). Drug and gene targeting to brain with molecular trojan horses. *Nat. Rev. Drug Discov.* 1:131–139.

Parkinson, F. E., Friesen, J., Krizanac-Bengez, L., and Janigro, D. (2003). Use of three-dimensional in vitro model of the rat blood–brain barrier to assay nucleoside efflux from brain. *Brain Res.* 980:233–241.

Pirro, J. P., Di Rocco, R. J., Narra, R. K., and Nunn, A. D. (1994). Relationship between in vitro transendothelial permeability and in vivo single-pass brain extraction. *J. Nucl. Med.* 35:1514–1519.
Plateel, M., Dehouck, M.-P., Torpier, G., Cecchelli, R., and Teissier, E. (1995). Hypoxia increases the susceptibility of oxidant stress and the permeability of the blood–brain barrier endothelial cell monolayer. *J. Neurochem.* 65:2138–2145.
Plateel, M., Teissier, E., and Cecchelli, R. (1997). Hypoxia dramatically increases the nonspecific transport of blood-borne proteins to the brain. *J. Neurochem.* 68:874–877.
Prat, A., Biernacki, K., Wosik, K., and Antel, J. P. (2001). Glial cell influence on the human blood–brain barrier. *Glia* 36:145–155.
Ramsohoye, P. V., and Fritz I. B. (1998). Preliminary characterization of glial-secreted factors responsible for the induction of high electrical resistances across endothelial monolayers in a blood–brain barrier model. *Neurochem. Res.* 23:1545–1551.
Raub, T. J. (1996). Signal transduction and glial cell modulation of cultured brain microvessel endothelial cell tight junctions. *Am. J. Physiol. Cell Physiol.* 271:C495–C503.
Raub, T. J., Kuentzel, S. L., and Sawada, G. A. (1992). Permeability of bovine brain microvessel endothelial cells in vitro: Barrier tightening by a factor released from astroglioma cells. *Exp. Cell Res.* 199:330–340.
Reese, T. S., and Karnovsky, M. J. (1967). Fine structural localization of a blood–brain barrier to exogenous peroxidase. *J. Cell Biol.* 34:207–217.
Reichel, A., Begley, D. J., and Abbott, N. J. (2003). An overview of in vitro techniques for blood–brain barrier studies. In Nag, S. (ed.), *The Blood–Brain Barrier: Biology and Research Protocols. Methods in Molecular Medicine, Vol. 89*, Humana Press, Totowa, NJ, pp. 307–324.
Rist, R. J., Romero, I. A., Chan, M. W. K., and Abbott, N. J. (1996). Effects of energy deprivation induced by fluorocitrate in immortalised rat brain microvessel endothelial cells. *Brain Res.* 730:87–94.
Rist, R. J., Romero, I. A., Chan, M. W. K., Couraud, P.-O., Roux, F., and Abbott, N. J. (1997). F-Actin cytoskeleton and sucrose permeability of immortalised rat brain microvascular endothelial cell monolayers: Effects of cyclic AMP and astrocytic factors. *Brain Res.* 768:10–18.
Romero, I. A., Prevost, M.-C., Perret, E., Adamson, P., Greenwood, J., Couraud, P.-O., and Ozden, S. (2000). Interactions between brain endothelial cells and human T-cell leukemia virus type 1-infected lymphocytes: Mechanisms of viral entry into the central nervous system. *J. Virol.* 74:6021–6030.
Romero, I. A., Radewicz, K., Jubin, E., Michel, C. C., Greenwood, J., Couraud, P.-O., and Adamson, P. (2003). Changes in cytoskeletal and tight junctional proteins correlate with decreased permeability induced by dexamethasone in cultured rat brain endothelial cells. *Neurosci. Lett.* 344:112–116.
Romero, I. A., Rist, R. J., Aleshaiker, A., and Abbott, N. J. (1997a). Metabolic and permeability changes caused by thiamine deficiency in immortalized rat brain microvessel endothelial cells. *Brain Res.* 756:133–140.
Romero, I. A., Rist, R. J., Chan, M W., and Abbott, N. J. (1997b). Acute energy deprivation syndromes: Investigation of m-dinitrobenzene and alpha-chlorhydrin toxicity on immortalized rat brain microvessel endothelial cells. *Neurotoxicology* 18:781–791.
Roux, F., and Couraud, P.-O. (2005). Rat brain endothelial cell lines for the study of blood–brain barrier permeability and transport functions. *Cell. Mol. Neurobiol.* 25:41–58.
Rubin, L. L., Hall, D. E., Porter, S., Barbu, K., Cannon, C., Horner, H. C., Janatpour, M., Liaw, C. W., Manning, K., Morales, J., Tanner, L. I., Tomaselli, K. J., and Bard, F. (1991). A cell culture model of the blood–brain barrier. *J. Cell Biol.* 115:1725–1735.
Rubin, L. L., and Staddon, J. M. (1999). The cell biology of the blood–brain barrier. *Annu. Rev. Neurosci.* 22:11–28.
Ruchoux, M.-M., Brulin, P., Brillault, J., Dehouck, M.-P., Cecchelli, R., and Bataillard, M. (2002). Lessons from CADASIL. *Ann. N. Y. Acad. Sci.* 977:224–231.
Rutten, M. J., Hoover, R. L., and Karnovsky, M. J. (1987). Electrical resistance and macromolecular permeability of brain endothelial monolayer cultures. *Brain Res.* 425:301–310.
Sahagun, G., Moore, S. A., and Hart, M. N. (1990). Permeability of neutral vs. anionic dextrans in cultured brain microvascular endothelium. *Am. J. Physiol.* 259:H162–H166.
Schaddelee, M. P., Voorwinden, H. L., van Tilburg, E. W., Pateman, T. J., Ijzerman, A. P., Danhof, M., and de Boer, A. G. (2003). Functional role of adenosine receptor subtypes in the regulation of blood–brain barrier permeability: Possible implications for the design of synthetic adenosine derivatives. *Eur. J. Pharm. Sci.* 19:13–22.
Schirmacher, A., Winters, S., Fischer, S., Goeke, J., Galla, H. J., Kullnick, U., Ringelstein, E. B., and Stogbauer, F. (2000). Electromagnetic fields (1.8 GHz) increase the permeability to sucrose of the blood–brain barrier in vitro. *Bioelectromagnetics* 21:338–345.
Schulze, C., Smales, C., Rubin, L. L., and Staddon, J. M. (1997). Lysophosphatidic acid increases tight junction permeability in cultured brain endothelial cells. *J. Neurochem.* 68:991–1000.

Scism, J. L., Laska, D. A., Horn, J. W., Gimple, J. L., Pratt, S. E., Shepard, R. L., Dantzig, A. H., and Wrighton, S. A. (1999). Evaluation of an in vitro coculture model for the blood–brain barrier: Comparison of human umbilical vein endothelial cells (ECV304) and rat glioma cells from two commercial sources. *In Vitro Cell Dev. Biol. Anim.* 35:580–592.

Semenza, G. L. (2001). Hypoxia-inducible factor 1: Oxygen homeostasis and disease pathophysiology. *Trends Mol. Med.* 7:345–350.

Sharp, C. D., Hines, I., Houghton, J., Warren, A., Jackson, T. H. IV, Jawahar, A., Nanda, A., Elrod, J. W., Long, A., Chi, A., Minagar, A., and Alexander, J. S. (2003). Glutamate causes a loss in human cerebral endothelial barrier integrity through activation of NMDA receptor. *Am. J. Physiol. Heart Circ. Physiol.* 285:H2592–H2598.

Smith, K. R., and Borchardt, R. T. (1989). Permeability and mechanism of albumin, cationized albumin, and glycosylated albumin transcellular transport across monolayers of cultured bovine brain capillary endothelial cells. *Pharm. Res.* 6:466–473.

Sobue, K., Yamamoto, N., Yoneda, K., Hodgson, M.E., Yamashiro, K., Tsuruoka, N., Tsuda, T., Katsuya, H., Miura, Y., Asai, K., and Kato, T. (1999). Induction of blood–brain barrier properties in immortalized bovine brain endothelial cells by astrocytic factors. *Neurosci. Res.* 35:155–164.

Song, H. S., Son, M. J., Lee, Y. M., Kim, W. J., Lee, S.-W., Kim, C. W., and Kim, K.-W. (2002). Oxygen tension regulates the maturation of the blood–brain barrier. *Biochem. Biophys. Res. Commun.* 290:325–331.

Staddon, J. M., Herrenknecht, K., Smales, C., and Rubin, L. L. (1995). Evidence that tyrosine phosphorylation may increase tight junction permeability. *J. Cell Sci.* 108:609–619.

Stanness, K. A., Neumaier, J. F., Sexton, T. J., Grant, G. A., Emmi, A., Maris, D. O., and Janigro, D. (1999). A new model of the blood–brain barrier: Co-culture of neuronal, endothelial, and glial cells under dynamic conditions. *Neuroreport* 10:3725–3731.

Sîms, M. F., Badger, J., and Kim, K. S. (2001). Bacterial invasion and transcytosis in transfected human brain microvascular endothelial cells. *Microb. Pathog.* 30:19–28.

Suda, K., Rothen-Rutishauser, B., Gunthert, M., and Wunderli-Allenspach, H. (2001). Phenotypic characterization of human umbilical vein endothelial (ECV304) and urinary carcinoma (T24) cells: Endothelial versus epithelial features. *In Vitro Cell Dev. Biol. Anim.* 37:505–514.

Tamai, I., Yamashita, J., Kido, Y., Ohnari, A., Sai, Y., Shima, Y., Naruhashi, K., Kouzumi, S., and Tsuji, A. (2000). Limited distribution of new quinolone antibacterial agents into brain caused by multiple efflux transporters at the blood–brain barrier. *J. Pharmacol. Exp. Ther.* 295:146–152.

Tan, K. H., Dobbie, M. S., Felix, R. A., Barrand, M. A., and Hurst, R. D. (2001). A comparison of the induction of immortalized endothelial cell impermeability by astrocytes. *Neuroreport* 12:1329–1334.

Tao-Cheng, J. H., Nagy, Z., and Brightman, M. W. (1987). Tight junctions of brain endothelium in vitro are enhanced by astroglia. *J. Neurosci.* 7:3293–3299.

Tatsuta, T., Naito, M., Oh-hara, T., Sugawara, I., and Tsuruo, T. (1992). Functional involvement of P-glycoprotein in blood–brain barrier. *J. Biol. Chem.* 267:20383–20391.

Terasaki, T., and Hosoya, K. (2001). Conditionally immortalized cell lines as a new in vitro model for the study of barrier functions. *Biol. Pharm. Bull.* 24:111–118.

Thomas, S. A., Abbruscato, T. J., Hau, V. S., Gillespie, T. J., Zsigo, J., Hruby, V. J., and Davis, T. P. (1997). Structure-activity relationships of a series of [D-Ala^2]deltorphin I and II analogues: in vitro blood–brain barrier permeability and stability. *J. Pharmacol. Exp. Ther.* 281:817–825.

Tilling, T., Korte, D., Hoheisel, D., and Galla, H.-J. (1998). Basement membrane proteins influence brain capillary endothelial barrier function in vitro. *J. Neurochem.* 71:1151–1157.

Trottein, F., Descamps, L., Nutten, S., Dehouck, M.-P., Angeli, V., Capron, A., Cecchelli, R., and Capron, M. (1999). *Schistosoma mansoni* activates host microvascular endothelial cells to acquire an anti-inflammatory phenotype. *Infect. Immun.* 67:3403–3409.

Tsuji, A., and Tamai, I. (1999). Carrier-mediated or specialized transport of drugs across the blood–brain barrier. *Adv. Drug Deliv. Rev.* 36:277–290.

Tunkel, A. R., Rosser, S. W., Hansen, E. J., and Scheld, W. M. (1991). Blood–brain barrier alterations in bacterial meningitis: Development of an in vitro model and observations on the effects of lipopolysaccharide. *In Vitro Cell Dev. Biol.* 27A:113–120.

Utepbergenov, D. I., Mertsch, K., Sporbert, A., Tenz, K., Paul, M., Haseloff, R. F., and Blasig, I. E. (1998). Nitric oxide protects blood–brain barrier in vitro from hypoxia/reoxygenation-mediated injury. *FEBS Lett.* 424:197–201.

van Bree, J. B. M. M., de Boer, A. G., Danhof, M., Ginsel, L. A., and Breimer, D. D. (1988). Characterization of an "in vitro" blood–brain barrier: Effects of molecular size and lipophilicity on cerebrovascular endothelial transport rates of drugs. *J. Pharmacol. Exp. Ther.* 247:1233–1239.

van Bree, J. B. M. M., de Boer, A. G., Verhoef, J. C., Danhof, M., and Breimer, D. D. (1989). Transport of vasopressin fragments across the blood–brain barrier: "In vitro" studies using monolayer cultures of bovine brain endothelial cells. *J. Pharmacol. Exp. Ther.* 249:901–905.

Villacara, A., Kempski, O., and Spatz, M. (1990). Arachidonic acid and cerebromicrovascular endothelial permeability. In Long, D. (ed.), *Advances in Neurology, Vol. 52*, Raven Press, New York, NY, pp. 195–201.

Wang, W., Dentler, W. L., and Borchardt, R. T. (2001). VEGF increases BMEC monolayer permeability by affecting occludin expression and tight junction assembly. *Am. J. Physiol. Heart Circ. Physiol.* **280**:H434–H440.

Wang, W., Merrill, M. J., and Borchardt, R. T. (1996). Vascular endothelial growth factor affects permeability of brain microvessel endothelial cells in vitro. *Am. J. Physiol. Cell Physiol.* **271**:C1973–C1980.

Wolburg, H., and Lippoldt, A. (2002). Tight junctions of the blood–brain barrier: Development, composition and regulation. *Vascul. Pharmacol.* **38**:323–337.

Wolburg, H., Neuhaus, J., Kniesel, U., Krauß, B., Schmid, E.-M., Öcalan, M., Farrell, C., and Risau, W. (1994). Modulation of tight junction structure in blood–brain barrier endothelial cells. Effects of tissue culture, second messengers and cocultured astrocytes. *J. Cell Sci.* **107**:1347–1357.

Yamagata, K., Tagami, M., Nara, Y., Fujino, H., Kubota, A., Numano, F., Kato, T., and Yamori, Y. (1997). Faulty induction of blood–brain barrier functions by astrocytes isolated from stroke-prone spontaneously hypertensive rats. *Clin. Exp. Pharmacol. Physiol.* **24**:686–691.

Yamagata, K., Tagami, M., Takenaga, F., Yamori, Y., Nara, Y., and Itoh, S. (2003). Polyunsaturated fatty acids induce tight junctions to form in brain capillary endothelial cells. *Neuroscience* **116**:649–656.

Yang, J., Mutkus, L. A., Sumner, D., Stevens, J. T., Eldridge, J. C., Strandhoy, J. W., and Aschner, M. (2001). Transendothelial permeability of chlorpyrifos in RBE4 monolayers is modulated by astrocyte-conditioned medium. *Mol. Brain Res.* **97**:43–50.

Youdim, K. A., Dobbie, M. S., Kuhnle, G., Proteggente, A. R., Abbott, N. J., and Rice-Evans, C. (2003). Interaction between flavonoids and the blood–brain barrier: In vitro studies. *J. Neurochem.* **85**:180–192.

Zenker, D., Begley, D., Bratzke, H., Rübsamen-Waigmann, H., and von Briesen, H. (2003). Human blood-derived macrophages enhance barrier function of cultured brain capillary endothelial cells. *J. Physiol.* **551**:1023–1032.

Zysk, G., Schneider-Wald, B. K., Hwang, J. H., Bejo, L., Kim, K. S., Mitchell, T. J., Hakenbeck, R., and Heinz, H.-P. (2001). Pneumolysin in the main inducer of cytotoxicity to brain microvascular endothelial cells caused by *Streptococcus pneumoniae*. *Infect. Immun.* **69**:845–852.

ELSEVIER

Neurobiology of Disease

www.elsevier.com/locate/ynbdi
Neurobiology of Disease 16 (2004) 1–13

Review

The blood–brain barrier: an overview Structure, regulation, and clinical implications

Praveen Ballabh,* Alex Braun, and Maiken Nedergaard

Departments of Pediatrics, Anatomy and Cell Biology, and Pathology, New York Medical College and Westchester Medical Center, Valhalla, NY 10595, USA

Received 18 June 2003; revised 21 November 2003; accepted 10 December 2003

Available online 9 April 2004

The blood–brain barrier (BBB) is a diffusion barrier, which impedes influx of most compounds from blood to brain. Three cellular elements of the brain microvasculature compose the BBB—endothelial cells, astrocyte end-feet, and pericytes (PCs). Tight junctions (TJs), present between the cerebral endothelial cells, form a diffusion barrier, which selectively excludes most blood-borne substances from entering the brain. Astrocytic end-feet tightly ensheath the vessel wall and appear to be critical for the induction and maintenance of the TJ barrier, but astrocytes are not believed to have a barrier function in the mammalian brain. Dysfunction of the BBB, for example, impairment of the TJ seal, complicates a number of neurologic diseases including stroke and neuroinflammatory disorders. We review here the recent developments in our understanding of the BBB and the role of the BBB dysfunction in CNS disease. We have focused on intraventricular hemorrhage (IVH) in premature infants, which may involve dysfunction of the TJ seal as well as immaturity of the BBB in the germinal matrix (GM). A paucity of TJs or PCs, coupled with incomplete coverage of blood vessels by astrocyte end-feet, may account for the fragility of blood vessels in the GM of premature infants. Finally, this review describes the pathogenesis of increased BBB permeability in hypoxia–ischemia and inflammatory mechanisms involving the BBB in septic encephalopathy, HIV-induced dementia, multiple sclerosis, and Alzheimer disease.

Keywords: Blood–brain barrier; Tight junction; Germinal matrix; Astrocyte; Pericyte

Introduction

The blood–brain barrier (BBB) is a diffusion barrier essential for the normal function of the central nervous system. The BBB endothelial cells differ from endothelial cells in the rest of the body by the absence of fenestrations, more extensive tight junctions (TJs), and sparse pinocytic vesicular transport. Endothelial cell tight junctions limit the paracellular flux of hydrophilic molecules across the BBB. In contrast, small lipophilic substances such as O_2 and CO_2 diffuse freely across plasma membranes along their concentration gradient (Grieb et al., 1985). Nutrients including glucose and amino acids enter the brain via transporters, whereas receptor-mediated endocytosis mediates the uptake of larger molecules including insulin, leptin, and iron transferrin (Pardridge et al., 1985; Zhang and Pardridge, 2001). In addition to endothelial cells, the BBB is composed of the capillary basement membrane (BM), astrocyte end-feet ensheathing the vessels, and pericytes (PCs) embedded within the BM (Fig. 1A). Pericytes are the least-studied cellular component of the BBB but appear to play a key role in angiogenesis, structural integrity and differentiation of the vessel, and formation of endothelial TJ (Allt and Lawrenson, 2001; Balabanov and Dore-Duffy, 1998; Bandopadhyay et al., 2001; Lindahl et al., 1997). It is believed that all the components of the BBB are essential for the normal function and stability of the BBB.

The building blocks of the BBB

Tight junctions

Junction complex in the BBB comprises TJ and adherens junction (AJ). The TJs ultrastructurally appear as sites of apparent fusion involving the outer leaflets of plasma membrane of adjacent endothelial cells (Fig. 1B). Freeze fracture replica electron micrographs depict TJs as a set of continuous, anastomosing intramembranous strands or fibrils on P-face with a complementary groove on the E-face. The number of TJ strands as well as the frequency of their ramifications is variable. Adherens junctions are composed of a cadherin–catenin complex and its associated proteins. The TJ consists of three integral membrane proteins, namely, claudin, occludin, and junction adhesion molecules, and a number of cytoplasmic accessory proteins including ZO-1, ZO-2, ZO-3, cingulin, and others (Fig. 1C). Cytoplasmic proteins link membrane proteins to actin, which is the primary cytoskeleton protein for the maintenance of structural and functional integrity of the endothelium.

Claudins

Claudins-1 and -2 were identified as integral component of TJ strands in 1998 (Furuse et al., 1998). So far, at least 24 members

* Corresponding author. Neonatal Intensive Care Unit, 2nd Floor, Main Building, Westchester Medical Center, Valhalla, NY 10595. Fax: +1-914-594-4453.

E-mail address: pballabh@msn.com (P. Ballabh).

Available online on ScienceDirect (www.sciencedirect.com.)

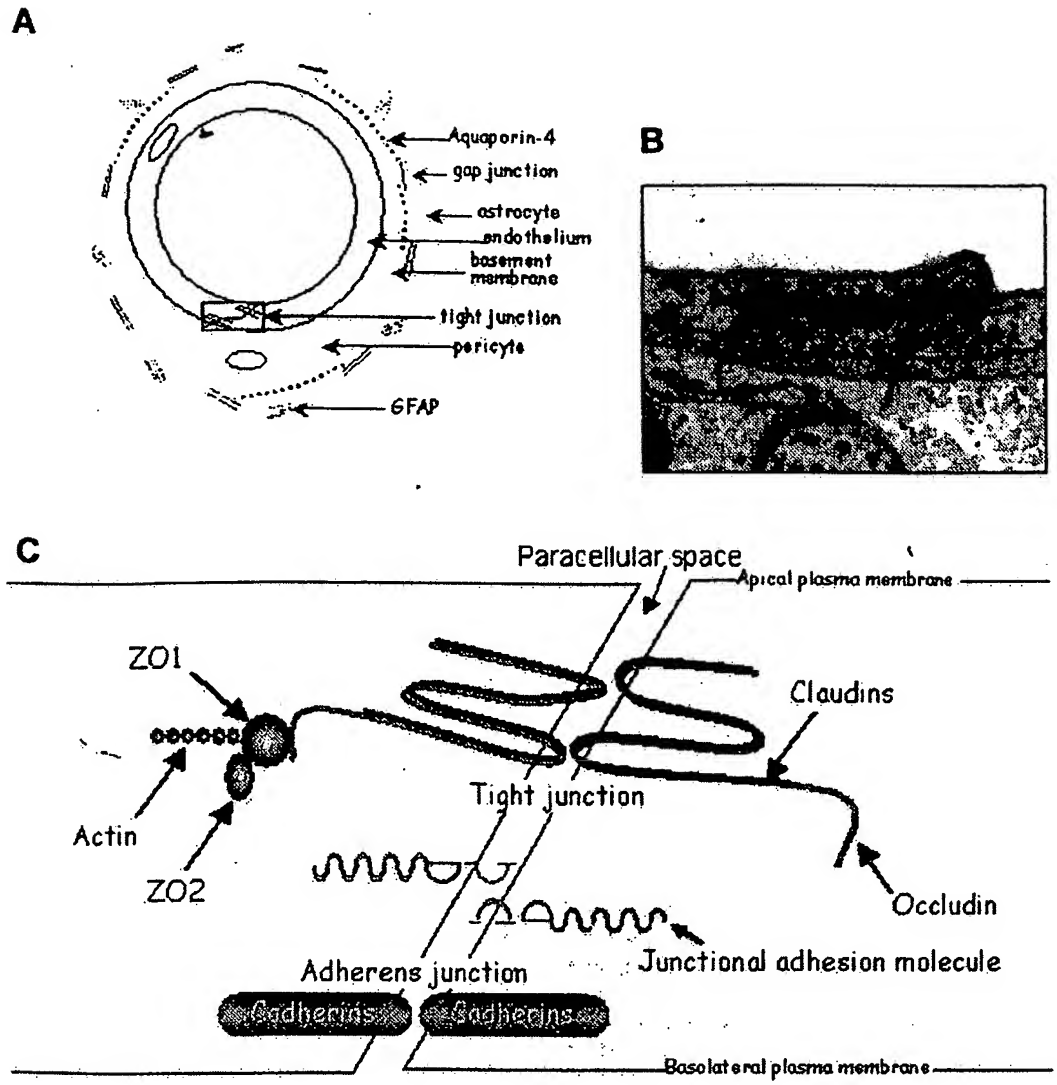

Fig. 1. Blood–brain barrier and the tight junction. (A) Schematic drawing of the blood–brain barrier in transverse section showing endothelium, basement membrane, pericytes, astrocytes, and tight junctions. The localization of gap junction, GFAP, and aquaporin-4 are shown. (B) Electron micrograph of mammalian blood–brain barrier showing endothelial tight junction. [Adapted from: The Blood–Brain Barrier Cellular and Molecular Biology. Pardridge, W.M. (Ed.). Raven Press]. (C) Schematic representation of protein interaction associated with tight junctions at the blood–brain barrier. Claudin, occludin, and junction adhesion molecule are the transmembrane proteins, and ZO-1, ZO-2, and ZO-3, cingulin, and others are the cytoplasmic proteins. Claudins are linked to actins through intermediary cytoplasmic proteins.

of claudin family have been identified in mouse and human, mainly through database searches (Morita et al., 1999a). They are 22 kDa phosphoprotein and have four transmembrane domains. Claudins are the major components of TJ and are localized exclusively at TJ strands as revealed by immunoreplica electron microscopy. Claudins bind homotypically to claudins on adjacent endothelial cells to form primary seal of the TJ (Furuse et al., 1999). Carboxy terminal of claudins binds to cytoplasmic proteins including ZO-1, ZO-2, and ZO-3 (Furuse et al., 1999). In brain, claudins-1 and -5, together with occludin, have been described to be present in endothelial TJs forming the BBB (Liebner et al., 2000a; Morita et al., 1999b). Fig. 2 depicts expression of claudin-5 in cerebral blood vessels of a term newborn. Claudin-11, also known as oligodendrocyte protein (OSP), is a major component of CNS myelin. Loss of claudin-1, but not claudin-5, from cerebral vessels was demonstrated under pathologic conditions such as tumor, stroke, inflammation (Liebner et al., 2000a,b; Lippoldt et al., 2000), as well as in vitro (Liebner et al., 2000b).

Occludin

Occludin was identified in 1993 as the first integral protein localized at the TJ by immunogold freeze fracture microscopy in chickens (Furuse et al., 1993) and then in mammals (Ando-Akatsuka et al., 1996). It is a 65-kDa phosphoprotein, significantly larger than claudin. Occludin shows no amino acid sequence similar to the claudins. Occludin has four transmembrane domains, a long COOH-terminal cytoplasmic domain, and a short NH_2-terminal cytoplasmic domain. The two extracellular loops of occludin and claudin originating from neighboring cells form the paracellular barrier of TJ. The cytoplasmic domain of occludin is directly associated with ZO proteins. The expression of occludin has also been documented in rodents (Hirase et al., 1997) and adult human brain (Papadopoulos et al., 2001) but not in normal human newborn and fetal brain. Occludin expression is much higher in brain endothelial cells compared to nonneural tissues. Occludin appears to be a regulatory protein that can alter paracellular permeability (Hirase et al., 1997).

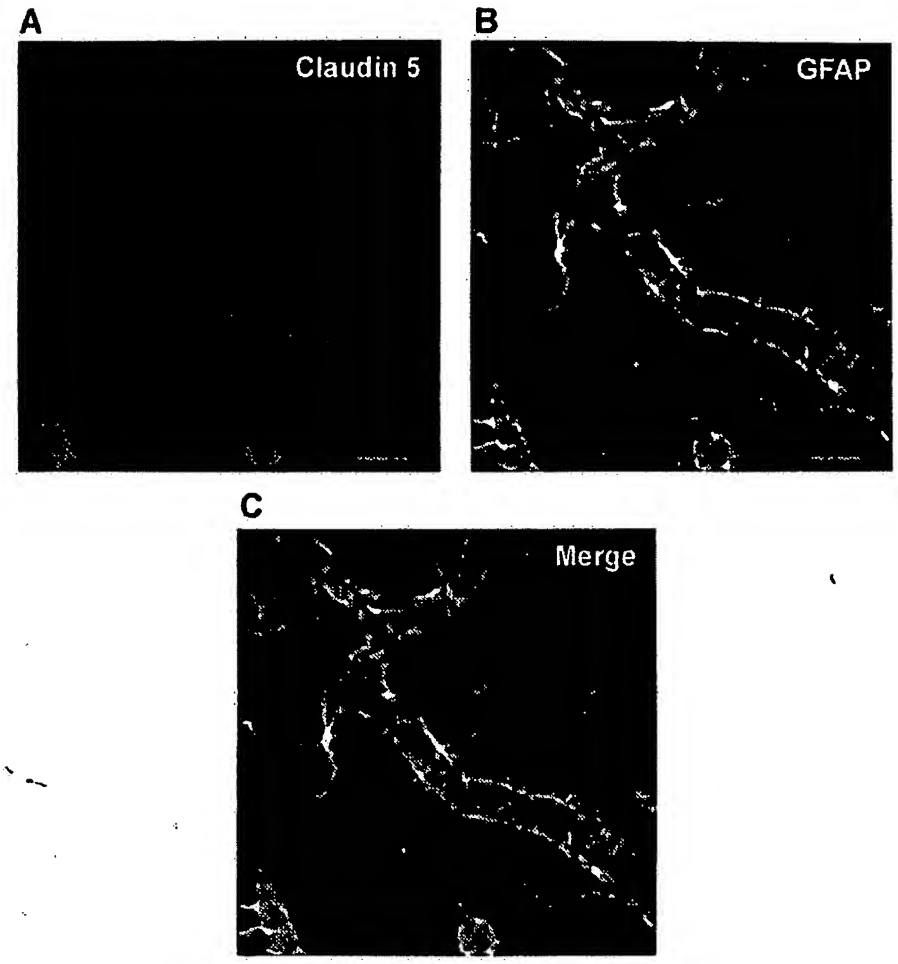

Fig. 2. Claudin-5 (red in A) and GFAP (white in B) immunolabeling of cerebral blood vessels of a term newborn. This infant with cardiomyopathy died in our neonatal intensive care unit on day 2 of life. Coronal section of frontal cortex was immunostained with claudin-5 and GFAP in our laboratory. Claudin-5 is strongly expressed in blood vessels. Astrocyte end-feet, visualized by GFAP-staining, closely cover the blood vessels. Colocalization by double-labeling of claudin-5 and GFAP (Fig. 3C). Scale bar = 20 μm.

Occludins and claudins assemble into heteropolymers and form intramembranous strands, which have been visualized in freeze-fracture replicas. These strands have been proposed to contain fluctuating channels allowing the selective diffusion of ions and hydrophilic molecules (Matter and Balda, 2003). Breakdown of the BBB in tissue surrounding brain tumors occurs with concomitant loss of a 55-kDa occludin expression (Papadopoulos et al., 2001). Together, claudins and occludins form the extracellular component of TJs and are both required for formation of the BBB (Sonoda et al., 1999).

Junctional adhesion molecules

The third type of TJ-associated membrane protein, junctional adhesion molecules (JAM; approximately 40 kDa), has recently been identified (Martin-Padura et al., 1998). They belong to the immunoglobulin superfamily. They have a single transmembrane domain and their extracellular portion has two immunoglobulin-like loops that are formed by disulfide bonds. Three JAM-related proteins, JAM-1, JAM-2, and JAM-3, have been investigated in rodent brain sections. It was observed that JAM-1 and JAM-3 are expressed in the brain blood vessels but not JAM-2 (Aurrand-Lions et al., 2001). The expression of JAM in human BBB is yet to be explored. It is involved in cell-to-cell adhesion and monocyte transmigration through BBB (Aurrand-Lions et al., 2001; Bazzoni et al., 2000). However, our knowledge on function of JAM is incomplete, and more investigations are required to unfold its function in the BBB.

Cytoplasmic accessory proteins

Cytoplasmic proteins involved in TJ formation include zonula occludens proteins (ZO-1, ZO-2, and ZO-3), cingulin, 7H6, and several others. ZO-1 (220 kDa), ZO-2 (160 kDa), and ZO-3 (130 kDa) have sequence similarity with each other and belong to the family of proteins known as membrane-associated guanylate kinase-like protein (MAGUKs). They contain three PDZ domains (PDZ1, PDZ2, and PDZ3), one SH3 domain, and one guanyl kinaselike (GUK) domain. These domains function as protein binding molecules and thus play a role in organizing proteins at the plasma membrane. The PDZ1 domain of ZO-1, ZO-2, and ZO-3 has been reported to bind directly to COOH-terminal of claudins (Itoh et al., 1999). Occludin interacts with the GUK domain on ZO-1 (Mitic et al., 2000). JAM was also recently shown to bind directly to ZO-1 and other PDZ-containing proteins (Ebnet et al., 2000). Importantly, actin, the primary cytoskeleton protein, binds

to COOH-terminal of ZO-1 and ZO-2, and this complex cross-links transmembrane elements and thus provides structural support to the endothelial cells (Haskins et al., 1998).

Adherens junctions

These junctions consist the membrane protein cadherin that joins the actin cytoskeleton via intermediary proteins, namely, catenins, to form adhesive contacts between cells. AJs assemble via homophilic interactions between the extracellular domains of calcium-dependent cadherin on the surface of adjacent cells. The cytoplasmic domains of cadherins bind to the submembranal plaque proteins β- or γ-catenin, which are linked to the actin cytoskeleton via α-catenin. AJ components including cadherin, alpha-actinin, and vinculin (α-catenin analog) have been demonstrated in intact microvessels of the BBB in rat. TJ and AJ components are known to interact, particularly ZO-1 and catenins, and influence TJ assembly (Matter and Balda, 2003).

Brain structures lacking a BBB

The BBB is present in all brain regions, except for the cirumventricular organs including area postrema, median eminence, neurohypophysis, pineal gland, subfornical organ, and lamina terminalis. Blood vessels in these areas of the brain have fenestrations that permit diffusion of blood-borne molecules across the vessel wall. These unprotected areas of the brain regulate autonomic nervous system and endocrine glands of the body.

Notably, choroid plexus epithelial cells possess both TJ and AJ. Claudins-1, -2, -11, occludin, and ZO-1 are present in epithelial TJs of choroid plexus, whereas claudins-1, -5, -11, occludin, and ZO-1 form the TJ of the BBB (Wolburg, 2001). Thus, the difference in molecular composition of TJ between choroid plexus (blood–CSF barrier) and the BBB is with respect to claudins-2 and -5.

Role of astrocytes in the formation of the blood–brain barrier

A number of grafting and cell culture studies have suggested that the ability of CNS endothelial cells to form a BBB is not intrinsic to these cells, but CNS environment induces the barrier property into the blood vessels. Avascular tissue was transplanted from 3-day-old quail brain into the coelomic cavity of chick embryos; and it was observed that the chick endothelial cells vascularizing the quail brain grafts formed a competent BBB (Stewart and Wiley, 1981). In contrast, when avascular embryonic quail coelomic grafts were transplanted into embryonic chick brain, the chick endothelial cells that invaded the mesenchymal tissue grafts formed leaky capillaries and venules. Cultured astrocytes implanted into areas with normal leaky vessels have induced tightening of endothelium (Janzer and Raff, 1987). Blood vessels from solid CNS and peripheral tissues grafted to brain sustained and maintained their morphologic and permeability characteristics (Broadwell et al., 1990). However, peripheral neural and nonneural tissues not possessing BBB properties did not acquire such characteristics on transplantation to the CNS. Direct contact between endothelial cells and astrocytes was deemed necessary to generate an optimal BBB (Rubin et al., 1991). High trans-endothelial resistance can be reintroduced in human or bovine endothelial cell monolayers that are cultured in astrocyte-conditioned media, suggesting that an astrocyte-derived soluble factor may be responsible for induction of BBB characteristics in endothelial cells (Neuhaus et al., 1991).

However, subsequent investigators criticized the culture and transplantation experiments on methodologic grounds and also disagreed with the view that mature astrocytes play a significant role in the initial expression of the BBB (Holash et al., 1993). It was reported that intact neuronal or glial cells were not necessary for the maintenance of the BBB properties (Krum et al., 1997). They induced neuronal and glial injury by injecting immunotoxin OX7-SAP and the ribosome-inactivating protein saporin into the adult rat striatum. The microvasculature was noted to be intact, allowing a qualitative immunohistochemical analysis of several BBB markers at time points ranging from 3 to 28 days postinjection (Krum et al., 1997). These contradictions may be resolved by additional experiments using host animals of different ages, standard grafting methodology, and systematic analysis of grafts after vascularization. The role of astrocytes in the formation of the BBB is of great interest to scientists and may have therapeutic implications.

Astrocyte–endothelial interaction and signaling pathways

Intercellular signaling: inductive influence of astrocytes on endothelial cells

Numerous efforts have been directed on defining agents that mediate the induction and maintenance of the BBB. We are reviewing only selected studies here. It has demonstrated in astrocyte–endothelial coculture experiments that TGF-β produced by astrocytes is responsible for the down-regulation of tissue plasminogen activator (tPA) and anticoagulant thrombomodulin (TM) expression in cerebral endothelial cells (Tran et al., 1999). It is plausible that TGF-β secreted by astrocytes may have a role in protecting the brain against intracerebral bleeding in children and adults and against intraventricular hemorrhage in premature infants by decreasing the levels of these anticoagulant factors. In another experiment involving TGF-β, the influence of astrocytes and TGF β on differentiation of endothelium and PCs was studied in an in vitro culture mode (Ramsauer et al., 2002). This study suggested that a close association of astrocytes and endothelium was required for the induction and organization of endothelial cells into capillary-like structure (CLS). In contrast to the influence of astrocytes, TGF-β1 led to the formation of a defective CLS, which lacked PCs, recruited fewer endothelial cells, and was shorter in length. Thus, astrocytes have a significant influence on the morphogenesis and the organization of the vessel wall, and the effect of TGF-β1 is different from the astrocytic effect. Glial cell-derived neurotropic growth factor (GDNF), a member of TGF-β family, seems to be involved in postnatal maturation of the BBB (Utsumi et al., 2000). Cerebral endothelial cells are a major source of adrenomedullin, which regulates the cerebral circulation and BBB function (Kis et al., 2003). Other chemical agents that have been shown to differentiate BBB are interleukin-6 (IL-6), hydrocortisone (Hoheisel et al., 1998), and basic fibroblast growth factor (bFGF) (Sobue et al., 1999).

In summary, due to technical limitations associated with live tissues, only culture methods have been utilized so far to describe agents that are involved in BBB maturation. A number of factors

have been shown to induce formation of CLS in culture studies, but it is not known whether similar mechanisms apply in vivo.

Intercellular signaling: inductive influence of endothelial cells on neuronal precursors and astrocytes

Intriguingly, there are also reports about the inductive influence of endothelial cells on astrocytes and on neuronal precursors. It appears that astrocytes and endothelial cells cross talk with each other and regulate each other's function. Endothelial cells seem to be the primary source of leukemia-inhibiting factor (LIF), which helps to induce astrocyte differentiation in vivo (Mi et al., 2001). Changes in the morphology of neonatal mouse cortical astrocytes following their coculture with mouse brain capillary endothelial cells (bEnd 3) have been observed. bEnd 3 cells altered the morphology of astrocytes by transforming them from confluent monolayers into a network of elongated multicellular columns (Yoder, 2002). In addition, astrocytes in cocultures showed increased Ca^{2+} responsiveness to bradykinin and glutamate. Furthermore, the glial–endothelial partnership has been shown to up-regulate aquaporin-4 expression in astrocyte end-feet (Rash et al., 1998) and increase synthesis of antioxidant enzymes in both astrocytes and endothelium (Schroeter et al., 1999).

It has been observed that dividing neuronal cells are found in dense clusters associated with the vasculature, and roughly 37% of all dividing cells are immunoreactive for endothelial markers. This suggests that neurogenesis is intimately associated with active vascular recruitment and subsequent remodeling (Palmer et al., 2000). Recent observations suggest that there is a causal interaction between testosterone-induced angiogenesis and neurogenesis in the adult forebrain (Louissaint et al., 2002). This study has demonstrated that testosterone up-regulates vascular endothelial growth factor (VEGF) and its endothelial receptor in the higher vocal center of adult canaries, which leads to angiogenesis. Angiogenic stimulation induces synthesis of brain-derived growth factor, which stimulates neurogenesis. Hence, these studies indicate that there is an instructive role of endothelial cells on neurogenesis, gliogenesis, and CNS development.

Calcium signaling between astrocyte and endothelium

Calcium waves that propagate in an astrocyte network have been demonstrated in primary cell culture experiments, hippocampal slices, and in isolated retina. However, only few studies have addressed the issue of dynamic signaling between endothelium and astrocyte. This astrocyte–endothelium calcium signaling mechanism has been investigated in two in vitro coculture models: (1) rat cortical astrocytes with ECV304 cells and (2) rat cortical astrocyte with primary rat brain capillary endothelial cells (Braet et al., 2001; Paemeleire, 2002). They have demonstrated that intercellular calcium waves mediate bidirectional astrocyte–endothelial calcium signaling in both culture models. Their experiments suggest that two signaling mechanisms are involved. First, astrocytes and endothelial cells can exchange calcium signals by an intracellular IP3- and gap junction-dependent pathway. Second, pathway involves extracellular diffusion of purinergic messenger. However, in situ, the basement membrane is interposed in between the endothelium and astrocytes. Furthermore, PCs are embedded in the basement membrane and thereby not in direct contact with either endothelium or astrocyte. These findings therefore need confirmation in brain slices. Interestingly, a recent elegant study performed on rat cortical slices has shown that dilatation of arterioles triggered by neuronal activity is dependent on glutamate-mediated $[Ca^{2+}]$ oscillations in astrocytes (Zonta et al., 2003). Inhibition of calcium responses resulted in impairment of activity-dependent vasodilatation. In addition, direct astrocyte stimulation triggered vasodilatation and astrocyte-mediated dilatation was mediated by cyclooxygenase (COX) product. In conclusion, neuron–astrocyte signaling is central to the dynamic control of brain microcirculation. Since up-regulation of COX expression leads to increase in prostaglandin and since prostaglandin may influence BBB permeability, we speculate that neuron–astrocyte signaling may be a mechanism in regulation of BBB permeability.

Signaling pathways associated with tight junctions

There are two principal types of signal transduction processes associated with TJ: (1) signals transduced from the cell interior towards TJ to guide their assembly and regulate paracellular permeability and (2) signals transmitted from TJ to the cell interior to modulate gene expression, cell proliferation, and differentiation (Matter and Balda, 2003). The mechanism of signal transduction is not completely understood. Multiple signaling pathways and proteins have been implicated in the regulation of TJ assembly including calcium, protein kinase A, protein kinase C, G protein, calmodulin, cAMP, and phospholipase C (Balda et al., 1991; Izumi et al., 1998). Calcium acts both intracellularly and extracellularly to regulate TJ activity, and several of the molecules modulating BBB permeability seem to act by alteration of intracellular calcium. Intracellular calcium plays a role in increasing transendothelial resistance as well as in ZO-1 migration from intracellular sites to plasma membrane and thus restoring the TJ assembly (Stevenson and Begg, 1994). Raising extracellular calcium triggers a series of molecular events, which increases resistance across the membrane and decreases the permeability (Stevenson and Begg, 1994). These events are mediated through heterotrimeric G protein and protein kinase C (PKC) signaling pathways. Furthermore, tyrosine kinase activity is necessary for TJ reassembly during ATP repletion, and the tyrosine phosphorylation of occludin, ZO-2, and p130/ZO-3 has roles to play in TJ reformation (following TJ disruption) (Tsukamoto and Nigam, 1999). Based on the studies done so far, it appears that ZO and occludin molecules are primary regulatory proteins of TJ that modulates BBB permeability. However, the role of claudins in regulation of TJ has yet to be explored.

Pericytes and the BBB

Pericytes (PCs) are cells of microvessels including capillaries, venules, and arterioles that wrap around the endothelial cells. They are thought to provide structural support and vasodynamic capacity to the microvasculature. Importantly, PC loss and microaneurysm formation in PDGF-B-deficient mice have been observed (Lindahl et al., 1997). This suggests that PCs play a key role in the structural stability of the vessel wall. Metabolic injury to PCs in diabetes mellitus is associated with microaneurysm formation in the retina (Kern and Engerman, 1996), and PC

degeneration is seen in hereditary cerebral hemorrhage with amyloidosis (Verbeek et al., 1997). This evidence supports the view that PCs play an essential role in the structural integrity of microvessels. PCs express a number of receptors for chemical mediators such as catecholamines (Elfont et al., 1989), angiotensin II (Healy and Wilk, 1993), vasoactive intestinal peptides (Benagiano et al., 1996), endothelin-1 (Dehouck et al., 1997), and vasopressin (van Zwieten et al., 1988), indicating that PCs may also be involved in cerebral autoregulation.

The role of PCs in angiogenesis and differentiation of the BBB has been studied in an in vitro culture model (Ramsauer et al., 2002). This study suggests that PCs stabilize CLS formed by endothelial cells in culture with astrocytes by preventing apoptosis of endothelium. The fact that endothelial cells associated with PCs are more resistant to apoptosis than isolated endothelial cells further supports the role of PCs in structural integrity and genesis of the BBB. A number of experimental observations support the concept that PCs regulate angiogenesis and may play a role in BBB differentiation (Balabanov and Dore-Duffy, 1998; Hirschi and D'Amore, 1997). An ultrastructural study in embryonic mouse brain has shown that endothelial cells together with PCs start invading the neural tissues around E10 (Bauer et al., 1993). Lastly, PCs exhibit phagocytic activity and may be involved in neuroimmune functions (Balabanov et al., 1996).

Fetal brain anatomy, geriminal matrix, and development of BBB

Fetal brain anatomy and germinal matrix

The wall of the fetal cerebral hemisphere consists the ventricular zone, subventricular zone, intermediate zone, cortical plate, and marginal zone, as described by the Boulder Committee (1970). A localized thickening medial to the basal ganglia in the subventricular zone, which bulges into the lateral ventricle, is referred as the germinal matrix. This periventricular germinal matrix (GM) in human fetuses, located in the region of the thalamostriate groove beneath the ependyma, is densely packed with neuroblasts and glioblasts and is richly supplied with capillaries. It undergoes progressive decrease in size from a width of 2.5 mm at 23–24 weeks to 1.4 mm at 32 weeks and to complete involution by approximately 36 weeks (Hambleton and Wigglesworth, 1976; Szymonowicz et al., 1984).

Development of the BBB in the GM has been studied in baboon and beagle pup models at the developmental stage, during which premature infants develop GM hemorrhage. Electron microscopic examination of germinal matrix capillaries in baboons at 100 days (54%) of gestational age has revealed continuous endothelium, prominent tight junctions, uninterrupted basement membrane, and clearly identifiable astrocyte end-feet (Bass et al., 1992). GM capillaries in the beagle model showed a significant increase in basement membrane area, tight junction length, and coverage of capillary perimeter by glial end-feet (from 79% to 95%) on day 10 compared to day 1 (Ment et al., 1995). In contrast, microvessels of the white matter showed no changes in these parameters during this time period, which suggests that blood vessels in the white matter mature earlier than those of vasculature in the GM. Subsequent investigators have studied cortical plate vasculature in human fetus telencephalon of gestational age 12 and 18 weeks, and their findings are consistent with the observations made in the beagle pup model. They observed that perivascular coverage by astrocytes and radial glia was more extensive for 18-week fetuses compared to 12-week fetuses (Bertossi et al., 1999). Thus, it seems that coverage of blood vessels by astroctye end-feet, tight junction length, and basal lamina area in the GM increases as a function of conceptional and postnatal age and that their maturation in GM possibly lags behind the white matter.

Development of the BBB

The temporal development of the BBB varies with species and this has been best studied in rodents. The first blood vessels invade the outer surface of the developing neural tube at E10 in the mouse and E11 in the rat (Bauer et al., 1993; Stewart and Hayakawa, 1994). Neurogenesis in the developing mouse neocortex occurs between embryonic days 11 and 17 and up to E21 in rats (Jacobson, 1991). Gliogenesis starts from E17 in rodents and continues in subventricular zone even in the adult period (Jacobson, 1991). The invasion of blood vessels into the developing nervous tissue is therefore associated with neurogenesis rather than with gliogenesis (Rakic, 1971). The formation of the BBB starts shortly after intraneural neovascularization, and the neural microenvironment seems to play a key role in inducing BBB function in capillary endothelial cells. Fenestrations in the intraparenchymal cerebral vessels are frequent at E11, decline rapidly, and are not seen after E17 (Stewart and Hayakawa, 1994). Thus, the BBB seems to develop between E11 and E17. This also suggests that development of TJ may precede the development of astrocyte end-feet. Occludin expression has been reported to be low in rat brain endothelial cells at postnatal day 8 but clearly detectable on postnatal day 70 (Hirase et al., 1997). Development of other TJ molecules has not been investigated. At present, there is no systemic study of the development of TJ, astrocyte end-feet, and PCs in the developing human brain.

GFAP, vimentin, and aquaporin 4

In rodents, astrocytes, as assessed by glial fibrillary acidic protein (GFAP) immunoreactivity, are first detected at E16 (Liu et al., 2002). In humans, vimentin has been demonstrated in the ventricular zone at 7 weeks and older, and GFAP-positive cells start to appear at 9 weeks in the spinal cord and at 15 weeks in the cerebrum (Sasaki et al., 1988). Ependymal tanycytes are GFAP-positive with their radial processes extending into subventricular zone (SVZ) at 19 weeks (Gould and Howard, 1987). However, GFAP-positive astrocyte differentiation in GM occurred progressively only after 28 weeks, which led to dense network of fibers by 31 weeks. Hence, GFAP immunostaining is not an effective method to evaluate astrocytes in GM before 28 weeks.

Aquaporin 4 (AQP4) immunostaining is an excellent tool to evaluate astrocyte end-feet and the BBB (Fig. 3). Immunogold electron microscopy has demonstrated that AQP4 is restricted to glial membranes and ependymal cells. AQP4 is particularly strongly expressed in glial membranes that are in direct contact with capillaries (Nielsen et al., 1997). We have also shown that AQP4 expression is highly polarized and most immunoreactivity is present in astrocyte end-feet. AQP4 expression had been demonstrated on embryonic day 14 in chick embryos (Nico et al., 2001).

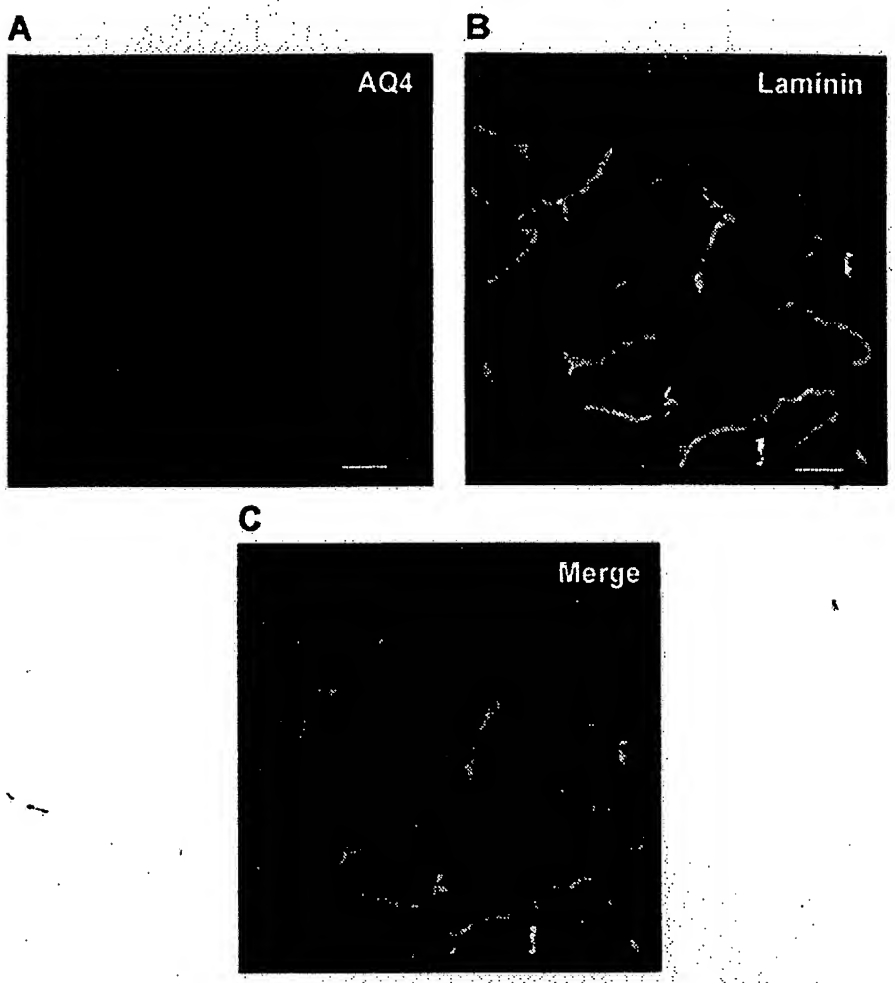

Fig. 3. Aquaporin-4 (A) and laminin (B) expression in cerebral blood vessel of a term human newborn. Coronal section of cerebral cortex (frontal lobe) immunostained in our laboratory for aquaporin-4 and laminin. (A) Aquaporin-4-staining of astrocyte end-feet seems to be continuous. (B) Laminin stains the basement membrane of the blood vessels. (C) Colocalization of aquaporin-4 and laminin. Laminin expression is on luminal side, and aquaporin-4 labels the astrocyte end-feet covering the blood vessels. Scale bar = 50 μm.

We have seen AQP-4 staining of astrocyte end-feet in premature infants as early as 23 weeks of gestation.

Clinical implications

Opening of the BBB in pathophysiology

As discussed earlier, under physiologic conditions, the BBB is relatively impermeable. In pathologic conditions, a number of chemical mediators are released that increase BBB permeability. Several of these mediators of BBB opening have been studied in both in vivo and in vitro experiments and include glutamate, aspartate, taurine, ATP, endothelin-1, ATP, NO, MIP-2, tumor necrosis factor-α (TNF-α), MIP2, and IL-β, which are produced by astrocytes (Abbott, 2000, 2002; Chen et al., 2000; Kustova et al., 1999; Magistretti et al., 1999). Other humoral agents reported to increase BBB permeability are bradykinin, 5HT, histamine, thrombin, UTP, UMP, substance P, quinolinic acid, platelet-activating factor, and free radicals (Abbott, 2002; Annunziata et al., 1998; Pan et al., 2001; St'astny et al., 2000). The source of these BBB-modulating mediators is of interest. Some of these agents are released by endothelium and endothelium itself responds to the released agents. For example, endothelin (ET-1) acts on ETA receptors. In physiologic conditions, nerve terminals of neurons running close to blood vessels release mediators, such as histamine, substance P, and glutamate, which influence BBB permeability.

Germinal matrix hemorrhage and the BBB

GM hemorrhage commonly affects premature infants and has an incidence of 1.45% of live births or approximately 5800 cases per year in the United States (Anstrom et al., 2002). Intraventricular hemorrhage (IVH) occurs when hemorrhage in the GM ruptures through the ependyma into the lateral ventricles (Fig. 4).

The etiopathogenesis of GM hemorrhage is multifactorial, and a combination of vascular and intravascular factors is considered to be responsible. Perinatal and postnatal events, such as vaginal delivery (Ment et al., 1992), chorioamnionitis (DiSalvo, 1998), hypoxia (Antoniuk and da Silva, 2000), hypercarbia (Kenny et al., 1978), pneumothorax, patent ductus arteriosus (Volpe, 1989a), seizures, and respiratory distress syndrome (Volpe, 1989b), lead to significant fluctuation in cerebral blood flow or blood pressure inside the blood vessels (intravascular) and may participate in rupture of the GM microvasculature. Vascular risk factors relate to fragility of the immature thin-walled GM vasculature. Since TJ, astrocyte end-feet, PCs, and BM potentially stabilize the cerebral blood vessels, we speculate that the reason for fragility of the GM vasculature is incomplete coverage of GM capillaries by astrocyte end-feet, poorly developed TJ joining cerebral endothelial cells and

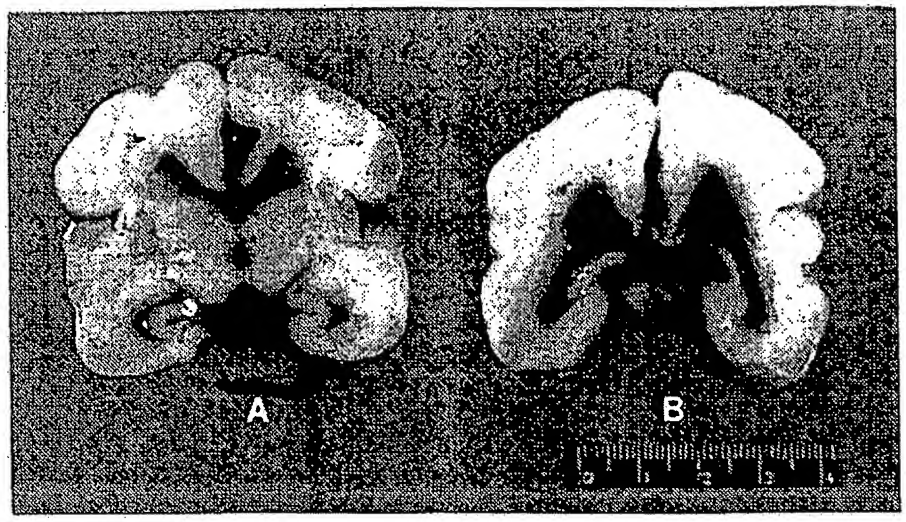

Fig. 4. Intraventricular hemorrhage. Coronal sections of the brain of a premature newborn of 26 weeks of gestational age who died in our neonatal intensive care unit. Lateral ventricles are filled with blood and are mildly dilated (A and B).

immaturity of BM, and/or PCs. Interestingly, a recent investigation has suggested that GM hemorrhage is primarily venous in origin (Ghazi-Birry et al., 1997). However, this report based on postmortem study of brain from four premature infants with IVH needs confirmation by studying larger group of subjects.

The GM hemorrhage may lead to hydrocephalus and other long-term sequelae. Hemorrhage in GM presumably destroys neuron and glial cell precursors that are destined to populate layers II to VI of cerebral cortex. Infants with a history of IVH have a higher incidence of seizures, neurodevelopmental delay, cerebral palsy, and death. Understanding the reason for vulnerability of GM microvessels to hemorrhage will definitely help in developing therapeutic strategies.

Hypoxic–ischemic insult of the BBB

The effect of hypoxia–ischemia on the BBB has been extensively investigated. Hypoxia–ischemia sets in motion a series of events, which leads to disruption of TJ and increased BBB permeability. These events seem to be mediated by cytokines, VEGF, and NO.

Elevated levels of proinflammatory cytokines, IL-1β, and TNF-α have been demonstrated in animal brains after focal and global ischemia (Feuerstein et al., 1994) and in cerebrospinal fluid of stroke patients (Tarkowski et al., 1997). In an in vitro model of the BBB consisting human cerebrovascular endothelial cells and astrocytes, it has been observed that simulated ischemia stimulates IL-8 and MCP-1 secretion from endothelial cells and astrocytes (Zhang et al., 1999). In a further study, the same group of investigators provided evidence that human astrocytes subjected to in vitro hypoxia release inflammatory mediators that are capable of up-regulating genes of IL-8, ICAM-1, E-selectin, IL-1β, TNF-α, and MCP-1 in human cerebrovascular endothelial cells (Zhang et al., 2000). Increased cytokines and subsequent up-regulation of endothelial and neutrophil adhesion molecules lead to transmigration of leukocytes across the endothelium and the BBB. Blood vessels associated with neutrophil recruitment display increase in phosphotyrosine staining, loss of TJ molecules including occludin and zonula occludens, and apparent redistribution of adherens junctions protein vinculin (Bolton et al., 1998). Thus, leukocyte recruitment seems to trigger signal transduction cascades that lead to disorganization of TJ and BBB breakdown.

Hypoxia induces permeability in porcine brain microvascular endothelial cells via VEGF and NO (Fischer et al., 1999). VEGF enhances transcytosis and gap formation between endothelial cells and induces fenestration in unfenestrated human and porcine endothelial monolayers in vitro (Hippenstiel et al., 1998). Subsequent studies have shown that hypoxia-increased release of VEGF led to decreased expression, dislocalization, and increased phosphorylation of ZO-1 (Fischer et al., 2002). In another study, hypoxia induced a 2.6-fold increase in [(14) C] sucrose, a marker of paracellular permeability, increased expression of actin, and changes in occludin, ZO-1, and ZO-2 protein localization in primary bovine brain microvessel endothelial cells (Mark and Davies, 2002). Interestingly, astrocytes protect the BBB against hypoxia-induced disruption of tight junction protein, zonula occludens, and paracellular permeability changes by decreasing VEGF expression in porcine brain microvascular endothelial cells (Fischer et al., 2000). Other investigators have made similar observations (Kondo et al., 1996).

In conclusion, these investigations suggest that increased BBB permeability induced by hypoxia–ischemia involves a cascade of events in which cytokines, VEGF, and NO are the main players and astrocytes appear to play a protective role. Most of these conclusions based on in vitro experiments need further confirmation by performing experiments in vivo and in intact tissues.

Break down of BBB in septic encephalopathy

The pathophysiology of septic encephalopathy including decreased cerebral blood flow and oxygen extraction by the brain, cerebral edema, and breakdown of the BBB may be related to several reasons—the effect of inflammatory mediators on the cerebrovascular endothelium, abnormal neurotransmitter composition of the reticular activating system, impaired astrocyte function, and neuronal degeneration (Papadopoulos et al., 2000). A variety of evidence demonstrates that the BBB is compromised in septic encephalopathy. Colloidal iron oxide (Clawson et al., 1966), ^{14}C amino acid (Jeppsson et al., 1981), and ^{125}I-albumin (Deng et al., 1995) have been shown to enter brain parenchyma from the circulation in rodents. In addition, elevated CSF protein has been observed. Cellular pathology underlying this blood–brain disruption has been reported by several investigators including (1) increased pinocytosis in cerebral microvessel endothelium and

swelling of astrocytes in rabbit with endotoxemia (Clawson et al., 1966); (2) perivascular edema, swollen astrocyte end-feet with ruptured membranes, and detachment from microvessel walls in septic pigs (Norenberg, 1994); and (3) dark shrunken neurons in pigs 8 h after inducing peritonitis (Papadopoulos et al., 1999). The adrenergic system has been implicated in the inflammatory response to sepsis (Tighe et al., 1996). β_2 adrenoreceptor stimulation appears to be suppressed, and α_1 adrenoreceptor stimulation seems to induce an inflammatory response and hence influence BBB permeability.

Disruption of BBB in brain tumor

The BBB is poorly developed in brain tumor leading to increased vascular permeability (Groothuis et al., 1991). Investigations have shown that there is opening of interendothelial TJ in human gliomas (Long, 1970) and metastatic adenocarcinoma (Long, 1979). The expression of the TJ protein claudin-1 is lost in the microvessels of glioblastoma multiforme, whereas claudin-5 and occludin are significantly down-regulated and ZO-1 expression is unaffected (Liebner et al., 2000a). A loss of 55 kDa occludin expression in microvessels, observed in astrocytoma and metastatic adenocarcinoma, may also contribute to endothelial TJ opening (Papadopoulos et al., 2001).

The explanation for loss of TJ molecules in brain tumor microvessels is not clear. However, VEGF, cytokines (de Vries et al., 1996), and Scatter factor or hepatocyte growth factor (Lamszus et al., 1999) secreted by astrocytoma and other brain tumors may be involved in down-regulating TJ molecules leading to TJ opening, increased vascular permeability, and cerebral edema. It is also possible that poorly differentiated neoplastic astrocytes do not release factors necessary for BBB function.

Since cerebral edema is an important consequence of brain tumor, water channel molecule, AQP4, has been examined in brain tumor by several investigators. AQP4 is massively up-regulated in astrocytoma and metastatic adenocarcinoma and this correlates with blood–brain barrier opening assessed by contrast-enhanced computed tomograms (Saadoun et al., 2002). Mice deficient in AQP4 have a much better survival than wild-type mice in a model of brain edema caused by acute water intoxication. Up-regulation of AQP4 has also been noted in rat models of ischemia (Taniguchi et al., 2000) and brain injury (Vizuete et al., 1999). Thus, it seems that breakdown of the BBB associated with brain tumors and other forms of brain injury increases the expression of AQP4. However, the exact mechanism of AQP4 up-regulation in different clinical situations is not known.

Inflamed BBB: HIV-induced dementia, multiple sclerosis, and Alzheimer disease

In normal brain, highly specialized cerebral endothelial cells limit entry of leukocytes and circulating substances into the brain. Neurologic conditions including HIV-associated dementia, multiple sclerosis, and Alzheimer disease alter the integrity of the BBB with consequent migration of leukocytes into the brain (Lou et al., 1997; Minagar et al., 2002). Leukocyte migration into brain has been shown to trigger signal transduction cascades leading to loss of TJ molecules including occludin and zonula occludens and BBB breakdown (Bolton et al., 1998).

Astrocytes and microglia play a significant role in host defense as well as in the pathogenesis of infectious and autoimmune diseases of CNS. They ordinarily protect the CNS but in pathologic circumstances can amplify inflammation and mediate cellular damage. Interaction of astrocyte, microglia, and immune system leads to an altered production of neurotoxins and neurotropins by these cells, which have roles to play in the pathogenesis of HIV-induced dementia, multiple sclerosis, and Alzheimer disease (Minagar et al., 2002). HIV encephalitis is associated with immune activation of astrocytes and macrophages. HIV-infected macrophages or microglia and astrocytes release cytokines, chemokines, reactive oxygen species, and a number of neurotoxins, which impair cellular functioning, modify transmitter action, and cause leukoencephalopathy and neuronal loss (Sharer, 1992). The neurotoxins include TNF-α, arachidonic acid, nitric oxide, platelet-activating factor, and quinolinic acid. TNF-α is released by HIV-infected macrophages, which particularly affect oligodendrocytes (Johnson, 1988). Nitric oxide is synthesized by macrophages, endothelial cells, and neurons, which react with superoxide anion to produce peroxynitrite (Boven, 1999). In addition, nitric oxide is associated with NMDA-type glutamate-induced neurotoxicity. Quinolinic acid also plays a major role in pathogenesis of neuronal damage in HIV-induced dementia.

In Alzheimer disease, microglia and astrocyte are activated by β-amyloid protein and related oligopeptides, leading to a cascade of events producing toxic molecules, neuronal damage, and synaptic dysfunction (Giulian et al., 1995). Reactive macrophages or microglia closely associated with neuritic and β-amyloid plaque, and interaction of macrophages and astrocyte possibly leads to release of interleukin-1 β (IL-1 β), TNF-α, transforming growth factor-β, neurotropic factors such as NGF and bNGF, and reactive oxygen species (Klegeris, 1997a,b). In addition, it has been shown that β-amyloid stimulates NF-κB that induces transcription of TNF-α, IL-1, IL-6, monocyte chemoattractant protein-1, and nitric oxide synthetase (Akama, 1998). The details of the signal transduction pathway that mediates neurotoxicity in Alzheimer disease are not known.

Most investigators believe that multiple sclerosis is an autoimmune disease in which reactive T cells recognize and destroy myelin sheath and the underlying axons (Wekerle, 2003). An antigen-specific T cell receptor called Hy.2E11 has been isolated from a T cell line from a patient with multiple sclerosis (Lang, 2002). This receptor recognizes two peptides, one derived from myelin basic protein, which is bound to HLA-DR2b, and other derived from the Epstein–Barr virus, which is bound to HLA-DR2a. The reactive T cell interacts with the antigen presented by macrophages- or microglia-expressing HLA-DR2a and HLA-DR2b. Activated macrophages synthesize and secrete nitric oxide and cytokines including interferon-γ, TNF-α, and IL-3, which damage oligodendrocytes causing interference with myelination and myelin gene expression (Chao et al., 1995; Merrill et al., 1993). Disruption of the BBB is one of the initial key steps in multiple sclerosis, which follows massive infiltration of T cells and the formation of demyelinative foci.

In conclusion, the pathogenesis of HIV-associated dementia, multiple sclerosis, and Alzheimer disease involves activation of inflammatory mechanisms, production of toxins and neurotropins, and the breakdown of the BBB.

Future directions

Rapid progress in the BBB research has led to a better understanding of BBB morphology and physiology. However, several key questions related to normal human development of the BBB are unanswered. Data on expression of claudins-1, -2, -5, and -11 in brain endothelial cells in human fetuses, preterm, and

term infants are lacking. Morphology of the gliovascular interface of germinal matrix compared to other areas of human brain cortex has not been adequately studied. This may be critical to understanding why the blood vessels of GM are fragile and prone to bleeding in premature infants. In addition, a number of puzzles with respect to functional property of the BBB are yet to be resolved: How do TJ molecules assemble? How are they regulated in different physiologic conditions? How do they interact with several mediators, neurotransmitters, and medications? How do they alter in disease conditions? Over the coming years, emerging information on the mechanism of BBB disruption may help in formulating strategies to protect BBB and to prevent and treat BBB-related pathologies.

References

The Boulder Committee, 1970. Embryonic vertebrate central nervous system: revised terminology. Anat. Rec. 166, 257–261.

Abbott, N.J., 2000. Inflammatory mediators and modulation of blood–brain barrier permeability. Cell. Mol. Neurobiol. 20, 131–147.

Abbott, N.J., 2002. Astrocyte–endothelial interactions and blood–brain barrier permeability. J. Anat. 200, 629–638.

Akama, K.T., Albanese, C., Pestell, R.G., Van Eldik, L.J., 1998. Amyloid beta-peptide stimulates nitric oxide production in astrocytes through an NFkappaB-dependent mechanism. Proc. Natl. Acad. Sci. U.S.A. 95, 5795–5800.

Allt, G., Lawrenson, J.G., 2001. Pericytes: cell biology and pathology. Cells Tissues Organs 169, 1–11.

Ando-Akatsuka, Y., Saitou, M., Hirase, T., Kishi, M., Sakakibara, A., Itoh, M., Yonemura, S., Furuse, M., Tsukita, S., 1996. Interspecies diversity of the occludin sequence: cDNA cloning of human, mouse, dog, and rat–kangaroo homologues. J. Cell Biol. 133, 43–47.

Annunziata, P., Cioni, C., Toneatto, S., Paccagnini, E., 1998. HIV-1 gp120 increases the permeability of rat brain endothelium cultures by a mechanism involving substance P. AIDS 12, 2377–2385.

Anstrom, J.A., Brown, W.R., Moody, D.M., Thore, C.R., Challa, V.R., Block, S.M., 2002. Anatomical analysis of the developing cerebral vasculature in premature neonates: absence of precapillary arteriole-to-venous shunts. Pediatr. Res. 52, 554–560.

Antoniuk, S., da Silva, R.V., 2000. Periventricular and intraventricular hemorrhage in the premature infants. Rev. Neurol. 31, 238–243.

Aurrand-Lions, M., Johnson-Leger, C., Wong, C., Du Pasquier, L., Imhof, B.A., 2001. Heterogeneity of endothelial junctions is reflected by differential expression and specific subcellular localization of the three JAM family members. Blood 98, 3699–3707.

Balabanov, R., Dore-Duffy, P., 1998. Role of the CNS microvascular pericyte in the blood–brain barrier. J. Neurosci. Res. 53, 637–644.

Balabanov, R., Washington, R., Wagnerova, J., Dore-Duffy, P., 1996. CNS microvascular pericytes express macrophage-like function, cell surface integrin alpha M, and macrophage marker ED-2. Microvasc. Res. 52, 127–142.

Balda, M.S., Gonzalez-Mariscal, L., Contreras, R.G., Macias-Silva, M., Torres-Marquez, M.E., Garcia-Sainz, J.A., Cereijido, M., 1991. Assembly and sealing of tight junctions: possible participation of G-proteins, phospholipase C, protein kinase C and calmodulin. J. Membr. Biol. 122, 193–202.

Bandopadhyay, R., Orte, C., Lawrenson, J.G., Reid, A.R., De Silva, S., Allt, G., 2001. Contractile proteins in pericytes at the blood–brain and blood–retinal barriers. J. Neurocytol. 30, 35–44.

Bass, T., Singer, G., Slusser, J., Liuzzi, F.J., 1992. Radial glial interaction with cerebral germinal matrix capillaries in the fetal baboon. Exp. Neurol. 118, 126–132.

Bauer, H.C., Bauer, H., Lametschwandtner, A., Amberger, A., Ruiz, P., Steiner, M., 1993. Neovascularization and the appearance of morphological characteristics of the blood–brain barrier in the embryonic mouse central nervous system. Brain Res. Dev. Brain Res. 75, 269–278.

Bazzoni, G., Martinez-Estrada, O.M., Mueller, F., Nelboeck, P., Schmid, G., Bartfai, T., Dejana, E., Brockhaus, M., 2000. Homophilic interaction of junctional adhesion molecule. J. Biol. Chem. 275, 30970–30976.

Benagiano, V., Virgintino, D., Maiorano, E., Rizzi, A., Palombo, S., Roncali, L., Ambrosi, G., 1996. VIP-like immunoreactivity within neurons and perivascular neuronal processes of the human cerebral cortex. Eur. J. Histochem. 40, 53–56.

Bertossi, M., Virgintino, D., Errede, M., Roncali, L., 1999. Immunohistochemical and ultrastructural characterization of cortical plate microvasculature in the human fetus telencephalon. Microvasc. Res. 58, 49–61.

Bolton, S.J., Anthony, D.C., Perry, V.H., 1998. Loss of the tight junction proteins occludin and zonula occludens-1 from cerebral vascular endothelium during neutrophil-induced blood–brain barrier breakdown in vivo. Neuroscience 86, 1245–1257.

Boven, L.A., Gomes, L., Hery, C., Gray, F., Verhoef, J., Portegies, P., Tardieu, M., Nottet, H.S., 1999. Increased peroxynitrite activity in AIDS dementia complex: implications for the neuropathogenesis of HIV-1 infection. J. Immunol. 162, 4319–4327.

Braet, K., Paemeleire, K., D'Herde, K., Sanderson, M.J., Leybaert, L., 2001. Astrocyte–endothelial cell calcium signals conveyed by two signalling pathways. Eur. J. Neurosci. 13, 79–91.

Broadwell, R.D., Charlton, H.M., Ebert, P., Hickey, W.F., Villegas, J.C., Wolf, A.L., 1990. Angiogenesis and the blood–brain barrier in solid and dissociated cell grafts within the CNS. Prog. Brain Res. 82, 95–101.

Chao, C.C., Hu, S., Sheng, W.S., Peterson, P.K., 1995. Tumor necrosis factor-alpha production by human fetal microglial cells: regulation by other cytokines. Dev. Neurosci. 17, 97–105.

Chen, Y., McCarron, R.M., Azzam, N., Bembry, J., Reutzler, C., Lenz, F.A., Spatz, M., 2000. Endothelin-1 and nitric oxide affect human cerebromicrovascular endothelial responses and signal transduction. Acta Neurochir., Suppl. 76, 131–135.

Clawson, C.C., Hartmann, J.F., Vernier, R.L., 1966. Electron microscopy of the effect of gram-negative endotoxin on the blood–brain barrier. J. Comp. Neurol. 127, 183–198.

Dehouck, M.P., Vigne, P., Torpier, G., Breittmayer, J.P., Cecchelli, R., Frelin, C., 1997. Endothelin-1 as a mediator of endothelial cell-pericyte interactions in bovine brain capillaries. J. Cereb. Blood Flow Metab. 17, 464–469.

Deng, X., Wang, X., Andersson, R., 1995. Endothelial barrier resistance in multiple organs after septic and nonseptic challenges in the rat. J. Appl. Physiol. 78, 2052–2061.

de Vries, H.E., Blom-Roosemalen, M.C., van Oosten, M., de Boer, A.G., van Berkel, T.J., Breimer, D.D., Kuiper, J., 1996. The influence of cytokines on the integrity of the blood–brain barrier in vitro. J. Neuroimmunol. 64, 37–43.

DiSalvo, D., 1998. The correlation between placental pathology and intraventricular hemorrhage in the preterm infant. The Developmental Epidemiology Network Investigators. Pediatr. Res. 43, 15–19.

Ebnet, K., Schulz, C.U., Meyer Zu Brickwedde, M.K., Pendl, G.G., Vestweber, D., 2000. Junctional adhesion molecule interacts with the PDZ domain-containing proteins AF-6 and ZO-1. J. Biol. Chem. 275, 27979–27988.

Elfont, R.M., Sundaresan, P.R., Sladek, C.D., 1989. Adrenergic receptors on cerebral microvessels: pericyte contribution. Am. J. Physiol. 256, R224–R230.

Feuerstein, G.Z., Liu, T., Barone, F.C., 1994. Cytokines, inflammation, and brain injury: role of tumor necrosis factor-alpha. Cerebrovasc. Brain Metab. Rev. 6, 341–360.

Fischer, S., Clauss, M., Wiesnet, M., Renz, D., Schaper, W., Karliczek, G.F., 1999. Hypoxia induces permeability in brain microvessel endothelial cells via VEGF and NO. Am. J. Physiol. 276, C812–C820.

Fischer, S., Wobben, M., Kleinstuck, J., Renz, D., Schaper, W., 2000. Effect of astroglial cells on hypoxia-induced permeability in PBMEC cells. Am. J. Physiol.: Cell Physiol. 279, C935–C944.

Fischer, S., Wobben, M., Marti, H.H., Renz, D., Schaper, W., 2002. Hypoxia-induced hyperpermeability in brain microvessel endothelial cells involves VEGF-mediated changes in the expression of zonula occludens-1. Microvasc. Res. 63, 70–80.

Furuse, M., Hirase, T., Itoh, M., Nagafuchi, A., Yonemura, S., Tsukita, S., 1993. Occludin: a novel integral membrane protein localizing at tight junctions. J. Cell Biol. 123, 1777–1788.

Furuse, M., Fujita, K., Hiiragi, T., Fujimoto, K., Tsukita, S., 1998. Claudin-1 and -2: novel integral membrane proteins localizing at tight junctions with no sequence similarity to occludin. J. Cell Biol. 141, 1539–1550.

Furuse, M., Sasaki, H., Tsukita, S., 1999. Manner of interaction of heterogeneous claudin species within and between tight junction strands. J. Cell Biol. 147, 891–903.

Ghazi-Birry, H.S., Brown, W.R., Moody, D.M., Challa, V.R., Block, S.M., Reboussin, D.M., 1997. Human germinal matrix: venous origin of hemorrhage and vascular characteristics. AJNR Am. J. Neuroradiol. 18, 219–229.

Giulian, D., Haverkamp, L.J., Li, J., Karshin, W.L., Yu, J., Tom, D., Li, X., Kirkpatrick, J.B., 1995. Senile plaques stimulate microglia to release a neurotoxin found in Alzheimer brain. Neurochem. Int. 27, 119–137.

Gould, S.J., Howard, S., 1987. An immunohistochemical study of the germinal layer in the late gestation human fetal brain. Neuropathol. Appl. Neurobiol. 13, 421–437.

Grieb, P., Forster, R.E., Strome, D., Goodwin, C.W., Pape, P.C., 1985. O_2 exchange between blood and brain tissues studied with $18O_2$ indicator-dilution technique. J. Appl. Physiol. 58, 1929–1941.

Groothuis, D.R., Vriesendorp, F.J., Kupfer, B., Wamke, P.C., Lapin, G.D., Kuruvilla, A., Vick, N.A., Mikhael, M.A., Patlak, C.S., 1991. Quantitative measurements of capillary transport in human brain tumors by computed tomography. Ann. Neurol. 30, 581–588.

Hambleton, G., Wigglesworth, J.S., 1976. Origin of intraventricular haemorrhage in the preterm infant. Arch. Dis. Child. 51, 651–659.

Haskins, J., Gu, L., Wittchen, E.S., Hibbard, J., Stevenson, B.R., 1998. ZO-3, a novel member of the MAGUK protein family found at the tight junction, interacts with ZO-1 and occludin. J. Cell Biol. 141, 199–208.

Healy, D.P., Wilk, S., 1993. Localization of immunoreactive glutamyl aminopeptidase in rat brain. II. Distribution and correlation with angiotensin II. Brain Res. 606, 295–303.

Hippenstiel, S., Krull, M., Ikemann, A., Risau, W., Clauss, M., Suttorp, N., 1998. VEGF induces hyperpermeability by a direct action on endothelial cells. Am. J. Physiol. 274, L678–L684.

Hirase, T., Staddon, J.M., Saitou, M., Ando-Akatsuka, Y., Itoh, M., Furuse, M., Fujimoto, K., Tsukita, S., Rubin, L.L., 1997. Occludin as a possible determinant of tight junction permeability in endothelial cells. J. Cell. Sci. 110, 1603–1613.

Hirschi, K.K., D'Amore, P.A., 1997. Control of angiogenesis by the pericyte: molecular mechanisms and significance. EXS 79, 419–428.

Hoheisel, D., Nitz, T., Franke, H., Wegener, J., Hakvoort, A., Tilling, T., Galla, H.J., 1998. Hydrocortisone reinforces the blood–brain properties in a serum free cell culture system. Biochem. Biophys. Res. Commun. 247, 312–315.

Holash, J.A., Noden, D.M., Stewart, P.A., 1993. Re-evaluating the role of astrocytes in blood–brain barrier induction. Dev. Dyn. 197, 14–25.

Itoh, M., Furuse, M., Morita, K., Kubota, K., Saitou, M., Tsukita, S., 1999. Direct binding of three tight junction-associated MAGUKs, ZO-1, ZO-2, and ZO-3, with the COOH termini of claudins. J. Cell Biol. 147, 1351–1363.

Izumi, Y., Hirose, T., Tamai, Y., Hirai, S., Nagashima, Y., Fujimoto, T., Tabuse, Y., Kemphues, K.J., Ohno, S., 1998. An atypical PKC directly associates and colocalizes at the epithelial tight junction with ASIP, a mammalian homologue of *Caenorhabditis elegans* polarity protein PAR-3. J. Cell Biol. 143, 95–106.

Jacobson, M., 1991. Developmental Neurobiology, third ed. Plenum, New York.

Janzer, R.C., Raff, M.C., 1987. Astrocytes induce blood–brain barrier properties in endothelial cells. Nature 325, 253–257.

Jeppsson, B., Freund, H.R., Gimmon, Z., James, J.H., von Meyenfeldt, M.F., Fischer, J.E., 1981. Blood–brain barrier derangement in sepsis: cause of septic encephalopathy? Am. J. Surg. 141, 136–142.

Johnson, R.T., McArthur, J.C., Narayan, O., 1988. The neurobiology of human immunodeficiency virus infections. FASEB J. 2, 2970–2981.

Kenny, J.D., Garcia-Prats, J.A., Hilliard, J.L., Corbet, A.J., Rudolph, A.J., 1978. Hypercarbia at birth: a possible role in the pathogenesis of intraventricular hemorrhage. Pediatrics 62, 465–467.

Kern, T.S., Engerman, R.L., 1996. Capillary lesions develop in retina rather than cerebral cortex in diabetes and experimental galactosemia. Arch. Ophthalmol. 114, 306–310.

Kis, B., Abraham, C.S., Deli, M.A., Kobayashi, H., Niwa, M., Yamashita, H., Busija, D.W., Ueta, Y., 2003. Adrenomedullin, an autocrine mediator of blood–brain barrier function. Hypertens. Res. 26, S61–S70 (supplement).

Klegeris, A., McGeer, P.L., 1997. Beta-amyloid protein enhances macrophage production of oxygen free radicals and glutamate. J. Neurosci. Res. 49, 229–235.

Klegeris, A., Walker, D.G., McGeer, P.L., 1997. Interaction of Alzheimer beta-amyloid peptide with the human monocytic cell line THP-1 results in a protein kinase C-dependent secretion of tumor necrosis factor-alpha. Brain Res. 747, 114–121.

Kondo, T., Kinouchi, H., Kawase, M., Yoshimoto, T., 1996. Astroglial cells inhibit the increasing permeability of brain endothelial cell monolayer following hypoxia/reoxygenation. Neurosci. Lett. 208, 101–104.

Krum, J.M., Kenyon, K.L., Rosenstein, J.M., 1997. Expression of blood–brain barrier characteristics following neuronal loss and astroglial damage after administration of anti-Thy-1 immunotoxin. Exp. Neurol. 146, 33–45.

Kustova, Y., Grinberg, A., Basile, A.S., 1999. Increased blood–brain barrier permeability in LP-BM5 infected mice is mediated by neuroexcitatory mechanisms. Brain Res. 839, 153–163.

Lamszus, K., Laterra, J., Westphal, M., Rosen, E.M., 1999. Scatter factor/hepatocyte growth factor (SF/HGF) content and function in human gliomas. Int. J. Dev. Neurosci. 17, 517–530.

Lang, H.L., Jacobsen, H., Ikemizu, S., Andersson, C., Harlos, K., Madsen, L., Hjorth, P., Sondergaard, L., Svejgaard, A., Wucherpfennig, K., Stuart, D.I., Bell, J.I., Jones, E.Y., Fugger, L., 2002. A functional and structural basis for TCR cross-reactivity in multiple sclerosis. Nat. Immunol. 3, 940–943.

Liebner, S., Fischmann, A., Rascher, G., Duffner, F., Grote, E.H., Kalbacher, H., Wolburg, H., 2000a. Claudin-1 and claudin-5 expression and tight junction morphology are altered in blood vessels of human glioblastoma multiforme. Acta Neuropathol. (Berl.) 100, 323–331.

Liebner, S., Kniesel, U., Kalbacher, H., Wolburg, H., 2000b. Correlation of tight junction morphology with the expression of tight junction proteins in blood–brain barrier endothelial cells. Eur. J. Cell Biol. 79, 707–717.

Lindahl, P., Johansson, B.R., Leveen, P., Betsholtz, C., 1997. Pericyte loss and microaneurysm formation in PDGF-B-deficient mice. Science 277, 242–245.

Lippoldt, A., Kniesel, U., Liebner, S., Kalbacher, H., Kirsch, T., Wolburg, H., Haller, H., 2000. Structural alterations of tight junctions are associated with loss of polarity in stroke-prone spontaneously hypertensive rat blood–brain barrier endothelial cells. Brain Res. 885, 251–261.

Liu, Y., Wu, Y., Lee, J.C., Xue, H., Pevny, L.H., Kaprielian, Z., Rao, M.S., 2002. Oligodendrocyte and astrocyte development in rodents: an in situ and immunohistological analysis during embryonic development. Glia 40, 25–43.

Long, D.M., 1970. Capillary ultrastructure and the blood–brain barrier in human malignant brain tumors. J. Neurosurg. 32, 127–144.

Long, D.M., 1979. Capillary ultrastructure in human metastatic brain tumors. J. Neurosurg. 51, 53–58.

Lou, J., Chofflon, M., Juillard, C., Donati, Y., Mili, N., Siegrist, C.A., Grau, G.E., 1997. Brain microvascular endothelial cells and leukocytes derived from patients with multiple sclerosis exhibit increased adhesion capacity. NeuroReport 8, 629–633.

Louissaint Jr., A., Rao, S., Leventhal, C., Goldman, S.A., 2002. Coordinated interaction of neurogenesis and angiogenesis in the adult songbird brain. Neuron 34, 945–960.

Magistretti, P.J., Pellerin, L., Rothman, D.L., Shulman, R.G., 1999. Energy on demand. Science 283, 496–497.

Mark, K.S., Davies, T.P., 2002. Cerebral microvascular changes in permeability and tight junctions induced by hypoxia-reoxygenation. Am. J. Physiol.: Heart Circ. Physiol. 282, H1485–H1494.

Martin-Padura, I., Lostaglio, S., Schneemann, M., Williams, L., Romano, M., Fruscella, P., Panzeri, C., Stoppacciaro, A., Ruco, L., Villa, A., et al., 1998. Junctional adhesion molecule, a novel member of the immunoglobulin superfamily that distributes at intercellular junctions and modulates monocyte transmigration. J. Cell Biol. 142, 117–127.

Matter, K., Balda, M.S., 2003. Signalling to and from tight junctions. Nat. Rev., Mol. Cell Biol. 4, 225–236.

Ment, L.R., Oh, W., Philip, A.G., Ehrenkranz, R.A., Duncan, C.C., Allan, W., Taylor, K.J., Schneider, K., Katz, K.H., Makuch, R.W., 1992. Risk factors for early intraventricular hemorrhage in low birth weight infants. J. Pediatr. 121, 776–783.

Ment, L.R., Stewart, W.B., Ardito, T.A., Madri, J.A., 1995. Germinal matrix microvascular maturation correlates inversely with the risk period for neonatal intraventricular hemorrhage. Brain Res. Dev. Brain Res. 84, 142–149.

Merrill, J.E., Ignarro, L.J., Sherman, M.P., Melinek, J., Lane, T.E., 1993. Microglial cell cytotoxicity of oligodendrocytes is mediated through nitric oxide. J. Immunol. 151, 2132–2141.

Mi, H., Haeberle, H., Barres, B.A., 2001. Induction of astrocyte differentiation by endothelial cells. J. Neurosci. 21, 1538–1547.

Minagar, A., Shapshak, P., Fujimura, R., Ownby, R., Heyes, M., Eisdorfer, C., 2002. The role of macrophage/microglia and astrocytes in the pathogenesis of three neurologic disorders: HIV-associated dementia, Alzheimer disease, and multiple sclerosis. J. Neurol. Sci. 202, 13–23.

Mitic, L.L., Van Itallie, C.M., Anderson, J.M., 2000. Molecular physiology and pathophysiology of tight junctions I. Tight junction structure and function: lessons from mutant animals and proteins. Am. J. Physiol.: Gastrointest. Liver Physiol. 279, G250–G254.

Morita, K., Sasaki, H., Fujimoto, K., Furuse, M., Tsukita, S., 1999a. Claudin-11/OSP-based tight junctions of myelin sheaths in brain and Sertoli cells in testis. J. Cell Biol. 145, 579–588.

Morita, K., Sasaki, H., Furuse, M., Tsukita, S., 1999b. Endothelial claudin: claudin-5/TMVCF constitutes tight junction strands in endothelial cells. J. Cell Biol. 147, 185–194.

Neuhaus, J., Risau, W., Wolburg, H., 1991. Induction of blood–brain barrier characteristics in bovine brain endothelial cells by rat astroglial cells in transfilter coculture. Ann. N.Y. Acad. Sci. 633, 578–580.

Nico, B., Frigeri, A., Nicchia, G.P., Quondamatteo, F., Herken, R., Errede, M., Ribatti, D., Svelto, M., Roncali, L., 2001. Role of aquaporin-4 water channel in the development and integrity of the blood–brain barrier. J. Cell Sci. 114, 1297–1307.

Nielsen, S., King, L.S., Christensen, B.M., Agre, P., 1997. Aquaporins in complex tissues. II. Subcellular distribution in respiratory and glandular tissues of rat. Am. J. Physiol. 273, C1549–C1561.

Norenberg, M.D., 1994. Astrocyte responses to CNS injury. J. Neuropathol. Exp. Neurol. 53, 213–230.

Paemeleire, K., 2002. The cellular basis of neurovascular metabolic coupling. Acta Neurol. Belg. 102, 153–157.

Palmer, T.D., Willhoite, A.R., Gage, F.H., 2000. Vascular niche for adult hippocampal neurogenesis. J. Comp. Neurol. 425, 479–494.

Pan, W., Kastin, A.J., Gera, L., Stewart, J.M., 2001. Bradykinin antagonist decreases early disruption of the blood–spinal cord barrier after spinal cord injury in mice. Neurosci. Lett. 307, 25–28.

Papadopoulos, M.C., Lamb, F.J., Moss, R.F., Davies, D.C., Tighe, D., Bennett, E.D., 1999. Faecal peritonitis causes oedema and neuronal injury in pig cerebral cortex. Clin. Sci. (Lond.) 96, 461–466.

Papadopoulos, M.C., Davies, D.C., Moss, R.F., Tighe, D., Bennett, E.D., 2000. Pathophysiology of septic encephalopathy: a review. Crit. Care Med. 28, 3019–3024.

Papadopoulos, M.C., Saadoun, S., Woodrow, C.J., Davies, D.C., Costa-Martins, P., Moss, R.F., Krishna, S., Bell, B.A., 2001. Occludin expression in microvessels of neoplastic and non-neoplastic human brain. Neuropathol. Appl. Neurobiol. 27, 384–395.

Pardridge, W.M., Eisenberg, J., Yang, J., 1985. Human blood–brain barrier insulin receptor. J. Neurochem. 44, 1771–1778.

Rakic, P., 1971. Guidance of neurons migrating to the fetal monkey neocortex. Brain Res. 33, 471–476.

Ramsauer, M., Krause, D., Dermietzel, R., 2002. Angiogenesis of the blood–brain barrier in vitro and the function of cerebral pericytes. FASEB J. 16, 1274–1276.

Rash, J.E., Yasumura, T., Hudson, C.S., Agre, P., Nielsen, S., 1998. Direct immunogold labeling of aquaporin-4 in square arrays of astrocyte and ependymocyte plasma membranes in rat brain and spinal cord. Proc. Natl. Acad. Sci. U.S.A. 95, 11981–11986.

Rubin, L.L., Barbu, K., Bard, F., Cannon, C., Hall, D.E., Horner, H., Janatpour, M., Liaw, C., Manning, K., Morales, J., et al., 1991. Differentiation of brain endothelial cells in cell culture. Ann. N.Y. Acad. Sci. 633, 420–425.

Saadoun, S., Papadopoulos, M.C., Davies, D.C., Krishna, S., Bell, B.A., 2002. Aquaporin-4 expression is increased in oedematous human brain tumours. J. Neurol. Neurosurg. Psychiatry 72, 262–265.

Sasaki, A., Hirato, J., Nakazato, Y., Ishida, Y., 1988. Immunohistochemical study of the early human fetal brain. Acta Neuropathol. 76, 128–134.

Schroeter, M.L., Mertsch, K., Giese, H., Muller, S., Sporbert, A., Hickel, B., Blasig, I.E., 1999. Astrocytes enhance radical defence in capillary endothelial cells constituting the blood–brain barrier. FEBS Lett. 449, 241–244.

Sharer, L.R., 1992. Pathology of HIV-1 infection of the central nervous system. A review. J. Neuropathol. Exp. Neurol. 51, 3–11.

Sobue, K., Yamamoto, N., Yoneda, K., Hodgson, M.E., Yamashiro, K., Tsuruoka, N., Tsuda, T., Katsuya, H., Miura, Y., Asai, K., Kato, T., 1999. Induction of blood–brain barrier properties in immortalized bovine brain endothelial cells by astrocytic factors. Neurosci. Res. 35, 155–164.

Sonoda, N., Furuse, M., Sasaki, H., Yonemura, S., Katahira, J., Horiguchi, Y., Tsukita, S., 1999. *Clostridium perfringens* enterotoxin fragment removes specific claudins from tight junction strands: evidence for direct involvement of claudins in tight junction barrier. J. Cell Biol. 147, 195–204.

St'astny, F., Skultetyova, I., Pliss, L., Jezova, D., 2000. Quinolinic acid enhances permeability of rat brain microvessels to plasma albumin. Brain Res. Bull. 53, 415–420.

Stevenson, B.R., Begg, D.A., 1994. Concentration-dependent effects of cytochalasin D on tight junctions and actin filaments in MDCK epithelial cells. J. Cell Sci. 107, 367–375.

Stewart, P.A., Hayakawa, K., 1994. Early ultrastructural changes in blood–brain barrier vessels of the rat embryo. Brain Res. Dev. Brain Res. 78, 25–34.

Stewart, P.A., Wiley, M.J., 1981. Developing nervous tissue induces formation of blood–brain barrier characteristics in invading endothelial cells: a study using quail-chick transplantation chimeras. Dev. Biol. 84, 183–192.

Szymonowicz, W., Schaflet, K., Cussen, L.J., Yu, V.Y., 1984. Ultrasound and necropsy study of periventricular haemorrhage in preterm infants. Arch. Dis. Child. 59, 637–642.

Taniguchi, M., Yamashita, T., Kumura, E., Tamatani, M., Kobayashi, A., Yokawa, T., Maruno, M., Kato, A., Ohnishi, T., Kohmura, E., et al., 2000. Induction of aquaporin-4 water channel mRNA after focal cerebral ischemia in rat. Brain Res. Mol. Brain Res. 78, 131–137.

Tarkowski, E., Rosengren, L., Blomstrand, C., Wikkelso, C., Jensen, C., Ekholm, S., Tarkowski, A., 1997. Intrathecal release of pro- and anti-inflammatory cytokines during stroke. Clin. Exp. Immunol. 110, 492–499.

Tighe, D., Moss, R., Bennett, D., 1996. Cell surface adrenergic receptor stimulation modifies the endothelial response to SIRS. Systemic inflammatory response syndrome. New Horiz. 4, 426–442.

Tran, N.D., Correale, J., Schreiber, S.S., Fisher, M., 1999. Transforming growth factor-beta mediates astrocyte-specific regulation of brain endothelial anticoagulant factors. Stroke 30, 1671–1678.

Tsukamoto, T., Nigam, S.K., 1999. Role of tyrosine phosphorylation in the reassembly of occludin and other tight junction proteins. Am. J. Physiol. 276, F737–F750.

Utsumi, H., Chiba, H., Kamimura, Y., Osanai, M., Igarashi, Y., Tobioka, H., Mori, M., Sawada, N., 2000. Expression of GFRalpha-1, receptor for GDNF, in rat brain capillary during postnatal development of the BBB. Am. J. Physiol.: Cell Physiol. 279, C361–C368.

van Zwieten, E.J., Ravid, R., Swaab, D.F., Van de Woude, T., 1988. Immunocytochemically stained vasopressin binding sites on blood vessels in the rat brain. Brain Res. 474, 369–373.

Verbeek, M.M., de Waal, R.M., Schipper, J.J., Van Nostrand, W.E., 1997. Rapid degeneration of cultured human brain pericytes by amyloid beta protein. J. Neurochem. 68, 1135–1141.

Vizuete, M.L., Venero, J.L., Vargas, C., Ilundain, A.A., Echevarria, M., Machado, A., Cano, J., 1999. Differential upregulation of aquaporin-4 mRNA expression in reactive astrocytes after brain injury: potential role in brain edema. Neurobiol. Dis. 6, 245–258.

Volpe, J.J., 1989a. Intraventricular hemorrhage in the premature infant-current concepts. Part I. Ann. Neurol. 25, 3–11.

Volpe, J.J., 1989b. Intraventricular hemorrhage in the premature infant-current concepts. Part II. Ann. Neurol. 25, 109–116.

Wekerle, H., Hohlfeld, R., 2003. Molecular mimicry in multiple sclerosis. N. Engl. J. Med. 349, 185–186.

Wolburg, H., Wolburg-Buchholz, K., Liebner, S., Engelhardt, B., 2001. Claudin-1, claudin-2 and claudin-11 are present in tight junctions of choroid plexus epithelium of the mouse. Neurosci. Lett. 307, 77–80.

Wolburg, H., Wolburg-Buchholz, K., Liebner, S., Engelhardt, B., 2001. Claudin-1, claudin-2 and claudin-11 are present in tight junctions of choroid plexus epithelium of the mouse. Neurosci. Lett. 307, 77–80.

Yoder, E.J., 2002. Modifications in astrocyte morphology and calcium signaling induced by a brain capillary endothelial cell line. Glia 38, 137–145.

Zhang, Y., Pardridge, W.M., 2001. Rapid transferrin efflux from brain to blood across the blood–brain barrier. J. Neurochem. 76, 1597–1600.

Zhang, W., Smith, C., Shapiro, A., Monette, R., Hutchison, J., Stanimirovic, D., 1999. Increased expression of bioactive chemokines in human cerebromicrovascular endothelial cells and astrocytes subjected to simulated ischemia in vitro. J. Neuroimmunol. 101, 148–160.

Zhang, W., Smith, C., Howlett, C., Stanimirovic, D., 2000. Inflammatory activation of human brain endothelial cells by hypoxic astrocytes in vitro is mediated by IL-1beta. J. Cereb. Blood Flow Metab. 20, 967–978.

Zonta, M., Angulo, M.C., Gobbo, S., Rosengarten, B., Hossmann, K.A., Pozzan, T., Carmignoto, G., 2003. Neuron-to-astrocyte signaling is central to the dynamic control of brain microcirculation. Nat. Neurosci. 6, 43–50.

MECHANISMS OF DISEASE: THE BLOOD-BRAIN BARRIER

Edward A. Neuwelt, M.D.
Departments of Neurology and Neurosurgery, Oregon Health & Science University, Portland, Oregon

Reprint requests:
Edward A. Neuwelt, M.D., Oregon Health & Science University, 3181 SW Sam Jackson Park Road, L603, Portland, OR 97201.
Email: neuwelte@ohsu.edu

Received, June 16, 2003.
Accepted, September 3, 2003.

OBJECTIVE: The blood-brain barrier (BBB) is often perceived as a passive membrane. However, evidence has demonstrated that the BBB plays an active role in normal homeostasis and in certain disease processes.

METHODS: Approximately 300 peer-reviewed publications that discussed normal or abnormal BBB function were reviewed.

RESULTS: The role of the BBB and how it contributes to disorders of the central nervous system vary, depending on the specific disease process.

CONCLUSION: In health and disease and extending to old age, endothelial cells, neurons, and glia constitute a neurovascular unit that regulates the BBB. Advances toward penetrating the BBB must account for both normal and abnormal functions of the neurovascular unit.

KEY WORDS: Barrier, Blood-Brain, Central nervous system delivery

Neurosurgery 54:131–142, 2004 DOI: 10.1227/01.NEU.0000097715.11966.8E www.neurosurgery-online.com

The blood-brain barrier (BBB) consists of a layer of endothelial cells that line the blood vasculature throughout the brain (*Fig. 1*). This layer is held together by tight junctions produced in response to signals from astrocytes. These tight junctions prevent small molecules from diffusing through the gaps between the cells (i.e., the paracellular route) (*Fig. 2*). Because the diffusion of molecules across the cells via other means (e.g., pinocytosis) is minimal, these tight junctions and their inherent impermeability to water-soluble molecules or molecules larger than M_r 200 to 400 create the BBB.

The BBB permeability of most molecules can be predicted on the basis of their octanol/water partition coefficients (68, 83, 84). For example, diphenhydramine (Benadryl), which has a high coefficient, easily accesses the brain, whereas water-soluble loratadine (Claritin) does not cross the BBB and has little effect on the central nervous system (CNS) (30). However, permeability is not absolute and diffusion across the BBB reflects the octanol/water partition coefficient, although it may be low. Therefore, virtually all albumin (30 mg/100 ml) in cerebrospinal fluid (CSF) is from the ultrafiltration of serum (3 g/100 ml), as is the small amount of immunoglobulin M (approximately M_r 1,000,000) that is normally present in the CNS.

Substances with low partition coefficients that easily penetrate the CNS are generally ushered across the BBB via active or facilitated transport (*Fig. 2*). Transport is often asymmetric, depending on ion channels, specific transporters, energy-dependent pumps, and a limited amount of receptor-mediated endocytosis. Glucose, amino acids, and small intermediate metabolites, for example, are carried into the brain via facilitated transport mediated by specific proteins, whereas larger molecules, such as insulin, transferrin, and other plasma proteins, are carried across the endothelial layer via receptor-mediated or adsorptive endocytosis (55).

Some small solutes with high octanol/water partition coefficients are observed to poorly penetrate the BBB. Recent studies demonstrated that these molecules are actively transported back into the blood by efflux systems (55). These systems can be particularly troublesome for drug delivery across the BBB. For example, P-glycoprotein (P-gp), which is a member of the adenosine triphosphate-binding cassette family of exporters and is found in brain capillaries, has been demonstrated to be a potent energy-dependent transporter. P-gp contributes greatly to the efflux of xenobiotics from the brain and has increasingly been recognized as having a protective role and conferring drug resistance by impeding the delivery of therapeutic agents (70) (*Fig. 2*). The organic anion transporters and glutathione-dependent multidrug resistance-associated proteins (MRP) also contribute to the efflux of organic anions from the brain and CSF, and many (if not most) drugs with CNS permeability that is lower than predicted are substrates for these efflux proteins (*Fig. 2*).

Recent research suggested that blocking of these transporters, some of which can be inhibited by probenecid, for example (9), could improve delivery across the BBB. *MDR1*-deficient mice, for example, are phenotypically normal unless exposed to drugs that are normally pumped out of the endothelial cells by P-gp (70). Furthermore, it was observed that a colony of dogs that exhibited unexpected neurotoxicity with the administration of ivermectin, which is an excellent P-gp substrate, were deficient in the transporter (44). Attention has

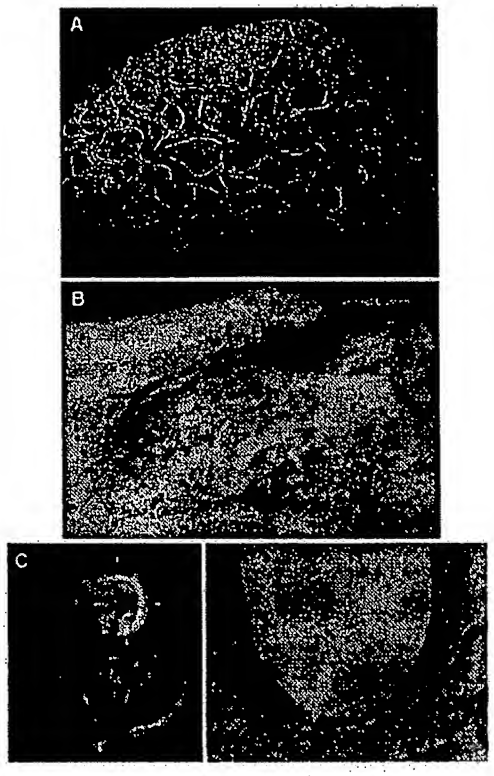

FIGURE 1. *Blood vessels in the human brain (A and B) and imaging of the BBB (C and D). There are approximately 400 miles of capillaries in the brain, with a surface area of approximately 12 m², which is 1000 times larger than the surface area of the choroid plexus, the origin of the blood-CSF barrier. A, photograph of blood vessels. A plastic emulsion was injected into the brain vessels, and brain parenchymal tissue was dissolved (from, Zlokovic BV, Apuzzo MLJ: Strategies to circumvent vascular barriers of the central nervous system. Neurosurgery 43:877–878, 1998 [92]). B, electron micrograph demonstrating electron-dense lanthanum (dark areas in the vessel lumen) that is unable to penetrate beyond a tight junction (arrows) between endothelial cells (E) (courtesy of Dr. Milton Brightman, National Institutes of Health). C and D, imaging with superparamagnetic iron oxide particles partially coated with dextran (Feridex; Berlex Laboratories, Inc., Wayne, NJ), which are the size of adeno-associated virus virions and can be observed at the light and electron microscopic levels and with MRI. C, MRI scan obtained after reversible BBB opening and intravascular infusion of superparamagnetic iron oxide particles. Distribution of the superparamagnetic iron oxide particles throughout the right cerebral hemisphere (arrows) is indicated by increased MRI signal. D, electron micrograph demonstrating that all of the particles are trapped in the basement membrane (arrows) and are not exposed to brain parenchyma. Thereby MRI can suggest global CNS delivery across the BBB when the contrast agent (iron particles) is actually trapped at the basement membrane (46) (D, original magnification, ×19,000). V, vessel lumen; MA, myelinated axon.*

also been focused on other efflux transporters, particularly nucleoside transporters (21).

Inhibition of P-gp may also have consequences independent of drug delivery. Some glial tumors, for example, demonstrate increased levels of P-gp, which has generated interest in the development of inhibitors of this transporter as chemotherapeutic agents (70). Unfortunately, effective doses of P-gp inhibitors, such as cyclosporin and verapamil, are often toxic. More detailed information on the BBB can be found elsewhere (5, 7, 26, 40, 48, 49, 55).

CHOROID PLEXUS AND OTHER CIRCUMVENTRICULAR ORGANS

In addition to the endothelium of the BBB, tight junctions are found in the epithelium of the choroid plexus (28) and in the arachnoid membrane that surrounds the surface of the brain and the spinal cord. These tight junctions limit the movement of solutes into and out of the CSF. Microvilli give the small choroid plexus a large surface area (48, 55), ensuring that the brisk blood flow through the plexus can replace the total CSF volume every 3 to 4 hours. Net sodium transport across the plexus from the blood is a cardinal feature of CSF production, with concomitant chloride and bicarbonate transport. Potassium and calcium ions, urea, and some drugs (such as penicillin) are pumped out of the CSF (48, 55) and micronutrients such as ascorbic acid are specifically pumped into the CSF at the plexus. After solutes enter the CSF, they can theoretically proceed to the brain unimpeded; however, the small extracellular space in the CNS ensures that diffusion into the brain is limited.

The CSF acts as a "sink," draining proteins and other metabolites from the interstitial fluid flowing from the ventricles over the surface of the brain; protein levels are generally approximately 5 mg/100 ml in the ventricles, compared with 30 to 40 mg/100 ml in the subarachnoid CSF. The brain is drained by the CSF as it egresses, mainly via arachnoid granulations but also, at least in animal models, via nerve roots, the carotid sheath, and olfactory tracts. The volume of CSF that leaves the CNS via these pseudolymphatic pathways may nearly equal the volume of CSF that leaves via arachnoid granulations (47). Although influx into the CNS via tight junctions is very restricted, this egressing fluid may contain components up to the size of intact white blood cells. These contrasting properties ensure that the brain is highly protected by a unidirectional barrier (48, 55).

The circumventricular organs of the hypothalamus, which lack a BBB, and the choroid plexus may also play key roles in metabolism. Both are densely packed with leptin receptors, which, after binding leptins produced by peripheral adipocytes, initiate a signal cascade that results in appetite suppression (90). Exactly how leptins access the hypothalamus is not well understood (43), but evidence suggests that decreased access across the hypothalamus BBB mediates obesity (93).

Because of these blood-CNS barriers and the lack of true lymphatic vessels, the CNS is often considered immunologically privileged. This privileged status is readily demonstrated by the fact that allogenic and even xenogenic grafts, which would be rapidly rejected if placed systemically, survive in the

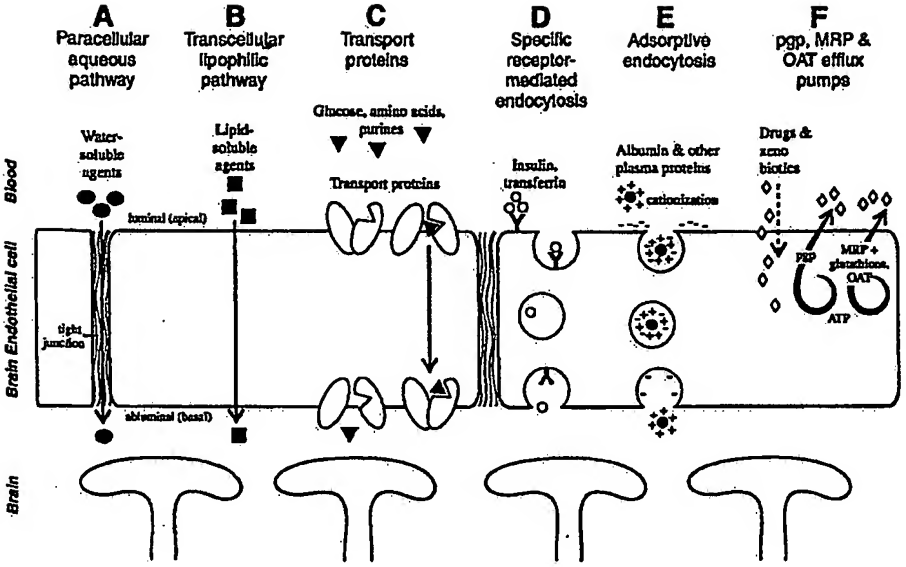

FIGURE 2. *Mechanisms and routes through the BBB (1, 22, 41, 58, 67, 81, 89). For normal homeostasis, carrier-mediated transport systems exist for hexoses (glucose, mannose, and galactose), monocarboxylic acids (acetic, lactic, and pyruvic acids), large neutral amino acids (tyrosine, phenylalanine, and isoleucine), acidic amino acids (glutamate and aspartate), basic amino acids (arginine and lysine), nucleic acid precursors (adenine, adenosine, and guanine), choline, and thyroid hormones (via transthyretin) (22). Concern regarding the consumption of sucrose and/or the artificial sweetener aspartame by children leading to increased delivery across the BBB via transporters, resulting in hyperactivity, was not documented with assessments of behavior and cognition, even after unusually high intake (89). The large neutral amino acid transporter, like the glucose transporter, is present on both the luminal and abluminal membranes of endothelial cells (67). At least 10 neutral amino acids compete for transport via the large neutral amino acid transporter, as indicated in a recent study of phenylketonuria, a disorder that causes extremely high levels of the neutral amino acid phenylalanine in the CNS, resulting in retardation unless dietary restriction is implemented (58). Transporters such as the monocarboxylic acid transporter for lactate and ketone bodies are particularly important during the neonatal period, with seizures, and during long-term fasts, when lactate and ketone bodies are important energy sources for the brain and levels of the transporter increase 8- to 25-fold (41). Whereas the glucose transporter and large neutral amino acid transporter are bidirectional (although they are most important for influx), other transporters are unidirectional efflux systems. For example, the inhibitory neurotransmitters glutamate and glycine are present in blood at concentrations 1000-fold greater than those in the CNS. Such levels in the CNS would be highly neurotoxic, as they are when the BBB is compromised after craniocerebral trauma or stroke (81). Therefore, the carrier for small neutral amino acids is primarily located on the abluminal membrane and allows only efflux. Similarly, brain extracellular potassium levels are maintained at approximately two-thirds the levels in blood, so as to not interfere with neural transmission. Potassium efflux is also accomplished with an energy-dependent process exchanging sodium for potassium at the abluminal membrane, with adenosine triphosphate (ATP) as the energy source (Na^+/K^+-adenosine triphosphatase). Encoded by the multidrug resistance gene (MDR1), P-gp is localized to the luminal membrane of endothelial cells and pumps amphipathic organic cations or neutral compounds out into the capillaries. Multidrug resistance-associated protein (MRP) and organic anion transporter (OAT) pump anions out of the CNS as efflux proteins* (modified from, *Abbott NJ, Romero IA: Transporting therapeutics across the blood-brain barrier. Mol Med Today 2:106–113, 1996 [1]).*

CNS. However, extracellular fluid and CSF can flow to superior cervical lymph nodes, via the olfactory nerves, to activate the systemic immune system (particularly the humoral arm) against antigens such as albumin (32). In addition, although transport across the BBB is tightly regulated, a slow influx of white blood cells into the CNS after bone marrow transplantation has been noted, and findings of 1 to 3 lymphocytes/mm^3 of CSF are considered normal. These findings indicate that the immunological privilege is only partial and may be subject to changes in disease states. The infiltration of white blood cells into the CNS after bone marrow transplantation, for example, can have a major effect in preventing neurological symptoms among children with globoid leukodystrophy and metachromatic leukodystrophy (35); lymphoma cells can preferentially target the CNS via the choroid plexus and cranial nerves (25).

OUTWITTING THE BBB

The treatment of Parkinson's disease represents a model of successful treatment using the BBB (38). The introduction of L-dopa revolutionized therapy for Parkinson's disease, because L-dopa crosses the BBB via the neutral amino acid transporter (which is normally only half-saturated) and is then converted by dopa decarboxylase to biologically active dopamine. Treatment with L-dopa also demonstrates the "metabolic BBB." The dopa decarboxylase inhibitor carbidopa, which cannot enter endothelial cells, systemically blocks the metabolism of L-dopa. However, the precursor (dopa) can be metabolized to dopamine as it crosses the endothelium and can be trapped there (i.e., the metabolic BBB).

Unfortunately, analogous therapies using acetylcholine precursors, such as phosphatidylcholine or diaminoethanol, have not been effective for the treatment of movement disorders such as Huntington's chorea (48). However, direct infusion into CSF of the γ-aminobutyric acid agonist baclofen has been effective for the treatment of spinal spasticity (48). Intranasal administration is another promising avenue, allowing drugs to access the CNS via the olfactory nerves (7).

Sometimes the formulation and route of delivery can be modified to increase BBB permeability. Smith et al. (78) demonstrated that intra-arterial infusion of chlorambucil, which is normally tightly bound to proteins, in a protein-free infusate increased delivery to the CNS, because of the high lipophilicity of the drug. The opposite approach is also sometimes successful. Drugs bound to cationized albumin bind to the negatively charged cerebral endothelium and are transported

across the BBB by adsorption-mediated transcytosis. Other delivery vectors also demonstrate promise (54). Friden et al. (19) shuttled nerve growth factor across the rat BBB by conjugating it to the monoclonal antibody Ox-26, which targets the transferrin transporter. Avidin linked to an insulin fragment or an antibody to the BBB insulin receptor allowed Shi and Pardridge (54, 73) to shuttle biotin-coupled drugs or imaging agents (up to 4% of the injected dose) across the endothelium. Even an intact enzyme (β-galactosidase) has been delivered across the BBB, by being coupled to the human immunodeficiency virus (HIV) TAT protein (71).

For decades, direct instillation into the brain and CSF produced only modest benefits; however, this approach is currently undergoing a resurgence of interest. Prophylactic intrathecal or intraventricular infusion of methotrexate and/or cytosine arabinoside has been demonstrated to markedly reduce the rates of death attributable to leukemic meningitis, which was virtually unknown in the 1950s but, with the advent of effective systemic chemotherapy, has become a major cause of death for children with lymphocytic leukemia. This approach is less effective for the treatment of overt CNS leukemia or lymphomas, because tumor cells fill the perivascular Virchow-Robin spaces, which limits the ability of drugs placed in the CSF to reach the cells (8). Another strategy that has demonstrated little success to date but is promising involves direct injection of fetal neuronal precursor cells or neurons directly into the brain for treatment of clinical movement disorders such as Parkinson's disease (18).

The major limitation with the instillation of drugs, proteins, viruses, and cells directly into the brain is the small extracellular space available. Secondary impediments to success include agent size, adsorptive properties, and efflux. For example, treatment of gliomas with surgical implantation of polifeprosan 20 with wafer carmustine (10), a polymer that slowly degrades and releases the lipophilic nitrosurea *N,N'*-bis(2-chloroethyl)-*N*-nitrosourea, has demonstrated only limited success because of the slow diffusion of *N,N'*-bis(2-chloroethyl)-*N*-nitrosourea and its high lipophilicity, which permits efflux back across the BBB. Similar diffusion problems were encountered when fibroblasts that released retroviruses carrying cytotoxic genes were placed in the brain; infected tumor cells were observed only within a few cell diameters of the injection site (64). However, direct injection into rodent brains could reverse symptoms of genetic neurodegenerative disease (77). The key problem with direct intracerebral injection models is that drugs with good therapeutic efficacy in 1-g rat brains usually do not demonstrate the same efficacy in human brains, which weigh more than 1000 g, unless the target volume is small (i.e., basal ganglia in Parkinson's disease).

One approach to solving delivery problems involves coupling the direct instillation of drugs or vectors with mechanical manipulation, to maximize the distribution of the agent. Arterial pulsations, for example, may accelerate drug movement in the brain and along perivascular spaces by increasing bulk flow. Chen et al. (13) promoted the use of this strategy, which is currently referred to as convection or clysis, to increase the volume of distribution. Testing in animals and among patients with brain tumors has demonstrated that chronic convection can increase brain sucrose levels up to 10,000-fold, compared with intravenous infusion (23). Convection may be best suited for treatment of focal rather than global CNS disease, because global delivery is not possible with current clysis methods (*Fig. 3, A* and *B*).

An alternative to direct instillation or the use of vectors is reversible opening of the BBB. Focal and global BBB openings have been attempted with a variety of strategies (49, 51). Chemicals such as dimethyl sulfoxide, bradykinin or its stable potent analog RMP-7, and the antineoplastic agent etoposide and mechanical stresses such as hypertension and hypercapnia have all been used, but none has been as consistent and safe as osmotic BBB disruption (BBBD). Osmotic BBBD is facilitated by hypertonic nonmetabolizable solutes that are injected intra-arterially and can open the BBB to components from small drugs to proteins and even the herpesvirus (180 nm in diameter). Intra-arterial infusion at a rate to yield a pressure just higher than the blood pressure for at least 20 seconds reversibly opens the BBB in the region of the infused arterial circulation for approximately 30 minutes. This increases delivery of drugs to the CNS up to 100-fold, compared with levels achieved with intravenous infusion; even greater relative increases are achieved for proteins and viruses (16, 34). An advantage of BBBD is that, after the BBB has closed, drugs in the systemic circulation can be neutralized (cleared) with chelators or modifying agents (60), because the resealed BBB once again creates two distinct compartments (*Fig. 3, C* and *D*).

IMAGING OF THE BBB

Standard imaging of BBB integrity is performed with small, water-soluble, contrast agents with short plasma half-lives (usually <1 h). Iodinated contrast agents produce enhancement in the brain on computed tomographic (CT) scans, which indicates where there is a loss of BBB integrity (such as with malignant tumors, abscesses, or other lesions that cause vasogenic edema). The degree of enhancement on CT scans (measured in Hounsfield units) increases linearly with the amount of contrast agent entering the brain. For magnetic resonance imaging (MRI), chelated gadolinium is used as a water-soluble, paramagnetic, contrast agent. As with enhanced CT scanning, BBB breaches can be observed as enhancement on T1-weighted MRI scans, but with greater sensitivity than on CT scans. Signal intensity changes attributable to gadolinium enhancement on MRI scans are not linear, unlike CT scanning results.

A new class of MRI contrast agents, namely, superparamagnetic iron oxide compounds (ultra-small-particle iron oxide), are now being used to assess BBB integrity (*Fig. 1, C* and *D*). One such agent, ferumoxtran-10 (Combidex; Advanced Magnetics, Cambridge, MA), has a long plasma half-life (1–2 d) and is taken up by phagocytic cells (microglia and reactive

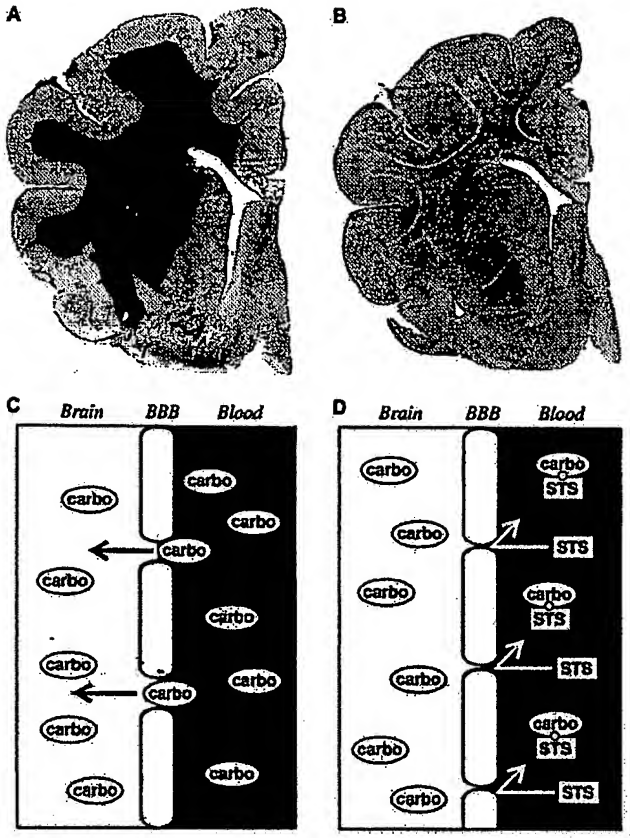

FIGURE 3. *Novel approaches for drug delivery. With a current focus on dose intensity and targeted delivery in CNS therapy, there is an increasing need to protect non-CNS tissues. The BBB permits novel approaches for dose-intensive and/or targeted delivery, with minimization of systemic toxicity (16). One method of targeted delivery that minimizes systemic toxicity is administration of therapeutic agents directly into the brain via convection. A and B, sections in which iron was infused into the cerebral hemisphere of a cat (A and B, original magnification, ×5). A, staining for iron, showing distribution (black areas) throughout the white matter (A, modified from, Muldoon LL, Nilaver G, Kroll RA, Pagel MA, Breakefield XO, Chiocca EA, Davidson BL, Weissleder R, Neuwelt EA: Comparison of intracerebral inoculation and osmotic blood-brain barrier disruption for delivery of adenovirus, herpesvirus and iron oxide particles to normal rat brain. Am J Pathol 147:1840–1851, 1995 [45]). B, hematoxylin and eosin staining, showing no evidence of tissue damage. Myelin staining yielded similar results (data not shown). C and D, diagrams indicating that the BBB offers a unique two-compartment model to separate cytotoxic drugs aimed at killing CNS tumors from chemoprotectant agents designed to protect tissues such as the cochlea and bone marrow. For example, carboplatin (carbo) can be administered intra-arterially after opening of the BBB (C) and then, 4 to 8 hours after BBB closure, high doses of thiols such as sodium thiosulfate (STS) can be administered intravenously (D). Sodium thiosulfate does not cross the BBB and covalently binds non-CNS carboplatin, preventing most ototoxicity and even mitigating thrombocytopenia (16) (C and D, modified from, Neuwelt EA, Brummett RE, Doolittle ND, Muldoon LL, Kroll RA, Pagel MA, Dojan R, Church V, Remsen LG, Bubalo JS: First evidence of otoprotection against carboplatin-induced hearing loss with a two compartment system in patients with central nervous system malignancy using sodium thiosulfate. J Pharmacol Exp Ther 286:77–84, 1998 [50]).*

astrocytes) and generally not by tumor cells. Therefore, despite their large size, relative to standard gadolinium contrast agents, these compounds facilitate imaging of brain tumors with slow leakage into the tumor and brain tissue around the tumor and uptake (trapping) by reactive cells in and around the tumor. With this approach, additional and/or larger lesions (*Fig. 4*) have been identified among some patients with brain tumors, in comparison with standard gadolinium-based scans (86). These agents may also facilitate imaging of inflammatory brain lesions, including multiple sclerosis (MS) and stroke. A National Institutes of Health-sponsored clinical trial of iron oxide MRI agents for observation of intracerebral tumors and other CNS lesions is ongoing.

ROLE OF THE BBB IN DISEASE

Infections

Much is known about bacterial infections of the CNS (62). Bacteria such as meningococci (61) colonize the nose, enter the vascular system, and bind, via pili, to the endothelium of both the brain and the choroid plexus. In particular, the PilC protein, which is found on the tip of the pilus, is up-regulated in bacteria isolated from CSF, compared with bacteria in the blood, and this protein may play a crucial role in adhesion.

In the case of pneumococci (65), bacteria bind to the endothelial cell surface via platelet-activating factor receptors. The ensuing CNS infection induces increased vesicular transport across cells and separation of tight junctions, leading to the release of inflammatory peptides such as interleukin-1, tumor necrosis factor, and metalloproteinases (56). To decrease the inflammatory damage, corticosteroids are sometimes administered, but they can restore the BBB integrity, thus decreasing antibiotic delivery and slowing bacterial clearance from the

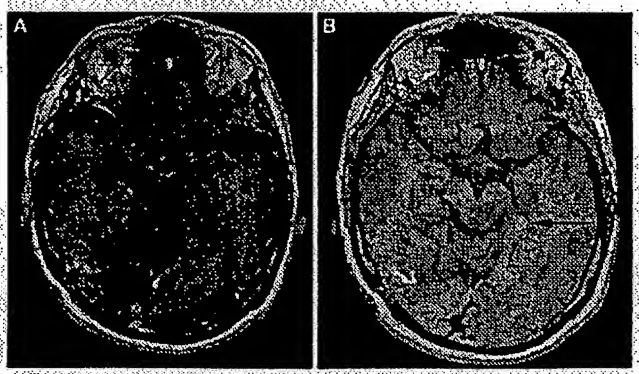

FIGURE 4. *MRI scans for a patient with a glioblastoma after an excellent response to temozolomide, a new oral chemotherapeutic drug that crosses the BBB very well. Residual disease was assessed on T1-weighted MRI scans, with two intravenously administered contrast agents. A, gadolinium-enhanced scan. B, ferumoxtran-10-enhanced scan. The residual lesion in the right hemisphere, which can be clearly observed with both gadolinium and ferumoxtran-10, should be noted. A left-side lesion that is not well detected with gadolinium but is easily observed with iron (arrows) should also be noted.*

CNS. However, corticosteroids can also decrease the rates of morbidity, such as hearing loss among young children with *Haemophilus influenzae* meningitis, and the benefits of adjunctive corticosteroid treatment thus remain controversial. Antioxidants such as *N*-acetylcysteine may be safer for decreasing CNS injury (4).

Some viruses (such as herpesvirus) enter the CNS via the olfactory nerves, and others (such as rabies virus) enter via spinal nerves (48). Some may enter via the circumventricular organs, but most probably cross the brain endothelium or the choroid plexus. In the case of HIV, brain endothelial cells lack the CD4 and galactosylceramide binding sites that are used by the virus to enter most cells. There is evidence that adsorptive endocytosis in response to cytokines can mediate uptake, although most HIV entry is via infected monocytes (57), which traverse abnormal tight junctions (14) and/or penetrate endothelial cells. After HIV has penetrated the BBB, it can proliferate in microglia and other non-neuronal parenchymal cells, to be released systemically to the venous blood via the arachnoid granulations and to the cervical lymph nodes via the olfactory tracts and nerves. Therefore, the CNS can function as both a reservoir and an HIV factory that releases the virus to the systemic circulation and the cervical lymph nodes, while being protected from systemically administered antiviral drugs by the BBB (82).

It is fortunate that infection may facilitate the influx of antibiotics, such as penicillin, across the BBB. For example, the CSF concentrations of penicillin G are usually approximately 0.4% of the steady-state serum levels in normal animals but CSF levels increase approximately 10-fold in animals with pneumococcal meningitis (48). BBB integrity varies with the type of infective agent; viruses cause minimal BBB damage, making delivery of antiviral agents a greater challenge for physicians. In general, BBB integrity may be better correlated with CSF protein levels than with CSF white blood cell counts, and CSF analyses may facilitate selection of appropriate doses of therapeutic agents. Monitoring of the CSF may also be prudent, because the BBB may be quickly reestablished as the infection subsides, reducing the permeability to antiinfective agents severalfold. The keys to the treatment of CNS bacterial infections are rapid establishment of bactericidal antibiotic levels and maintenance of such levels throughout the course of therapy (62).

Inflammatory CNS Disorders and MS

Lymphoid cells normally circulate in the vasculature, extravasate into tissues (including brain tissue), traffic through the lymphatic vessels (via arachnoid granulations or the olfactory nerves [32] in the CNS), and return to the circulation. Extravasation into the brain through the BBB may be influenced by weak inflammatory stimuli such as pain (27) and can be accentuated by stronger stimuli such as complete Freund's adjuvant, which can open the BBB to albumin, immunoglobulin G, and immunoglobulin M, without concomitant extravasation of lymphoid cells and without gliosis (63). Such extravasation may underlie CNS lupus, in which there is usually minor vasculopathy despite profound encephalopathy.

Infections and other immunological stimuli, such as Freund's adjuvant plus myelin basic protein, can cause experimental allergic encephalomyelitis (EAE) in animals (48). Experimental allergic encephalomyelitis is widely, but not uniformly, considered to be a model of MS. In both MS and experimental allergic encephalomyelitis, increased BBB permeability and lymphoid cell extravasation (59) across the BBB (*Fig. 5*) are early events (52). Extravasation of $CD4^+$ T cells sensitized to several self-myelin and nonmyelin MS antigens mediate the hallmark of MS, namely, demyelination. Lymphoid cells may transverse the cerebral capillaries through and/or between endothelial cells; the exact route is not clear. Locally produced antibodies are also involved and result in

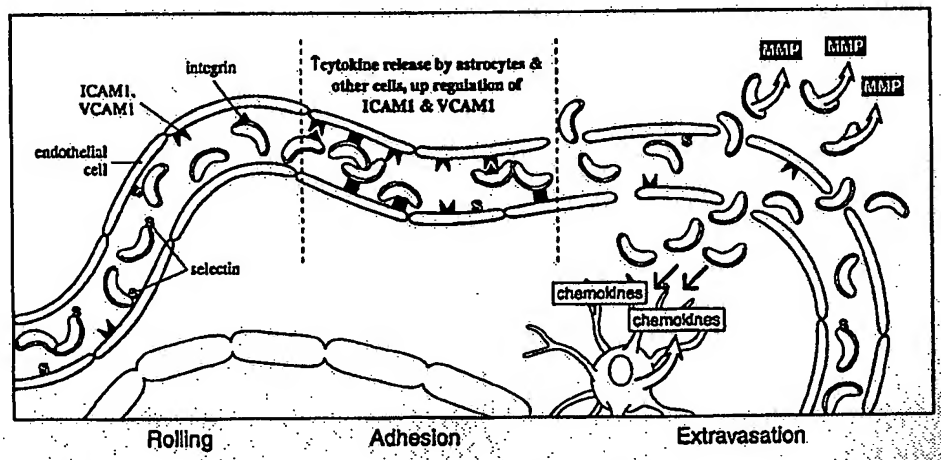

FIGURE 5. *Diagram of the extravasation process. Lymphoid cells roll along the endothelium in the body because of binding between selectins and their carbohydrate ligands, leading to firm adhesion of integrins to an immunoglobulin G-like superfamily, including intercellular adhesion molecule-1 (ICAM1) and vascular cell adhesion molecule-1 (VCAM1). Molecules such as intercellular adhesion molecule-1 are normally only barely detectable on the cerebral endothelial surface, but their expression is up-regulated in response to proinflammatory cytokines released by astrocytes and other cells (2). Such cytokines include tumor necrosis factor-α, interleukin-1β, and interferon-γ. Lymphoid cell adhesion results in rearrangement of the actin cytoskeleton of endothelial cells via a number of mediators, opening the BBB to lymphoid cell extravasation. Lymphoid cells and macrophages are attracted to the CNS by low-molecular weight chemokines (chemotactic cytokines), some of which are released by astrocytes. As the lymphoid cells ($CD4^+$ T cells) and macrophages extravasate, they release matrix metalloproteinases (MMP), which digest the extracellular matrix (31). Inhibitors of metalloproteinases represent an effective treatment for experimental allergic encephalomyelitis. Recent studies emphasized integrin binding to adhesion molecules but questioned the role of selectins in the brain (3, 85).*

oligoclonal bands with CSF electrophoresis, which represents an important diagnostic finding (48). Corticosteroids decrease the BBB leakiness in MS (20), whereas the three major therapeutic agents (15) (interferon-1β, interferon-1α, and glatiramer acetate) all decrease the passage of immune cells across the BBB. BBB compromise and extravasation of lymphoid cells (59) via adhesion molecules, with modulation by cytokines and chemokines, are key events early in the pathogenesis of MS and autoimmune inflammatory diseases.

Cerebrovascular Disease

The integrity of the BBB in cerebrovascular disease attributable to hypertension (29) or cardiac bypass (72) is variable, because the underlying cerebral ischemia varies with respect to mechanism, severity, and duration (11, 66). During ischemia, decreasing nutrient levels can lead to endothelial membrane failure, as can nitric oxide, which may be produced by the free radicals formed as a result of oxygen deprivation. Ischemia can also have effects similar to those of inflammatory disorders, leading, as noted, to the activation of cytokines such as tumor necrosis factor and interleukin-1 and the upregulation of cell adhesion molecules. White blood cells can then penetrate the BBB, releasing proteases (particularly metalloproteinases) and resulting in both cytotoxic and vasogenic edema; the latter is attributable to BBB opening, which can be detected on enhanced CT and/or MRI scans. Unlike with vasogenic edema observed in CNS tumors, corticosteroids have little effect on ischemia-induced edema, just as they have little effect on edema produced by trauma. Ischemia may also compromise the BBB by increasing vesicular transport across the BBB and by opening tight junctions. Transient ischemia is normally worse than permanent occlusion attributable to reperfusion injury (66). Hyponatremia, hyperglycemia, and fever can all exacerbate the process.

Cerebral insults such as stroke and trauma illustrate two basic concepts of BBB biological processes (6, 39, 66). The first is that BBB opening in and around the stroke or trauma can be biphasic, particularly after reperfusion injury (37). The second is that BBB opening is different for small versus large molecules. Among patients with ischemic infarctions, technetium-labeled diethylenetriamine penta-acetic acid (M_r 398) can penetrate the BBB, whereas technetium-labeled albumin (approximately M_r 68,000) cannot (24). More severe infarctions, however, can induce opening to both large and small molecules (48), suggesting that ischemic patients with more BBB damage may have greater risks of hemorrhage after fibrinolysis (i.e., reperfusion). In such cases, the administration of neurotropins with genetic delivery vectors may be neuroprotective if performed within 60 minutes (79).

Finally, the location of the BBB damage may depend on the type of cerebrovascular disease (48). Openings at capillaries are more likely with ischemia, whereas openings at arterioles are more often produced by diabetic vasculopathy, emboli, and hypertension and openings at venules can be induced by subarachnoid hemorrhage.

CNS Tumors

Therapeutic options for the treatment of primary and metastatic tumors have been limited because of the BBB. Perioperative corticosteroid administration has reduced the mortality rates associated with brain tumor surgery from more than 50% to less than 5%, by rapidly restoring BBB integrity (12) and thus decreasing vasogenic cerebral edema and contrast agent enhancement. However, chemotherapy has proven only marginally successful (75, 87); for sensitive tumors such as small cell lung cancers, breast cancers, lymphomas, and germ cell tumors, there may be complete systemic responses to chemotherapy concomitant with tumor progression in the CNS (16).

There are several reasons for this difference in systemic versus CNS responses (36). The BBB is extremely heterogeneous and is frequently more permeable in the center of a malignant tumor, whereas the well-vascularized, actively proliferating, infiltrating edge, which is sometimes referred to as the brain tissue adjacent to the tumor, exhibits a variable degree of BBB integrity (*Fig. 6*) (75). These different permeabilities result in sharply reduced concentrations of chemotherapeutic agents at the rapidly growing periphery, because of limited diffusion from the central leaky hypoxic tumor (88). This is termed the sink effect, and it can contribute to chemotherapy failure.

In addition, because the bulk of a tumor gradually decreases with treatment, BBB integrity often recovers. In the case of primary CNS lymphomas, positron emission tomographic scans demonstrated that BBB integrity may be reestablished after 6 weeks of chemotherapy (53), but responses are short-lived unless high-dose chemotherapy and/or BBB modification techniques are used to enhance delivery as the BBB recovers. Indeed, BBBD-enhanced delivery of chemotherapeutic agents was observed to increase survival rates for patients with primary CNS lymphomas, with outcomes being statistically correlated with the number and degree of BBBDs (33).

BBBD has led to responses that are durable for primary CNS lymphomas and, although the approach is invasive, it has been used with relatively little toxicity. Kraemer et al. (33) reported an association between total dose intensity and survival times among 74 patients with primary CNS lymphomas (highly chemosensitive brain tumors) treated with BBBD (42). Using the total number of disruptions as a surrogate measure of total dose intensity (a weighted quality of disruption score is also discussed [33]), those authors demonstrated a statistically significant association between the number of disruptions (as a time-dependent covariate) and overall survival times for the patients, after adjustment for age, performance status, sex, and prior chemotherapy. *Figure 7* presents a Kaplan-Meier plot of overall survival times among patients grouped according to the number of BBBDs (corresponding to approximately 3-mo intervals). After accounting for survival bias, this analysis confirms the importance of total dose intensity (delivered in many courses, rather than in a short period) in the treatment of primary CNS lymphomas with BBBD.

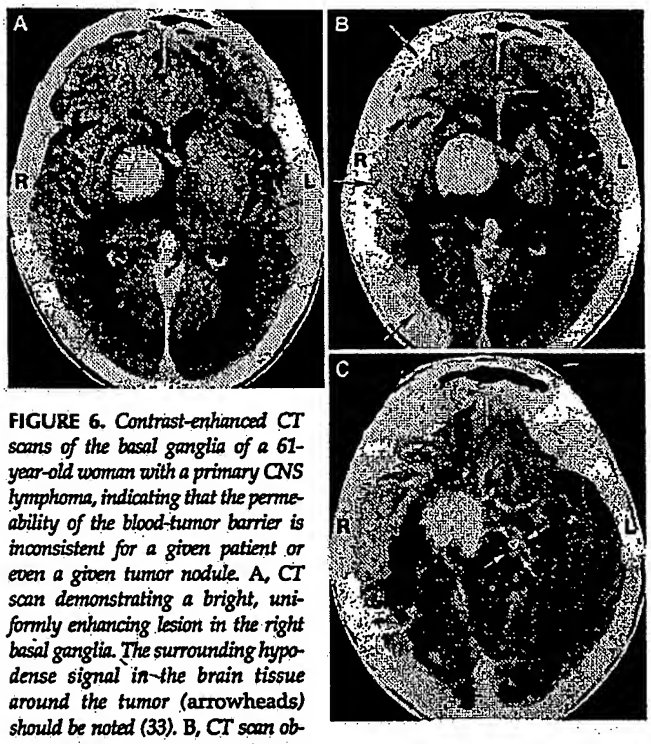

FIGURE 6. *Contrast-enhanced CT scans of the basal ganglia of a 61-year-old woman with a primary CNS lymphoma, indicating that the permeability of the blood-tumor barrier is inconsistent for a given patient or even a given tumor nodule. A, CT scan demonstrating a bright, uniformly enhancing lesion in the right basal ganglia. The surrounding hypodense signal in the brain tissue around the tumor (arrowheads) should be noted (33). B, CT scan obtained after contrast agent administration. Contrast material was administered immediately after osmotic BBBD and CT scans were obtained 30 minutes after the first BBBD treatment, to confirm and assess the grade of BBBD. The patient underwent right internal carotid artery disruption in the anterior and middle cerebral artery distributions (arrows). Opening of the brain tissue around the tumor in the area of the peritumoral hypodense signal evident in the CT scan in A should be noted (33). C, CT scan obtained after BBBD in a patient with a right hemiparesis that was unexplained, because the only visible tumor was in the right cerebrum (A). BBBD the day after the CT scan in A extended into the posterior circulation via the posterior communicating artery. A left-side brainstem lesion not apparent in pre-BBBD imaging studies was noted. The right hemiparesis was thus attributable to a brainstem tumor (arrows) on the left that was not apparent on pre-BBBD MRI scans (intact BBB and no edema). Silbergeld and Chicoine (76) demonstrated tumor cells 4 cm from T2-weighted abnormalities among patients undergoing stereotactic biopsies.*

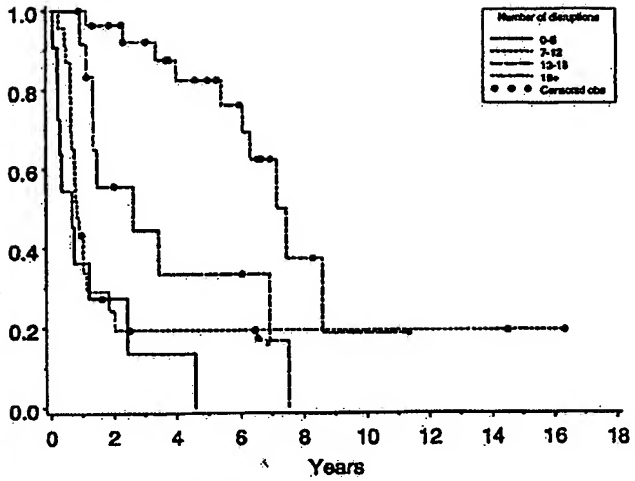

FIGURE 7. *Kaplan-Meier plot of overall survival rates for patients with non-AIDS primary CNS lymphomas treated with BBBD-delivered methotrexate. Patients were grouped according to the total number of courses; the groups represent approximate treatment periods of less than 3 months, 3 to 6 months, 6 to 9 months, or 9 to 12 months (33). Circles, censored observations. These results confirm the importance of dose intensity in the treatment of CNS neoplasms.*

Other BBB-bypass methods that may help patients with tumors include stem cell rescue in the treatment of oligodendrogliomas, as a means to avoid radiotherapy, which too often impairs cognitive function (17), and dendritic cell vaccines, which induce T cells to cross the BBB to the brain (91).

CONCLUSION

Endothelial cells, in addition to glia and neurons, should be considered integral components of the CNS. Indeed, in both health and disease and extending to old age (69, 74, 80), these three cell types should be studied mechanistically as a neurovascular unit. Attention currently directed toward delivery of neurotherapeutic agents across the cerebral endothelium is modest, compared with studies of the other two components of the neurovascular unit. More research is needed to allow us to better understand and exploit the endothelium and to develop desperately needed therapeutic agents.

DISCLOSURE

EAN and the Oregon Health & Science University have significant financial interests in Adherex, a company that has a commercial interest in the results of this research and technology. This potential conflict of interest has been reviewed and managed by the Oregon Health & Science University Conflict of Interest in Research Committee. For more information, contact the Oregon Health & Science University Research Integrity Office (telephone: 503/494-7887).

REFERENCES

1. Abbott NJ, Romero IA: Transporting therapeutics across the blood-brain barrier. Mol Med Today 2:106–113, 1996.
2. Adamson P, Etienne S, Couraud PO, Calder V, Greenwood J: Lymphocyte migration through brain endothelial cell monolayers involves signaling through endothelial ICAM-1 via a rho-dependent pathway. J Immunol 162:2964–2973, 1999.
3. Alon R: Encephalitogenic lymphoblast recruitment to resting CNS microvasculature: A natural immunosurveillance mechanism? J Clin Invest 108: 517–519, 2001.
4. Auer M, Pfister LA, Leppert D, Täuber MG, Leib SL: Effects of clinically used antioxidants in experimental pneumococcal meningitis. J Infect Dis 182:347–350, 2000.
5. Balabanov R, Dore-Duffy P: Role of the CNS microvascular pericyte in the blood-brain barrier. J Neurosci Res 53:637–644, 1998.
6. Baldwin SA, Fugaccia I, Brown DR, Brown LV, Scheff SW: Blood-brain barrier breach following cortical contusion in the rat. J Neurosurg 85:476–481, 1996.

7. Begley D, Kreuter JE: Drug delivery and targeting to the CNS. J Drug Target 10:261–358, 2002.
8. Bokstein F, Lossos A, Lossos JS, Siegal T: Central nervous system relapse of systemic non-Hodgkin's lymphoma: Results of treatment based on high-dose methotrexate combination chemotherapy. Leuk Lymphoma 43:587–593, 2002.
9. Bradbury M: *The Concept of a Blood-Brain Barrier*. Chichester, John Wiley & Sons, 1979.
10. Brem H, Gabikian P: Biodegradable polymer implants to treat brain tumors. J Control Release 74:63–67, 2001.
11. Brott T, Bogousslavsky J: Treatment of acute ischemic stroke. N Engl J Med 343:710–722, 2000.
12. Cairncross JG, Macdonald DR, Pexman JHW, Ives FJ: Steroid-induced CT changes in patients with recurrent malignant glioma. Neurology 38:724–726, 1988.
13. Chen MY, Lonser RR, Morrison PF, Governale LS, Oldfield EH: Variables affecting convection-enhanced delivery to the striatum: A systematic examination of rate of infusion, cannula size, infusate concentration, and tissue-cannula sealing time. J Neurosurg 90:315–320, 1999.
14. Dallasta LM, Pisarove LA, Esplen JE, Werley JV, Moses AV, Nelson JA, Achim CL: Blood-brain barrier tight junction disruption in human immunodeficiency virus-1 encephalitis. Am J Pathol 155:1915–1927, 1999.
15. Dhib-Jalbut S: Mechanisms of action of interferons and glatiramer acetate in multiple sclerosis. Neurology 58[Suppl 4]:S3–S9, 2002.
16. Doolittle ND, Abrey LE, Ferrari N, Hall WA, Laws ER Jr, McLendon RE, Muldoon LL, Peereboom D, Peterson DR, Reynolds CP, Senter P, Neuwelt EA: Targeted delivery in primary and metastatic brain tumors: Enhanced delivery versus neurotoxicity. Clin Cancer Res 8:1702–1709, 2002.
17. Doolittle ND, Anderson CP, Bleyer WA, Cairncross JG, Cloughesy T, Eck SL, Guastadisegni P, Hall WA, Muldoon LL, Patel SJ, Peereboom D, Siegal T, Neuwelt EA: Importance of dose intensity in neuro-oncology clinical trials: Summary report of the Sixth Annual Meeting of the Blood-Brain Barrier Disruption Consortium. Neuro-oncol 3:46–54, 2001.
18. Freed CR, Greene PE, Breeze RE, Tsai WY, DuMouchel W, Kao R, Dillon S, Winfield H, Culver S, Trojanowski JQ, Eidelberg D, Fahn S: Transplantation of embryonic dopamine neurons for severe Parkinson's disease. N Engl J Med 344:710–719, 2001.
19. Friden PM, Walus LR, Watson P, Doctrow SR, Kozarich JW, Backman C, Bergman H, Hoffer B, Bloom F, Granholm AC: Blood-brain penetration and in vivo activity of an NGF conjugate. Science 259:373–377, 1993.
20. Gasperini C, Pozzilli C, Bastianello S, Koudriavtseva T, Galgani S, Millefiorini E, Paolillo A, Horsfield MA, Bozzao L, Fieschi C: Effect of steroids on Gd-enhancing lesions before and during recombinant β interferon 1a treatment in relapsing remitting multiple sclerosis. Neurology 50:403–406, 1998.
21. Goldman D: Membrane transport of chemotherapeutics and drug resistance: Beyond the ABC family of exporters to the role of carrier-mediated processes. Clin Cancer Res 8:4–6, 2002.
22. Goldstein GW, Betz AL: The blood-brain barrier. Sci Am 255:74–83, 1986.
23. Groothuis DR, Ward S, Itskovich AC: Comparison of D-sucrose delivery to the brain by intravenous, intraventricular, and convection-enhanced intracerebral infusion. J Neurosurg 90:321–331, 1999.
24. Gumerlock MK: Cerebrovascular disease and the blood-brain barrier, in Neuwelt EA (ed): *The Clinical Impact of the Blood-Brain Barrier and Its Manipulation*. New York, Plenum Press, 1989, pp 495–565.
25. Hochman J, Assaf N, Deckert-Schlüter M, Wiestler OD, Pe'er J: Entry routes of malignant lymphoma into the brain and eyes in a mouse model. Cancer Res 61:5242–5247, 2001.
26. Huber JD, Egleton RD, Davis TP: Molecular physiology and pathophysiology of tight junctions in the blood-brain barrier. Trends Neurosci 24:719–725, 2001.
27. Huber JD, Witt KA, Hom S, Egleton RD, Mark KS, Davis TP: Inflammatory pain alters blood-brain barrier permeability and tight junctional protein expression. Am J Physiol 280:H1241–H1248, 2001.
28. Johanson CE, Jones HC: Promising vistas in hydrocephalus and cerebrospinal fluid research. Trends Neurosci 24:631–632, 2001.
29. Johansson BB: Hypertension mechanisms causing stroke. Clin Exp Pharmacol Physiol 26:563–565, 1999.
30. Kay GG: The effects of antihistamines on cognition and performance. J Allergy Clin Immunol 105[Suppl 6]:S622–S627, 2000.
31. Kieseler BC, Seifert TS, Giovannoni G, Hartung HP: Matrix metalloproteinases in inflammatory demyelination: Targets for treatment. Neurology 53:20–25, 1999.
32. Knopf PM, Harling-Berg CJ, Cserr HF, Basu D, Sirulnick EJ, Nolan SC, Park JT, Keir G, Thompson EJ, Hickey WF: Antigen-dependent intrathecal antibody synthesis in the normal rat brain: Tissue entry and local retention of antigen-specific B cells. J Immunol 161:692–701, 1998.
33. Kraemer DF, Fortin D, Doolittle ND, Neuwelt EA: Association of total dose intensity of chemotherapy in primary central nervous system lymphoma (human non-acquired immunodeficiency syndrome) and survival. Neurosurgery 48:1033–1041, 2001.
34. Kraemer DF, Fortin D, Neuwelt EA: Chemotherapeutic dose intensification for treatment of malignant brain tumors: Recent developments and future directions. Curr Neurol Neurosci Rep 2:216–224, 2002.
35. Krivit W, Shapiro EG, Peters C, Wagner JE, Cornu G, Kurtzberg J, Wenger DA, Kolodny EH, Vanier MT, Loes DJ, Dusenbery K, Lockman LA: Hematopoietic stem-cell transplantation in globoid-cell leukodystrophy. N Engl J Med 338:1119–1126, 1998.
36. Kroll RA, Neuwelt EA: Outwitting the blood-brain barrier for therapeutic purposes: Osmotic opening and other means. Neurosurgery 42:1083–1100, 1998.
37. Kuroiwa T, Ting P, Martinez H, Klatzo I: The biphasic opening of the blood-brain barrier to proteins following temporary middle cerebral artery occlusion. Acta Neuropathol (Berl) 68:122–129, 1985.
38. Lang AE, Lozano AM: Parkinson's disease: First of two parts. N Engl J Med 339:1044–1053, 1998.
39. Laohaprasit V, Silbergeld DL, Ojemann GA, Eskridge JM, Winn HR: Postoperative CT contrast enhancement following lobectomy for epilepsy. J Neurosurg 73:392–395, 1990.
40. Leeds NE, Kieffer SA: Evolution of diagnostic neuroradiology from 1904 to 1999. Radiology 217:309–318, 2000.
41. Leino RL, Gerhart DZ, Drewes LR: Monocarboxylate transporter (MCT1) abundance in brains of suckling and adult rats: A quantitative electron microscopic immunogold study. Brain Res Dev Brain Res 113:47–54, 1999.
42. McAllister LD, Doolittle ND, Guastadisegni PE, Kraemer DF, Lacy CA, Crossen JR, Neuwelt EA: Cognitive outcomes and long-term follow-up after enhanced chemotherapy delivery for primary central nervous system lymphomas. Neurosurgery 46:51–61, 2000.
43. McCarthy TJ, Banks WA, Farrell CL, Adamu S, Derdeyn CP, Snyder AZ, Laforest R, Litzinger DC, Martin D, LeBel CP, Welch MJ: Positron emission tomography shows that intrathecal leptin reaches the hypothalamus in baboons. J Pharmacol Exp Ther 301:878–883, 2002.
44. Mealey KL, Bentjen SA, Gay JM, Cantor GH: Ivermectin sensitivity in collies is associated with a deletion mutation of the *mdr1* gene. Pharmacogenetics 11:727–733, 2001.
45. Muldoon LL, Nilaver G, Kroll RA, Pagel MA, Breakefield XO, Chiocca EA, Davidson BL, Weissleder R, Neuwelt EA: Comparison of intracerebral inoculation and osmotic blood-brain barrier disruption for delivery of adenovirus, herpesvirus and iron oxide particles to normal rat brain. Am J Pathol 147:1840–1851, 1995.
46. Muldoon LL, Pagel MA, Kroll RA, Roman-Goldstein S, Jones RS, Neuwelt EA: A physiological barrier distal to the anatomic blood-brain barrier in a model of transvascular delivery. AJNR Am J Neuroradiol 20:217–222, 1999.
47. Muldoon LL, Varallyay P, Kraemer DF, Kiwic G, Pinkston K, Walker-Rosenfeld SL, Neuwelt EA: Trafficking of superparamagnetic iron oxide particles (Combidex) from brain to lymph nodes in the rat. Neuropathol Appl Neurobiol (in press).
48. Neuwelt EA: *Implications of the Blood-Brain Barrier and Its Manipulation*. New York, Plenum Press, 1989.
49. Neuwelt EA, Abbott NJ, Drewes L, Smith QR, Couraud PO, Chiocca EA, Audus KL, Greig NH, Doolittle ND: Cerebrovascular biology and the various neural barriers: Challenges and future directions. Neurosurgery 44: 604–609, 1999.
50. Neuwelt EA, Brummett RE, Doolittle ND, Muldoon LL, Kroll RA, Pagel MA, Dojan R, Church V, Remsen LG, Bubalo JS: First evidence of otoprotection against carboplatin-induced hearing loss with a two compartment system in patients with central nervous system malignancy using sodium thiosulfate. J Pharmacol Exp Ther 286:77–84, 1998.

51. Ningaraj NS, Rao M, Hashizume K, Asotra K, Black KL: Regulation of the blood-brain barrier permeability by calcium-activated potassium channels. J Pharmacol Exp Ther 301:838–851, 2002.
52. Noseworthy JH, Lucchinetti C, Rodriguez M, Weinshenker BG: Multiple sclerosis. N Engl J Med 343:938–952, 2000.
53. Ott RJ, Brada M, Flower MA, Babich JW, Cherry SR, Deehan BJ: Measurements of blood-brain barrier permeability in patients undergoing radiotherapy and chemotherapy for primary cerebral lymphoma. Eur J Cancer 27: 1356–1361, 1991.
54. Pardridge WM: CNS drug design based on principles of blood-brain barrier transport. J Neurochem 70:1781–1792, 1998.
55. Pardridge WM: *Introduction to the Blood-Brain Barrier: Methodology, Biology and Pathology*. Cambridge, Cambridge University Press, 1998.
56. Paul R, Lorenzl S, Koedel U, Sporer B, Vogel U, Frosch M, Pfister HW: Matrix metalloproteinases contribute to the blood-brain barrier disruption during bacterial meningitis. Ann Neurol 44:592–600, 1998.
57. Persidsky Y, Ghorpade A, Rasmussen J, Limoges J, Liu XJ, Stins M, Fiala M, Way D, Kim KS, Witte MH, Weinand M, Carhart L, Gendelman HE: Microglial and astrocyte chemokines regulate monocyte migration through the blood-brain barrier in human immunodeficiency virus-1 encephalitis. Am J Pathol 155:1599–1611, 1999.
58. Pietz J, Kreis R, Rupp A, Mayatepek E, Rating D, Boesch C, Bremer HJ: Large neutral amino acids block phenylalanine transport into brain tissue in patients with phenylketonuria. J Clin Invest 103:1169–1178, 1999.
59. Prat A, Biernacki K, Lavoi JF, Poirier J, Duquette P, Antel JP: Migration of multiple sclerosis lymphocytes through brain endothelium. Arch Neurol 59:391–397, 2002.
60. Press OW, Corcoran M, Subbiah K, Hamlin DK, Wilbur DS, Johnson T, Theodore L, Yau E, Mallett R, Meyer DL, Axworthy D: A comparative evaluation of conventional and pretargeted radioimmunotherapy of CD20-expressing lymphoma xenografts. Blood 98:2535–2343, 2001.
61. Pron B, Taha MK, Rambaud C, Fournet JC, Pattey N, Monnet JP, Musilek M, Beretti JL, Nassif X: Interaction of *Neisseria meningitidis* with the components of the blood-brain barrier correlates with an increased expression of PilC. J Infect Dis 176:1285–1292, 1997.
62. Quagliarello VJ, Scheld WM: Treatment of bacterial meningitis. N Engl J Med 336:708–716, 1997.
63. Rabchevsky AG, Degos JD, Dreyfus PA: Peripheral injections of Freund's adjuvant in mice provoke leakage of serum proteins through the blood-brain barrier without inducing reactive gliosis. Brain Res 832:84–96, 1999.
64. Ram Z, Culver KW, Oshiro EM, Viola JJ, DeVroom HL, Otto E, Long Z, Chiang Y, McGarrity GJ, Muul LM, Katz D, Blaese RM, Oldfield EH: Therapy of malignant brain tumors by intratumoral implantation of retroviral vector-producing cells. Nat Med 3:1354–1361, 1997.
65. Ring A, Weiser JN, Tuomanen EI: Pneumococcal trafficking across the blood-brain barrier: Molecular analysis of a novel bidirectional pathway. J Clin Invest 102:347–360, 1998.
66. Rosenberg GA: Ischemic brain edema. Cardiovasc Dis 42:209–216, 1999.
67. Sanchez del Pino MM, Hawkins RA, Peterson DR: Neutral amino acid transport by the blood-brain barrier. J Biol Chem 270:14913–14918, 1995.
68. Sawchuk RJ, Elmquist WF: Microdialysis in the study of drug transporters in the CNS. Adv Drug Deliv Rev 45:295–307, 2000.
69. Schenk D, Barbour R, Dunn W, Gordon G, Grajeda H, Guido T, Hu K, Huang J, Johnson-Wood K, Khan K, Kholodenko D, Lee M, Liao Z, Lieberburg I, Motter R, Mutter L, Soriano F, Shopp G, Vasquez N, Vandevert C, Walker S, Wogulis M, Yednock T, Games D, Seubert P: Immunization with amyloid-β attenuates Alzheimer-disease-like pathology in the PDAPP mouse. Nature 400:173–177, 1999.
70. Schinkel AH, Wagenaar E, Mol C, van Deemter L: P-glycoprotein in the blood-brain barrier of mice influences the brain penetration and pharmacological activity of many drugs. J Clin Invest 97:2517–2524, 1996.
71. Schwarze SR, Ho A, Vocero-Akbani A, Dowdy SF: In vivo protein transduction: Delivery of a biologically active protein into the mouse. Science 285:1569–1572, 1999.
72. Selnes OA, McKhann GM: Coronary-artery bypass surgery and the brain. N Engl J Med 344:451–452, 2001.
73. Shi N, Pardridge WM: Noninvasive gene targeting to the brain. Proc Natl Acad Sci U S A 97:7567–7572, 2000.
74. Shibata M, Yamada S, Kuma SR, Calero M, Bading J, Frangione B, Holtzman DM, Miller CA, Strickland DK, Ghiso J, Zlokovic BV: Clearance of Alzheimer's amyloid peptide from brain by LDL receptor-related protein-1 at the blood-brain barrier. J Clin Invest 106:1489–1499, 2000.
75. Siegal T, Zylber-Katz E: Strategies for increasing drug delivery to the brain. Clin Pharmacokinet 41:171–186, 2002.
76. Silbergeld DL, Chicoine MR: Isolation and characterization of human malignant glioma cells from histologically normal brain. J Neurosurg 86:525–531, 1997.
77. Sly WS, Vogler C: Brain-directed gene therapy for lysosomal storage disease: Going well beyond the blood-brain barrier. Proc Natl Acad Sci U S A 99:6216–6221, 2002.
78. Smith QR, Fisher C, Parepally J: Kinetics of in vivo chlorambucil efflux from brain. Pharm Res 4:W4238, 2002 (abstr).
79. Song BW, Vinters HV, Wu D, Pardridge WM: Enhanced neuroprotective effects of basic fibroblast growth factor in regional brain ischemia after conjugation to a blood-brain barrier delivery vector. J Pharmacol Exp Ther 301:605–610, 2002.
80. Steinberg D: Companies halt first Alzheimer vaccine trial. Scientist 16:22, 2002.
81. Stover JF, Kempski OS: Glutamate-containing parenteral nutrition doubles plasma glutamate: A risk factor in neurosurgical patients with blood-brain barrier damage? Crit Care Med 27:2252–2256, 1999.
82. Strelow LI, Janigro D, Nelson JA: The blood-brain barrier and AIDS. Adv Virus Res 56:355–388, 2001.
83. Takasato Y, Rapoport SI, Smith QR: An in situ brain perfusion technique to study cerebrovascular transport in the rat. Am J Physiol 247[Suppl 3]:H484–H493, 1984.
84. Tofteng F, Larsen FS: Monitoring extracellular concentrations of lactate, glutamate, and glycerol by in vivo microdialysis in the brain during liver transplantation in acute liver failure. Liver Transplant 8:302–305, 2002.
85. Vajkoczy P, Laschinger M, Engelhardt B: α4-integrin-VCAM-1 binding mediates G protein-independent capture of encephalitogenic T cell blasts to CNS white matter microvessels. J Clin Invest 108:557–565, 2001.
86. Varallyay P, Nesbit G, Muldoon LL, Nixon RR, Delashaw J, Cohen J, Petrillo A, Rink D, Neuwelt EA: Comparison of two superparamagnetic viral-sized iron oxide particles ferumoxides and ferumoxtran-10 with a gadolinium chelate in imaging intracranial tumors. AJNR Am J Neuroradiol 23:510–519, 2002.
87. Vick NA, Khandekar JD, Bigner DD: Chemotherapy of brain tumors. Ann Neurol 34:523–526, 1977.
88. Walker MD, Weiss H: Chemotherapy in the treatment of malignant brain tumors. Adv Neurol 13:149–191, 1975.
89. Wolraich ML, Lindgren SD, Stumbo PJ, Stegink LD, Appelbaum MI, Kiritsy MC: Effects of diets high in sucrose or aspartame on the behavior and cognitive performance of children. N Engl J Med 330:301–307, 1994.
90. Yanovski SZ, Yanovski JA: Drug therapy: Obesity. N Engl J Med 346:591–602, 2002.
91. Yu JS, Wheeler CJ, Zeltzer PM, Ying H, Finger DN, Lee PK, Yong WH, Incardona F, Thompson RC, Riedinger MS, Zhang W, Prins RM, Black KL: Vaccination of malignant glioma patients with peptide-pulsed dendritic cells elicits systemic cytotoxicity and intracranial T-cell infiltration. Cancer Res 61:842–847, 2001.
92. Zlokovic BV, Apuzzo MLJ: Strategies to circumvent vascular barriers of the central nervous system. Neurosurgery 43:877–878, 1998.
93. Zlokovic BV, Jovanovic S, Miao W, Samara S, Verma S, Farrell CL: Differential regulation of leptin transport by the choroid plexus and blood-brain barrier and high affinity transport systems for entry into hypothalamus and across the blood-cerebrospinal fluid barrier. Endocrinology 141:1434–1441, 2000.

Acknowledgments

This work was supported by the Veterans Administration and the National Institutes of Health (Grants NS34608, NS33618, and NS44687). We especially thank Drs. Thomas Jacobs, Thomas Davis, Quentin Smith, and William Elmquist for constructive suggestions and Dr. Tom Fagan for editing expertise.

COMMENTS

This is a superb review of the current status of the blood-brain barrier (BBB) in health and disease. It is packed with the most up-to-date information and is both well written and extremely easy to read. Basic research findings are translated into clinical relevance, and the article provides the reader an in-depth understanding of the physiology and pharmacology of how solutes (nutrients, endogenous peptides, proteins, and immune cells as well as exogenous drugs) either gain access to or are limited from the brain and cerebrospinal fluid in both health and disease. The status of the barrier changes vastly depending on the disease state, as critically reviewed by the author. Nevertheless, this physiological, pharmacological, and enzymatic barrier remains a nemesis in effective treatment of numerous neurological diseases. In many cases, effective drugs have been designed that incorporate the appropriate physicochemical features to maintain efficacious concentrations at the disease target within either the brain or cerebrospinal fluid; for other diseases, such drugs are not available and may never be developed. Entrepreneurial strategies to outwit the BBB have become crucial, and the most interesting have been critically reviewed. Such techniques have allowed innovative clinicians and scientists, as exemplified by the author, to make better use of currently available drugs whose conventional use in the treatment of brain-sequestered diseases is associated with poor outcome.

Nigel H. Greig
Baltimore, Maryland

In this excellent review, Neuwelt has described the BBB in terms of both anatomy and physiology. He has also described techniques used to break down the BBB to allow for passage of large-molecular-weight compounds. Neuwelt has published extensively on this subject and has presented a large body of data suggesting that BBB breakdown can include the efficacy of therapy using large-molecular-weight compounds, especially for the treatment of central nervous system (CNS) lymphoma.

I believe this review is useful in bringing a reader up to date in a concise fashion. One can only hope that these techniques can be applied to the treatment of other diseases with the goal of increasing efficacy.

Corey Raffel
Rochester, Minnesota

In this insightful review, Neuwelt presents current knowledge about the BBB and its role in the pathogenesis of various disorders of the CNS. Clearly, the physiological activity of the BBB affects virtually all aspects of brain function in both health and disease. Awareness of this fact compels us to revise previous concepts about the CNS and embrace a more encompassing notion of the neurovascular unit, which considers the endothelial cell of brain capillaries to be just as integral to neurophysiology as the neuron and glial cell.

As the author shows, the BBB has traditionally been an impediment to treatment of CNS disorders. It is estimated that more than 98% of all potential CNS drugs do not cross this partition (2). In a previous article, however, he labeled the BBB the "Achilles' heel of CNS therapeutics" and presaged potential opportunities for outwitting it (3).

For instance, adsorptive endocytosis allows the ingress of specific peptides and proteins across the BBB. Approximately 15 transporters have been characterized so far, and more than 50 may exist (2). Drug conjugation to ligands or antibodies directed against these receptors can enhance entry into the brain via transcytosis. This "Trojan horse" strategy has successfully escorted therapeutic molecules across the BBB in animal models of stroke and brain tumors. The BBB can also be transiently opened with brief intra-arterial infusions of hypertonic solutions, such as mannitol or arabinose, that produce osmotic shrinkage of the endothelial cells and mechanical separation of the tight junctions, or with the infusion of various inflammatory mediators.

When coupled with these techniques of permeabilizing the BBB, selective intra-arterial delivery of genetic or cellular therapeutic agents to the CNS may circumvent many of the limitations imposed by conventional routes of access (1). The advantages of this strategy over craniotomy or stereotactic instillation include the potential for widespread distribution, the ability to deliver large volumes, limited perturbation of neural tissue, and the feasibility of repeated administration. Therapeutic agents may be injected into the CNS arterial system as liquid suspensions or may be integrated into mechanical scaffolds (such as stents or coils) that are deposited intravascularly, allowing release of the biological mediator with regulated temporal and spatial profiles. Polymers such as poly-L-lactic acid and polyglycolic acid have been engineered with mechanical properties, porosity, and degradation rates favorable for their use as reservoirs for intravascular delivery of therapeutic agents. Biodegradable polymeric coils and stents have provided the platforms for local delivery of recombinant growth factors, cell cytokines, recombinant viruses, and other gene therapy vectors after endovascular placement. Incorporation of gene therapy vectors into resorbable endoluminal stents and coils has allowed site-specific, sustained transduction of cells of vessel walls, including the adventitia. Impregnating these devices with more mobile vehicles, such as neural progenitor cells, may allow gene transfer into the surrounding parenchyma as well.

Therefore, it is reasonable to envision catheter-based deposition of molecular, genetic, and cellular therapies that treat both the arterial wall and neighboring tissues of the brain and that are based on emerging understanding of the physiology of the BBB (1). Thus, the review that Neuwelt has provided is both timely and vital.

Arun Paul Amar
New Haven, Connecticut
Michael L.J. Apuzzo
Los Angeles, California

1. Amar AP, Zlokovic BV, Apuzzo MLJ: Endovascular restorative neurosurgery: A novel concept for molecular and cellular therapy of the nervous system. Neurosurgery 52:402–413, 2003.

2. Miller G: Breaking down barriers. Science 297:1116–1118, 2002.
3. Neuwelt EA, Abbott NJ, Drewes L, Smith QR, Couraud PO, Chiocca EA, Audus KL, Greig NH, Doolittle ND: Cerebrovascular biology and the various neural barriers: Challenges and future directions. Neurosurgery 44:604–609, 1999.

This authoritative review covers a broad range of issues related to the BBB, ranging from basic principles of function under physiological conditions to disrupted or altered function in selected disease states. Some of the highlights of the section on physiological function include the description of the multiple contributors that determine the extent of movement of soluble molecules into and out of the CNS. These include passive diffusion and active influx and efflux transport mechanisms that are operative at the level of the BBB, the choroid plexus, and the selected CNS regions that lack a BBB (circumventricular organs of the hypothalamus). These are all of central importance for the issue of drug delivery into the CNS. The review describes the challenges of how to "outwit" the BBB by manipulating transport systems and using novel vector delivery systems and/or direct intrathecal injections. The latter bypasses the restrictions imposed by the BBB but not the problem of diffusion within the CNS tissue. Illustrated in the review are emerging neuroimaging techniques that will enhance our capacity to evaluate the status of the BBB in vivo.

The section on disease includes consideration of infectious, inflammatory, vascular, and neoplastic disorders, each of which is affected by function and dysfunction of the BBB. Important issues raised include how infections access the CNS, the regulation of autoreactive immune cell trafficking across the BBB, the effect of ischemia on the BBB, and how to sustain tumor-directed chemotherapy responses. As the review concludes, an enhanced understanding of the biology of the BBB will enhance our opportunities to manipulate its properties for therapeutic purposes.

Jack P. Antel
Neurologist
Montreal, Quebec, Canada

There is a resurgence of interest in the biology of the BBB. Disruption of the BBB is an early event in many neuroinflammatory conditions, including bacterial meningitis and multiple sclerosis, and occurs secondary to cell damage in ischemia and trauma. Astrocytes, neurons, and pericytes around the endothelial cells form a neurovascular unit. Between the endothelial cells and the astrocytic end feet is a basal lamina. Damage to any of the components affects the function of the entire unit. Many laboratories are attempting to discover novel ways to alter BBB permeability transiently to allow drugs to pass from the blood into the brain. In this review, Neuwelt describes a wide range of experimental approaches. Some are based on the action of drugs, whereas others use changes in serum osmolality.

Gary A. Rosenberg
Neurologist
Albuquerque, New Mexico